

\$20.95



This document was produced  
by scanning the original publication.

Ce document est le produit d'une  
numérisation par balayage  
de la publication originale.

GEOLOGICAL SURVEY OF CANADA  
COMMISSION GÉOLOGIQUE DU CANADA

**CURRENT RESEARCH 1995-C  
CANADIAN SHIELD**

---

**RECHERCHES EN COURS 1995-C  
BOUCLIER CANADIEN**



1995



Natural Resources Canada  
Ressources naturelles Canada

Canada

### **NOTICE TO LIBRARIANS AND INDEXERS**

The Geological Survey's Current Research series contains many reports comparable in scope and subject matter to those appearing in scientific journals and other serials. Most contributions to Current Research include an abstract and bibliographic citation. It is hoped that these will assist you in cataloguing and indexing these reports and that this will result in a still wider dissemination of the results of the Geological Survey's research activities.

### **AVIS AUX BIBLIOTHÉCAIRES ET PRÉPARATEURS D'INDEX**

La série Recherches en cours de la Commission géologique contient plusieurs rapports dont la portée et la nature sont comparables à ceux qui paraissent dans les revues scientifiques et autres périodiques. La plupart des articles publiés dans Recherches en cours sont accompagnés d'un résumé et d'une bibliographie, ce qui vous permettra, on l'espère, de cataloguer et d'indexer ces rapports, d'où une meilleure diffusion des résultats de recherche de la Commission géologique.

**GEOLOGICAL SURVEY OF CANADA  
COMMISSION GÉOLOGIQUE DU CANADA**

**CURRENT RESEARCH 1995-C  
CANADIAN SHIELD**

---

**RECHERCHES EN COURS 1995-C  
BOUCLIER CANADIEN**

**1995**

©Minister of Energy, Mines and Resources Canada 1995

Available in Canada from

Geological Survey of Canada offices:

601 Booth Street  
Ottawa, Canada K1A 0E8

3303-33rd Street N.W.,  
Calgary, Alberta T2L 2A7

100 West Pender Street  
Vancouver, B.C. V6B 1R8

or from

Canada Communication Group - Publishing  
Ottawa, Canada K1A 0S9

and through authorized bookstore agents  
and other bookstores

A deposit copy of this publication is also available for reference  
in public libraries across Canada

Cat. No. M44-1995/3E  
ISBN 0-660-15810-8

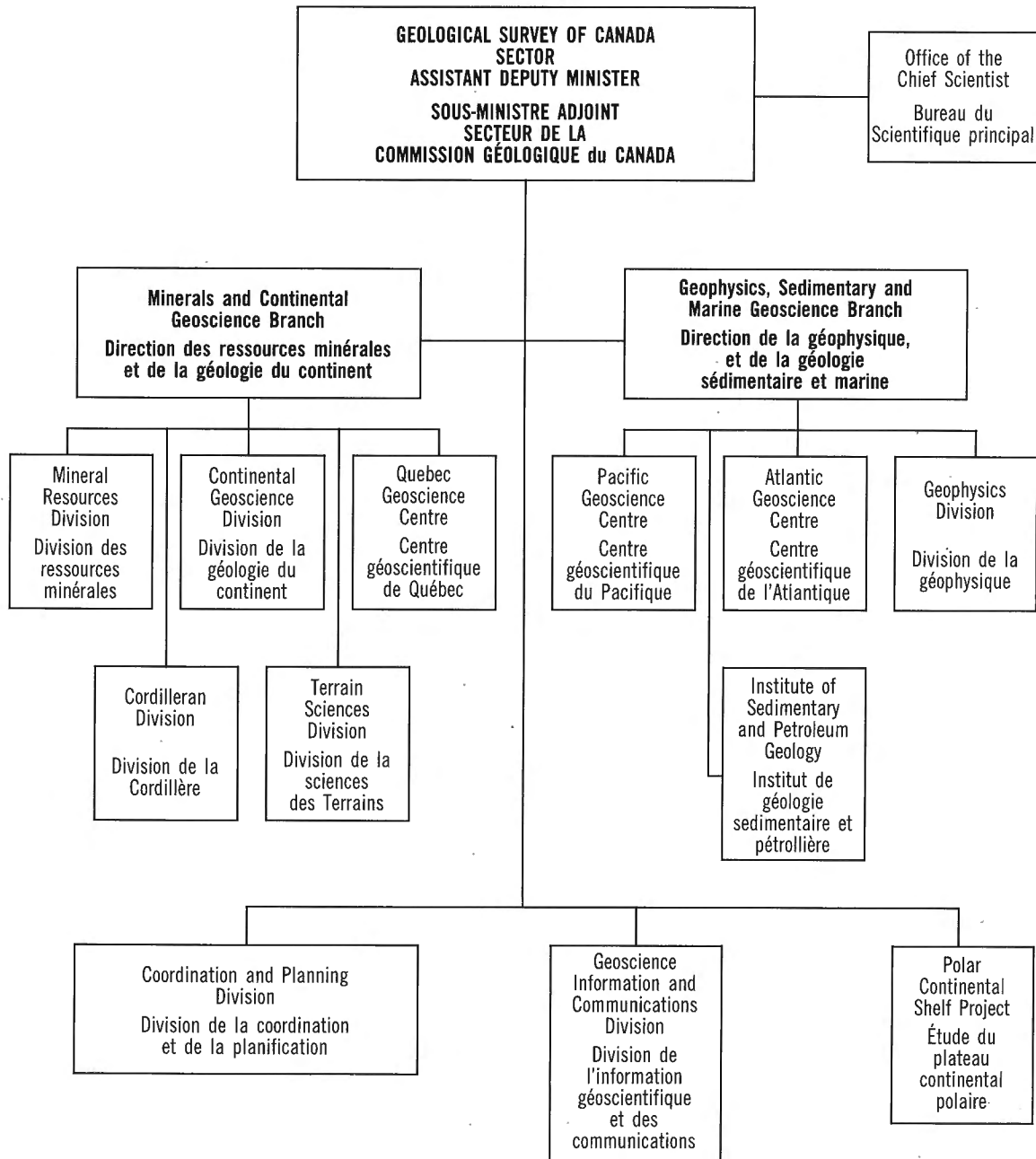
Price subject to change without notice

#### **Cover description**

Silicified pillow basalt, semi-conformable alteration zone, near Spi Lake, Kaminak Lake map area (55L/4), Northwest Territories. See report in this volume by Miller and Tella. (Photo by A.R. Miller; GSC 1994-791).

#### **Description de la photo couverture**

Basalte en coussin silicifié, zone d'altération semi-concordante, près du lac Spi, région cartographique du lac Kaminak (55L/4), Territoires du Nord-Ouest. Voir le rapport de Miller et Tella dans ce volume. (Photo prise par A.R. Miller; GSC 1994-791).



## Separates

A limited number of separates of the papers that appear in this volume are available by direct request to the individual authors. The addresses of the Geological Survey of Canada offices follow:

601 Booth Street  
OTTAWA, Ontario  
K1A 0E8  
(FAX: 613-996-9990)

Institute of Sedimentary and Petroleum Geology  
3303-33rd Street N.W.  
CALGARY, Alberta  
T2L 2A7  
(FAX: 403-292-5377)

Cordilleran Division  
100 West Pender Street  
VANCOUVER, B.C.  
V6B 1R8  
(FAX: 604-666-1124)

Pacific Geoscience Centre  
P.O. Box 6000  
9860 Saanich Road  
SIDNEY, B.C.  
V8L 4B2  
(Fax: 604-363-6565)

Atlantic Geoscience Centre  
Bedford Institute of Oceanography  
P.O. Box 1006  
DARTMOUTH, N.S.  
B2Y 4A2  
(FAX: 902-426-2256)

Québec Geoscience Centre  
2700, rue Einstein  
C.P. 7500  
Ste-Foy (Québec)  
G1V 4C7  
(FAX: 418-654-2615)

When no location accompanies an author's name in the title of a paper, the Ottawa address should be used.

## Tirés à part

On peut obtenir un nombre limité de «tirés à part» des articles qui paraissent dans cette publication en s'adressant directement à chaque auteur. Les adresses des différents bureaux de la Commission géologique du Canada sont les suivantes:

601, rue Booth  
OTTAWA, Ontario  
K1A 0E8  
(facsimilé : 613-996-9990)

Institut de géologie sédimentaire et pétrolière  
3303-33rd St. N.W.,  
CALGARY, Alberta  
T2L 2A7  
(facsimilé : 403-292-5377)

Division de la Cordillère  
100 West Pender Street  
VANCOUVER, British Columbia  
V6B 1R8  
(facsimilé : 604-666-1124)

Centre géoscientifique du Pacifique  
P.O. Box 6000  
9860 Saanich Road  
SIDNEY, British Columbia  
V8L 4B2  
(facsimilé : 604-363-6565)

Centre géoscientifique de l'Atlantique  
Institut océanographique Bedford  
B.P. 1006  
DARTMOUTH, Nova Scotia  
B2Y 4A2  
(facsimilé : 902-426-2256)

Centre géoscientifique de Québec  
2700, rue Einstein  
C.P. 7500  
Ste-Foy (Québec)  
G1V 4C7  
(facsimilé : 418-654-2615)

Lorsque l'adresse de l'auteur ne figure pas sous le titre d'un document, on doit alors utiliser l'adresse d'Ottawa.

---

# CONTENTS

---

The convoluted "layer-cake": an old recipe with new ingredients for the Swayze greenstone belt, southern Superior Province, Ontario <b>K.B. Heather, G.T. Shore, and O. van Breemen</b> . . . . .	1
Pre-Dubawnt plutonism and deformation in the Nicholson Lake-Dubawnt Lake area, Northwest Territories <b>T.D. Peterson and C. Lee</b> . . . . .	11
A potassic phreatomagmatic volcanic centre in the Thelon Basin (Northwest Territories): implications for diamond exploration <b>T.D. Peterson</b> . . . . .	19
Geology and structure of the Barbour Bay region, District of Keewatin, Northwest Territories, and its potential for industrial garnets <b>S. Tella, U. Mader, and M. Schau</b> . . . . .	27
Geological and age relationships of the margins of the Manitouwadge greenstone belt and the Wawa-Quetico subprovince boundary, northwestern Ontario <b>E. Zaleski, V.L. Peterson, and O. van Breemen</b> . . . . .	35
The Auyuittuq carving stone study project, eastern Baffin Island, Northwest Territories: a geological report <b>I. Ermanovics</b> . . . . .	45
Archean and Proterozoic lithology, structure, and metamorphism in the vicinity of Ege Bay, Baffin Island, Northwest Territories <b>R.J. Scammell and K.M. Bethune</b> . . . . .	53
Preliminary geological investigation of the Lake Harbour Group and surrounding gneissic rocks near Lake Harbour and Markham Bay, southern Baffin Island, Northwest Territories <b>D.J. Scott and L. Godin</b> . . . . .	67
A reconnaissance of the high grade metamorphic terrane south of Ghost Lake, southwestern Slave Province, Northwest Territories <b>J.B. Henderson and T. Chacko</b> . . . . .	77

Thematic structural studies in the Slave Province: preliminary results and implications for the Yellowknife Domain, Northwest Territories <b>W. Bleeker and C. Beaumont-Smith</b> . . . . .	87
Geology, geochronology, and metallogeny of High Lake greenstone belt, Archean Slave Structural Province, Northwest Territories <b>J.R. Henderson, J.A. Kerswill, M.N. Henderson, M. Villeneuve, C.A. Petch, J.F. Dehls, and M.D. OKeefe</b> . . . . .	97
Regional geology and mineral potential of the Winter Lake-Lac de Gras area, central Slave Province, Northwest Territories <b>P.H. Thompson, I. Russell, D. Paul, J.A. Kerswill, and E. Froese</b> . . . . .	107
Structural evolution of the Vizienz and Kogaluc greenstone belts in Minto block, northeastern Superior Province, northern Quebec <b>S. Lin, J.A. Percival, P.A. Winsky<sup>1</sup>, T. Skulski, and K.D. Card</b> . . . . .	121
Archean unconformity in the Qalluviartuuq greenstone belt, Goudalie domain, northern Quebec <b>P.A. Winsky, T.M. Kusky, J.A. Percival, and T. Skulski</b> . . . . .	131
Granite-greenstone terranes of the northern Goudalie domain, northeastern Superior Province, Quebec <b>J.A. Percival, T. Skulski, S. Lin, and K.D. Card</b> . . . . .	141
Polymetallic unconformity-related uranium veins in lower Proterozoic Amer Group, Pelly Lake map area, northern Thelon Basin, Churchill Province, Northwest Territories <b>A.R. Miller</b> . . . . .	151
Oxide iron-formation-hosted lode gold, Meliadine Trend, Rankin Inlet Group, Churchill Province, Northwest Territories <b>A.R. Miller, M.J. Balog, and S. Tella</b> . . . . .	163
Stratigraphic setting of semiconformable alteration in the Spi Lake area, Kaminak greenstone belt, Churchill Province, Northwest Territories <b>A.R. Miller and S. Tella</b> . . . . .	175
Lamprophyre dykes of the Christopher Island Formation, Thirty Mile Lake, District of Keewatin, Northwest Territories <b>A.L. Jones, A.R. Miller, A.E. Armitage, and N.D. MacRae</b> . . . . .	187



Paleomagnetism of 779 Ma Hottah gabbro sheets of the Wopmay Orogen, Northwest Territories <b>J.K. Park, K.L. Buchan, and S.S. Gandhi</b> . . . . .	195
Geological setting of Bode copper and Damp polymetallic prospects, central Great Bear magmatic zone, Northwest Territories <b>S.S. Gandhi and N. Prasad</b> . . . . .	201
Geological setting of the Sandhill Zn-Cu-Pb-Ag prospect in the Gibson-MacQuoid Lake area, District of Keewatin, Northwest Territories <b>A.E. Armitage, A.R. Miller, and N.D. MacRae</b> . . . . .	213
Granitoid plutons and major structures in the Iskwasum Lake sheet, Manitoba: a portion of the Flin Flon Domain of the Trans-Hudson Orogen <b>D.W. Morrison and J.B. Whalen</b> . . . . .	225
Preliminary diatom analysis of selected samples from Lake Abitibi and Glacial Lake Ojibway, Ontario and Quebec <b>C.L. Prévost, J.J. Veillette, and P.B. Hamilton</b> . . . . .	235
The spectacular cross-striated outcrops of James Bay, Quebec <b>J.J. Veillette and M. Roy</b> . . . . .	243
New evidence for northwestward glacial ice flow, James Bay region, Quebec <b>J.J. Veillette</b> . . . . .	249
Séquence des écoulements glaciaires dans le secteur de Chibougamau-Némiscau, Québec <b>S.J. Paradis et E. Boisvert</b> . . . . .	259
Accuracy of low porosity measurements in granite <b>T.J. Katsube and N. Scromeda</b> . . . . .	265
Author Index . . . . .	271

# The convoluted "layer-cake": an old recipe with new ingredients for the Swayze greenstone belt, southern Superior Province, Ontario<sup>1</sup>

Kevin B. Heather, Geoff T. Shore<sup>2</sup>, and Otto van Breemen  
Continental Geoscience Division

*Heather, K.B., Shore, G.T., and van Breemen, O., 1995: The convoluted "layer-cake": an old recipe with new ingredients for the Swayze greenstone belt, southern Superior Province, Ontario; in Current Research 1995-C; Geological Survey of Canada, p. 1-10.*

---

**Abstract:** Lithological and structural mapping, in conjunction with U-Pb zircon geochronology, indicates that a regionally coherent, upward facing, pre-D<sub>2</sub> stratigraphic sequence (i.e., the "layer-cake") is locally preserved in low strain domains within the Swayze greenstone belt. This stratigraphic sequence has undergone regional, upright F<sub>2</sub> folding which can be characterized as thick-skinned, involving large, sheet-like synvolcanic tonalite and diorite intrusions. The F<sub>2</sub> folds are doubly plunging and produce a distinctive cusped-lobate fold geometry. Recognition of a coherent pre-D<sub>2</sub> stratigraphic sequence will allow for the deciphering of the earlier D<sub>1</sub> regional structures and to extrapolate economically favourable packages of rocks into areas affected by D<sub>2</sub> folding, and overprinted by D<sub>3</sub> and D<sub>4</sub> structures (i.e., "convoluted"). The northeast-striking Wakami high-strain zone is a sinistral, extensional shear that may be analogous to the gold producing, northeast-striking, Kirkland Lake break. New age dates establish the presence of an older package of rocks along the southern margin of the Swayze belt.

**Résumé :** Une cartographie lithologique et structurale, en conjonction avec une géochronologie U-Pb sur zircon, indique qu'une séquence stratigraphique pré-D<sub>2</sub> (c'est-à-dire «le gâteau à étages»), cohérente sur le plan régional, orientée vers le haut, est préservée localement dans des domaines de faible contrainte au sein de la ceinture de roches vertes de Swayze. Cette séquence a subi un plissement régional F<sub>2</sub> droit, que l'on peut qualifier d'endodermique et qui a touché de vastes intrusions feuilletées de diorite et de tonalite hypovolcaniques. Les plis F<sub>2</sub> sont caractérisés par un plongement double et présentent une géométrie lobée-arquée distinctive. L'identification d'une séquence stratigraphique pré-D<sub>2</sub> cohérente permettra de déchiffrer des structures régionales D<sub>1</sub> plus anciennes et d'extrapoler des ensembles de roches économiquement favorables dans des régions affectées par un plissement D<sub>2</sub> et surimprimées par des structures D<sub>3</sub> et D<sub>4</sub> (c'est-à-dire «en volutes»). La zone de Wakami, fortement déformée et à orientation nord-est, est le résultat d'un cisaillement par distension senestre qui peut être analogue à la fracture de Kirkland Lake, à orientation nord-est, d'où l'on extrait de l'or. De nouvelles datations signalent la présence d'un ensemble de roches plus anciennes le long de la bordure sud de la ceinture de Swayze.

---

<sup>1</sup> Contribution to Canada-Ontario Subsidiary Agreement on Northern Ontario Development (1991-1995), under the Canada-Ontario Economic and Regional Development Agreement.

<sup>2</sup> Department of Geology, University of Western Ontario, London, Ontario, N6A 5B7

## INTRODUCTION

The Swayze greenstone belt and surrounding granitoid rocks represent the western extension of the mineral-rich Abitibi greenstone belt (Fig. 1). This summary is the third installment of results from the Swayze bedrock mapping program being conducted by the Geological Survey of Canada under the auspices of the Northern Ontario Development Agreement (NODA) for minerals. The project area encompasses approximately 12 000 km<sup>2</sup> southwest of Timmins, Ontario centred on the Swayze greenstone belt and surrounding granitoid terranes (Fig. 1). Additional geological, structural, and radiometric ages are reported in Heather (1993) and Heather and van Breemen (1994).

## GENERAL GEOLOGY

### *Metavolcanic-Metasedimentary Rocks of the biscotasing Arm*

The Biscotasing arm of the Swayze greenstone belt, herein referred to as the Biscotasing arm, extends for over 50 km (Fig. 2). Current mapping indicates the presence of amphibolite-facies mafic and felsic metavolcanic rocks in Hong Kong Township, joined by chert-magnetite iron-formation and metasedimentary rocks in Carew and Joffre townships. Rocks of the Biscotasing arm appear to be a southeastward extension of units exposed in the Cunningham and Blamey township area. Mafic metavolcanic rocks are predominant in the Biscotasing arm and consist of massive, medium- to

coarse-grained flows and pillowed flows with local flow top breccia zones; top indicators are not preserved. Felsic rocks consist of massive flows, lapilli tuffs, feldspar-quartz crystal tuffs and volcanoclastic sediments. The massive flows range from fine grained to quartz porphyritic and commonly contain biotite and locally garnet. Felsic fragmental and volcanoclastic rocks constitute the majority of the felsic package and commonly contain garnet, epidote, hornblende, and minor diopside. Narrow, chert-magnetite iron-formation occurs locally near the mafic-felsic contact, however its presence is significant for both regional stratigraphic correlation and base-metal exploration. A narrow iron-formation located on the Hollinger road contains abundant coarse grained garnet and re-folded folds (Fig. 3). Mafic metavolcanic and metasedimentary rocks of the Biscotasing arm cannot be traced across Biscotasi Lake, however they appear to grade into zones of complex diorite and a body of quartz-porphyritic biotite tonalite (Fig. 2).

### *Ramsey-Algoma granitoid complex*

The vast Ramsey-Algoma granitoid complex (Heather, 1993; Heather and van Breemen, 1994) is located south of the main Swayze greenstone belt (Fig. 2). During 1994 that part of the complex lying south and east of the Biscotasing arm was mapped at 1:50 000 scale, building on previous mapping by Rogers (1962). Granitoid rock names used in this report follow Streckeisen (1976) and are based on field estimates of the proportions of quartz, plagioclase, potassium feldspar, and mafic minerals.

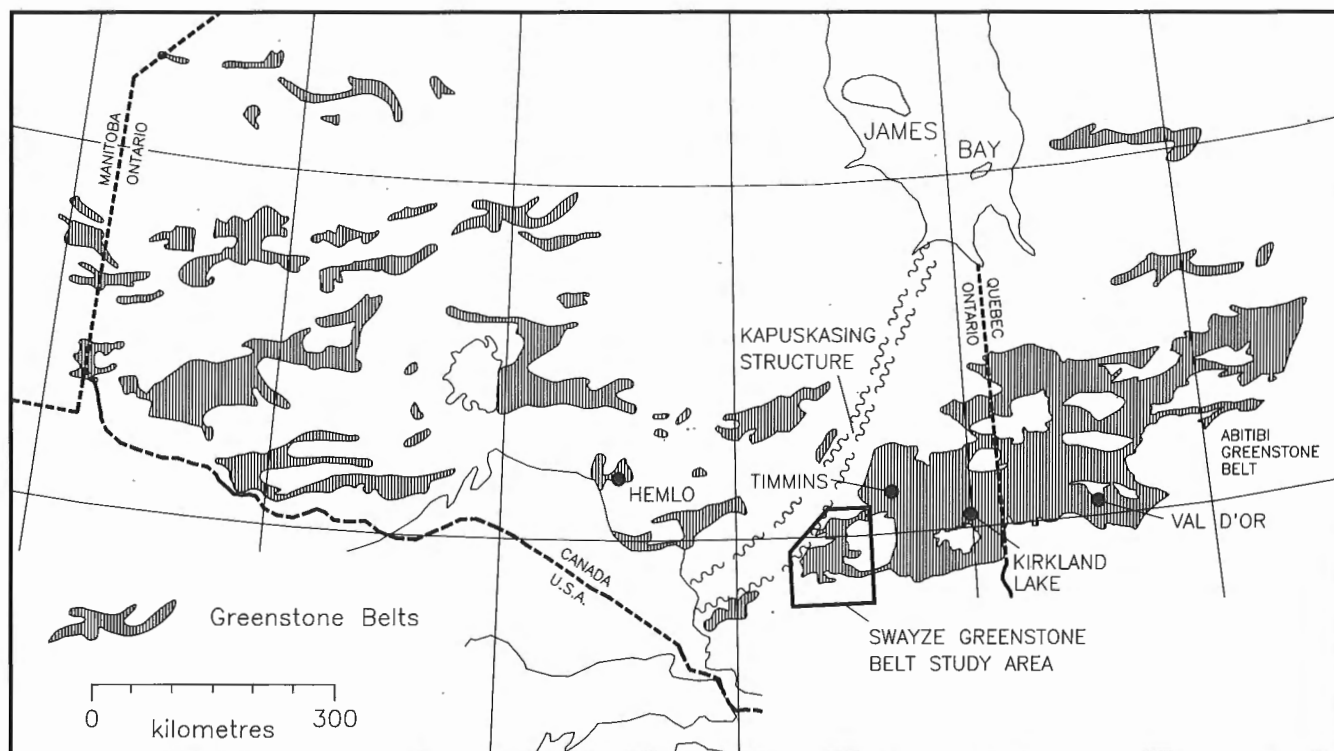
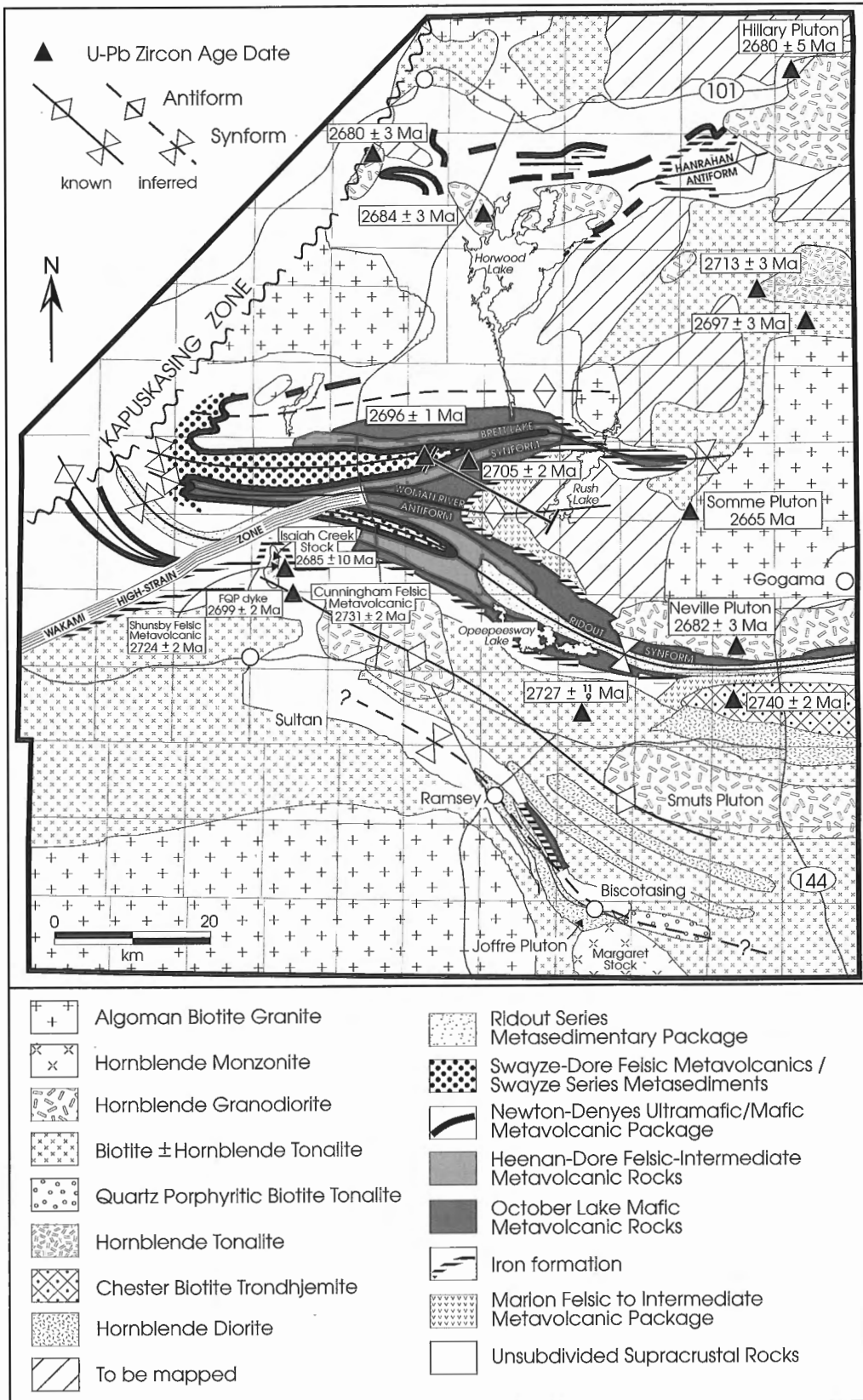


Figure 1. Regional setting of the Swayze greenstone belt study area.



**Figure 2.** Simplified bedrock and structural geology map for the Swayze study area depicting major  $F_2$  fold axes and high-strain zones. Location of the stratigraphic section depicted in Figure 5 is indicated by the bar (black) on the north limb of the Woman River Antiform. Late diabase dykes have been omitted for clarity.

Several complex diorite zones were identified: 1) two linear, east-southeast-striking, 1 km wide zones along the northern margin of the Biscotasing arm and extending east to Bisotasi Lake, and 2) isolated outcrops in Alcona Township. These diorite zones are texturally and mineralogically similar to those described by Heather and van Breemen (1994) and they commonly occur proximal to the supracrustal greenstone rocks. Despite diverse textures, the diorites are generally massive to weakly foliated, medium- to coarse-grained, and dominated by varying proportions of amphibole and plagioclase.

The Joffre pluton is a distinctive linear body, approximately 3 km by 18 km, adjacent to the southern margin of the Biscotasing arm (Fig. 2). This weakly to strongly foliated unit consists of abundant melanocratic hornblende diorite enclaves within a more leucocratic, medium- to coarse-grained, hornblende diorite to quartz diorite. The melanocratic enclaves are characterized by igneous textures, cusped margins, and are variably assimilated, all suggestive of magma mingling (Fig. 4).



**Figure 3.** Z-shaped  $F_2$  fold re-folding an  $F_1$  fold within a chert-magnetite iron-formation. From the Biscotasing arm of the Swayze greenstone belt, Carew Township. Scale card indicates north. (GSC 1994-771G)

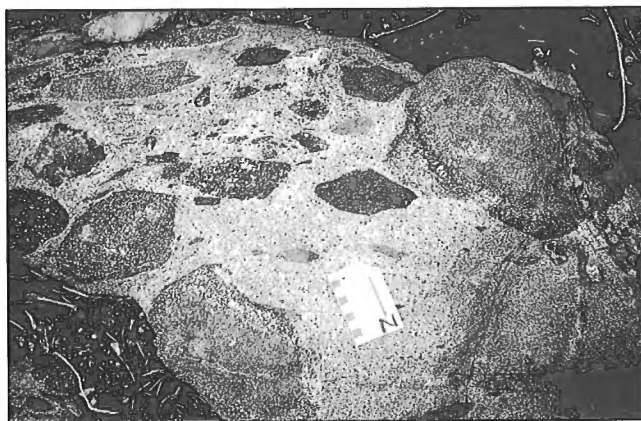


**Figure 4.** Melanocratic hornblende diorite enclaves within leucocratic hornblende diorite of the Joffre pluton. Scale card indicates north. (GSC 1994-771F)

Foliated biotite±hornblende tonalites are volumetrically the most significant and among the oldest granitoids in the map area (Heather and van Breemen, 1994). Geochronological studies indicate that some of the tonalites are coeval with felsic metavolcanic rocks in the Swayze greenstone belt (Heather and van Breemen, 1994; this report). A large body of biotite±hornblende tonalite occurs in the northern part of the Ramsey-Algoma complex (Fig. 2). These tonalites form a complex zone characterized by moderately to strongly foliated (locally gneissic) rocks and heterogeneous breccia zones consisting of biotite and amphibole tonalite, melatonalites and diorites intruded by leucocratic, aplitic biotite tonalites which impart a "swirly" texture to the rocks.

A foliated, quartz-porphyrific biotite granodiorite to tonalite unit forms an east-southeast-striking, linear zone, approximately 5 km wide by 13 km long, extending as far west as Biscotasing and as far south as the Margaret stock (Fig. 2). Westward this unit appears to be transitional into the Biscotasing arm supracrustal rocks suggesting that it is cogenetic. Smoky quartz phenocrysts form distinctive resistant "knots" on the weathered surface.

The 100 km<sup>2</sup> Margaret stock is a texturally and mineralogically distinct hornblende monzonite is located at the eastern terminus of the Biscotasing arm (Fig. 2). The monzonite is massive, pink to red weathering, coarse grained (K-feldspar crystals up to 3 cm), homogeneous and locally contains an igneous foliation defined by alignment of amphibole (±secondary biotite) and tabular feldspar.

A 25 km long by 10 km wide body of leucocratic, biotite granodiorite centred in Smuts Township is herein referred to as the Smuts pluton (Fig. 2). This massive to weakly foliated, medium grained, equigranular unit contains few crosscutting dykes and is extensively hematized. The western and southern margins of the pluton are tonalitic and contains xenoliths of older, foliated biotite tonalite. The Smuts pluton is similar to other granitoids belonging to the circa 2680 Ma suite of intrusions (Heather and van Breemen, 1994).

Massive biotite granite belonging to the Algonian Suite is the youngest (circa 2665-2660 Ma) phase in the area occurring as large mappable plutons as well as numerous crosscutting dykes in older units (Heather, 1993; Heather and van Breemen, 1994). A large body of Algonian biotite granite, southwest of Ramsey (Fig. 2), extends eastward across Ramsey Lake, where a massive phase of equigranular biotite granite is transitional with heterogeneous breccia zones containing xenoliths of biotite±amphibole tonalite, diorite and foliated amphibolite.

## STRATIGRAPHIC RELATIONSHIPS

The Abitibi Subprovince, including the Swayze greenstone belt, has recently been subdivided into a number of assemblages (Jackson and Fyon, 1991). In an attempt to test the validity of the assemblage subdivisions proposed for the Swayze belt, mappable rock units were assigned "package" names (Fig. 5) based on rock type, composition, and age (when available).

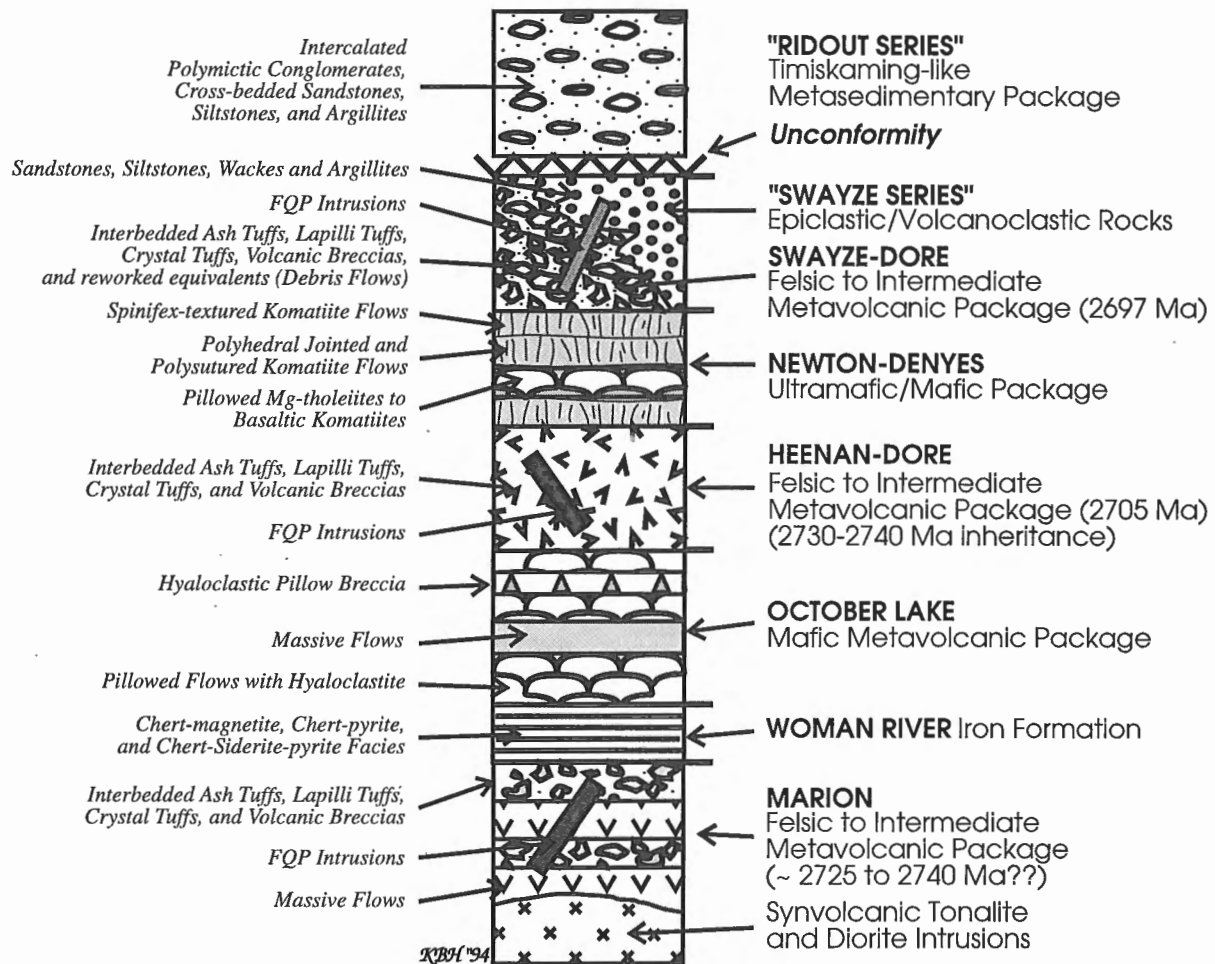


**Figure 5.** An idealized vertical section depicting the pre- $D_2$ ,  $D_1$  lithotectonic stratigraphic sequence'. Note that there is no true thickness implied for the packages, nor is any intra-package stratigraphy. See Figure 2 for location of this 'stratigraphic sequence'. The Ridout Series occurs within the Ridout synform and does not occur on the north limb of the Woman antiform.

Within the Swayze greenstone belt a coherent, continuously upward facing, pre- $D_2$  panel of rocks (i.e.,  $D_1$  lithotectonic stratigraphic sequence) is preserved in a low strain domain on the north limb of the regional  $F_2$  Woman River antiform (Fig. 2, 5). Stratigraphic sequences have been recognized elsewhere in the Abitibi subprovince (e.g., Pyke, 1982; MERQ-OGS, 1983), however this is the first formal recognition of such a pre- $D_2$  'stratigraphic sequence' within the Swayze belt. Preservation of this coherent 'stratigraphic sequence' is interpreted to be the result of a regional strain shadow effect created by the large Kenogamissi Batholith to the east (Fig. 2). The effect of  $D_1$  deformation on the 'stratigraphic sequence' preserved on the north limb of the Woman River antiform appears to be minimal, however this relationship is not well understood and is best referred to as a  $D_1$  lithotectonic stratigraphic sequence (Fig. 5).

The regional  $F_2$  Woman River antiform is cored by felsic to intermediate metavolcanic and metaplutonic rocks of the Marion package (Heather, 1993) of which the lower portion of the package is characterized by felsic to intermediate metavolcanic rocks and abundant, apparently coeval tonalite

to diorite intrusions. The upper portion of the package is dominated by variably chloritized and sulphidized felsic to intermediate lapilli tuffs, volcanic breccias (Fig. 6), and feldspar-quartz porphyries that form the footwall rocks to the Woman River iron-formation (Goodwin, 1965). The strong chloritic alteration, incipient zones of hydrothermal brecciation and crackle breccias are likely related to hydrothermal fluids responsible for formation of the exhalative Woman River iron-formation. Elsewhere, the Marion package consists of massive, felsic to intermediate flows, as well as ash and crystal tuffs interbedded with lapilli tuffs and volcanic breccias. Mafic and ultramafic dykes are common and are interpreted to represent feeders to the overlying mafic to ultramafic metavolcanic rock packages. The Marion package is thought to be one of the oldest in the Swayze belt. It is likely correlative with rocks of the  $2727 \pm 1.5$  Ma Bartlett assemblage (Corfu et al., 1989), located east of the Kenogamissi Batholith, and with rocks of the upper part of the Deloro Group, near Timmins (Pyke, 1982). It may also be correlative with older rocks in the Shunsby-Cunningham area of the Swayze belt (see Geochronology section).

Overlying the Marion metavolcanic package (Fig. 2, 5), in an apparently conformable relationship, is the large and regionally extensive Woman River iron-formation. The Woman River iron-formation is a regionally significant unit that can be traced for tens of kilometres around the Woman River antiform and beyond.

Overlying the Woman River iron-formation is a thick, monotonous package of massive to pillowed, Fe-tholeiitic to Mg-tholeiitic, mafic metavolcanic rocks. Rock types and textures typical of this package occur immediately east of October Lake and herein this package will be informally referred to as the October Lake mafic metavolcanic package (Fig. 2, 5). A preliminary evaluation of the contact between the iron-formation and this mafic metavolcanic package, in the vicinity of the Woman River antiform closure, suggests it is not highly strained and may thus be a conformable stratigraphic contact rather than a significant tectonic contact. Along the northern limb of the F<sub>2</sub> Woman River antiform, top indicators from pillow facings and flow top breccia units are consistently to the northwest, whereas in the vicinity of the axial trace they are to the west, consistent with the observations of Goodwin (1965).

Overlying the October Lake mafic package is the Heenan-Dore felsic metavolcanic package (Fig. 2, 5) that consists predominantly of felsic to intermediate pyroclastic and volcanoclastic rocks, as well as synvolcanic feldspar-quartz porphyry (FQP) intrusions (Heather, 1993). A quartz-phyric rhyolite from this package yielded an U-Pb zircon age of 2705 ± 2 Ma (Heather and van Breemen, 1994). Significantly, the rhyolite contained a second, concordant population of older inherited zircons that yielded ages of ~2740-2730 Ma, indicating that the 2705 Ma felsic package was extruded through a substrate of ~2740-2730 Ma aged rocks. Facing indicators were not observed within this poorly exposed package. The contact between the October Lake and the Heenan-Dore packages has not been observed, however regional deformation intensity data indicate low strain in the vicinity of the inferred contact. Although a narrow, regionally

significant high strain zone along this contact cannot be ruled out, the presence of older inherited zircons within the Heenan-Dore package intimates a parautochthonous, if not an autochthonous, relationship with the underlying volcanics.

Overlying the Heenan-Dore felsic metavolcanic package is a regionally extensive package of mafic and ultramafic metavolcanic flows and intrusions, herein informally referred to as the Newton-Denyes ultramafic/mafic metavolcanic package. The package extends across the belt (Fig. 2) and forms a prominent airborne magnetic anomaly that defines a regional F<sub>2</sub> synform, which is apparently doubly plunging and cored by rocks of the Swayze-Dore felsic package. This package consists of pillowed Mg-tholeiites and basaltic komatiites that are intercalated with polysutured, polygonal jointed, and spinifex-textured picritic komatiites. The pillowed Mg-tholeiites and basaltic komatiites exhibit well developed hyaloclastic breccias, variolites and flow top breccias. Polysutured flow top breccias, pillow facings, and downward fanning spinifex sheaths all indicate northward facing.

Overlying the Newton-Denyes package (Fig. 2, 5) are rocks of the Swayze-Dore package (Heather, 1993), a mixed group of felsic to intermediate pyroclastic and volcanoclastic rocks (Fig. 7) intercalated with epiclastic metasedimentary rocks of the 'Swayze Series' (Furse, 1932; Rickaby, 1935). Cattell et al. (1984) dated this package at 2697 ± 1.5 Ma and interpreted it to underlie the komatiite-dominated Newton-Denyes package. Previous maps of the area (summarized on Map 2543, Ontario Geological Survey, 1991), and descriptions by Jackson and Fyon (1991), indicate that rocks of the Swayze-Dore package extend from Halcrow Township in the west to Newton Township in the east and only occur north of the Newton-Denyes package. Our mapping suggests a different geometry with the Swayze-Dore package occupying the core of the regional, doubly plunging F<sub>2</sub> Brett Lake synform (Fig. 2) that is outlined by prominent magnetic anomalies related to ultramafic rocks of the Newton-Denyes package. In addition to being surrounded, and hence underlain by rocks of the Newton-Denyes ultramafic/mafic metavolcanic

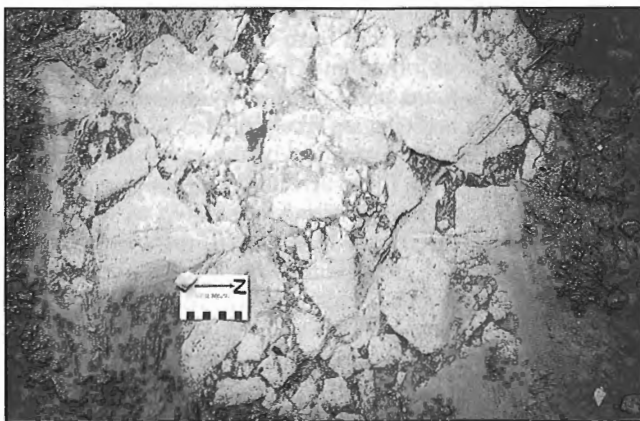


**Figure 6.** Chloritized felsic volcanic breccia from the Marion package, Heenan Township. Located near the fold closure of the F<sub>2</sub> Woman River antiform, note the low strain state. Scale card indicates north. (GSC 1994-771B)



**Figure 7.** Poorly sorted, felsic volcanic breccia (debris flow?) from the Swayze-Dore package, Swayze Township. Note the low strain state. D. Anderson for scale. (GSC 1994-771A)

package, facing indicators from the Swayze-Dore rocks also define a synformal geometry consistent with the regional magnetic pattern. Furthermore, the Swayze-Dore package can only be traced as far as Dore Township and does not extend into Newton Township as previously depicted, a geometry that requires transgression across several regional, magnetic anomalies. In fact the felsic metavolcanic rocks in Newton Township look very similar to those of the Heenan-Dore package and may be a fold repetition of that same package. Based on the current geometry, the age of the ultramafic/mafic Newton-Denyes package is bracketed by 2705 Ma rocks of the Heenan-Dore package and 2697 Ma rocks of the Swayze-Dore package (Fig. 5).

## STRUCTURAL GEOLOGY

A refined and updated structural chronology of that presented in Heather (1993) is outlined here and, also in light of new geochronological and stratigraphic information, implications for regional fold geometries. The discussion is restricted to the southern Swayze belt where the bulk of the structural work has been done to-date. The character and style of the  $D_1$  deformation is poorly understood, however recognition of the coherent pre- $D_2$ , 'lithotectonic stratigraphic sequence' will help in deciphering the earlier  $D_1$  structural framework. The  $D_1$  structures consist of a penetrative foliation and isoclinal, commonly intrafolial  $F_1$  folds. Currently, neither the geochronology nor the regional structure indicate either a young over old relationship (i.e., thrust) or any regional, downward facing folds (i.e.,  $F_1$  nappes). There are small, outcrop-scale reclined and downward facing  $F_2$  folds, however their regional significance remains equivocal. Future work will focus on identification of  $D_1$  stratigraphic cutoffs as well as regional  $F_1$  folds.

The map pattern preserved within the Swayze greenstone belt is dominated by regional  $F_2$ , antiforms and synforms with an associated  $S_2$  axial planar foliation. Many of these folds were previously recognized (e.g., Furse, 1932; Rickaby, 1935; Donovan, 1965; Goodwin, 1965); however, they were interpreted as  $F_1$  folds. Results from the current mapping indicate that in many cases a penetrative  $S_1$  foliation, along with the  $D_1$  lithotectonic stratigraphic sequence, is folded about  $F_2$  folds. The antiforms (e.g., Woman River antiform) tend to be open to tight, whereas the synforms (e.g., Brett Lake synform) are tight to isoclinal. The limbs of the  $F_2$  antiforms are highly attenuated, whereas the noses are structurally thickened. The  $D_1$  lithotectonic stratigraphic sequence has undergone regional, upright to locally inclined  $F_2$  folding that can be characterized as thick-skinned, because it involves large, sheet-like synvolcanic tonalite and diorite intrusions. The  $F_2$  folds such as the Brett Lake synform are doubly plunging (i.e., noncylindrical) resulting in distinctive fold patterns in map view (Fig. 2). Involvement of competent crystalline synvolcanic intrusions in the folding produces a distinctive cusped-lobate fold geometry (Fig. 2) owing to the high rheological contrast between the greenstones and the intrusive rocks.

The  $F_2$  synforms are the locus of intense deformation characterized by profound flattening, tight to isoclinal folding, transposition, and locally a component of dextral simple shear in the east-southeast-striking zones. These zones are interpreted to be syn- to late- $D_2$  because they are localized within  $F_2$  synforms and no overprinting relationships are documented to support a distinct deformation event. These high-strain zones are thought to be correlative with the major "breaks" documented elsewhere in the Abitibi greenstone belt. The Timiskaming-like, Ridout Series metasedimentary rocks are localized within the core of the  $F_2$  Ridout synform (Fig. 2) and are thought to unconformably overlie the older metavolcanic and metasedimentary rock packages. Both the Ridout metasedimentary rocks and the older metavolcanic and metasedimentary rocks have undergone folding and shearing. Stratigraphic relationships within these high-strain zones are strongly disrupted making regional correlations difficult, but not necessarily impossible. These east-southeast-striking high-strain zones commonly are overprinted by a northeast-striking crenulation cleavage associated with outcrop-scale, Z-shaped  $F_4$  crenulation folds.

A major, northeast-striking  $D_3$  structure, referred to here as the Wakami high-strain zone (Fig. 2), sinistrally displaces regional magnetic anomalies by 10-15 km. This feature appears to be a greenstone-belt-scale, sinistral, extensional shear band that apparently dies out to the northeast by bending into the regional foliation in Dore Township. Outcrop evidence of a sinistral, extensional crenulation cleavage overprinting  $D_2$  strained rocks is found locally within this zone (Fig. 8). The relationship between the northeast-striking dextral, crenulation cleavage ( $S_4$ ) and this sinistral, extensional cleavage is not well constrained. The sinistral,  $D_4$  Wakami high-strain zone appears to overprint and deflect the syn- to late- $D_2$  high-strain zones. At one locality, the northeast-striking, dextral cleavage ( $S_4$ ) overprints a sinistrally extended quartz vein, however the relation between the sinistral extension recorded by the vein and that recorded by the Wakami zone is not clear. As reported in Heather (1993) a rare,

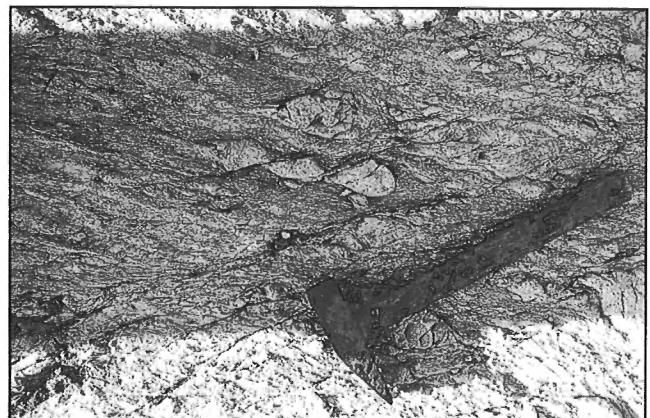


**Figure 8.** Sinistral extensional shear bands ( $S_3$  crenulation cleavage) overprinting a strong  $S_2$  foliation within an intermediate volcanoclastic lapilli tuff, Dore Township. Note the sinistral extension of the lapilli fragments. Hammer for scale. (GSC 1994-771A)



subhorizontal cleavage ( $S_5/D_5$ ) overprints the syn- to late- $D_2$  high strain zones and the  $D_4$  dextral, northeast-striking cleavage but its relation to the northeast-striking,  $D_3$  sinistral structures is not known. Conjugate kink-bands ( $D_6$ ) and late, northeast- and northwest-striking brittle faults ( $D_7$ ) round out the regional structural chronology. The major northwest-striking, sinistral faults are spaced in the order of 5-10 km.

## GEOCHRONOLOGY

Preliminary U-Pb geochronological results are presented for five samples collected during the 1993 field season and an updated age for a phase of the Kenogamissi Batholith (Fig. 2). These new ages and those reported in Heather and van Breemen (1994) are depicted graphically in a time/space diagram along with structural and mineral deposit information (Fig. 9). A felsic volcanoclastic tuff from the stratigraphic footwall of the Shunsby base-metal occurrence yielded an age of  $2724 \pm 2$  Ma. Approximately 3 km south of the Shunsby occurrence, in Cunningham Township, a felsic lapilli tuff containing flow banded rhyolite and pumiceous fragments yielded an age of  $2731 \pm 2$  Ma. A feldspar-quartz porphyry (FQP) dyke cutting

a strong  $S_1$  foliation and axial planar to  $F_2$  folds of that same foliation is dated at  $2699 \pm 3/-2$  Ma, placing an upper limit on  $D_1$  deformation. A preliminary age of  $2685 \pm 10$  Ma for the Isaiah Creek stock, long thought to be synvolcanic, shows it to be some 30 to 40 Ma younger than the felsic metavolcanic rocks in the footwall to the Shunsby mineralization. A biotite tonalite from immediately south of the Swayze greenstone belt yields a preliminary age of  $2727 \pm 11/-9$  Ma. A refined age of  $2680 \pm 5$  Ma was obtained for the Hillary hornblende granodiorite, located along the northern margin of the Kenogamissi Batholith (Fig. 2).

## DISCUSSION

The time/space diagram presented in Figure 9 summarizes our understanding of the volcanic, plutonic, and deformation histories based on available geochronological and structural data for the Swayze belt and surrounding granitoid complexes. The recognition of a coherent, upward facing, pre- $D_2$  'stratigraphic sequence' preserved in low strain domains can be thought of as a  $D_1$  lithotectonic "layer-cake". A feldspar quartz porphyry (FQP) dyke cutting a strong  $S_1$  foliation and

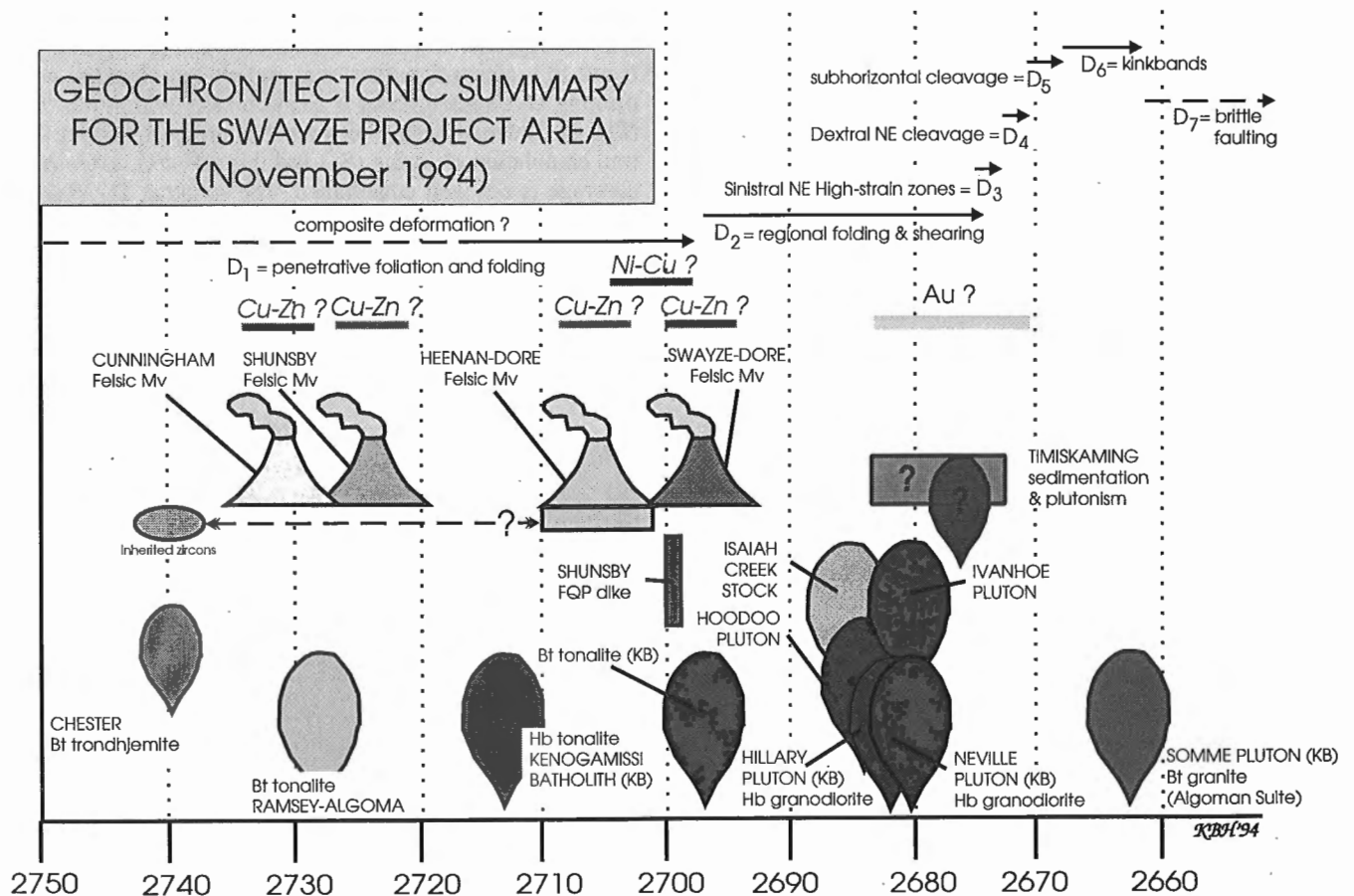


**Figure 9.** Schematic time/space diagram summarizing the volcanic, plutonic, and deformation histories in light of the new geochronological and structural data collected to-date for the Swayze greenstone belt and surrounding granitoid complexes.

axial planar to  $F_2$  folds of that same foliation is dated at  $2699 \pm 3/-2$  Ma, placing an upper limit on  $D_1$  deformation (Fig. 9). This 'stratigraphic sequence' has undergone regional, upright to inclined  $F_2$  folding, which can be characterized as thick-skinned, involving large, sheet-like synvolcanic tonalite and diorite intrusions. The  $F_2$  folds are doubly plunging and produce a distinctive cusped-lobate fold geometry.

The south limb of the Woman River antiform is highly attenuated with the Woman River iron-formation being dislocated into isolated boudins that are strung out to the east. The October Lake mafic metavolcanic package faces northwest on the north limb of the Woman River antiform, west in the axial region of the fold and west to southwest on the south limb. Early workers (e.g., Laird, 1932, 1936; Moorhouse, 1951) recognized that the narrow band of greenstone belt rocks located south of the Kenogamissi Batholith defined a synclinal structure. The Ridout synform is now interpreted as a regional, isoclinal  $F_2$  fold that is offset 10-15 km sinistrally along the major, northeast-striking,  $D_3$  Wakami high-strain zone (Fig. 2).

Mafic pillowed metavolcanic rocks located north of the Ridout metasedimentary rocks are interpreted to be the southeast strike extension of the October Lake package which stratigraphically overlies the Woman River iron-formation (Fig. 2, 5). The pillows are moderately to strongly deformed in this region, however, shape fabrics at several localities suggest tops to the west, parallel to the strong foliation, or to the southwest. A similar looking mafic metavolcanic package, located to the south of the Ridout package, faces north and locally west, parallel to a strong foliation, which is consistent with these mafic metavolcanics being on the south limb of the  $F_2$  Ridout synform and possibly part of the October Lake package. Although highly attenuated, and possibly cut out due to shearing, the closure of the  $F_2$  Ridout synform is interpreted to occur in the vicinity of Schist Lake, near the Potier-Yeo township boundary. This interpreted closure is based on the distribution of iron-formation (i.e., magnetic highs and regional electromagnetic conductors) within the southern mafic package, which appears to outline a fold that hooks to the north before being truncated by the Ridout metasedimentary package. Rocks to the east of this inferred  $F_2$  synform should be correlative with the Marion felsic to intermediate metavolcanic package.

Similar intermediate pyroclastic rocks occur immediately north of the  $2740 \pm 2$  Ma synvolcanic Chester granitoid complex, the oldest dated rock within the Swayze greenstone belt (Fig. 9). Similar intermediate to felsic metavolcanic rocks can be traced discontinuously for nearly 50 km to the west along the southern margin of the Swayze greenstone belt. Felsic to intermediate metavolcanic rocks associated with the large Shunsby iron-formations, in Cunningham, Garnet and Blamey townships, are thought to be correlative with those along the southern margin of the greenstone belt. Two of these felsic metavolcanic rocks in Cunningham Township yielded ages of  $2724 \pm 2$  Ma and  $2731 \pm 2$  Ma (Fig. 9) consistent with this regional correlation. A foliated biotite tonalite (Fig. 2), immediately south of intermediate crystal and lapilli tuffs within the Swayze greenstone belt, is preliminarily dated as  $2727 \pm 11/-9$  Ma (Fig. 9), again consistent with the regional

correlation. Rocks in the Biscotasing arm of the Swayze belt contain a strong  $S_1$  foliation that is consistently overprinted by a counterclockwise  $S_2$  foliation, axial planar to metre-scale Z-shaped  $F_2$  folds that plunge moderately to the northwest. The vergence of these folds is consistent with them being on the south limb of a regional,  $F_2$  antiform and hence part of the circa 2730 Ma package of rocks (Fig. 2). The Joffre pluton also contains an  $S_2$  foliation, consistently clockwise to an  $S_1$  foliation (Heather and van Breemen, 1994). Locally, compositional banding and an early tectonic foliation ( $S_1$ ) within tonalites of the Ramsey-Algoma granitoid complex are overprinted by a prominent east-southeast-striking foliation ( $S_2$ ), producing folds ( $F_2$ ) that plunge shallowly to moderately west to northwest.

Both the October Lake mafic package and the overlying 2705 Ma Heenan-Dore felsic package are repeated to the north of the  $F_2$  Brett Lake synform in Newton Township (Fig. 2). Pillows in the mafic package consistently face south and felsic fragmental rocks to the south are identical to those of the Heenan-Dore package. These felsic rocks have previously been correlated with the 2697 Ma Swayze-Dore felsic rocks (Donovan, 1965; Jackson and Fyon, 1991); however, this hypothesis would require crossing several airborne magnetic anomalies, which outline komatiites of the Newton-Denyes package on the north limb of the  $F_2$  Brett Lake synform.

## CONCLUSIONS AND IMPLICATIONS FOR EXPLORATION

A coherent  $D_1$  lithotectonic stratigraphic sequence (i.e., the "layer-cake") that has undergone upright to locally inclined  $F_2$  folding is recognized in the Swayze greenstone belt. The  $F_2$  folding can be characterized as thick-skinned, involving large, sheet-like synvolcanic tonalite and diorite intrusions of the surrounding granitoid complexes. Involvement in the folding of competent crystalline synvolcanic intrusions produces a distinctive cusped-lobate fold geometry. The distribution of major rock packages is strongly controlled by the north- to northeast-trending,  $F_2$ -fold enveloping surface. Major rock packages can be traced along strike, around regional  $F_2$  folds, and most importantly across the dominantly east-striking assemblage boundaries of Jackson and Fyon (1991).  $D_3$  and  $D_4$  high-strain zones have further modified this folded,  $D_1$  lithotectonic stratigraphic sequence. Despite this structural complexity, it may be possible to correlate packages of rocks across the regional high-strain zones (i.e., the "breaks") in the Swayze belt. This study has attempted to show, based on new structural and geochronological information, that the assemblage boundaries proposed by Jackson and Fyon (1991) require revision. We also suggest that the assemblage boundaries within the adjoining Abitibi greenstone belt and, perhaps, across the entire Superior Province need to be re-evaluated in light of the results presented.

Implications of this study for mineral exploration are: (1) recognition of a  $D_1$  lithotectonic stratigraphic sequence allows more accurate extrapolation of favourable rock packages (e.g., VMS Cu-Zn, Ultramafic Ni-Cu) into structurally

complex areas, affected by  $F_2$  folding,  $D_3$  and  $D_4$  high strain zones (i.e., "convoluted"), and (2) delineation of several regional, high-strain zones ("breaks") as potential hosts for gold mineralization. The similarity in regional setting between the Kirkland Lake break (Abitibi belt) and the Wakami high-strain zone (Swayze belt) is believed to be significant.

## ACKNOWLEDGMENTS

D. Anderson contributed to the mapping and along with J. Aubry and B. Baran provided conscientious and pleasant field assistance. S. Fumerton, K. Houle, and B. Yee are thanked for all their help over the course of the summer. Staff of the Timmins Resident Geologists Office provided many essential services and logistical support when necessary. The strong support and interest by the exploration industry is acknowledged in particular: B. Jeffery, K. Watson, R. Ban, and M. Houle (Falconbridge, Timmins); R. Dahn and J. Wakeford (Noranda, Timmins); and J. Perry and T. Hart (Inco, Sudbury). D. Panagapko (Cameco, Sudbury) is thanked for his support and for taking the senior author on guided tours of rocks in portions of Halcrow, Tooms, and Benton townships. Geological discussions with J. Ayer, M. Bernier, and A. Fyon (OGS) are acknowledged. Visits to the field by C. van Staal, J.A. Percival, E. Zaleski, and G. Peterson (GSC) provided different perspectives on a variety of geological problems which is always welcomed. Cees van Staal and John A. Percival provided constructive reviews of this report.

## REFERENCES

- Cattell, A.C., Krogh, T.E., and Arndt, N.T.**  
1984: Conflicting Sm-Nd whole-rock and U-Pb zircon ages for the Archean lavas from Newton Township, Abitibi Belt, Ontario; *Earth and Planetary Science Letters*, v. 70, p. 280-290.
- Corfu, F., Krogh, T.E., Kwok, Y.Y., and Jensen, L.S.**  
1989: U-Pb zircon geochronology in the southwestern Abitibi greenstone belt, Superior Province; *Canadian Journal of Earth Sciences*, v. 26, p. 1747-1763.
- Donovan, J.F.**  
1965: Geology of Swayze and Dore Townships, District of Sudbury, Ontario; Ontario Department of Mines, Geological Report No. 33, 25 p., includes Map 2070, scale 1:31 680.
- Furse, G.D.**  
1932: Geology of the Swayze area; Ontario Department of Mines, Annual Report, 1932, v. 41, pt. 3, p. 35-53.
- Goodwin, A.M.**  
1965: Geology of Heenan, Marion and the northern part of Genoa townships, District of Sudbury, Ontario; Ontario Department of Mines, Geological Report No. 38, 60 p., includes Map 2067, scale 1:31 680.
- Heather, K.B.**  
1993: Regional geology, structure, and mineral deposits of the Archean Swayze greenstone belt, southern Superior Province, Ontario; in *Current Research, Part C*; Geological Survey of Canada, Paper 93-1C, p. 295-305.
- Heather, K.B. and van Breemen, O.**  
1994: An interim report on geological, structural, and geochronological investigations of granitoid rocks in the vicinity of the Swayze greenstone belt, southern Superior Province, Ontario; in *Current Research 1994-C*; Geological Survey of Canada, p. 259-268.
- Jackson, S.L. and Fyon, A.J.**  
1991: The western Abitibi subprovince in Ontario; in *Geology of Ontario*, Ontario Geological Survey, Special Volume 4, pt. 1, p. 405-482.
- Laird, H.C.**  
1932: Geology of the Three Duck Lakes area, District of Sudbury; Ontario Department of Mines, Annual Report, 1932, v. 41, pt. 3, p. 1-34, includes Map 41d, scale 1:47 520.  
1936: Geology of the Opepeesway Lake area, District of Sudbury; Ontario Department of Mines, Annual Report, 1936, v. 44, p. 31-37, accompanying 1:63,360 scale Map 44g.
- MERQ-OGS**  
1983: Lithostratigraphic map of the Abitibi Subprovince; Ontario Geological Survey/Ministère de l'Énergie et des Ressources, Québec, 1:500 000, catalogued as "Map 2484" in Ontario and "DV 83-16" in Quebec.
- Moorhouse, W.W.**  
1951: Geology of Osway Township, District of Sudbury; Ontario Department of Mines, Annual Report, 1949, v. 58, pt. 5, p. 1-27, includes Map 1949-2, scale 1:12 000.
- Ontario Geological Survey**  
1991: Bedrock geology of Ontario, east-central sheet; Ontario Geological Survey, Map 2543, scale 1:1 000 000.
- Pyke, D.R.**  
1982: Geology of the Timmins area, Ontario; Ontario Geological Survey Report 219, 141 p. includes Map 2455, scale 1:50 000, 3 charts.
- Rickaby, H.C.**  
1935: Geology of the Swayze gold area, District of Sudbury; Ontario Department of Mines, Annual Report, 1934, v. 43, pt. 3, p. 1-36, includes Map 43b, scale 1:63,360.
- Rogers, D.P.**  
1962: Geology of the Biscotasing area, District of Sudbury; Ontario Department of Mines, Geological Report No. 7, 35 p., includes Map 2013, scale 1:63 360.
- Streckheisen, A.**  
1976: To each plutonic rock its proper name; *Earth-Science Reviews*, v. 12, p. 1-33.

# Pre-Dubawnt plutonism and deformation in the Nicholson Lake-Dubawnt Lake area, Northwest Territories

T.D. Peterson and C. Lee<sup>1</sup>  
Continental Geoscience Division

*Peterson, T.D. and Lee, C., 1995: Pre-Dubawnt plutonism and deformation in the Nicholson Lake-Dubawnt Lake area, Northwest Territories; in Current Research 1995-C; Geological Survey of Canada, p. 11-18.*

---

**Abstract:** Almandine-bearing granodiorite, and slightly younger granites (Snow Island suite), intruded a polydeformed mixed gneiss terrane (Snow River gneiss) at ca. 2.6 Ga. Remelting of previously migmatized arkosic gneiss produced the youngest, biotite leucogranite, which was released during a late extensional event. The sequence of deformation and intrusion closely parallels that in the central Slave Province, and is consistent with crustal thickening, lithosphere delamination, and lower-lithosphere melting, all subsequent to poorly constrained collisional tectonic activity.

**Résumé :** Une granodiorite almandinifère et des granites légèrement plus jeunes (suite de Snow Island), ont recoupé un terrane de gneiss mixte polydéformé (gneiss de Snow River) vers 2,6 Ga. La refusion de gneiss arkosique préalablement migmatisé a produit le plus jeune leucogranite à biotite, qui a été libéré au cours d'un événement d'extension tardif. La séquence de déformation et d'intrusion s'est déroulée parallèlement à celle de la partie centrale de la Province des Esclaves, et elle est compatible avec l'épaississement de la croûte, la délamination de la lithosphère et la fusion de la lithosphère inférieure, tous subséquents à une activité tectonique de collision peu documentée.

---

<sup>1</sup> Department of Earth Sciences, Memorial University of Newfoundland, St. John's, Newfoundland A1B 3X5

## **INTRODUCTION**

Previous studies in the Dubawnt Lake area focussed on Proterozoic sedimentary and volcanic basins (Dubawnt Supergroup, ca. 1.85-1.7 Ga) and their margins (Peterson et al., 1989; Peterson and Rainbird, 1990; Rainbird and Peterson, 1990). The basement to these basins consists of Archean gneisses with minor early Proterozoic (ca. 2.1 Ga) quartzites and phyllites of the Amer Group. The Archean gneisses are dominated by the Snow Island intrusive suite, which consists of granites (U-Pb zircon ages from 2605-2602 Ma) and granodiorite, with minor diorite and peridotite. Very similar granites of identical age are widespread throughout the Churchill Province (LeCheminant and Roddick 1991). The presence of these granites poses difficult problems, since they are not associated with any regional linear features which might be interpreted as the roots of late Archean volcanic arcs; rather, they represent a continent-scale, postorogenic or anorogenic event of uncertain origin.

The pre-Dubawnt Supergroup rocks of the Dubawnt Lake region were moderately to strongly affected by early Proterozoic deformation, which produced basement-cover folding and thrusting, narrow metre-scale mylonite bands (mostly east-northeast-trending), and a pervasive south-southwest-plunging stretching lineation, all developed at upper greenschist facies. Although strong, late Archean (and earlier) deformation was recognized locally (e.g., Peterson and Born, 1994), it has been partly obscured in the vicinity of Dubawnt Lake by Proterozoic overprinting.

Here, we report on the results of 1:50 000 scale mapping southwest of Dubawnt Lake (NTS 65 L/16) in an area contiguous to earlier mapping, but well outside Dubawnt Supergroup basins. The map area covers most of the Dubawnt River between Nicholson Lake and Dubawnt Lake. This area was only slightly affected by Proterozoic deformation, yielding a clear picture of late Archean deformation. In this work, the stratigraphy and deformational history of pre-2.6 Ga gneisses was clarified, and the source, and heat trigger, of the granites of the Snow Island suite were identified. An occurrence of upper Dubawnt Supergroup potassic, phreatomagmatic volcanism is described by Peterson (1995).

## **SNOW RIVER GNEISS**

The southwest half of the map area (Fig. 1) is underlain by a migmatized paragneiss, intruded by mafic orthogneiss. This mixed gneiss unit is named after the Snow River. Except for small areas containing variably folded amphibolite horizons and centimetre- to metre-scale amphibolite boudins, the paragneiss protolith was arkosic psammite, converted to coarsely crystalline, white-weathering granite (averaging over 50% by volume) in concordant sheets separated by narrow, biotite-rich melanosomes which lack amphibole. Minor pelitic layers are abundant in the northwest part of the map area. Large sills, up to 5 m thick and pale pink-weathering, are most commonly concordant to the main layering, but locally cut the layers at a high angle. Pink-weathering granitic dykes (5-15 cm wide) are ubiquitous and variably deformed;

they may be folded into, or cut across, the dominant gneissic fabric. A compositional transition from the very leucocratic, thin concordant sills to the pink granite sills and dykes was locally observed, and attributed in the field to increasing iron content due to additional melting of biotite. The pink granite is identical in all respects to adjacent plutons of biotite leucogranite, which is an important member of the Snow Island intrusive suite (Peterson, 1993); small plutons of biotite leucogranite are also scattered within the paragneiss. The biotite leucogranite from north Dubawnt Lake has been dated at 2602 Ma (U-Pb zircon, C. Roddick, pers. comm., GSC).

The orthogneiss is a strongly foliated augen gneiss consisting of quartz-feldspar segregations in a schistose, melanocratic matrix rich in biotite and amphibole. Typically, this orthogneiss is separated from the paragneiss by a decimetre-scale band of feldspar pegmatite which cuts the migmatitic layering and presumably formed by limited partial melting. The pink leucogranite dykes intrude this orthogneiss. This orthogneiss was therefore emplaced prior to mobilization of the leucocratic granite (at 2.6 Ga), but post-dates initial migmatization of the paragneiss. A second orthogneiss, observed in small dyke-like bodies, is weakly or nondeformed, and consists of plagioclase phenocrysts in a dark green, aphanitic matrix.

At the north end of the map area, the arkosic paragneiss is structurally overlain by interbedded biotite schist and quartz-rich metasandstone with minor iron-formation. The transition zone contains interlayered gneiss and schist. Although disrupted by granite intrusions, these rocks were probably contiguous with schist and iron-formation-bearing gneiss farther north (NTS 65 M/1). These schists are here termed the Clarke River schist, after a small river which empties into Dubawnt Lake (65 M/1). It is not clear if the contact represents a transition to deeper-water sedimentation, or is a strongly folded unconformity. The Clarke River schist is rich in hydrous minerals, but it is not migmatized to the same extent as the Snow River gneiss and underwent only one migmatitic event, producing undeformed pods of two-mica leucogranite which forms no plutons in the area. The schist may therefore have been unconformably deposited on the Snow River gneiss some time after the gneiss was first migmatized, but before 2.6 Ga.

## **SNOW ISLAND INTRUSIVE SUITE**

The Snow Island intrusive suite (Fig. 2) is named after an island in west-central Dubawnt Lake; all previously identified members of the suite were found in the present map area but peridotite and diorite are scarce. Most of the map area not underlain by the Snow River gneiss is underlain by a hornblende granodiorite, locally almandine-bearing. The granodiorite ranges from strongly to nondeformed, with a foliation mainly parallel to the foliation/migmatitic banding in the paragneisses. The northern limit of the granodiorite coincides closely with the transition between the Snow River gneiss and the Clarke River schist; this north-south limit is also seen on the opposite (east) side of Dubawnt Lake, where few metasedimentary enclaves were identified (Peterson, 1993).

Aphyric, deformed mafic dykes within the granodiorite, and less commonly within megacrystic granite, are presumed to represent a minor basaltic phase of this suite.

Two granitic derivatives of the granodiorite were identified. A grey-weathering, quartz-rich granite containing hornblende and resorbed plagioclase phenocrysts forms isolated plutons, with gradational contacts, well away from the arkosic paragneisses. No strongly deformed outcrops of this granite, interpreted as a simple igneous differentiate of the granodiorite, were found. Adjacent to the arkosic paragneiss, the granodiorite grades into megacrystic granite by the gradual development of potassium feldspar phenocrysts. The megacrystic granite is a volumetrically important member of the Snow Island suite along the northern shores of Dubawnt Lake. This member is highly variable, in places being rich in biotite and elsewhere in hornblende; its composition also extends to monzonite. The megacrystic granite is here interpreted as a contaminated differentiate of the granodiorite, with saturation in K-feldspar induced by dissolution of meta-arkose or by mixing with leucogranite melt derived from the meta-arkose. The megacrystic granite from northern Dubawnt Lake has been dated at 2605 Ma (LeCheminant and Roddick, 1991).

## **BAKER LAKE GROUP**

The Baker Lake Group, consisting of ultrapotassic volcanic rocks and dykes (Christopher Island Fm.), and alluvial fan sequences (Kunwak Fm.) is well represented in all quadrants of Dubawnt Lake except the southwest quadrant. The complete absence of lamprophyre dykes in the present map area was unexpected. It may indicate that the southwest quadrant lies within a block unaffected by the ca. 1.85 Ga brittle faulting which induced dyke emplacement and basin formation throughout much of the central Churchill Province (Peterson, 1994).

## **NUELTIN INTRUSIVE SUITE**

The Nueltin Suite in the Churchill Province consists mainly of quartz and feldspar porphyritic plutons of granodiorite to high-silica granite (commonly rapakivi-textured), with associated rhyodacite to rhyolite extrusive rocks (Pitz Formation). It is a classic anorogenic suite. One body of Nueltin granite in northern Dubawnt Lake yielded a U-Pb (zircon) age of 1740 Ma (C. Roddick, pers. comm., GSC). Several small intrusive bodies of nondeformed brick-red weathering porphyritic granite rich in quartz phenocrysts are in the map area; these are spatially associated with 1-2 metre grey, aphanitic dykes bearing quartz and (rarely) K-feldspar phenocrysts. It is not clear if the dykes, which usually are aligned parallel to the regional fabric, are less siliceous than the granites, but they are tentatively interpreted as coeval dacites.

One porphyry body, located in a northwest-southeast shear zone in the centre of the map area, has a very strong stretching lineation plunging shallowly south-southwest. The porphyry clearly post-dates the Snow Island suite, since it is

highly discordant to the fabric of the strongly deformed granodiorite it intrudes. Deformation has not been observed in Nueltin Suite granites elsewhere, and its presence here may indicate tectonic activity to the east or southeast at about 1.75 Ga. Alternatively, the porphyry may predate the Early Proterozoic deformation which affected the Amer Group, but porphyries of this age have not been previously recognized in the region.

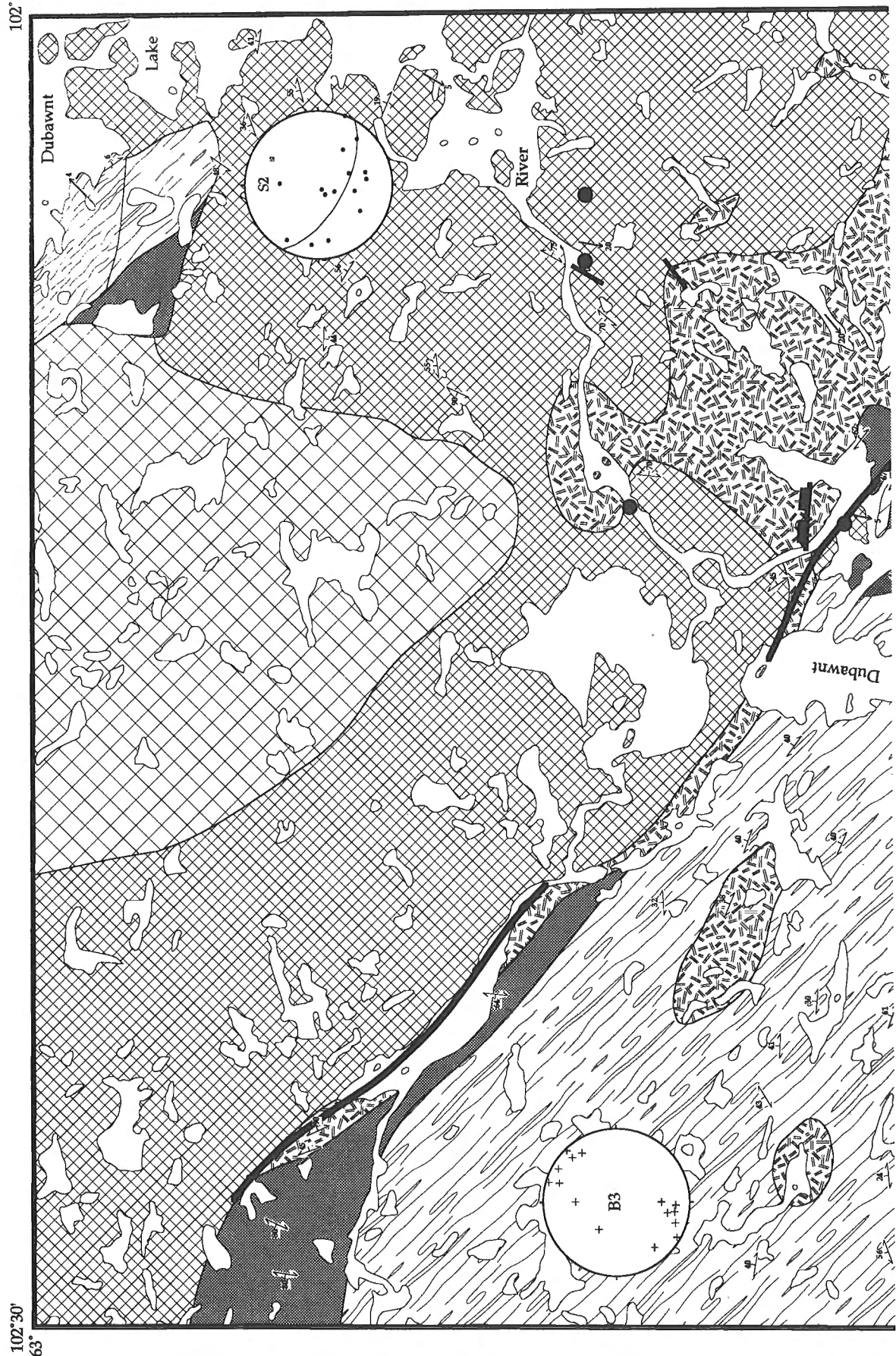
## **DESCRIPTION OF THE STRUCTURES**

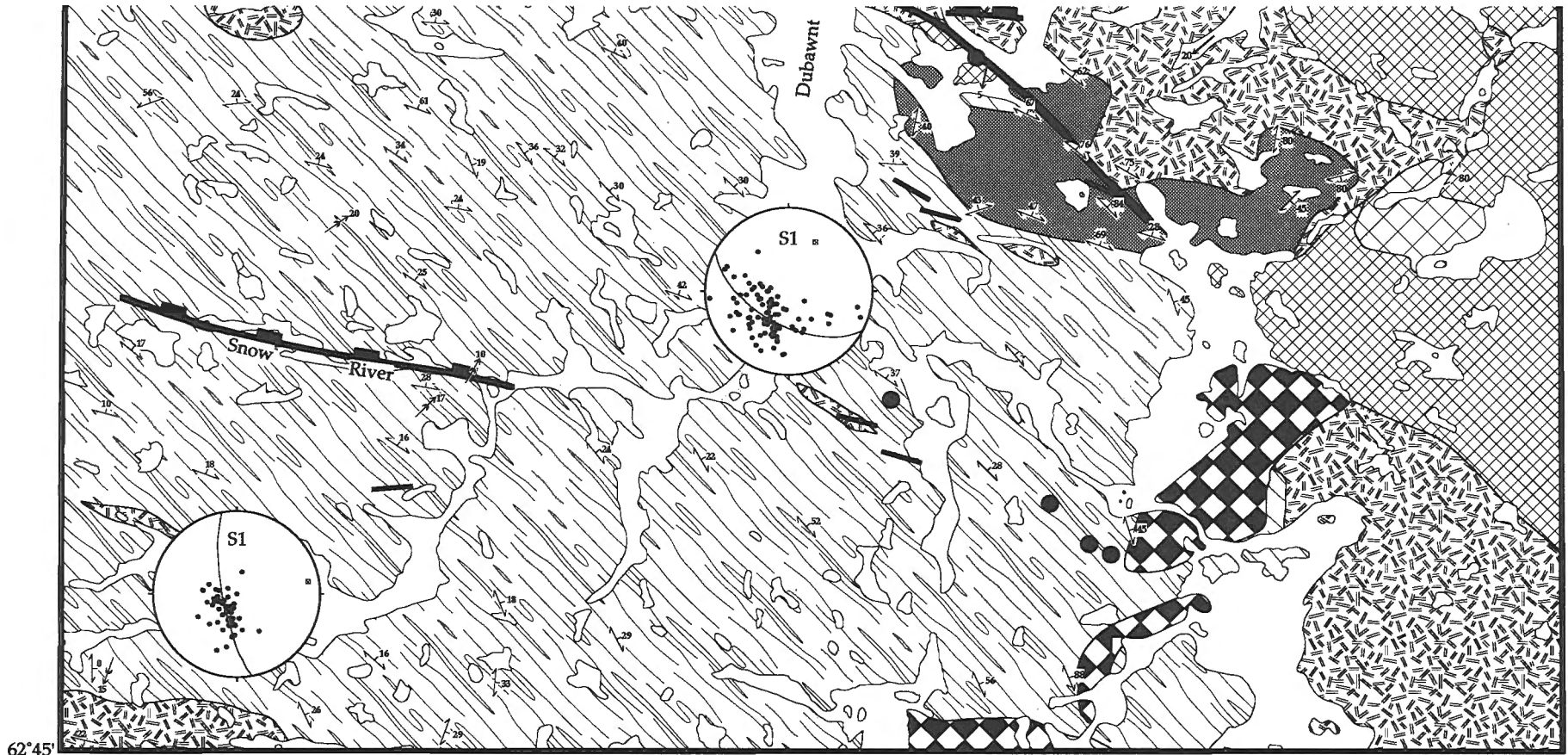
Four phases of deformation can be distinguished in the map area. The first (D1), coincided with the development of a strong, possibly bedding parallel, foliation in the arkosic paragneiss, which is concordant with the compositional layering resulting from migmatization. In pelitic layers, the S1 fabric is well-developed in an amphibolite facies metamorphic assemblage (bio+musc+gnt+plag+qtz).

S1 and the associated migmatitic layering were transposed into a northwest-striking, north-dipping foliation (S2), during the second phase of deformation (D2). This transposition locally produced asymmetrical, mainly 'S' shaped, isoclinal folds in the paragneiss, and a strong anastomosing fabric in the augen orthogneiss. A parallel fabric is commonly well-developed in the granodiorite, but is weakly developed in both the hornblende and biotite granites. Leucogranite dykes in the paragneiss are variably affected by D2; they commonly cut the S2 fabric at high angles, but have also been locally folded and rotated into the main trend. The transposition is therefore interpreted as synintrusive. Fold vergence in the paragneiss, together with well-developed shear bands in the orthogneiss fabric are all compatible with north over south crustal thickening at this time.

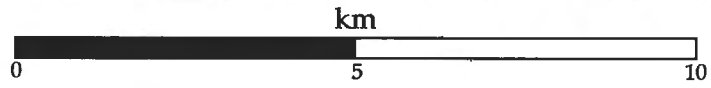
Foliations and migmatitic bands are close to flat-lying in the southwest corner of the map area, and steepen toward the northeast margin of the gneisses (Fig. 1). At well-exposed areas near the Dubawnt River, the northeast margin is a high-strain zone about 100 m wide where paragneiss, orthogneiss, and granodiorite have unusually strong and steep, anastomosing S2 fabrics. In most areas, the high-strain zone contains large numbers of leucogranite dykes both folded into and crosscutting the S2 fabric; leucogranite also forms a large pluton contacting the northeast side of this shear zone. Steepening of S2 toward this contact may reflect monoclinical folding as a result of extension and normal movement (north side down), however no kinematic indicators were noted. Regardless of the direction of motion, activity on this shear zone is interpreted as concurrent with the release of large volumes of leucogranite from the arkosic gneiss.

The Proterozoic D3 event is well defined elsewhere near Dubawnt Lake, particularly along the western shoreline. There, basement-cover thrusting and folding involving the Amer Group, mylonite bands, and a pervasive south-southwest-plunging stretching lineation are interpreted as post-2.1 Ga, pre-1.85 Ga structures related to the Slave-Churchill collision at ca. 2.0-1.9 Ga (Peterson and Born, 1994). D3 structures in the present map area, particularly in the granodiorite and larger leucogranite bodies, are mainly represented by a





62°45'



- Nueltin granite (small pluton)
- ▬ Nueltin dacite dyke
- ▬ Normal fault (decoration on downthrown side)
- ↖<sup>29</sup> transposed S1
- ↖<sup>36</sup> S2
- ↖<sup>30</sup> L3 (D3 lineation)
- ↖<sup>30</sup> B3 (D3 fold axis)
- ~ High strain zone

Figure 1. Geology, 65L/16. See Figure 2 for lithological legend.



north-northeast stretching lineation. This lineation is commonly associated with a conjugate set (sinistral: 303°/90°; dextral: 049°/45°) of narrow (10-200 cm wide) mylonite zones, which accommodated east-west shortening, and north-south extension. D3 deformation in the paragneiss is in part represented by broad, open folds of S2, with amplitudes of about 1 m. These folds are doubly (northeast-southwest) plunging, probably due to an undulating S1/S2 surface. Locally, low angle, northwest verging thrusts with associated isoclinal folds have developed in the paragneiss, with throws of approximately 5-10 m.

In the northwest portion of the map area, the northwest-trending high strain zone appears to have been reactivated at greenschist facies during D3. The main S2 fabric has been strongly overprinted by metre scale 'S' shaped folds, and minor crenulations with the same vergence. En-echelon, right-stepping quartz veins, approximately 5 m long, are very common in this area, possibly due to extension in a sinistral strain field. Unequivocal kinematic indicators were not found, but regional considerations of metamorphism, structures, and timing of events, lead us to believe that this zone was reactivated through sinistral-oblique, normal faulting, during D3.

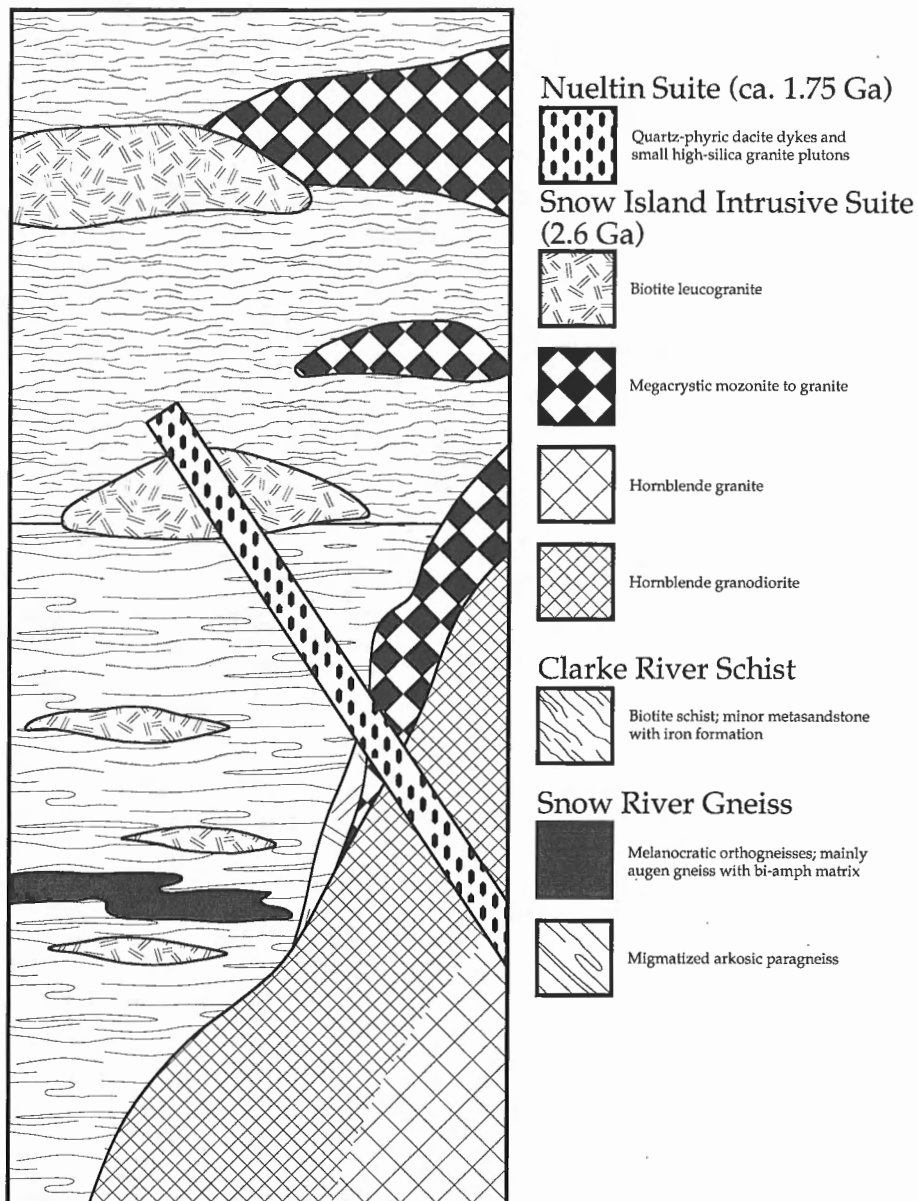


Figure 2. Stratigraphy and intrusive sequences in 65L/16 and 65M/1.

A D4 event is tentatively equated with the development of a stretching lineation in Nueltin suite porphyry. This event may be identical with D3, in which case the porphyry is substantially older than the Nueltin Suite. Confirmation of a D4 event must await geochronological results from the porphyry.

## DISCUSSION

This study was intended as preliminary to a more extensive examination of 2.6 Ga igneous activity in the Churchill Province. Widespread 2.6 Ga activity is characteristic of some other Archean cratons, for example the Yilgarn (West Australia) and the Slave Province (Davis et al., 1994). There may be close parallels between Churchill and Slave plutonism at this time. Davis et al. (1994) interpreted relatively young, 2-mica leucogranites of the central Slave Province (Contwoyto Suite) as partial melts of metasedimentary rocks, produced by intrusion of slightly older granodioritic melts (Concession Suite), themselves derived by partial melting of lower lithosphere. Megacrystic granite is present in the related Yamba suite; geochemical data strongly indicate this is a mixture of lower crustal and upper crustal melts. In this study, megacrystic granite was interpreted as a mixture of granodiorite and leucogranite or paragneiss. A working hypothesis could be that, where K-feldspar megacrystic granites are found elsewhere in the Churchill Province, older high-K sediments may have been present.

The areal and temporal distribution of the 2.6 Ga suites of the Slave Province is inconsistent with quasi-linear arc systems, a factor even more problematical in the Churchill Province. Because this plutonism was dispersed over a large area, Davis et al. (1994) preferred to attribute it to widespread heating of the lower crust induced by delamination of lithospheric mantle (there is no geochemical evidence for hotspot magmatism, and the small volume of gabbroic rocks is inconsistent with large-scale melting of peridotite). Thickening may have been consequent to the assembly of numerous microcontinents with intervening arc assemblages, at about 2.7 Ga. Intrusion of the younger Contwoyto/Yamba suites in the Slave Province, and of biotite leucogranite in the Dubawnt Lake area, may both have been coincident with extension, which is consistent with a delamination model.

A related, more speculative model, would suggest that several stabilized Archean cratons assembled shortly before 2.6 Ga and were thickened by convergence accommodated on intracontinental shear zones. Some evidence in support of the involvement of continental (as opposed to microcontinental) convergent tectonics has been obtained from the Snowbird tectonic zone, which runs diagonally southwest-northeast through the central Churchill Province (Hanmer and Kopf, 1993). Much of the penetrative deformation in this zone coincided with intrusion of 2.6 Ga granitoids and the formation of mylonites bounding crustal-scale boudins containing granulite-facies rocks. The zone is clearly not a late Archean

suture (though it may be superimposed on a suture of ca. 3.2 Ga vintage) and may be best interpreted as a discontinuous intracontinental shear zone (Hanmer, pers. comm., 1994).

Typically, intermediate intrusive rocks with calc-alkaline geochemical signatures are interpreted as subduction-related. Available geochemical data for the 2.6 Ga suites in the Churchill Province indicate a calc-alkaline heritage. However, if lower lithospheric rocks – themselves formed by subduction-related processes at an earlier date – were extensively remelted, they could hardly produce melts with anything but subduction-related features. Further studies on late Archean Churchill plutonic rocks must focus on syn-intrusive deformation, geochemistry (to constrain source rocks), and Nd model ages (to constrain the antiquity of the source region, and to indirectly map variations in deep lithosphere).

## ACKNOWLEDGMENTS

We gratefully acknowledge field and computer drafting assistance by Alex Ivanoff. Westminner Canada provided helicopter support for collecting geochronology samples.

## REFERENCES

- Davis, B., Fryer, B.J., and King, J.E.**  
1994: Geochemistry and evolution of Late Archean plutonism and its significance to the tectonic development of the Slave Craton; *Precambrian Research*, v. 67, p. 207-241.
- Gall, Q., Peterson, T.D., and Donaldson, J.A.**  
1992: Early Proterozoic stratigraphy of the Thelon and Baker Lake basins, District of Keewatin: a proposed revision; *in* Current Research, Part C; Geological Survey of Canada, Paper 92-1C, p. 129-137.
- Hanmer, S. and Kopf, C.**  
1993: The Snowbird tectonic zone in District of Mackenzie, Northwest Territories; *in* Current Research, Part C; Geological Survey of Canada, Paper 93-1C, p. 41-52.
- LeCheminant, A.N. and Roddick, C.**  
1991: U-Pb zircon evidence for widespread 2.6 Ga felsic magmatism in the central District of Keewatin, Northwest Territories; *in* Radiogenic Age and Isotopic Studies: Report 4; Geological Survey of Canada, Paper 90-2, p. 91-99.
- Peterson, T.D.**  
1993: Geology, Dubawnt Lake; Geological Survey of Canada, Open File 2551, 1:100 000.  
1994: Early Proterozoic ultrapotassic volcanism of the Keewatin Hinterland, Canada; *in* Proceedings, 5th International Kimberlite Conference; vol. 1, Kimberlites, related rocks and mantle xenoliths, (ed.) H.O.A. Meyer and O.H. Leonardos; *Campanhia de Pesquisa de Recursos Minerais, Brasilia*, p. 221-235.  
1995: A potassic phreatomagmatic volcanic centre in the Thelon Basin, Northwest Territories: implications for diamond exploration; *in* Current Research 1995-C; Geological Survey of Canada, this volume.
- Peterson, T.D. and Born, P.**  
1994: Archean and lower Proterozoic geology of western Dubawnt Lake, Northwest Territories; *in* Current Research 1994-C; Geological Survey of Canada, p. 157-164.
- Peterson, T.D. and Rainbird, R.H.**  
1990: Tectonic and petrological significance of regional lamproite-minette volcanism in the Thelon and Trans-Hudson hinterlands, Northwest Territories; *in* Current Research, Part C; Geological Survey of Canada, Paper 90-1C, p. 69-79.

**Peterson, T.D., LeCheminant, A.N., and Rainbird, R.H.**

1989: Preliminary report on the geology of northwestern Dubawnt Lake area, District of Keewatin, Northwest Territories; in Current Research, Part C; Geological Survey of Canada Paper 89-1C, p. 173-183.

**Rainbird, R.H. and Peterson, T.D.**

1990: Physical volcanology and sedimentology of lower Dubawnt Group strata, Dubawnt Lake, District of Keewatin, Northwest Territories; in Current Research, Part C; Geological Survey of Canada, Paper 90-1C, p. 207-217.

---

Geological Survey of Canada Project 880012

# A potassic phreatomagmatic volcanic centre in the Thelon Basin (Northwest Territories): implications for diamond exploration

T.D. Peterson

Continental Geoscience Division

*Peterson, T.D., 1995: A potassic phreatomagmatic centre in the Thelon Basin (Northwest Territories): implications for diamond exploration; in Current Research 1995-C; Geological Survey of Canada, p. 19-26.*

---

**Abstract:** An exposure of the strongly potassic and magnesian Kuungmi Formation (less than 1.72 Ga) within the Thelon Basin has the characteristics of a phreatomagmatic volcanic centre, including vesicular sandy tuffs and phlogopite-rich accretionary lapilli. This centre demonstrates that the geological conditions which permit development of diamondiferous lamproite vents were present in the early to mid-Proterozoic, when the Thelon Formation was much more extensive.

**Résumé :** Un affleurement de la Formation de Kuungmi (moins de 1,72 Ga) à forte teneur en potassium et en magnésium au sein du bassin de Thelon présente les caractéristiques d'un centre volcanique phréatomagmatique, y compris des tufs sableux vésiculaires et des lappilis accrétiés riches en phlogopite. Ce centre démontre que les conditions géologiques qui permettent la formation de conduits de lamproïte diamantifère étaient présentes du Protérozoïque précoce à moyen, alors que la Formation de Thelon était beaucoup plus étendue.

## INTRODUCTION

The Churchill Province is notable for containing an areally and volumetrically, very extensive potassic igneous province (Peterson, 1994). Nearly all of these potassic rocks are within the 1.85 Ga Christopher Island Formation (CIF) (part of the Baker Lake group: Gall et al., 1992). Many extrusive and intrusive igneous facies have been recorded within this formation, but notably lacking have been recorded instances of phreatomagmatic centres. Identifying such centres is potentially important, since portions of the Christopher Island Formation are lamproitic in character, and phreatomagmatic lamproite centres are important exploration targets for diamond deposits. Unlike kimberlites, which exsolve dissolved CO<sub>2</sub> in the upper mantle and crust and hence are self-propelling, lamproite magmas are strongly alkaline (usually peralkaline); peralkaline magmas maintain a high solubility of CO<sub>2</sub> and H<sub>2</sub>O at all pressures (e.g., Kjarsgaard and Hamilton, 1989). Therefore, in order to develop explosive intrusive centres which can erupt entrained mantle xenoliths and xenocrysts to the surface, lamproite magmas typically must intersect the water table. This will often occur during eruption through thick deposits of poorly indurated and water-saturated sediments (e.g., the Australian Ellendale field: Stachel, 1992) or, as in the case of the very diamond-rich Argyle intrusion of northern Australia, into a brittly faulted zone which acts as an aquifer (Boxer et al., 1989).

Continued investigation of potassic volcanism in the Churchill Province is revealing that lamproitic rocks are not restricted solely to the Christopher Island Formation. Younger dykes are being found, most notably a swarm of lamproite dykes from Baffin Island which are too fresh to be Proterozoic (they contain unaltered leucite: D. Hogarth, University of Ottawa, pers. comm., 1994) and may well be Tertiary. Gall et al. (1992) reported the presence of potassic rocks within the Kuungmi Formation, an extrusive volcanic

formation which overlies the Thelon Formation (1.72 Ga: Miller et al., 1989). Outcrops of the Kuungmi Formation have been found in widely separated locations within the Thelon Basin, and also at the south end of Dubawnt Lake. Rocks of the Kuungmi Formation were initially described by Donaldson (1968) as basaltic flows, and tentatively correlated with the Mackenzie dyke swarm, at 1267 Ma (LeCheminant and Heaman, 1989). Detailed study of samples of the "basalts" collected during regional mapping (T. Peterson and S. Tella, unpub. data) revealed that the rocks are strongly potassic, and closely resemble some Christopher Island Formation rocks in composition. I considered that the Kuungmi Formation warranted re-examination, with the view that its diamond potential should be assessed.

## LOCATION AND FIELD DESCRIPTION

The outcrops investigated were those indicated by Donaldson (1968) as being the most accessible exposures within the Thelon Basin. They can be reached by floatplane, landing on a large, unnamed lake southwest of Retort Lake, at latitude 64°04' N, longitude 102°58' W (NTS 66D/2). The outcrops cap a series of low (10-20 m) flat-topped hills, which presumably once comprised a continuous blanket of deposits (Fig. 1). The total area encompassed by these hills is about 5 km<sup>2</sup>. They are 6 km east of an excellent exposure of the Pine Point Formation, which is the dolomitic cap at the top of the Barrenland Group, of which the Thelon Formation is the dominant and lowermost member (Gall et al., 1992). The Thelon Formation consists of very clean, well-sorted, kaolinite-cemented pebbly quartz arenite (mostly planar or trough crossbedded) with a basal quartzite-bearing conglomerate unit.

The Kuungmi outcrops are almost entirely restricted to the fringes of the tops of the hills. There, very homogeneous, medium grained, purplish grey weathering volcanic rocks



**Figure 1.**

*Aerial view of outcrop area (facing south-east), with lapilli tuff site indicated by the arrow. GSC 1994-741A.*



**Figure 2.** Outcrop of crystal tuff, weathering into crude slabs parallel to bedding. GSC 1994-741E.

superficially resembling flows are disintegrating into blocky rubble which forms aprons below the hills (Fig. 2). Some blocks of this material contain very distinct, brick-red weathering bands about 2 cm thick with sharp boundaries on one side and gradational boundaries on the other. Beyond the gradational boundaries, 1-2 mm red specks are scattered throughout the purple-grey matrix. The bands strongly indicate that these outcrops are of crystal tuff, not lava flows.

Numerous blocks of silica-cemented sandstone, with abundant interstitial hematite (including specular hematite and chalcedony in pore spaces) are also scattered below the hills. These do not resemble rocks from the Thelon Formation, since they have strongly contorted millimetre to centimetre-scale bedding, large numbers of smooth, rounded pores ( $\leq 5$  mm), and highly rounded lithic fragments which are usually exceptionally rich in hematite. The finest beds have a higher proportion of hematite, and typically are truncated, or bifurcate around lenses of coarser, more quartz-rich sand. Only one outcrop of hematitic sandstone was discovered, at the topographic level of the base of the hills (Fig. 3). It consists of three beds, each about 6 cm thick, with the amount of hematite increasing upwards.

Most of the lithic fragments are 2-5 mm in diameter, but some others, dominated by quartz sand grains, reach diameters of 2 cm. The small lithic fragments form discontinuous thin beds; larger fragments either accumulated in depressions or caused depression of the underlying sand by loading (Fig. 4). On broken surfaces, the smaller fragments appear to have a concentric structure. The field interpretation of these hematized sandstones was as volcanic lapilli tuffs (with hematite replacing mafic minerals) heavily contaminated by Thelon sand grains, subjected to considerable soft-sediment deformation. They are overlain by the better-outcropping crystal tuffs, which lack a quartz sand contaminant.

**Figure 3.**

Outcrop of dark, hematitic vesicular tuff, overlying 2 beds of more quartz-rich sandy tuff. Note the load feature (small arrow) and tabular breccia body (large arrow). GSC 1994-741C.



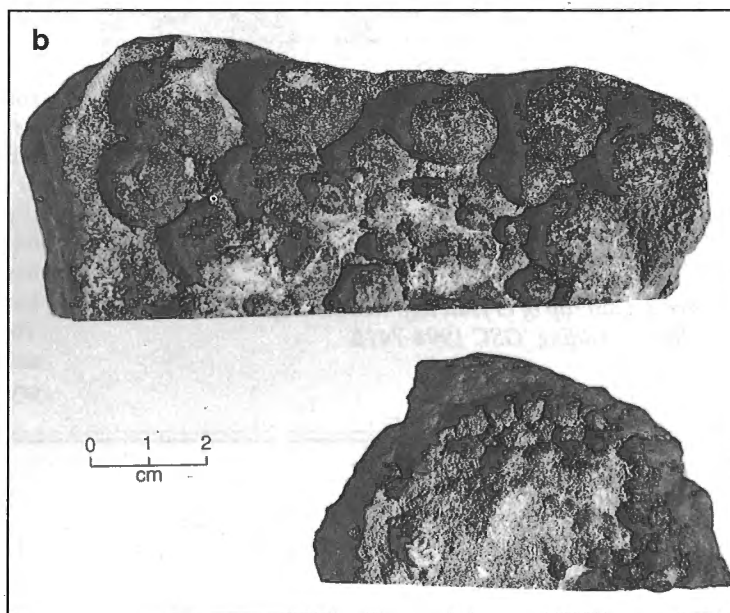
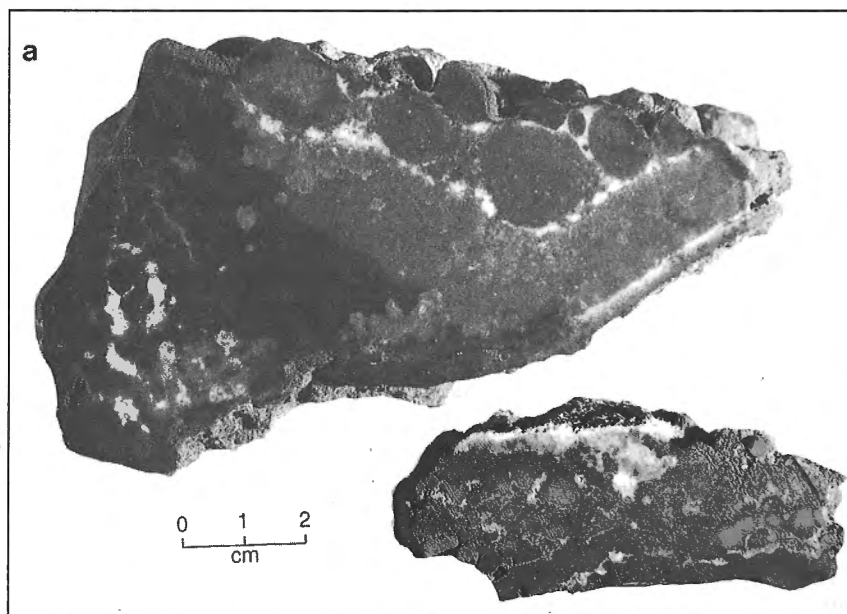


**Figure 4.**

*Front (a) and top (b) views of hematitic lapilli tuffs. The smaller sample in photograph (a) is upside down. GSC 1994-753A,B.*

## **THIN SECTION DESCRIPTIONS**

### ***Sandstones and lapillistones***

In the thinnest edges of thin sections, the fine grained (average 0.02 mm) hematite-rich sandstones are seen to consist of 6 components. In order of abundance, they are: (1) quartz sand grains, with hematite rims; (2) ovoid grains altered to very fine aggregates of hematite+ others; (3) sanidine sand grains (identified by scanning electron microscope, SEM); (4) phlogopite laths (occasionally altered to chlorite), commonly contorted and strongly oxidized; (5) equant grains which are nearly opaque but are translucent dark brown on the edges, some are faceted octahedra; (6) primary igneous fragments, most less than 1 mm but some up to 2 mm long. At least some void spaces represent pressurized gas pockets, since the sand laminae are bulged outward on either side of them.

Within the hematite-rich sands are thin lenses and beds of relatively hematite-poor sand which are slightly coarser (0.06 mm). Thicker (centimetre-scale) beds of hematite-poor sand are coarser still (0.2 mm). Size sorting in all sandy beds is excellent. Irregular voids are common in the coarser sand lenses. Some have linings of euhedral quartz, and all except the largest are filled with a later generation of sparry carbonate. Both hematite-rich and poor sands were initially cemented by silica, however, near some void spaces, very fine grained carbonate has partly replaced the silica cement.

Three varieties of igneous fragments are present. Most common in the hematitic sands are small, angular to rounded, transparent yellow-brown grains with very low birefringence and undulose extinction; these appear to have been volcanic glass. Many of the hematized, ovoid grains may also have been glass. Fragments in the coarser

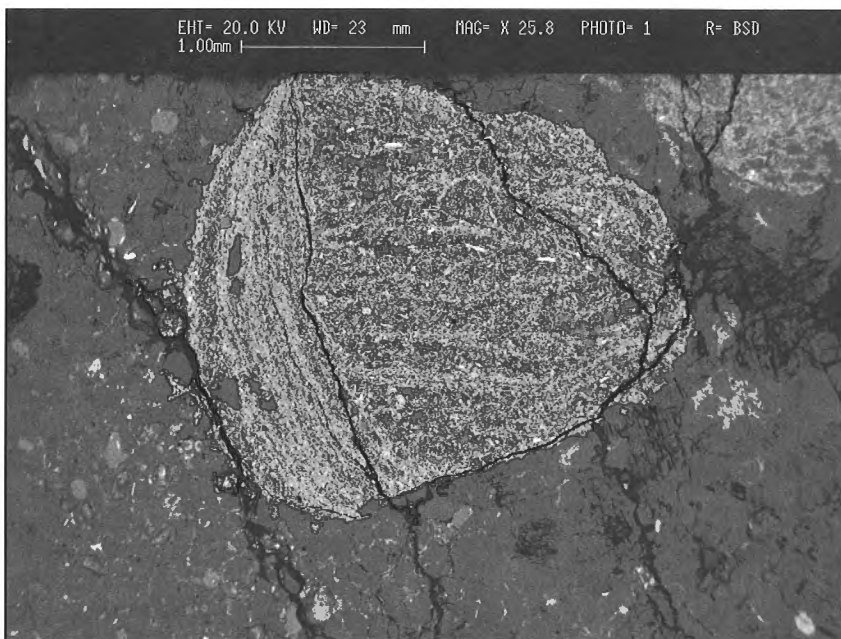


**Figure 5.**

*Backscattered electron image of quartz (dark) and hematite (bright) rich lapillus. Note the bright laths of phlogopite in the older laminae, which are truncated by an erosional surface coated on one end by accreted quartz-hematite sand. The matrix consists mostly of quartz with minor interstitial hematite; grey grains in the matrix are sanidine.*

sand laminae are highly glassy (again yellow-brown) with abundant microphenocrysts of phlogopite and a colourless mineral with low birefringence which appears to be sanidine. One fragment was found with abundant skeletal, swallow-tail sanidine crystals in a strongly oxidized, nearly opaque matrix; the hollow sanidine cores trapped a dark orange-brown glass.

The smaller, hematite-rich lapilli clearly display a banded structure defined by laminae of quartz, sanidine, and hematite, incorporating aligned phlogopite laths (Fig. 5). They consist of the same material as the hematite-rich sandstones, except that the ratio of quartz:sanidine is about 1:1 in the lapilli, and greater than 10:1 in the sands. The banding may be planar, extending across the entire lapillus, or concentric. Some grains have a central planar-banded region surrounded by a concentric rind. The large, quartz-rich lapilli are only faintly concentrically structured, if at all. Although they are silica-cemented, they occur within a carbonate-cemented quartz sand, and some of the sand grains in the matrix consist of fine grained, polygonal silica cement.

### **Crystal tuffs**

In thin section, additional bedding planes marked by changes in mineral and glass content are visible, confirming that the tuff unit is not composed of flows. The crystal tuffs were formed from two magma types. The principal type had a mineral assemblage of plagioclase (normally zoned from An<sub>50</sub> to An<sub>20</sub>, determined optically), sanidine, pyroxene, and olivine. Olivine occurs as subhedral to anhedral grains about 0.1 mm wide, replaced by ochre-brown masses of hematite plus hydrous silicates. The pyroxene is replaced by fibrous talc, and was probably orthopyroxene. Glassy mesostases, and glassy matrices in rare lithic fragments, are mainly devitrified to sanidine and contain abundant acicular microphenocrysts (probably pyroxene) and opaque octahedra (probably magnetite). Some glass pockets partly crystallized

before cooling; these consist of rosettes of silica (tridymite?) intermixed with magnetite+ilmeneite, and tabular sanidine crystals, in a dark red-brown microcrystalline matrix of sanidine+silica+Fe-oxide+an unknown Mg-bearing phase.

The red-weathering bands and spots within the tuff consist of the above plus an additional, earlier generation of resorbed Mg-rich olivines, replaced by colourless serpentine (these commonly have Fe-enriched rims partly replaced by Fe oxides). Notably lacking from either crystal tuff variety is phlogopite. Irregular voids in both types of tuff are mainly filled with sparry carbonate, and rarely with yellow-green chlorite(?).

### **INTERPRETATION**

The sandy tuffs and the crystal tuffs clearly represent two different magma types, distinguished mainly by the presence of phlogopite (sandy tuffs) and plagioclase (crystal tuffs). Although olivine was not positively identified in the sandy tuffs, it is possible that many of the hematized, ovoid grains in them were olivine. There is clear evidence that more than one eruption phase is represented in the sandy tuffs. The lapilli in the sandy tuffs probably originated as fragments of silica-cemented tuff which were abraded in an eruption column, then enlarged by concentric accretion of additional hematitic sand. These were redeposited, and recemented by carbonate. Although fluvial re-working of the sandy tuffs cannot be discounted, it is considered that their complex, contorted bedding, and the presence of accretionary lapilli, are more consistent with a second eruption phase; ripple marks, mud cracks, and other indications of fluvial deposition were not observed. Further observations in outcrop would be desirable; however, the size sorting and bedforms are consistent with fallout from base surge (Fischer and Schmincke, 1984).



The non-igneous content of the sandy tuffs and lapilli is usually well over 50%, and strongly indicates deposition by an eruption mechanism which disrupted and entrained large volumes of country rock (Thelon sandstone). Also, the absence of macroscopic fragments of juvenile igneous material (e.g., bombs and melt lapilli) is consistent with a very violent eruption and a small volume of magma. These

observations, together with the presence of accretionary lapilli, vesicular tuffs with expanding gas bubbles, and soft-sediment deformation, strongly indicate a phreatomagmatic eruption through water-saturated sand or sandstone (Fischer and Schmincke, 1984). It is possible that the Thelon Formation was not indurated at the time of eruption, since no sand grains coated with kaolinite, nor any lithic clasts from the Thelon Formation, were recognized in any of the samples.

**Table 1.** Whole-rock analyses of potassic rocks.

	CIF,hi-Mg average	Kuungmi average	shoshonite SH-241
SiO <sub>2</sub>	53.26	50.30	60.00
TiO <sub>2</sub>	0.77	1.84	0.53
Al <sub>2</sub> O <sub>3</sub>	11.50	16.23	17.30
Fe <sub>2</sub> O <sub>3</sub>	4.19	4.33	2.14
FeO	2.56	6.03	3.39
MnO	0.10	0.21	0.10
MgO	9.28	6.65	2.10
CaO	5.52	3.16	3.76
Na <sub>2</sub> O	1.65	2.60	3.37
K <sub>2</sub> O	6.85	4.01	4.38
P <sub>2</sub> O <sub>5</sub>	0.81	0.29	0.37
H <sub>2</sub> O	1.57	3.90	2.30
CO <sub>2</sub>	0.85	0.20	
sum	98.90	99.75	99.74
mg#	0.719	0.545	0.413
Rb	311	120	210
Sr	1301	553*	543
Ba	4092	1689	
Y	26	19*	37
Zr	354	209*	364
V	114	220*	80
Nb	21	42*	27
Cr	352	34*	31
Ni	196	23*	10
La	101	53*	80
Ce	211	110*	151
Nd	104	42*	64
Sm	17.3	7.6*	11.1
Eu	3.87	2.3*	1.91
Gd	12.21	5.8*	
Dy	6.29	4.3*	
Tm	0.32		0.48
Yb	1.64	1.9*	2.82
Column 1: average of 56 samples (T. Peterson and A. LeCheminant, unpublished data).			
Column 2: average of 3 samples, except (*) (1 sample)			
Column 3: Venturelli et al., 1984			

## DISCUSSION

The field relationships between the lapillistones/quartz sand tuffs and the crystal tuffs are unclear, but it is unlikely that the olivine-rich crystal tuffs represent differentiates of the phlogopite- and sanidine-bearing magma which produced the sandy tuffs. Insufficient mineralogical data are available to characterize the phlogopite-bearing magma, which could have been minette, leucitite, or lamproite magma. The crystal tuffs have mineral assemblages most similar to rocks of the shoshonite/banakite/absarokite series (Carmichael et al., 1974). In the most comprehensive study of shoshonites to date, Meen (1987) concluded that shoshonitic magma can form by fractionation of anhydrous basaltic andesite at close to 10 kbar pressure. Alternatively, shoshonites may represent highly potassic magma (for example, minette magma) mixed with dacitic or andesitic magma, or contaminated by crustal rocks. Therefore, at this stage, all that can be said of the primary magma at this eruption site is that it was strongly potassic and Mg-rich.

The similarity of the crystal tuffs to shoshonites may be peculiar to this centre. No chemical analyses are available from this site, however, Kuungmi flows from the south end of Dubawnt Lake do not resemble shoshonites. In particular (Table 1), they are much more magnesian and have substantially lower silica contents (T. Peterson and S. Tella, unpub. data). The analyses are suspect, since all available samples of the Kuungmi Formation are altered, but the samples resemble average Christopher Island Formation rocks in having high Al<sub>2</sub>O<sub>3</sub> and very low CaO. There is no generally accepted rock name for this composition, which is typical of early Proterozoic Churchill potassic rocks (including the microdiamond-bearing dyke reported by MacRae and Armitage, 1994). The Kuungmi Formation is also exceptionally Fe-rich (>10% total FeO), which is reflected in the very iron-rich glasses of the crystal tuffs and the large quantity of hematite in the sandy tuffs.

These outcrops of the Kuungmi Formation physically resemble those of some diamondiferous lamproites. The volcanology of such deposits is well known. Using the well-exposed diamond-bearing intrusives of the Ellendale field as examples, the first eruptive phase produces a flaring vent filled with inward-dipping olivine lamproite tuffs, deposited by base surge (Stachel, 1992). These are invariably highly contaminated with xenolithic material from the level of the water table (in the case of the Argyle pipe, the tuffs contain at least 50% by volume of aquifer quartzite). Common features of these tuffs include accretionary lapilli, glassy fragments, soft-sediment deformation, and cementation/replacement by silica derived from heated groundwater. The

second, quieter phase results in the formation of a central intrusive plug of differentiated lamproite, commonly olivine-poor and rich in the low-pressure phase leucite.

In a tectonic context, other relevant features of diamondiferous lamproites were noted by Mitchell and Bergman (1991). They stated: "Although Proterozoic lamproites are relatively rare.....they are apparently the most diamondiferous, compared with their Phanerozoic counterparts." (p. 107). And: "The vast majority of lamproites were intruded through, or extruded over, relatively undeformed flat-lying platform sedimentary rocks." (p. 117). The conditions necessary to form diamondiferous lamproite centres are well known from the study of examples in Australia (Jaques et al., 1986) and also from India (Scott Smith, 1989) and Africa (Scott Smith et al., 1989). These are: (1) a phlogopite-rich, lithospheric mantle source region must be present beneath the site, with enrichment probably occurring as a consequence of subduction at least tens of millions of years before eruption of the lamproites; (2) partial melting is triggered by relatively modest thermal events which induce very limited partial melting, yielding no basaltic melts; (3) an extensive, trans-lithospheric fault system must be present to permit rapid ascent of the magma; and (4) the water table must be intersected.

The Thelon Basin is a potential exploration target for phreatomagmatic lamproite centres for the following reasons: (1) the older ultrapotassic Christopher Island Formation lamprophyre dyke swarm extends to the basin's eastern margin, and (together with phlogopite-enriched mantle) presumably extends underneath it. Additionally, the youngest rocks of the basin are strongly potassic and mafic volcanic rocks. (2) The basin overlies an extensive fault system. The intersection of the Bathurst and MacDonald fault systems lies beneath the centre of the basin. Indeed, the basin is probably preserved today because it is underlain by downfaulted crust. (3) The Thelon Formation is at present quite porous, and must have been so throughout its history; it likely has always contained substantial meteoric water.

Similarly, the Proterozoic basins of the eastern Churchill Province, in the Baker Lake region, are also excellent targets for phreatomagmatic centres, including some of early Dubawnt age (ca. 1.85 Ga). Recently, single microdiamonds have been found (with varying degrees of certainty) in a lamprophyre dyke (MacRae and Armitage, 1994) and a welded ultrapotassic intrusive breccia (J. Davis, Taiga Consultants, pers. comm., 1993) which are presumed to be correlative with the Christopher Island Formation, although this has not been demonstrated by geochronology. Both of these occurrences contact crystalline basement at the present level of exposure; they would be more significant if it could be demonstrated that they lie within the root zones of volcanic vents which intersected sedimentary rocks.

Based on a transition from minette-like to lamproite-like compositions with increasing stratigraphic height within the Christopher Island Formation, Peterson et al. (in press) suggested that progressively younger ultrapotassic rocks within the Churchill Province could be increasingly lamproitic. Some support for this hypothesis has recently been found, in the form of young, true lamproites containing leucite,

perovskite, K-Ti richterite, and other lamproite indicator minerals, at southern Baffin Island (Hogarth and Peterson, in prep.). The importance of the Kuungmi Formation is that it demonstrates that some Proterozoic potassic volcanism post-dated all subduction-collisions on the margins of the Churchill Province by at least 80 Ma; such extended delays between metasomatism and melt generation seem to be an important factor for lamproite generation (Mitchell and Bergman, 1991). Tantalizing evidence for diamondiferous lamproites within the Churchill Province is present. It remains to be seen whether the correct age, source, and volcanic facies can be wedded at the same location.

## REFERENCES

- Boxer, G.L., Lorenz, V., and Smith, C.B.**  
1989: The geology and volcanology of the Argyle (AK1) lamproite diatreme, Western Australia; in *Kimberlites and Related Rocks*, (ed.) J. Ross et al.; Geological Society of Australia, Special Publication 14, p. 140-152
- Carmichael, I.S.E., Turner, F.J., and Verhoogen, J.**  
1974: *Igneous Petrology*; McGraw-Hill, New York, 739 p.
- Donaldson, J.A.**  
1968: Descriptive notes (with particular reference to the late Proterozoic Dubawnt Group) to accompany a geological map of central Thelon Plain, Districts of Keewatin and Mackenzie; Geological Survey of Canada, Paper 68-49.
- Fischer, R.V. and Schmincke, H.-U.**  
1984: *Pyroclastic Rocks*; Springer-Verlag, New York, 472 p.
- Gall, Q., Peterson, T.D., and Donaldson, J.A.**  
1992: Early Proterozoic stratigraphy of the Thelon and Baker Lake basins, District of Keewatin: a proposed revision; in *Current Research, Part C*; Geological Survey of Canada, Paper 92-1C, p. 129-137.
- Jaques, A.L., Lewis, J.D., and Smith, C.B.**  
1986: The kimberlites and lamproites of western Australia; Geological Survey of Australia, Bulletin 132.
- Kjarsgaard, B.A. and Hamilton, D.L.**  
1989: The genesis of carbonatites by immiscibility; in *Carbonatites, Genesis and Evolution* (ed.) K. Bell; Unwin Hyman, London, p. 388-404.
- LeCheminant, A.N. and Heaman, L.**  
1989: Mackenzie igneous events, Canada: Middle Proterozoic hotspot magmatism associated with ocean opening; *Earth and Planetary Science Letters*, v. 96, p. 38-48.
- MacRae, N.D. and Armitage, A.E.**  
1994: Diamond-bearing potential of alkaline dykes in the Gibson Lake area, District of Keewatin, N.W.T.; Geological Association of Canada-Mineralogical Association of Canada, Program with Abstracts; v. 19, p. A69.
- Meen, J.**  
1987: Formation of shoshonites from calcalkaline basalt magmas: geochemical and experimental constraints from the type locality; *Contributions to Mineralogy and Petrology*, v. 97, p. 333-351.
- Miller, A.R., Cumming, G.L., and Krstic, D.**  
1989: U-Pb, Pb-Pb, and K-Ar isotopic study and petrography of uraniumiferous phosphate-bearing rocks in the Thelon Formation, Dubawnt Group, Northwest Territories Canada; *Canadian Journal of Earth Sciences*, v. 26, p. 867-880.
- Mitchell, R.H. and Bergman, S.C.**  
1991: *Petrology of Lamproites*; Plenum Press, New York, 447 p.
- Peterson, T.D.**  
1994: Early Proterozoic ultrapotassic volcanism of the Keewatin Hinterland, Canada; in *Proceedings, 5th International Kimberlite Conference; volume 1, Kimberlites, related rocks and mantle xenoliths*, (ed.) H.O.A. Meyer, O.H. Leonardos; Companhia de Pesquisa de Recursos Minerais, Brasilia, p. 221-235.
- Peterson, T.D., Esperança, S., and LeCheminant, A.N.**  
in press: Geochemistry and origin of Early Proterozoic ultrapotassic rocks of the Churchill Province, Canada; *Mineralogy and Petrology*.

**Scott Smith, B.H.**

1989: Lamproites and kimberlites in India; Neues Jahrbuch Mineralogie Abhandlung, v. 161, p. 193-225.

**Scott Smith, B.H., Skinner, E.M.W., and Loney, P.E.**

1989: The Kapamba lamproites of the Luangwa Valley, eastern Zambia; in Kimberlites and Related Rocks, (ed.) J. Ross et al.; Geological Society of Australia, Special Publication 14, p. 189-205.

**Stachel, T.**

1992: The olivine and leucite lamproite pipes of the Ellendale volcanic field; Zeitschrift der Deutschen Geologischen Gesellschaft, v. 143, p. 133-158.

**Venturelli, G., Thorpe, R.S., Dal Piaz, G.V., Del Moro, A., and Potts, P.J.**

1984: Petrogenesis of calc-alkaline, shoshonitic and associated ultrapotassic Oligocene volcanic rocks from the Northwestern Alps, Italy; Contributions to Mineralogy and Petrology, v. 86, p. 209-220.

---

Geological Survey of Canada Project 880012

# Geology and structure of the Barbour Bay region, District of Keewatin, Northwest Territories, and its potential for industrial garnets

S. Tella, U. Mader<sup>1</sup>, and Mikkel Schau  
Continental Geoscience Division

*Tella, S., Mader, U., and Schau, M., 1995: Geology and structure of the Barbour Bay region, District of Keewatin, Northwest Territories, and its potential for industrial garnets; in Current Research 1995-C; Geological Survey of Canada, p. 27-34.*

---

**Abstract:** Archean supracrustal rocks in the Barbour Bay region form a northeast-trending, synformal remnant within a granitoid gneiss terrane. They are composed of a conformable sequence of mafic metavolcanic rocks and semipelitic schists that are deformed and metamorphosed under amphibolite facies conditions. The semipelitic rocks contain garnet±biotite±cordierite±sillimanite+plagioclase+quartz assemblages. Interlayers of garnetite with up to 80% garnet porphyroblasts, and sillimanite-rich layers are common within the schists. They reflect highly Al- and Fe-rich compositions of a metasedimentary protolith. P-T estimates for metamorphism are in the order of 2.8-3.6 kb and 520°C-650°C.

The garnetite layers appear to offer a potential source of industrial garnets. The garnets occur in three forms (idiomorphic glassy, idiomorphic dull, poikiloblastic), and contain 70-90 mol% almandine, 5-12 mol% pyrope, and 2-8 mol% grossular. Further work is necessary to determine the grade, tonnage, milling and separation characteristics, abrasive quality of different garnet-types, and the commercial viability of the potential deposit.

**Résumé :** Les roches archéennes supracrustales dans la région de la baie Barbour forment un résidu synforme, à direction nord-est, au sein d'un terrane de gneiss granitoïde. Elles se composent d'une séquence concordante de métavolcanites mafiques et de schistes semi-pélitiques qui sont déformés et métamorphisés dans des conditions propres au faciès des amphibolites. Les roches semi-pélitiques contiennent des assemblages de grenat±biotite±cordiérite±sillimanite+plagioclase+quartz. Les intercalations de grenatite contenant jusqu'à 80 % de porphyroblastes de grenat et les couches riches en sillimanite sont fréquentes au sein des schistes. Elles reflètent les compositions très riches en Al et Fe d'un protolithe métasédimentaire. Les estimations de P-T pour le métamorphisme sont de l'ordre de 2,8 kbar à 3,6 kbar et de 520 °C à 650 °C.

Les couches de grenatite pourraient être une source de grenats industriels. Les grenats se présentent sous trois formes (idiomorphe vitreux, idiomorphe sombre, poeciloblastique) et contiennent 70-90 % M d'almandine, 5-12 % M de pyrope et 2-8 % M de grossulaire. D'autres travaux sont nécessaires pour déterminer la teneur, le tonnage, les caractéristiques liées au broyage et à la séparation, la qualité abrasive de différents types de grenats et la rentabilité du gisement potentiel.

---

<sup>1</sup> Rock-water Interaction Group, University of Bern, Geology, Baltzerstrasse 1, CH-3012 Bern, Switzerland

## INTRODUCTION

The Barbour Bay region (Fig. 1, 2) is underlain by deformed and metamorphosed Archean volcanic-sedimentary gneiss and schist intruded by early Proterozoic, post-tectonic, two-mica leucogranite. The purpose of this note is to present preliminary results of a structural and petrological study undertaken in a supracrustal remnant that is exposed along the south shore of Barbour Bay (Fig. 2), and to outline the economic potential for industrial garnets in this supracrustal remnant. The results of most recent regional bedrock mapping studies in the region, at a scale of 1:250 000, were reported by Tella et al. (1992, 1993) and Tella and Schau (1994). The reader is referred to the above publications and references therein for an overview of the geology and tectonometamorphic history of the region.

## GEOLOGY, STRUCTURE, AND METAMORPHISM

In the Barbour Bay region, metavolcanic and metasedimentary rocks are exposed in a synform which plunges shallowly (20°-30°) towards the northeast (Fig. 3). Local plunge reversals toward the southwest are common. The metasedimentary gneisses conformably overlie the metavolcanic rocks which in turn structurally overlie a quartzofeldspathic granitoid gneiss terrane. The distribution of rock units is shown in Figure 2, and the orientations of selected fabric elements are shown in Figure 3. The regional planar fabric within the belt is concordant with that in the granitoid gneiss for the most part, but discontinuous shear fabrics in both rock units along the southern margin suggest a tectonic break. Abundant mafic inclusions, probably derived from the metavolcanic rocks, in the granitoid gneiss suggest that they were intruded, and subsequently

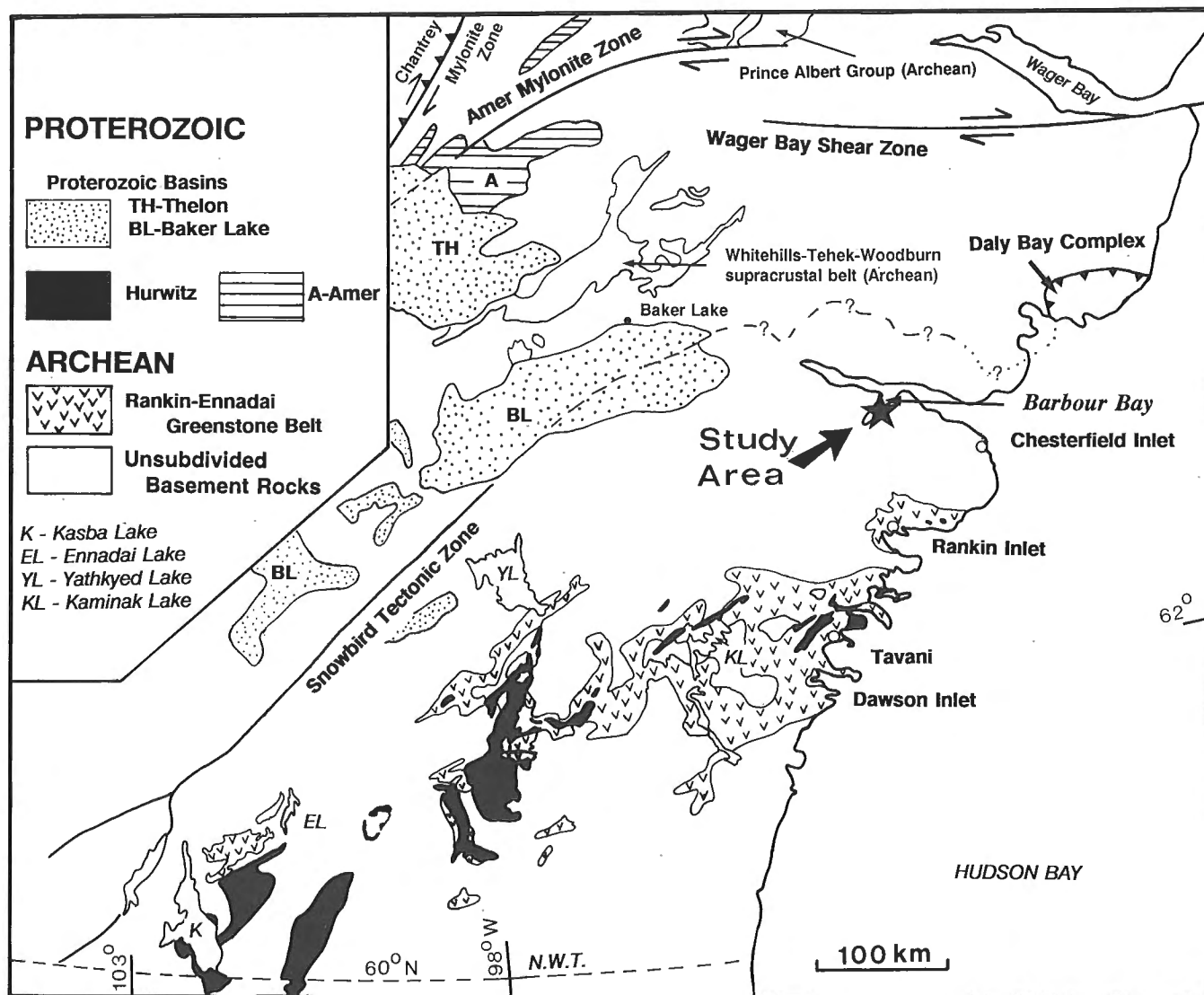


Figure 1. Sketch map showing location of the Barbour Bay region, and the distribution of major supracrustal belts, and shear zones, District of Keewatin.

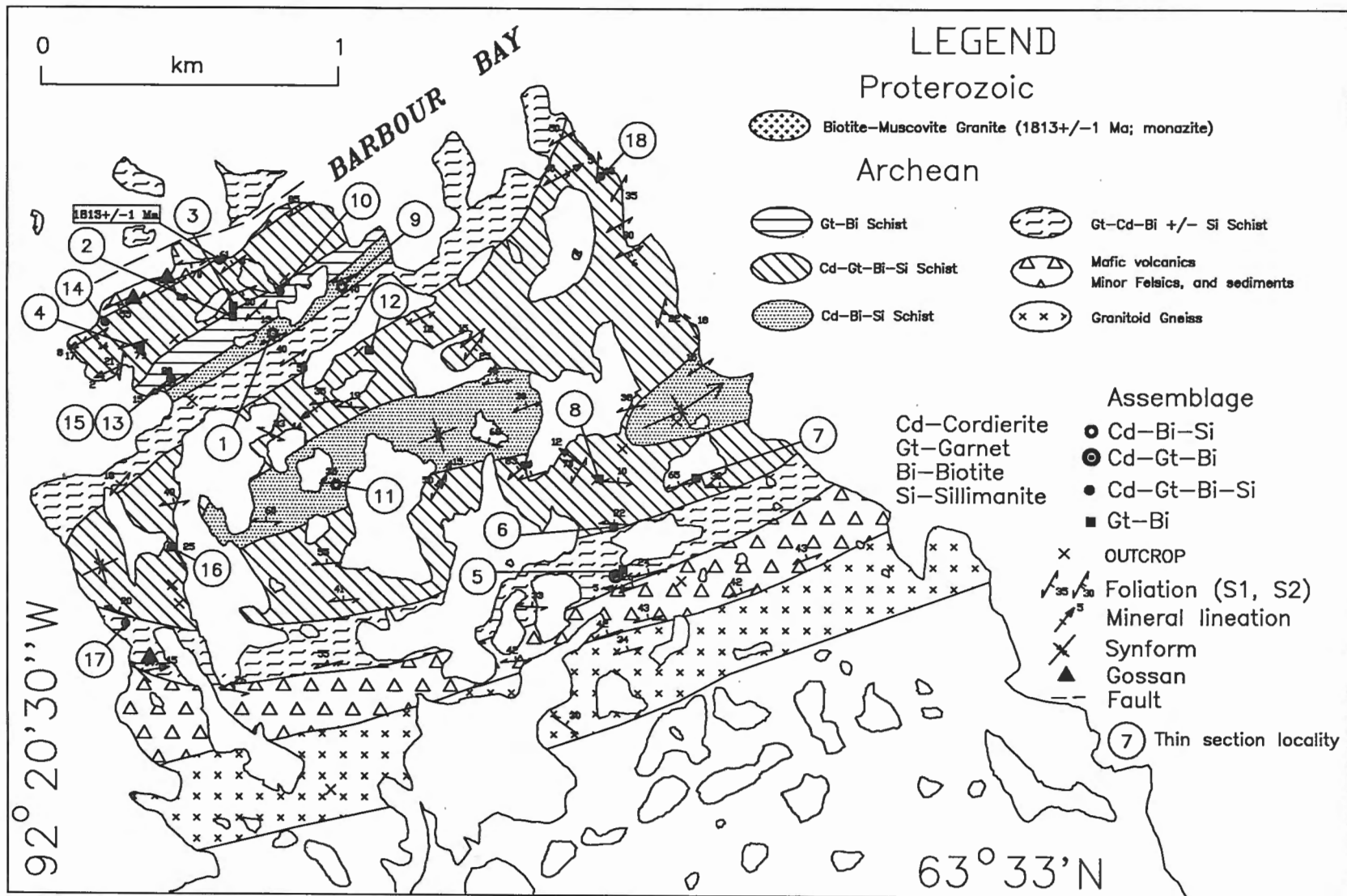


Figure 2. Detailed geological map of the Barbour Bay region (see Figure 1 for location).

sheared. The regional foliation within the metavolcanic rocks and schists is folded about a mesoscopic, northeast-plunging regional  $F_2$  fold axis. The northern contact is not exposed. In the adjoining regions to the east, south, and west these pelitic rocks form narrow belts that wrap around, and dip away from, domal masses of younger felsic plutons (Tella et al., 1992, 1993; Tella and Schau, 1994).

Poles to Foliation (S1) ; N=73 (circles)  
 Mineral lineation (L1) ; N=7 (squares)

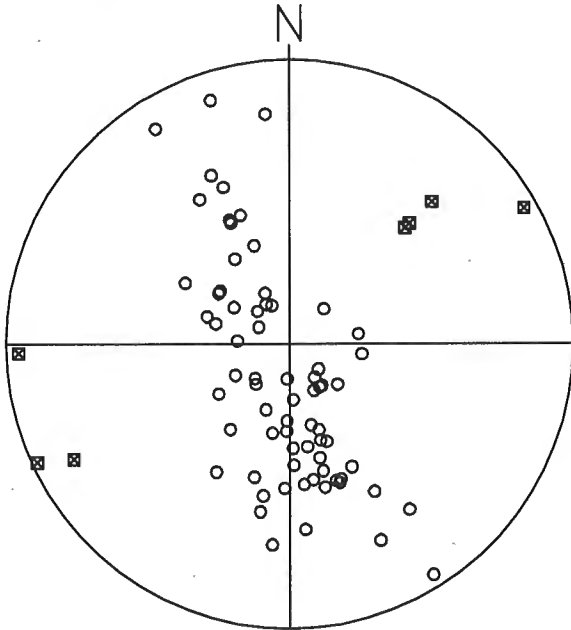


Figure 3. Orientation selected fabric elements (S1, L1) from the Barbour Bay region.

The metavolcanic rocks are fine- to medium-grained, well foliated mafic rocks interlayered with minor felsic rocks, and finely laminated volcanoclastics that contain disseminated magnetite. Some centimetre-scale magnetite-rich horizons may represent lean iron-formation. Adjacent to the Barbour Bay shore line, a 2-m thick mafic dyke (hornblende-biotite-plagioclase bearing) cuts the metavolcanics and overlying semipelitic schists. The mafic metavolcanic rocks, on both limbs of the synform, contain abundant plagioclase and quartz replacement textures (pseudomorphous after garnet?). Discontinuous psammitic layers are also common within the metavolcanic rocks.

The metasedimentary schist belt in the Barbour Bay region contains biotite-plagioclase-quartz±sillimanite±cordierite±garnet±tourmaline±K-feldspar assemblages. Relict staurolite was noted at two localities (13, 17; Fig. 2). There, and at locality 10, garnet, sillimanite, cordierite and biotite appear to coexist as stable phases. The semipelitic schists are subdivided into several distinct, structurally conformable compositional layers based on their metamorphic assemblages (Fig. 2, Table 1). Characteristic are the lack of K-feldspar and muscovite, and the relative abundance of tourmaline. Sillimanite and garnet porphyroblasts up to 4 cm long (Fig. 4) are present throughout the semipelitic belt. Garnetite layers containing up to 80% almandine garnet (Fig. 5, 6, 7; Table 1) are interlayered with biotite-sillimanite-quartz, and cordierite-biotite-sillimanite schists. Individual layers range from a few centimetres to up to 100 m thick. At one locality (14, Fig. 2), sillimanite occurs both as needles and fibres within the regional fabric planes. Most sillimanite needles exhibit preferred orientation within the planar fabric defined by biotite, but some random orientations were also noted. At the same locality, a few sillimanite needles with a preferred orientation are completely enclosed by a cordierite porphyroblast.



Figure 4.

Sillimanite porphyroblasts in garnet-cordierite-biotite-sillimanite schist, Barbour Bay. Diameter of the lens cap is 5 cm. GSC 1994-723F

**Table 1.** Metamorphic mineral assemblages from the Barbour Bay region.

Sample # Map Loc.	Paragenesis	Accessories	Range of garnet compositions (Mole %)				
			gr	pyr	alm	sp	M/F
92TXU-026A (1)	Cd-Bi-Si-Pl-Qz	Ap-II-Zr-Py					
92TXU-026B (1)	Cd-Bi-Si-Pl-Qz-Tm	Cl					
92TXU-027B (2)	Cm-Pl-Qz						
92TXU-028A (3)	Gt-Bi-Pl-Qz		8.97- 13.47	12.35- 13.18	71.60- 76.63	1.74- 2.04	0.14- 0.15
92TXU-030 (4)	Gt-Bi-Pl-Qz	Ap-II	6.97- 7.32	10.27- 12.16	76.67- 78.25	3.86 4.29	0.12- 0.14
92TXU-039A (5)	Gt-Cd-Bi-Pl-Qz-Tm	Zr	4.18- 4.33	12.50- 13.45	70.13- 70.69	11.55 13.18	0.15- 0.16
92TXU-039B (5)	Gt-Bi-Pl-Qz		8.56- 8.70	8.24- 8.32	75.95- 76.34	6.86- 6.87	0.10
92TXU-040 (6)	Gt-Bi-Pl-Qz Bt-Pl-Mt-Qz-Tm		3.32- 4.79	4.57- 5.76	88.11- 88.93	1.72- 2.32	0.05- 0.06
92TXU-041 (7)	Gt-Bi-Pl-Qz-Tm	Mt-Ap-Cpy	6.50- 7.13	8.22- 9.79	81.74- 83.61	1.41- 1.88	0.09- 0.11
92TXU-042A (8)	Gt-Bi-Pl-Cm-Qz	Ap	1.94- 16.13	3.49- 7.70	76.99- 90.15	0.15 3.39	0.07- 0.08
92TXU-044A (9)	Cd-Bi-Si-Pl-Qz	Il-Py-Ap-Mz					
92TXU-044B (9)	Cd-Bi-Si-Pl-Qz-Tm	Py-Ap-Cpy					
92TXU-046 (10)	Gt-Cd-Bi-Si-Pl-Qz-Tm	Mz	2.86- 3.13	7.74- 10.05	82.22- 89.48	4.19- 4.93	0.08- 0.11
92TXU-047 (11)	Cd-Bi-Si-Pl-Qz-Tm						
92TXU-048A(12)	Gt-Bi-Pl-Qz-Kf-Tm		2.56- 3.02	7.90- 8.27	88.27- 88.90	0.78- 0.81	0.08- 0.09
92TX-185C (13)	Gt-Cd-Bi-Si-Pl-Qz-Tm	Il-Py-Ap-Mz-St	2.43- 3.31	8.43- 11.09	82.98- 84.90	3.06- 3.93	0.09- 0.11
94TX-025 (14)	Cd-Bi-Si-Pl-Qz-Tm	Ap-II-Zr-Cl					
94TX-034 (15)	Cd-Bi-Si-Pl-Qz-Tm	Ap-II-Zr					
94TX-037 (16)	Gt-Bi-Pl-Qz	Ap-Mt-Cl					
94TX-038 (17)	Gt-Cd-Si-Bi-Pl-Qz-Tm	Ap-II-Zr-Cl-St					
94TX-043 (18)	Gt-Bi-Pl-Qz	Il-Cl					

Bi-biotite; Cd-cordierite; Cm-cummingtonite; Gt-garnet; Kf-potassium feldspar; Pl-plagioclase; Si-sillimanite; St-staurolite; Tm-tourmaline; Zr-zircon; Cpy-chalcopyrite; Ap-apatite; Cl-chlorite; Il-illemenite; Mt-magnetite; Mz-monazite; Py-pyrite; Qz-quartz; gr-grossular; prp-pyrope; alm-almandine; sps-spessartine; M/F-  
Mg/(Mg+Fe<sub>tot</sub>)



Garnet occurs in three different habits in the semipelitic lithologies: (a) idiomorphic, glassy, with few large inclusions; (b) idiomorphic, dull, with abundant small inclusions; and (c) highly poikiloblastic. Habit (a) is typical for the coarse grained biotite-cordierite±sillimanite schists. Habits (b) and (c) are common in biotite schists, with (b) being typical for garnet-rich layers that form the topographic highs of the area. Inclusions comprise quartz, plagioclase, and biotite in order of abundance. The abundance of garnet porphyroblasts (<1 mm to up to 5 cm; Fig. 5, 6) within the semipelitic layers reflect the highly Al- and Fe-rich original bulk composition of the metasediments. Internal grading of garnet porphyroblasts may reflect variations in original composition and/or grain size, or nucleation at different times during the

metamorphic history. The garnet compositions are listed in Table 1. They range from almandine 70-90 mol% and pyrope 5-12 mol%. Grossular content varies from 2-8 mol% but does reach 12-16 mol% in the cores of some grains from the garnet-rich sample TXU-042A. Spessartine content is highest (4-13 mol%) in samples containing little garnet, but is below 2 mol% in garnet-rich lithologies, except for cores of the largest grains.

Rocks within the supracrustal belt are considered to be higher grade equivalents of aluminous and iron-rich sedimentary successions of the Rankin Inlet Group (Tella et al., 1986). The presence of sillimanite, garnet, and biotite in gneisses together with locally developed quartzofeldspathic melt pods attest to middle to upper amphibolite facies conditions of

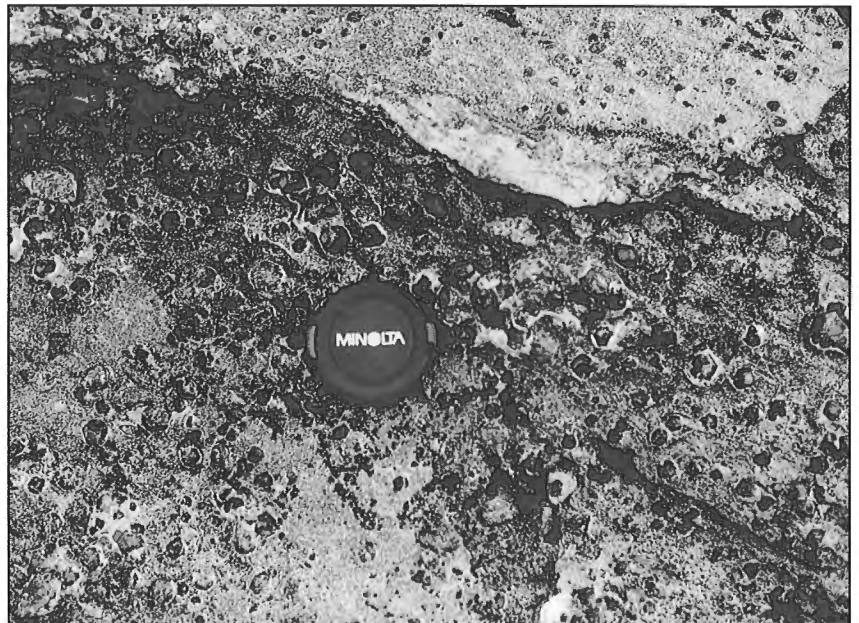


**Figure 5.**

*Graded garnet-rich layers in garnet-cordierite-biotite-sillimanite schist. Euhedral to subhedral peppered throughout the unit form pseudo-graded beds that reflect original bulk composition, Barbour Bay region; garnets represent up to 80% by volume. Diameter of the lens cap is 5 cm. GSC 1994-723G*

**Figure 6.**

*Porphyroblasts of euhedral garnets in cordierite-garnet-biotite-sillimanite schist. Note replacement-rims of quartz around garnets. Diameter of the lens cap is 5 cm. GSC 1994-723A*



regional metamorphism. Preliminary thermobarometric calculations yield 520°-650°C from the garnet-biotite Fe-Mg exchange reaction, and 2.8-3.6 kbar pressure from the anorthite = grossular+sillimanite+quartz equilibrium, using thermodynamic data and software of Berman (1988, 1990, 1991). The temperature estimates were calculated from both rim and core compositions of garnets, and represent the total range for ten analyzed samples. The spread is fairly large, and there does not appear to be a clear separation between core and rim temperatures. High temperatures are in the 600-650°C range, and low temperatures are 520-570°C range. Thermobarometric calculations, based on a number of different mineral equilibria, from the adjoining region to the southeast that contains similar lithologies (but containing kyanite instead of sillimanite), yielded P-T estimates of ca 4.9 kb and 545°C for the assemblages (Tella et al., 1992).

The origin of these rocks is currently under study. They may represent sediments with a source region of highly weathered aluminous- and iron-rich materials. Alternatively, an origin of the protolith as the consequence of extensive hydrothermal alteration of an acid and/or intermediate volcanoclastic sequence is possible. A few gossans adjacent to the metavolcanics occur within the cordierite-bearing layers. Commonly, magnesium enrichment is associated with hydrothermal activity, not with deep weathering. Metasomatic alteration has affected thin mafic dykes in adjacent supracrustal remnants, forming a 10-cm-wide alteration zone along the edges of the dykes indicating at least some post-dyke alteration. Several kilometres to the west, in similar rocks, metasomatic alteration has produced a gahnite-rich zone within a Cu-Zn massive sulphide prospect (Armitage et al., 1994).

The age of deformation, metamorphism of the country rock, and subsequent development and folding of ductile strain zones, are all believed to be Archean. Approximately 7 km along strike to the northeast of the present study area, sillimanite-bearing pelitic schists occur as inclusions within

a ductile mylonite zone. There, a syntectonic pegmatite, emplaced during the mylonitic event, yielded a U-Pb zircon age of ca 2.65 Ga confirming that the pelitic rocks are Archean (J.C. Roddick, GSC, pers. comm., 1994).

A massive to weakly foliated, biotite-muscovite leucogranite is exposed as dykes and small intrusive plugs adjacent to the south shore of the Barbour Bay (Fig. 2). The granite is coarse to medium grained and grey to white weathering. Textural and mineralogical characteristics suggest that the granite is peraluminous S-type. A monazite fraction from this granite yielded a U-Pb concordia intercept age of  $1813 \pm 1$  Ma, interpreted as the crystallization age for the granite (Roddick, pers. comm., 1994). The granite post-dates the deformation and metamorphic events recorded in the volcanic and sedimentary schists. Contact metamorphic effects related to the granite emplacement are not obvious.

## ECONOMIC GEOLOGY

Garnet-rich semipelitic rocks are exposed in the Barbour Bay region over a 2 km<sup>2</sup> area. The area is easily accessible by water along Chesterfield Inlet. The garnet occurrence may have a potential for an industrial garnet deposit, and for mineral collectors. As mentioned previously, garnets in the semipelites form three textural groupings – (a) subhedral to rounded garnets with inclusion trails of quartz, plagioclase and biotite in the cores, and with inclusion-free overgrowths; (b) angular to subrounded porphyroblasts with strong, preferentially oriented inclusion trails (qz-bi-pl), no overgrowths, and external fabric discordant with the internal fabric defined by the inclusion-trails; and (c) randomly oriented inclusions of quartz, biotite, and plagioclase in subrounded to euhedral porphyroblasts with inclusion-free overgrowth; external fabric wraps around the porphyroblasts. All garnet types may occur within one lithology, and the relative proportions in each lithology have not been estimated. Garnets with

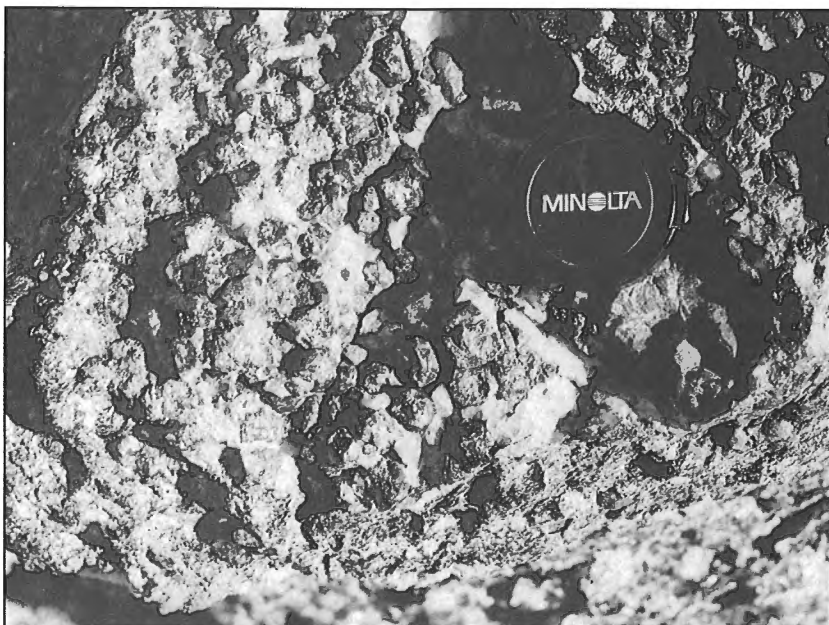


**Figure 7.**

*Euhedral garnets in garnet-biotite schist layers, Barbour Bay region. Diameter of the lens cap is 5 cm. GSC 1994-723J*

**Table 2.** Whole-rock assays of gossan samples.

Sample	94TX-030	94TX-038
Au	41 ppb	4 ppb
Ag	0.8 ppm	0.9 ppm
Zn	89 ppm	92 ppm
Cu	177 ppm	23 ppm
Ni	18 ppm	8 ppm
Pb	4 ppm	16 ppm
As	<3 ppm	<3 ppm
Co	15 ppm	8 ppm
(ICP analyses; XRAL Laboratories)		

abundant inclusions may not be suitable for abrasives. Further detailed work is necessary to obtain quantitative estimates of different garnet types, to determine the type and composition of internal impurities, and other physical properties (e.g., specific gravity, magnetic susceptibility) in order to determine the commercial potential of the deposit.

Discontinuous, rusty weathering, sulphide-rich gossan zones up to 2 m thick that contain chalcopyrite, pyrite, and arsenopyrite are present along the contact between the meta-volcanics and the garnet-sillimanite schist on both limbs of the F<sub>2</sub> synform. No anomalous base or precious metal concentrations were detected in the analyzed samples from these zones (see Table 2 for analytical data).

## ACKNOWLEDGMENTS

S. Alvarado is thanked for his assistance in the field during 1994 season and for digital processing of field data. The manuscript was reviewed by R.G. Berman and K.D. Card.

## REFERENCES

- Armitage, A.E., Miller, A.R., and MacRae, N.D.**  
1994: Geology of the Sandhill Zn-Cu showing in the Gibson Lake area, District of Keewatin, Northwest Territories; in *Current Research 1994-C*; Geological Survey of Canada, p. 147-155.
- Berman, R.G.**  
1988: Internally consistent thermodynamic data for minerals in the system Na<sub>2</sub>O-K<sub>2</sub>O-CaO-MgO-FeO-Fe<sub>2</sub>O<sub>3</sub>-Al<sub>2</sub>O<sub>3</sub>-SiO<sub>2</sub>-TiO<sub>2</sub>-H<sub>2</sub>O-CO<sub>2</sub>; *Journal of Petrology*, v. 29, p. 445-522.  
1990: Mixing properties of Ca-Fe-Mg-Fe-Mn garnets; *American Mineralogist*, v. 75, p. 328-344.  
1991: Thermobarometry using multi-equilibrium calculations – a new technique, with petrological applications; *Canadian Mineralogist*, v. 29, p. 833-855.
- Tella, S. and Schau, M.**  
1994: Geology, Gibson Lake east-half, District of Keewatin, Northwest Territories; Geological Survey of Canada, Open File 2737, scale 1:250 000.
- Tella, S., Annesley, I.R., Borradaile, G.J., and Henderson, J.R.**  
1986: Precambrian geology of Tavani, Marble Island and Chesterfield Inlet map areas, District of Keewatin, Northwest Territories; Geological Survey of Canada, Paper 86-13, 20 p.
- Tella, S., Schau, M., Armitage, and Loney, B.C.**  
1993: Precambrian geology and economic potential of the northeastern parts of Gibson Lake map area, District of Keewatin, Northwest Territories; in *Current Research, Part C*; Geological Survey of Canada, Paper 93-1C, p. 197-208.
- Tella, S., Schau, M., Armitage, A.E., Seemayer, B.E., and Lemkow, D.**  
1992: Precambrian geology and economic potential of the Meliadine Lake – Barbour Bay region, District of Keewatin, Northwest Territories; in *Current Research, Part C*; Geological Survey of Canada, Paper 92-1C, p. 1-11.

Geological Survey of Canada Project 850002

# Geological and age relationships of the margins of the Manitouwadge greenstone belt and the Wawa-Quetico subprovince boundary, northwestern Ontario<sup>1</sup>

E. Zaleski, V.L. Peterson<sup>2</sup>, and O. van Breemen  
Continental Geoscience Division

*Zaleski, E., Peterson, V.L., and van Breemen, O., 1995: Geological and age relationships of the margins of the Manitouwadge greenstone belt and the Wawa-Quetico subprovince boundary, northwestern Ontario; in Current Research 1995-C; Geological Survey of Canada, p. 35-44.*

---

**Abstract:** The Manitouwadge greenstone belt and its Cu-Zn deposits occur within a highly deformed remnant of upper amphibolite-facies supracrustal rocks adjacent to the Wawa-Quetico subprovince boundary. On the basis of structural and lithological criteria, the Wawa-Quetico boundary in the Manitouwadge area is transitional. New mapping shows that migmatitic metasedimentary rocks can be traced as semicontinuous enclaves from the Quetico subprovince, through a series of map-scale folds, to the Manitouwadge belt in the Wawa subprovince. Metagreywackes in the Manitouwadge belt are indistinguishable from those in the Quetico subprovince, except for the higher metamorphic grade and migmatization of the latter. U-Pb zircon provenance study of Manitouwadge metagreywackes places a maximum age limit on deposition of 2693 Ma, at least 25 Ma younger than felsic metavolcanic rocks associated with base metal mineralization.

**Résumé :** La ceinture de roches vertes de Manitouwadge et ses gisements de Cu-Zn sont situés au sein d'un vestige hautement déformé de roches supracrustales du faciès des amphibolites supérieur adjacentes à la frontière de la sous-province de Wawa-Quetico. Selon des critères structuraux et lithologiques, la frontière de Wawa-Quetico dans la région de Manitouwadge en est une de transition. Une nouvelle cartographie montre que des roches métasédimentaires migmatitiques peuvent être retracées sous forme d'enclaves semi-continues depuis la sous-province de Quetico, à travers une série de plis d'échelle cartographique jusqu'à la ceinture de Manitouwadge, dans la sous-province de Wawa. Les métagrauwackes dans la ceinture de Manitouwadge ne se distinguent guère de ceux de la sous-province de Quetico, sauf que ces derniers sont plus fortement métamorphisés et migmatisés. Une étude sur la provenance basée sur des datations U-Pb sur zircon des métagrauwackes de Manitouwadge fixe une limite d'âge maximale du dépôt à 2 693 Ma, soit au moins 25 Ma de moins que pour les métavolcanites felsiques associées à une minéralisation en métaux communs.

---

<sup>1</sup> Contribution to Canada-Ontario Subsidiary Agreement on Northern Development (1991-1995), under the Canada-Ontario Economic and Regional Development Agreement.

<sup>2</sup> Department of Geosciences and Anthropology, Western Carolina University, Cullowhee, North Carolina, 28723, U.S.A.

## INTRODUCTION

The Manitowadge greenstone belt lies in the volcano-plutonic Wawa subprovince, immediately south of the major tectonic boundary with the metasedimentary-migmatitic Quetico subprovince (Fig. 1). Stockwell (1964) originally used structural trends and style to distinguish the subprovinces, contrasting the linear east-west trends of the Quetico subprovince with the curvilinear trends of the Wawa and Wabigoon subprovinces, the latter defined by remnants of greenstone belts lying between domical batholiths (also see discussion in Percival, 1989). Subsequently, lithological features were incorporated into subprovince definitions by contrasting the dominantly volcanic origin of supracrustal rocks in the volcano-plutonic terranes with the sedimentary origin of the Quetico subprovince (Stockwell, 1970; Card and Ciesielski, 1986). In some cases, boundaries were defined to exclude mafic metavolcanic rocks from the Quetico subprovince (Williams, 1991). Regardless of whether structural or lithological criteria are used, the Wawa-Quetico boundary in the Manitowadge area is transitional in nature.

This contribution presents highlights of the 1994 field season, in particular those pertinent to the marginal relationships of the Manitowadge greenstone belt, including the subprovince boundary to the north, and the plutonic rocks of various ages that engulf the greenstone belt. The field observations are combined with ongoing structural analysis and geochronology. Especially in the area of structural analysis, the summary given here anticipates a more thorough interpretation and presentation currently in preparation. This work builds on previous field seasons (1991-1993) while minimizing repetition of previously published findings (Zaleski and Peterson, 1993a, b; Zaleski et al., 1994; Peterson and Zaleski, 1994a, b).

## GEOLOGICAL SETTING

The Manitowadge greenstone belt is a remnant of volcanic and sedimentary rocks, highly deformed and metamorphosed to upper amphibolite facies. Williams et al. (1991) considered the belt as possibly correlative with the Black River assemblage of the Schreiber-Hemlo belt, and the Dayohessarah-Kabinagami belt, representing dismembered parts of an originally continuous greenstone terrane (Fig. 1). The belt comprises felsic to mafic metavolcanic rocks, metamorphosed iron-formation, metasedimentary rocks, and foliated intrusive rocks (Fig. 2). The regional structure is dominated by the D3 Manitowadge synform, and the greatest thickness of supracrustal rocks lies in the hinge region of this fold. Away from the hinge region, supracrustal units are attenuated and invaded by plutonic rocks. Despite its relatively small size and high metamorphic grade, the Manitowadge belt hosts major Cu-Zn deposits, of which the Geco mine (Noranda Inc.) is the only one still in production.

### Structure

In a preliminary structural interpretation, we suggested that five phases of ductile deformation have affected the Manitowadge belt (Peterson and Zaleski, 1994a). D1 and D2 were based on the interpretation of pre- to syn-metamorphic ductile thrust faults and associated folds. D2 was the main fabric-forming event, producing the dominant foliations and lineations which were subsequently folded about the east-northeasterly plunging D3 Manitowadge synform (Fig. 2). The Blackman Lake and Jim Lake folds were assigned to D4 based on the interpretation that they re-fold the axial trace and southern limb of the Manitowadge synform. The Banana Lake antiform was assigned to D5 deformation. Although this model is still

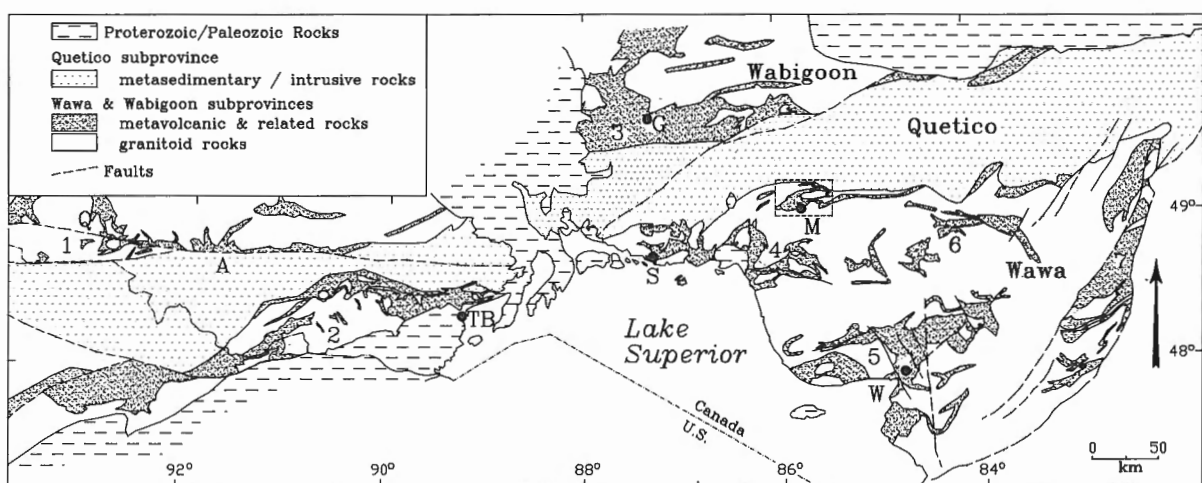


**Figure 1.** Tectonic map of the southwestern Superior Province showing the Wawa, Quetico and Wabigoon subprovinces. The area of Figure 2 is outlined. 1 = Rainy Lake area; 2 = Shebandowan greenstone belt; 3 = Beardmore-Geraldton belt; 4 = Schreiber-Hemlo greenstone belt; 5 = Michipicoten greenstone belt; 6 = Dayohessarah-Kabinagami greenstone belt; 7 = Kapuskasing structural zone; Q = Quetico fault; A = Atikokan; TB = Thunder Bay; S = Schreiber; M = Manitowadge; W = Wawa. Adapted from Williams et al. (1991) and Percival (1989).

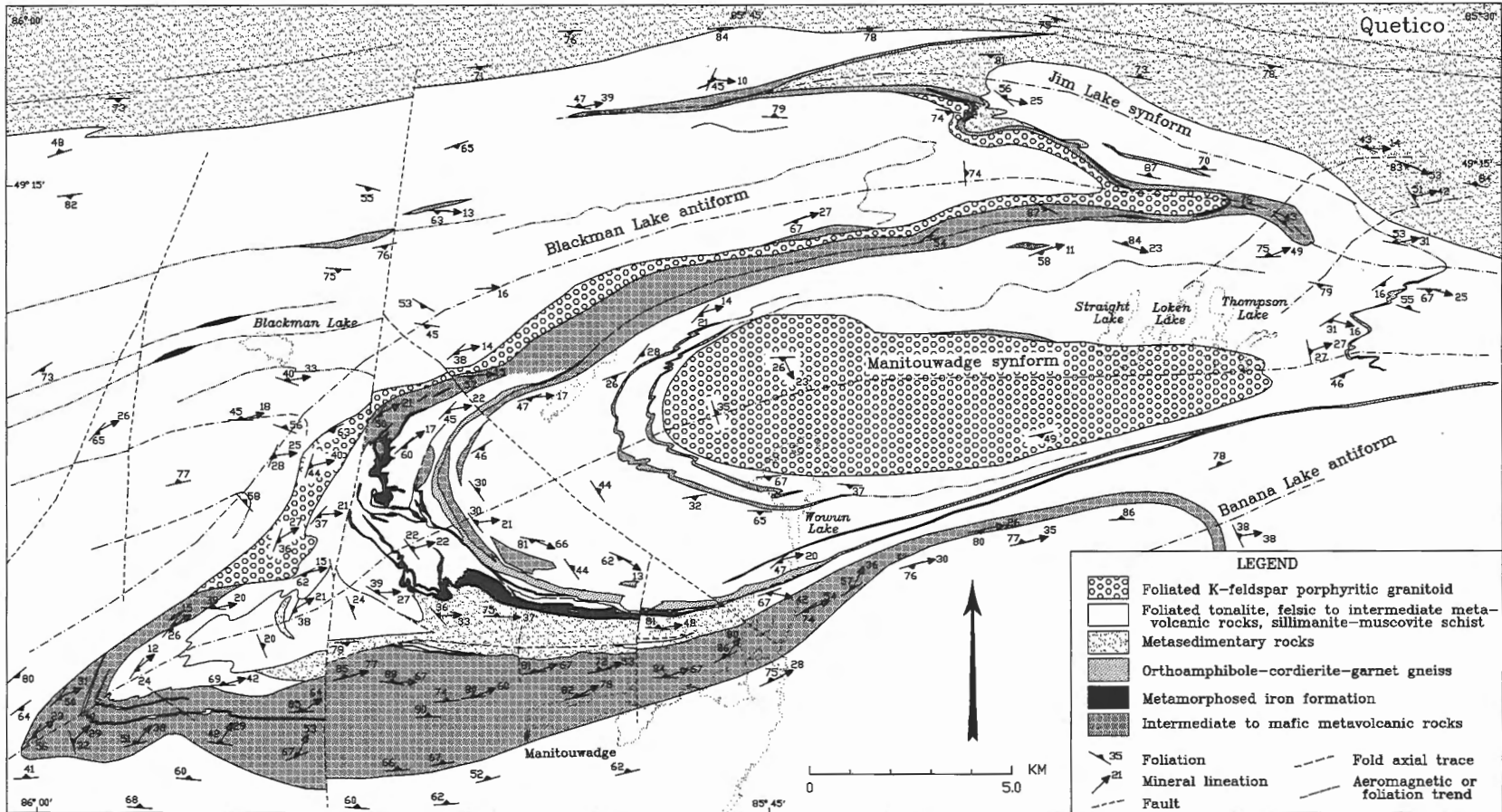


Figure 2. Generalized geology of the Manitowadge greenstone belt, omitting diabase dykes. See Peterson and Zaleski, 1994a, Fig. 3 for corresponding aeromagnetic map.

permitted on the basis of the available data, we now prefer a simpler model that accounts for the observations in a 4-stage deformation history (Peterson and Zaleski, 1994b). Details of this model are being prepared for publication and only a brief summary is given is here.

The two models have many elements in common, in particular the interpretation of mappable zones of laminated straight gneiss as annealed mylonite lying on D1 ductile thrust faults. In our preferred model, D2 deformation produced sheath folds (map and outcrop scale), the dominant foliation, and mineral lineations parallel to fold axes. The 'Manitouwadge syncline', previously proposed to account for repetition of metavolcanic rocks about a central zone of metasedimentary rocks on the southern limb of the D3 Manitouwadge synform (Touborg, 1973; Robinson, 1979), is interpreted as a D2 fold. Orthoamphibole-cordierite-garnet gneisses east of Thompson Lake (Fig. 2), correlated with the 'Geco mine horizon' and defining a series of folds with a northerly trending enveloping surface (Zaleski and Peterson, 1993b; Zaleski et al., 1994; Peterson and Zaleski, 1994a), are reinterpreted as the 'keel' of a D2 fold involved in a D2/D3 fold interference pattern. The major map-scale folds; the Manitouwadge synform, Blackman Lake antiform and Jim Lake synform, are D3 folds that formed in a dextral transpressive regime. The Banana Lake antiform may be a D3 or D4 structure.

### **Metamorphism**

There is a regional metamorphic gradient from amphibolite facies in the Schreiber-Hemlo greenstone belt (Fig. 1; Corfu and Muir, 1989b), through upper amphibolite at Manitouwadge, to upper amphibolite and granulite facies in the southern Quetico subprovince (Williams and Breaks, 1989). In the Manitouwadge belt, metamorphic grade increases to the north, with muscovite-sillimanite-quartz schists near the Geco mine on the southern limb of the Manitouwadge synform, giving way to sillimanite-microcline-quartz schists. Migmatites are ubiquitous north of the Blackman Lake antiform. Metagreywackes in the core of the 'Manitouwadge syncline' contain garnet-sillimanite-biotite in pelitic layers, but are not migmatitic. Similar rocks near the Quetico boundary contain tonalitic segregations, in some cases with cordierite and garnet. In the Manitouwadge belt, dominant D2 fabrics are defined by high grade minerals and deformed by D3 folds; hence, peak metamorphism was broadly synchronous with D2. Petrographic evidence of decompression reactions (e.g., cordierite mantling sillimanite and orthoamphibole) suggests that cooling was protracted and that high temperatures persisted during D3 deformation.

### **Geochronological constraints**

In the Manitouwadge belt, felsic metavolcanic rocks, including barren rocks and rocks associated with Cu-Zn mineralization, give primary volcanic ages of circa 2720 Ma (Zaleski et al., 1994; Davis et al., 1994). The age of zircon ( $2720 \pm 3$  Ma) from foliated quartz-rich tonalite north of the Willroy and Geco mines confirmed our field interpretation of synvolcanic intrusion. In the Schreiber-Hemlo belt, felsic volcanism

ranges in age from  $2772 \pm 2$  Ma near the Hemlo gold camp to  $2695 \pm 2$  Ma for the Heron Bay volcanic complex (Corfu and Muir, 1989a), but felsic metavolcanic rocks associated with the Winston Lake Zn-Cu mine near Schreiber are  $2723 \pm 2$  Ma (Schandl et al., 1991).

South of the Schreiber-Hemlo belt, marginal rocks of the Pukaskwa batholith were intruded at  $2719 \pm 6/-4$  Ma (Corfu and Muir, 1989a), broadly coeval with felsic volcanism at Winston Lake and Manitouwadge. Near Hemlo, several granodiorite plutons cluster closely around 2688-2687 Ma, but amphibolite-facies metamorphism dated by titanite, peaked around 2678-2676 Ma, coeval with the late tectonic Gowan Lake pluton at  $2678 \pm 2$  Ma (Corfu and Muir, 1989b). Synmetamorphic monazites gave ages of  $2675 \pm 1$  Ma at Geco and  $2677 \pm 1$  Ma at Winston Lake (Schandl et al., 1991), suggesting synchronous metamorphism throughout most of this part of the Wawa subprovince. Younger monazite ( $2661 \pm 1$  Ma) in biotite schist at Geco was interpreted to date local K-metasomatism (Davis et al., 1994).

Metagreywackes of the Quetico subprovince have been interpreted as an accretionary complex continuous with the Wawa subprovince at least since 2689-2684 Ma (Percival and Williams, 1989). Geochronological studies of Quetico metasedimentary rocks have been mainly confined to west and north of Thunder Bay (Fig. 1). Detrital zircons constrain the maximum age of sedimentation to  $2702 \pm 4$  Ma for the southern Quetico near Thunder Bay (Percival and Sullivan, 1988), and to  $2698 \pm 3$  Ma for the northern Quetico near Atikokan (Davis et al., 1990). Minimum ages were constrained by intrusion ages of  $2687 \pm 19/-13$  Ma and  $2688 \pm 4$  Ma, respectively for each area. In both cases, zircons older than 3000 Ma indicated input from old sources (Davis et al., 1990). In the Atikokan area, the zircons could have relatively proximal sources to the north, including the  $3003 \pm 5$  Ma Marmion Lake batholith (Davis et al., 1990). In the case of zircons greater than 2800 Ma in the southern Quetico, no local potential sources are known (Percival and Sullivan, 1988). The Coutchiching metagreywackes in the Rainy Lake area of the Wabigoon subprovince (Fig. 1) contain detrital zircon populations similar to those of Quetico rocks (Davis et al., 1989). The maximum depositional age was established at  $2704 \pm 3$  Ma and the minimum age at  $2692 \pm 2$  Ma, the age of a crosscutting intrusion. The presence of zircons as old as 3059 Ma indicated a Mesoarchean source.

## **INTRUSIVE ROCKS AND THEIR INCLUSIONS**

### **Black Pic batholith**

Supracrustal rocks of the Manitouwadge belt are bounded to the west and south by foliated multiphase plutonic rocks, collectively known as the Black Pic batholith. Near the southern contact, at least three intrusive phases are recognized (Fig. 3). The contact is a transitional zone of interleaved mafic metavolcanic rocks, diorite and younger tonalite, all involved in tight intrafolial folds. The oldest phase, foliated hornblende-biotite diorite with plagioclase augen, is found mainly as

blocky inclusions in foliated tonalite to granite. The youngest phase forms crosscutting dykes of weakly foliated granite, aplite, and pegmatite.

South of the Manitouwadge belt, plutonic rocks of the Black Pic batholith are continuous to the Schreiber-Hemlo greenstone belt (Fig. 1; Williams et al., 1991) and foliations define a structural dome (Williams and Breaks, 1990a, b). D2 foliations in Black Pic rocks are deformed by the Manitouwadge synform (D3), and the Blackman Lake (D3) and Banana Lake (D3/D4?) antiforms (Fig. 2). West of the Manitouwadge belt in the hinge region of the Blackman Lake antiform, abundant screens of mafic to intermediate supracrustal rocks are likely derived from the main supracrustal belt. A few screens of quartz-magnetite iron-formation are present; also mafic inclusions are commonly strongly magnetic. Aeromagnetic maps show a pronounced striping parallel to foliation trends (Geological Survey of Canada, 1993a, b; Fig. 3 in Peterson and Zaleski, 1994a), interpreted to reflect the presence of semicontinuous supracrustal septa. The aeromagnetic striping and the linear map pattern are transitional across the Quetico boundary, becoming straighter and trending more nearly east-west toward the north. In contrast, the Black Pic batholith to the south contains few supracrustal inclusions and the aeromagnetic signature is low and flat (Geological Survey of Canada, 1993a, b; Fig. 3 in Peterson and Zaleski, 1994a).

### *K-feldspar porphyritic granitoids*

Two bodies of foliated K-feldspar porphyritic granitoid can be distinguished from the multiphase Black Pic suite (Fig. 2). These lie near the margins of the greenstone belt (including

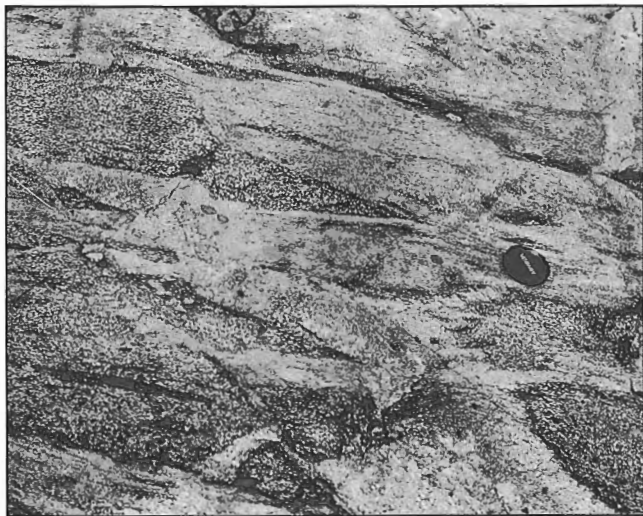


**Figure 3.** Relationships between phases of the Black Pic batholith. The oldest phase, forming angular inclusions in foliated tonalite, is plagioclase-porphyritic diorite containing elongate mafic enclaves. The youngest phase is weakly foliated aplite cutting both diorite and tonalite (e.g. on the right). The lens cap in this and the following photographs is about 5 cm in diameter.

probable synvolcanic intrusions), and have been involved in D3 folding. The westernmost body, here called the Nama Creek pluton, lies along the contact between supracrustal rocks and foliated Black Pic tonalites within the Blackman Lake antiform. It forms a long sinuous body of foliated hornblende-biotite (up to 25%) granitoid. Microcline phenocrysts, typically 1 to 2 cm in length, vary in abundance from sparse (or none) to about 25%. A moderate to strong tectonic fabric defined by mafic minerals and augen-shaped phenocrysts is folded by outcrop-scale Z-folds (D3). This, and the presence of folded pegmatite-aplite dikes, suggests that the intrusion is pre- to syn-D2.

Microcline porphyritic granitoid, here called the Loken Lake pluton, occupies the innermost area of the Manitouwadge synform (Fig. 2). Except for the western part of this body, exposure is poor, and its distribution was interpreted to coincide with an elliptical area of low flat aeromagnetic expression (Geological Survey of Canada, 1993a, b; Fig. 3 in Peterson and Zaleski, 1994a). The rock is characterized by microcline megacrysts, typically 5 to 15 cm long, varying in abundance from sparse to 25% (Fig. 4). Large areas of the intrusion consist of non-porphyritic rock resembling the matrix of porphyritic varieties. In comparison to the Nama Creek pluton, the Loken Lake pluton has larger phenocrysts and is more leucocratic, generally containing about 5 to 10% biotite. A strong tectonic fabric, commonly L>S, is delineated by quartz, feldspars, biotite, and microcline augen. Variations in fabric orientation suggest folding by the D3 Manitouwadge synform implying that, like the Nama Creek pluton, the intrusion is pre- to syn-D2.

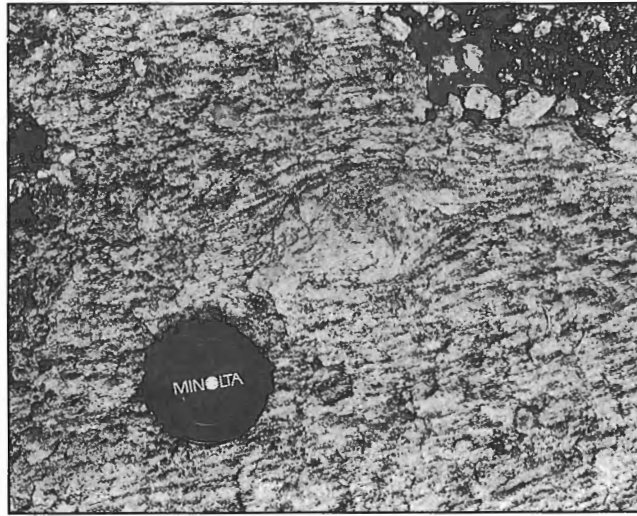


**Figure 4.** K-feldspar megacrystic granitoid of the Loken Lake intrusion in the inner area of the Manitouwadge synform. The strong mineral lineation is partly defined by microcline augen; in this case delta-tails indicate apparent sinistral rotation.



### *Inner Manitouwadge synform, Dead Lake suite*

Within the Manitouwadge synform, synvolcanic foliated quartz-rich tonalite (Zaleski et al., 1994) grades inward to more potassic rocks. In general, although the more potassic rocks are texturally and compositionally similar to the tonalite, it is not clear in outcrop whether they are comagmatic with synvolcanic rocks or a different and possibly younger intrusion. At least two continuous zones of mafic rocks can be mapped within the synform (Fig. 2) corresponding to zones of high variable aeromagnetic relief (Fig. 3 in Peterson and Zaleski, 1994a). These rocks, here called the Dead Lake suite, comprise a complex association of interleaved foliated gabbro, diorite, and layered mafic to intermediate rocks of probable supracrustal origin (Fig. 5-7).

The Dead Lake suite includes a distinctive group of strongly magnetic rocks characterized by hornblende-magnetite± plagioclase±garnet±clinopyroxene±sulphide minerals with variable amounts of quartz (minor to 50%), commonly in eyes or lenticules. The rocks are usually fine to medium grained and homogeneous, at hand-sample scale. However, in many cases, thin layering (1-5 cm) and grading, interpreted as modified bedding, is defined by variations in grain size and mineral abundances (Fig. 5). Locally, these are associated with magnetite-bearing quartzites (metachert?) and mafic metavolcanic rocks with garnet-cummingtonite(?) concentrated in interconnected ganglions (Fig. 6). An origin as metamorphosed and digested (by intrusion) ferruginous chert (G. Stott, Ontario Geological Survey, pers. comm., 1994) and iron-formation (H. Lockwood, Noranda Inc., pers. comm., 1994) has been proposed.

The Dead Lake suite is intruded by multiphase tonalite, granite and pegmatite-aplite. At least some of the tonalite (Fig. 7) is similar to the synvolcanic quartz-rich tonalite that forms the outer margin of the intrusive centre of the Manitouwadge synform. However, most tonalites in this area differ from those of the outer margin in their higher content of mafic minerals, including hornblende. Some of the hornblende, coarse grained (0.5 to 1 cm), randomly to moderately oriented poikiloblasts, appears secondary.

The relationship of the Dead Lake suite to the main supracrustal assemblage is problematic. The two zones of the suite are indistinguishable and may represent a structural repetition. They are similar to mafic rocks elsewhere in the Manitouwadge belt, especially garnetiferous mafic rocks, but the abundance of iron-formation and related rocks implied by the volume of hornblende-magnetite-garnet assemblages is unusual. It is possible that the Dead Lake suite represents another refolded 'keel' of a D2 fold, analogous to that proposed for the orthoamphibole-cordierite-garnet rocks east of Thompson Lake.

### WAWA-QUETICO BOUNDARY

The northern part of the Manitouwadge belt, in the vicinity of the Blackman Lake and Jim Lake folds, comprises foliated diorite, gabbro and thinly layered, fine- to medium-grained, mafic to intermediate metavolcanic rocks. The diorite and

gabbro may be recrystallized homogeneous volcanic or sub-volcanic rocks. These rocks are commonly strongly magnetic and contain minor interleaved iron-formation (Fig. 2). The easternmost exposure of orthoamphibole-garnet gneiss on the northern limb of the Manitouwadge synform lies 2 km north of Straight Lake and is associated with a new find (Paul Degagne, Noranda Inc., pers. comm., 1994) of sphalerite-bearing iron-formation. To the north, the Jim Lake synform is defined by mappable zones of screens and inclusion

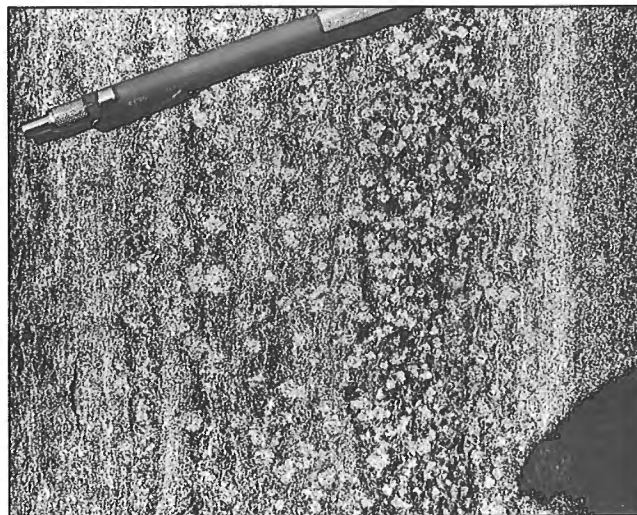


**Figure 5.** Layering in the Dead Lake suite defined by garnet, magnetite, hornblende and plagioclase abundance. The light-coloured spots are plagioclase porphyroblasts riddled with magnetite and garnet inclusions.

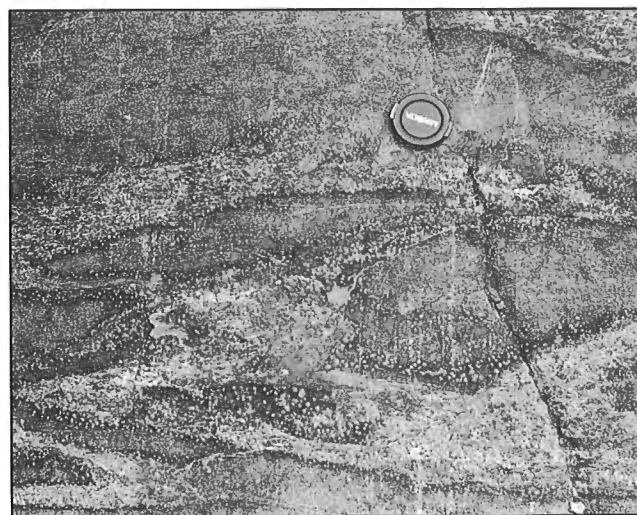


**Figure 6.** Mafic metavolcanic rocks, Dead Lake suite; garnet-cummingtonite(?) in interconnected quartz-rich enclaves (light-coloured) suggest metasomatic alteration. Note the darker hornblende-rich selvages and decreasing garnet abundance and grain size toward the interior of mafic enclaves.

swarms of mafic to intermediate rocks in foliated tonalite and pegmatite (Fig. 8, 9). Locally, rotated mafic to intermediate blocks (with discordant foliation trends) in an intrusive matrix resemble agmatite or intrusion breccia.

The Quetico subprovince to the north is characterized by migmatitic metagreywackes and biotite schists, compositionally layered (typically 2-50 cm) and locally with pelitic to psammitic grading (Fig. 10). Pelitic layers commonly contain garnet, and less commonly, sillimanite. The metasedimentary rocks contain abundant migmatitic segregations including

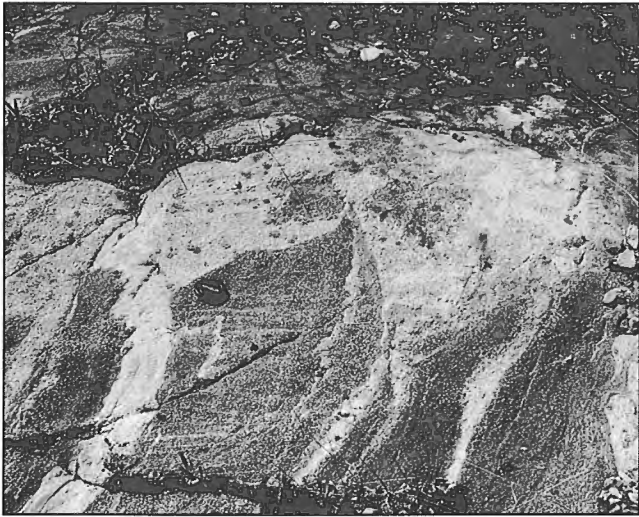


**Figure 7.** Hornblende-garnet-magnetite rocks (dark) of the Dead Lake suite intruded by foliated tonalite.

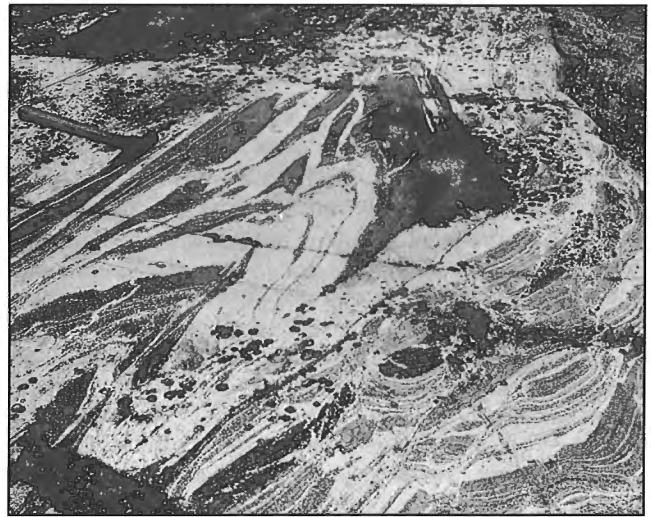


**Figure 9.** Interleaved folded and sheared tonalite and mafic rocks (metavolcanic?) near the hinge of the Jim Lake synform.

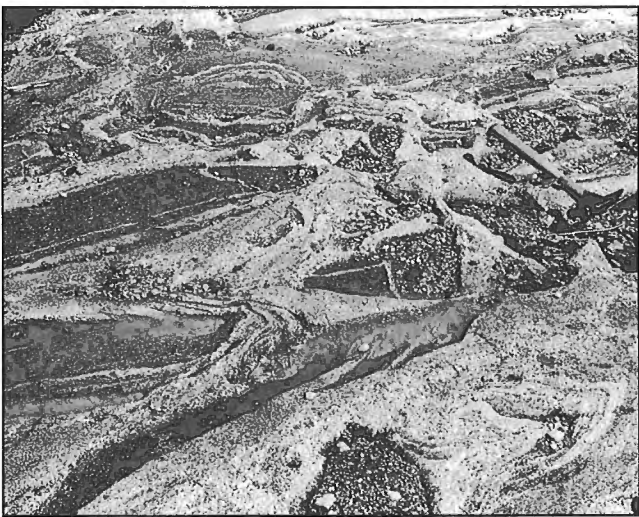


**Figure 8.** Mafic to intermediate rocks, interpreted as metavolcanic, form blocky inclusions in foliated tonalite on the northern limb of the Jim Lake synform. The tonalite truncates layering and foliation in the inclusions. The inclusions are strongly magnetic, containing hornblende, plagioclase and magnetite.



**Figure 10.** Folded contact (modified bedding) in Quetico metasedimentary rocks between schist containing coarse grained garnet (bottom) and fine grained more quartzofeldspathic layers.

Metasedimentary rocks similar to those in the Quetico subprovince are also present along the southern limb of the Manitowadge synform, coring the D2 'Manitouwadge syncline' (see above, Fig. 2). The main differences are in the lower metamorphic grade and the absence of migmatitic segregations in the rocks of the southern limb. Locally, the Manitowadge metagreywackes contain quartz- and plagioclase-crystal clasts, evidence for a volcanogenic component. The Manitowadge metasedimentary rocks are interpreted to be involved in map-scale D2 folds and the dominant foliation is ascribed to a D2 axial-planar fabric.

## GEOCHRONOLOGY

This section is a brief progress report of data available from our ongoing geochronological studies. U-Pb analyses of zircons extracted from felsic volcanic and subvolcanic rocks of the Manitowadge belt have yielded ages of  $2722 \pm 2$  Ma,  $2720 \pm 3$  Ma (Zaleski et al., 1994a) and  $2720 \pm 2$  Ma (Davis et al., 1994). We have attempted to bracket deformation by sampling dykes showing timing relationships relative to various generations of tectonic fabrics and structures. The samples include: pre- to syn-D1 pegmatite, and syn-D2 and syn-D3 tonalite dykes. We have had limited success at dating these intrusions because, either they did not contain zircon, or the zircon was highly fractured and vulnerable to secondary Pb loss. The intrusions do contain monazite, apparently of igneous morphology, analyzed in the expectation that it would give primary crystallization ages. Monazites from the syn-D1 pegmatite and the syn-D2 tonalite dyke were concordant or nearly so, and gave the same age (within error) of  $2669 \pm 3$  Ma and  $2671 \pm 3$  Ma (Zaleski et al., 1994), respectively, just younger than the age of  $2675 \pm 1$  Ma reported for metamorphic monazite from the Geco mine (Davis et al., 1994). Four

monazite fractions from the syn-D3 tonalite dike gave a scatter of discordant ages. Given the results, we regard the monazite ages from the syn-D1 and D2 intrusions as probably of secondary origin, despite their igneous morphology and near-concordance. They may record metamorphic crystallization or isotopic reequilibration during protracted cooling. We are continuing our efforts to extract zircon from syntectonic dykes.

From the larger plutonic bodies, only a sample of the K-feldspar porphyritic Nama Creek pluton has been processed; a U-Pb zircon age of  $2680 \pm 3$  Ma places a maximum limit on D2 deformation.

A sample of metagreywacke from the southern limb of the Manitowadge synform (3 km north of Manitowadge, Fig. 2; see Fig. 4 in Zaleski and Peterson, 1993a for an outcrop photograph), yielded concordant or slightly discordant analyses of detrital zircons ranging in age from  $2719 \pm 2$  Ma to  $2679 \pm 11$  Ma (Fig. 13). The youngest zircon, together with another grain of  $2692 \pm 1$  Ma, provides a maximum limit on deposition of 2693 Ma, at least 25 Ma younger than the age of felsic rocks to the north and south. Several zircons cluster about 2700 Ma, an age not known elsewhere in the Manitowadge belt. The oldest zircon of  $2719 \pm 2$  Ma could be derived from local volcanic rocks, which would imply their exposure at the time of sedimentation.

## INTERPRETATION

Metagreywackes in the Manitowadge belt are correlative with those in the Quetico subprovince, on the basis of: 1) lithological similarity, and 2) involvement of Quetico rocks in map-scale D3 folds, suggesting that they originally extended farther south. Zircon provenance studies on Quetico



**Figure 11.** Quetico metasedimentary rocks south of the Jim Lake synform; a pelitic layer has abundant tonalitic leucosome defining eye-shaped folds. Axial planes and biotite schistosity are oblique to the dominant layering.

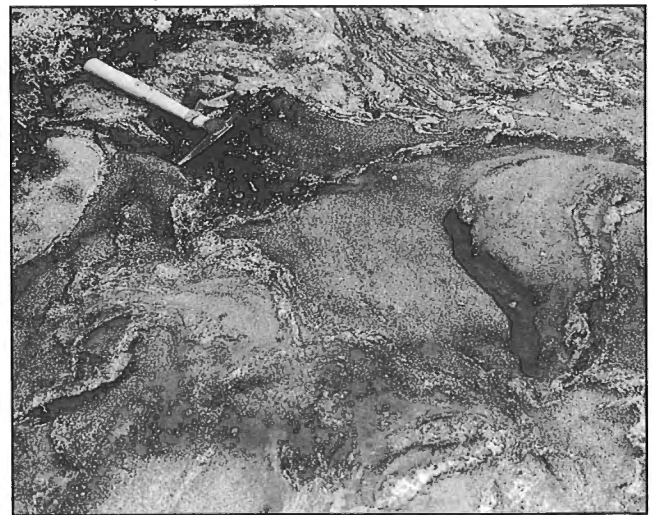


**Figure 12.** Quetico metasedimentary rocks south of the Jim Lake synform. Thin iron-formation (e.g., lower left along from the hammer pick) highly contorted in a migmatitic garnet-biotite schist.

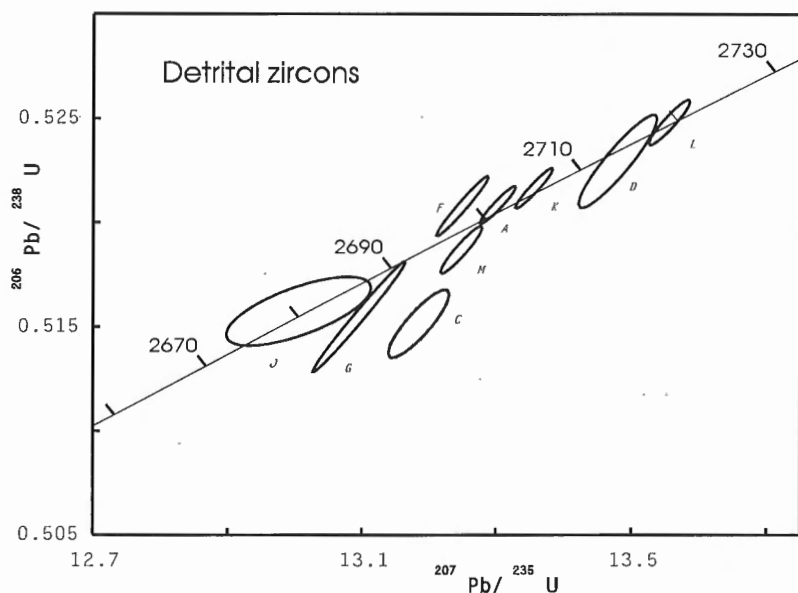


**Figure 13.**

*U-Pb Concordia diagram showing analyses of detrital zircons from Manitowadge meta-sedimentary rocks. All analyses are from single abraded crystals, except 'A' which represents a fraction of about 20 grains. The maximum age of deposition is constrained to 2693 Ma by the two youngest grains.*

metasedimentary rocks have established age brackets of circa 2700 to 2688 Ma (Percival and Sullivan, 1988; Davis et al., 1990), somewhat older than those of the Manitowadge meta-greywackes, and zircons older than 2720 Ma were not found in our sample. However, the Quetico studies were done at least 200 km to the west, and source areas and timing of sedimentation could be expected to vary.

The position of metasedimentary rocks on the southern limb of the Manitowadge synform is most easily explained by a D2 fold, the 'Manitouwadge syncline'. The axial trace lies within the metasedimentary rocks, and repeats the older metavolcanic sequence to the north and south (Fig. 2). Field evidence is inconclusive, but the 25 Ma age difference between volcanic and sedimentary sequences suggests that deposition post-dated D1 deformation; in this case, the contact would be an unconformity or a fault with metasedimentary rocks emplaced during or prior to D2. Based on this interpretation, the maximum age limit on sedimentation of 2693 Ma also provides a minimum age limit on D1 deformation, hence, bracketed between 2720 Ma (volcanism) and 2693 Ma. The presence of straight gneiss (annealed mylonite) on D1 thrust faults indicates ductile deformation and somewhat elevated temperatures. Two post-D1 pre-D2 temperature-time paths are possible for the Manitowadge belt (Fig. 14): one assuming erosion and unconformable deposition of sedimentary rocks, the other consistent with tectonic emplacement of an allochthonous sequence by pre- or syn-D2 faulting. Our observations suggest that the two subprovinces experienced similar deformation paths since D2. In the Manitowadge belt, regional metamorphism was broadly synchronous with D2 deformation (Zaleski and Peterson, 1993a, Zaleski et al., 1994). The timing of D2 deformation is constrained by the  $2680 \pm 3$  Ma age of the pre- to syn-D2 Nama Creek pluton, and magmatic activity could have contributed to metamorphic heating. The ages of younger events are poorly constrained. Metamorphic monazite ages, ranging from 2675 Ma to 2669 Ma could record either near-peak metamorphism or prolonged cooling of the Manitowadge

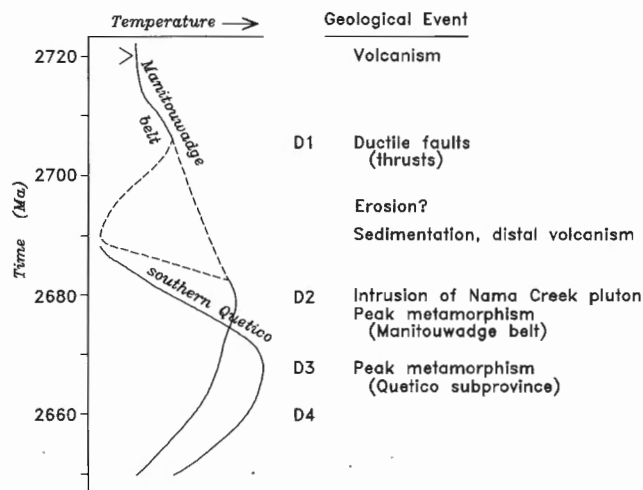


**Figure 14.** *Temperature-time plot showing relationships between the deformation sequence and metamorphism in the Manitowadge belt and the Quetico subprovince. The dashed line shows alternative paths for the Manitowadge belt assuming either, unconformable deposition of sedimentary rocks or, emplacement by early faulting.*

belt. In the Quetico subprovince, field observations indicate that peak metamorphism and migmatization were synchronous with progressive deformation and the map-scale folds (D3) near the boundary (Peterson and Zaleski, 1994a). Peak metamorphism in the Quetico could have been coeval with granitic magmatism at 2670-2650 Ma (Percival, 1989), consistent with diachronous development of peak metamorphism between the Quetico and Wawa subprovinces.

The Wawa-Quetico boundary in the Manitowadge area is transitional on structural and lithological criteria. Firstly, there is a gradational change to the south, from dominantly east-west structural trends, to map-scale folds with broader hinge regions; secondly, Manitowadge and Quetico

metasedimentary rocks are indistinguishable. A transitional subprovince boundary is not unique to the Manitouwadge area. Similar relationships have been described between the Quetico subprovince and Coutchiching metasedimentary rocks in the Rainy Lake area of the Wabigoon subprovince (Davis et al., 1989), and Kehlenbeck (1985) considered the Beardmore-Geraldton belt to be a structural and lithological transition zone between the Quetico and Wabigoon subprovinces. The thesis that the Beardmore-Geraldton belt developed through deformation involving the margins of both subprovinces (Kehlenbeck, 1985) is equally applicable to the Wawa-Quetico boundary and the Manitouwadge greenstone belt.

## ACKNOWLEDGMENTS

Noranda Minerals Inc. (Geco Division), Granges Inc., Minnova Inc. and Al Turner contributed to this project by providing access to unpublished maps and reports. Special thanks go to Hugh Lockwood, Noranda Minerals Inc., for discussions, ideas, and all around support of our efforts during the field season. The geochronology sample of the Nama Creek pluton was collected by Rob Reukl and Jody Hache. We benefited from field trips and/or discussions with Mark Smyk, Bernie Schnieders, Andy Fyon and Greg Stott, Ontario Geological Survey; Kevin Heather, Geological Survey of Canada; and Paul Degagne, Hugh Lockwood and John Londry, Noranda Minerals Inc. Field work was greatly assisted by David Copeland. The manuscript was improved by comments from Ken Card and John Percival.

## REFERENCES

- Card, K.D. and Ciesielski, A.**  
1986: Subdivisions of the Superior Province of the Canadian Shield; *Geoscience Canada*, v. 13, p. 5-13.
- Corfu, F. and Muir, T.L.**  
1989a: The Hemlo-Heron Bay greenstone belt and Hemlo Au-Mo deposit, Superior province, Ontario, Canada 1. Sequence of igneous activity determined by zircon U-Pb geochronology; *Chemical Geology (Isotope Geology Section)*, v. 79, p. 183-200.  
1989b: The Hemlo-Heron Bay greenstone belt and Hemlo Au-Mo deposit, Superior province, Ontario, Canada 2. Timing of metamorphism, alteration and Au mineralization from titanite, rutile and monazite U-Pb geochronology; *Chemical Geology (Isotope Geology Section)*, v. 79, p. 201-223.
- Davis, D.W., Pezzutto, F., and Ojakangas, R.W.**  
1990: The age and provenance of metasedimentary rocks in the Quetico subprovince, Ontario, from single zircon analyses: implications for Archean sedimentation and tectonics in the Superior Province; *Earth and Planetary Science Letters*, v. 99, p. 195-205.
- Davis, D.W., Poulsen, K.H., and Kamo, S.L.**  
1989: New insights into Archean crustal development from geochronology in the Rainy Lake area, Superior Province, Canada; *Journal of Geology*, v. 97, p. 379-398.
- Davis, D.W., Schandl, E.S., and Wasteneys, H.A.**  
1994: U-Pb dating of minerals in alteration halos of Superior province massive sulphide deposits: syngensis vs. metamorphism; *Contributions to Mineralogy and Petrology*, v. 115, p. 427-437.
- Geological Survey of Canada**  
1993a: Total field aeromagnetic map of the Manitouwadge greenstone belt; Geological Survey of Canada, Open File 2754, scale 1:25 000.  
1993b: Shaded relief aeromagnetic map of the Manitouwadge greenstone belt; Geological Survey of Canada Open File 2755, scale 1:25 000.
- Kehlenbeck, M.M.**  
1985: Folds and folding in the Beardmore-Geraldton fold belt; *Canadian Journal of Earth Sciences*, v. 23, p. 158-171.  
1988: A fault-bounded outlier of Archean clastic rocks near Thunder Bay, Ontario; *Canadian Journal of Earth Sciences*, v. 25, p. 152-157.
- Percival, J.A.**  
1989: A regional perspective of the Quetico metasedimentary belt, Superior Province, Canada; *Canadian Journal of Earth Sciences*, v. 26, p. 677-693.
- Percival, J.A. and Sullivan, R.W.**  
1988: Age constraints on the Quetico belt, Superior Province, Ontario; in *Radiogenic and Isotope Studies: Report 2*; Geological Survey of Canada, Paper 88-2, p. 97-107.
- Percival, J.A. and Williams, H.R.**  
1989: The late Archean Quetico accretionary complex, Superior Province, Canada; *Geology* v. 17, p. 23-25.
- Peterson, V.L. and Zaleski, E.**  
1994a: Structure and tectonics of the Manitouwadge greenstone belt and Wawa-Quetico subprovince boundary, Superior Province, northwestern Ontario; in *Current Research 1994-C*; Geological Survey of Canada, p. 237-247.  
1994b: Structural history of the Archean Manitouwadge greenstone belt, southwestern Superior Province: implications for the setting of mineralization and tectonic evolution (abstract); *Geological Society of America, Abstracts with Programs* v. 26, p. A50.
- Robinson, P.C.**  
1979: *Geology and evolution of the Manitouwadge migmatite belt, Ontario, Canada*; PhD. thesis, University of Western Ontario, London, Ontario, 367 p.
- Schandl, E.S., Davis, D.W., Gorton, M.P., and Wasteneys, H.A.**  
1991: Geochronology of hydrothermal alteration around volcanic-hosted massive sulphide deposits in the Superior Province; Ontario Geological Survey, Miscellaneous Paper 156, p. 105-120.
- Stockwell, C.H.**  
1964: Fourth report on structural provinces, orogenies and time-classification of rocks of the Canadian Precambrian Shield; in *Age Determinations and Geological Studies, Part II*; Geological Survey of Canada, Paper 64-17, p. 1-21.  
1970: *Geology of the Canadian Shield, introduction*; in *Geology and Economic Minerals of Canada, Part A*; (ed.) R.J.W. Douglas; Geological Survey of Canada, Economic Geology Report 1, p. 44-54.
- Touborg, J.F.**  
1973: Structural and stratigraphical analysis of the Geco sulphide deposit in Manitouwadge, northwestern Ontario (abstract); 19th Annual Institute on Lake Superior Geology, p. 38-39.
- Williams, H.R.**  
1991: Quetico subprovince; in *Geology of Ontario*; Ontario Geological Survey, Special Volume 4(1), p. 383-403.
- Williams, H.R. and Breaks, F.W.**  
1989: Geological studies in the Manitouwadge-Hornpayne area; Ontario Geological Survey, Miscellaneous Paper 146, p. 79-91.  
1990a: *Geology of the Manitouwadge-Hornpayne area*; Ontario Geological Survey, Open File Map 142, scale 1:50 000.  
1990b: Geological studies in the Manitouwadge-Hornpayne area; Ontario Geological Survey, Miscellaneous Paper 151, p. 41-47.
- Williams, H.R., Stott, G.M., Heather, K.B., Muir, T.L., and Sage, R.P.**  
1991: Wawa subprovince; in *Geology of Ontario*; Ontario Geological Survey, Special Volume 4(1), p. 485-539.
- Zaleski, E., Peterson, V.L., and van Breemen, O.**  
1994: Geological, geochemical and age constraints on base metal mineralization in the Manitouwadge greenstone belt, northwestern Ontario; in *Current Research 1994-C*; Geological Survey of Canada, p. 225-235.
- Zaleski, E. and Peterson, V.L.**  
1993a: Lithotectonic setting of mineralization in the Manitouwadge greenstone belt, Ontario: preliminary results; in *Current Research, Part C*; Geological Survey of Canada, Paper 93-1C, p. 307-317.  
1993b: *Geology of the Manitouwadge greenstone belt*; Geological Survey of Canada, Open File 2753, scale 1:25 000.

# The Auyuittuq carving stone study project, eastern Baffin Island, Northwest Territories: a geological report

I. Ermanovics

Continental Geoscience Division

*Ermanovics, I., 1995: The Auyuittuq carving stone study project, eastern Baffin Island, Northwest Territories: a geological report; in Current Research 1995-C; Geological Survey of Canada, p. 45-51.*

---

**Abstract:** Deposits of potential carving stone in south and eastern Baffin Island include mainly serpentinitized ultramafic rocks (soapstone) and marble. A search of the published and unpublished geological literature revealed no reports of carving stone deposits within Auyuittuq Park or within a few kilometres of its boundary. Assessment of the principally high-grade Proterozoic terrane of the Cumberland batholithic complex, which underlies the park, indicated a low potential for carving stone within the park compared to other areas of Baffin Island. Fieldwork in 1994 bore out this prediction.

**Résumé :** Des gisements de pierre à sculpter potentielle dans le sud et l'est de l'île de Baffin comprennent principalement des roches ultramafiques serpentinisées (stéatite) et du marbre. Une recherche portant sur la documentation géologique publiée et non publiée n'a révélé aucune mention de gisement de pierre à sculpter dans le parc Auyuittuq ou dans un rayon de quelques kilomètres de ses limites. Une évaluation du terrane fortement métamorphisé et principalement protérozoïque du complexe batholithique de Cumberland, sur lequel s'étend le parc, indiquait un faible potentiel de pierre à sculpter dans les limites du parc comparativement à d'autres secteurs de l'île de Baffin. La campagne 1994 sur le terrain a confirmé cette prédiction.

## BACKGROUND

The Nunavut Land Claims Final Agreement provides that, prior to the establishment of a National Park in the Nunavut Settlement Area, Parks Canada shall undertake "...a detailed study to determine the location, the extent and quality of any deposit of carving stone within the proposed boundaries of the Park." (part of Clause 19.9.7, p. 129, Inuit Ratification Committee, 1992). Parks Canada accordingly approached the author in January 1994 with a draft protocol outlining the terms of reference by which assessment of the carving stone potential in the Auyuittuq Park reserve could proceed (B. Tyrchniewicz, Terms of reference of the Auyuittuq carving stone study project; Environment Canada, Parks Service, Iqaluit, unpublished correspondence with I. Ermanovics, January 1994). The present report summarizes

two unpublished geological accounts submitted in 1994 to the Land Claims Implementation Co-ordinator of Parks Canada in Iqaluit, NWT, regarding deposits of carving stone within Auyuittuq National Park (I. Ermanovics, two unpublished geological reports to B. Tyrchniewicz, Land Claims Implementation Co-ordinator, Parks Canada, Iqaluit, N.W.T., April 1994, 11 p., and September 1994, 7 p.).

### The study area

The park (Auyuittuq, land that never melts) essentially surrounds the Penny ice cap on southeastern Baffin Island (Fig. 1). Park boundaries are indicated on NTS maps 16M and L, 26I, J, K, N, O and P, and 27A and B (the pre-1992 boundary). Additionally, a more current document shows modified park boundaries of a smaller potential park area

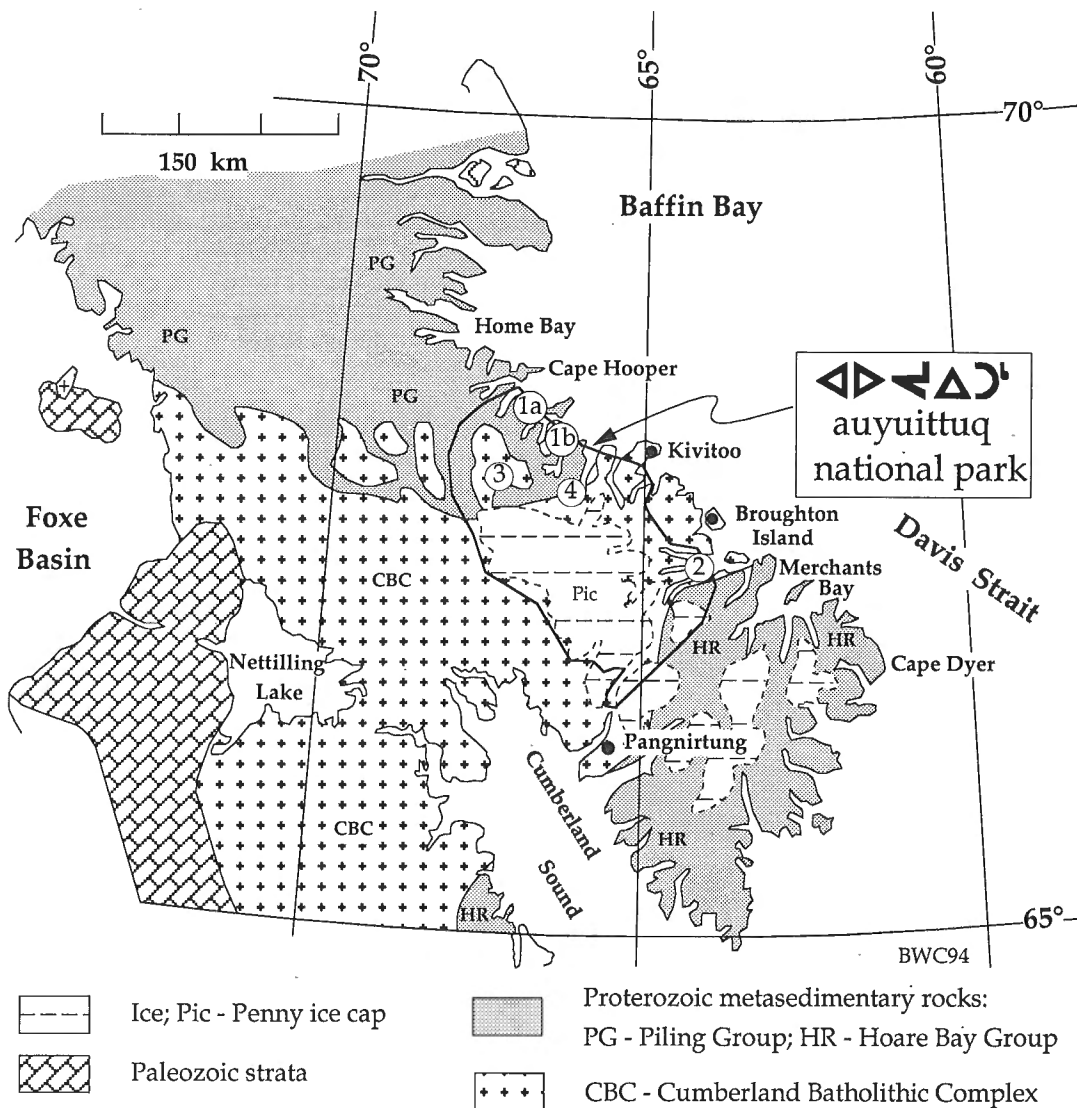


**Figure 1.** Southeastern Baffin Island showing some of the lithotectonic elements of the Baffin orogen (after Jackson et al., 1990) and the approximate pre-1992 boundary of the Auyuittuq National Park. Numbers refer to the study areas discussed in text.

(Environment Canada Parks, 1992). The pre-1992 boundaries were used in delineating the park area for purposes of the present study (Fig. 2 in I. Ermanovics, unpublished report to B. Tyrchniewicz, Land Claims Implementation Co-ordinator, Parks Canada, Iqaluit, N.W.T., April 1994, 11 p.).

### *Terms of reference of the study*

The terms of reference stipulated a two-phase approach to the work. Phase 1 comprised identification of potential for the occurrence of carving stone and Phase 2 involved field assessment of any carving stone identified in Phase 1. Phase 1 entailed the collation of map information derived from published and unpublished geological information and location of proven and potential carving stone deposits. Significantly, Phase 1 included consultation with residents of Broughton Island (Fig. 1, 2) as well as special interest groups to explain the geological information gathered and to solicit comment and additional information based on local knowledge. The need for Phase 2 field work became evident when it was agreed that the geological database might be inadequate for the identification of carving stone deposits.

### *Definition of carving stone*

The Nunavut Final Agreement defines carving stone as "utkuhighak and hananguagahaq, which means serpentine, argillite and soapstone in the Nunavut Settlement Area where those substances are suitable for use for carving purposes." (p. 2, in B. Tyrchniewicz, Terms of reference of the Auyuittuq carving stone study project; Environment Canada, Parks Service, Iqaluit, unpublished correspondence with I. Ermanovics, January 1994). In practical terms this definition required field identification of ultramafic rocks (protoliths of serpentinite and soapstone), marble, serpentine marble (verde antique) and low-grade metamorphic mudstone (argillite).

## **PHASE 1: GEOLOGICAL ASSESSMENT**

### *Sources of information*

The geology and the interpretation of it for the park area is based on reports by Jackson and Taylor (1972), Jackson and Morgan (1978), Jackson et al. (1990) and on maps by Henderson (1985) and by G.D. Jackson (in prep.). The



**Figure 2.** Aerial view of Broughton Island community; sea ice fills part of the bay at left. Photographed August 25, 1994. GSC 1994-740A.



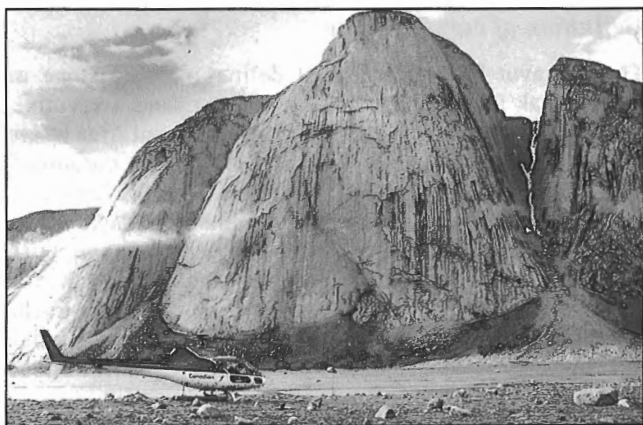


**Figure 3.** Typical exposure (about 1300 m high) of granite of the Cumberland batholithic complex; vertical bands are surface discoloration. North Pangnirtung Fiord, view westward from 64°41'W, 66°16'N. GSC 1994 - 740B.

condition of reported soapstone localities and the state of alteration of ultramafic rock in the vicinity of the park area (none is known within the park reserve) are given by Tippett (1980), Gibbins (1982), and I. Ermanovics (unpublished report for M. Cunningham, Minerals Policy Advisor, GNWT, Yellowknife, N.W.T., October 13, 1992, 10 p.).

An open file map of the geology of the park area at a scale of 1:250 000 is in preparation by G.D. Jackson. His work and that of Henderson (1985) to the immediate north of the park show that ultramafic rocks and of course marble are more likely to be preserved in areas of supracrustal rocks than in plutonic rocks. Thus until a geological map of the park is published, an interim geological information map was prepared at the same scale, showing the few areas of metasedimentary rocks and amphibolite exposed in the park (I. Ermanovics, unpublished report to B. Tychniewicz, Land Claims Implementation Co-ordinator, Parks Canada, Iqaluit, N.W.T., April 1994, 11 p.). This map aided consultation with residents of Broughton Island and special interest groups and served as an incentive for them to contribute local knowledge to the map.

### Geological summary

Rocks underlying the park and its surrounds comprise plutonic and high-grade metasedimentary units of the ca. 1.8-1.9 Ga Baffin Orogen. In this area, mainly granitic rocks (Fig. 3) of the Cumberland batholithic complex intrude higher level, dominantly metasedimentary units of the lower Proterozoic Piling, Hoare Bay, and Lake Harbour groups (Jackson and Taylor, 1972).

The Piling and Hoare Bay groups, respectively northwest and east of the park, record periods of early Proterozoic sedimentation at ca. 2.0 Ga. Limestone, mudstone, quartz-rich sandstone, and muddy quartz-feldspar sandstone (greywacke) are the predominant shelf and basin sedimentary rocks of both groups. These were deposited as a cover on, and in part transported onto, a basement composed of Archean

rocks. (Jackson and Taylor, 1972; Henderson, 1985). During a subsequent continental collision event (Jackson and Hegner, 1991), the Archean basement and its Proterozoic sedimentary cover were deformed and metamorphosed and intruded by voluminous granitic rocks of the Cumberland batholithic complex. The sedimentary rocks were metamorphosed to amphibolite and granulite facies rocks (Jackson and Morgan, 1978), veined by granitic magmas, intercalated with basement rocks and subjected to anatexis. Metamorphism was too high to allow preservation of argillite, forming rusty-weathering schist and gneiss instead. The intensity of metamorphism and granitization of the metasedimentary rocks increases toward the Cumberland batholithic complex which ultimately exposes mainly granitic rocks and only sparse remnants of a granitized sedimentary rock cover.

Early phases of the orogenic activity included mafic and ultramafic magmas emplaced in the metasedimentary rocks and provided the protolith for serpentinite and soapstone. Large exposures of these rocks occur west of Dewar Lakes, 150 km west of Home Bay (Fig. 1), where the metasedimentary rocks of the Piling Group are relatively unaffected by the Cumberland batholithic complex (Jackson and Taylor, 1972; Tippett, 1980). Small, isolated, metre-scale bodies in zones up to 1 km long occur in the Merchant's Bay area (80 km southeast of Broughton Island, Fig. 1), invariably located in metasedimentary rocks (Jackson, pers. comm., 1992; I. Ermanovics, unpublished report for M. Cunningham, Minerals Policy Advisor, GNWT, Yellowknife, N.W.T., October 13, 1992, 10 p.). Elsewhere they occur peripherally to the park reserve, also associated with smaller supracrustal rock remnants, but none is known within the park.

Detailed examination of a number of the smaller ultramafic rock occurrences within the Cumberland batholithic complex (Gibbins, 1982; I. Ermanovics, unpublished report for M. Cunningham, Minerals Policy Advisor, GNWT, Yellowknife, N.W.T., October 13, 1992, 10 p.) and of the large mass west of Dewar Lakes (Tippett, 1980; Henderson et al., 1988) showed that hydration (alteration) to talc, serpentine and similar soft minerals is variable and at best poorly developed. The alteration tends to be confined to narrow fractures or is restricted to margins of the ultramafic masses, centimetres to decimetres wide, making quarrying impractical and unprofitable. Similar observations of the lack of serpentinitization of ultramafic rocks were made by Henderson (1985 and pers. comm., 1992) who, in an area of 14 000 km<sup>2</sup> adjacent to the northwestern part of the park, found no soapstone or notable serpentinitization in the sparse ultramafic rocks that were located.

In summary, the park is largely underlain by a high-temperature, deep-seated, granitic batholithic complex that would preclude good preservation of supracrustal rocks and associated ultramafic rocks. Ultramafic rocks were intruded into supracrustal rocks early in the tectonic history of the area and the subsequent formation of the batholithic complex has simply left little trace of these early units. However, even the few isolated occurrences of ultramafic rocks that do occur marginal to the park reserve did not undergo the hydration required for formation of soapstone. Marble, an increasingly popular carving stone, not included in the terms of reference

as carving stone, is also absent from the park. In this respect, the geology of the park reserve differs from the geological environments to the northwest and south which are more favourable for the formation of soapstone and marble. Another practical consideration is the rugged terrain in parts of the park area, where quarrying and procurement of stone could be difficult, hazardous and uneconomic.

### **Conclusions of Phase 1**

The Auyuittuq National Park area contains no known deposits of carving stone. Additionally, the terrain in general, and within reach of Broughton Island and Pangnirtung communities in particular, offers only a low potential for such deposits to be detected with respect to other areas of Baffin Island (I. Ermanovics, unpublished report to B. Tyrchniewicz, Land Claims Implementation Co-ordinator, Parks Canada, Iqaluit, NWT, April 1994, 11 p.). The reason for this relatively low potential rests with the observation that supracrustal rocks, considered to be the main hosts of marble, argillite, ultramafic rock and its derivative, soapstone, are only sparsely present in the park but are more plentiful outside it (Jackson et al., 1990). Thus the chances of finding carving stone are correspondingly greater outside the park.

## **PHASE 2: GEOLOGICAL FIELDWORK VERIFICATION**

Three areas (areas 1 to 3, Fig. 1) were identified as being underlain by metasedimentary rock within the park, representing remnants of a once extensive cover of supracrustal rocks (I. Ermanovics, unpublished report to B. Tyrchniewicz, Land Claims Implementation Co-ordinator, Parks Canada, Iqaluit, NWT, April 1994, 11 p.). Areas 1 and 2 (Fig. 1) were investigated to verify the conclusions of Phase 1. These offered reasonable access from the sea. Area 3 (Fig. 1), being relatively inaccessible, was considered too costly to survey in detail and hence was not investigated. Additionally, two specific sites (4a and 4b), identified by Broughton Island residents, were included in the field work.

### **Method of investigation**

The total area of rock identified within the park was 40 km<sup>2</sup> comprising 10 separate sites (see Appendix). The extent and strike of these rock units was confirmed in the field at each site and the units were then traversed either on foot or by helicopter at about 10-m altitude at a line spacing of about 100 m. Landings were effected to establish rock types and to check whenever the rock unit changed appearance. Outcrops were tracked to the edge of the fresh snow cover at elevations of about 400 to 600 m. The rise of land at the study sites is generally too steep to be walkable so that shoreline exposures or outcrops on small plateaus commonly provide the only places where direct observations could be made.

Shoreline outcrops in particular were examined in detail. Additionally, sections of shoreline were walked in the hope of finding soapstone or marble as local, glacially transported debris, or rock fall which might reflect local bedrock sources.

### **Results**

Areas 1a and 1b (Fig. 1) each represent about 10 km<sup>2</sup> of terrain of which about 60 per cent is accessible from the shore. The terrain is underlain by pelitic and psammitic schists and gneisses. The rocks are layered, dip moderately to steeply and contain garnet, muscovite, biotite and sillimanite in addition to quartz and feldspar. Some thin layers of metapelite weather rusty to ochre locally which can discolour the underlying rocks for several hundreds of metres in spectacular fashion. Weakly foliated granitic rocks, occasionally garnet-bearing, have intruded or are intercalated with the metasedimentary rocks and constitute up to 50 per cent of some outcrops. The rocks in areas 1a and 1b are correlated with more extensive units in the Home Bay area (Fig. 1) where they are assigned to the Piling Group (Henderson, 1985). However, the metasedimentary rocks of the study area lack marble which is locally present in the Piling rocks in Home Bay suggesting that rocks of the study area represent the upper metasediments (turbiditic wackes) of the group in which marble is only sparsely present (Jackson and Taylor, 1972; Henderson, 1985). Marble, ultramafic rock and its derivative, soapstone, were not found.

Area 2 (Fig. 1) contains eight smaller occurrences (Appendix), each about 2 km<sup>2</sup>, composed of elongate rafts of layered gneiss in granitic rock. The layers are composed of quartzofeldspathic rock, rusty mafic rock, granitic injections and metre-scale pods of amphibolite all highly metamorphosed, containing garnet, muscovite, biotite, hornblende, pyroxene, quartz and feldspar. The layered gneisses, correlated with Hoare Bay Group (Jackson et al., 1990), are readily distinguished from the granites by steeply oriented, variegated layering and commonly by rusty and yellow-ochre discoloration. Although most of the layered rocks are exposed in cliff sections up to 600 m high and are thus inaccessible, some are exposed near the shorelines and on elevated plateaus. Locally, black, fresh diabase dykes have intruded the gneisses and granites. Marble, soapstone or other ultramafic rock was not found. A brief search of the detritus along the shorelines below some of these sites in areas 1 and 2 revealed no marble or soapstone.

The two sites of area 4, identified from community hearsay information, comprise "black rock" on extremely steep rock faces at about 600 to 700 m elevation. Freshly fallen snow made landing and walking in the broken rock debris hazardous. One site was found to be granite covered with an 1 cm-thick black moss. Apparently water from firm snow above trickling over the rock causes moss to grow in a micro-niche (10 by 30 m), making the otherwise grey granite appear black. The other site could not be reached, but since the black rock at this locality was confined to the cliff face immediately below a v-shaped stream bed within grey granite, this rock probably is also moss-covered granite. Although the black talus immediately below the cliff face was also not

accessible, it too may be assumed to be moss covered resulting from intermittent water cascading from the hanging valley during early summer run-off. A brief search of the stream bed emanating from beneath the talus uncovered no stone other than granite.

### **Conclusion of Phase 2**

Verification of the geology and more detailed observation in areas 1a and 1b confirmed the absence of marble, ultramafic rock and derived soapstone. As well, the grade of metamorphism is too high for argillite to have been preserved. Marble, not uncommon in the lower units of the Piling Group in Home Bay, is absent from the metasedimentary rocks of the study sites. This leads to the conclusion that only the upper turbiditic greywackes of the group, generally barren of marble, are exposed in the park area.

Verification of the geology and more detailed observations in area 2, south of Broughton Island, yielded similar negative results with respect to carving stone. The marble and the protoliths of soapstone are absent. Even if the protoliths were present, the high regional metamorphic grade would preclude formation of soapstone which requires hydration at low grades of metamorphism.

The sites in area 4, comprising "black rock" in southwestern Okoa Bay, were probably located correctly from the hearsay information and are superficially discoloured granite. However, even though no record exists of any stone having been recovered from here, some doubt remains because I could not investigate the area as well as I would have liked. Nevertheless, if carving stone does exist in this area it would have to be of exceptional quality to merit venturing into the southern reaches of Okoa Bay and vicinity.

### **SUMMARY**

The 1994 fieldwork confirmed the prediction, based on existing geological information, that carving stone is probably absent from the rocks within Auyuittuq National Park. The park reserve is underlain by a plutonic granitic complex and sparse remnants of metamorphosed, supra-crustal rock that constitute an environment unfavourable for the preservation of marble, ultramafic rock and its derivative, soapstone. As well, metamorphic temperatures far exceeded the threshold for preservation of argillite.

### **ACKNOWLEDGMENTS**

Operating funds for this study were provided by Parks Canada, Iqaluit. I am indebted to Betty Tyrchniewicz, Land Claims Implementation Co-ordinator, Parks Canada for assuring the timely conclusion of the study. I thank David Kooneeliusie, Parks Canada, Broughton Island for help with logistics during the fieldwork. I am indebted to Garth Jackson for geological information and interpretation used in preparing this report. I acknowledge, with thanks, reviews of the manuscript by Thomas Frisch and Marc St-Onge.

### **REFERENCES**

- Environment Canada, Parks.**  
1992: Auyuittuq National Park Map, scale 1: 250 000; taken from map showing lands identified for withdrawal according to agreement between Tungavik Federation of Nunavut and Canada.
- Gibbins, W.**  
1982: DIAND - GNWT - COOP - Soapstone Project Baffin Island 1981; unpublished report, Geology Section, Department of Indian Affairs and Northern Development, Yellowknife, NWT, 7 p.
- Henderson, J.R.**  
1985: Geology, Ekalugad Fiord-Home Bay, District of Franklin, Northwest Territories; Geological Survey of Canada, Map1606A, scale 1: 250 000.
- Henderson, J. R., Grocott, J., Henderson, M.N., Falardeau, F., and Heijke P.**  
1988: Results of fieldwork in Foxe Fold Belt near Dewar Lakes, Baffin Island, N.W.T.; in *Current Research, Part C*; Geological Survey of Canada, Paper 88-1C, p. 101-108.
- Inuit Ratification Committee**  
1992: Agreement between the Inuit of the Nunavut Settlement Area and Her Majesty in Right of Canada; Tungavik Federation of Nunavut and Department of Indian Affairs and Northern Development, Yellowknife, NWT, 229 p.
- Jackson, G.D. and Hegner, E.**  
1991: Evolution of late Archean to early Proterozoic crust based on Nd isotopic data for Baffin Island and northern Quebec and Labrador; Joint Annual Meeting, Geological Association of Canada/Mineralogical Association of Canada, Program With Abstracts, v. 16, p. A59.
- Jackson, G.D. and Morgan, W.C.**  
1978: Precambrian metamorphism on Baffin and Bylot islands; in *Metamorphism in the Canadian Shield*; Geological Survey of Canada, Paper 78-10, p. 249-267.
- Jackson, G.D. and Taylor, F.C.**  
1972: Correlation of major Aphebian rock units in the northeastern Canadian Shield; *Canadian Journal of Earth Sciences*, v. 9, p. 1659-1669.
- Jackson, G. D., Hunt, P.A., Loveridge, W.D., and Parrish, R.R.**  
1990: Reconnaissance geochronology of Baffin Island, N.W.T.; in *Radiogenic Age and Isotopic Studies, Report 3*; Geological Survey of Canada, Paper 89-2, p. 123-148.
- Tippett, C.R.**  
1980: A geological cross-section through the southern margin of the Foxe Fold Belt Baffin Island, Arctic Canada, and its relevance to the tectonic evolution of the northeastern Churchill Province; Ph.D. thesis, Queen's University, Kingston, Ontario, 490 p.

## Appendix

### Location of Study Areas

Areas 1a and 1b (Fig.1) between Brodie Bay and Nudlung Fiord, 150 km northwest of Broughton.

- 1a. The mainland shore (and 1 km inland) located 10 km south of Nadlung Island between 66°46' to 67°00'W and 68°12' to 68°17'N.
- 1b. The mainland shore (and 2 km inland), located 10 km west of Nedlukseak Island between 66°12' to 66°15'W and 68°00' to 68°05'N.

Area 2, circumscribing the junction of Maktak, Coronation and North Pangnirtung fiords located 30 to 40 km south of Broughton Island. In addition to the sites listed below, North Pangnirtung Fiord was surveyed at the level where the fiord rock walls meet the sea or the valley floor as far south as the third emergency hut at about 64°41'W, 66°16'N.

- 2a. South of Kingnelling Fiord, 3 km inland, centred at 64°10'W, 67°25'N.
- 2b. Tip of land between Maktak and Coronation fiords, centred at 64°11'W, 67°17'N.
- 2c. North side of Pangnirtung Fiord, centred at 64°20'W, 67°11'30"N.
- 2d. Five kilometres south of the mouth of North Pangnirtung Fiord, centred at 63°57'W, 67°07'N.

2e. Point of land between Coronation and North Pangnirtung fiords centred at 63°58'W, 67°16'N.

2f. Western end of island at mouth of Maktak Fiord at 64°00'W, 67°19'N.

2g. North side of Maktak Fiord centred at 64°14'W, 67°19'30"N.

2h. Near the mouth of North Pangnirtung Fiord at 63°59'45"W, 67°10'30"N.

Area 3 (Fig. 1) was not investigated (see text).

Area 4 consists of two sites of "black rock" located on a 1:250 000 scale topographic map by an anonymous resident of Broughton Island, inland from the western side of Okoa Bay (David Kooneeliusie, Parks Canada, Broughton, pers. comm., August 1994).

4a. Five kilometres inland from the western shore of Okoa Bay at 66°08'W, 67°42'45"N at an elevation of 700 m. The locality is described as black broken rock strewn from a cliff face of a hanging V-shaped valley floored by an intermittent stream.

4b. Seven kilometres inland from the western shore of Okoa Bay at 66°12'W, 67°39'30"N at an elevation of 700 m. The locality is described as flat rock above two small lakes.



# Archean and Proterozoic lithology, structure, and metamorphism in the vicinity of Ege Bay, Baffin Island, Northwest Territories<sup>1</sup>

R.J. Scammell and K.M. Bethune  
Continental Geoscience Division

*Scammell, R.J. and Bethune, K.M., 1995: Archean and Proterozoic lithology, structure, and metamorphism in the vicinity of Ege Bay, Baffin Island, Northwest Territories; in Current Research 1995-C; Geological Survey of Canada, p. 53-66.*

---

**Abstract:** Bedrock mapping and preliminary laboratory studies have provided new insights on the geological evolution of northwest Baffin Island, between the Archean Committee Orogen and the Proterozoic Foxe Fold Belt. Two greenschist to upper amphibolite facies greenstone belts near Ege Bay and Grant Suttie Bay contain 3-50 m thick, laterally continuous (>10 km), volcanic- and turbidite-hosted banded iron formations which have potential for gold mineralization. Greenstone belts record ~2.72 Ga granitic plutonism, felsic volcanism, and deformation. Gneisses bordering the greenstone belts record ~2.77 Ga plutonism and Archean deformation. These gneisses, the greenstone belts, and Proterozoic metasedimentary rocks have been affected by northwest-southeast-directed contractional strain associated with ~1.82 Ga regional metamorphism and granitic plutonism. Structural and metamorphic events are related to tectonic events associated with the ~2.7 Ga Committee Orogen, the Proterozoic Foxe Fold Belt, and possibly the late Early Proterozoic Northeast Baffin Thrust Zone.

**Résumé :** La cartographie du substratum rocheux et les études préliminaires en laboratoire ont fourni de nouvelles données sur l'évolution géologique du nord-ouest de l'île de Baffin, entre l'orogène archéen de Committee et la ceinture de plissement protérozoïque de Foxe. Deux ceintures de roches vertes du faciès des schistes verts au faciès des amphibolites supérieur, à proximité de la baie Ege et de la baie Grant Suttie, contiennent des formations ferrifères rubanées de 3-50 m d'épaisseur, continues latéralement (>10 km), encaissées dans des volcanites et des turbidites; elles présentent un potentiel de minéralisation aurifère. Les ceintures de roches vertes présentent un plutonisme granitique, un volcanisme felsique et une déformation d'environ 2,72 Ga. Les gneiss bordant les ceintures de roches vertes présentent un plutonisme d'environ 2,77 Ga et une déformation archéenne. Ces gneiss, les ceintures de roches vertes et les roches métasédimentaires du Protérozoïque ont été affectés par une déformation par contraction dans la direction nord-ouest-sud-est associée à un métamorphisme régional et à un plutonisme granitique d'environ 1,82 Ga. Les événements structuraux et métamorphiques sont liés à des événements tectoniques associés à l'orogène de Committee d'environ 2,7 Ga, à la zone de plissement protérozoïque de Foxe et, peut-être, à la zone de charriage de la fin du Protérozoïque précoce dans le nord-est de l'île de Baffin.

---

<sup>1</sup> Contribution to Canada-Northwest Territories Mineral Initiatives (1991-1996), an initiative under the Canada-Northwest Territories Economic Development Cooperation Agreement.

## INTRODUCTION

Mapping during the 1994 field season completed the field component of a three-year project on rocks near Ege Bay, north-central Baffin Island (NTS 37C, NE; Fig. 1). The aim of this mapping agreement is to provide a 1:100 000 geological map, and to assess the mineral resource potential of the map area. Important previous studies in the area include a brief report by Morgan et al. (1975), a 1:250 000 map (Morgan, 1982), and limited, detailed mapping and petrographic studies (Crawford, 1973). Previous work done under the current mapping agreement was summarized by Bethune and Scammell (1993). The present paper provides additional observations and conclusions based on mapping during 1994, and on preliminary laboratory work.

## GEOLOGICAL FRAMEWORK

A general geological framework for the map area is presented in Jackson (1966; in press), Jackson and Taylor (1972), Morgan et al. (1975), Jackson and Morgan (1978), Morgan (1982), Henderson et al. (1989), Jackson et al. (1990a, b), and Jackson and Hegner (1991). This work indicates that the map area lies between two Precambrian orogenic belts, which trend northeast across northwestern Baffin Island and adjacent Melville Peninsula (Fig. 1). The Committee Orogen lies mainly north of the map area, and is characterized by strongly deformed Archean greenstone belts (Mary River and Prince Albert groups), which are bounded by a wide variety of granitic and gneissic rocks. To the south, the Foxe Fold Belt consists of early Proterozoic supracrustal rocks of the Piling and Penrhyn groups which unconformably overlie rocks of the Committee Orogen. The Foxe Fold Belt formed by northwest-directed thrusting in the early Proterozoic before intrusion of the ~1.89-1.85 Ga Cumberland batholith.

Within the map area, metamorphosed mafic and felsic volcanic rocks, semipelitic to pelitic sedimentary rocks, and banded iron formation form two northeast-trending belts referred to as the 'Ege Bay' and the 'Isortoq' greenstone belts (Fig. 2). Based on lithological similarity and two bulk U-Pb zircon ages, Morgan (1982) correlated these rocks with the Archean Mary River Group (Jackson, 1966) of the Committee Orogen. Another supracrustal succession northwest of Isortoq Fiord in the map area (Fig. 2), characterized by the association of quartzite, metapelite, marble, and calc-silicate rock, was correlated by Morgan with the Proterozoic Piling Group. Bulk zircon U-Pb dating, compositional and structural relationships also led Morgan to subdivide orthogneisses and plutonic rocks into Archean or Proterozoic age groups. Jackson (in press) interprets the northwest limit of Proterozoic thrusting associated with the Foxe Fold Belt to be marked by the Isortoq Fault Zone (Fig. 2), coinciding with marked changes in aeromagnetic pattern and metamorphic grade, which strikes northeast across Baffin Island from Isortoq Fiord (Fig. 2). Fieldwork in 1994 concentrated mainly on gneissic, plutonic, and supracrustal rocks near Ege Bay (Fig. 2, 3).

## ROCK TYPES

Figures 4 to 10 and Table 1 provide summary descriptions of rocks outside the Ege Bay greenstone belt. Rocks within the Ege Bay greenstone belt have been described by Bethune and Scammell (1993).

## MAP UNITS

Rocks north and south of the Ege Bay greenstone belt comprise a wide variety of granitoid rocks, gneisses, and migmatites (Fig. 3). In many places a single rock type is dominant. Elsewhere, a wide variety of rocks are subdivided on the basis of the predominance of a particular rock type, or of a consistent association of rock types. Most rock types described in Table 1 form map units in Figure 3. In addition there are two composite map units which are described below.

### *Granodiorite-tonalite and mafic gneisses (Unit Gn)*

This unit is well exposed on the eastern side of Ege Bay (Fig. 3). It is composed primarily of granodiorite-tonalite orthogneiss (Table 1), which is interlayered with, or includes, quartzofeldspathic gneiss, and mafic gneiss and schist (Table 1) that comprise 10-50 per cent of the rock. A compositional range between biotite granodiorite gneiss to hornblende-rich (>75% Hbl) amphibolite is present at many locations. Mafic rocks comprise medium- to coarse-grained amphibolite ( $\pm$  Bt, Grt), and biotite schist, each commonly forming centimetre- to metre-thick layers (Fig. 5). Mafic and quartzofeldspathic gneisses are generally well foliated parallel to foliation in surrounding granodiorite-tonalite gneisses. However, in many locations there are discordances between gneissosity in boudins of mafic and polydeformed quartzofeldspathic gneisses, and an external foliation in the enclosing granodiorite-tonalite gneiss. In some places these relationships can be attributed to differential shear strain. In others, the discordances suggest an original intrusive relationship, especially where quartzofeldspathic gneisses preserve earlier structures, such as multiple sets of folds, that are not evident in the enclosing granodiorite-tonalite gneiss. These latter observations indicate that this composite unit is composed of previously deformed mafic and quartzofeldspathic gneisses and later granodiorite-tonalite gneisses.

### *Heterogeneous gneiss and plutonic rock complex (Unit HPgn)*

In 1992 a sheet-like body of megacrystic granite (Table 1) was mapped on the north side of Ege Bay (Fig. 3). This summer's mapping established that this rock is present south of Ege Bay; however, associated with it almost everywhere are one or two phases of later, intrusive, dark grey biotite granodiorite and light grey biotite ( $\pm$ Ms) tonalite (Fig. 7, 8; Table 1). Rather than forming a readily mappable unit, as to the north, the distribution of the megacrystic granite and associated grey granitoids is irregular. Together they are

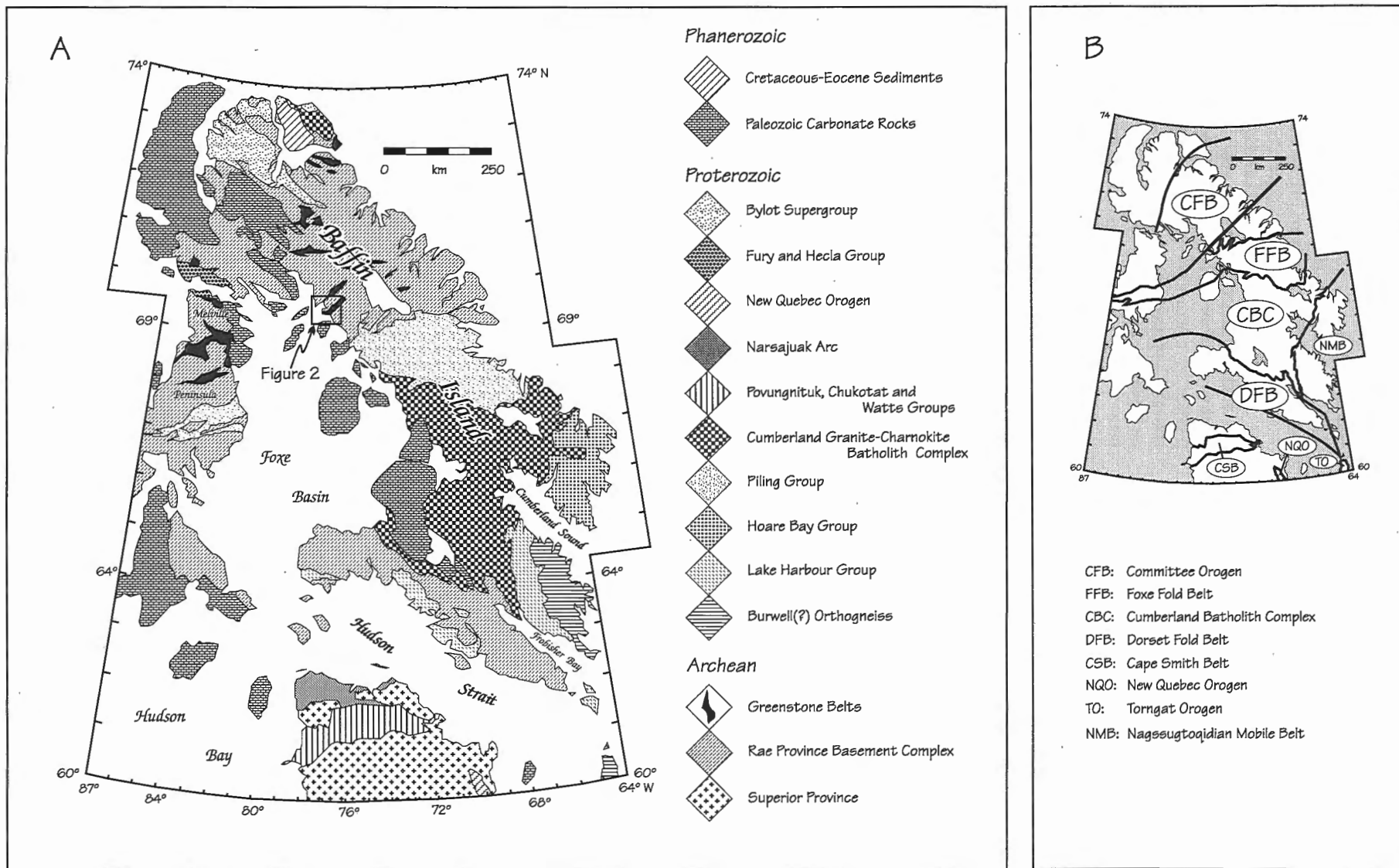


Figure 1. General geology and tectonic subdivisions of Baffin Island (after Hoffman, 1988; Jackson et al., 1990b).



commonly intercalated with older quartzofeldspathic and mafic gneisses, and metasedimentary rocks, including ortho-quartzite, quartz-granule to quartz-pebble conglomerate, and micaceous schist. This heterogeneous association is labelled "HPgn" on Figure 3. Areas where the megacrystic granite predominates are outlined, as are layers of metasedimentary rocks.

Well exposed shoreline outcrop has shown that the megacrystic granite and associated grey granitoid rocks are intruded in turn by metre- to decimetre-scale irregular bodies of pink biotite ( $\pm$ Ms) granite and by two-mica pegmatites (Fig. 7, 8; Table 1). These late phases also cut other gneisses (unit Gn).

**Eqe Bay greenstone belt**

Detailed mapping in the northeast part of the Eqe Bay greenstone belt identified all of the units described by Bethune and Scammell (1993). Several key observations were made which are summarized below in point form, and in the section "Economic geology" below. (1) The map of Morgan (1982) shows a narrow band of iron-formation immediately northeast of the southeast-trending valley linking Eqe Bay with Grant Suttie Bay. Our observations this summer indicate that, rather than iron-formation, the elongate high in the aeromagnetic

pattern at this location reflects a diabase dyke. (2) Crawford (1973) and Morgan (1982) delineated a northeast-striking quartzite within mafic volcanic rocks near the base of the Eqe Bay greenstone belt (Fig. 3). Although this quartzite was mapped in the southwestern part of the belt, detailed field-work failed to confirm its extension along strike, northeast of the aforementioned valley. (3) In the Eqe Bay greenstone belt the contact between primarily volcanogenic rocks to the northwest and turbiditic siliciclastic rocks to the southeast is marked by a transition from felsic volcanoclastic rocks to paraconglomerates (Bethune and Scammell, 1993). Bethune and Scammell (1993) suggested that the large-scale map pattern, in which northeast-striking units in the underlying volcanic succession are truncated by slightly more northerly striking turbidites, indicates that this contact represents an angular unconformity (Fig. 3). However, the possibility of a fault could not be ruled out. The latter possibility is supported by the fact that this long (>20 km) linear contact separates two successions of polydeformed rocks, yet is apparently not folded. With this problem in mind we again examined in detail nearly continuous outcrop across this contact in the central part of the Eqe Bay belt. At this location, steeply southeast-dipping felsic volcanoclastic rocks, breccias, and paraconglomerates are strongly flattened, with down dip elongation of clasts; they are also conformable and gradational into one another at outcrop scale, with no discernible

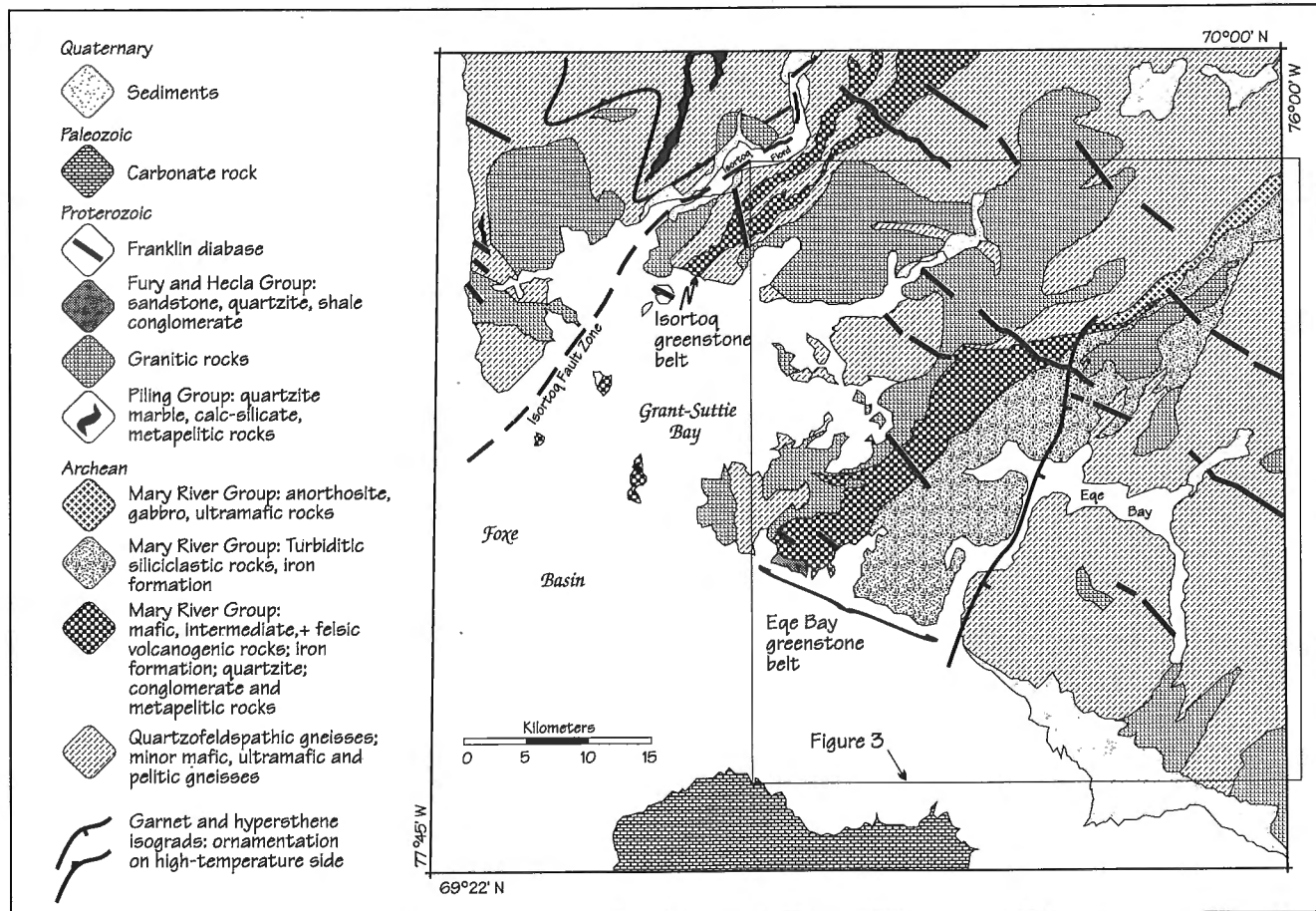
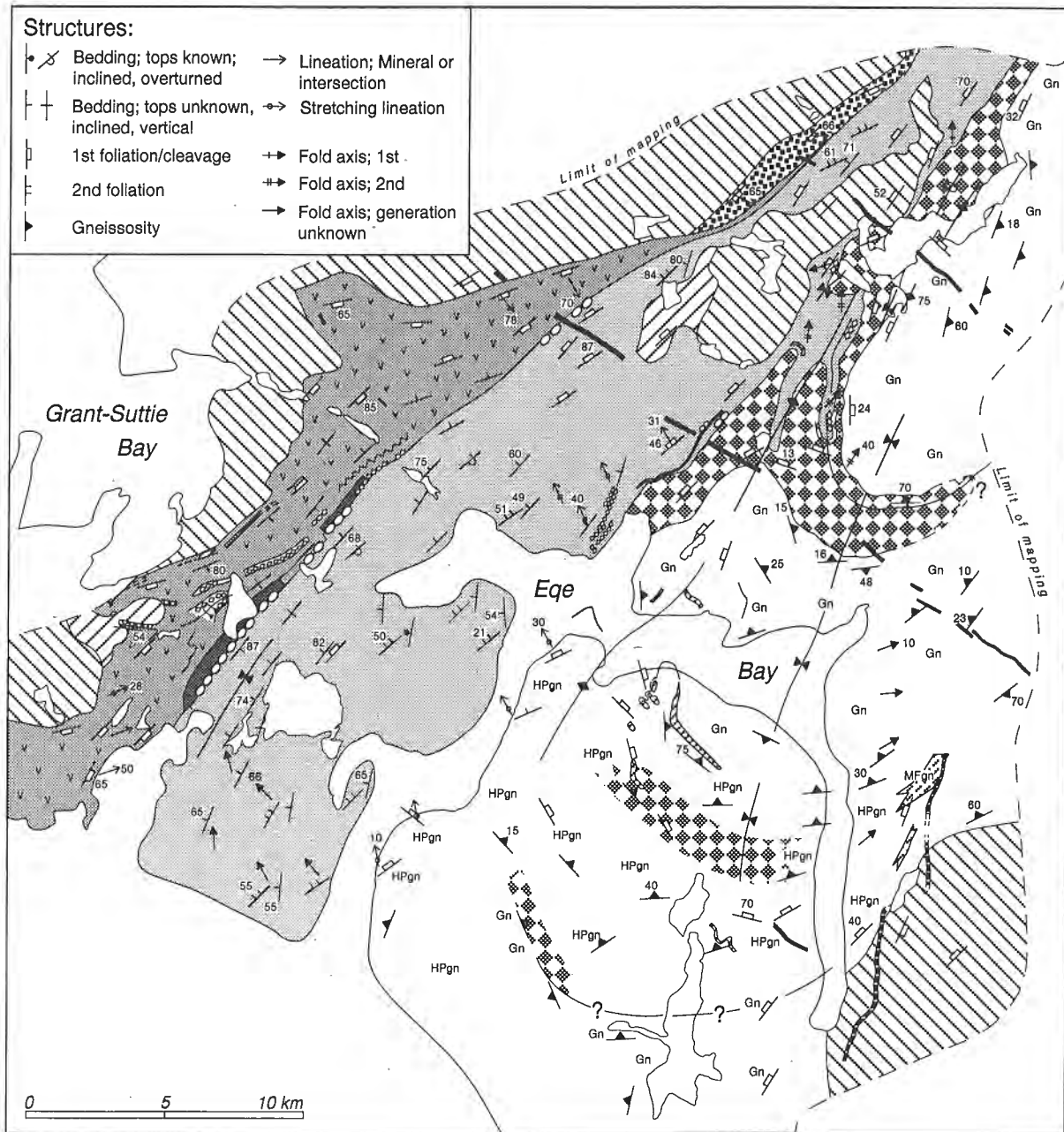


Figure 2. Geology of the Eqe Bay area (modified after Morgan, 1982).



**Mary River Group  
Supracrustal Rocks**

- Mafic Volcanic rocks
- Felsic volcanic rocks
- Iron Formation
- Orthoquartzite/micaceous schist
- Conglomerate/Volcaniclastic rocks
- Siliclastic sedimentary rocks (Turbidites)
- Gossan

**Gneisses and Granitoid Rocks**

- Gn** Granodiorite-Tonalite and Mafic Gneisses: dominantly Bt +/- Hbl orthogneiss with remnants of older? quartzofeldspathic (QF)-mafic(MF) gneisses, some of tonalitic composition; abundant late pink granite
- Mafic gneiss-Amphibolite (MFgn)
- HPgn** Heterogeneous Gneiss and Plutonic rock association: Kfs-meg granite and associated grey granitoid rocks interlayered with older(?) gneisses; intruded by late pink Bt ( $\pm$ Ms) granite and pegmatite
- Megacrystic granite
- Anorthosite (Mary River Gp)
- Diorite/Qtz-diorite (Mary River Gp)
- Granodiorite and granite (Table 1)
- Metagabbro dykes
- Diabase dykes (Franklin)

**Figure 3. Geology of the Ege Bay area.**

**Table 1.** Descriptions of rock types.

Rock and Description	Contact Relationships
<p><input type="checkbox"/> <b>Granodiorite-tonalite gneisses (part of unit "Gn" in Figure 3)</b></p> <p>These gneisses are characterized by the dominance of light grey- to white-weathering, medium-grained, quartzofeldspathic gneisses. They are composed primarily of quartz, plagioclase and K-feldspar, with subordinate amounts of biotite and less commonly hornblende, and vary in composition from granite to tonalite, and are most commonly granodioritic. They are typically well foliated, layered on a centimetre- to decimetre-scale, and are commonly migmatitic with 5-30% layer-parallel granitic leucosome. The foliation in these gneisses is defined by either leucosomes, thin biotite seams, or both, and can be wispy and discontinuous (Fig. 4). At some locations the leucosome cross-cuts the foliation, but has been involved in deformation which folds the gneisses, and is also cross-cut by undeformed granite dikes and sheets described below. At one location, along the east shore of Ege Bay, relict K-feldspar megacrysts have been observed indicating that the protolith of some of the grey granodiorite-tonalite gneiss is a plutonic rock. Coarse-grained hornblende tonalitic gneisses are also a common component of these gneisses. These gneisses display multiple sets of folds described below.</p>	<p>Commonly obscured by strain. Cut by most rocks described below.</p>
<p><input type="checkbox"/> <b>Mafic gneisses (unit "MFgn" and part of unit "Gn" in Figure 3)</b></p> <p>Mafic gneisses are composed primarily of amphibolites (<math>\pm</math> Bt, Grt) and biotite (<math>\pm</math> Grt) schists interlayered at centimetre- to metre-scales (Fig. 5). Coarse-grained amphibolites can contain 50-90% hornblende, form discrete decimetre- to metre-thick layers, and while most have sharp contacts they can be gradational with hornblende tonalitic gneisses. Black biotite schists are well foliated, and range from very fine- to coarse-grained layers that are centimetres to several metres in thickness.</p>	<p>Commonly obscured by strain. Cut by most rocks described below. Gradational and sharp with granodiorite-tonalite gneisses.</p>
<p><input type="checkbox"/> <b>Metasedimentary rocks</b></p> <p>Metasedimentary rocks include a variety of rocks. White quartzites range from several centimetres to several metres thick, and commonly contain muscovite. They are commonly interlayered with subordinate amounts of quartzofeldspathic meta-arenites and biotite schists. Decimetre- to metre-thick layers of metamorphosed quartz-pebble-granule conglomerates are occasionally associated with the quartzites. Metapelitic rocks are commonly stromatic metatexites layered on a centimetre-scale. They are composed of biotite, feldspar, quartz and less commonly garnet, and are interlayered with semipelitic schists. At one location previously mapped by Morgan (1982) northeast of Trident Lake (Fig. 3), paragneisses are dominated by feldspar-rich biotite semipelite interlayered with minor quartzite. All paragneisses display multiple sets of folds described below.</p>	<p>Commonly obscured by strain. Interlayered with mafic gneisses. Sharp with granodiorite-tonalite gneisses and intrusive rocks described below. Some quartzites are mylonitic at sheared contacts and crosscut trends in surrounding gneisses.</p>
<p><input type="checkbox"/> <b>Megacrystic granite (unit "K" in Figure 3)</b></p> <p>Pink megacrystic K-feldspar granite gneiss is a very distinctive rock type. This gneiss is medium- to coarse-grained, and is generally composed of 10-40% dispersed, 1-5 centimetre long megacrysts of K-feldspar, which are set in a matrix composed primarily of biotite (15-25% of the rock) with lesser amounts of quartz, plagioclase and rare hornblende. Megacrysts of K-feldspar are commonly recrystallized, forming sheared augen (Fig. 6) that define a mineral elongation lineation (Fig. 7). Rocks that are considered to be comagmatic with the megacrystic K-feldspar biotite granite include: (i) well lineated, pink, biotite-rich (15-25%) granites in which K-feldspar grains form phenocrysts less than 1 centimetre in diameter, and (ii) medium- to coarse-grained K-feldspar-bearing amphibolites that have small amounts (&lt;10%) of evenly distributed pink K-feldspar phenocrysts (Fig. 8). This suite of lineated granites clearly cross-cut older migmatitic granodioritic-tonalite and mafic gneisses. These latter gneisses are lithologically and structurally similar to the grey granodiorite-tonalite and mafic gneisses described above, and consequently presumed to be correlatives. The megacrystic K-feldspar biotite granite unit is cross-cut by undeformed granitic units (described below).</p>	<p>With the above gneisses the contacts are: (i) sharp and discordant, (ii) discordant with an intervening m-thick layer of sheared chlorite schist and or rusty schist, and (iii) mylonitic. The Ksp-bearing amphibolites have been observed in sharp contact with the megacrystic K-feldspar biotite granite along the south shore of Ege Bay. Crosscut by rocks described below.</p>

**Rock and Description****Contact Relationships** **Dark grey biotite granodiorite**

Fine-grained biotite granodiorite(?) is primarily dark grey. It is composed of white feldspar, quartz and biotite. It has light-grey centimetre-thick layers that are discontinuous and common where in contact with the megacrystic K-feldspar biotite granite (Fig. 7). This gneissic rock also has centimetre-thick white feldspar-rich leucosomes. All layering is tightly folded in this rock.

Cross-cuts the megacrystic Ksp Bt granite above.

 **Hornblende diorite**

Grey-green diorite is found in close proximity to the Ege Bay greenstone belt. It is composed primarily of quartz and plagioclase, contains up to 10% hornblende, is medium grained, and has subhedral granular igneous texture.

Cross-cuts greenstones along the northwest margin of the Ege Bay belt.

 **Grey-biotite ( $\pm$  muscovite) tonalite**

This light grey rock is composed of very fine-grained feldspar, quartz, biotite and on occasion muscovite. The fine grain size does not allow an accurate determination of the quantities of these minerals, but it is generally feldspar-rich and tentatively interpreted to be a tonalite. It is usually undeformed with a subhedral granular igneous texture, but can have a weak foliation, and most commonly forms small 100 metre wide stocks and metre-scale intrusive dikes and sills.

Cross-cuts granodiorite gneisses, mafic gneisses, megacrystic Ksp Bt granite, and dark grey biotite granodiorite.

 **Weakly foliated biotite-granite**

This light grey, white-weathering granite contains 10-15% biotite, which in many places defines a weak to moderately-well developed foliation that is discontinuous and commonly wispy in nature (Fig. 9). This granite is medium-grained, and it contains muscovite at some locations where it is cross-cut by later pegmatites.

Cross-cuts trends in all above gneisses.

 **North-trending mafic dykes**

A large, vertical mafic dyke east of Ege Bay is one of several north-trending dykes shown by Morgan (1982) in this area. It is coarse-grained and is generally composed of subequal amounts of hornblende and plagioclase, but can have up to 20% biotite. The dike is ~150 m thick and >5 km long. Aphanitic chilled margins have been observed at the contacts with host gneisses. Metre-scale black aphanitic dikes that are north-trending are present elsewhere.

Cross-cuts all above gneisses and the weakly foliated biotite granite.

 **Pink biotite ( $\pm$  muscovite) granite**

Medium-grained pink granite generally contains <5% biotite with trace amounts of muscovite. This granite is usually undeformed, homogeneous and exhibits a subhedral granular igneous textures (Fig. 7).

Cross-cut all of the above.

 **Biotite ( $\pm$  hornblende) granodiorite**

White weathering biotite granodiorite is medium- to coarse-grained, and commonly contains dispersed megacrysts of white K-feldspar that comprise <10% of the rock. Biotite is the main accessory mineral. Hornblende can also be present. In some locations the granodiorite grades into a K-feldspar-rich granite with distinctive blebs of quartz that are 0.5-2 cm in diameter, and evenly distributed (Fig. 10).

Intrudes rocks of the Ege Bay greenstone belt along its northwest margin.

 **Two-mica ( $\pm$  garnet, tourmaline) granitic pegmatites**

Very coarse-grained, white, granitic pegmatites are present throughout the area and cross-cut most of the rock types above. They contain very coarse grains of biotite and muscovite. Garnet and tourmaline have been observed at some locations as accessory minerals.

Cross-cut all of the above.

 **Diabase dikes**

Brown weathering, northwest-striking diabase dikes are present throughout the area. They range from 10 to 100 m in thickness, and are considered to be Franklin dykes by Fahrig et al. (1971).

Cross-cut all of the above rock types.



**Figure 4.**

*Biotite granodiorite-tonalite gneiss. Note wispy discontinuous layering. View to the southeast; scale in inches and centimetres.*

**Figure 5.**

*Interlayered mafic gneisses and biotite granodiorite-tonalite gneiss. View to the southeast; scale in inches and centimetres.*

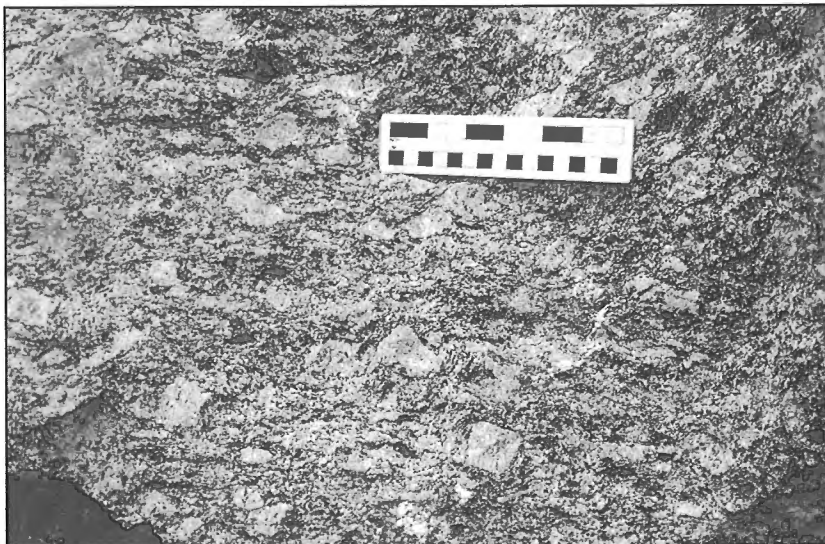
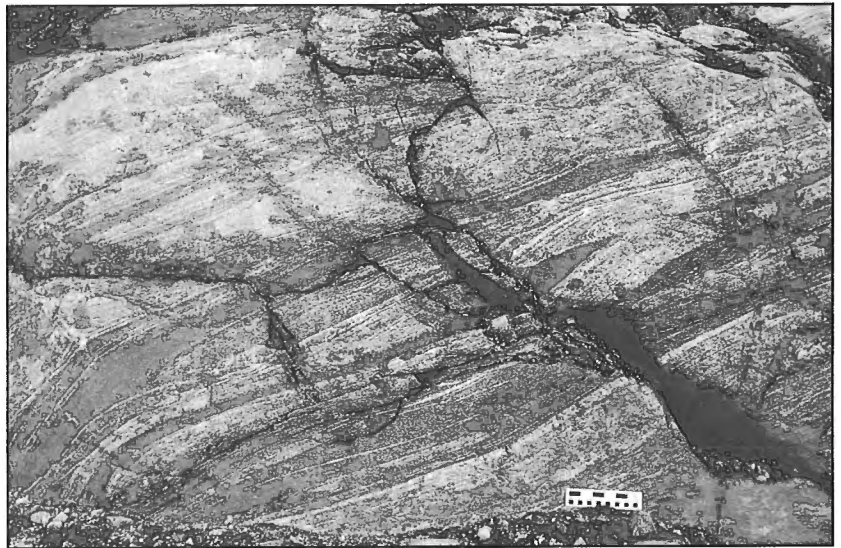


**Figure 6.**

*Sheared megacrystic granite. View to the northwest; scale in inches and centimetres.*

**Figure 7.**

*Intrusive relationships in the heterogeneous gneiss and plutonic rock unit (Hpgn). Lineated megacrystic granite (speckled black and white) is crosscut by dark grey biotite granodiorite gneiss with light grey layers. Both rocks are crosscut by pink biotite granite (light grey). View looking down, top of photograph is southwest; scale in inches and centimetres.*

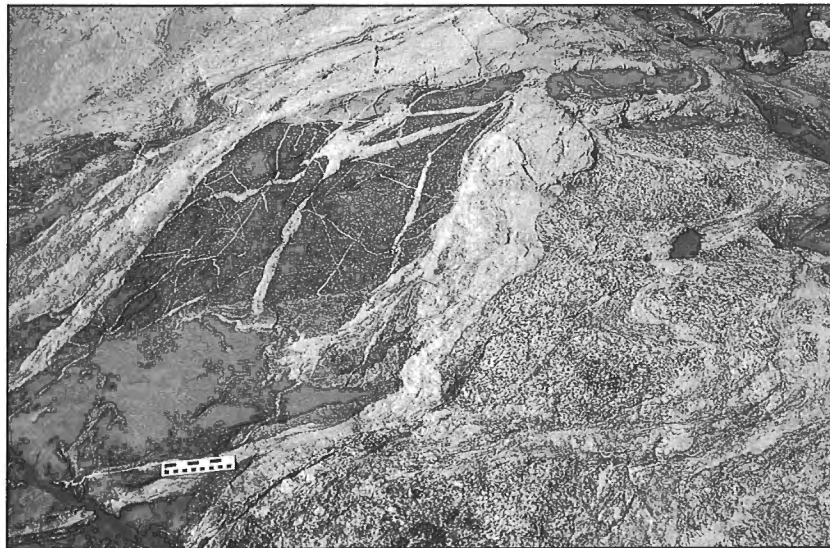


**Figure 8.**

*Contact relationships in the heterogeneous gneiss and plutonic rock unit (Hpgn). Lineated and folded megacrystic granite (speckled black and white rock on right), boudin of dark grey biotite granodiorite gneiss (dark grey unit above the scale) and K-feldspar-bearing amphibolite (darkest grey rock in dark boudin), all crosscut by white pegmatite and pink biotite granite. View to the northwest; scale in inches and centimetres.*

**Figure 9.**

*Weakly foliated biotite ( $\pm$  muscovite) granite. View to the north.*



discontinuity. We therefore interpret this contact as an angular unconformity, but one that was oriented in such a way that it escaped some of the folding recorded in the sequences of rocks it separates. For further discussion, see "Structure" below.

## STRUCTURE

### Mesoscale structures

#### Gneissic foliation

The most noticeable outcrop-scale structure in granodiorite-tonalite gneisses, mafic gneisses, and paragneisses southeast of the Eqe Bay greenstone belt is a composite gneissic foliation. It is defined by one or more of the following structural elements: (i) compositional layering, (ii) schistosity, and (iii) concordant layers of leucosome. Minerals that define the foliation are commonly partly to fully annealed, such that the

degree of strain recorded by individual minerals is not commensurate with that recorded in the rock, as indicated for example by boudins or folds. Tight to isoclinal folding of the gneissic foliation about shallow to moderately plunging, northeast-trending fold axes is common. Rootless isoclinal folds that have axial planes coplanar with the gneissic foliation, as well as local Type-3 interference patterns (Fig. 11), demonstrate a relatively high degree of flattening within the plane of gneissic foliation, as well as multiple phases of folding. The rocks are not well enough exposed to allow chronological designation to individual folds (e.g.  $F_2$  or  $F_3$ ). However, crosscutting relationships indicate that significant folding of the tonalitic-granodioritic and mafic gneisses occurred before intrusion of the megacrystic granite.

The schistose to gneissic foliation in metasedimentary rocks is defined by alternating coplanar schistose layers and millimetre- to centimetre-scale leucosomes, and is commonly concordant with gneissic foliation in surrounding gneisses. In several places schistose layers display a crenulation about



**Figure 10.**

*Undeformed biotite granite with millimetre- to centimetre-diameter round quartz "blebs". View to the southeast.*

**Figure 11.**

*Type-3 interference pattern in interlayered mafic gneisses and biotite granodiorite-tonalite gneisses. The black line outlines a refolded layer. Axial plane of oldest fold marked by folded white line. View to the north; scale in inches and centimetres.*



northeasterly-trending axes and subhorizontal axial planes. These crenulations deform chlorite and biotite, and were generated at low metamorphic grade.

### Fabrics in megacrystic granite

Shear foliation and mineral elongation lineation are present within most of the megacrystic granite. These structural elements are defined by the dimensionally preferred orientation of recrystallized feldspar augen, quartz, and biotite (Fig. 6). The degree of development of L or S fabric elements appears to be a function of large-scale folding (described below), i.e. L-tectonites in fold hinges and S>L-tectonites along limbs. Locally the foliation is mylonitic with asymmetric porphyroclasts of K-feldspar set in a matrix of ribbon quartz and biotite. In most cases unequivocal shear sense cannot be determined systematically.

### Shear zones

At several locations north of Ege Bay, shearing is localized at the contacts between the megacrystic granite and bounding gneisses. At one place mylonitization affected both granite and underlying granodiorite-tonalite gneisses. The stretching lineation associated with these mylonites is annealed, and unequivocal shear sense could not be determined. In general, folds associated with these mylonite zones are intrafolial isoclinal folds with northeast-trending axes.

Quartzite, occurring either in association with schists or as isolated layers within gneisses, commonly shows strong mylonitic fabrics with partly annealed quartz ribbons. Layers of mylonitized quartzite at two locations dip shallowly and strike southwest, and also contain boundary-parallel isoclinal folds (Fig. 12). Fabrics in these mylonitic quartzites are similar to those associated with shear zones at the margin of the megacrystic granite in that they are annealed, and shear sense is equivocal in outcrop. If intrafolial folds in quartzites

**Figure 12.**

*Transposed intrafolial (transport-parallel?) folds in partly annealed mylonitic quartzite. View to the northeast; scale in inches and centimetres.*



**Figure 13.**

*Southwest-verging sheath fold in a metre-thick mylonite zone developed in biotite granodiorite-tonalite gneisses. Long axis of the sheath is parallel to the scale, which is in inches and centimetres. Fold is cut by pink biotite granite. View is down toward the southeast.*



and megacrystic granite are transport-parallel folds, then the shear sense is either southwest-directed (thrusting) or northeast-directed (normal faulting).

Metre-thick, steeply southwest-dipping ductile shear zones, marked by mylonitic biotite schists, locally crosscut all structural elements in gneissic rocks. Where shear sense indicators are unequivocal, they indicate that displacements are primarily right-lateral with a subordinate reverse component (Fig. 13). These ductile shear zones are cut by undeformed biotite granite.

Several high-angle, chlorite-grade shear zones also cut the gneisses. These later structures are marked by biotite-chlorite schists, and record metre-scale down-to-the-southeast displacements. The schists in these shear zones also display crenulations of similar orientation and style to those found locally in schistose metasedimentary rocks.

#### Additional observations

The marble-metapelite assemblage (Bethune and Scammell, 1993), northwest of Isortoq Fiord, and neighbouring granodiorite-tonalite gneisses are tightly folded together about northeasterly trending axes. Folds are tight to isoclinal with subhorizontal axes that are coaxial with aligned sillimanite. Type-3 interference patterns are also present. Despite folding, a high-angle discordance exists between metamorphic foliation in quartzite and that in underlying gneisses at one locality, suggesting an original unconformable relationship (Fig. 14).

A thick gabbroic dyke has been mapped east of Ege Bay (Morgan, 1982). The dyke crosscuts all structures in the host gneisses and weakly foliated biotite granite. It is generally undeformed, but is locally cut by small brittle faults.

#### Macroscale structure

The northwest margin of the Ege Bay greenstone belt is intruded by several biotite granite-granodiorite plutons. For the most part these are undeformed (Fig. 10), although locally they acquire a moderately to steeply southeast-dipping foliation within several hundred metres of the contact.

In the northwest part of the Ege Bay greenstone belt, layers of iron-formation in predominantly mafic volcanic rocks display complex, refolded folds whose axial planes and steeply southeast-dipping limbs appear to be truncated by the unconformity with structurally overlying turbidites. These rocks, the unconformity, as well as turbidites and gneisses to the southeast are folded about northeast-trending axes, forming a regional syncline-anticline-syncline triplet. The most northwesterly syncline is cored by greenstones and overlying turbidites, and has an axial surface trace lying just southeast of the unconformity. These relationships support the tentative interpretation that volcanic rocks and iron-formation of the greenstone belt were subjected to deformation before deposition of the siliciclastic turbidite sequence. Both successions, as well as bordering gneisses, were then deformed during a later event characterized by northwest-directed contractional strain, which led to formation of the syncline-anticline-syncline triplet. In general, orientations of gneissic foliation within the megacrystic granite, granodiorite-tonalite gneiss, mafic gneisses, and associated metasedimentary rocks outline this fold pattern. Additional complexity occurs within the anticline-syncline pair southeast of the Ege Bay belt where the contact between megacrystic granite and turbidites outlines earlier tight to isoclinal folds, indicating that there are at least two phases of folding in this part of the greenstone belt. Southeast of the Ege Bay belt metasedimentary rocks are preserved in synformal keels within the gneisses.

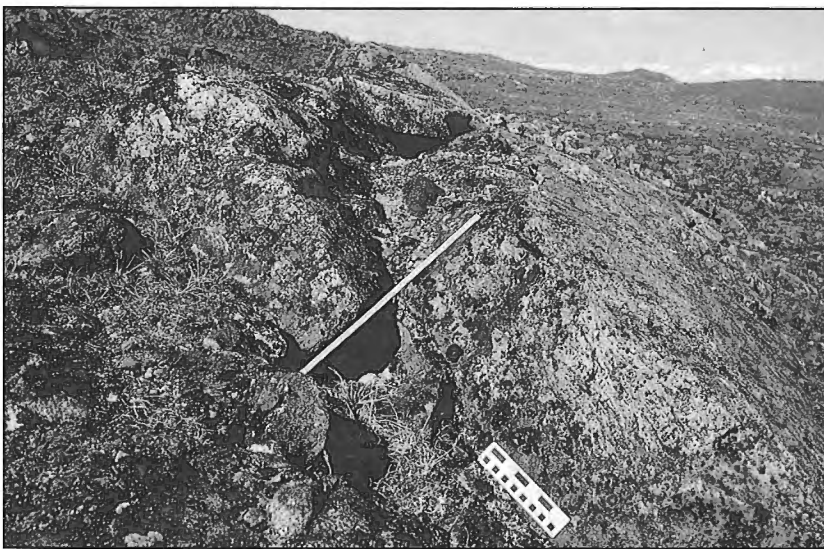


**Figure 14.**

*Looking north at the angular unconformity, marked by the left-dipping white line, between foliated biotite granodiorite-tonalite gneisses, and quartzite in the quartzite-metapelite succession north of Isortoq Fiord. The east-dipping foliation in gneisses is parallel to the scale, and the west-dipping foliation in quartzite is parallel to the unconformity.*

## METAMORPHISM

Bethune and Scammell (1993) observed that rocks northwest of Isortoq Fiord have been metamorphosed to low-pressure granulite facies, and confirmed the observations of Morgan et al. (1975) that metamorphic grade decreases to the southeast to a greenschist facies metamorphic low within the Ege Bay greenstone belt. Continuing southeast they observed that metamorphic grade increases to garnet grade with local porphyroblasts of cordierite, staurolite, and andalusite. This general trend in metamorphism was reconfirmed in 1994. In addition, and also in accord with Morgan (1982), it was established that turbiditic rocks are metamorphosed to sillimanite grade in the northeast part of the Ege Bay greenstone belt. The uniformly higher metamorphic grade on the southeast side of the belt is probably related to crustal thickening by folding (see above) as well as later intrusion of granite. Thin section studies of metapelitic rocks near the Isortoq greenstone belt have documented the presence of rare porphyroblasts of andalusite replaced by sillimanite, indicating that metamorphism in both greenstone belts is likely related, and represents a low-pressure facies series.

Gneisses and metasedimentary rocks southeast of the Ege Bay belt contain biotite and rare garnet, indicating that they are at least at garnet grade. In general though, it is believed that these rocks are at upper amphibolite facies based on several lines of reasoning. First, the gneisses and metasedimentary rocks are commonly migmatitic with granitic leucosome, which may be a product of partial melting. Second, these rocks are deformed by folds that are characteristic of high-temperature ductile flow. Third, these gneisses and metasedimentary rocks do not appear to have bulk compositions that contain enough aluminium to generate metamorphic index minerals typical of higher grades of metamorphism.

The gabbroic dyke mapped east of Ege Bay appears to have plagioclase and hornblende in recrystallized ophitic texture. It locally contains zones of metamorphic biotite, particularly along the margins, some of which are sheared.

## TIMING CONSTRAINTS

In an effort to improve our understanding of the geological evolution of the area, new U-Pb zircon and monazite dating has been initiated. Some tentative conclusions can be drawn from preliminary data (Scammell, unpub. data, 1994). The oldest rocks are ~2.84 Ma granitic cobbles found within the basal conglomerate of the turbidite succession in the Ege Bay belt. Granodiorite-tonalite gneisses northwest of Isortoq Fiord appear to have in part an igneous protolith that was emplaced at ~2.77 Ga. In the Ege Bay greenstone belt felsic volcanism and plutonism occurred at ~2.72 Ga, and one ~2.72 Ga pluton crosscuts structures in the mafic volcanic succession, implying that the structures are older. In the vicinity of Isortoq Fiord, upper-amphibolite to granulite facies metamorphism and intrusion of syn- to post-kinematic granite occurred at ~1.82 Ga.

## ECONOMIC GEOLOGY

New findings with respect to economic mineralization include the following. Within the Ege Bay greenstone belt the thick band of iron-formation closest to the contact with turbidites strikes farther northeast than shown on the map of Morgan (1982). A 1-3 m thick gossan zone, composed primarily of massive pyrite set in a matrix of variable amounts of quartz and calcite, was discovered in mafic rocks just northwest of this iron-formation. It strikes northeast and has been traced for ~5 km. Northwest of Isortoq greenstone belt a ~50 m thick and >2 km long zone of late, vertical, quartz-carbonate veining with copper-bearing mineralization was discovered along a late fracture zone that cuts Archean gneisses and Proterozoic granite.

Preliminary geochemical analyses of one sample of oxide-facies iron-formation from the lowest grade part of the Ege Bay greenstone belt, and another of silicate-facies iron-formation within mafic volcanic rocks nearby, have relatively high gold and silver values (320 and 170 ppb Au, 3.0 and 0.7 ppm Ag, respectively) correlating with elevated concentrations of arsenic (1200 and 36 000 ppm). Mineralization in the latter sample is clearly related to visible arsenopyrite and pyrite associated with quartz and quartz-carbonate veins cutting the rock. Other geochemical analyses indicate that significant amounts of gold, silver, and base metals (Cu, Cr, Zn, Ni) occur locally within mafic and felsic volcanic rocks, both at Ege Bay and within the Isortoq belt. It is of interest that an analysis of oxide-facies iron-formation metamorphosed to upper amphibolite facies in the Isortoq belt, does not show the same abundances of gold and silver as greenschist facies iron-formation in the Ege Bay belt.

## DISCUSSION

Regional correlation of supracrustal rocks of the Isortoq and Ege Bay belts with the Mary River Group is a reasonable proposal based on similarity in rock types (Jackson and Taylor, 1972; Crawford, 1973; Morgan, 1982; Jackson et al., 1990b; Bethune and Scammell, 1993; Jackson, in press). The preliminary ~2.72 Ga U-Pb zircon dating reported above is very similar to a U-Pb zircon age from dacite within the Mary River Group (2718 ±5/-3 Ma; Jackson et al., 1990b) supporting the proposed correlation. U-Pb dating also has some important implications for the timing of deformation in the Ege Bay greenstone belt. For example, a relatively massive biotite-hornblende granodiorite that crosscuts rock units and structures within the Ege Bay volcanogenic sequence was emplaced at ~2.72 Ga. This age, and an age of 2.71 Ga for a leucomonzodiorite body with similar crosscutting relationships to structures in greenstone belts in the Mary River area (Jackson et al., 1990b), implies that major deformation preceded plutonism at ~2.72-2.71 Ga, and most likely reflects deformation associated with the 2.7 Ga Committee Orogen. Other evidence for Archean deformation in the map area includes: (i) the presence, northwest of Isortoq Fiord, of a suspected angular unconformity between inferred Proterozoic quartzite and structure in underlying ~2.77 Ga gneisses,

(ii) the fact that early folds in gneisses southeast of the Ege Bay greenstone belt are cut by megacrystic granite which is lithologically similar to, and tentatively correlated with, a ~2.72 Ga granite that underlies the Isortoq Belt.

At present the age of the turbidite sequence within the Ege Bay greenstone belt remains unknown, although it must be younger than the ~2.84 Ga age of granitic clasts in the basal conglomerate. If the lowermost contact of the turbidites is an angular unconformity, as interpreted above, the turbidites would then be ~2.72 Ga or younger. The timing of later large-scale northeast-trending folds which deform turbidites, volcanic rocks, and gneisses in the Ege Bay area is similarly ill constrained. To the northwest near Isortoq Fiord, similarly oriented folds affect gneisses, the Isortoq greenstone belt, and Proterozoic(?) supracrustal rocks, and regional metamorphism appears to have occurred at ~1.82 Ga, all of which point to major tectonism in the Proterozoic. It is therefore likely that large-scale folds in the Ege Bay area are also Proterozoic. The orientation of these folds indicates northwest-directed contractional strain which is likely related to development of the Foxe Fold Belt.

Possible southwest-verging shear zones in the map area may be associated with the Northeast Baffin Thrust Belt (Jackson, in press). This thrust belt, located along the northeast coast of Baffin Island, comprises southwest-directed ductile fold and thrust nappes that overprint structures of the Foxe Fold Belt.

## ACKNOWLEDGMENTS

We thank Katherine Venance, Hillar Pintson, and Iain Boyle for their assistance in mapping, culinary experiments, and camp organization. Deb MacKean and Shey Scammell provided additional assistance. Aircraft and logistical field support were provided mainly by Polar Continental Shelf Project (PCSP). Our thanks are extended to Dave Malloley and Jim Godin at PCSP, Pat Power, Al MacDonald, and Ray Baumbury at First Air, and Luke Gauthier and David Totaram from Canadian Helicopters. We especially thank Garth Jackson for his guidance, mapping, and discussions regarding the geology of Baffin Island. Garth Jackson and Tony Davidson provided critical reviews of early drafts of this paper. This report summarizes ongoing work related to Visiting Fellowships awarded the authors at the Geological Survey of Canada.

## REFERENCES

- Bethune, K.M. and Scammell, R.J.**  
1993: Preliminary Precambrian geology in the vicinity of Ege Bay, Baffin Island, N.W.T.; *in* Current Research, Part C; Geological Survey of Canada, Paper 93-1C, p. 19-28.
- Crawford, W.J.**  
1973: Metamorphic iron formations of Ege Bay and adjacent parts of northern Baffin Island, PhD. thesis, University of Washington, 76 p.
- Fahrig, W.F., Irving, E., and Jackson, G.D.**  
1971: Paleomagnetism of the Franklin diabases; Canadian Journal of Earth Sciences, v. 8, p. 455-467.
- Henderson, J.R., Grocott, J., Henderson, M.N., and Perrault, S.**  
1989: Tectonic history of the Lower Proterozoic Foxe-Rinkian belt in central Baffin Island, N.W.T.; *in* Current Research, Part C; Geological Survey of Canada, Paper 89-1C, p. 185-197.
- Hoffman, P.F.**  
1988: United plates of America, the birth of a craton; Early Proterozoic assembly and growth of Laurentia; Annual Reviews of Earth and Planetary Sciences, v. 16, p. 543-603.
- Jackson, G.D.**  
1966: Geology and mineral possibilities of the Mary River region, northern Baffin Island; Canadian Mining Journal, v. 87, p. 57-61.  
in press: Geology of the Clyde-Cockburn Land map area; Geological Survey of Canada, Memoir 440.
- Jackson, G.D. and Hegner, E.**  
1991: Evolution of Late Archean and Early Proterozoic crust based on Nd isotopic data for Baffin Island and northern Quebec and Labrador; *in* Geological Association of Canada, Program with Abstracts, 1991, v. 16, p. A59.
- Jackson, G.D. and Morgan, W.C.**  
1978: Precambrian metamorphism on Baffin and Bylot islands; *in* Metamorphism in the Canadian Shield, (ed.) J.A. Fraser and W.W. Heywood; Geological Survey of Canada, Paper 78-10, p. 249-267.
- Jackson, G.D. and Taylor, F.C.**  
1972: Correlation of major Aphebian rock units in the Canadian Shield; Canadian Journal of Earth Sciences, v. 9, no. 12, p. 1650-1669.
- Jackson, G.D., Frisch, T., Hegner, E., and Hunt, P.A.**  
1990a: U-Pb geochronology, Nd model ages and tectonics of the eastern Arctic Canadian Shield; *in* Forum 1990, Program with Abstracts, Geological Survey of Canada, p. 12.
- Jackson, G.D., Hunt, P.A., Loveridge, W.D., and Parrish, R.R.**  
1990b: Reconnaissance geochronology of Baffin Island, N.W.T.; *in* Radiogenic Age and Isotopic Studies: Report 3; Geological Survey of Canada, Paper 89-2, p. 123-148.
- Morgan, W.C.**  
1982: Koch Island, District of Franklin, Northwest Territories; Geological Survey of Canada, Map 1535A, scale 1:250 000.
- Morgan, W.C., Bourne, J., Herd, R.K., Pickett, J.W., and Tippet, C.R.**  
1975: Geology of the Foxe Fold Belt, Baffin Island, District of Franklin; *in* Current Research, Part A; Geological Survey of Canada, Paper 75-1, p. 343-347.

Geological Survey of Canada Project 690061-KG

# Preliminary geological investigation of the Lake Harbour Group and surrounding gneissic rocks near Lake Harbour and Markham Bay, southern Baffin Island, Northwest Territories

David J. Scott<sup>1</sup> and Laurent Godin<sup>2</sup>

Continental Geoscience Division

*Scott, D.J. and Godin, L., 1995: Preliminary geological investigation of the Lake Harbour Group and surrounding gneissic rocks near Lake Harbour and Markham Bay, southern Baffin Island, Northwest Territories; in Current Research 1995-C; Geological Survey of Canada, p. 67-76.*

---

**Abstract:** Preliminary examination of Paleoproterozoic siliciclastic and carbonate supracrustal rocks of the Lake Harbour Group and surrounding tonalitic gneisses was undertaken in two small areas south and west of Iqaluit. North of Lake Harbour, the Lake Harbour Group consists of siliciclastic schists, marble, and calcsilicate schists preserved in a tight synform surrounded by younger granitoid rocks. At Markham Bay, similar supracrustal rocks grade into migmatitic rocks. Preliminary U-Pb geochronological results from the Lake Harbour area suggest that penetrative deformation of the Lake Harbour Group occurred prior to, or during, peak metamorphic conditions at ca. 1845-1840 Ma. Folding of the S1 fabric, possibly synchronous with emplacement of the adjacent tonalitic rocks, occurred ca. 1840-1830 Ma. The age of monazite from an undeformed granitic dyke,  $1760 \pm 2$  Ma, brackets the time of final regional tectonic activity.

**Résumé :** Un examen préliminaire des roches supracrustales du Groupe de Lake Harbour et des gneiss environnants a été entrepris dans deux petites régions au sud et à l'ouest d'Iqaluit. Au nord du village de Lake Harbour, le Groupe de Lake Harbour, séquence de schistes silicoclastiques et calcosilicatés et de marbres, représente une structure synforme fermée, entourée de roches granitoïdes plus jeunes. Dans la région de la baie Markham, on retrouve une séquence de roches supracrustales similaires qui passent à des roches migmatitiques. Dans la région de Lake Harbour, les données préliminaires de géochronologie U-Pb suggèrent que la déformation pénétrative du Groupe de Lake Harbour s'est produite avant ou pendant le développement des conditions métamorphiques paroxismales il y a environ 1845-1840 Ma. Le plissement de la schistosité S1 semble être synchrone à la période de mise en place des tonalites adjacentes, il y a 1840-1830 Ma. L'âge de la dernière phase d'activité tectonique régionale est déterminé grâce à la datation d'une monazite provenant d'un dyke granitique non déformé, laquelle monazite remonte à  $1760 \pm 2$  Ma.

---

<sup>1</sup> GEOTOP, Université du Québec à Montréal, C.P. 8888, Succursale centre-ville, Montréal (Québec) H3C 3P8

<sup>2</sup> Department of Earth Sciences, Carleton University, Ottawa, Ontario K1S 5B6

## INTRODUCTION

The Baffin Orogen, exposed on southern Baffin Island, is characterized by granitoid gneisses of presumed Archean and Paleoproterozoic age, and supracrustal and meta-igneous rocks of known Paleoproterozoic age (Davison, 1959; Blackadar, 1967a; Jackson et al., 1990; Scott and Godin, 1994). The bedrock geology of the region was last investigated, at reconnaissance-scale, in 1965 (Blackadar, 1967a). This pioneering work by the Geological Survey of Canada successfully identified the major geological elements of the region, and suggested that the Precambrian rocks belong to the Churchill Structural Province and may in part be correlative with rocks across Hudson Strait in northeastern Quebec and northern Labrador in the Torngat Orogen (Jackson and Taylor, 1972). Recent geological investigations on the Ungava Peninsula (Ungava Orogen, St-Onge et al., 1992, and references within) and in the Torngat Orogen (Ermanovics and Van Kranendonk, 1990; Bertrand et al., 1993; Wardle et al., 1994; Van Kranendonk et al., 1994; Scott and Machado, in press), have increased our understanding of the tectonic evolution of this part of northeastern Laurentia (Hoffman, 1989; Van Kranendonk et al., 1993; Wardle et al., 1990). The present initiative on southern Baffin Island builds on this foundation, and is an initial contribution toward a more complete understanding of the tectonic evolution of this region.

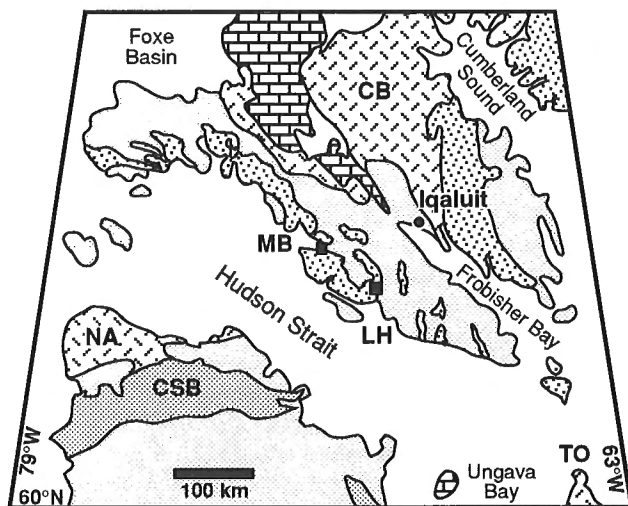


**Figure 1.** Generalized geology of northern Quebec and southern Baffin Island (modified from Blackadar, 1967a; Hoffman, 1989; St-Onge et al., 1992), showing location of Lake Harbour (LH) and Markham Bay (MB) study areas. Rocks of the Lake Harbour Group are shown in stippled pattern along the south coast of Baffin Island, CB - Cumberland batholith, Ordovician sediments shown in brick pattern. Cape Smith Belt (CSB) and Narsajuaq magmatic arc (NA) are shown in northern Quebec, and Torngat Orogen (TO) in northernmost Labrador.

Field work we initiated in 1993 and continued in 1994 has begun to address some of the first-order uncertainties of the Precambrian geology of southern Baffin Island through a program of detailed geological mapping and precise U-Pb geochronology applied in areas of regional importance (Fig. 1). The principal objectives of this work are to 1) investigate the tectonostratigraphy, timing of deposition, metamorphism and deformation of the metasedimentary rocks of the Lake Harbour Group (LHG), and 2) characterize the granitoid gneisses of the Meta Incognita Peninsula adjacent to the Lake Harbour Group. This work is a direct contribution to the LITHOPROBE Eastern Canadian Shield Onshore-Offshore Transect (ECSOOT), and should facilitate a more detailed comparison of geological events in southern Baffin with those in northernmost Quebec and Labrador as well as other parts of the Baffin Orogen. Field observations, based on three weeks of field work in a ca. 100 km<sup>2</sup> area north of Lake Harbour (130 km southwest of Iqaluit) and five days in a ca. 70 km<sup>2</sup> area at Markham Bay (160 km west-southwest of Iqaluit), and initial U-Pb results are presented in the following sections.

## GEOLOGY OF THE LAKE HARBOUR AREA (NTS 25K/13)

### *Paleoproterozoic supracrustal rocks*

Rocks assigned to the Lake Harbour Group are preserved as a continuous belt along the south Baffin coast, northwestward from the hamlet of Lake Harbour for more than 500 km; they are discontinuously exposed southeast of Lake Harbour for more than 150 km along the Meta Incognita Peninsula (Blackadar, 1967a). Jackson and Taylor (1972) have correlated rocks of the Lake Harbour Group with similar units as far southeast as eastern Ungava Bay and to the west onto Southampton Island. They comprise pelitic schists, micaceous quartzite, quartzite, and extensive marble and calcisilicate schists as well as subordinate amounts of mafic and ultramafic rock and iron formation containing bands of high-grade iron oxide (Blackadar, 1967b). They are well exposed in the lower Soper River valley, ca. 3 km north of the hamlet of Lake Harbour where we have subdivided them into three map units (Fig. 2), described below.

### **Semi-pelite and micaceous quartzite**

Biotite-garnet-quartz-feldspar schist is the dominant rock type in the eastern part of the area examined (Fig. 2). The generally rusty weathering rocks of this unit are characterized by heterogeneous compositional layering, ranging from quartz- and feldspar-rich to more micaceous. The layering ranges from 1-2 mm to tens of centimetres in thickness, and individual layers can be traced for up to tens of metres in length (Fig. 3a). A strong foliation is defined by the alignment of mica (S1), parallel to the compositional layering that is considered to reflect primary compositional variation. A lamination composed of elongated quartz-feldspar grain aggregates is widely observed on S1 (Fig. 3b). The more micaceous layers commonly contain disseminated, 1-3 mm flakes of

graphite and rare grains of pyrite and chalcopyrite. Sillimanite occurs throughout the unit, but is restricted to relatively rare, thin, more aluminous layers. It generally occurs as mats of randomly oriented needles confined to the S1 plane; aligned bundles of sillimanite needles were rarely seen (mineral lineations; Fig. 2). Ubiquitous garnet ranges from lilac pink to pale

red, and generally occurs as 1-4 mm subhedral poikiloblasts which overgrow the schistosity. Closures of folds of compositional layering with S1 parallel to the fold axial plane (F1) have only rarely been observed (Fig. 3c), whereas open, minor folds of compositional layering and S1 (F2) are common at all scales. White granitic pegmatite dykes are an

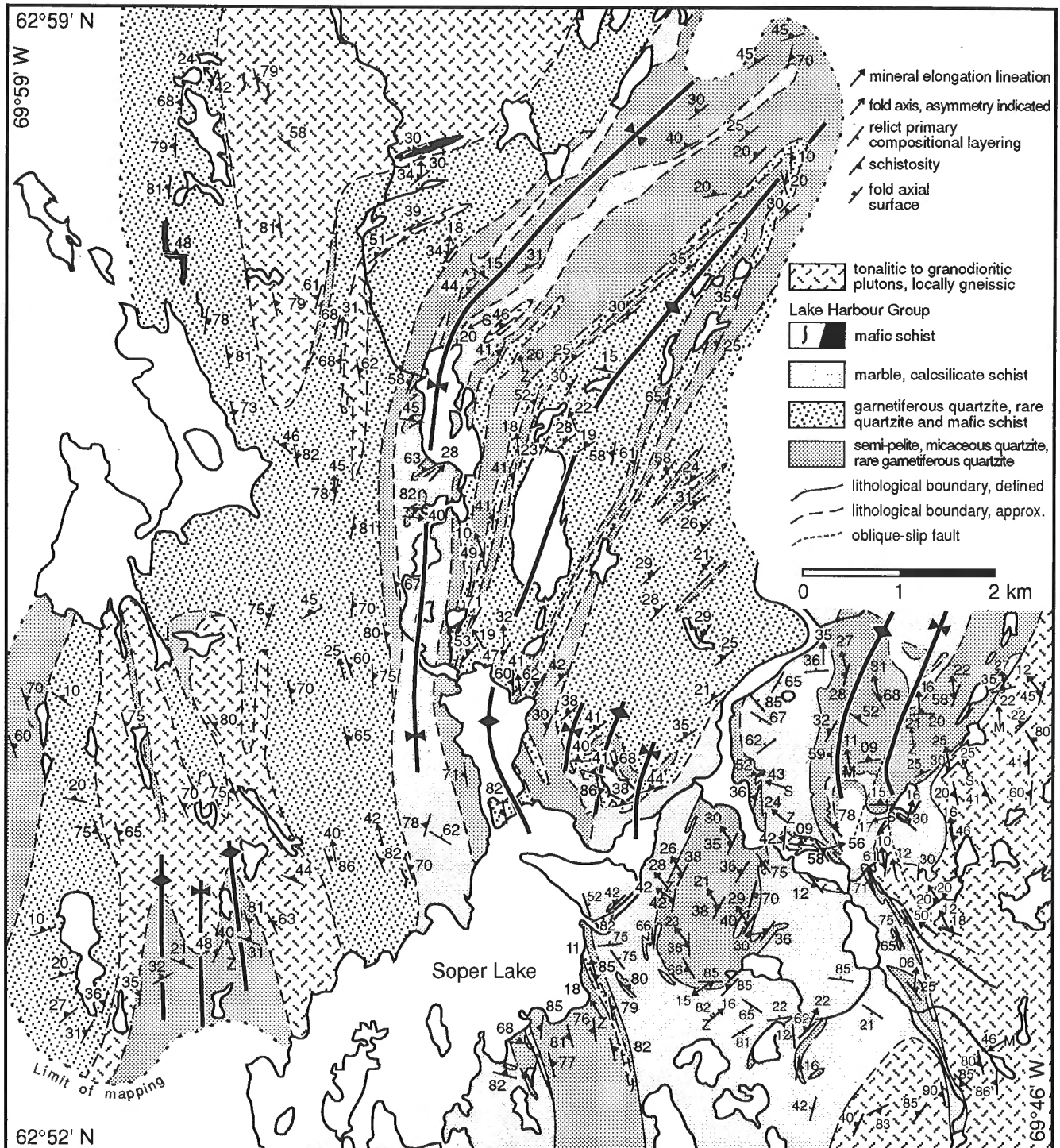


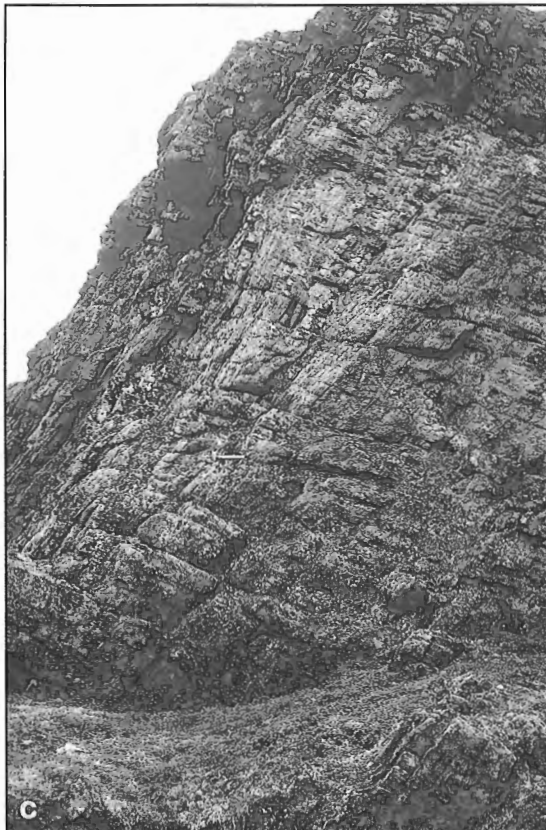
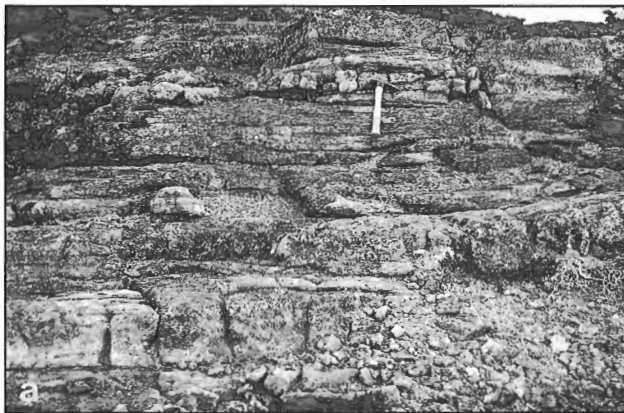
Figure 2. Geological map of the study area, lower Soper River valley. Community of Lake Harbour is ca. 3 km south of the southern edge of the map. See Figure 1 for location.

important constituent of this map unit, occurring both as discrete, tabular bodies and more diffuse, irregular pods or seams. Both types, with various relationships to deformation events, have been sampled for U-Pb geochronology and are discussed in a subsequent section.

### Garnetiferous quartzite

Fine grained quartz-feldspar schist, commonly with up to 20 per cent garnet, forms a robust, grey-weathering, generally leucocratic unit in the study area (Fig. 4a). Typically, thin micaceous layers (<1 cm) are intercalated with thicker (5-15 cm) quartz- and feldspar-rich layers, and minor amounts of disseminated biotite are present in all but the most

quartzose layers, which range up to 1 m thick (Fig. 4b). Compositional layering is laterally continuous for tens of metres, and is interpreted as relict primary layering. Development of S1 is moderate throughout much of this unit, but strong in micaceous layers. Quartz-feldspar mineral aggregate lineations are more widespread in occurrence and strongly developed in the eastern part of the area examined than in rocks of similar composition in the central and western parts. Despite favourable composition and the general lack of penetrative deformation, other primary depositional features, such as crossbedding or graded bedding, were not recognized. Parallel-sided granitic pegmatite dykes are present throughout this map unit, both parallel and oblique to S1. Fine- to medium-grained tonalitic to granodioritic sheets up to several



- a) typical rubbly outcrop of interbedded semi-pelite and micaceous quartzite, 35 cm hammer for scale (GSC1994-719B)
- b) quartz-feldspar elongation lineation developed on S1, 15 cm pen for scale (GSC1994-719AA)
- c) isoclinal fold of compositional layering (S0) with axial planar S1 foliation, 35 cm hammer for scale (GSC1994-719H).

**Figure 3.** Semi-pelite and micaceous quartzite.

metres thick are common in the northwestern part of the map area, where they locally comprise up to 50 per cent of individual outcrops.

### Marble and calcsilicate schist

White, light grey to tan-weathering marble and calcsilicate rocks are abundant in the study area, and are a characteristic feature of the Lake Harbour Group regionally. They are dominantly composed of coarsely recrystallized dolomite, diopside, and phlogopite, with trace amounts of titanite and apatite. Compositional layering, defined by varying proportions of carbonate and silicate minerals, is commonly preserved (Fig. 5). The layers range from centimetres to metres in thickness, can locally be traced for tens of metres, and commonly are highly contorted. The layering is interpreted as relict primary compositional variation, possibly reflecting varying degrees of input of siliciclastic material. The irregular folding of the compositional layering is interpreted to be a result of ductile flow. The lack of penetratively distributed platy minerals has resulted in negligible development of S<sub>1</sub>, and mineral lineations are rare.

Isolated inclusions of micaceous siliciclastic rocks, from metres to hundreds of metres in length, have been recognized throughout this map unit, commonly near contacts with adjacent, continuous panels of siliciclastic rocks (Fig. 2). Books of mica, up to 20 cm in longest dimension, are typically found at interfaces between isolated inclusions of siliciclastic rocks and host marbles. The extraordinary size of the mica crystals and their restricted occurrence are probably related to fluid

interaction along the marble/siliciclastic rock contacts. Numerous excavation pits attest to mining activity in the 1910s when the mica was extracted for use as windows in stoves and furnaces (S. Akavak, pers. comm., 1993).

### Mafic schist

Fine- to medium-grained schist consisting of hornblende, plagioclase and garnet, with locally preserved cores of clinopyroxene or orthopyroxene surrounded by hornblende, is found in the garnetiferous quartzite unit, becoming increasingly abundant toward the northwest part of the study area. These rocks occur as conformable layers which are generally <10 m thick, locally exceed 100 m in length, and may represent thin sills or volcanic flows. As the surrounding metasedimentary rocks are not strongly deformed, we consider it unlikely the mafic rocks represent highly deformed, structurally transposed dykes.

### Granitoid plutons and gneisses

The rocks which occupy much of the Meta Incognita peninsula of southern Baffin Island and surround the Lake Harbour Group consist of various quartz-feldspar gneisses, migmatites, and migmatitic and granitic gneisses and plutons (Davison, 1959; Blackadar, 1967a), interpreted as in part Archean with extensive Paleoproterozoic reworking and assigned to the Churchill Structural Province (Jackson and Taylor, 1972; Jackson et al., 1990). Hoffman (1989) has interpreted these rocks as the southeastern arm of the Rae craton. In the Soper

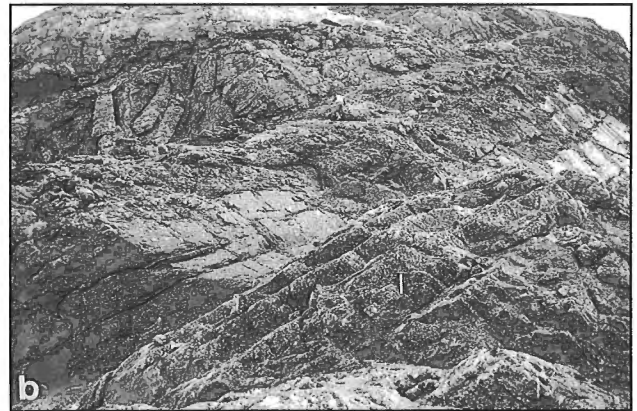


**Figure 4.** *a*) garnetiferous quartzite, 15 cm pen for scale (GSC1994-719N); *b*) typical outcrop of garnetiferous quartzite, beds up to ~1m thick, 35 cm hammer for scale (GSC1994-719A).



Lake area (Fig. 2), these rocks are tonalitic to granodioritic plutons, locally gneissic, which contain discontinuous mafic layers, concordant granitic layers and late, crosscutting granitic pegmatites.

Three kilometre-scale plutonic masses were identified in the western half of the map area (Fig. 2). They are medium to coarse grained, and appear to comprise two principal, relatively homogeneous phases (not subdivided on Fig. 2). A buff- to white weathering, pale olive-green tonalitic phase (Fig. 6) contains minor amounts of hornblende with locally preserved cores of orthopyroxene. A pink-weathering granodioritic phase (Fig. 6) is locally pegmatitic, and occurs as dykes and sheets within the buff tonalite as well as bodies hundreds of metres across. Both are generally massive to weakly foliated, with schistosity development increasing toward the margins. The contact with the rocks of the Lake Harbour Group is gradational across a distance of up to several hundred metres. Metre-scale sheets of tonalite and dykes of granodiorite intrude rocks of the Lake Harbour Group, becoming volumetrically more abundant toward the main plutonic mass as metasedimentary rock becomes less abundant. Laterally continuous outcrops of metasediment yield to isolated panels and ultimately to narrow, contorted and partially melted rafts within the tonalite and granodiorite.

On the east side of the area examined (Fig. 2), fine- to medium-grained, relatively homogeneous tonalitic rocks contain rare, discontinuous mafic layers, minor granitic- to granodioritic sheets and late, cross-cutting granitic pegmatites. Orthopyroxene, usually mantled by hornblende, occurs rarely throughout the tonalite; hornblende is a minor but widespread constituent. The contact between rocks of the Lake Harbour Group and the tonalitic rocks to their east is abrupt, occurring over a distance of < 1 m in contrast to the gradational contact described above. Dykes of tonalite were not identified in the adjacent Lake Harbour Group rocks, nor were screens or rafts of metasedimentary rock identified within the tonalite along its margin. Penetrative schistosity

and mineral extension lineations along the margin the tonalite are coplanar and collinear, respectively, to similar fabric elements in rocks of the Lake Harbour Group. At one stream-washed exposure of the tonalite/Lake Harbour Group contact, the coplanarity of the foliated tonalite, granodioritic sheets and mafic layers gives the outcrop a gneissic appearance. We suggest that the igneous and supracrustal rocks have been affected by the same deformation event, and that the contact between the tonalite and the Lake Harbour Group, originally intrusive, has been strongly tectonized.

### MARKHAM BAY AREA (25M)

Supracrustal rocks of the Lake Harbour Group and their contact with adjacent migmatitic granitic gneisses are well exposed in the vicinity of Markham Bay, about 130 km northwest of the hamlet of Lake Harbour (Blackadar, 1967a). Extensive wave-washed outcrop is accessible along the coastline.

Supracrustal rocks similar to those in Lake Harbour area occur in the southern part of the area examined (Fig. 7). The dominant rock type is a garnetiferous quartzite, interlayered with more micaceous semi-pelite; quartz-rich layers were only rarely observed. Biotite and centimetre-scale granitic dykelets are ubiquitous in the rocks examined. Marble and calcsilicate schist are present as lenticular bodies less than 1 km in length. Diopside and phlogopite are the dominant silicate minerals in the calcsilicate schist. A conformable layer of ultramafic rocks, up to 100 m thick, occurs in micaceous quartzite and semi-pelite near the southern limit of the area examined. The rocks are dominantly clinopyroxene, variably hydrated to hornblende, with trace amounts of olivine. Narrow, irregular dykes and/or thicker sheets of granitic to tonalitic material are present in most outcrops. Much of this material is parallel to compositional layering and the principal schistosity (S1), but discrete, crosscutting aplitic to pegmatitic granitic sheets are also present. The principal



**Figure 5.** Well-developed compositional layering in siliceous marble, dark bands are diopside rich, light bands are dolomite rich (GSC1994-719U).

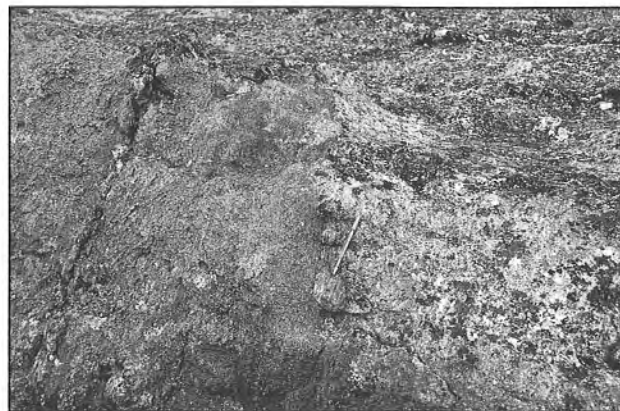


**Figure 6.** Contact between buff-weathering ortho pyroxene-bearing tonalite (left) and pink granodiorite, 15 cm pen (GSC1994-719G).

schistosity (S1), coplanar with compositional layering, generally strikes west-northwest. A quartz-plagioclase aggregate elongation lineation is locally well developed on S1, and invariably plunges shallowly to the west-northwest. Folds of compositional layering to which S1 is axial planar (F1) were not observed, and folds of S1 (F2) were only rarely noted.

The northern part of the area examined at Markham Bay is composed mostly of granitoid rocks which have intruded one another and the metasediments to form a migmatitic complex. The igneous rocks range from tonalitic to granodioritic, and from massive and only weakly foliated to gneissic. Biotite and hornblende are common accessory phases, whereas garnet is less common, and cordierite is only rarely observed. Metasedimentary rocks are widespread, as continuous kilometre-scale panels (Fig. 7), screens metres to tens of metres thick and hundreds of metres long (Fig. 8a), and smaller rafts or irregularly shaped xenoliths (Fig. 8b). Intimate veining relationships between the igneous and metasedimentary rocks (Fig. 8c) suggest that much of the igneous material is of relatively local derivation. Numerous sheets of homogeneous, leucocratic granodiorite to tonalite,

essentially free of metasedimentary material, are present; the largest sheet is shown in the northern part of Figure 7. Its southern contact is abrupt, occurring as a sharp contact against the compositionally more complex migmatitic rocks. The northern contact is gradational; screens of migmatite become more numerous northward, and discrete sheets of leucotonalite less common. We suggest that leucotonalite is a discrete intrusive phase which post-dates development of much of the migmatitic material.

The contact between the migmatitic rocks and the southern supracrustal rocks (Fig. 7) is gradational over a distance of less than 1 km. The distinction between them has been drawn at the northern limit of essentially continuous supracrustal rock. The volume of igneous rock within the garnetiferous quartzite unit increases northward; outcrops locally comprise up to 40-50 per cent granitoid dykes and sheets. The southernmost outcrops shown as part of the granitic migmatite unit (Fig. 7) comprise up to 30-40 per cent screens or disrupted panels of metasedimentary rock in various states of assimilation; elsewhere in the unit, metasedimentary material typically comprises 10-20 per cent of any one outcrop.

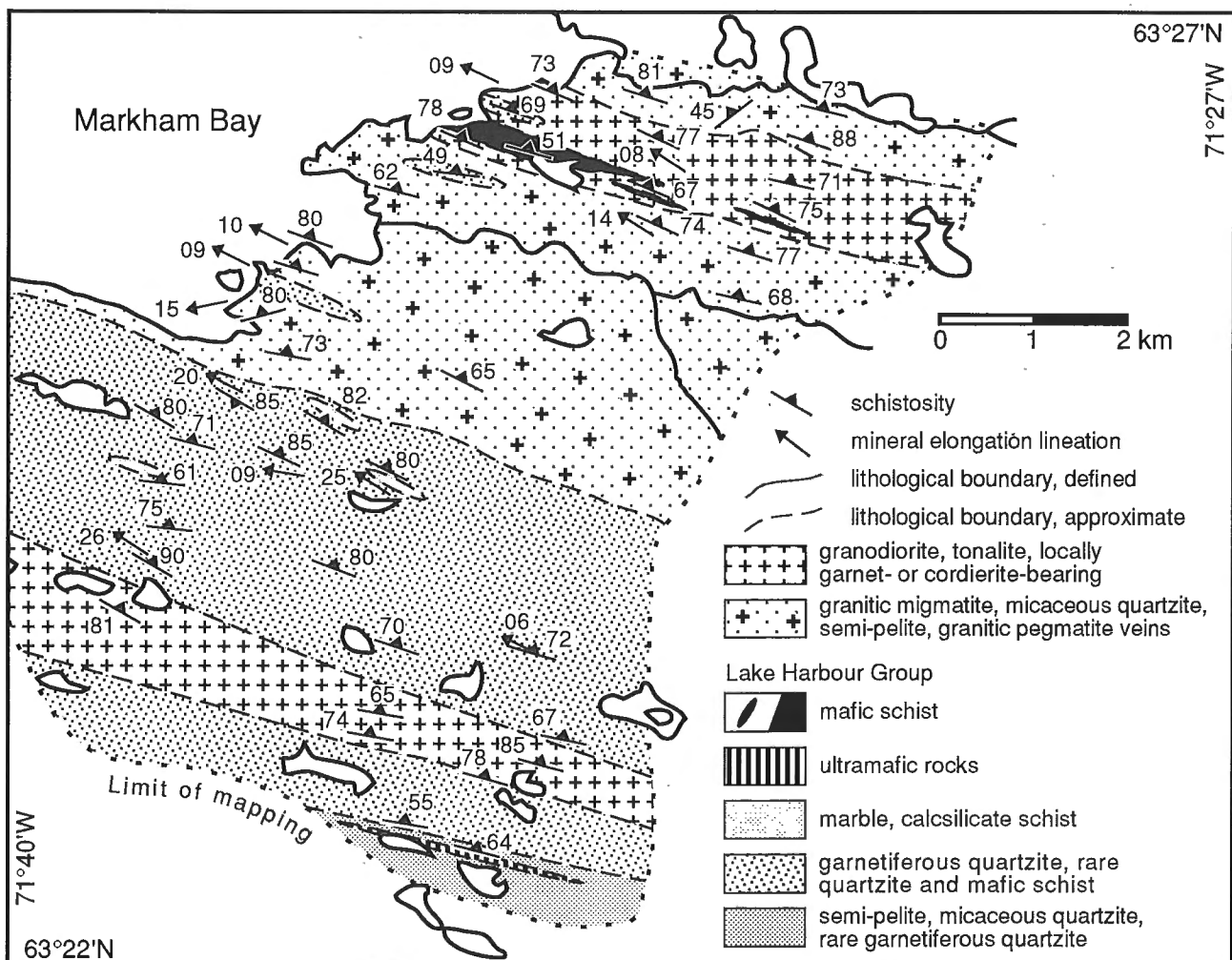


Figure 7. Geological map of the Markham Bay area. See Figure 1 for location.

## DISCUSSION

### *Structure and metamorphism*

Metamorphic assemblages in pelitic rocks in the Soper Lake area (Fig. 2) contain biotite, garnet, sillimanite and melt pods, indicative of mid- to upper-amphibolite facies conditions. Although sillimanite has not been observed in similar rocks in the Markham Bay area, the widespread occurrence of granitic melt pods is consistent with upper-amphibolite facies conditions across this part of southern Baffin (Jackson and Morgan, 1978).

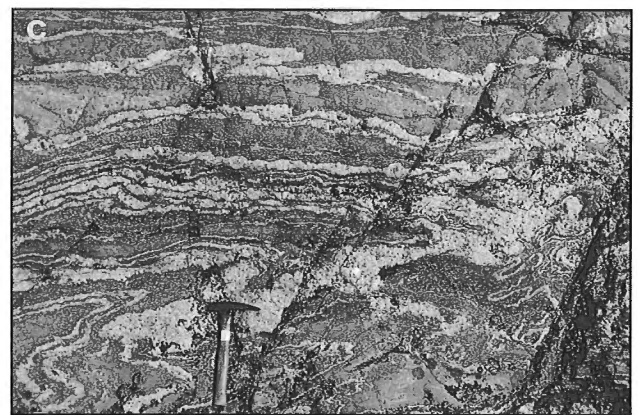
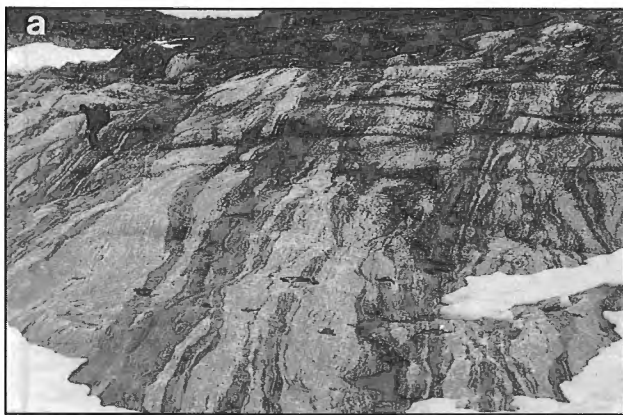
Garnet porphyroblast overgrowths of the penetrative S1 schistosity, and sillimanite generally not aligned parallel to L1 suggest that peak thermal conditions post-dated this phase of deformation. These observations are consistent with the interpretation that crustal thickening led to the development of S1, followed by thermal re-equilibration. S1 has been systematically folded into a series of open- to tight F2 synforms and antiforms across the study area (Fig. 2). As tonalitic rocks truncate S1 fabrics but appear to be folded by F2 (southwest corner of Fig. 2), we suggest that much of the plutonism in the area immediately preceded or accompanied this second phase of deformation. Subsequent ductile flow of the carbonate rocks in the eastern part of the study area has truncated high-strain fabrics developed in quartzofeldspathic units (Fig. 9), dislodged kilometre-scale panels of metasedimentary rocks and re-oriented L1 mineral lineations and F2 fold axes (southeast corner of Fig. 2), and, we believe,

complicated the original stratigraphic sequence of the Lake Harbour Group. This ductile flow may have occurred as a consequence of loading and heating due to crustal thickening, facilitated by additional heat associated with plutonism.

Based on our examination of the small area north of Lake Harbour (Fig. 2), we suggest that the lowest unit in the Lake Harbour Group tectonostratigraphic sequence consists of semi-pelitic schists and micaceous quartzite, overlain by garnetiferous quartzite, followed by marble and calcisilicate schist. Mafic rocks appear to be confined to the western part of the study area, corresponding to higher tectonostratigraphic levels if the sequence postulated above is correct. Due to the tentative nature of this proposed tectonostratigraphic sequence and highly deformed and metamorphosed state of these rocks, we believe it would be premature to offer an interpretation of the primary depositional environment of the Lake Harbour Group.

### *Preliminary U-Pb geochronology*

The following is an overview of the preliminary results of conventional U-Pb isotopic analyses performed at the GEOTOP laboratories, Université du Québec à Montréal, on samples collected during 1993 fieldwork in the vicinity of Soper Lake (Fig. 2). The age of monazite from a melt pod in a semi-pelitic layer southeast of Soper Lake is  $1845 \pm 2$  Ma, suggesting that peak metamorphic conditions may have existed immediately prior this time. The age of monazite in a granitic dyke which



- a) screens of semi-pelitic metasediment in granodioritic host (GSC1994-719Z);
- b) disrupted screens and xenoliths of metasediments (GSC1994-719Q);
- c) agmatitic veining, 35 cm hammer (GSC1994-719S);

**Figure 8.** Granitic migmatite, Markham Bay.



**Figure 9.** Ductile deformation of carbonate rocks (light) has led to the disruption of S1-foliated panels of siliciclastic schist (dark). Height of cliff is 30 m (GSC1994-719W).

truncates the principal deformation fabric in its host micaceous quartzite, but is itself foliated, has been determined as  $1840 \pm 3$  Ma. These observations are consistent with the suggestion that much of the penetrative deformation (S1) preceded or was synchronous with peak metamorphic conditions. Zircon from a granitic sheet parallel to schistosity in tonalitic rocks east of the Lake Harbour Group yielded an age of ca. 1837 Ma, with evidence of an inherited, Archean zircon component, suggesting that this Paleoproterozoic intrusive may have interacted with older crustal material. A zircon fraction from a sample of tonalite from the southeast part of Figure 2 is ca. 1830 Ma, whereas a single monazite grain from this reworked gneiss yielded a concordant age of  $1808 \pm 2$  Ma; we tentatively suggest these ages may correspond to intrusive and cooling events, respectively, and that ductile flow of the carbonate rocks is bracketed by these ages. Monazite from an undeformed granitic dyke which truncates all earlier deformation in its host micaceous quartzite is  $1760 \pm 2$  Ma, indicating that much of the tectonothermal activity in the area had ceased by this time. This preliminary quantitative history must be elaborated in order that the primary stratigraphic sequence and tectonic significance of the Lake Harbour Group can be better understood.

### ***Tectonic interpretation***

The present results, although preliminary and based on an examination of two relatively small areas, are important to an improved understanding of the tectonic evolution of southern Baffin Island. These observations are consistent with previous assertions that the rocks of the Lake Harbour Group are Paleoproterozoic, and have been affected by Paleoproterozoic thermotectonism (e.g., Hoffman, 1989; Jackson et al., 1990). The geometry of the supracrustal succession is insufficiently known at present to assess either primary depositional aspects or kinematics of deformation.

The extant U-Pb data, whose preliminary nature must be emphasized, suggest that the principal deformation of the supracrustal rocks (D1) occurred prior to, or possibly synchronous with, peak metamorphic conditions at ca. 1845-1840 Ma. This is coincident with high-grade

deformation in the Abloviak shear zone (Bertrand et al., 1993; Scott and Machado, 1994); we suggest that these two deformation events may be related.

Emplacement of the tonalitic rocks which surround the rocks of the Lake Harbour Group, possibly synchronous with the second phase of deformation (D2), occurred at least in part during the period ca. 1840-1830 Ma. Rocks of this age are known from the younger (1844-1826 Ma) magmatic suite of the Narsajuaq Arc in the Ungava Orogen (St-Onge et al., 1992), on the opposite side of Hudson Strait; the present results suggest the possibility that the magmatic activity in these two areas is related. In contrast, the present magmatism is distinctly younger than that associated with both the >1.90-1.85 Ga Cumberland Batholith (Pidgeon and Howie, 1975; Henderson, 1985; Jackson et al., 1990), about 100 km north of the present area, and the 1.91-1.87 Ga magmatic arc (Scott and Machado, 1994, in press) in the Torngat Orogen in northernmost Labrador.

The  $1808 \pm 2$  Ma monazite from a tonalitic gneiss sample immediately east of the Lake Harbour Group suggests that high-temperature conditions, possibly accompanied by deformation, prevailed at this time. Deformation at the supracrustal sequence/tonalite interface may therefore have outlasted penetrative deformation within the Lake Harbour Group. The  $1760 \pm 2$  Ma undeformed granitic dyke suggests that much of the regional tectonic activity had ceased by this time, comparable to cessation of events in the Ungava Orogen (1758 Ma; St-Onge et al., 1992).

It appears, from limited field and U-Pb geochronological observations, that much of the tonalitic and granodioritic material adjacent to the supracrustal rocks of the Lake Harbour Group is younger than the metasedimentary rocks. The question of the nature and/or existence of older (Archean?) rocks which were the depositional basement to the Lake Harbour Group has yet to be resolved. Regional mapping and additional isotopic analyses are required to address this question, as well as to establish a more solid understanding of the significance of the rocks of the Lake Harbour Group and their tectonic history.

### **ACKNOWLEDGMENTS**

Funding for this investigation has been provided by NSERC Operating and LITHOPROBE Supporting Geoscience Grants to Nuno Machado. Fixed-wing aircraft support was generously supplied by the Polar Continental Shelf Project through Bradley Air Services, Iqaluit. Special thanks to Dick Deblicquy, whose skillful flying to off-strip destinations got us where we needed to go. Logistical support and radio contact provided by Lynn Peplinski and the staff of the Iqaluit Research Centre (Science Institute of the Northwest Territories) and additional logistical support provided by the GSC are gratefully acknowledged. Lake Harbour residents Sandy Akavak and Matthew Akavak are thanked for their assistance with boats and ATVs, and Sam Pitsiulak for his generous hospitality. Discussions and/or reviews of this manuscript by Jean David, Simon Hanmer, Garth Jackson and Marc St-Onge have contributed to the evolution of the ideas presented here.

## REFERENCES

- Bertrand, J.-M., Roddick, J.C., Van Kranendonk, M.J., and Ermanovics, I.**  
1993: U-Pb geochronology of deformation and metamorphism across a central transect of the Early Proterozoic Torngat Orogen, North River map area, Labrador; *Canadian Journal of Earth Sciences*, v. 30, p. 1470-1489.
- Blackadar, R.G.**  
1967a: Geological reconnaissance, southern Baffin Island, District of Franklin; Geological Survey of Canada, Paper 66-47, 32 p.  
1967b: Geology of Mingo Lake-Macdonald Island map area, Baffin Island, District of Franklin; Geological Survey of Canada, Memoir 345, 54 p.
- Davison, W.L.**  
1959: Geology, Lake Harbour, Baffin Island, District of Franklin, Northwest Territories; Geological Survey of Canada, Map 29-1958, 1:63 360, 1 sheet.
- Ermanovics, I. and Van Kranendonk, M.J.**  
1990: The Torngat Orogen in the North River-Nutak transect area of Nain and Churchill provinces; *Geoscience Canada*, v. 17, p. 279-283.
- Henderson, J.R.**  
1985: Geology, Ekalugad Fiord-Home Bay, District of Franklin, Northwest Territories; Geological Survey of Canada, Map 1606A, 1:250 000, 1 sheet.
- Hoffman, P.F.**  
1989: Precambrian geology and tectonic history of North America; in *The geology of North America - An overview*, (ed.) A.W. Bally and A.R. Palmer; *The Geology of North America*, Volume A, p. 447-512.
- Jackson, G.D., Hunt, P.A., Loveridge, W.D., and Parrish, R.R.**  
1990: Reconnaissance geochronology of Baffin Island, N.W.T.; in *Radiogenic Age and Isotopic Studies: Report 3*; Geological Survey of Canada, Paper 90-3, p. 123-148.
- Jackson, G.D. and Morgan, W.C.**  
1978: Precambrian metamorphism on Baffin and Bylot Islands; in *Metamorphism in the Canadian Shield*, (ed.) J.A. Fraser and W.W. Heywood; Geological Survey of Canada, Paper 78-10, p. 249-267.
- Jackson, G.D. and Taylor, F.C.**  
1972: Correlation of major Aphebian rock units in the northeastern Canadian Shield; *Canadian Journal of Earth Sciences*, v. 9, p. 1650-1669.
- Pidgeon, R.T. and Howie, R.A.**  
1975: U-Pb age of zircon from a charnockitic granulite from Pangnirtung on the east coast of Baffin Island; *Canadian Journal of Earth Sciences*, v. 12, p. 1046-1047.
- Scott, D.J. and Godin, L.**  
1994: Preliminary geological and geochronological investigation of the Lake Harbour Group and surrounding gneissic rocks near Lake Harbour, NWT; in *Report of 1993 ECSOOT Transect Meeting*, (ed.) R.J. Wardle and J. Hall; Report 36, p. 156-162.
- Scott, D.J. and Machado, N.**  
1994: U-Pb geochronology of the northern Torngat Orogen: results from work in 1993; in *Report of 1993 ECSOOT Transect Meeting*, (ed.) R.J. Wardle and J. Hall; Report 36, p. 141-155.  
in press: U-Pb geochronology of the northern Torngat Orogen, Labrador Canada: A record of Paleoproterozoic magmatism and deformation; *Precambrian Research*, v. 70.
- St-Onge, M.R., Lucas, S.B., and Parrish, R.R.**  
1992: Terrane accretion in the internal zone of the Ungava orogen, northern Quebec; *Canadian Journal of Earth Sciences*, v. 29, p. 746-764.
- Van Kranendonk, M.J., Wardle, R.J., Mengel, F.C., Campbell, L.M., and Reid, L.**  
1994: New results and summary of the Archean and Paleoproterozoic geology of the Burwell domain, northern Torngat Orogen, Labrador, Quebec, and Northwest Territories; in *Current Research 1994-C*; Geological Survey of Canada, p. 321-332.
- Van Kranendonk, M.J., Wardle, R.J., Mengel, F.C., Scott, D.J., Bridgwater, D., Godin, L., and Campbell, L.M.**  
1993: Geology and tectonic evolution of the northernmost part of the Paleoproterozoic Torngat Orogen, Labrador, Quebec, and Northwest Territories; in *Report of 1992 ECSOOT Transect Meeting*, (ed.) R.J. Wardle and J. Hall; Report 32, p. 6-20.
- Wardle, R.J., Bridgwater, D., Mengel, F., Campbell, L., Van Kranendonk, M.J., Hauman, A., Churchill, R., and Reid, L.**  
1994: Mapping in Torngat Orogen, northernmost Labrador; Report 3, the Nain craton, including a note on ultramafic dyke occurrences in northernmost Labrador; in *Current Research (1994)*; Newfoundland Department of Mines and Energy, p. 399-407.
- Wardle, R.J., Ryan, B., and Ermanovics, I.**  
1990: The eastern Churchill Province, Torngat and New Québec orogens: An overview; *Geoscience Canada*, v. 17, p. 217-222.

---

 Geological Survey of Canada Project 770013

# A reconnaissance of the high grade metamorphic terrane south of Ghost Lake, southwestern Slave Province, Northwest Territories<sup>1</sup>

J.B. Henderson and T. Chacko<sup>2</sup>  
Continental Geoscience Division

*Henderson, J.B. and Chacko, T., 1995: A reconnaissance of the high grade metamorphic terrane south of Ghost Lake, southwestern Slave Province, Northwest Territories; in Current Research 1995-C; Geological Survey of Canada, p. 77-85.*

---

**Abstract:** A series of isolated fixed wing landings were made throughout much of an 80 km long by up to 35 km wide, triangular shaped, high metamorphic grade terrane that is outlined by a prominent aeromagnetic signature. It is underlain by Archean granitoid gneisses, massive to foliated plutons, and migmatitic to diatexitic supracrustal rocks of the Yellowknife Supergroup. Granulite grade mineral assemblages occur throughout most of the northern, east-central and south-central parts of the terrane. Megascopic orthopyroxene was not observed in the high grade rocks in a zone along the southwestern part. The terrane is fault bounded and has been interpreted as an asymmetric block uplift with most displacement taking place along a major low grade cataclastic shear zone on the east side of the uplift. The maximum age of uplift of the block is interpreted to be 2.1 Ga.

**Résumé :** Une série d'atterrissages isolés par aéronef à voilure fixe ont été effectués sur la grande partie d'un terrane fortement métamorphisé mesurant jusqu'à 80 km de longueur sur 35 km de largeur, de forme triangulaire et délimité par une signature aéromagnétique distincte. Ce terrane repose sur des gneiss granitoïdes archéens, des plutons massifs à feuilletés et des roches supracrustales migmatitiques à diatexitiques du Supergroupe de Yellowknife. Des assemblages minéraux du faciès des granulites sont présents dans presque toutes les parties nord, centre est et centre sud du terrane. Aucune orthopyroxène mégascopique n'a été observée dans les roches très métamorphisées d'une zone longeant la partie sud-ouest du terrane. Le terrane est limité par des failles et on croit qu'il s'agit d'un soulèvement de bloc asymétrique dont le plus grand déplacement s'est effectué le long d'une importante zone de cisaillement cataclastique faiblement métamorphisée sur le côté est du soulèvement. L'âge maximal du soulèvement du bloc est de 2,1 Ga.

---

<sup>1</sup> Contribution to the Slave NATMAP Project

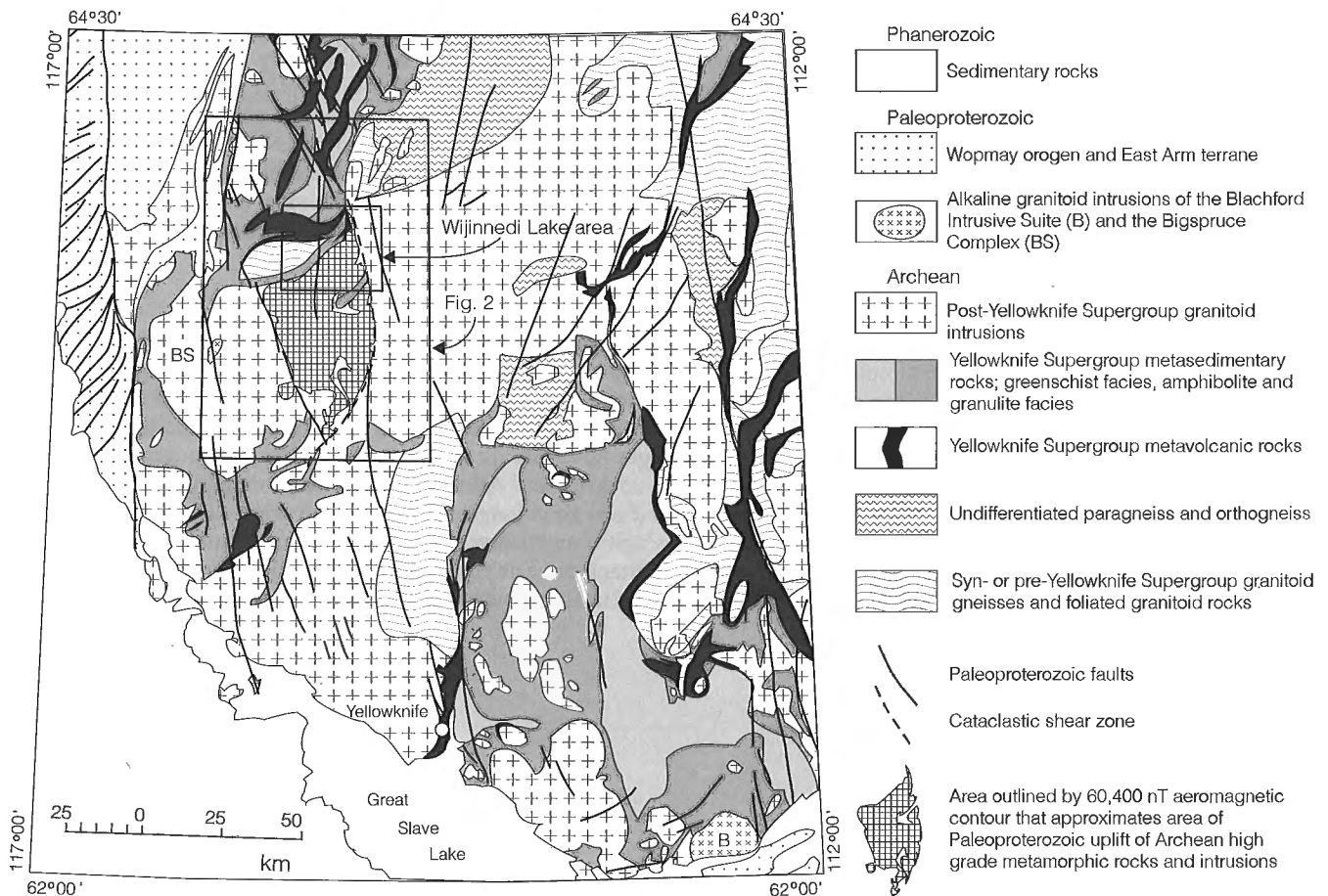
<sup>2</sup> Department of Geology, University of Alberta, Edmonton, Alberta, T6G 2E3

## INTRODUCTION

Regional geological mapping of the Wijinnedi Lake map area in the southwestern Slave Province, together with detailed petrological studies in parts of it, resulted in the recognition of an extensive granulite terrane in the southeastern third of the area (Farquhar et al., 1993; Henderson and Schaan, 1993; Henderson, 1994; Fig. 1). Reported occurrences of granulite grade rocks in the Slave Province are rare. Robertson and Folinsbee (1974) first recognized orthopyroxene in both granite and metasedimentary rocks south of Ghost Lake. Metamorphic orthopyroxene also occurs in several localities in the Winter Lake area 125 km northeast of Ghost Lake (Thompson, 1978, Thompson et al., 1995) and in the northeasternmost part of the supracrustal terrane northeast of Yellowknife (Stubley et al., 1994). Granulite grade assemblages are also reported 15 km north of the northeast corner of the Wijinnedi map area (S.J. Pehrsson, pers. comm., 1994).

Within the Wijinnedi Lake map area, there is a close correspondence between the granulite grade rocks and a generally elevated, as well as high relief, aeromagnetic

expression for the terrane relative to the surrounding region (Fig. 2). As this anomalous magnetic pattern extends some 50 km to the south of the area mapped, Henderson and Schaan (1993) speculated that the high grade rocks may also extend that far. They suggested that the regional anomaly pattern and the exposure of high grade rocks at the present erosion level is the product of a Paleoproterozoic block uplift that juxtaposed the Archean rocks, formed under mid- to lower-crustal granulite grade conditions, against the higher level granitoid and metasedimentary rocks that are characteristic of most of the Slave Province. Their suggestion concerned only an uplift event that took place during the Proterozoic as, in the Wijinnedi Lake map area, the Archean history also includes the relative uplift of a series of domains, whose metamorphic grade varies from greenschist to granulite (Henderson and Schaan, 1993). This Archean uplift took place along a series of wide, ductile, high-grade shear zones that separate the various domains. Preliminary metamorphic pressure-temperature estimates on the ca. 2.6 Ga granulite grade rocks also suggest decompression quickly followed peak metamorphic conditions (Farquhar et al., 1993). In order to confirm the suggestion that exposure of the high grade rocks continues



to the south, float plane landings were made, independently by the two authors, at a variety of locations within the magnetically anomalous area south of Ghost Lake.

The only previous geological mapping in the region was by Lord (1942) and Yardley (1949). The aeromagnetically anomalous terrane was included in their undifferentiated granitoid unit in each case. The area is very well exposed, particularly in the western parts of the terrane where fires in the early seventies have resulted in extensive lichen-free areas of outcrop that rival the quality of coastal exposures.

## **REGIONAL AEROMAGNETIC PATTERN**

The southwesternmost Slave Province is characterized by low amplitude and long wavelength aeromagnetic anomalies that are in strong contrast with the relatively higher amplitude, shorter wavelength anomalies characteristic of much of the province. Geological units within this area have, for the most part, no specific magnetic expression, exceptions being units with unusually high magnetite content such as part of the Gamey Lake volcanic belt west of Damoti Lake (Pehrsson and Beaumont-Smith, 1994; S.J. Pehrsson, pers. comm., 1994), parts of a metagabbro body northwest of Ghost Lake (Henderson, 1994) and phases of the Bigspruce Lake alkalic complex (Cavell and Badsgaard, 1986). The greatest departure from this generally quiet pattern is the triangular region of relatively elevated magnetic field characterized by high amplitude - short wavelength anomalies that is thought to outline the proposed high-grade uplift at the eastern margin of this anomalously flat aeromagnetic terrane (Fig. 2).

## **MARGINS OF THE STRUCTURE**

### *Eastern margin*

The structure as outlined by the aeromagnetic pattern is roughly triangular in shape (Fig. 2). The eastern margin corresponds to a prominent, gently curved, topographic lineament that, where mapped, is the locus of a locally complex, low grade, cataclastic shear zone (Henderson, 1994). The contact of the shear zone with the minimally deformed and altered high grade rocks to the west is quite abrupt with granites containing altered pyroxene occurring within 50 m of the main fault zone. The rocks to the east of the lineament, however, are intensely deformed and altered with the degree of cataclastic breakdown and chloritization of the dominantly granitoid rocks decreasing over a distance up to several kilometres. This asymmetry of the shear zone is reflected in aeromagnetic profiles across it with the locally very high magnetic expression of some of the high grade rocks in the west dropping abruptly at the western margin of the shear zone before more gradually increasing again to the east (Fig. 3).

To the north, the trend of the shear zone becomes north-northwesterly, similar to that of the Indin - West Bay faults that are so abundant at and north of Indin Lake and in and

west of the Yellowknife region (Brown, 1955) (Fig. 1). The cataclastic shear zone appears to be traceable as far north as Damoti Lake along a fault previously mapped by Tremblay et al. (1953). Where seen on the northwest shore of Daran Lake, it has an asymmetric chlorite alteration zone, over a kilometre wide, similar to that east and south of Ghost Lake. This cataclastic fault, with its prominent alteration zone, is distinct from the Indin - West Bay faults which tend to be narrow and brittle with minor alteration. While the Indin faults have sinistral strike separation, the cataclastic fault, as noted by Tremblay (1948), has apparent dextral strike separation on the basis of the metamorphic zonation pattern in the vicinity of Ranji Lake. From a more regional perspective, however, the Archean metamorphic pattern northeast of the fault and the fault's hypothetical projection to the northwest through Indin Lake is quite distinct from that to the southwest. A possible explanation for the much greater proportion of greenschist grade rocks at the present erosion level to the northeast could be that the terrane to the southwest has moved up with respect to that to the northeast (Frith, 1993) (Fig. 1).

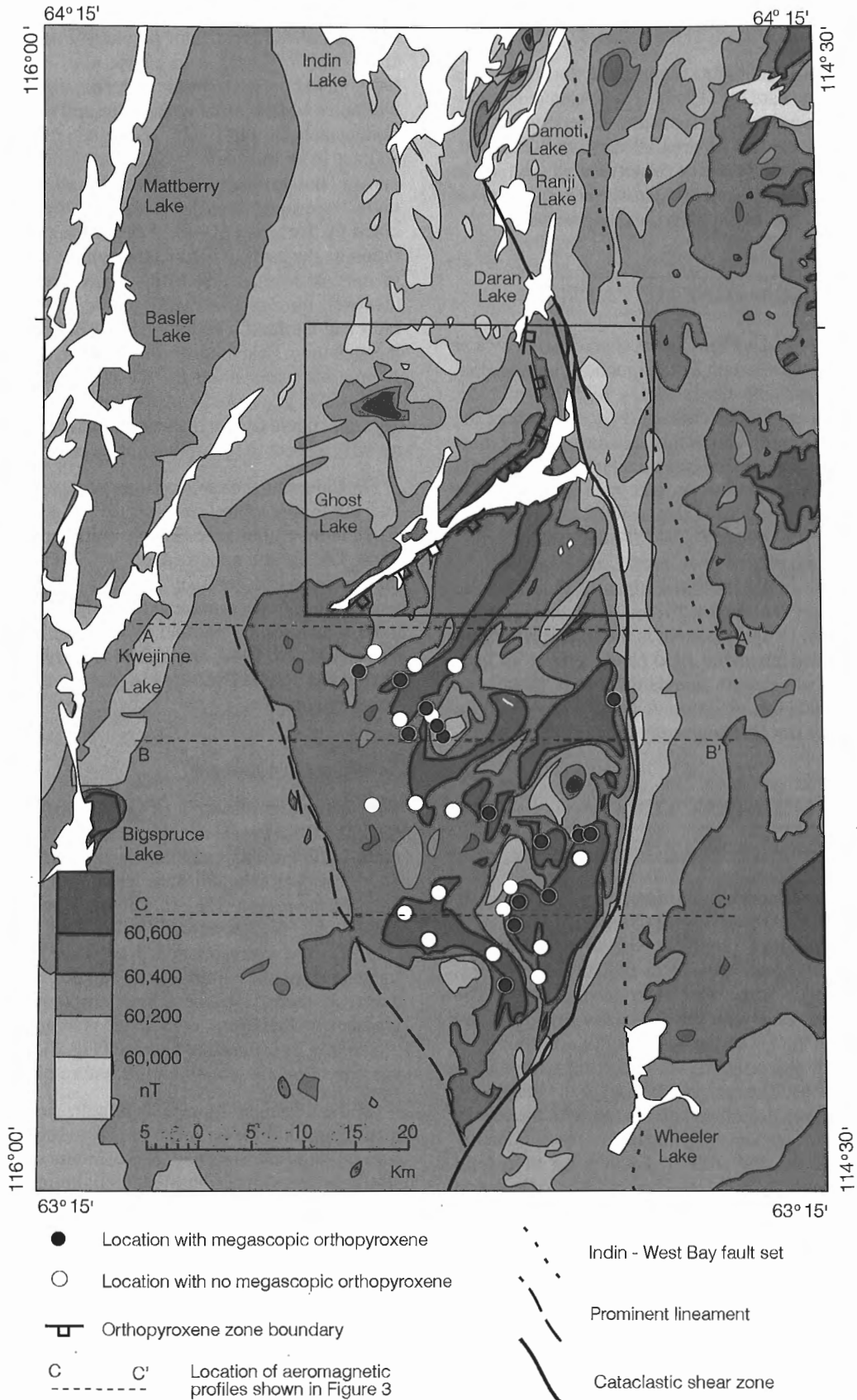
To the south, the shear zone assumes a southwesterly trend and the topographic lineament by which it is expressed is much more pronounced, locally being up to half a kilometre wide. The lineament extends some 5 km beyond the extent of the aeromagnetic anomaly where it splays into several lineaments that have a more west-southwesterly trend. These latter structures are parallel to Archean lithological units in that area (Lord, 1942) and also to the major Paleoproterozoic dextral McDonald Fault that in part bounds the southeastern Slave Province.

### *Southwestern margin*

The southwestern margin of the anomaly as defined by the 60 400 nT contour also corresponds to a relatively straight, north-northwesterly trending lineament that is well defined on air photographs and, to a lesser degree, the topographic maps of the region (Fig. 2). The lineament is also similar in trend to the Paleoproterozoic Indin-West Bay series of faults (Fig. 1). The correspondence between the position of the lineament and the aeromagnetic contour is more than coincidental as there is either a break in slope of the magnetic gradient at the linear or a local increase in the magnetic gradient in its immediate vicinity (Fig. 3). This structure was not visited on the ground and its nature remains unknown.

If the lineament represents a fault, the sense of displacement appears to be largely vertical as there is no horizontal translation of the aeromagnetic contours across the line. The similarly trending Indin-West Bay series of faults have a dominant sinistral component of movement (e.g., Brown, 1955). This is based on the separated lithological contacts apparent in map views and the work of Campbell (1948) who, in an attempt to determine the location of an offset gold ore body at Yellowknife, determined an approximately 10:1 ratio of horizontal to vertical displacement on the West Bay fault, an estimate subsequently confirmed by drilling.





### Northwestern margin

The geology in the vicinity of the northwestern margin of the uplift is better known as most of it is within the Wijinnedi Lake map area (Henderson and Schaan, 1993; Henderson, 1994). The boundary zone, at least as defined by the aeromagnetic pattern, occurs well within the Ghost domain, which consists of high grade rocks including migmatitic supracrustal rocks, granitoid gneisses and granitoid rocks (Henderson and Schaan, 1993). This high grade domain is separated from lower grade domains to the north by high grade ductile shear zones that are considered to be Archean (Henderson and Schaan, 1993). The northwest side of the aeromagnetic anomaly is approximately parallel to the megascopic orthopyroxene zone boundary (Fig. 2), although in most places, the break in slope of the gradient between the anomaly and the regional field occurs 1 to 2 km to the north of this boundary. The Ghost domain rocks north of the zone boundary, while not orthopyroxene bearing, are also at high metamorphic grade. No low metamorphic grade shear zones have been recognized in this area although the contact between the dominantly metasedimentary migmatites of the Ghost domain and the granitoid gneisses of the adjacent Hinscliffe domain to the north, wherever crossed, was obscured by several metres of cover that could represent the locus of a shear zone formed under low metamorphic grade conditions.

The main part of the northwestern aeromagnetic anomaly boundary has a northeasterly trend parallel to the Archean structural and lithological grain of the Ghost domain. This is the dominant Archean structural trend seen in many areas in the southwestern Slave Province west of western Point Lake and Yellowknife. The aeromagnetic trend, along with the geological trends, including the orthopyroxene zone boundary, swings north as the eastern cataclastic margin of the uplifted block is approached. This bend is considered to be an Archean structure. The change in trend is coincident with a series of northerly to north-northwesterly trending faults within the uplift that are roughly parallel to the trend of the main cataclastic break to the east (Henderson, 1994). The high grade migmatitic metasedimentary rocks continue north

**Figure 2.**

Aeromagnetic map of the Ghost Lake region. The roughly triangular shaped, slightly elevated, high relief anomaly that outlines the uplift occurs at the eastern margin of a region characterized by aeromagnetic anomalies having low amplitudes and long wavelengths. This contrasts with the shorter wavelengths and higher relief of anomalies that are prevalent to the east and which are more characteristic of the Slave Province as a whole. The locations of outcrops seen in the course of the reconnaissance is shown with the presence or absence of megascopically identified orthopyroxene indicated. The Wijinnedi Lake map area that is outlined has been geologically mapped at 1:50 000 scale. The location of the cataclastic shear zone south of that area is based on interpretation of air photographs on which it is evident as a prominent lineament.

another 20 km from the point where the trend of the magnetic anomaly pattern swings north to the south shore of Ranji Lake (Fig. 2) (Tremblay et al., 1953).

### HIGH GRADE ROCKS WITHIN THE UPLIFT

The geology within the uplift south of the Wijinnedi Lake map area is known only from a series of fixed wing aircraft landings whose locations are indicated in Figure 2. These

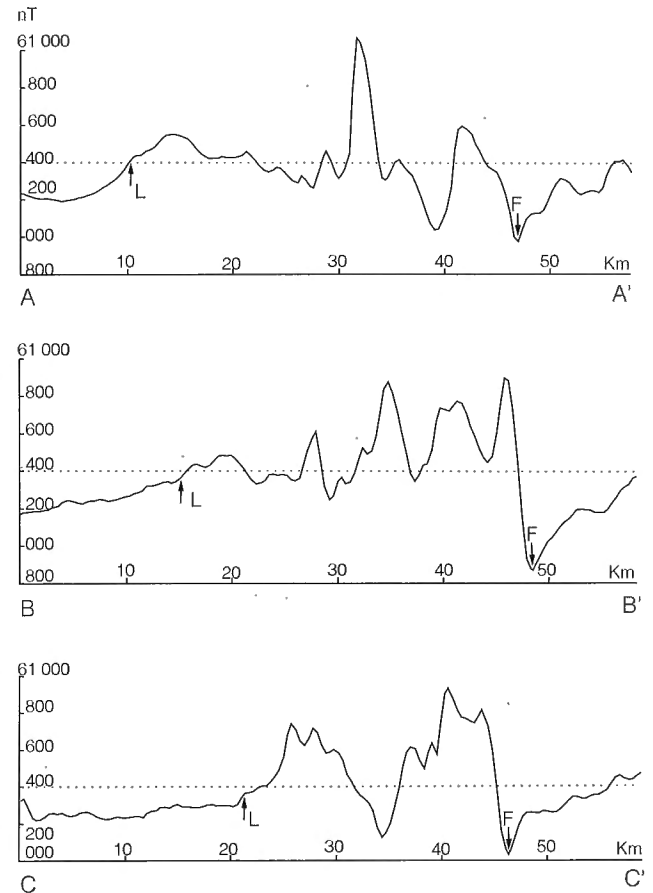


**Figure 3.** Aeromagnetic profiles across the uplift. The locations of the profiles are indicated in Figure 2. The dotted 60 400 nanoTesla line corresponds to the contour in Figure 2 that outlines the triangular shape of the uplift. Arrows at F in each profile indicate the position of the pronounced negative anomaly that in the Wijinnedi Lake area in the northern part of the uplift corresponds to the cataclastic shear zone that marks its eastern margin. The arrows at L in each profile represent the location of a prominent linear structure, possibly a fault, that closely corresponds to the western margin of the anomaly as outlined by the 60 400 nT contour. As can be seen in at least two of the profiles and on the more closely contoured aeromagnetic map of the region (Geological Survey of Canada, 1969), there is a slight break in the magnetic gradient at this point. In profile AA', the pronounced negative anomaly 8 km west of the uplift boundary negative anomaly (F) is due to a 2 km wide belt of metasedimentary rocks.

outcrops can be classified into three general categories consisting of granitoid gneisses, metasedimentary rocks, and massive to weakly foliated granitoid rocks. In many cases more than one type is present at any given locality. Given the small number of isolated observations and the apparent complexity of the geology, it is not possible to outline the distribution of the various lithological units.

### **Granitoid gneisses**

Weakly to moderately foliated granitoid gneisses appear to be the dominant rock type within the uplift (Fig. 4). The generally medium grained, even grained rocks have a typical pinkish buff to buff weathered colour and greasy green to yellow brown fresh colour where at granulite grade. At lower grades they are an intermediate to light grey colour. The gneisses are moderately heterogeneous in composition with granodioritic to tonalitic compositions dominating. Layering on a 10 to 40 cm scale is expressed by commonly subtle compositional and textural variations although amphibolitic layers and inclusions within the gneiss are common. Layers and inclusions of metasedimentary origin are rare, although one example of possible iron-formation was noted. Mafic minerals include varied proportions of biotite, hornblende and, at higher grades, clino and orthopyroxene. The heterogeneous granitoid gneisses are generally garnet-free.

The gneisses contain or are intruded by a variety of pods, lenses and veins of pegmatitic granite. Where associated with granulite grade gneisses, these bodies can either contain pyroxene or locally retrogress the adjacent gneiss, reflecting perhaps more a variation in the water content of these intrusions at the time of their formation, than their emplacement

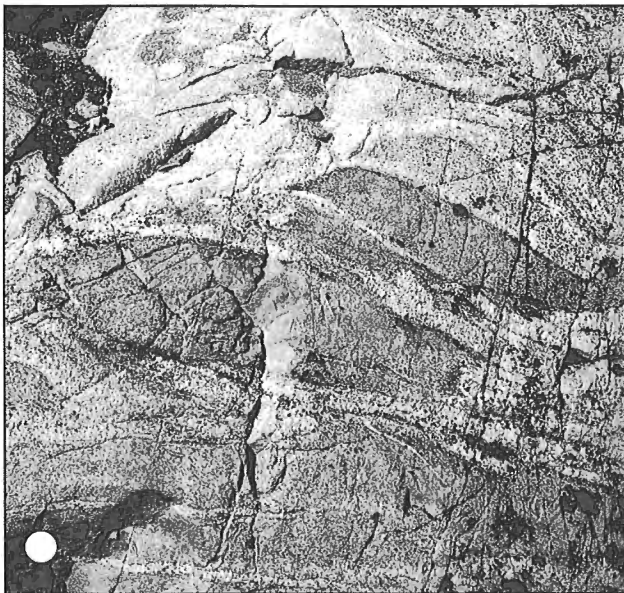


**Figure 4.** Complex granitoid orthogneisses intruded by leucocratic granite-pegmatite phases from the western part of the uplift. Orthopyroxene was not recognized in these rocks at least at the outcrop or hand specimen scale. White dot is 4 cm in diameter. (GSC 1994-716C)

at different times under different conditions. Also present in some areas are intrusions of larger bodies of massive to weakly foliated granite to granodiorite that are related to the larger bodies of plutonic rocks discussed below.

Some of these rocks bear a strong resemblance to layered orthogneiss complexes elsewhere in the Slave Province such as the Hinscliffe complex immediately northwest of Ghost Lake (Henderson and Schaan, 1993), the Cotterill Lake complex 20 km north northeast of Ghost Lake (Frith, 1993; Pehrsson and Beaumont-Smith, 1994) and the Anton Complex north of Yellowknife.

### **Metasedimentary rocks**

Metasedimentary rocks were seen in only a few localities south of the Wijinnedi Lake map area within which they are quite abundant. They may be more abundant than would be indicated by this reconnaissance survey. The prominent, up to 2.5 km wide, southwest-trending metasedimentary belt near the southeast corner of the Wijinnedi Lake area (Henderson, 1994) has a pronounced low aeromagnetic expression that extends at least another 10 km into the uplift south of the Wijinnedi Lake map area (Fig. 2, 3). Several other areas of low aeromagnetic expression may also be due to the occurrence of metasedimentary rocks.

Migmatitic metasedimentary rocks ranging from layered metatexite to homogeneous diatexite are similar to those described in the high grade parts of the Wijinnedi Lake area (Farquhar et al., 1993; Henderson and Schaan, 1993; Henderson, 1994) where they are thought to have been derived from a particularly pelite-rich facies of the Yellowknife Supergroup. The typically well-layered migmatites (Fig. 5) contain

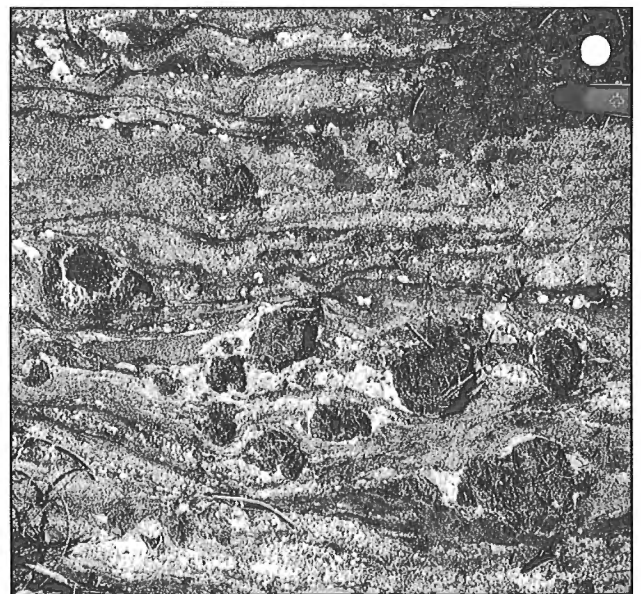


**Figure 5.** Metasedimentary migmatite with coarse garnet from the north central part of the uplift. White dot is 3 cm in diameter. (GSC 1994-716E)

assemblages of the minerals quartz, plagioclase, biotite, cordierite, garnet, and less commonly microcline and sillimanite. Pyroxene-bearing metasedimentary migmatites, although noted, are rare. The more leucocratic diatexites are more homogeneous and can be distinguished from the massive to weakly foliated granitoids by their distinctive texture and the common occurrence of garnet and cordierite. In the few exposures of metasedimentary diatexite seen to the south, psammitic layers and inclusions, in places containing pyroxene, are common.

No rocks that could be interpreted as representing meta-volcanic rocks were identified. The only mafic material recognized are relatively thin layers of amphibolite associated with some of the granitoid gneisses and these are thought more likely to represent transposed and metamorphosed mafic dykes or sills than volcanic remnants.

### *Massive to weakly foliated granitoid rocks*

Massive to weakly foliated granitoid rocks, which dominate the northern part of the uplift in the Wijinnedi Lake area, appear to be less abundant to the south. These rocks can be divided into microcline megacrystic granite and equigranular granitoid intrusions. In the Wijinnedi Lake area preliminary U-Pb (zircon) analyses have been completed from examples from each of these types, both having been emplaced under granulite grade conditions. The large megacrystic granite south of Ghost Lake has an age of  $2598 \pm 2$  Ma while an equigranular granite at the eastern margin of the uplift has an age of  $2589 \pm 1$  Ma (Villeneuve and van Breemen, 1994). In both cases the zircons had simple igneous crystal morphology. These ages are near the young end of the 2.62-2.58 Ga age spectrum for post-Yellowknife Supergroup granitoid rocks of the Slave Province (van Breemen et al., 1992).

Megacrystic granite also occurs as two large bodies south of the Wijinnedi Lake map area. The northern occurrence is the extension of the large elongate body south of Ghost Lake and indicates this body is in excess of 20 km in length. Towards the southern end of the uplift, several landings were made on a second similar megacrystic granite that has an extent of at least 5 km. The granites are densely megacrystic with microcline crystals in the order of 8 cm. Biotite is the dominant mafic mineral; orthopyroxene and garnet are more sporadically present. Pegmatitic lenses containing pyroxenes up to 2 cm in size occur locally (Fig. 6). The granite locally contains abundant inclusions of dominantly psammitic metasedimentary rocks that commonly contain orthopyroxene at their margins.

The equigranular granites are more heterogeneous in composition, ranging from granite to tonalite. Their colour varies from yellow to greenish brown to pink depending on metamorphic grade or degree of retrogression or alteration. On the whole these rocks are medium grained. Their mafic mineral content consists of assemblages of biotite, hornblende, and pyroxene, again depending on grade. In the Wijinnedi Lake area, these intrusions dominate along the eastern margin of the uplift where they are at granulite grade although a few small sub-granulite grade plugs are also present locally. Most

of the examples seen south of the Wijinnedi Lake area are either sub-granulite grade or are altered. At several localities these granitoid intrusions are intimately associated with the granitoid gneisses, containing inclusions of them. The inclusions are mainly granitoid gneisses but also include a one location in the southwest part of the uplift, amphibolite, amphibolitic gneiss, and anorthositic metagabbro. The granitoid gneiss inclusions at this locality are strongly assimilated with poorly defined ghost-like outlines.

## METAMORPHIC PATTERN

Although little can be said about the distribution of the lithological units without further, more systematic mapping at a fairly detailed scale, a general pattern is emerging regarding the extent of granulite grade rocks. Most of the rocks observed in the eastern and central parts, extending almost to the southern end of the uplift (Fig. 2), are at granulite grade, defined for this purpose by the recognition of orthopyroxene in hand specimen or on the outcrop. There appears to be a zone along the western side of the uplift where the rocks are not at granulite grade although it should be emphasized the coverage is by no means complete or evenly distributed. These rocks which are lithologically similar to the granulite grade rocks may represent either the retrogressed equivalents of the granulite grade rocks to the east or may never have reached that grade. Even within the area dominated by granulite grade rocks there are occurrences where the rocks are sub-granulite. In some cases this may be related to post metamorphic alteration as some of the localities are near prominent lineaments that are possibly due to faults related to the uplift of the block.



*Figure 6. Coarse pyroxene in a pegmatitic sweat within megacrystic granite from the southern part of the uplift. Knife is 10 cm long. (GSC 1994-716D)*

## DISCUSSION

A reconnaissance of the southern part of the poorly known, aeromagnetically anomalous terrane at and south of Ghost Lake in the southwestern Slave Province indicates that it is underlain primarily by high grade gneisses, plutons and migmatitic to diatexitic supracrustal rocks that are in large part at granulite grade. As such it is similar to the southern part of the recently mapped Wijinnedi Lake area at the north end of the terrane. The terrane appears to be fault bounded with a dominant, wide, low grade cataclastic shear zone on the east side that extends to both north and south, well beyond the extent of the anomaly. The southwestern margin of the anomaly corresponds to a topographic lineament whose trend is similar to the mainly transcurrent West Bay - Indin faults that occur throughout the southwestern Slave Province. The northwestern margin is more cryptic but may be coincident with similarly trending high grade Archean ductile shear zones.

It was previously suggested that the uplift of this terrane was mainly along the eastern low grade cataclastic fault and that therefore the uplift of the block was asymmetric (Henderson and Schaan, 1993). The evidence for this was the perceived asymmetry of the magnetic anomaly (Fig. 3) but is also supported by the distribution of granulite grade rocks in the eastern, central, and southern part of the uplift with an apparent sub-granulite zone along the southwestern side of the uplift. Supporting this sense of asymmetry is the attitude of the Indin dykes within the Wijinnedi Lake area at the northern end of the uplift. About 80 per cent of the dominantly northeasterly and northwesterly trending dykes that were measured have an average dip of 82° in an easterly direction. If this is related to tilting of the uplift subsequent to their emplacement, it would suggest the east side may have risen in the order of 3 or 4 km higher than the west side. Mafic dykes are deformed in the main cataclastic shear zone as well as in subsidiary structures associated with it, further evidence that the dykes predate the uplift.

There would appear to be an association between the uplift and the West Bay-Indin fault set in that the north end of the cataclastic shear zone on the east side of the uplift becomes parallel to the West Bay-Indin fault trend and the topographic lineament at the southwestern margin of the uplift is also parallel to these faults (Fig. 2). The Indin-West Bay faults everywhere have a dominant sinistral strike slip component and the vertical component of displacement, where determined, has been shown to be relatively minor (Campbell, 1948). On the other hand, there is little evidence to suggest that the uplift of the high grade terrane involved anything other than vertical movement. It is possible then that the uplift of the high grade terrane postdated the dominantly transcurrent West Bay-Indin faulting event but these pre-existing structures may have acted as zones of weakness along which the subsequent, largely vertical, movement could take place. There is no direct evidence as to the age of uplift but the maximum age can be constrained to some degree. As argued above, the Indin dykes predate the uplift but the only age information on them is K-Ar whole rock data suggesting an age of about 2.0 Ga (Leech, 1966). The Indin dykes are offset by the West Bay-Indin faults at Yellowknife

(Henderson and Brown, 1966) which are constrained in time by their relations with the Blatchford Lake Intrusive Suite and the Great Slave Supergroup of the East Arm of Great Slave Lake. These have been dated at 2.09 and 1.87 Ga respectively (Bowring et al., 1984; Fig. 1). If the uplift is synchronous with or postdates West Bay - Indin faulting, uplift took place during or after this time period. The maximum age of uplift would therefore be about 2.1 Ga while the only minimum age constraint is the 1268 Ma Mackenzie dyke swarm (LeCheminant and Heaman, 1989) which cuts all structures in the Slave Province. Only one probable Mackenzie dyke has been recognized within the uplift but its dip has not been observed.

Previously Henderson and Schaan (1993) suggested that the uplift may have been a consequence of the indentation of most of the Slave Province into the western Churchill Province along the Bathurst and McDonald faults between 1.84 and 1.74 Ga (Henderson et al., 1990), an interpretation that continues to fit with the maximum age constraints just outlined. Similar isotopic methods to those used to constrain the age of indentation in the eastern Slave Province (Henderson et al., 1990) might be attempted to more directly estimate the age of this uplift in the southwestern Slave Province.

## ACKNOWLEDGMENTS

The data used for Figure 3 were provided by the Geophysical Data Centre and the plot made by D. Abbinett of the Potential Fields Section. The hospitality extended by S.J. Pehrsson and discussions on the geology of the Indin Lake region during a visit to Daran Lake by J.B.H. was greatly appreciated. T.C. thanks M. Perks and P. Wagner for good company and able assistance in the field. The paper has benefited from reviews by Sally J. Pehrsson, Mike D. Thomas, and Peter H. Thompson.

## REFERENCES

- Bowring, S.A., van Schmus, W.R., and Hoffman, P.F.**  
1984: U-Pb zircon ages from Athapuscow aulacogen, East Arm of Great Slave Lake, N.W.T., Canada; *Canadian Journal of Earth Sciences*, v. 21, p. 1315-1324.
- Brown, I.C.**  
1955: Late faults in the Yellowknife area; *Geological Association of Canada, Proceedings*, v. 7, p. 123-138.
- Campbell, N.**  
1948: West Bay fault; in *Structural Geology of Canadian Ore Deposits*; Canadian Institute of Mining and Metallurgy, Symposium Volume, p. 244-259.
- Cavell, P.A. and Baadsgaard, H.**  
1986: Geochronology of the Big Spruce Lake alkaline intrusion; *Canadian Journal of Earth Sciences*, v. 23, p. 1-10.
- Farquhar, J., Stavely, J.A., and Chacko, T.**  
1993: Granulite facies metamorphism near Ghost Lake, Slave Province, N.W.T.; *Geological Association of Canada / Mineralogical Association of Canada, Program and Abstracts*, 1993, v. 18, p. A28.
- Frith, R.A.**  
1993: Precambrian geology of the Indin Lake map area, District of Mackenzie, Northwest Territories; *Geological Survey of Canada, Memoir 424*, 63 p.
- Geological Survey of Canada**  
1969: Wecho River, District of Mackenzie, Northwest Territories; *Geological Survey of Canada, Geophysics Paper 7196, Map 7196G*, scale 1:253 440.

**Henderson, J.B.**

1994: Geology of the Wijinnedi Lake area - a Paleoproterozoic(?) asymmetric uplift of Archean rocks on the southwestern Slave Province, District of Mackenzie, Northwest Territories; in *Current Research 1994-C*, Geological Survey of Canada, p. 71-79.

**Henderson, J.B. and Schaan, S.E.**

1993: Geology of the Wijinnedi Lake area: a transect into mid-crustal levels in the western Slave Province, District of Mackenzie, Northwest Territories; in *Current Research, Part C*; Geological Survey of Canada, Paper 93-1C, p. 83-91.

**Henderson, J.B., McGrath, P.H., Theriault, R.J., and van Breemen, O.**

1990: Intracratonic indentation of the Archean Slave Province into the early Proterozoic Thelon Tectonic Zone of the Churchill Province, northwestern Canadian Shield; *Canadian Journal of Earth Sciences*, v. 27, p. 1699-1713.

**Henderson, J.F. and Brown, I.C.**

1966: Geology and structure of the Yellowknife Greenstone Belt, District of Mackenzie; Geological Survey of Canada, Bulletin 141, 87 p.

**Hoffman, P.F. and Hall, L.**

1993: Geology, Slave craton and environs, District of Mackenzie, Northwest Territories; Geological Survey of Canada, Open File 2559, scale 1:1 000 000.

**LeCheminant, A.N. and Heaman, L.M.**

1989: Mackenzie igneous events, Canada; middle Proterozoic hotspot magmatism associated with ocean opening; *Earth and Planetary Science Letters*, v. 96, p. 38-48.

**Leech, A.P.**

1966: Potassium-argon dates of basic intrusive rocks of the District of Mackenzie, N.W.T.; *Canadian Journal of Earth Sciences*, v. 3, p. 389-412.

**Lord, C.S.**

1942: Snare River and Ingray Lake map-areas, Northwest Territories; Geological Survey of Canada, Memoir 235, 55 p.

**McGlynn, J.C.**

1977: Geology of the Bear-Slave Structural Provinces, District of Mackenzie; Geological Survey of Canada, Open File 445.

**Pehrsson, S.J. and Beaumont-Smith, C.**

1994: Preliminary report on the geology of the Indin Lake supracrustal belt, western Slave Province, Northwest Territories; in *Current Research 1994-C*, Geological Survey of Canada, p. 91-102.

**Robertson, D.K. and Folinsbee, R.E.**

1974: Lead isotope ratios and crustal evolution of the Slave craton at Ghost Lake, Northwest Territories; *Canadian Journal of Earth Sciences*, v. 11, p. 819-827.

**Stubley, M.P., Cairns, S.R., King, J.E., Jaegli, K., and Tyler, T.**

1994: Geology of the Ames Lake area, south-central Slave Province (NTS 85 P/6&11); Indian and Northern Affairs, Canada, EGS 1994-11, 1:50 000 scale.

**Thompson, P.H.**

1978: Archean regional metamorphism in the Slave Structural Province - a new perspective on some old rocks; in *Metamorphism in the Canadian Shield*, (ed.) J.A. Fraser and W.W. Heywood; Geological Survey of Canada, Paper 78-10, p.85-102.

**Thompson, P.H., Russell, I., Paul, D., Kerswill, J.A., and Froese, E.**

1995: Regional geology and mineral potential of the Winter Lake - Lac de Gras area, central Slave Province, District of Mackenzie, Northwest Territories; in *Current Research 1995-C*; Geological Survey of Canada, this volume.

**Tremblay, L.P.**

1948: Ranji Lake map-area, Northwest Territories; Geological Survey of Canada, Paper 48-10, 7 p.

**Tremblay, L.P., Wright, G.M., and Miller, M.L.**

1953: Ranji Lake, District of Mackenzie, Northwest Territories; Geological Survey of Canada, Map 1022A, scale 1:63 360.

**van Breemen, O., Davis, W.J., and King, J.E.**

1992: Temporal distribution of granitoid plutonic rocks in the Archean Slave Province, northwest Canadian Shield; in *The Tectonic Evolution of the Superior and Slave Provinces of the Canadian Shield*, (ed.) K.D. Card and J.E. King; *Canadian Journal of Earth Sciences*, v. 29, p. 2186-2199.

**Villeneuve, M.E. and van Breemen, O.**

1994: A compilation of U-Pb age data from the Slave Province; Geological Survey of Canada, Open File 2972, 53 p.

**Yardley, D.H.**

1949: Wecho River (east half), Northwest Territories; Geological Survey of Canada, Paper 49-14, scale 1:126 720.

---

Geological Survey of Canada Project 870008-JB



# Thematic structural studies in the Slave Province: preliminary results and implications for the Yellowknife Domain, Northwest Territories

Wouter Bleeker<sup>1</sup> and Chris Beaumont-Smith<sup>2</sup>

Continental Geoscience Division

*Bleeker, W. and Beaumont-Smith, C., 1995: Thematic structural studies in the Slave Province: preliminary results and implications for the Yellowknife Domain, Northwest Territories; in Current Research 1995-C; Geological Survey of Canada, p. 87-96.*

---

**Abstract:** Preliminary results indicate that the structure of the area is dominated by two phases of regional folding that produce mushroom-type interference patterns. The Sleepy Dragon Complex is such a regional-scale interference structure. Its geometry and timing of formation contradict the hypothesis that the complex represents a core complex. They also cast doubt on previous kinematic studies. F<sub>2</sub> folding was a response to dextral transpression during which both the Defeat Suite and Prosperous Suite granitoids were emplaced. Regional low-pressure metamorphism is largely late-D<sub>2</sub> and associated with granitoid emplacement. Following F<sub>2</sub> folding, D<sub>2</sub> dextral transpression became localized in discrete dextral shear zones that record retrograde metamorphism.

**Résumé :** Les résultats préliminaires révèlent que la structure de la région est dominée par deux phases de plissement régional qui produisent des motifs d'interférence en forme de champignon. Le Complexe de Sleepy Dragon est une structure d'interférence d'échelle régionale de ce genre. Sa géométrie et l'époque de sa formation contredisent l'hypothèse selon laquelle le complexe représenterait un complexe interne. Elles jettent aussi un doute sur les études cinématiques antérieures. Le plissement F<sub>2</sub> a été une réponse à une transpression dextre durant laquelle se sont mis en place les granitoïdes de la Suite de Defeat et de la Suite de Prosperous. Le métamorphisme régional de basse pression date en majeure partie de la fin de D<sub>2</sub> et est associé à la mise en place des granitoïdes. Après le plissement F<sub>2</sub>, la transpression dextre D<sub>2</sub> est devenue locale, dans des zones de cisaillement dextres distinctes qui témoignent d'un métamorphisme rétrograde.

---

<sup>1</sup> Geological Survey of Canada, Continental Geoscience Division, 5013-51st Street, Yellowknife, Northwest Territories X1A 1S5

<sup>2</sup> Department of Geology, University of New Brunswick, Box 4400, Fredericton, New Brunswick E3B 5A3



## INTRODUCTION

In recent years, generalized accretionary models have been developed to explain the tectonic history of the Archean Slave Structural Province (e.g., Fyson and Helmstaedt, 1988; Hoffman, 1990; Kusky, 1990). Too few of these models are firmly based on field data. Where detailed field data have been used to support tectonic hypotheses, controversy remains as to the correct interpretation of the structural and stratigraphic relationships (e.g., thrusts, fold vergences, kinematic indicators, etc.). Other scholars of the Slave province, including those who have been involved in mapping large parts of the province, favour less mobilistic views in which the volcanic and associated sedimentary sequences are thought to have been deposited in ensialic rifts (e.g., Henderson, 1985).

A central issue to the controversy, which is as current for the Slave province as for greenstone belts worldwide (e.g., de Wit and Ashwal, 1986; Bickle et al., 1994), is the relationship between older "basement" rocks and overlying supracrustal sequences. In accretionary models, volcanic sequences, some of which may be of oceanic affinity, were accreted onto older continental crust – hence horizontal translations were large, contacts between gneisses and volcanic sequences are dominantly structural, and processes are thought to have been similar to those associated with Phanerozoic-style plate tectonics. In ensialic rift models, although contacts may have been modified, horizontal translations are thought to have been insignificant – hence stratigraphic relationships should be largely preserved with gneiss-volcanic contacts signifying extrusion of thick greenstone piles onto pre-existing continental crust. Marginal basin or back-arc basin models (Tarney et al., 1976) are attractive because they have the potential of reconciling both views – the evolution of (ensialic) rift basins within overall convergent plate margin settings.

The aim of our study is to resolve some of these first-order tectonic questions for greenstone belts in the Slave Province. The Yellowknife Domain, and in particular the Sleepy Dragon Complex and its associated greenstone belts (Fig. 1), were selected as a starting point because of their accessibility and because many of the fundamental questions come together here. The relevance of this area is further enhanced by planned acquisition of the SNORCLE Lithoprobe transect (see Lithoprobe Phase IV Proposal, p. 4-21...4-41, Clowes, 1993). Also, a wealth of detailed data exists for the Yellowknife Domain (e.g., Henderson, 1985 and references therein), which could be synthesized into a unified view if some of the outstanding questions can be resolved.

An underlying premise of this work is that with the above average level of exposure, detailed and integrated stratigraphic, structural, and metamorphic work, supported by high-precision U-Pb dating, should be able to provide unique solutions to critical field relationships. For an overview of the geology of the eastern Yellowknife Domain and the Sleepy Dragon Complex the reader is referred to Davidson (1972), Henderson (1985), Lambert (1988), Kusky (1990), Stublely and Bégin (1993) and references therein.

## DATA COLLECTION

Figure 1 shows a simplified geological map of the Yellowknife Domain (modified after Henderson, 1985). Structural and stratigraphic data were collected from Hearne and Watta Lake in the south to Ross and Upper Ross Lake in the north, and across the southern flank of the Sleepy Dragon Complex to Tumpline Lake. Regional observations were complemented with detailed mapping of selected key areas and concentrated data collection along selected transects. Results of one such transect, section B-B'''' in Figure 1, are shown in Figure 2. The 32 km cross-section transects folded Burwash Formation metagreywackes in the central part of the domain and is constrained by essentially continuous shoreline for much of its length. Although the Yellowknife Domain has been affected by polyphase folding (e.g., Fyson, 1984; Henderson, 1985, and references therein; this study); the section occurs on a single limb of regional  $F_2$  folds and runs almost perpendicular to the trends of upright  $F_1$  folds (Fig. 3). Results from several other detailed sections throughout the area are currently being analyzed and will be presented elsewhere.

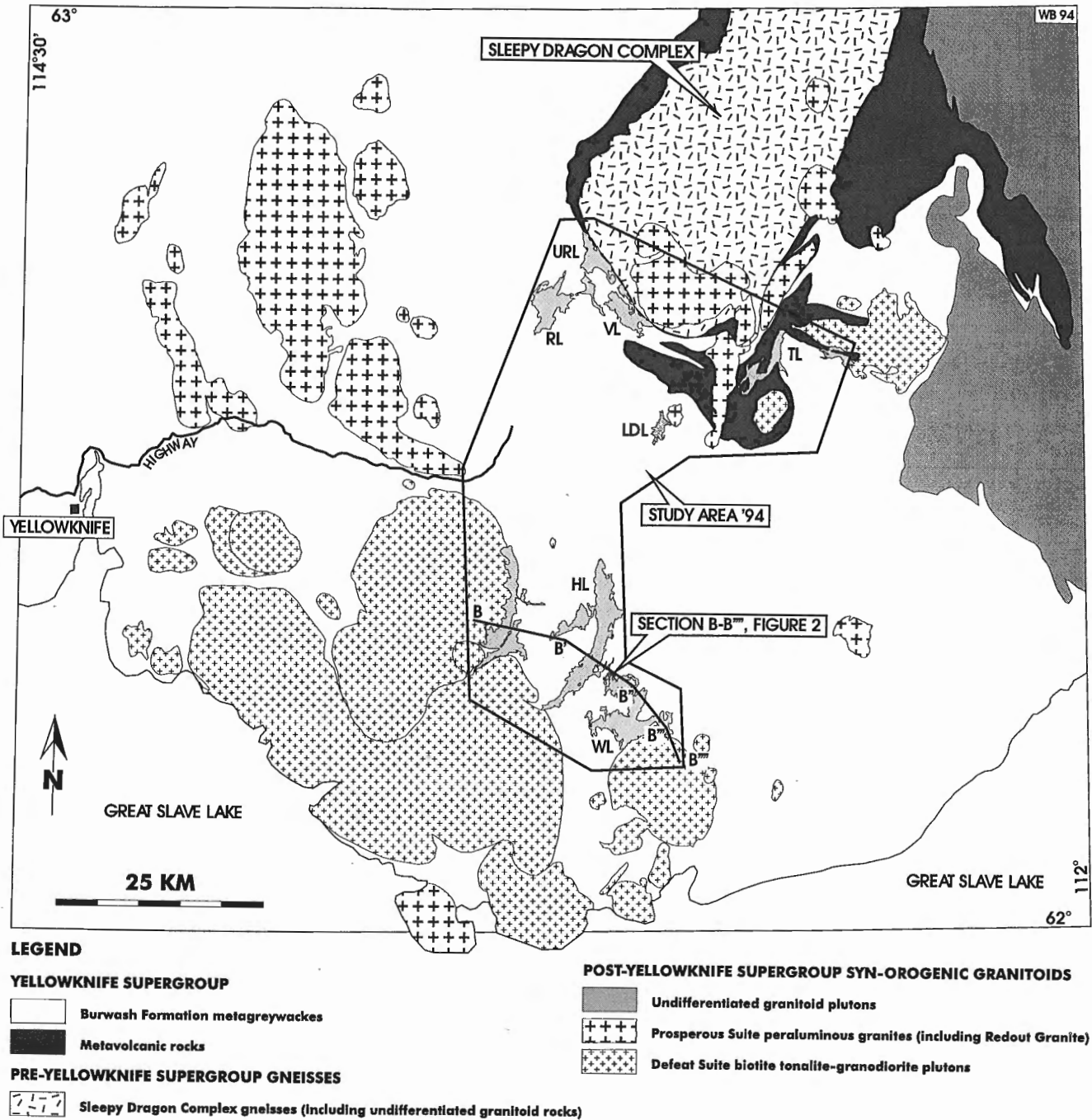
## PRELIMINARY RESULTS

### Introduction

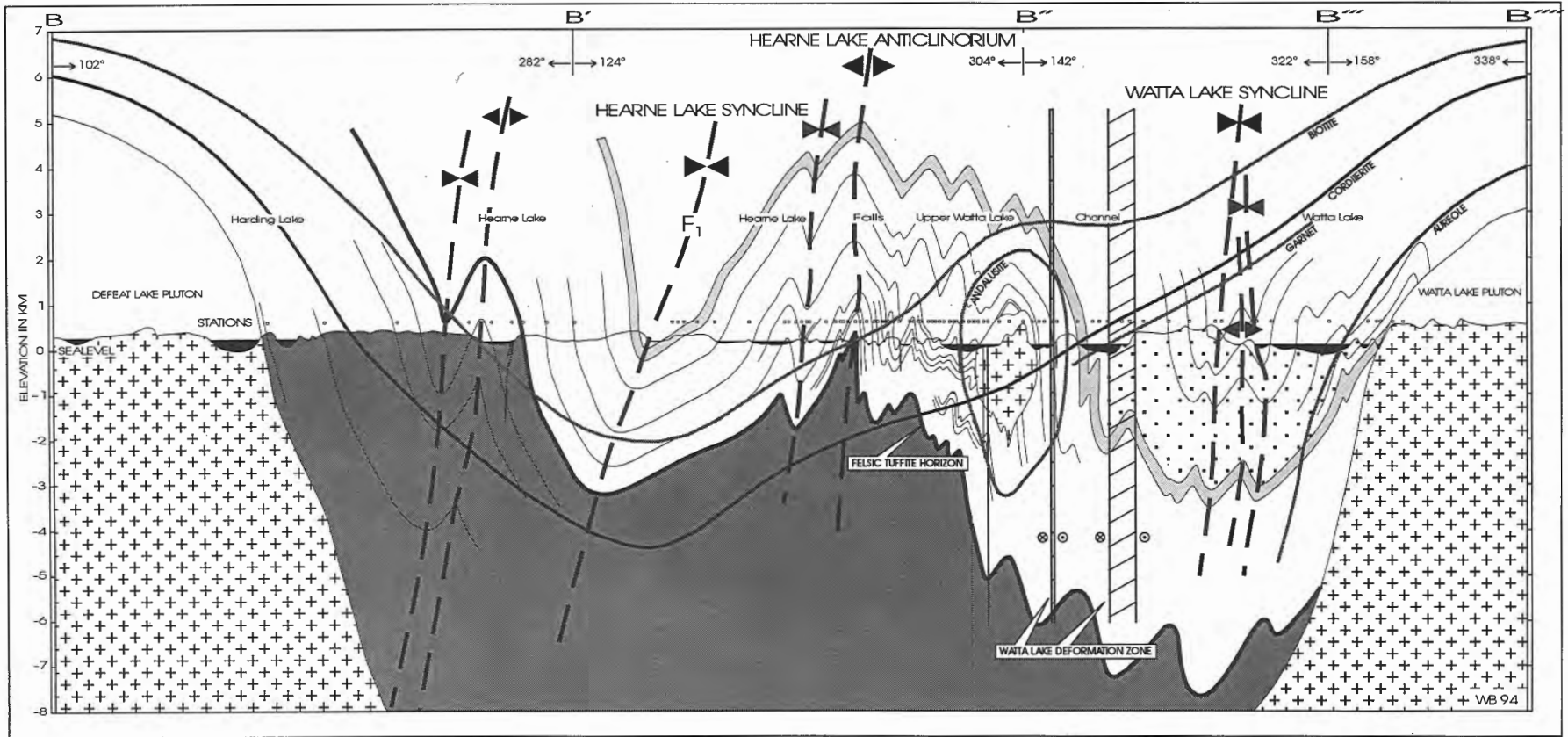
Apart from the detailed observations along section B-B''''', which highlight the relationships between  $F_1$  folding, granitoid intrusion, and metamorphic isograds, regional results on the geometry of the two major fold generations ( $F_1$  and  $F_2$ ) are compiled in Figure 3. Our results are similar to, but expand on, analyses by Fortier (1946, 1947), Henderson (1985), and Lambert (1988).

### The large-scale structure

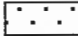
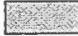



A critical result is that  $F_1$  fold trends in general, as well as specific upright  $F_1$  synclines and anticlines, can be followed continuously around the southern flank of the Sleepy Dragon Complex in what is a coherent  $F_1$ - $F_2$  interference structure: a regional scale "mushroom fold" (type 2 interference, see Ramsay, 1967). The southern termination of the Sleepy Dragon Complex is a steeply plunging  $F_2$  fold. The regional  $S_2$  cleavage, which is parallel to the  $F_2$  axial plane traces (Fig. 3), shows systematic vergence changes from the southwestern flank of the complex (where it is statistically clockwise to lithological contacts) to the southeastern flank (where it is statistically anticlockwise to lithological contacts). On each of these flanks, structural and stratigraphic data indicate a major  $F_1$  anticline towards the north. The only possible location for this major  $F_1$  anticlinal trace through the Sleepy Dragon Complex, compatible with the structural systematics, is as shown in Figure 3. A comparison with Kusky's (1990) analysis shows that his "unfolding" of the complex is geometrically incorrect. As a consequence, the kinematic analysis presented in Kusky (1990) is internally inconsistent.



*Figure 1. Simplified geological map (modified after Henderson, 1985) of the southern Yellowknife Domain. The Yellowknife greenstone belt has been omitted for simplicity. Marked are the Sleepy Dragon Complex, the area covered during the 1994 field season, and the location of section B-B'''' (see Fig. 2). Locality names: Watta Lake (WL), Hearne Lake (HL), lower Donore Lake (LDL), Ross Lake (RL), Upper Ross Lake (URL), Victory Lake (VL), and Tumpline Lake (TL).*



**BURWASH FORMATION METATURBIDITES**

-  Thickly bedded metaturbidites, typically including coarse sands and grits
-  Arbitrary marker unit
-  Medium to thickly bedded metaturbidites
-  Thin felsic tuffite horizon, graded, cyclic, interlayered with black pelite seams
-  Lowermost package of metaturbidites in the Hearne-Watta Lakes area

**SYN-OROGENIC GRANITOID INTRUSIONS**

-  Defeat Suite biotite tonalite-granodiorite intrusion, ~2618 Ma
-  Early Defeat Suite porphyry dykes

**PROTEROZOIC DIABASE DYKES**

-  North to northeasterly trending swarm at Watta Lake

0 1 5 SCALE: 5 KM

WB 94

### Core complex?

Results show that the Sleepy Dragon structure is part of a regionally coherent  $F_1$ - $F_2$  fold interference pattern. The basement uplift is first of all a basement-cored, southerly plunging  $F_1$  anticline (anticlinorium), which was subsequently refolded by northwest-southeast trending, subvertically plunging  $F_2$  folds. Similar  $F_1$ - $F_2$  mushroom interference patterns can be observed throughout the Yellowknife Domain. One such interference pattern was mapped and analyzed in detail at Lower Donore Lake (locality LDL in Fig. 3). Hence, we found no supporting evidence that the Sleepy Dragon basement "high" represents a late-stage extension-related core complex (James and Mortensen, 1992). Specifically, we have not found any evidence for a late-stage detachment fault along the basement contact. The coherent structure throughout the metaturbidites around the complex also precludes the presence of complex block faulting typically seen in the stretched hanging wall of core complexes (cf. Brun et al., 1994).

## A BRIEF DESCRIPTION OF STRUCTURES AND SEQUENCE OF EVENTS

### $F_1$ folds

$F_1$  folds are the dominant fold structures in the domain and form high amplitude upright folds with doubly plunging axes (0 to 50°). Section B-B'''' (Fig. 2) shows a detailed profile through several major  $F_1$  folds, where they are least modified by superimposed strain. In such areas of above average preservation,  $F_1$  folds are open to tight chevron folds. Distributed  $F_2$ -related strain, associated with  $S_2$  cleavage formation, may have produced as much as ~25 per cent additional horizontal

shortening across this section, so that the original  $F_1$  fold profile must have been considerably less tight. For instance, the interlimb angle of the Hearne Lake Syncline, currently ~45°, would open up to ~68° by restoring 25 per cent  $F_2$  shortening. Interlimb angles of ~60° are typical for tight chevron folds. At this angle flexural slip becomes ineffective – the folds "lock up" – and further shortening can only be accommodated by bulk strain (Ramsay, 1974).

Prominent quartz saddle reefs and en échelon vein arrays typically accompany  $F_1$  hinges, and hinge zones are commonly complicated by other accommodation structures such as limb thrusts (Ramsay, 1974). Figure 3 shows the axial traces of some of the specific  $F_1$  folds that have been followed as part of the present study and are critical to the overall geometrical understanding.

A well-developed slaty cleavage is axial planar to  $F_1$  folds and is locally preserved in the lowest grade areas such as at Hearne Lake. Concretions, loadcasts, flames, and shale clasts are strongly flattened parallel to  $S_1$  and elongated parallel to a steeply plunging stretching lineation in the plane of the foliation ( $L_1$ ). In most areas, however, strong development of the regional  $S_2$  cleavage has obliterated  $S_1$ , at least on an outcrop scale. Nevertheless,  $S_1$  vergence can still be deduced from the asymmetry and en échelon arrangement of concretions and shale clasts relative to bedding and has been used, together with changes in younging direction, to define individual  $F_1$  folds.  $F_1$  folds developed under low-grade (burial) metamorphic conditions and entirely predate all granitoid intrusions (except for synvolcanic plutons).

Although refolded by  $F_2$ , the Yellowknife Domain clearly preserves a systematic fold belt of upright, doubly plunging (periclinal)  $F_1$  folds. In the present study area,  $F_1$  folds show a weak vergence that is dominantly towards the southeast (see Fig. 2). Where  $F_2$  refolding is intense,  $F_1$  folds are passively tightened to nearly isoclinal profiles and axes are rotated to more steeply doubly plunging attitudes (~70°). Despite this superimposed strain,  $F_1$  folds throughout the study area remain upright and upward facing. Early recumbent folds or nappes (cf. Kusky, 1990) were not observed in the Burwash Formation metaturbidites of the study area.

Contrary to previous workers (e.g. Fyson, 1982), who argue for the presence of regional  $F_0$  folds, we found no evidence for significant pre- $F_1$  deformation, neither on a mesoscopic nor a macroscopic scale. The doubly plunging nature of  $F_1$  folds is thought to be produced during  $F_1$  rather than inherited from earlier regional folds.  $F_1$  folds were observed to be doubly plunging on all scales – a natural consequence of a system of relaying upright chevron folds.

Timing constraints on the formation of the  $F_1$  fold belt are currently not very precise.  $F_1$  post-dates deposition of the Burwash Formation metaturbidite sequence, which overlies ~2660 Ma rhyolites at the top of the volcanic stratigraphy (e.g., the Turnback Rhyolite dated at 2663 ± 7/-5 Ma, Henderson et al., 1987). A thin felsic tuffite intercalation within the Burwash Formation metaturbidites (Fig. 4, see also Fig. 2) is currently being dated.  $F_1$  also post-dates intrusion of gabbroic sill complexes that intruded into the Burwash Formation (Henderson, 1985; this study). A minimum age for

**Figure 2.** A detailed structural-stratigraphic section from west of Harding Lake (B) to the southeastern shore of Watta Lake (B'''). Its location is shown in Figures 1 and 3. The section is close to a true profile through high-amplitude  $F_1$  chevron folds and is constructed without vertical exaggeration (only the topographic surface is drawn with a 10x vertical exaggeration, centred on the +200 m level, to facilitate correlation with topographic features). The section is constrained by well over a 100 stations and in critical areas by essentially continuous shoreline exposure. Most of the detailed features shown occur right on or near the section, but some have been constructed by down- or up-plunge projection.

$F_1$  folds are high amplitude, upright doubly plunging folds, with a weak easterly vergence in this area. The section shows ± 10-12 km of turbidite stratigraphy, which, for the purpose of this section, has been subdivided in a number of informal members. The top of the Burwash Formation turbidite sequence, characterized by thickly bedded, sand-dominated units including coarse grits, is exposed in the cores of the Hearne and Watta Lake synclines. Note the location of a thin felsic tuffite horizon lower in the sequence. Dating of this unit is in progress.

$F_1$  is provided by crosscutting felsic porphyry dykes that precede the main Defeat Suite intrusive event (2618  $\pm$  7/-20 Ma, Henderson et al., 1987). As a tentative age for the formation of the  $F_1$  fold belt we suggest ~2640-2630 Ma.

**$F_2$  folds**

Folds of this generation (Fig. 5) are developed throughout the area and are invariably steeply plunging.  $F_2$  fold axes are parallel to intersection lineations between the prominent, subvertical, northwest-southeast trending  $S_2$  axial plane

cleavage (schistosity) and the pre- $F_2$  fold geometry produced by  $F_1$ . In many areas,  $F_2$  folds axes and associated  $L_2$  intersection lineations show steeply plunging, bimodal groupings reflecting the opposing limbs of  $F_1$  chevron folds.

$F_2$  folds and the associated  $S_2$  cleavage (Fig. 6) overprint felsic porphyry dykes, which represent the earliest manifestations of the intrusion of Defeat Suite tonalites to granodiorites. The larger biotite-tonalite to granodiorite plutons, which represent the bulk of the Defeat Suite intrusive event (Henderson, 1985), may show a weak  $S_2$  foliation or none at all. Late pegmatite dykes cut  $F_2$  folds, but are themselves

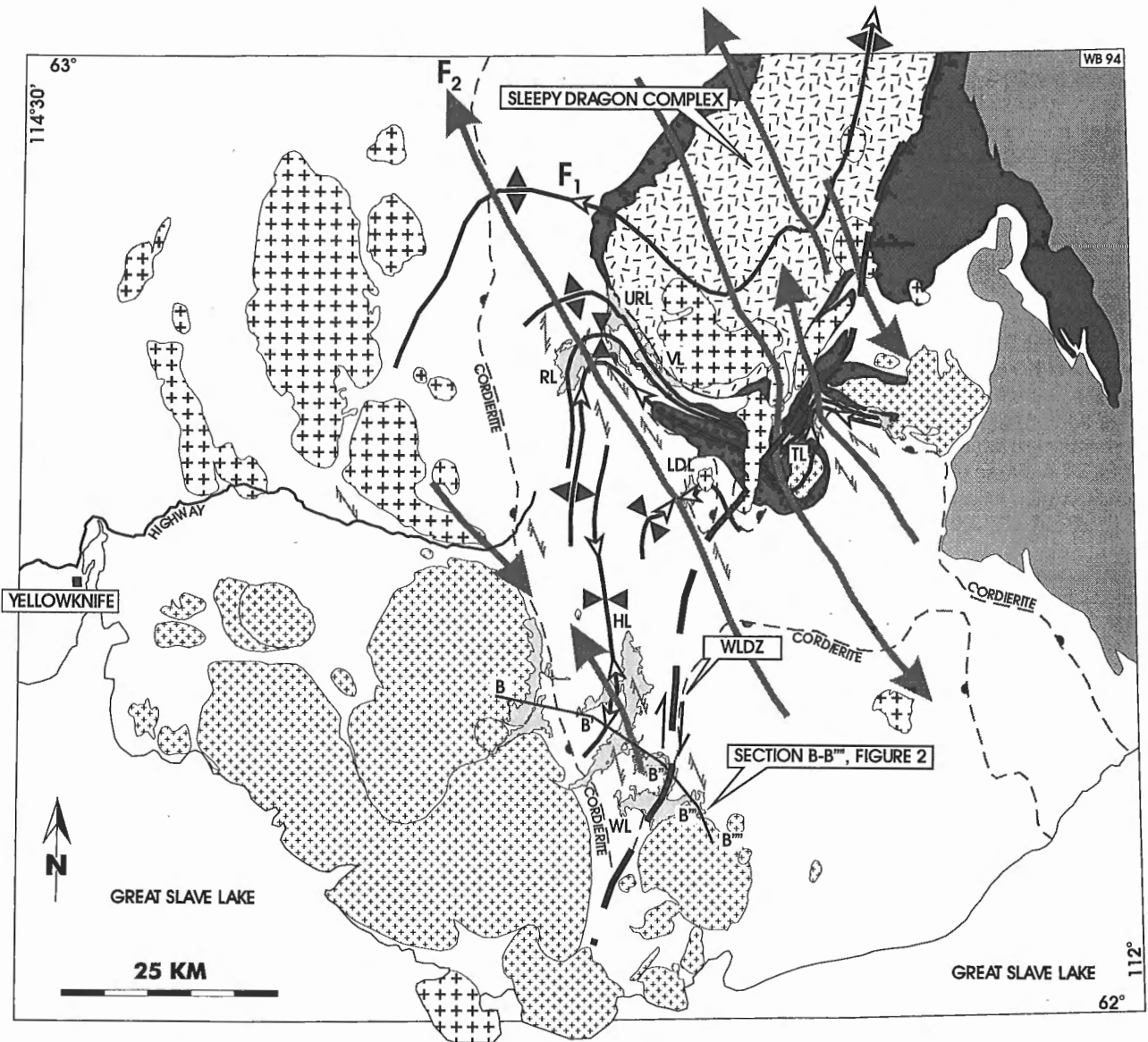


**Figure 3.** Simplified geological map similar to Figure 1, showing some of the first-order  $F_1$  and  $F_2$  fold structures. The Sleepy Dragon Complex is a regional-scale type 2 ("mushroom") interference pattern.  $F_1$  synclinal and anticlinal traces are shown in black, with arrows along the traces indicating plunge direction.  $F_2$  traces are in grey. Foliation symbols mark the regional  $S_2$  cleavage (schistosity). The dextral Watta Lake Deformation Zone (WLDZ) is indicated by the heavy dashed line. The regional cordierite-in isograd is indicated by a dashed line, with symbols marking its high-grade side.

deformed (open folding, boudinage) by the latest increments of  $F_2$  folding. The  $D_2$  event can thus be dated accurately, using the various manifestations of Defeat Suite plutonism. A currently available, rather imprecise U-Pb zircon age for one of the Defeat Suite plutons (Henderson et al., 1987) indicates that  $F_2$  deformation occurred at ~2620-2600 Ma. High-precision U-Pb zircon dating of the various phases of the Defeat Suite intrusive event is being planned. Precise dating of  $D_2$  is important for correlation of events between the study area and other domains of the Slave Province.

### Late- $D_2$ shear zones

During or after the late stages of  $F_2$  folding,  $D_2$  deformation became localized in discrete shear zones that record dextral strike-slip. The Watta Lake Deformation Zone

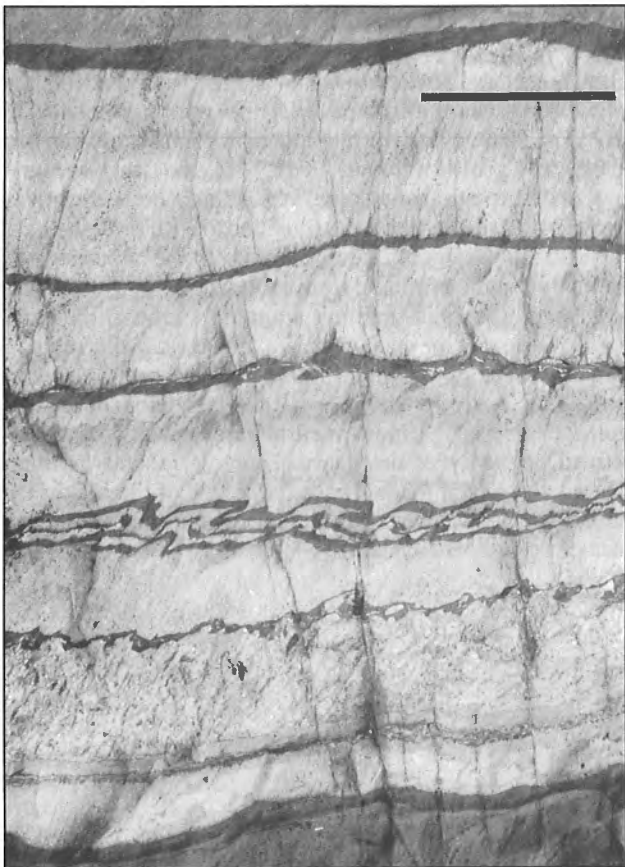


**Figure 4.** Close-up of a thin, laterally continuous felsic tuffite horizon (scale bar in upper right corner is 10 cm) intercalated in the central section of the Burwash Formation metaturbidite sequence, Watta Lake. See Figure 2 for location in section B-B'''. The horizon consists of yellow, cyclic, weakly graded beds of lapilli to silt-size tuffaceous material, intercalated by black (graphitic) pelitic seams. The latter suggest that the background turbidite sedimentation was interrupted by a period of quiescence. Dating of this horizon is currently in progress. Stratigraphic top is towards the top of the page. Note the small-scale  $F_2$  folds.



**Figure 5.** Mesoscopic  $F_1$ - $F_2$  fold interference structure. The strong regional cleavage ( $S_2$ ) is axial planar to steeply plunging  $F_2$  folds. Quartz veins were introduced late- $F_1$ , along bedding and parallel to the  $S_1$  slaty cleavage. Cameron River northwest of Ross Lake. Note 25 cent coin for scale.

(WLDZ; see Fig. 2, 3) is such a structure. It shows variable shear strains, a dextral shear band cleavage, and shallowly north-plunging stretching lineations over approximately 1 km width. Its extent is tentatively correlated with dextral shear zones along the eastern margin of the Sleepy Dragon Complex (e.g., Lambert and van Staal, 1987; this study). Late- $D_2$  dextral shear zones overprint Defeat Suite as well as Prosperous Suite granitoid plutons (Fig. 7).

In the Watta Lake Deformation Zone, cordierite porphyroblasts are deformed and retrograded. New growth of andalusite occurs, especially near abundant quartz veins. In the central part of the zone, these synkinematic quartz veins show tight dextral drag folds and andalusite porphyroblasts show boudinage with subhorizontal quartz fibres filling the necks.

### $S_3$ cleavage

A variety of mesoscopic structures overprint the regional  $S_2$  cleavage. Most prominent among these is a locally developed, coarsely spaced crenulation cleavage ( $S_3$ ).  $S_3$  attitudes are generally subvertical, and with northeast-southwest trends.

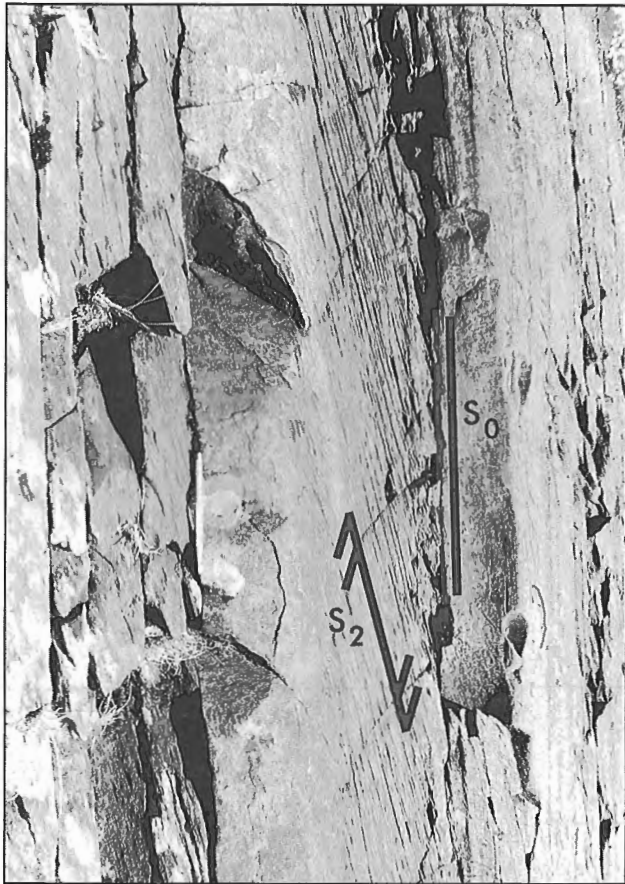


**Figure 6.** Vertical, easterly younging graded turbidite beds, transected by the strongly developed anticlockwise  $S_2$  cleavage, Hearne Lake. Note pen for scale; plan-view, east towards the right.

$S_3$  was observed in about 5 per cent of the outcrops and is usually developed in only one or a number of beds. The significance of the  $S_3$  cleavage is not well understood, but its presence may point to a third phase of deformation ( $D_3$ ) that refolds  $F_2$  and  $S_2$  about subvertical axes.  $F_3$  folds have not been observed on a mesoscopic scale, but macroscopic  $F_3$  folds do probably exist and are responsible for some of the dispersion in  $F_2$  axial planes and the  $S_2$  cleavage.

### **Post- $S_3$ structures**

Other late structures include locally developed small-scale kinks and a variety of late brittle fault sets. Throughout the area, late kinks have subvertical axes. In general, minor structures that postdate  $F_2$  do not appear to have produced major effects on the regional geometry.

## **METAMORPHISM**

Although a detailed description of the metamorphic findings is beyond the scope of this paper, a brief outline will be given here. The Hearne Lake-Watta Lake section (Fig. 2) shows a nearly true profile through several isograds that border a low-grade "trough" centred on Hearne Lake. From the lowest grade core of the Hearne Lake Syncline to eastern Watta Lake the following "isograds" are observed: 1) the appearance of distinct ~1 mm biotite porphyroblasts, 2) a conspicuous andalusite-in isograd defining an aureole around the small Defeat Suite pluton on Upper Watta Lake, 3) the regional cordierite-in isograd ("knot-in-grad"), 4) a garnet-in isograd, virtually coincident with the cordierite-in isograd, defined by the appearance of ~1 mm euhedral garnets, and 5) a loosely defined boundary of the thermal aureole around the main Watta Lake pluton marked by a darkening of the rocks. The latter corresponds to a colour change in biotite and the appearance of a granoblastic texture.

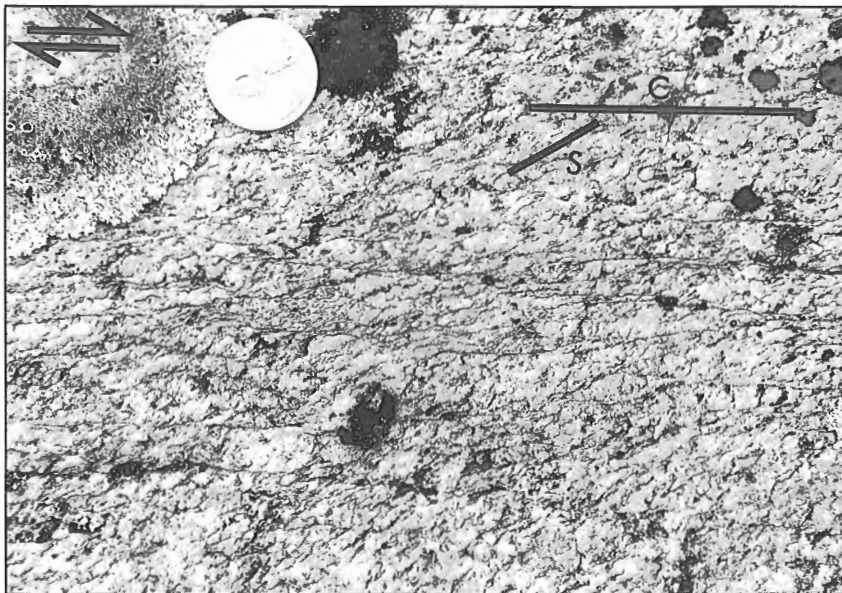


**Figure 7.**

Prosperous Suite muscovite-bearing granite on Tumpline Lake showing well-developed dextral  $S-C$  fabric (top to the right). Main phase Prosperous Suite granites intruded synkinematic with respect to  $D_2$  deformation. They are overprinted by  $S_2$  and late- $D_2$  dextral shear zones. Note 25 cent coin for scale.

All porphyroblasts show late to post- $S_2$  growth in this area – they passively overgrow and include the dominant  $S_2$  fabric. Hence, in the relatively low-grade areas associated with the metamorphic "troughs", the peak of low-pressure metamorphism was attained late to post- $F_2$ , following intrusion of the main phase Defeat Suite tonalite-granodiorite plutons. Similar observations were made all throughout the study area, but relationships change towards somewhat higher grade rocks close to the margin of the Sleepy Dragon Complex, where cordierite and andalusite porphyroblast growth occurred syn- $D_2$ . In these areas,  $S_2$  foliation planes are included in but also wrap around the porphyroblasts, which may show distinct pressure shadows. In higher grade rocks, the peak of metamorphism thus occurred slightly earlier.

Both observations can be explained if the peak of metamorphism in the area is syn- $D_2$  (coincident with Defeat and Prosperous Suite intrusive events): the latter stages of  $F_2$  caused regional folding of the isograd surfaces, followed by relaxation of the folded isograds with heat conducting from regional  $F_2$  culminations to  $F_2$  depressions. This would lead to a prograde readjustment and hence a somewhat later peak in the lower grade areas. The trough-shaped section through the isograds in section B-B'''' reflects frozen-in relaxation of  $F_2$ -folded regional metamorphic isograds.

## DISCUSSION AND CONCLUSIONS

Progress has been made in the understanding of the southeastern Yellowknife Domain. Our work agrees with and expands on earlier descriptions by Henderson (1985) and Lambert (1988). We do not see the need for the complex treatment presented by Fyson in a variety of papers (e.g., Fyson, 1975, 1982, 1984; Fyson and Helmstaedt, 1988), which tends to detract from the fact that the Yellowknife Domain preserves an upright, doubly plunging  $F_1$  chevron fold belt, refolded by regional, reclined  $F_2$  folds.

The Sleepy Dragon Complex is an integral part of the regional interference structure. It represents a mushroom-type  $F_1$ - $F_2$  fold. Correct interpretation of the geometry of the Sleepy Dragon Complex shows that Kusky's (1990) "unfolding" is wrong and his kinematic deductions internally inconsistent. Given the intense  $F_1$  and  $F_2$  folding and their associated strain, we also cast doubt on the robustness of the specific kinematic indicators presented by Kusky (1990). The claim that complex folds in the turbidites reflect "nappes" (Kusky, 1990) is not supported. All early folds in the turbidites belong to the  $F_1$  phase, all are upward facing, and originated as upright to moderately inclined doubly plunging (chevron) folds. This is an important result because it indicates that if there was an early accretionary phase, it must predate the deposition of the turbidites, unless they were riding on and deformed above a basal décollement. A basal décollement does not appear a viable option however, since both the underlying volcanic rocks as well as the basement rocks are involved in the upright  $F_1$  folding. The presence of strong  $L_1$  stretching lineations (possibly amplified by  $D_2$  strain) in the turbidites, at least locally, illustrates that an indiscriminate interpretation of strong stretching lineations as being due to accretionary tectonics is unjustified.

Nevertheless, it is important to note that the qualitative strain magnitude in the underlying volcanic sections is impressive, and at this point we do not want to rule out the possibility of a potentially more complex history in the volcanic sections than that recorded by the Burwash metaturbidites. More work is needed on this subject. Locally intense, early deformational fabrics were observed all through the volcanic belts, including the rhyolitic rocks near the top of the volcanic piles. Therefore, at the very least, deformation responsible for the variable but generally intense deformation in the volcanic rocks post-dated extrusion of the felsic centres. This observation presents a critical test for the accretion debate. The bimodal volcanic belts, and in particular the felsic centres, are associated with massive sulphide deposits. If their Pb-isotopes suggest significant involvement of older continental crust, as documented by Thorpe et al. (1992), it would indicate that the intense deformation overprinted rather than caused the association between volcanic piles and basement rocks.

The  $F_1$  fold belt was refolded by  $F_2$ . What is currently preserved is the refolded  $F_1$  trends, rather than the original  $F_1$  fold belt. Hence it is unclear to us what forms the basis for the north-south trends and westerly vergence that are implicit in published tectonic models (e.g., Fyson and Helmstaedt, 1988; Kusky, 1990). In the Yellowknife Domain,  $F_1$  folds show either no vergence or a weak vergence in variable directions (after unfolding  $F_2$ ). To highlight this point, in the present study area  $F_1$  folds show a weak but systematic easterly rather than a westerly vergence. Elsewhere in the Slave Province,  $F_1$  folds are less well preserved and vergence interpretations even less satisfactory (e.g., Kusky, 1989; see also King et al., 1989). Also, to interpret various domains as terranes is currently not justified.

If however the original  $F_1$  fold belt was oriented approximately north-south,  $F_2$  must reflect a large-scale dextral transpression event that has reoriented the  $F_1$  trends dramatically over the width of the Yellowknife Domain and beyond. A large, distributed dextral strike-slip displacement, in the order of ~100 km or more, would be required for this wholesale reorientation. Less dextral strike-slip is required if the original trend of the  $F_1$  fold belt was more northeasterly. Finally, no systematic dextral strike-slip would be required if the original trend was parallel to its current enveloping surfaces (i.e., east-northeasterly). We prefer the intermediate option in which the original fold belt ( $F_1$ ) was oriented northeasterly and was refolded by a dextral transpression event ( $F_2$ ), which terminated with discrete ductile to brittle, dextral strike-slip zones.

Although the Burwash metaturbidite sequence does not appear to record any early thrusting, we interpret its deposition as the result of a nearby orogenic event, producing rapid uplift and a prolific source of clastic material. Where this source was situated is currently unclear although preliminary paleocurrent indicators in the Hearne Lake area suggest a westerly source region. Given the systematic nature of the  $F_1$  folds in this area (e.g., Fig. 2) a dedicated sedimentological and detrital zircon study appears promising.



Both the Defeat and Prosperous Suite granitoids appear to have intruded broadly synchronous with the D<sub>2</sub> transpressional event. Possibly, strike-slip deformation played an important role in creating local upper crustal dilation to accommodate the voluminous granitoid intrusions (cf. Glazner, 1991). Low-pressure metamorphism in the study area is clearly linked, spatially as well as temporally, to intrusion of the main granitoid suites (cf. Lux et al., 1986) and peaked syn- to post-F<sub>2</sub>. The possibility of a cryptic earlier metamorphic event in the volcanic rocks remains to be evaluated.

## ACKNOWLEDGMENTS

We thank Bill Padgham for involving us in some of the field trips in the Yellowknife area, which helped in familiarizing ourselves with the geology of the Yellowknife Domain. Similar thanks goes to Rob Johnstone and Mike Stublely for arranging visits to their work areas. Cees van Staal, Janet King (GSC), Mike Stublely and Carolyne Relf (NWT Mineral Initiatives Office) critically read and provided helpful comments on an earlier draft of this paper.

## REFERENCES

- Bickle, M.J., Nisbet, E.G., and Martin, A.**  
1994: Archean greenstone belts are not oceanic crust; *The Journal of Geology*, v. 102, p. 121-138.
- Brun, J.P., Sokoutis, D., and van den Driessche, J.**  
1994: Analogue modeling of detachment fault systems and core complexes; *Geology*, v. 22, p. 319-322.
- Clowes, R.M. (ed.)**  
1993: LITHOPROBE Phase IV Proposal – Studies of the evolution of a continent; Lithoprobe Secretariat, University of British Columbia, Vancouver, 290 p.
- Davidson, A.**  
1972: Granite studies in the Slave province; in *Report of Activities, Part A*; Geological Survey of Canada, Paper 72-1A, p. 109-115.
- de Wit, M.J. and Ashwal, L.D.**  
1986: Workshop on tectonic evolution of greenstone belts; Lunar and Planetary Institute, Houston Technical Report 86-10, 227 p.
- Fortier, Y.O.**  
1946: Yellowknife-Beaulieu Region, Northwest Territories; Geological Survey of Canada, Paper 46-23, 1 map with marginal notes.  
1947: Ross Lake, Northwest Territories; Geological Survey of Canada, Paper 47-16, 4 p., 1 map.
- Fyson, W.K.**  
1975: Fabrics and deformation of Archean metasedimentary rocks, Ross Lake-Gordon Lake area, Slave Province, Northwest Territories; *Canadian Journal of Earth Sciences*, v. 12, p. 765-776.  
1982: Complex evolution of folds and cleavages in Archean rocks, Yellowknife, N.W.T.; *Canadian Journal of Earth Sciences*, v. 19, p. 878-893.  
1984: Fold and cleavage patterns in Archean metasediments of the Yellowknife domain, Slave Province; in *Precambrian Tectonics Illustrated*, (ed.) A. Kröner; Elsevier, Amsterdam, p. 281-293.
- Fyson, W.K. and Helmstaedt, H.**  
1988: Structural patterns and tectonic evolution of supracrustal domains in the Archean Slave Province, Canada; *Canadian Journal of Earth Sciences*, v. 25, p. 301-315.
- Glazner, A.F.**  
1991: Plutonism, oblique subduction, and continental growth: an example from the Mesozoic of California; *Geology*, v. 19, p. 784-786.
- Henderson, J.B.**  
1985: Geology of the Yellowknife-Hearne Lake area, District of MacKenzie: a segment across an Archean basin; Geological Survey of Canada, Memoir 414, 135 p., 1:250 000 map.
- Henderson, J.B., van Breemen, O., and Loveridge, W.D.**  
1987: Some U-Pb zircon ages from Archean basement, supracrustal and intrusive rocks, Yellowknife-Hearne Lake area, District of MacKenzie; in *Radiogenic Age and Isotopic Studies: Report 1*, Geological Survey of Canada, Paper 87-2, p. 111-121.
- Hoffman, P.F.**  
1990: On accretion of granite-greenstone terranes; in *Greenstone Gold and Crustal Evolution*, (ed.) F. Robert, P.A. Sheahan, and S.B. Green; Geological Association of Canada, NUNA 2, p. 32-45.
- James, D.T. and Mortensen, J.K.**  
1992: An Archean metamorphic core complex in the southern Slave Province: basement-cover structural relationships between the Sleepy Dragon Complex and the Yellowknife Supergroup; *Canadian Journal of Earth Sciences*, v. 29, p. 2133-2145.
- King, J.E., Davis, W.J., and Relf, C.**  
1989: Comment on "Accretion of the Archean Slave province"; *Geology*, v. 17, p. 963-964.
- Kusky, T.M.**  
1989: Accretion of the Archean Slave province; *Geology*, v. 17, p. 63-67.  
1990: Evidence for Archean ocean opening and closing in the southern Slave province; *Tectonics*, v. 9, no. 6, p. 1533-1563.
- Lambert, M.B.**  
1988: The Cameron River and Beaulieu River volcanic belts, District of MacKenzie, Northwest Territories; Geological Survey of Canada of Canada, Bulletin 382.
- Lambert, M.B. and van Staal, C.R.**  
1987: Archean granite-greenstone boundary relationships in the Beaulieu River volcanic belt, Slave province, N.W.T.; in *Current Research, Part A*; Geological Survey of Canada, Paper 87-1A, p. 605-618.
- Lux, D.R., DeYoreo, J.J., Guldotti, C.V., and Decker, E.R.**  
1986: Role of plutonism in low-pressure metamorphic belt formation; *Nature*, v. 323, p. 794-796.
- Ramsay, J.G.**  
1967: *Folding and Fracturing of Rocks*; McGraw-Hill, New York, 568 p.  
1974: Development of chevron folds; *Geological Society of America Bulletin*, v. 85, p. 1741-1754.
- Stublely, M.P. and Bégin, N.J.**  
1993: Geology of the Smoky Lake area, southern Slave province, parts of NTS 85P/3 and 6; Department of Indian and Northern Affairs Canada, Geology Division, Yellowknife, Report EGS 1993-5, 2 map sheets with marginal notes.
- Tarney, J., Dalziel, I.W.D., and de Wit, M.J.**  
1976: Marginal basin 'Rocas Verdes' Complex from S. Chile: a model for Archean greentone belt formation; in *The Early History of the Earth*, (ed.) B.F. Windley; Wiley, London, p. 131-146.
- Thorpe, R.I., Cumming, G.L., and Mortensen, J.K.**  
1992: A significant Pb-isotope boundary in the Slave province and its probable relation to ancient basement in the western Slave province; in *Project Summaries, Canada-Northwest Territories Mineral Development Subsidiary Agreement 1987-1991*, (ed.) D.G. Richardson and M. Irving; Geological Survey of Canada, Open File 2484, p. 179-184.

# Geology, geochronology, and metallogeny of High Lake greenstone belt, Archean Slave Structural Province, Northwest Territories<sup>1,2</sup>

J.R. Henderson, J.A. Kerswill<sup>3</sup>, M.N. Henderson<sup>3</sup>, M. Villeneuve, C.A. Petch<sup>4</sup>, J.F. Dehls<sup>5</sup>, and M.D. O'Keefe<sup>4</sup>

Continental Geoscience Division

*Henderson, J.R., Kerswill, J.A., Henderson, M.N., Villeneuve, M., Petch, C.A., Dehls, J.F., and O'Keefe, M.D., 1995: Geology, geochronology, and metallogeny of High Lake greenstone belt, Archean Slave Structural Province, Northwest Territories; in Current Research 1995-C; Geological Survey of Canada, p. 97-106.*

---

**Abstract:** High Lake greenstone belt, mapped along strike for 100 km, is subdivided into three domains based on lithological association, results of U-Pb zircon dating of volcanic rocks, and distribution of mineral occurrences. The oldest volcanic rocks (ca. 2.70 Ga) are felsic and predominate in the Western domain. Younger basaltic, andesitic, and dacitic flows and tuffs (ca. 2.67 Ga) are observed in the Eastern domain. The youngest rock interpreted to be volcanic, mapped in the Central domain, is a dacite (ca. 2.62 Ga) at the contact between greywacke and graphitic-sulphidic slate and siltstone. The belt is surrounded and intruded by 2.62-2.58 Ga granitic plutons and batholiths.

In the Western and Eastern domains, synvolcanic massive sulphides occur in intermediate to felsic volcanic rocks. In the Western domain, zones of hydrothermal alteration ("dalmatianite") are indicated by porphyroblastic knots of quartz-sericite-chlorite or cordierite. In the Central domain, epigenetic gold occurs with arsenopyrite-quartz in dilatant zones in mafic volcanic as well as metasedimentary rocks.

**Résumé :** La ceinture de roches vertes de High Lake, cartographiée sur une longueur de 100 km, est subdivisée en trois domaines basés sur les associations lithologiques, les résultats de datation U-Pb des roches volcaniques et la distribution des indices de minéralisation. Les roches volcaniques les plus anciennes (2,70 Ga) sont felsiques et prédominent dans le domaine occidental. Des coulées et tuffs basaltiques, andésitiques et dacitiques plus récents (environ 2,67 Ga) se rencontrent dans le domaine oriental. La roche volcanique la plus récente cartographiée dans le domaine central est une dacite (environ 2,62 Ga) au contact de grauwackes et d'ardoises graphitiques sulfurées et de siltstones. Des plutons et batholites granitiques de 2.62-2.58 Ga entourent et recourent la ceinture.

Dans les domaines occidental et oriental, des sulfures massifs synvolcaniques sont présents dans des roches volcaniques intermédiaires à felsiques. Dans le domaine occidental, des zones d'altération hydrothermale («dalmatianite») sont marquées par des porphyroblastes de quartz-séricite-chlorite ou de cordiérite. Dans le domaine central, on trouve de l'or épigénétique avec de l'arsénopyrite-pyrrhotite-quartz dans des zones dilatées dans des roches volcaniques mafiques et dans des roches métasédimentaires.

---

<sup>1</sup> Contribution to Canada-Northwest Territories Mineral Initiatives (1991-1996), an initiative under the Canada-Northwest Territories Economic Development Cooperation Agreement.

<sup>2</sup> Contribution to the Slave NATMAP Project

<sup>3</sup> Mineral Resources Division

<sup>4</sup> Queen's University, Kingston K7L 3N6

<sup>5</sup> Erindale College, University of Toronto, Mississauga L5L 1C6

## INTRODUCTION

Regional mapping in the High Lake greenstone belt (Fig. 1) and examination of known mineral occurrences were completed during the 1994 field season. Mapping in 1994 was done mainly at the north end of the belt in order to complete regional coverage, but parts of the belt mapped in 1992 and 1993 (Henderson et al., 1992, 1994a) were re-examined to address specific problems. Previous geological mapping in the area has been done by Fraser (1964), Padgham et al. (1973), Johnson (1974), Easton et al. (1982), Yeo et al. (1983), and Jackson et al. (1986a, b).

This report presents geological and metallogenic maps of the greenstone belt as well as new geological and geochronological data. A coloured geological map at 1:50 000 scale of the northern end of the belt (Fig. 2; 76M/10 and 15) will be released as a GSC Open File (Henderson et al., in press).

## SUMMARY OF GEOLOGY

High Lake greenstone belt comprises mafic, intermediate, and felsic volcanic rocks in the west and east, and a central domain of mixed volcanic and sedimentary rocks (Fig. 2). Along 70 km of strike, the belt is greenschist facies (chlorite zone), while amphibolite facies (andalusite zone) rocks occur in the south and north. Cordierite-bearing metagreywacke occurs north of James River, along the eastern margin of the belt. Granitic batholiths, emplaced late in the deformation

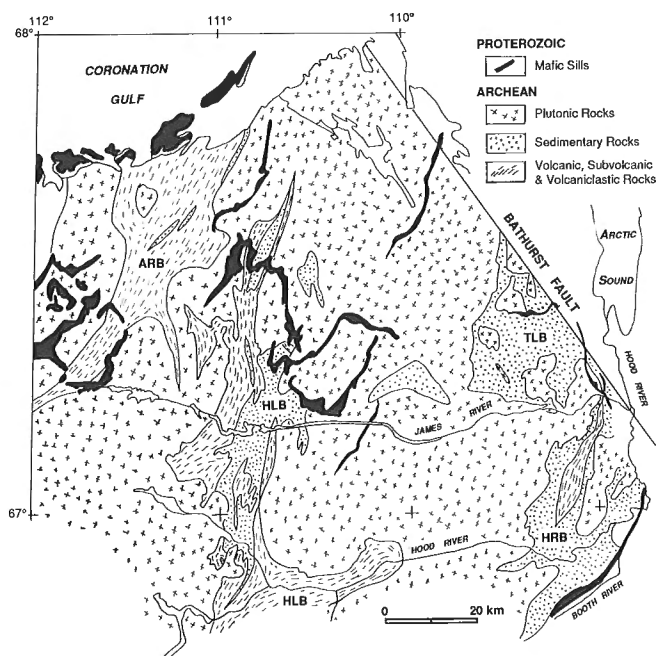


**Figure 1.** Location map showing simplified geology of northern Slave Structural Province, and locations of Hood River Belt (HRB), Torp Lake Belt (TLB), High Lake Belt (HLB), and Anialik River Belt (ARB).

history of the region, surround and intrude the belt. Rocks forming a basement terrane to the supracrustal rocks have not been recognized.

Near the western margin of the belt, in the Rush Lake area (Fig. 2), an angular discordance between older northwest-trending felsic and intermediate volcanic rocks, and younger, typically pillowed mafic volcanic rocks was mapped (Henderson et al., 1994b). Based on mapping in 1993, the authors included older felsic-intermediate volcanic rocks in the Rush Lake area in a "Rush Lake sequence", and younger volcanic and sedimentary rocks in the Snofield Lake area in a "Snofield Lake sequence". Although it appears that both sequences may extend beyond the area mapped in 1993, where to draw the apparent unconformity remains unclear. It seems expedient at this time to restrict the Rush Lake sequence to the area of its definition around Rush Lake, and to divide the entire High Lake greenstone belt into three domains (Western volcanic, Central mixed, and Eastern volcanic) based on lithological association, and the distribution of mineral occurrences (Fig. 3). Although limited geochronological results (see below) indicate that felsic volcanic rocks may occur in the Central domain that are significantly younger than felsic volcanic rocks in the Western and Eastern domains, there is no field evidence to indicate that Central domain boundaries are unconformities.

### Western volcanic domain

The Western domain of the High Lake belt, north of Canoe Lake and west of the Kennarctic River, is mainly intermediate and felsic volcanic and nonbedded volcanoclastic rocks. Subordinate basalt occurs in the area between High and Rush lakes. A few scattered pillowed andesites located north of the James River in 76M/2 young to the east. The eastern margin of the volcanic-dominated Western domain is marked by a horizon of chemical sedimentary rocks (banded iron-formation and marble) overlying a wide sequence of felsic volcanic rocks that can be traced discontinuously from Canoe Lake to High Lake.

### Central mixed domain

The Central domain contains chemical sedimentary rocks, black slate-grey siltstone, poorly bedded volcanic- and shale-clast conglomerate, and psammitic greywacke. Felsic volcanic and volcanoclastic rocks commonly occur interbedded with chemical and clastic sedimentary rocks. West of Snofield Lake, eastward-younging, thin bedded, grey silt-black shale turbidites overlie chemical sedimentary rocks along the western margin of the Central domain. A second prominent horizon of chemical sedimentary rocks (marble) occurs east of Snofield Lake at the top of an intermediate-felsic volcanic and nonbedded volcanoclastic sequence. Stromatolites described by J.B. Henderson (1975) occur in marble north of Snofield Lake. Sedimentary rocks in the Central domain are about 10 km wide at James River, narrow to several hundred metres south and north of High Lake, and widen to several kilometres north of High Lake along the Kennarctic River.

South of Canoe Lake, a 100 km<sup>2</sup> expanse of basalt flows with rare pillows is included in the Central domain. To the south in the Ulu area (Fig. 2), tan-weathering psammitic metagreywacke interlayered with basalt is the dominant lithological association.

### Eastern volcanic domain

An Eastern domain along the eastern margin of the High Lake belt from James River to south of Hood River is defined by mainly mafic and intermediate volcanic and volcanoclastic rocks, and a lack of sedimentary rocks. The Eastern domain is geologically similar to the Western volcanic domain, but lacks field evidence for more than one cycle of volcanism.

## AGES OF FELSIC VOLCANISM

U-Pb geochronology on zircons separated from five samples of dacite collected from the High Lake belt indicate ages of 2705 ± 1 Ma, 2696 +4/-3 Ma, 2695 ± 3 Ma, 2671 ± 3 Ma and 2616 ± 3 Ma (see methodology in Parrish et al., 1987). Sample localities are shown on Figure 2.

The four oldest dates are coeval with 2.71-2.66 Ga volcanic and turbiditic rocks of the Yellowknife Supergroup (van Breemen et al., 1992). The three oldest dates are from the Western domain, and it is noteworthy that the ca. 2705 Ma date is from the area assigned to the relatively old Rush Lake sequence, where field relationships suggest that these rocks rest unconformably beneath younger pillow basalts assigned to the base of the Snofield Lake sequence (Henderson et al., 1994b). The 2696 +4/-3 Ma and 2695 ± 3 Ma dates are from dacites in the Western domain near James River. The 2671 ± 3 Ma date is from a dacite in the Eastern domain. Except for the 2616 ± 3 Ma zircon described below, all radiometric ages mentioned in this report are preliminary.

### Ares dacite porphyry

The 2616 ± 3 Ma age is from a dacite porphyry collected from the south side of Ares Lake in the Central domain. This conformable unit occurs at the contact between andalusite grade psammitic metagreywacke and black slate. The fine grained matrix and stratiform geometry of the porphyry suggest that it is a flow rock, but it could also have originated as a hypabyssal sill. In hand sample 1-2 mm quartz and plagioclase phenocrysts are set in a 0.1-0.2 mm matrix. A thin section showed foliation-parallel muscovite with quartz and plagioclase in the matrix, plagioclase phenocrysts with calcite and sericite alteration, and quartz phenocrysts with some subgrains. Several quartz phenocrysts exhibit embayed euhedral outlines that are characteristic of felsic extrusive rocks. Zircons separated from this rock are extremely clear, prismatic crystals with typical igneous morphology.

Four single-grain fractions (Table 1) were analyzed. Each grain had about 100 ppm U, resulting in analyses with a high proportion of common Pb, and relatively large errors for individual fractions. However, three of the four error ellipses overlap concordia, and two of the four ellipses are centered on concordia with significant agreement. A weighted average of the four analyses yields an error of 3 Ma (Fig. 3).

Additional geochronology is in progress on other felsic volcanic, volcanoclastic, and sedimentary rocks from this area to determine whether the young age is characteristic of volcanism and sedimentation in the Central domain. Zircons from felsic volcanic and volcanoclastic rocks from the nearby ca. 2.67 Ga Hood River metasedimentary belt (Fig. 1) were dated at 2600 ± 2 Ma (van Breemen et al., 1994), and a conglomerate in the ca. 2.69 Ga Anialik River volcanic belt is less than 2600 Ma (Relf et al., 1994). In these two examples, younger rocks were shown to rest unconformably on older supracrustal rocks (Tirru and Bell, 1980; Jefferson et al., 1990), and to be the same age as nearby granitic intrusions. It would not be surprising if extrusive equivalents of some of the 2625 to 2580 Ma granitic intrusions that comprise more

Table 1. U-Pb isotopic data for the Ares dacite.

Fraction <sup>a</sup>	Wt. <sup>b</sup> mg	U ppm	Pb <sup>c</sup> ppm	Th <sup>d</sup> U	<sup>206</sup> Pb <sup>e</sup> <sup>204</sup> Pb	Pb <sup>f</sup> pg	Radiogenic ratios (±1σ, %) <sup>g</sup>			Age (Ma, ±2σ) <sup>h</sup>	
							<sup>206</sup> Pb <sup>238</sup> U	<sup>207</sup> Pb <sup>235</sup> U	<sup>207</sup> Pb <sup>206</sup> Pb	<sup>207</sup> Pb <sup>206</sup> Pb	Discord. <sup>i</sup> %
<b>ARESLAKE DACITE (UTM: Zone 12 Easting: 503592 Northing: 7434536N)</b>											
A	3	101	59	0.729	513	19	0.4970±0.22%	12.070±0.22%	0.17614±0.12%	2616.8±3.9	0.7
B	5	47	28	0.746	308	25	0.4996±0.55%	12.154±0.49%	0.17644±0.27%	2619.7±8.8	0.4
C	3	135	78	0.585	522	22	0.5000±0.26%	12.127±0.31%	0.17591±0.19%	2614.7±6.4	0.0
D	3	95	56	0.689	268	32	0.4998±0.50%	12.121±0.47%	0.17589±0.25%	2614.5±8.3	0.1

<sup>a</sup>All fractions are abraded except those marked with <sup>u</sup>; <sup>b</sup>Error on weight = ±1 μg; <sup>c</sup>Radiogenic Pb; <sup>d</sup>Th/U from <sup>208</sup>Pb\*/<sup>206</sup>Pb\* and <sup>207</sup>Pb/<sup>206</sup>Pb age; <sup>e</sup>Measured ratio corrected for spike and Pb fractionation of 0.09±0.03%/AMU; <sup>f</sup>Total common Pb on analysis corrected for fractionation and spike; <sup>g</sup>Corrected for blank Pb (10-20 pg) and U (0 pg) and common Pb (Stacey-Kramers model Pb composition at <sup>207</sup>Pb/<sup>206</sup>Pb age), 1 sigma error, in percent; <sup>h</sup>Corrected for blank and common Pb; <sup>i</sup>Discordance along a discordia to origin

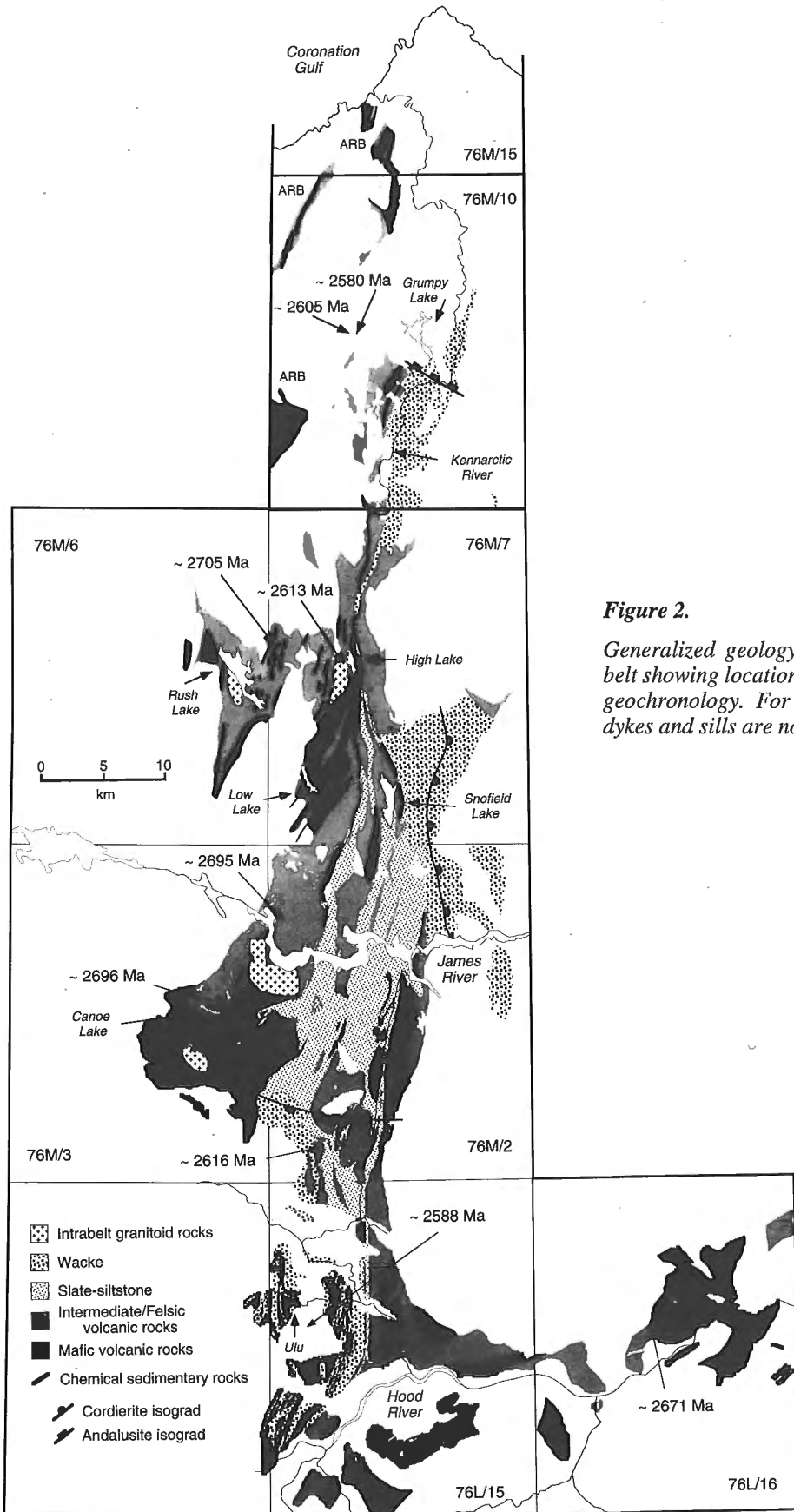


**Figure 2.**

Generalized geology of High Lake greenstone belt showing locations of sites sampled for U-Pb geochronology. For clarity, Proterozoic mafic dykes and sills are not shown.

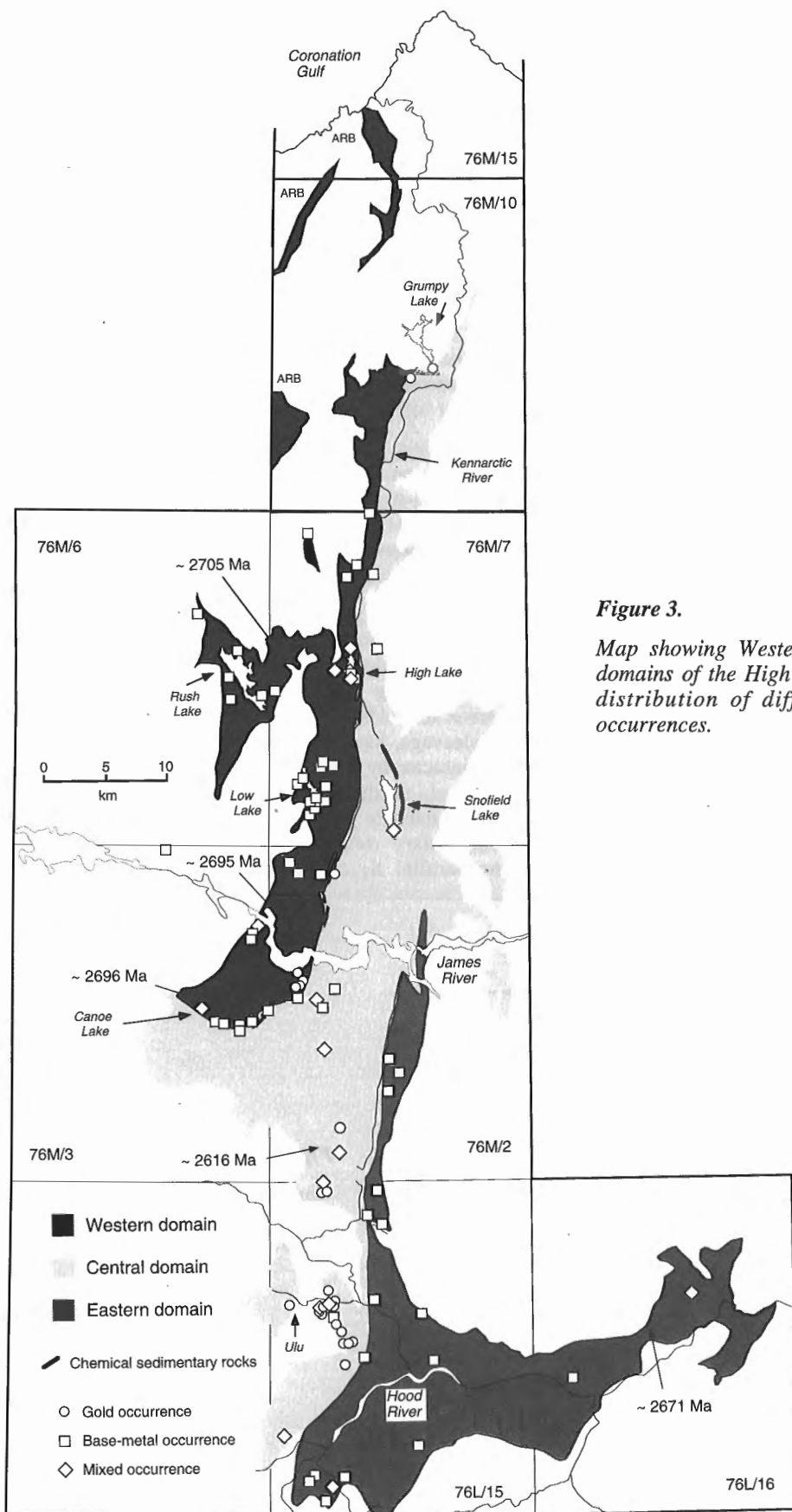


**Figure 3.**

Map showing Western, Central, and Eastern domains of the High Lake greenstone belt and distribution of different types of mineral occurrences.

than 80 per cent of the granitoids exposed in the Slave Province (van Breemen et al., 1992) are also preserved in the High Lake belt.

### AGES OF GRANITIC PLUTONISM

A granodiorite west of High Lake (Fig. 2) has been dated at  $2613 \pm 3$  Ma (U-Pb zircon) and is the oldest plutonic rock dated in the High Lake belt (Fig. 4). It intrudes and apparently truncates the High Lake polymetallic deposit. It is the same age as the  $2616 \pm 3$  Ma dacite collected about 30 km to the south (see above). About 25 km north of High Lake, two granitic rocks were dated. A foliated biotite granodiorite from a batholith was dated at  $2605 \pm 5/-3$  Ma (U-Pb zircon). The batholith is intruded by a massive two-mica granite pluton which gave a U-Pb zircon age of  $2580 \pm 8$  Ma. A similar-looking, unfoliated two-mica granite nearly surrounding the Ulu gold property of BHP Minerals Canada has been dated at  $2588 \pm 2$  Ma (U-Pb zircon). All these granite ages are consistent with ages of granitic magmatism determined elsewhere in Slave Province (cf. van Breemen et al., 1992).

### STRUCTURE AND METAMORPHISM

Contacts between supracrustal rock units dip very steeply, and folds generally plunge steeply. Finite flattening planes, and finite extension directions, indicated by the principal axes of deformed clasts, are also very steep. The geological map (Fig. 2) is therefore a good cross-sectional view of the High Lake greenstone belt. Where bedded rocks occur, their finite strain can be seen as the result of two or three heterogeneous deformations involving cleavage and folding.

In the Western domain, the angular discordance mapped in the Rush Lake area by Henderson et al. (1994b) separates ca. 2705 Ma felsic volcanic rocks from younger basalt. The regional tectonic significance of this discordance is not clearly understood because it occurs within an area of non-stratified volcanic and volcanoclastic rocks that are very difficult to subdivide and trace regionally. Felsic porphyries in the southern part of this domain have been dated at ca. 2696 and 2695 Ma. Where fragmental volcanic rocks in the Western domain have not been completely transposed, such as in the Rush Lake and Canoe Lake areas, flattened clasts are crenulated by the main northeast-striking cleavage, so the main fabric is at least an  $S_2$ .

Rocks in the Western domain are of greenschist grade, based on the common occurrence of quartz-sericite-chlorite knots in hydrothermally altered felsic volcanic rocks (see discussion of "dalmatianite" below).

In greenschist-grade sedimentary rocks of the Central domain,  $S_1$  is commonly the only cleavage, and it is axial-planar to north-south trending, steeply plunging folds. In several outcrops in the belt of turbiditic rocks east of Snofield Lake, an older deformation is indicated by reversals of younging directions observed on the  $S_1$  cleavage.

The Ulu gold property of BHP Minerals (Flood, 1991) occurs in amphibolite-grade terrane of the Central domain within a tightly folded basalt-greywacke succession trending north and plunging steeply (Henderson et al., 1993). The kilometre-scale folds locally are  $F_2$ , fold an  $S_1$  bedding-parallel cleavage, have no associated axial-plane cleavage, and are transected by the main cleavage which is an  $S_3$  fabric. This vertical, northeast-striking  $S_3$  cleavage overprints cordierite-andalusite porphyroblasts in the tightly folded metasedimentary rocks around Ulu, and crenulates the bedding-parallel  $S_1$  cleavage (Fig. 5). The strong

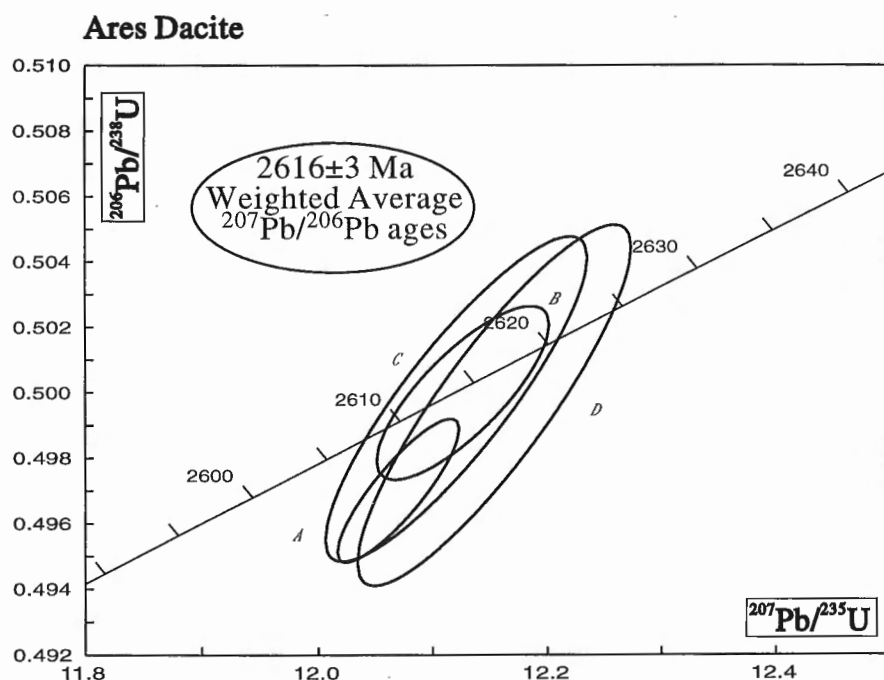


**Figure 4.**

Concordia diagram showing U-Pb zircon data for the Ares dacite, Central domain, High Lake belt.

northeast-trending  $S_3$  fabric is evident only in the southern part of the Central domain. About 10 km north of the Ulu gold property, regional metamorphism decreases to chlorite grade, and, near the andalusite isograd, coarse chiastolite porphyroblasts in graphitic slates randomly overprint the main cleavage, which is an  $S_1$  fabric (Fig. 6).

In the Eastern domain, near the southern limit of mapping along Hood River, an arm of volcanic and volcanoclastic rocks extends about 30 km east of the main part of the greenstone belt. Near the eastern limit of volcanic rocks, the dacite porphyry dated at  $2671 \pm 3$  Ma lies in the core of an east-closing vertical fold that is at least an  $F_2$  structure locally.  $S_1$  cleavage wraps around the fold closure, and the fold has no associated axial-plane cleavage. The two arms of the belt merge in a T-junction where the rocks show strong vertical lineation and no foliation. The sequence of deformations in the two arms of the belt, however, is not apparent from field relations.

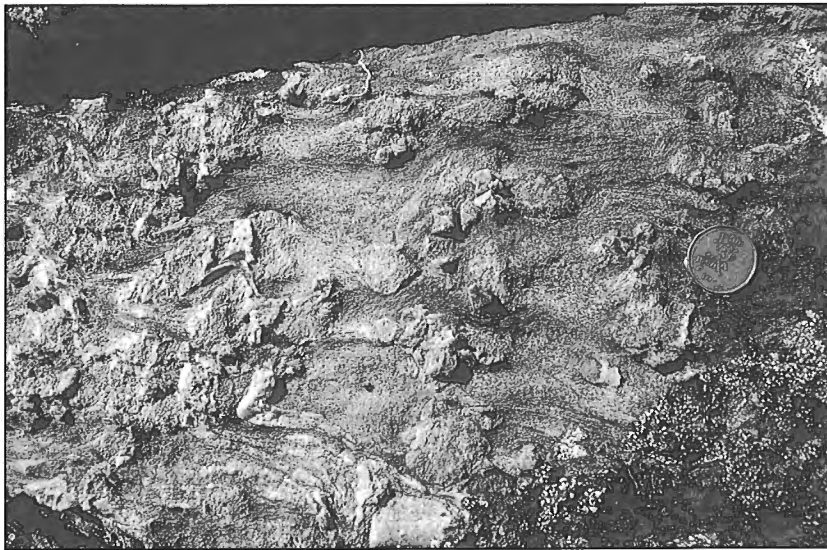


**Figure 5.**

*Photograph of metagreywacke beds (N-S in photo) with porphyroblasts of cordierite rimmed by andalusite and are wrapped by the main cleavage ( $S_3$ , E-W in photo). The blasts include an  $S_1$  cleavage. Located 500 m north of the Ulu gold property (Fig. 2). Two-centimetre diameter coin for scale.*

**Figure 6.**

*Photograph of graphitic slate beds with randomly oriented chiastolite porphyroblasts overprinting the main  $S_1$  cleavage (parallel to scale). Outcrop located about 1 km north of ca. 2616 Ma Ares dacite (Fig. 2). Four-centimetre long tweezers for scale.*





### ***Alteration zones associated with base metal mineralization***

Schists containing cordierite and/or quartz-sericite-chlorite porphyroblasts have been identified in association with known massive sulphide mineralization in several areas in the Western domain, including the High Lake AB, C, D, and E zones. These rocks appear to be chemically altered, subsequently metamorphosed intermediate to felsic volcanic and volcanoclastic rocks which are the principal hosts for the mineralization. They are thought to have been altered during synvolcanic hydrothermal activity that led to deposition of massive sulphide accumulations and/or subjacent stringer sulphide zones. Their spotted appearance has resulted in their being referred to as "dalmatianite" in the High Lake belt. Such rocks can be mistaken for metamorphosed pelitic sedimentary rocks, but their localized distribution and massive, rather than bedded, character suggest a volcanic derivation.

A preliminary assessment of lithogeochemical analyses from a suite of 13 dalmatianite samples from several areas of known massive sulphide mineralization indicates consistently low contents of Na<sub>2</sub>O, CaO, and Sr relative to a much larger suite of unaltered metavolcanic and metasedimentary rocks. These results are consistent with initial petrographic investigations, which indicate complete breakdown of plagioclase in the altered rocks. K<sub>2</sub>O and MgO contents are greater in many, but not all, of the altered samples, reflecting an increased abundance of sericite, chlorite, and/or cordierite. SiO<sub>2</sub> values do not appear to be consistently greater in the altered rocks, indicating that silicification may not have contributed significantly to dalmatianite development. CO<sub>2</sub> values are consistently low in the altered suite. Al<sub>2</sub>O<sub>3</sub>, TiO<sub>2</sub>, and Zr contents are widely variable in both suites and do not appear to be significantly different, suggesting that Al, Ti, and Zr abundances have not been greatly affected by alteration. Additional lithogeochemical studies are in progress to better define the character of the alteration zones, particularly with respect to determining the changes in mass and/or volume associated with alteration processes.

Exploration companies active in the High Lake area are currently mapping the distribution of dalmatianite as a pathfinder for synvolcanic base metal mineralization. The presence of dalmatianite and the associated depletion of Na, Ca, and Sr are clearly useful guides to hydrothermal alteration. Several zones of dalmatianite were recognized during the course of bedrock mapping in areas relatively distant from known mineralization. Such zones are clearly indicated on GSC Open File 2782 (Henderson et al., 1994a). Furthermore, as noted in Henderson et al. (1994b), the ca. 5 km<sup>2</sup> area that was mapped as metagreywacke in the Canoe Lake area (GSC Open File 2547; Henderson et al., 1992) is best described as dalmatianite, i.e. hydrothermally altered metavolcanic rocks.

### ***High Lake deposit***

The High Lake polymetallic massive sulphide deposits (AB, D, and E zones) consist of massive and stringer chalcopyrite+pyrite and sphalerite, with lesser pyrrhotite, galena, gold, and silver (Johnson, 1974; Covello, 1993). Recent work indicates

that: 1) the main AB zone contains poorly zoned (Cu vs. Zn) massive ore and chalcopyrite-rich stringer ore with apparent remobilization of chalcopyrite and lesser sphalerite and galena into fractures; 2) coarse, randomly oriented, acicular anthophyllite and subhedral magnetite define a unique massive zone or unit that is commonly intimately associated with the ore, and 3) dalmatianite occurs consistently outward of this zone. Work is in progress to better define the geometry, structural setting, mineralogy, and lithogeochemistry of the various ore zones.

### ***Geophysical anomalies associated with base metal mineralization***

Examination of assessment files indicates that known base metal occurrences produce greatly different geophysical anomalies. For example, strong to moderate coincident magnetic and electromagnetic (Mag-EM) airborne as well as ground anomalies are associated with the Ares and Ced lake occurrences (Henderson et al., 1993, Occurrences #32 and #48). In contrast, the High Lake AB, D, and E deposits are characterized by weak airborne Mag-EM responses. Furthermore, some very strong anomalies are associated with spectacular gossanous occurrences that show little evidence of base metal mineralization. The most notable example is the Pie occurrence (Henderson et al., 1994a, Occurrence #5).

### ***Age of gold mineralization***

The Flood gold zone on the Ulu gold property of BHP Minerals occurs in a northwest-striking dilatant zone in massive basalt. It is filled mainly with quartz-actinolite veins (Flood, 1991) and is approximately perpendicular to northeast-striking S<sub>3</sub> cleavage. This geometry suggests that gold mineralization may be synchronous with S<sub>3</sub> cleavage development (Henderson et al., 1993). The nearby two-mica granite dated at 2588 ± 2 Ma truncates S<sub>3</sub> cleavage, and if this model is correct, would provide a minimum age for the mineralization and S<sub>3</sub> cleavage. Abundant pre-S<sub>3</sub> metamorphic sphene occurs in mafic wall rocks of the Flood gold zone, and if amenable to U-Pb dating, they would indicate a maximum age for the mineralization and S<sub>3</sub> cleavage.

## **SUMMARY AND CONCLUSIONS**

The High Lake greenstone belt can be divided into three distinct domains on the basis of significant regional differences in lithology, types of mineral occurrences, and possibly age of volcanism. On this basis it is possible to predict that epigenetic gold deposits are most likely to be discovered in the Central domain.

Field relations and U-Pb zircon dating indicate that three or four volcanic sequences or cycles are present in High Lake belt: ca. 2705 Ma, 2696-2695 Ma, 2670 Ma, and possibly 2616 Ma. These ages are consistent with ages of volcanic rocks across the Slave Province (cf. Villeneuve et al. 1993; Isachsen and Bowring, 1994).

Hydrothermal alteration zones commonly associated with massive sulphide mineralization in the Western volcanic domain are characterized by the presence of spotted schist (dalmatianite), a sodium-depleted intermediate or felsic volcanic rock in which primary plagioclase has broken down to sericite.

## ACKNOWLEDGMENTS

Tom Wright mapped and resolved several problem areas where more information was required to delineate fold closures. Dave Graham diligently mapped the boundaries of Coronation Sills. Rod Kirkham examined several mineral occurrences and exposures of iron formation, and provided food for thought regarding their genesis (see Kirkham and Roscoe, 1993). We thank Bob Bell and Great Slave Helicopters for excellent logistical support, and Craig Nicholson for superior expediting service. Sharing of camp facilities at High Lake with Covello, Bryan and Associates significantly expedited our fieldwork. Doug Bryan, Jim Siddel, and Normand Bégin of Covello, Bryan and Associates are thanked for sharing their knowledge of High Lake belt mineral occurrences. Dave Thomas of Metall Mining is thanked for comparison of Run Lake and High Lake geology, as well as for sharing insights on dalmatianite genesis. Paul Cowley, Eugene Flood, and Greg McMaster of BHP Minerals Canada are thanked for sharing their knowledge on the geology of several parts of High Lake belt. We thank Bruce Kjarsgaard, Janet King and John B. Henderson for improvements to the draft manuscript.

## REFERENCES

- Covello, L.  
1993: High Lake-An Update; in Exploration Overview 1993, (ed.) S.P. Goff; Indian and Northern Affairs Canada, Geology Division, Yellowknife, p. 26-27.
- Easton, R.M., Ellis, C.E., Dean, M., Bailey, G., Bruneau, H.C., and Walroth, J.  
1982: Geology of the Typhoon Point map area, High Lake greenstone belt (76M/10 and 76M/15 south-half); Indian and Northern Affairs Canada, Northern Affairs Program, Geology Division, Yellowknife, EGS 1982-6, scale 1:31 680.
- Flood, E.  
1991: BHP-UTAH Mines Ltd. Ulu gold property; in Exploration Overview 1991, (ed.) J.A. Brophy; Indian and Northern Affairs Canada, Geology Division, Yellowknife, p. 22.
- Fraser, J.A.  
1964: Geology notes on the northeastern District of Mackenzie, NWT; Geological Survey of Canada, Paper 63-40, 20 p., Map 45-1963, scale 1:506 880.
- Henderson, J.B.  
1975: Archean stromatolites in the northern Slave Province, Northwest Territories; Canadian Journal of Earth Sciences, v. 12, p. 1619-1630.
- Henderson, J.R., Arias, Z., Henderson, M.N., Lemkow, D., Wright, T.O., Rice, R., and Kerswill, J.A.  
1992: Geology and mineral occurrences of the central High Lake greenstone belt, Slave Province, Northwest Territories; Geological Survey of Canada, Open File 2547, scale 1:100 000.
- Henderson, J.R., Henderson, M.N., Kerswill, J.A., Arias, Z., Lemkow, D., Wright, T.O., and Rice, R.  
1993: Geology and mineral occurrences of the southern part of High Lake greenstone belt, Slave Province, Northwest Territories; in Current Research, Part C; Geological Survey of Canada, Paper 93-1C, p. 125-136.
- Henderson, J.R., Henderson, M.N., and Kerswill, J.A.  
1994a: Preliminary geological map of north-central High Lake Greenstone Belt, N.W.T., NTS 76M/6 East, 76M/7; Geological Survey of Canada Open file 2782, scale 1:50 000.  
1994b: Geology and mineral occurrences of the central part of High Lake greenstone belt, Archean Slave Province, Northwest Territories; a preliminary account of an unconformity between two volcanic sequences; in Current Research 1994-C; Geological Survey of Canada, p. 81-90.
- Henderson, J.R., Kerswill, J.A., Henderson, M.N., Villeneuve, M., Petch, C.A., Dehls, J.F., and O'Keefe, M.D.  
in press: Preliminary geological map of northern High Lake greenstone belt, N.W.T., NTS 76M/10 and 15; Geological Survey of Canada, Open File, scale 1:50 000.
- Isachsen, C.E. and Bowring, S.A.  
1994: Evolution of the Slave craton; Geology, v. 22, p. 917-920.
- Jackson, V.A., Bell, R., Bishop, S., Daniels, A., Howson, S., Kerr, D.E., and Treganza, M.  
1986a: Preliminary geology of the eastern Hepburn Island area, NTS 76M/1, 2, 8, 9, 15, 16; Indian and Northern Affairs Canada, Geology Division, Yellowknife, EGS 1986-6, scale 1:50 000.  
1986b: Preliminary geology of the Hood River area, NTS 76L/10, 15, 16, NWT; Indian and Northern Affairs Canada, Geology Division, Yellowknife, EGS 1986-4, scale 1:50 000.
- Jefferson, C.W., Henderson, M.N., Henderson, J.R., and Schaan, S.  
1990: Geological setting of stratabound gold occurrences in the Archean Fish-hook-Turner lakes belt, Bathurst Inlet area, District of Mackenzie, N.W.T.; in Current Research, Part C; Geological Survey of Canada, Paper 90-1C, p. 349-361.
- Johnson, W.  
1974: Geology of two base metal deposits of the Slave structural province; Geological Survey of Canada, Open File 239, 16 p.
- Kerswill, J.A., Brophy, J.A., Thompson, P.H., Henderson, J.R., Henderson, M.N., Bretzlaff, R., Arias, Z., and Garson, D.G.  
1993: Recent developments in the metallogeny of Slave Province with emphasis on the Courageous Lake and High Lake greenstone belts; in Mining, Exploration and Geological Investigations, Exploration Overview 1993, Northwest Territories, (ed.) S.P. Goff; Northwest Territories Geology Division, Indian and Northern Affairs Canada, p. 39-40.
- Kirkham, R.V. and Roscoe, S.M.  
1993: Atmospheric evolution and ore deposit formation; Resource Geology Special Issue, No. 15, p. 1-17.
- Padgham, W.A., Jefferson, C.W., Hughes, D.R., and Shegelski, R.J.  
1973: Geology of the High Lake area N.W.T. (76M7); Geological Survey of Canada, Open File 208, scale 1:50 000.
- Parrish, R.R., Roddick, J.A., Loveridge, W.D., and Sullivan, R.W.  
1987: Uranium-lead analytical techniques at the geochronology laboratory, Geological Survey of Canada; in Radiogenic Age and Isotopic Studies: Report 2; Geological Survey of Canada Paper 87-2, p. 3-7.
- Relf, C., Chouinard, A., Sandeman, H., and Villeneuve, M.  
1994: Contact relationships between the Anialik River volcanic belt and the Kangguyak gneiss belt, northwestern Slave Province, Northwest Territories; in Current Research 1994-C; Geological Survey of Canada, p. 49-59.
- Tirrul, R. and Bell, I.  
1980: Geology of the Anialik River Greenstone Belt, Hepburn Island Map Area, District of Mackenzie; in Current Research, Part C; Geological Survey of Canada, Paper 80-1C, p. 157-164.
- van Breemen, O., Henderson, J.R., Jefferson, C.W., Johnstone, R.M., and Stern, R.  
1994: U-Pb age and Sm-Nd isotopic studies in Archean Hood River and Torp Lake supracrustal belts, northern Slave Province, Northwest Territories; in Radiogenic Age and Isotopic Studies: Report 8; Geological Survey of Canada, Current Research 1994-F, p. 1-16

**van Breemen, O., Davis, W.J., and King, J.E.**

1992: Temporal distribution of granitoid plutonic rocks in the Archean Slave Province, northwest Canadian Shield; Canadian Journal of Earth Sciences, v. 20, p. 2186-2199.

**Villeneuve, M., Hrabí, B., Jackson, V., and Relf, C.**

1993: Geochronology of supracrustal sequences in the central and northern Slave Province; in Mining, Exploration and Geological Investigations, Exploration Overview 1993, Northwest Territories, (ed.) S.P. Goff; Northwest Territories Geology Division, Indian and Northern Affairs Canada, p. 53-54.

**Yeo, G.M., Bailey, G., Crux, J., Fisher, B., Jackson, V., Relf, C., and Walroth, J.**

1983: Preliminary geology of the western Hepburn Island map area, NTS 76M/3, 4, 5, 6, 11, 12, 13, 14; Indian and Northern Affairs Canada, Geology Division, Yellowknife, EGS 1983-8.

---

Geological Survey of Canada Project 870008-KC

# Regional geology and mineral potential of the Winter Lake-Lac de Gras area, central Slave Province, Northwest Territories<sup>1,2</sup>

P.H. Thompson, I. Russell<sup>3</sup>, D. Paul, J.A. Kerswill<sup>4</sup>, and E. Froese  
Continental Geoscience Division

*Thompson, P.H., Russell, I., Paul, D., Kerswill, J.A., and Froese, E., 1995: Regional geology and mineral potential of the Winter Lake-Lac de Gras area, central Slave Province, Northwest Territories; in Current Research 1995-C; Geological Survey of Canada, p. 107-119.*

---

**Abstract:** Completion of regional mapping further emphasizes division of the area into one domain of metamorphosed sedimentary rocks and a second dominated by recrystallized, migmatitic, and gneissic granitoids. Discordant metamorphosed dykes, discordant isograds, and the change from curvilinear fold interference patterns to blocky, subrhombic structures indicate the metagranitoid complexes are older than Yellowknife Supergroup supracrustal rocks.

Interpreted as a relict of extensional structures related to basin formation, the subrhombic distribution of supracrustal rocks within and around large blocks of metagranitoid had a strong influence on later compressional structures.

Geothermal gradients associated with regional low pressure metamorphism are high enough to have generated syntectonic magmatism from moderately overthickened sialic crust and to preclude an Archean age for diamonds.

Metamorphosed hydrothermal alteration zones found near base metal occurrences in the Courageous Lake volcanic belt also occur in less well explored and in newly discovered supracrustal sequences. Sulphide banded iron-formation, not previously recognized, provides additional economic interest.

**Résumé :** La cartographie régionale accentue la division de la région en un domaine de roches sédimentaires métamorphosées et en un domaine dominé par des granitoïdes migmatitiques et gneissiques recristallisés. Des dykes métamorphosés discordants, les isogrades discordants et le passage de structures curvilignes d'interférence de plis à des structures subrhombiques en blocs indiquent que les complexes métagranitoïdes sont plus anciens que les roches supracrustales du Supergroupe de Yellowknife.

Interprétée comme un résidu de structures d'extension liées à la formation de bassins, la répartition subrhombique des roches supracrustales au sein et autour de gros blocs de métagranitoïdes a eu une forte influence sur les structures de compression ultérieures.

---

<sup>1</sup> Contribution to Canada-Northwest Territories Mineral Initiatives (1991-1996), an initiative under the Canada-Northwest Territories Economic Development Cooperation Agreement.

<sup>2</sup> Contribution to the Slave NATMAP Project

<sup>3</sup> University of Saskatchewan, Saskatoon

<sup>4</sup> Mineral Resources Division

Les gradients géothermiques associés au métamorphisme régional de faible pression sont suffisamment élevés pour avoir causé un magmatisme syntectonique à partir d'une croûte sialique modérément surépaissie et pour exclure la possibilité que les diamants remontent à l'Archéen.

Les zones d'altération hydrothermale métamorphisées observées près des occurrences de métaux communs dans la ceinture volcanique de Courageous Lake sont situées dans des séquences supracrustales moins bien explorées ou de découverte récente. Les formations de fer rubanées sulfurées, non décelées antérieurement, offrent un intérêt économique supplémentaire.

## INTRODUCTION

The Winter Lake-Lac de Gras area contains parts of two lithotectonic elements that recur across the Slave Province (Fig. 1). Metasedimentary rocks of the Yellowknife Supergroup, the first element, are predominant in the northeast. Recrystallized, migmatitic, and gneissic granitoid rocks in the southwest, here referred to collectively as older granitoids, make up the second. Younger, massive granitoid plutons intrude both elements. Narrow volcanic belts of the Yellowknife Supergroup commonly separate older granitoids from metasedimentary rocks.

The older granitoid domain is divided into large blocks, tens of kilometres wide, by supracrustal belts linking the northeastern sedimentary domain with the Yellowknife sedimentary domain 150 km to the southwest (Fig. 1). The characteristic distribution of volcano-sedimentary belts, straight line segments between sharply defined angles, extends beyond the map area to form a northwest-oriented zone about 300 km long and 150 km wide. This zone includes pre-Yellowknife basement rocks at Point Lake, 80 km southwest of Point Lake, in the Sleepy Dragon complex, and southwest of MacKay Lake.

Metasedimentary rocks in the map area join Padgham's (1990) MacKay-Aylmer Lake and Contwoyto-Itchen (Point) Lake basins to form an extensive metasedimentary element in the middle of the Slave Province here referred to as the "Contwoyto-MacKay sedimentary domain" (Fig. 1). The domain contains gold mines (one active, three inactive), base metal deposits, and most reported diamondiferous kimberlites. With only one known diamond occurrence and no reported occurrences of the other commodities, the older granitoid domain appears to have a much lower mineral potential. This report summarizes results of the last of three field seasons and considers briefly some implications for Archean evolution and mineral potential in the central Slave Province.

Current mapping (1:250 000 scale) extended and refined the regional geological framework outlined by Folinsbee (1949) in the east half of the area and by Fraser (1969) in the west half. Previous detailed mapping was limited to the Courageous Lake volcanic belt (Moore, 1956; Dillon-Leitch, 1981). Hrabí et al. (1994) are studying the stratigraphy and structure of the Winter Lake supracrustal belt (Fig. 1).

## ROCK UNITS

The completed preliminary map of the Winter Lake-Lac de Gras area (Fig. 2) was recently released as Open File 2740 (Thompson and Kerswill, 1994), which supersedes earlier versions (Thompson et al., 1993b). Previously published rock unit descriptions (Thompson et al., 1993a, 1994) are not repeated in this report. "Older granitoids" are considered, for the most part, to be older than the Yellowknife Supergroup (Henderson, 1970) on the basis of the occurrence of discordant metadykes, a change from curvilinear fold interference patterns to blocky, subrhombic structures, and discordant isograds (Thompson et al., 1993a, 1994). "Younger granitoids" are intrusive into supracrustal rocks and the older metaplutonic suite.

### *Older granitoids (units 1-4)*

Migmatitic quartzofeldspathic gneiss and granitoid migmatite north and south of Winter Lake have the same textural heterogeneity, simple mineralogy, and hornblende-bearing leucosomes that are found in the Jolly Lake complex (Thompson et al., 1994). The associated recrystallized, deformed granitoid rocks are also virtually identical. Gneissic, migmatitic, and foliated granitoids south of Winter Lake are part of a complex the extent of which is presently unknown. The Big Lake complex is bounded by the Winter Lake belt to the east, the newly recognized supracrustal package to the southwest (Fig. 2) and metavolcanic rocks to the north and northwest (Fig. 3).

### *Volcanic and related rocks (units 5, 6)*

In general, the scale and degree of lithological heterogeneity in this unit (Fig. 2) are such that differentiation of individual rock types is not possible at 1:250 000 scale. Where felsic volcanic rocks are sufficiently extensive, they are differentiated as unit 6.

Outcrops of Yellowknife Supergroup metavolcanic and meta-sedimentary rocks noted by Fraser (1969) north and east of Winter Lake were found to be part of an extensive supracrustal sequence that is essentially continuous with the Winter Lake supracrustal belt (Fig. 2). Reconnaissance traverses northwest of Winter Lake, outside the project area, indicate that these rocks may be continuous with volcanic belts at Point Lake (Fig. 3).

Southwest of Lake Providence, Quaternary cover obscures what is probably a complex intercalation of volcanic and related rocks (unit 5) with metagreywacke and foliated or migmatitic metagranitoid linking the northwest corner of the Jolly Lake complex to hornblende metagranite (unit 4). Mapping in 1994 led to recognition of more felsic volcanic rocks within the sequence and revealed granitoid migmatite within knotted schist immediately to the southwest. Intercalation of

supracrustal rocks, granitoid migmatite, and foliated metagranite northwest and southwest of Beauparlant Lake may be, at least in part, related to thrusting during the earliest stage of crustal shortening (Thompson, 1992).

Completion of regional mapping revealed the wide extent of metamorphosed sedimentary and felsic to intermediate volcanic rocks beneath the prominent mafic metavolcanic sequences within unit 5. The present mapping, together with Hrabí et al. (1994), confirm Fraser's (1969) recognition of felsic to intermediate supracrustal rocks within unit 5 along the western edge of the Winter Lake supracrustal belt. These rocks separate several hundred metres of pillowed mafic metavolcanic rocks from metagranitoid. Southeast of Winter Lake (Fig. 3), banded iron formation was found in a similar sequence, less than 150 m thick, that separates metatonalite from mafic metavolcanic rocks. Metamorphosed pelitic and quartz-rich sedimentary and felsic to intermediate volcanoclastic rocks also occur between mafic metavolcanics/metagabbro and quartzofeldspathic gneiss along the eastern border of the Winter Lake belt (Thompson, 1992). Thinner sequences of similar rocks underlie mafic volcanic rocks in the Desteffany Lake and Courageous Lake volcanic belts (Fig. 3). Felsic metavolcanic rocks were also deposited on top of pillowed mafic lavas. The thickest felsic sequence is south of Courageous Lake. Smaller felsic masses occur elsewhere at the upper contact of the volcanic belts with metasedimentary rocks or within these overlying rocks (Fig. 2, 7).

Periods of mafic volcanism bracketed by felsic events are a feature of parts of all the volcanic belts in the map area. Wherever the lower felsic sequence does occur, there is no structural discordance or contrast in metamorphic grade to indicate it is greatly older than overlying and intercalated mafic volcanic rocks. All volcanic and sedimentary rocks in unit 5 are therefore considered to be part of the Yellowknife Supergroup.

Several occurrences of quartz-rich metasedimentary rocks within volcanic and related rocks (unit 5) were found in addition to those reported by Thompson et al. (1993a) (Fig. 3). At the southernmost of two localities northwest of Big Lake, quartz arenite is several hundred metres thick. In most cases, however, they are centimetre- to metre-scale lenses or layers of quartz arenite, pebbly quartz-muscovite schist, and/or quartz-muscovite-chlorite schist. J.B. Henderson (pers. comm., 1993) considers similar sandstones that are associated with the unconformity at the base of the Keskarrah conglomerate (Point Lake) to be quartz lag deposits. North of Courageous Lake, an isolated outcrop of fuchsite-bearing quartz arenite appears to be an inclusion in pink megacrystic granite. A striking spatial relation exists between the distribution of these quartz-rich rocks and the contact between supracrustal rocks and the older granitoid domain (Fig. 3).

**Undivided granitoids (unit 9)**

Thompson et al. (1993 a,b) divided granitoids into older and younger suites, on the basis of texture and contact relations. As a result of field work in 1994, a third category was established. "Undivided granitoids" includes those that have the characteristics of older granitoids but may be the same age

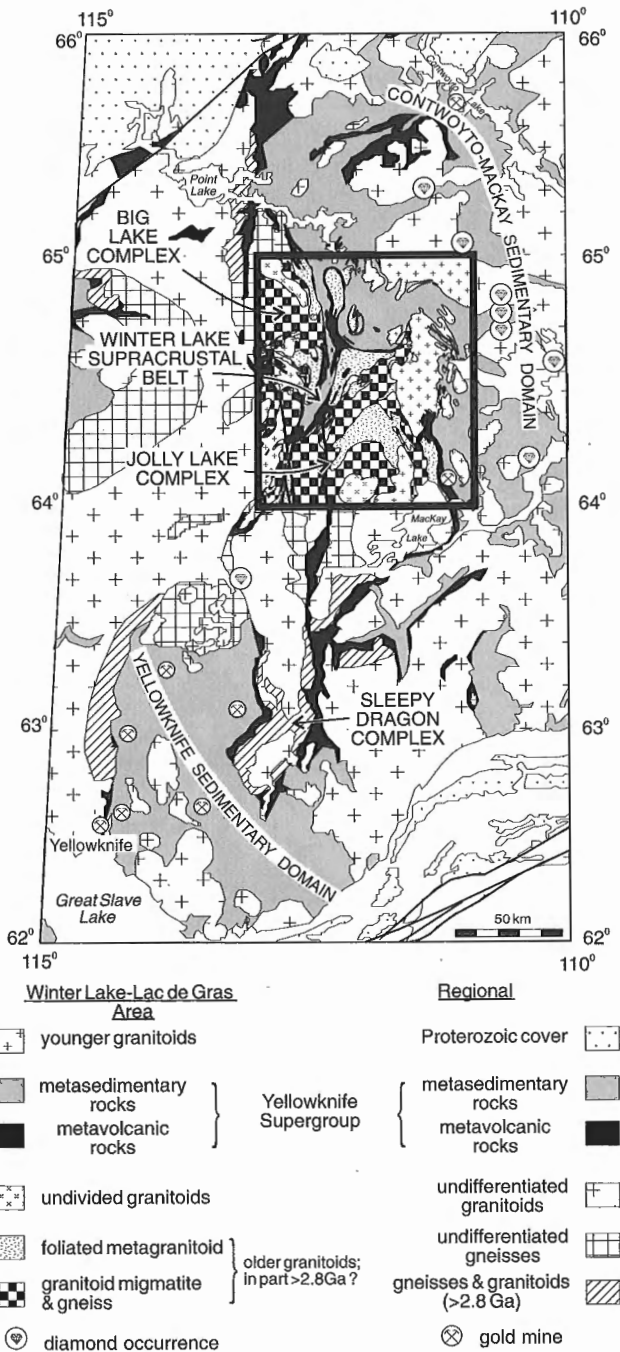


**Figure 1.** Location and Archean geological context of the Winter Lake-Lac de Gras area, southwestern Slave Province (after Henderson, 1985).

as the Yellowknife Supergroup and those that are old enough to be part of the older association but have not developed the metamorphic and deformational textures typical of other metagranitoids. For example, unit 9 includes mainly massive homogeneous plutons which occur in the middle of the Jolly Lake and Big Lake granitoid complexes (Fig. 2). Like foliated

metagranite-tonalite (unit 3), both plutons are conformable with structures in adjacent rocks, but unlike older granitoids they are apparently not recrystallized. Furthermore, the north-western pluton is continuous with a unit containing zircons 2685 Ma old (Bostock, 1980), a typical age of volcanism in the Yellowknife Supergroup (van Breemen et al., 1992).

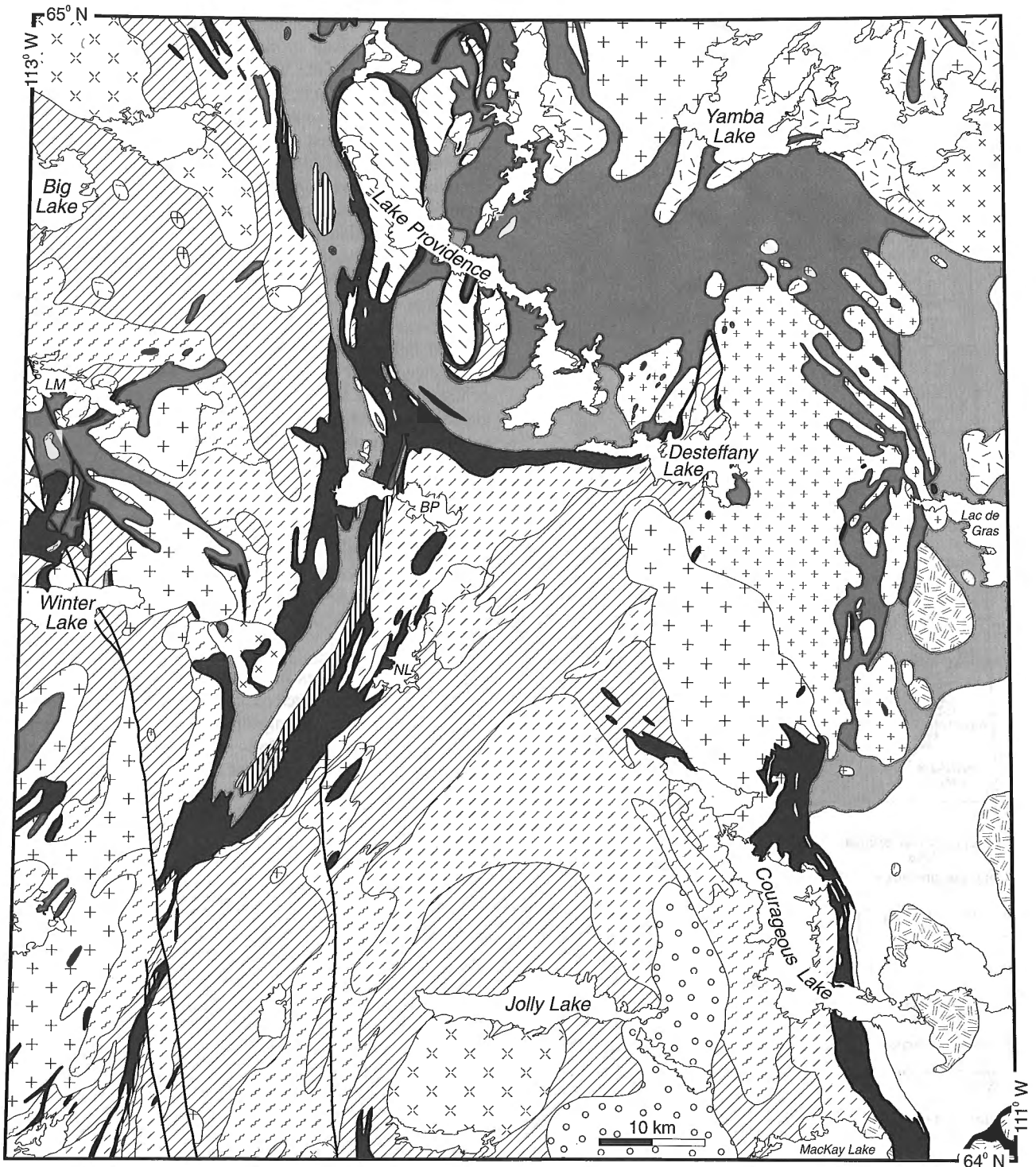


**Figure 2.** Preliminary geology of the Winter Lake-Lac de Gras map area (NTS 76D-W1/2, 86A-E1/2). Mafic dykes omitted for clarity. BP - Beuparlant Lake, NL - Newbigging Lake.

Therefore, the pluton was old enough to have been deformed and metamorphosed along with the Yellowknife Supergroup. The pluton's relatively well preserved state may indicate that it was protected from deformation by the surrounding granitoid complex. Alternatively, the pluton is a younger granitoid (Fraser, 1969) and the zircons are xenocrysts.

**Metamorphosed mafic dykes**

More examples of metamorphosed mafic dykes intrusive into granitoid migmatite and metagranitoid were found near the western contacts of metavolcanic sequences south of Point Lake, at Courageous Lake, and in the Winter Lake belt (Fig. 3). Considered to be equivalent to mafic magmatic rocks within the supracrustal sequence (Moore, 1956), these rocks are one aspect of the evidence (Thompson et al., 1994) indicating the older granitoids are basement to the Yellowknife Supergroup.

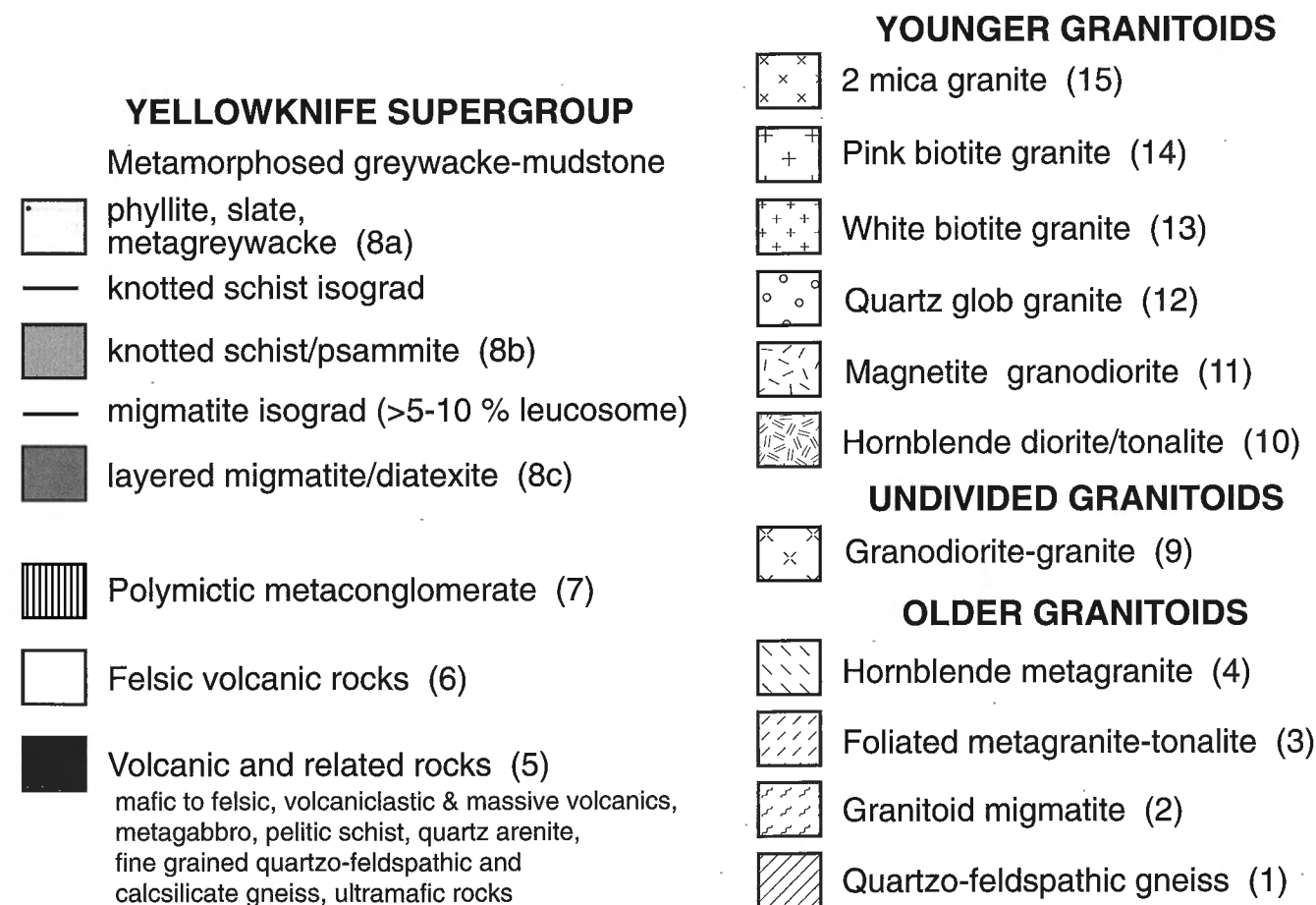
**GEOCHRONOLOGY AND STRATIGRAPHY**

At the regional scale of mapping in the study area, supracrustal rocks underlying mafic rocks within belts of unit 5 cannot be differentiated from the rest of the sequence. These

rock units are concordant with overlying rocks that exhibit similar degrees of strain. There is no contrast in metamorphic grade indicating different tectonic histories. Lithological variation may reflect different depositional environments rather than age differences. Zircons in felsic volcanic rocks associated with quartz arenite which underlie mafic volcanic sequences range from the age of basement rocks in the Winter Lake supracrustal belt (3.12 Ga, Villeneuve et al., 1993) to 2.668 Ga in the Beniah Lake area (J.K. Mortenson, pers. comm., 1992). The latter age is similar to that of zircons in a felsic porphyry that is younger than mafic volcanic rocks in the Courageous Lake belt (Villeneuve, 1993). In felsic volcanic rocks, the oldest zircons could be xenocrysts. Very old detrital zircons in quartz arenite (Villeneuve et al., 1993) could be derived from ancient granitoid crust or from weathered rhyolite containing xenocrysts inherited from that crust. In view of the age range and in the absence of geological evidence of significant age differences, it may be premature to remove from the Yellowknife Supergroup supracrustal rocks that underlie mafic rocks in volcanic belts of the central Slave Province, as proposed by Padgham (1990).

Polymictic metaconglomerate (Fig. 2) is intimately intercalated with metamorphosed volcanic rocks and greywacke-mudstone. It has been subjected to the same degree of metamorphism and deformation as that which affected

Legend for Figure 2.





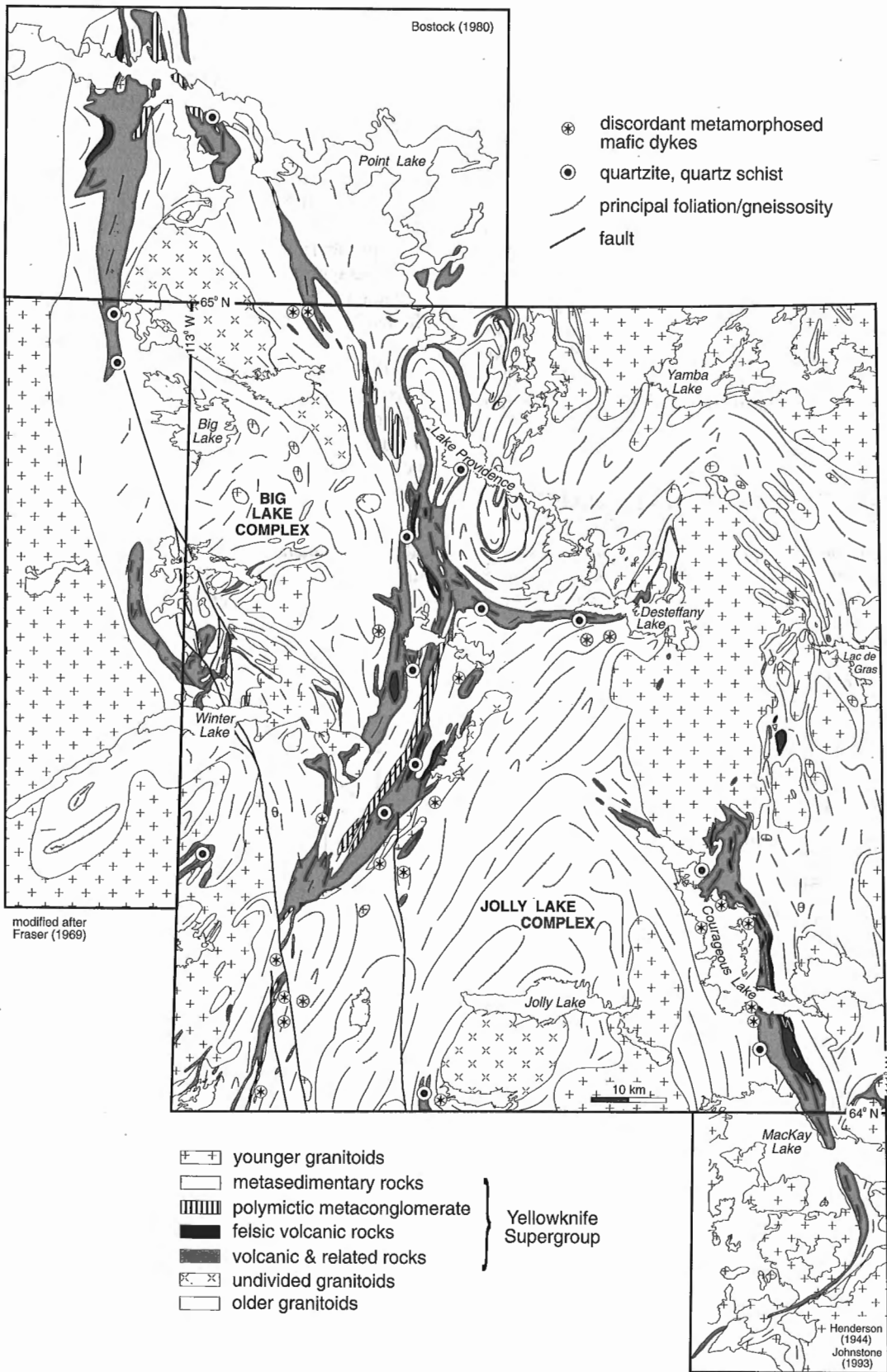


**Figure 3.** Trends of principal foliation and gneissosity. Note local discordance between structure in older granitoids and that in overlying Yellowknife Supergroup supracrustal rocks. Discordant metamorphosed mafic dykes occur in older granitoids near overlying volcanic belts.

adjacent supracrustal rocks. It appears to have been intruded by a foliated metatonalite. On this basis, Thompson et al. (1994) inferred that deposition of the conglomerate overlapped in time with Yellowknife Supergroup volcanism and sedimentation (2.66–2.69 Ga, van Breemen et al., 1992). Hrabi et al. (1993) suggested a much younger age and a Timiskaming-like depositional setting that is inconsistent with regional field evidence. Metaconglomerate elsewhere in the Slave Province contains zircons giving ages of 2.6 Ga (Villeneuve et al., 1993). In the map area such a young depositional age requires that regional metamorphism and the main phases of deformation occur in very short time. 2.6 Ga would be more compatible with the geological context of the metaconglomerate if it were the age of regional metamorphism. Thompson (1989) related metamorphism to 30–40 Ma of crustal shortening and overthickening which began soon after deposition of the Yellowknife Supergroup ended.

### CHANGE IN STRUCTURAL STYLE AT THE DOMAIN BOUNDARY

With the completion of regional mapping the contrast in structural styles between the older granitoid and the metasedimentary domains (Fig. 3) described by Thompson et al. (1994) is further emphasized. Where metasedimentary rocks are predominant, complex curvilinear fold interference patterns occur. In the domain dominated by granitoid rocks, narrow belts of supracrustal rocks outline angular to subangular folds around blocky masses of foliated, migmatitic, and gneissic granitoid. Thompson et al. (1994) suggested that this change marked the edge of an extensional ensialic basin and that the granitoid domain represents less thinned, relatively cool, sialic crust where relatively competent horsts of sialic crust are separated by thin troughs of volcanic and sedimentary rocks. In the basin (metasedimentary domain), less competent supracrustal rocks are thicker and underlying crust is presumably thinner. The contrast in competency could explain why the domains responded differently to horizontal shortening causing the observed change in structural style. A corollary of this explanation is that any interpretation of structures in the central Slave Province must consider interaction between a framework established during basin formation and subsequent shortening and overthickening.

### BRITTLE FAULTS

Brittle faults in the southwestern part of the map area (Fig. 3) do not cause major displacements of Archean structures. Most mylonitic fabrics in the vicinity of the faults are parallel to foliations and gneissosity of Archean age. These structures are commonly strongly oblique to topographic and aeromagnetic expressions of the faults. On the other hand, the faults appear to follow Archean structures at both regional and local scales wherever orientation of the older structures is appropriate. A prominent linear feature 10 km west of Jolly Lake corresponds to a fault with 2–3 km of sinistral offset south of the map area (Stubley, 1990). At the intersection with the Winter Lake belt, displacement is less than 300 m

(R.B. Hrabi, pers. comm., 1994). Just south of the intersection, the fault jogs parallel to the regional fabric for several hundred metres. North of Winter Lake, the main branch of the fault system probably splays along amphibolite facies Archean high strain zones. Farther northwest, the linear aeromagnetic anomaly that corresponds to the fault follows Archean foliation trends that curve into a northerly orientation across Point Lake.

### REGIONAL METAMORPHISM

On the completed metamorphic map (Fig. 4), metamorphic grade ranges from lower greenschist to upper amphibolite facies. Younger granitoids crosscut low-pressure, high-temperature isograds that are discordant to the older granitoid complex. Lowest grade rocks are adjacent to the northwest and east contacts of the Jolly Lake complex. Widely-distributed migmatitic metasedimentary rocks west of the Winter Lake supracrustal belt indicate that high-grade conditions prevailed at least as far west as the map boundary. Two occurrences of orthopyroxene-bearing gneiss in the southwest corner of the map area indicate that granulite facies conditions like those described by Henderson and Chacko (1995) 125 km to the southwest were attained locally.

### Geothermal gradients

The increase in temperature with depth in the lithosphere (geothermal gradient) during orogenesis is a critical factor with respect to granitoid magmatism and diamond genesis, among other things. Metamorphic mineral assemblages indicate that geothermal gradients were extremely high in the Slave Province in the late Archean (Fig. 5). Rocks metamorphosed at depths of 10–15 km and now at the surface of sialic crust of normal thickness (35 km) indicate that the crust was moderately overthickened during horizontal shortening associated with the main phases of folding (Thompson et al., 1994). Imposition of such high gradients on overthickened sialic crust can produce abundant magmatism. For example, experiments by Rutter and Wiley (1988) indicate that in crust 50 km thick with a composition of biotite tonalite, 30 per cent of the lowermost 15 km would be melt (inset, Fig. 5). The compositions of younger granitoids provide evidence of partial melting of various compositions, probably at different depths in the crust. On the other hand, lithospheric thicknesses on the order of 200 km, implying low geothermal gradients (Pollack and Chapman, 1977), are associated with many diamond fields. The high geothermal gradients required for low-pressure regional metamorphism (Fig. 5) imply much thinner lithosphere. Diamonds in the central Slave Province probably formed in the Late Proterozoic or later, long after thermal effects of Archean orogenesis had waned.

### Mineral assemblages and rock composition

The isograds shown in Figure 5 can be related to an erosion surface pressure-temperature array and a reaction grid for pelitic rocks (Fig. 6a). Many minerals, in the presence of quartz, can be represented in the system  $Al_2O_3$ -FeO-MgO. In

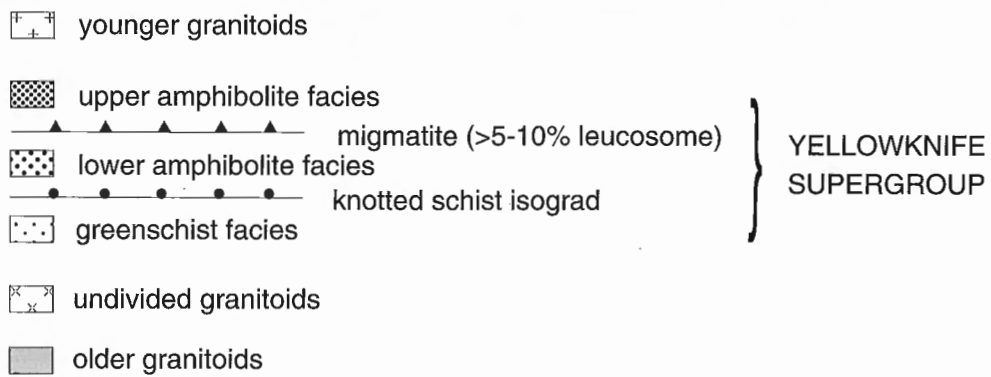
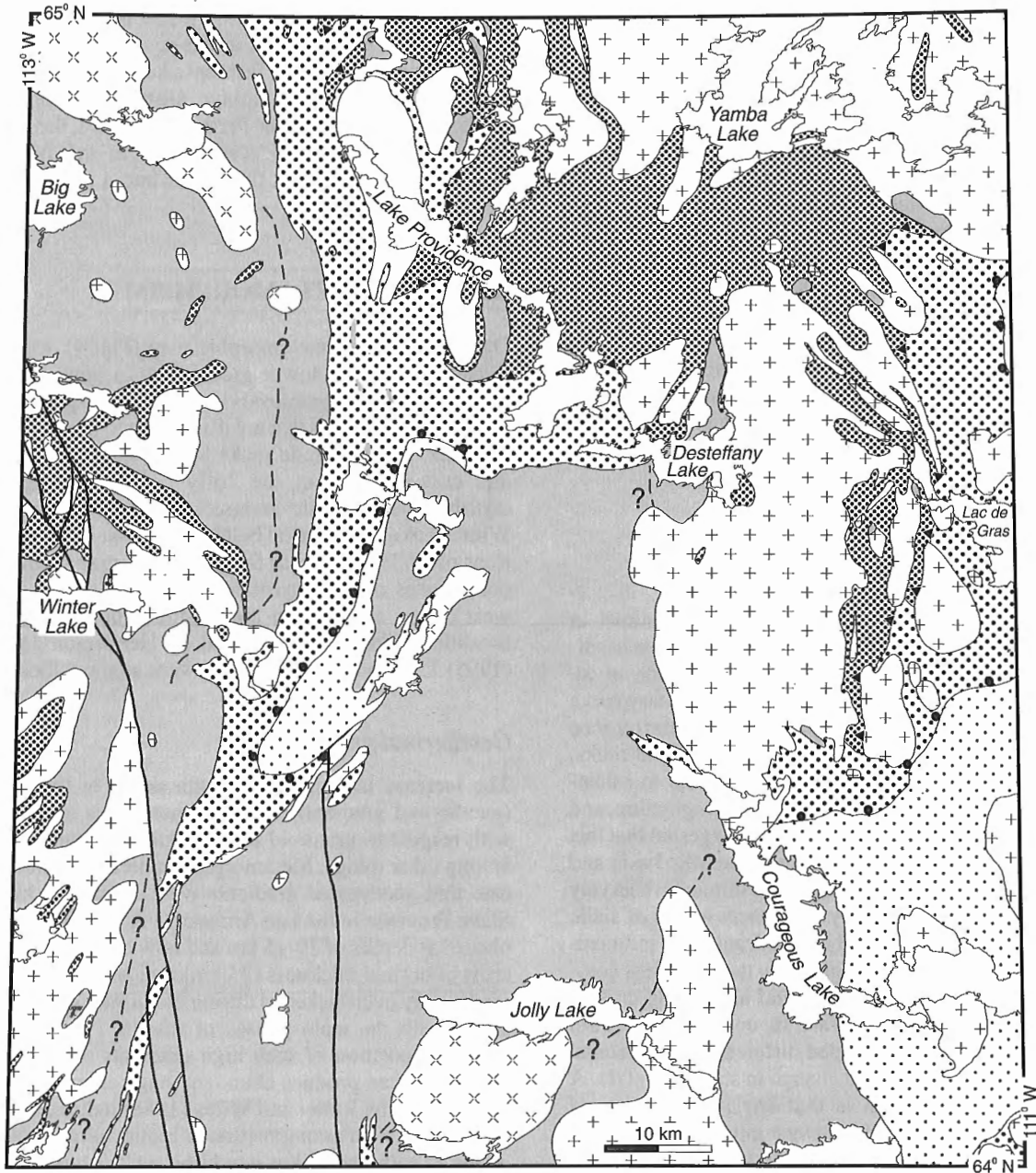


**Figure 4.** Distribution of low-pressure regional metamorphism. Isograds are discordant to older granitoids and intruded by younger granitoids indicating that neither suite is a likely source of heat for metamorphism. "?" indicates possible extrapolation of isograds.

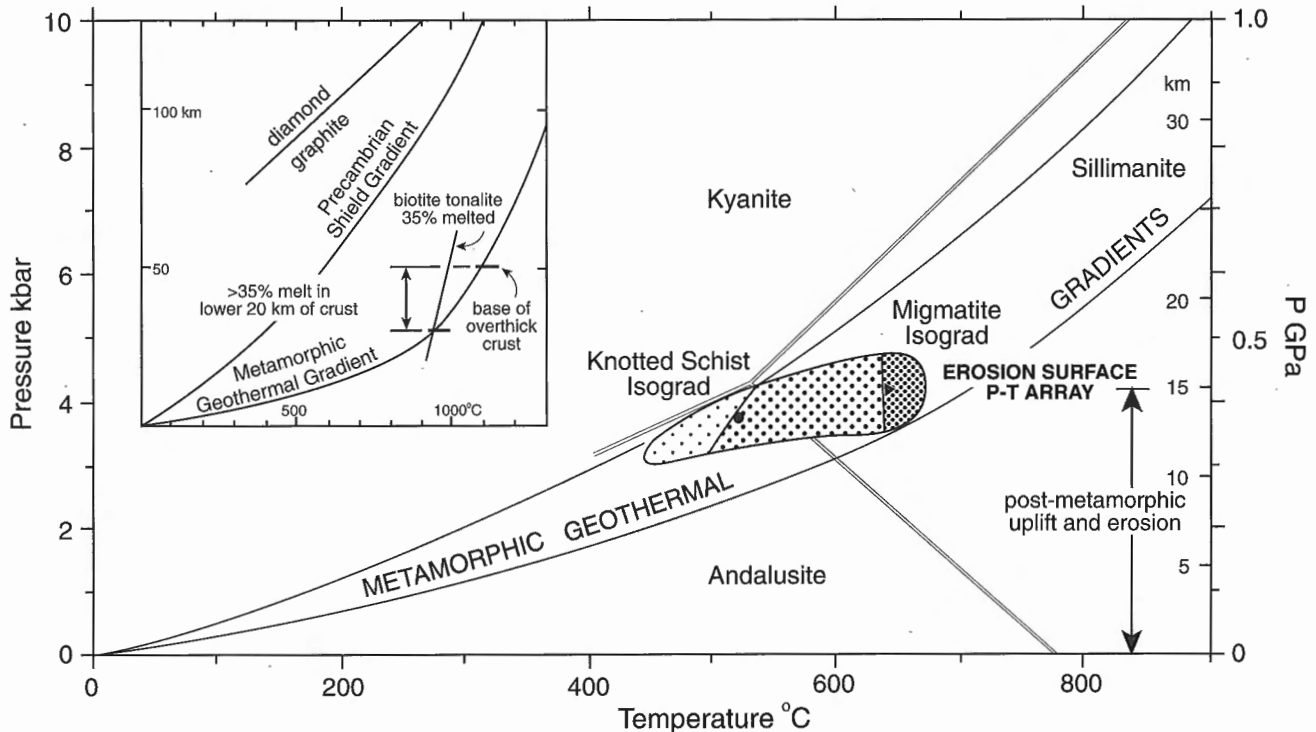


**Figure 5.** Pressure-temperature diagram indicating peak metamorphic conditions estimated from mineral assemblages in pelitic rocks on the erosion surface. Ten to fifteen kilometres of uplift and erosion have occurred since these conditions were attained. Associated geothermal gradients are high enough to have caused widespread melting in the lower and middle crust (inset).

order to include  $K_2O$ -bearing minerals,  $K_2O$  must be introduced as a component. In general, this will give rise to one additional mineral, either muscovite or biotite; fields of these can be shown on the  $Al_2O_3$ - $FeO$ - $MgO$  diagram. Such a diagram, valid for the knotted schist zone, is shown in Figure 6b. The typical mineral assemblage of metamorphosed greywacke-mudstone is represented in the andalusite-cordierite field on the muscovite-biotite boundary. Mineral assemblages in rocks of more unusual compositions can also be shown. Iron-formation in the map area plots in the cummingtonite-garnet field. Metasomatically altered volcanic rocks, in many instances associated with sulphide mineralization, plot in the cordierite-orthoamphibole and/or cordierite-cummingtonite fields.

## ECONOMIC GEOLOGY

### *Metallogeny of the Courageous Lake greenstone belt*

Eighty-two mineral occurrences are located and tabulated in GSC Open File 2740 (Thompson and Kerswill, 1994). Examination of the distribution of rock types and mineral occurrences in the Courageous Lake volcanic belt (Fig. 7) indicates well defined metallogenic zoning (Kerswill et al., 1993). All former gold mines and most gold occurrences are within an eastern zone that is either within or near the commonly gossanous transition between the top of the

volcanic-dominated belt and overlying turbidites. Most base metal occurrences, including both stratiform and vein-related mineralization, are within a western zone that is well within the volcanic/sedimentary transition. Recent field investigations and compilation of geophysical information strongly suggest that the largely synvolcanic base metal mineralization of the western zone occurs within an older volcanic sequence, and that much of the largely epigenetic gold-arsenopyrite mineralization of the eastern zone is associated with a younger volcanic sedimentary sequence. Both sequences are contained within unit 5 (Fig. 2, 7). This conclusion is consistent with previous work by Moore (1956), Dillon-Leitch (1981), Ransom and Robb (1986), Comeau et al. (1987), and Stanley and Seguin (1988).

The boundary between the eastern and western metallogenic zones is largely coincident with the Cycle 1/Cycle 2 contact as defined by Stanley and Seguin (1988) in four widely separated areas along the belt. It is characterized by a strong geophysical conductor that can be traced more than 60 km from the southern end of the belt to just north of the northern end of Courageous Lake. Although numerous gossans as well as several base metal occurrences are localized along the boundary, the principal massive sulphide deposit (Deb; #11, Fig. 7) and many other base metal occurrences and gossans are associated with strong, less extensive conductors within the western base metal zone. A solitary gold

occurrence (#77, Fig. 7) in arsenopyrite-bearing felsic volcanic rocks was discovered along the zone boundary by Noranda (Stanley and Seguin, 1988).

**Sulphide-bearing iron formation**

Sulphide-bearing iron formation (BIF) has been identified at six places within the eastern metallogenic domain of the Courageous Lake belt in the transition zone between upper felsic volcanic rocks and overlying turbidites (Fig. 7). The most notable occurrence is immediately south of the Tundra gold mine. At this locale, well laminated, pyrrhotite-rich, garnet- and amphibole-bearing rock is associated with black sulphidic mudstone. Elsewhere, iron formation is interlayered with thin units of felsic tuff. A single sample of sulphide-bearing iron formation from a gossan in a similar stratigraphic position in the Desteffany Lake area returned an assay of 220 ppb gold (Thompson et al., 1993a). Samples collected from the same gossan in 1992 returned gold assays of less than 20 ppb. Petrographic and lithochemical studies are in progress to better define the character and mineral potential of the transition zone.

Sulphide-bearing banded iron-formation was also recognized near the west margin of the central portion of the Winter Lake belt (#79, Fig. 7). Arsenopyrite was identified adjacent to late quartz veins in several old trenches that had been blasted in mixed sulphide-silicate-oxide-banded iron-formation. Although no information has been found in assessment reports, this occurrence has features similar to non-stratiform gold occurrences hosted by banded iron-formation. Assays from several samples indicate gold contents of between 343 and 5830 ppb. Gold assays up to 11.8 ppm (Boyd, 1988) and 2400 ppb (Yazdani, 1989) are associated with a thin unit of arsenopyrite-bearing mixed silicate- sulphide banded iron-formation that occurs in medium-grade metasedimentary rocks near the northern map boundary (#82, Fig. 7).

**Alteration zones**

Metamorphosed hydrothermal alteration zones similar to those described elsewhere (Franklin et al., 1981) were identified at the Deb, Ptarmigan, and Grizzly massive sulphide occurrences in the Courageous Lake belt (Fig. 7, #11, #2, and #1, respectively). Altered rocks were not

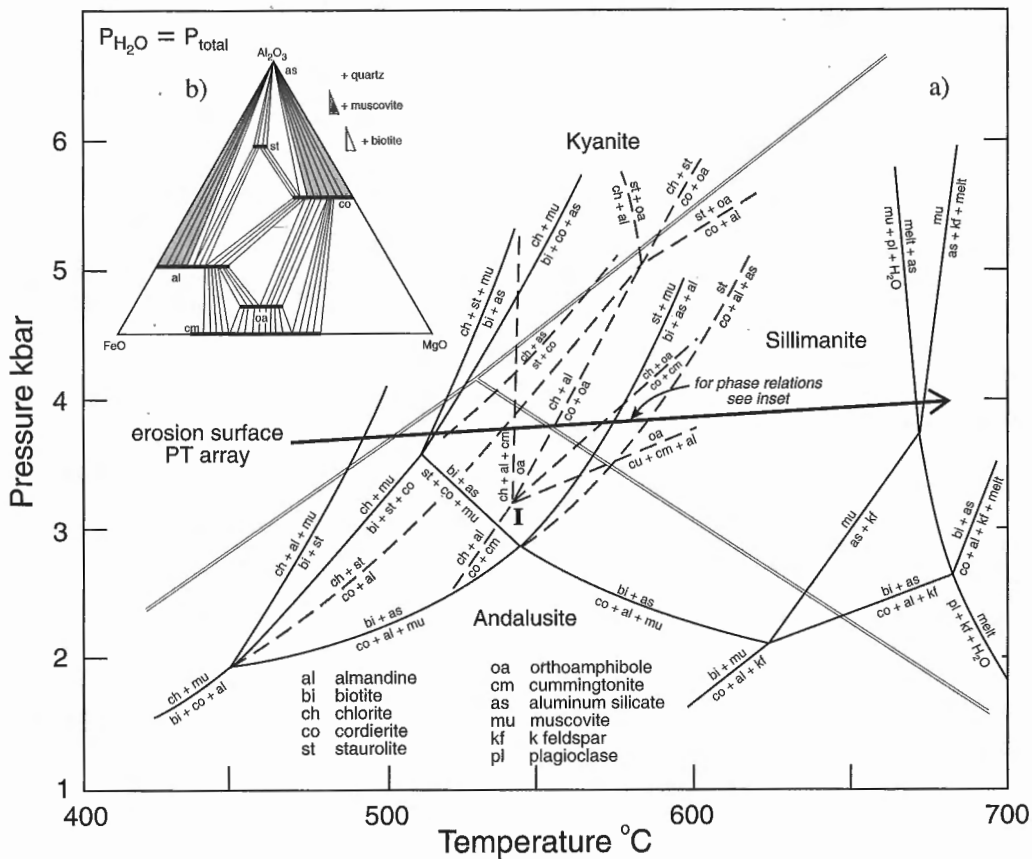


**Figure 6. a)** Petrogenetic grid (after D.M. Carmichael, in Davidson et al., 1990; with invariant point I from Spear and Rumble, 1986) shows relation between reactions in muscovite-bearing pelitic rocks (solid lines) and in muscovite-absent metamorphosed metasomatic alteration zones (dashed lines). **b)** Phase diagram illustrates relation between cordierite-(Fe-Mg) amphibole assemblages and typical cordierite-andalusite schist.

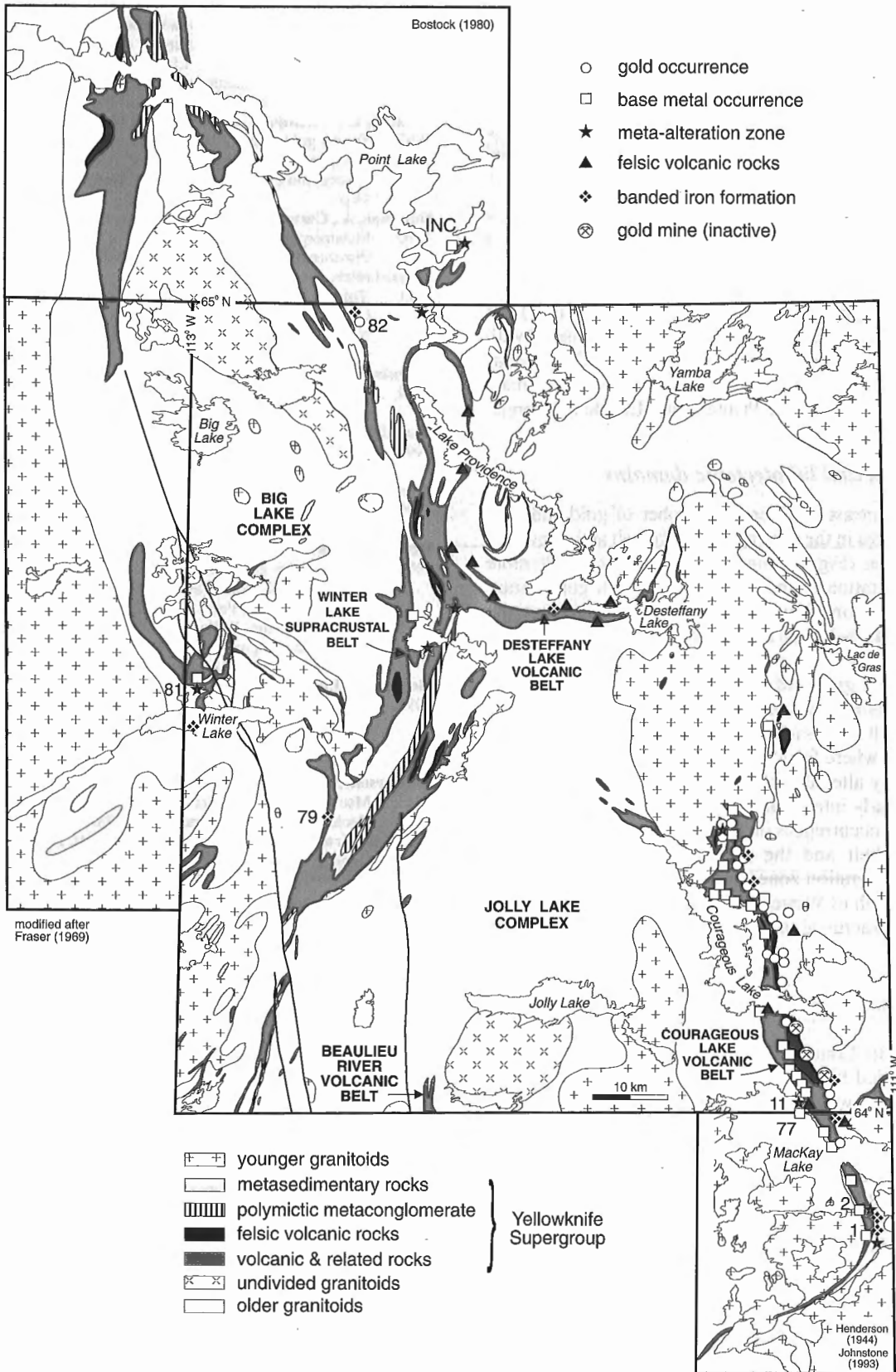


**Figure 7.** Distribution of mineral occurrences, metamorphosed alteration zones, banded iron formation, and small bodies of felsic volcanic rocks in Winter Lake-Lac de Gras area. Numbers refer to mineral occurrences from Thompson and Kerswill (1994) mentioned in text.

restricted to the stratigraphic footwall of known mineralization. Indeed, the best developed alteration at the Grizzly occurrence was in the stratigraphic hanging wall of the main gossan. Characteristic assemblages of cordierite-orthoamphibole and cordierite-cummingtonite with biotite and/or chlorite are present. Recognition of alteration in spite of regional metamorphism is a useful indicator of potential massive sulphide mineralization.

Similar cordierite-(Fe-Mg)amphibole rocks were identified at several other locations in the map area (Fig. 7). For example, rocks suggesting pre-metamorphic metasomatic alteration are prominent at the northwestern end of the Courageous Lake belt, north of Winter Lake (#81, Fig. 7) and south of Beuparlant Lake. This observation, combined with the potential for additional mineralization in the Courageous Lake belt, indicates potential for the discovery of new massive sulphide deposits in the Winter Lake-Lac de Gras area.

### *Mineralization and lithotectonic domains*

The striking contrast between the number of gold and base metal occurrences in the Courageous Lake belt and elsewhere in the map area (Fig. 7) may be a result of much more intensive exploration in the vicinity of known gold mines. With mapping complete, however, it is clear that the Courageous Lake belt is on the edge of an extensive sedimentary domain while most volcanic belts farther west occur within the older granitoid domain. From that perspective perhaps the Desteffany Lake belt and northern part of the Winter Lake belt merit more attention. The intersection of the latter two belts where felsic volcanic rocks, metamorphosed, metasomatically altered rocks, and prominent gossans coincide is particularly interesting. On the other hand, the banded iron-formation occurrences on the western edge of the central Winter Lake belt and the presence of metamorphosed hydrothermal alteration zones and garnet-amphibole-gossan rocks in and north of Winter Lake indicate some exploration potential in supracrustal rocks within the granitoid domain.

### ACKNOWLEDGMENTS

Sergio Alvarado, Lonnie Chin, Murray Gingras, and Robert Johnson provided first class field assistance. Our expeditor, Craig Nicholson, worked with his usual super competence. Ptarmigan Airways and Canadian Helicopters served us well. We thank the Polar Continental Shelf Project for helicopter time. Bill Padgham's generous offer of his house to an energetic crew of seven was much appreciated. Constructive critical reviews by Ken Card and John B. Henderson and comments by Janet King helped make this a better report.

### REFERENCES

**Bostock, H.H.**

1980: Geology of the Itchen Lake area, District of Mackenzie; Geological Survey of Canada, Memoir 391, 101 p.

**Boyd, T.**

1988: Geological report on the New Crow claims, New Crow 1-2, F17085, F17099, District of Mackenzie, Northwest Territories; Noranda Exploration Company, Limited, Assessment Report 082804, Department of Indian and Northern Affairs Mining Recorder, Yellowknife, Northwest Territories, 9 p. (maps, appendices).

**Comeau, R.L., Kemp, R., and Powers, D.H.R.**

1987: Tundra gold venture, Northwest Territories: an update; report that accompanied a talk presented at the 93rd Annual Northwest Mining Association Convention, Spokane, Washington, December 5, 1987, 14 p.

**Davidson, A., Carmichael, D.M., and Pattison, D.R.M.**

1990: Metamorphism and geodynamics of the southwestern Grenville Province, Ontario; Field Trip Guidebook, IGCP Project 235, p. 304.

**Dillon-Leitch, H.C.H.**

1981: Volcanic stratigraphy, structure and metamorphism in the Courageous-Mackay Lake Greenstone Belt, Slave Province, Northwest Territories; Msc. thesis, University of Ottawa, Ottawa, Canada, 169 p.

**Folinsbee, R.E.**

1949: Lac de Gras, District of Mackenzie, Northwest Territories; Geological Survey of Canada, Map 977A.

**Franklin, J.M., Lydon, J.W., and Sangster, D.F.**

1991: Volcanic-associated massive sulphide deposits; Economic Geology, 75th Anniversary Volume, p. 485-627.

**Fraser, J.A.**

1969: Winter Lake, District of Mackenzie; Geological Survey of Canada, Map 1219A.

**Henderson, J.B.**

1970: Stratigraphy of the Yellowknife Supergroup, Yellowknife Bay-Prosperous Lake area, District of Mackenzie; Geological Survey of Canada, Paper 70-26, 12 p.

1985: Geology of the Yellowknife-Hearne Lake area, District of Mackenzie: a segment across an Archean basin; Geological Survey of Canada, Memoir 414, 135 p.

**Henderson, J.B. and Chacko, T.**

1995: A reconnaissance of the high grade metamorphic terrane south of Ghost Lake, southwestern Slave Province, Northwest Territories; in Current Research 1995-C, Geological Survey of Canada, this volume.

**Henderson, J.F.**

1944: MacKay Lake, District of Mackenzie, Northwest Territories; Geological Survey of Canada Map 738A.

**Hrabi, B., Grant, J.W., Godin, P.D., Helmstaedt, H., and King, J.E.**

1993: Geology of the Winter Lake supracrustal belt, central Slave Province, District of Mackenzie, Northwest Territories; in Current Research, Part C; Geological Survey of Canada, Paper 93-1C, p. 71-81.

**Hrabi, R.B., Grant, J.W., Berclaz, A., Duquette, D., and Villeneuve, M.**

1994: Geology of the northern half of the Winter Lake supracrustal belt, Slave Province, Northwest Territories; in Current Research 1994-C; Geological Survey of Canada, p. 13-22.

**Johnstone, R.M.**

1993: Preliminary geology of the MacKay Lake area, District of Mackenzie (Parts of 75M/10, 11, 15, 16), EGS-1993-G.

**Kerswill, J.A., Brophy, J.A., Thompson, P.H., Henderson, J.R.,**

**Henderson, M.N., Bretzlaff, R., Arias, Z., and Garson, D.**

1993: Recent developments in the metallogeny of the Slave Province with emphasis on the Courageous Lake and High Lake greenstone belts; in Mining, exploration, and geological investigations, Exploration Overview 1993 Northwest Territories, (ed.) S.P. Goff; Northwest Territories Geology Division, Indian and Northern Affairs Canada, p. 39-40.

**Moore, J.C.G.**

1956: Courageous Lake - Matthews Lakes area, District of Mackenzie, Northwest Territories; Geological Survey of Canada, Memoir 283, 52 p.

**Padgham, W.A.**

1990: The Slave Province, an overview; in Mineral deposits of the Slave Province, Northwest Territories (Field Trip 13), (ed.) W.A. Padgham and D. Atkinson; Geological Survey of Canada Open File 2168, p. 1-40.

**Pollack, H.N. and Chapman, D.S.**

1977: On the regional variation of heat flow, geotherms and lithospheric thickness; *Tectonophysics*, v. 38, p. 279-296.

**Ransom, A.H. and Robb, M.E.**

1986: The Salmita gold deposit, Courageous Lake, Northwest Territories; in *Gold in the Western Shield*, (ed.) L.A. Clark; Proceedings of a symposium held in Saskatoon, September, 1985, p. 285-305.

**Rutter, M.J. and Wyllie, P.J.**

1988: Melting of vapour-absent tonalite at 10 kbar to simulate dehydration melting in the deep crust; *Nature*, v. 331, p. 159-160.

**Spear, F.S. and Rumble, D., III**

1986: Pressure, temperature, and structural evolution of the Orfordville belt, west-central New Hampshire; *Journal of Petrology*, v. 27, p. 1071-1093.

**Stanley, M.C. and Seguin, J.M.**

1988: Geological exploration report, Courageous-MacKay lake volcanic belt; District of Mackenzie, Northwest Territories; Noranda Exploration Company, Limited, Assessment Report 082777, Department of Indian and Northern Affairs Mining Recorder, Yellowknife, Northwest Territories, 57 p. (maps, appendices).

**Stubley, M.**

1990: Preliminary geology of the Prang Lake area, parts of NTS 85P/15,16; EGS 1990-19, Northwest Territories Geology Division, Department of Indian and Northern Affairs.

**Thompson, P.H.**

1989: Moderate overthickening of thinned sialic crust and the origin of granitic magmatism and regional metamorphism in low-pressure/high-temperature terranes; *Geology*, v. 17, p. 520-523.

1992: The Winter Lake-Lac de Gras regional mapping project, central Slave Province, District of Mackenzie, Northwest Territories; in *Current Research, Part A*; Geological Survey of Canada, Paper 92-1A, p. 41-46.

**Thompson, P.H. and Kerswill, J.A.**

1994: Preliminary geology of the Winter Lake-Lac de Gras area; Geological Survey of Canada Open File 2740 (revised) (1:250 000) (upgrade of Open File 2740 published in 1993).

**Thompson, P.H., Ross, D., Froese, E., Kerswill, J.A., and Peshko, M.**

1993a: Regional geology in the Winter Lake-Lac de Gras area, central Slave Province, District of Mackenzie, Northwest Territories; in *Current Research, Part C*; Geological Survey of Canada, Paper 93-1C, p. 61-70.

**Thompson, P.H., Ross, D.A., Davidson, A., Froese, E., and Pesko, M.**

1993b: Preliminary geological map of the Winter Lake - Lac de Gras area, central Slave Province, District of Mackenzie, NWT; Geological Survey of Canada, Open File 2740.

**Thompson, P.H., Ross, D., and Davidson, A.**

1994: Regional geology of the Winter Lake-Lac de Gras area, central Slave Province, District of Mackenzie, Northwest Territories; in *Current Research 1994-C*; Geological Survey of Canada, p. 1-12.

**van Breemen, O., Davis, W.D., and King, J.E.**

1992: Temporal distribution of granitoid plutonic rocks in the Archean Slave Province, northwest Canadian Shield; *Canadian Journal of Earth Sciences*, v. 29, p. 2186-2199.

**Villeneuve, M.**

1993: Preliminary geochronological results from the Winter Lake-Lac de Gras Slave Province NATMAP project, Northwest Territories; in *Radiogenic Age and Isotopic Studies: Report 7*; Geological Survey of Canada, Paper 93-2, p. 29-38.

**Villeneuve, M., Hrabi, B., Jackson, V., and Relf, C.**

1993: Geochronology of supracrustal sequences in the central and northern Slave Province; in *Exploration Overview, Northwest Territories*, (ed.) S.P. Goff; Northwest Territories Geology Division, Indian and Northern Affairs Canada, p. 83.

**Yazdani, K.**

1989: Geological report on the New Crow claims, New Crow 1-5, F17085, F17099, F17087-F17089, District of Mackenzie, Northwest Territories; Noranda Exploration Company, Limited, Assessment Report 082939, Department of Indian and Northern Affairs Mining Recorder, Yellowknife, Northwest Territories, 12 p. (maps, appendices).

---

Geological Survey of Canada Project 870008PT





# Structural evolution of the Vizien and Kogaluc greenstone belts in Minto block, northeastern Superior Province, northern Quebec

S. Lin, J.A. Percival, P.A. Winsky<sup>1</sup>, T. Skulski, and K.D. Card  
Continental Geoscience Division

*Lin, S., Percival, J.A., Winsky, P.A., Skulski, T., and Card, K.D., 1995: Structural evolution of the Vizien and Kogaluc greenstone belts in Minto block, northeastern Superior Province, northern Quebec; in Current Research 1995-C; Geological Survey of Canada, p. 121-130.*

---

**Abstract:** Structural analysis of the Vizien greenstone belt demonstrates five generations of ductile deformation (D1 to D5), as well as brittle faulting. D1 is indicated by the presence of a pre-D2 foliation. D2 is associated with a major shear zone with northeast-over-southwest(?) dip-slip movement. It is responsible for the main penetrative foliation, axial planar to tight to isoclinal F2 folds. Map-scale open to tight folds are F3 and F4, with north-northwest- and east-trending axial planes, respectively. D5 is associated with dextral transcurrent movement along a north-northwest-trending shear zone. A similar structural history is recognized in the Kogaluc area. The Kogaluc greenstone belt shows structural features similar to gold-mineralized breaks of the southern Superior Province. Map-scale doubly plunging (or proto-sheath) folds of an iron formation unit in the northern Kogaluc belt may be a favourable structural trap.

**Résumé :** Une analyse structurale de la ceinture de roches vertes de Vizien fait ressortir cinq générations de déformation ductile (D1 à D5), aussi bien que des failles cassantes. D1 se signale par la présence d'une foliation pré-D2. D2 est associée à une grande zone de cisaillement avec rejet nord-est-sur-sud-ouest(?). Elle est responsable des principaux plis F2 axiaux-planaires à serrés à isoclinaux de foliation pénétrative. Les plis ouverts à serrés d'échelle cartographique sont F3 et F4, dont la direction respective des plans axiaux est nord-nord-ouest et est. D5 est associée à un mouvement de coulissage dextre le long de la zone de cisaillement d'orientation nord-nord-ouest. Une histoire structurale similaire s'est déroulée dans la région de Kogaluc. La ceinture de roches vertes de Kogaluc possède des caractéristiques structurales semblables aux fractures à minéralisation aurifère dans le sud de la Province du lac Supérieur. Les plis à plongement double (ou fourreau initial) d'échelle cartographique d'une unité de formation ferrière dans le nord de la ceinture de Kogaluc pourraient constituer un piège structural favorable.

---

<sup>1</sup> Department of Earth Sciences, Boston University, Boston, Massachusetts 02215

## INTRODUCTION

The Minto block of northeastern Superior Province, characterized by northwesterly structural and aeromagnetic trends, has been divided into six domains: the Inukjuak, Tikkerutuk, Lake Minto, Goudalie, Utsalik, and Douglas Harbour domains (Fig. 1; Percival and Card, 1994). The Goudalie domain, a granite-greenstone terrane (Percival et al., 1995), was first identified on the basis of well preserved supracrustal sequences and associated tonalitic gneisses with a coincident negative aeromagnetic anomaly (Percival et al., 1992). Supracrustal sequences in the domain are best preserved in greenstone belts, including the Vizien, Kogaluc, Payne Lake, and Qalluviartuuq belts (Fig. 1). During our study of the Goudalie domain, we paid special attention to greenstone belts, not only for their potential for mineralization, but also because they contain a more complete structural record than associated granitoid rocks. In this paper, we report preliminary results of a structural study on two of the greenstone belts, the Vizien and Kogaluc belts, and discuss their implications for the structural evolution of the Goudalie domain.

## VIZIEN GREENSTONE BELT

### General geology

The Vizien greenstone belt consists of four structural panels (A, B, C, and X) with lithologically and chronologically distinct volcanic and sedimentary rocks, separated by shear zones (Fig. 2; Percival and Card, 1992a, 1992b; Skulski et al., 1994; Percival et al., 1994). A fifth panel, D, consists of a

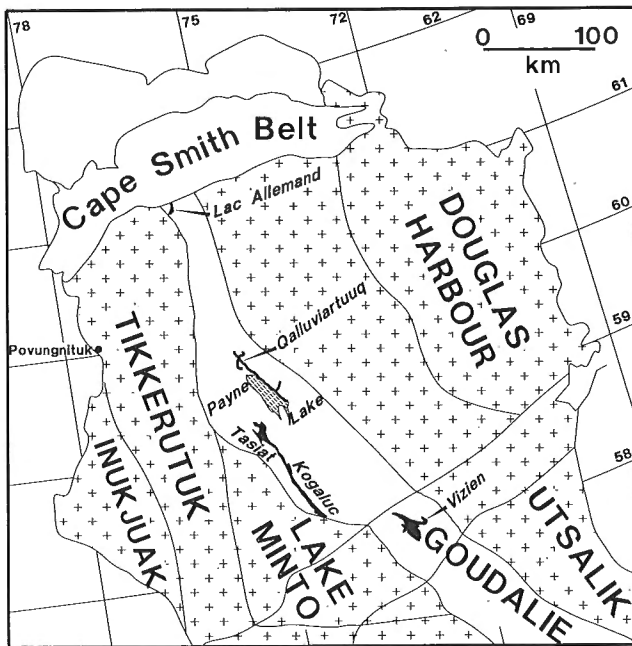


**Figure 1.** Domains of the Minto block and locations of greenstone belts in the Goudalie domain.

structurally dismembered assemblage of highly strained rocks of panels B, C, and X (Percival and Card, 1992a). Boundaries of panel D as shown in Figure 2 are drawn along two brittle faults, although true boundaries are gradational. Strong deformation and structural mixing in the panel makes it impossible to divide these rocks based on their panel affinity. The main features of individual panels are summarized below based on Percival et al. (1994) and Skulski et al. (1994).

Panel C, the oldest, consists of a bimodal sequence of subaerial tholeiitic lava flows of  $2793 \pm 8$  Ma (U-Pb age on zircon from rhyolite), which are interpreted to have evolved in a continental rift environment. Panel X consists of a sheet of peridotite and gabbro sills (U-Pb zircon age  $2786 \pm 1$  Ma) which intrude pillowed, nonvesicular, tholeiitic basaltic andesites, and is interpreted to be a fragment of transitional oceanic crust. Panel A consists of upward-shoaling calc-alkalic (submarine to shallow marine or subaerial) mafic, intermediate, and felsic volcanic rocks and minor sedimentary rocks (including conglomerate). A rhyolite in panel A yielded a concordant U-Pb zircon age of  $2724 \pm 1$  Ma (Percival et al., 1993). Panel A is interpreted to have formed in an island-arc environment. The youngest sequence, panel B,  $< 2718$  Ma based on the youngest U-Pb zircon age in a granite conglomerate clast (Percival et al., 1993), lies unconformably on saprolithic tonalitic basement of  $2940 \pm 5$  Ma (Percival et al., 1993). Basal conglomerate is overlain by greywacke and primitive tholeiitic picrites. The latter sequence faces downwards to the south, and is interpreted as a remnant of a continental marginal basin. Skulski et al. (1994) mapped a *mélange* exposed sporadically at the contact between panels X and B. It consists of mainly serpentine matrix with mafic blocks.

The tonalite and the unconformably overlying conglomerate and sandstone exposed north of volcanic rocks in panel C were previously mapped as the base of panel C (e.g., Percival and Card, 1992a). They are here interpreted as part of panel B because (1) they are identical to rocks of panel B, and (2) they are separated from panel C volcanic rocks by a strongly sheared peridotite sheet identical to that of panel X.

### Deformation history

Based mainly on overprinting relationships, the present study recognized five generations of ductile shearing and folding, as well as brittle faulting. For convenience in the following description, the five generations of ductile deformation are termed D1 to D5, and the associated foliation, lineations, and folds, where present, are correspondingly termed S1 to S5, L1 to L5, and F1 to F5. It should be noted that this terminology does not necessarily imply that D1 to D5 represent five discrete deformation episodes.

The earliest recognizable structure (D1) is indicated by local preservation in panel X of foliation (S1) that is folded by F2. The deformation fabrics preserved within blocks in *mélange* (Skulski et al., 1994) may also be related to D1. The scarcity of D1 structures renders its structural interpretation impossible. It is likely that D1 deformation was related to

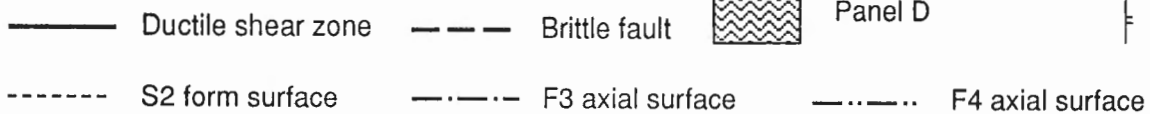
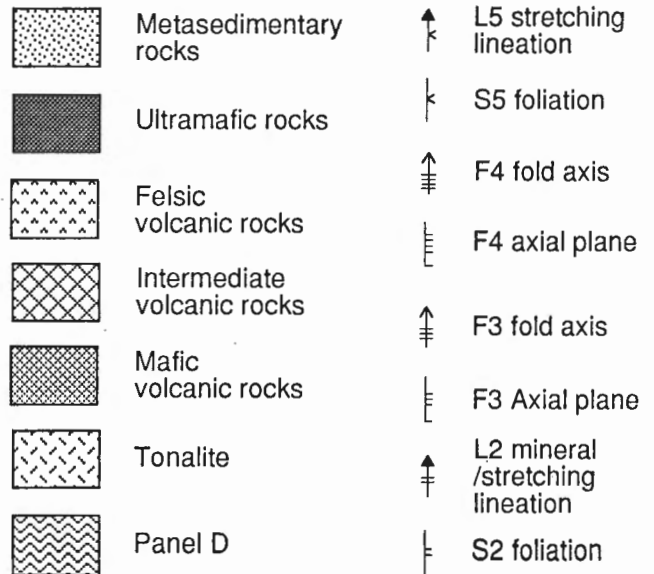
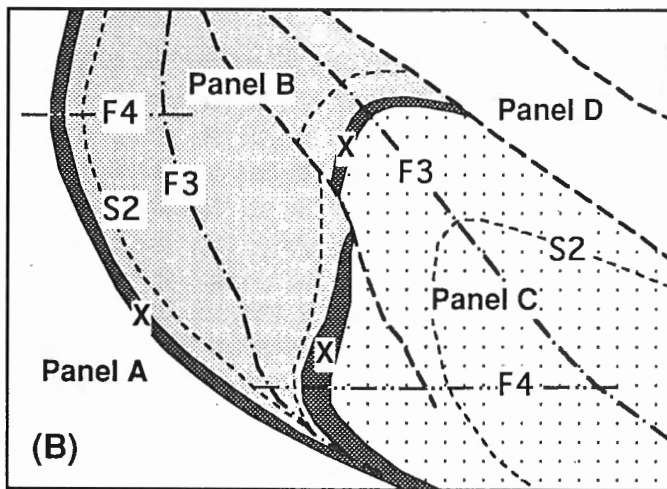
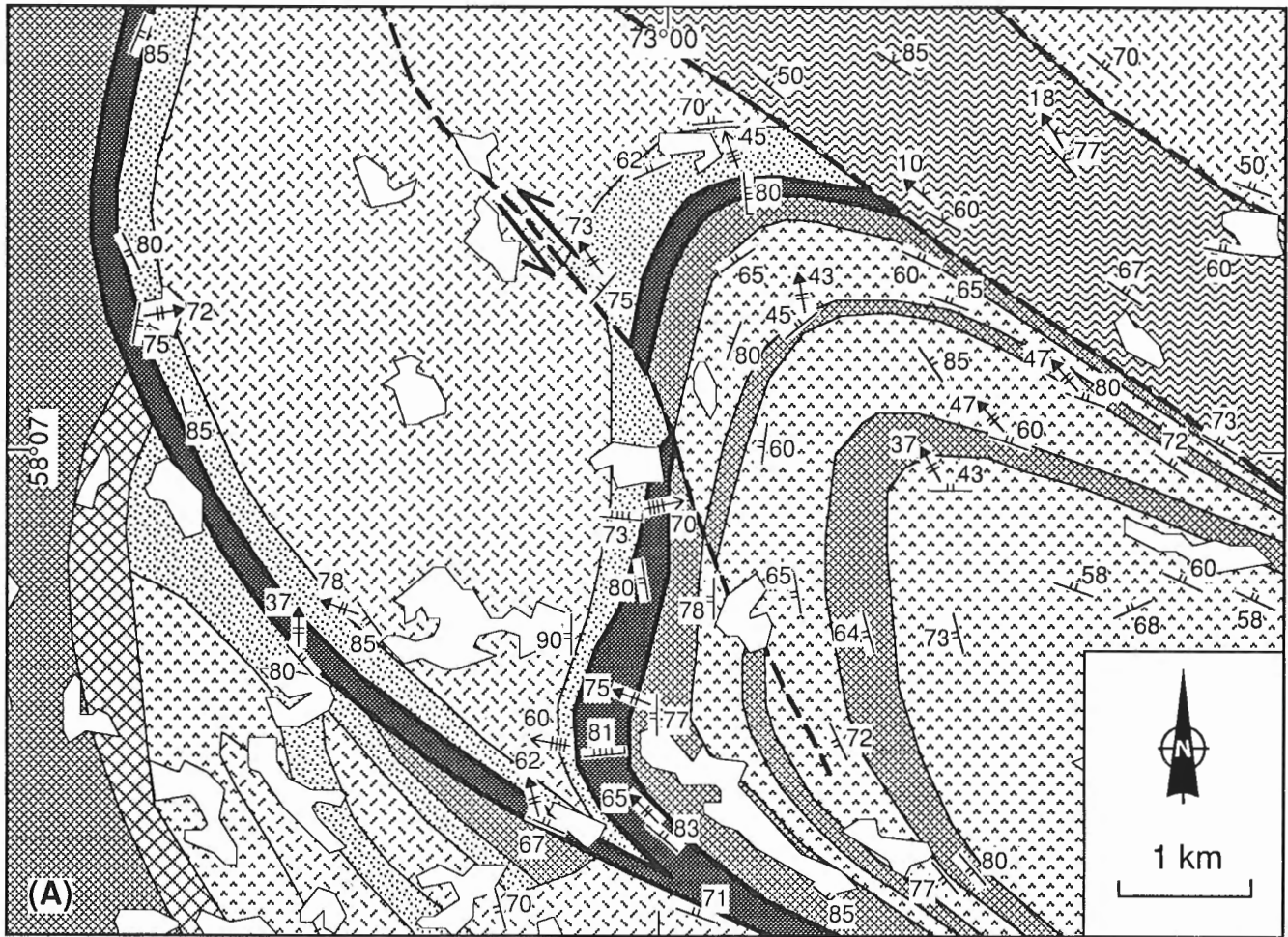


**Figure 2.** A) Geological map of the Vizie greenstone belt (modified from Percival and Card, 1994). B) Panel divisions and major structures of the belt (modified from Skulski et al., 1994). Note the overprinting relationship between S2, F3, and F4.

thrust emplacement of panel X over panel B, as inferred by Skulski et al. (1994) based on interpretation of the mélangé and map-scale truncation of panel B stratigraphy by panel X (Percival et al., 1993).

D2 deformation is responsible for formation of the dominant penetrative foliation (S2) in the Vizien belt. The foliation is axial planar to tight isoclinal F2 folds. It is defined by biotite, sillimanite, hornblende, serpentinite, and deformed conglomerate clasts, depending on rock types. The long dimension of minerals and deformed clasts also defines a strong lineation (L2) in the foliation (Fig. 3A). The S2 foliation generally has a strike subparallel to panel boundaries and lithological contacts (Fig. 2), and dips steeply. L2 lineations also plunge steeply (Fig. 2).

The S2 foliation and associated lineations are most pronounced in panel X and adjacent rocks in panels A, B, and C, and become much weaker towards the west in panel A, the north in panel B, and the south in panel C. The localization of D2 structures in and adjacent to panel X and the widespread presence of mylonite indicate that D2 deformation was a shear zone deformation. The centre of the shear zone, where deformation is most intense, is at the contact between panel X and panels A/C. Shear sense indicators, including shear bands, rotated clasts, and S-C structures (Fig. 3B), indicate that, in current coordinates, panels B/X moved upwards relative to both panels A and C.

F3 folds are open to tight with axial planes striking north-northwest and dipping steeply. They fold the S2 foliation and the L2 lineations. At map scale, they fold panel boundaries and lithological units (Fig. 2). In contrast to F2 folds, F3 folds lack axial planar foliation.

F4 folds are open. They overprint F3 and have axial planes that strike eastward (Fig. 2) and dip steeply. The map-scale bending of panel X between panels A and B in the western part and the crossfolds in the lower central part of Figure 2 are attributed to F4 folding.

D5 deformation is concentrated in panel D. The lack of F4 folds in panel D is interpreted to indicate that deformation in the panel possibly postdated F4 folding, although overprinting relationships between D4 and D5 structures were not observed. Panel D contains rock units of panels B, X, and C in the northeastern part of the map area (Fig. 2), and associated strong deformation has apparently resulted in structural mixing of rocks of the different panels. Where shearing in panel D is most intense, a new mylonitic foliation (S5) is developed with associated subhorizontal stretching lineations (L5). Drag folds and shear bands indicate dextral transcurrent movement (Fig. 4).

Brittle faults are observed at both outcrop scale and map scale. The map-scale fault in the middle of the map area sinistrally offsets panel and lithological boundaries by ~750 m (Fig. 2). Outcrop-scale sinistral faults observed in this map-scale fault zone support this sense of shear (Fig. 5). The sense of shear of the two faults that bound panel D is unknown. All map-scale brittle faults define clear topographic lineaments. Associated fault breccia zones are over 30 m wide.

### Age of deformation

The age of D1 cannot be definitely constrained due to limited preservation. However, if the interpretation is correct that D1 is associated with emplacement of panel X over panel B (see above), D1 should be younger than ca. 2718 Ma, age of the youngest zircon in a granite clast within a panel B conglomerate.

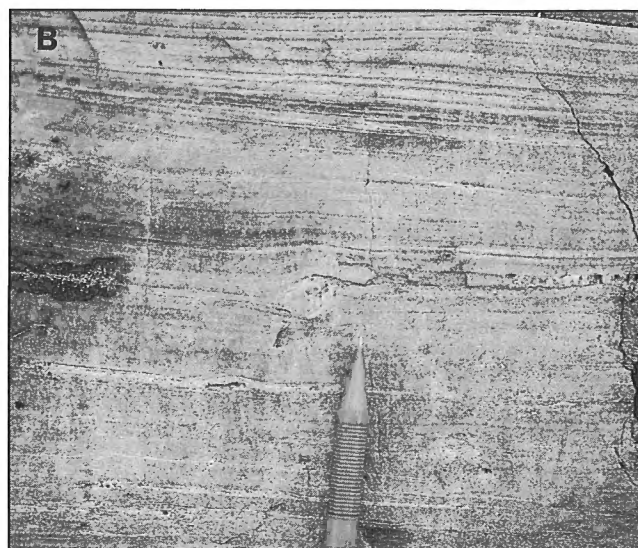
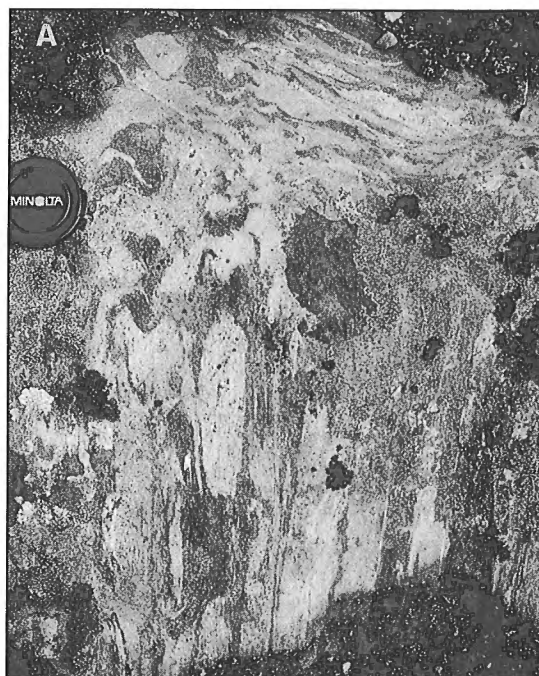


**Figure 3.** Examples of D2 structures in the Vizien belt. **A)** Deformed conglomerate clasts defining stretching lineations. **B)** Rotated clasts (close to the pencil tip) in a mylonite developed near the contact between panels X and A, indicating dextral shear on the outcrop surface. In three dimension, this indicates dominantly east-over-west (panel X-over-panel A) dip-slip with dextral transcurrent component.



**Figure 4.** Shear bands associated with D5 deformation in panel D of the Vizien belt, indicating dextral transcurrent movement. The fold closure in lower right is F2.

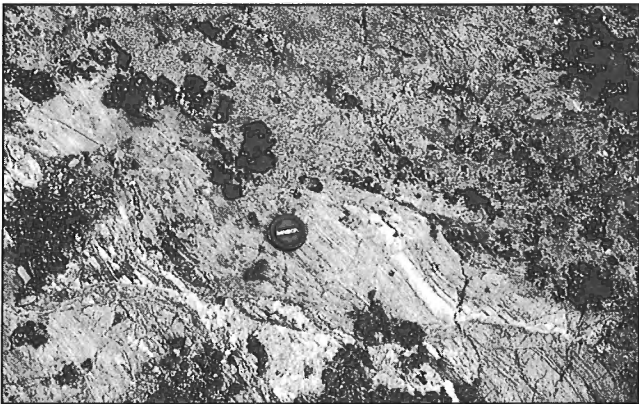


**Figure 5.** Outcrop-scale sinistral brittle fault developed in the fault zone shown in the middle of Figure 2A, the Vizien belt.

D2 is younger than ca. 2718 Ma because it deformed the conglomerate. It is older than ca. 2693 Ma, age of the oldest monazite in a pegmatite crosscutting S2 foliation. The ages of D3 to D5 relative to the dated pegmatite are not clear.

### Discussion

Skulski et al. (1994) and Percival et al. (1994) interpreted four sets of ductile structures, as well as brittle faulting, in the Vizien greenstone belt (D1 to D4). As described above, our recognition of pre-F2 foliation supports the existence of D1 deformation. Our data also substantiate that map-scale folds are F3 folds and crossfolds are F4 folds. We recognized an additional generation of deformation (D5) in panel D. We also determined the kinematics of D2 deformation.

As described above, S2 is the dominant foliation in the Vizien belt. It is axial planar to F2 and folded by F3, the map-scale folds. This differs from a previous interpretation (Skulski et al., 1994) that this foliation is S3 and is axial planar to F3 folds. These new observations suggest that D2 deformation was the dominant fabric-forming event, and therefore was probably the main panel amalgamation event. More importantly, it suggests that the current geometry of the greenstone belt is largely controlled by F3 and later folding. To restore D2 geometry, which is essential to understanding the kinematics of D2, the belt has to be unfolded.

Although the limited extent of the Vizien greenstone belt does not allow us to infer an unambiguous pre-F3 orientation of S2, it is reasonable to suggest that at the end of D2, S2 and the major panel boundaries were probably planar or nearly so. When this geometry is restored, the geometry of the Vizien belt is much simpler, with panel B on one side of panel X, and panels A/C on the other side (Fig. 6). A further inference from this is that panels A and C had probably been amalgamated, possibly with intervening 3.1 Ga tonalite, before they were juxtaposed with panels B/X. Field evidence indicates that during D2, panels B/X were partly overturned and thrust not only onto panel A as interpreted by Skulski et al. (1994), but also onto panel C. This order of panel amalgamation and sense of shear should be considered in further tectonic interpretation of the greenstone belt.

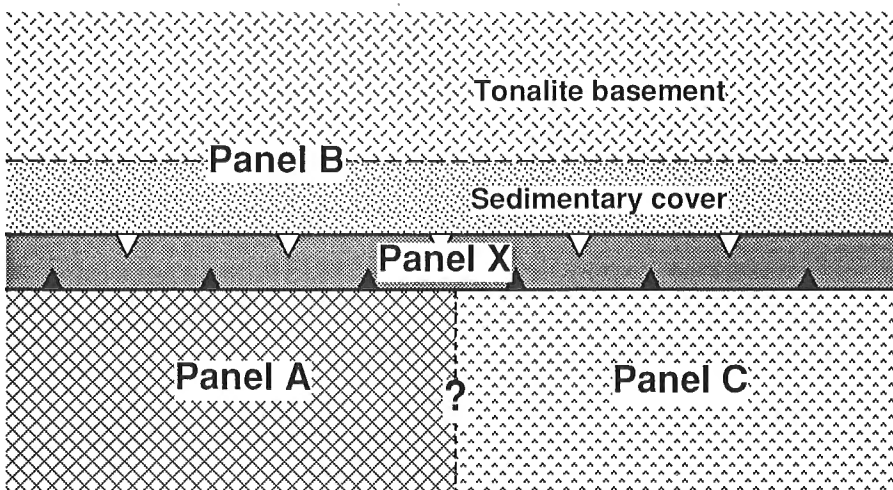


**Figure 6.**

Schematic diagram showing interpreted geometry of the Vizien belt at the end of D2 deformation. Solid and open thrust symbols represent D2 and D1(?) thrusts, respectively.

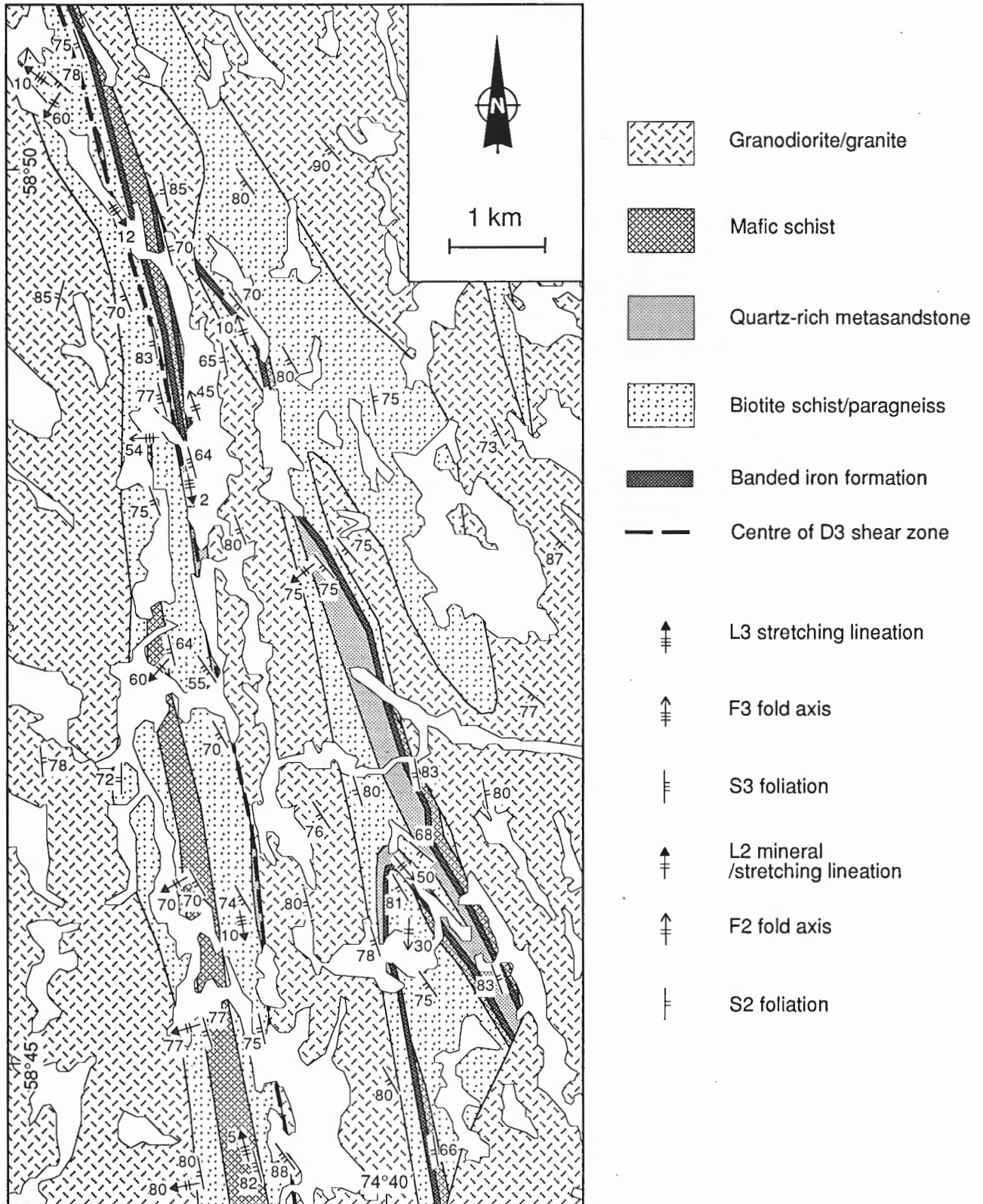


**Figure 7.** Geological map of northern Kogaluc belt. Note that the banded iron formation unit defines a map-scale "S" fold in the north (interrupted by a granodiorite sheet ) and a "Z" fold in the south. The two folds are interpreted as part of a doubly plunging (or proto-sheath) fold.

## KOGALUC GREENSTONE BELT

### General geology

The Kogaluc belt is over 100 km long and generally <1 km wide (it is wider in the north; Fig. 7). Three main supracrustal units can be distinguished: rocks of volcanic origin, metasedimentary rocks, and iron formation. Metavolcanic rocks are generally fine grained mafic schists, with stretched pillows recognizable locally (Percival et al., 1995). Felsic metavolcanic rocks are present in a few locations. One such unit gave a preliminary, imprecise U-Pb zircon age of ca. 2744 Ma (Percival et al., 1995). Metasedimentary rocks are for the most part fine grained biotite and/or muscovite schist. Primary structures, e.g., graded bedding, are preserved locally. Quartz-rich sandstones occur in association with rare conglomerate near the northern limit of metavolcanic units. A 5-10 m thick unit of quartz-magnetite banded iron formation with a strike length of ca. 15 km occurs in the northern part of the Kogaluc belt. Discontinuous units of silicate-facies iron formation (garnet-grunerite-quartz±magnetite rocks) occur sporadically throughout the belt (Percival et al., 1995).

Metamorphic grade in the Kogaluc Belt ranges from lower to middle amphibolite facies, based on local occurrences of both andalusite and sillimanite in pelitic schist and epidote-hornblende assemblages in mafic rocks. Plutonic rocks, mainly granodiorite containing biotite and/or hornblende, occur in 5 km wide zones flanking the belt (Percival et al., 1995).

### Deformation history

The following description of the structural history of the Kogaluc belt is based on mapping of the northern part of the belt. Reconnaissance work in other parts of the belt indicates a similar history.

Based on overprinting relationships, three generations of mainly ductile deformation are recognized in the Kogaluc belt. Without implying any one-to-one correlation to those in the Vizien belt described above, we refer to them as D1 to D3. (The correlation of structures of the two greenstone belts is discussed later.) Because the earliest recognizable structure, D1, is indicated only by locally preserved S1 foliation, no structural analysis is possible. For this reason, in the following description we are concerned only with D2 and D3.

D2 structures include a foliation (S2), lineations (L2), and folds (F2). Foliation and lineations are defined by preferred orientation of biotite, sillimanite, hornblende, and flattened and elongated mineral aggregates. The foliation strikes mainly north-northwest and dips steeply to the west. The lineation is mainly downdip. D2 deformation is most intense in a shear zone along the western margin of the greenstone belt, where foliation and lineations are very pronounced and mylonites are well developed.

F2 folds are tight to isoclinal with S2 as the axial plane foliation (Fig. 8A). Fold hinges vary from steeply plunging and subparallel to mineral lineations to shallowly plunging and highly oblique to mineral lineations, as is typical of folds

related to shear zone deformation. Examples of doubly plunging folds, possibly sheath folds, are widespread (Fig 8B). Fold vergence indicates east-over-west shearing.

The banded iron formation and associated mafic schist and quartz-rich sandstone define two map-scale folds, an "S" fold in the north (interrupted by a granodiorite sheet) and a "Z" fold in the south (Fig. 7). F2 mesoscale structures developed in the hinge areas of map-scale folds have a well developed axial planar cleavage (e.g., Fig. 8A), which suggests that both large-scale folds formed during F2. Field observations also indicate that the "S" fold plunges moderately to the north and the "Z" fold, to the south. Based on these observations, the two map-scale folds are interpreted as parts of a doubly plunging F2 fold, probably a proto-sheath fold, as shown schematically in Figure 9. This interpretation is supported by the presence of outcrop-scale F2 folds of similar style. This geometry is consistent with east-over-west shearing during D2 deformation.

D3 deformation is concentrated in a shear zone running through the middle of the greenstone belt. In the north of the map area, the shear zone is located along the western margin of the banded iron formation, and in the south, along the western margin of a granodiorite sheet (Fig. 7).



**Figure 8.** Examples of D2 structures in northern Kogaluc belt. A) F2 folds with an axial planar foliation. The folds are developed in the hinge area of the map-scale "Z" fold in Figure 7. B) A doubly plunging fold (possible sheath fold).



In the shear zone, mylonite with dynamic recrystallization structures is well developed. Mylonitic foliation (S3) dips steeply and stretching lineations plunge shallowly (Fig. 7), indicating dominantly transcurrent movement. Widespread shear sense indicators, including S-C structure, shear bands, and vergence of F3 folds, consistently indicate dextral movement (Fig. 10A).

Fault breccias, spatially closely associated with the mylonite, are also developed in the shear zone. The mylonite is brecciated, indicating that brittle deformation took place after ductile deformation. However, veins of brecciated mylonite are also observed to have been folded by F3 or themselves mylonitized (Fig. 10B), indicating that ductile deformation resumed after brittle deformation. These observations are interpreted to indicate that D3 deformation occurred under transitional ductile-brittle conditions, through intermittent ductile and brittle deformations or changes in strain rate.

On a regional scale the D3 shear zone in the Kogaluc Belt bends into an east-west orientation along southern Kogaluc River (Fig. 11). As in the D3 north-trending shear zone described above, mylonite and breccia are developed in close association and deformation took place in brittle-ductile conditions. C-surfaces in the mylonite dip moderately north and slickenside striae of the ridge-in-groove type, which lie on the C-surfaces and formed during ductile deformation

(Lin and Williams, 1992a), pitch moderately to steeply to the west. S-surfaces dip more steeply to the north than C-surfaces. These features indicate that the shear zone here dips moderately to the north and that movement was oblique with north-over-south dip-slip and dextral transcurrent components. During thrusting, rocks in the hanging (northern) wall, including mylonite formed during shearing, were uplifted relative to the footwall (southern). The observation that mylonite is located mainly north of the breccia is consistent with such a process.

The north- and east-trending shear zones merge into each other without crosscutting and movement in both zones occurred under ductile-brittle conditions. These observations indicate that the kinematics of the two shear zones were probably related. As shown in Figure 11, the general geometry and kinematics indicate that during D3 deformation the block east of the north-trending shear zone and north of the east-trending shear zone moved south relative to the block on the other side of the shear zones.

**Age of deformation**

A rhyolite in southern Kogaluc belt has yielded a U-Pb zircon age of ca. 2744 Ma, and a monzonite in central Kogaluc belt and a granodiorite in southern Kogaluc belt have yielded

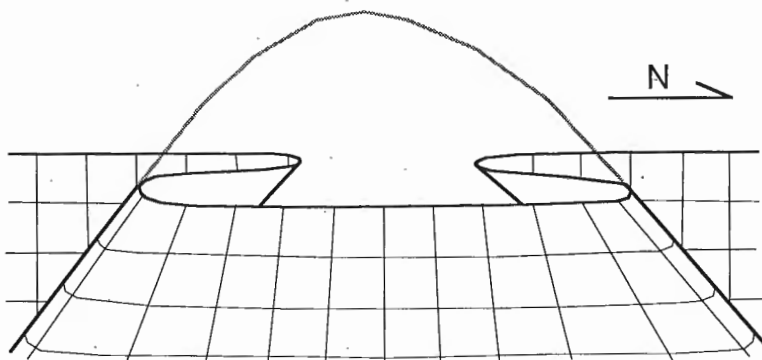


**Figure 9.** Schematic diagram showing interpreted geometry of the banded iron formation in the northern Kogaluc belt. The geometry is consistent with east-over-west shearing.



**Figure 10.** Examples of D3 structures in northern Kogaluc belt. **A)** Rotated boudins indicating dextral transcurrent movement. **B)** A vein of brecciated mylonite (light colored) associated with a D3 shear zone is folded by an F3 fold, indicating intermittent ductile and brittle deformations during D3.

U-Pb zircon ages of  $2725 \pm 5$  and  $2733 \pm 2$  Ma, respectively. Structures in the Kogaluc belt are interpreted to be younger than ca. 2744 Ma.

A granodiorite sheet is located in the middle of the northern Kogaluc belt (Fig. 7). It has not been dated directly, but is likely to be ca. 2735-2720 Ma, considering that all dated plutons of this lithology in the Leaf River transect (e.g., Percival and Card, 1994) and the Goudalie domain fall into this age range. The granodiorite bears a clear S2 foliation but is not folded by the map-scale doubly plunging F2 fold (Fig. 7). Mainly based on this, we suggest that the granodiorite sheet intruded at the late stages of D2 deformation. However, because the granodiorite sheet does not cut both limbs of the F2 fold, it cannot be ruled out that its intrusion was pre-D2. D3 deformation took place after intrusion of the granodiorite sheet, but its age is otherwise unconstrained.

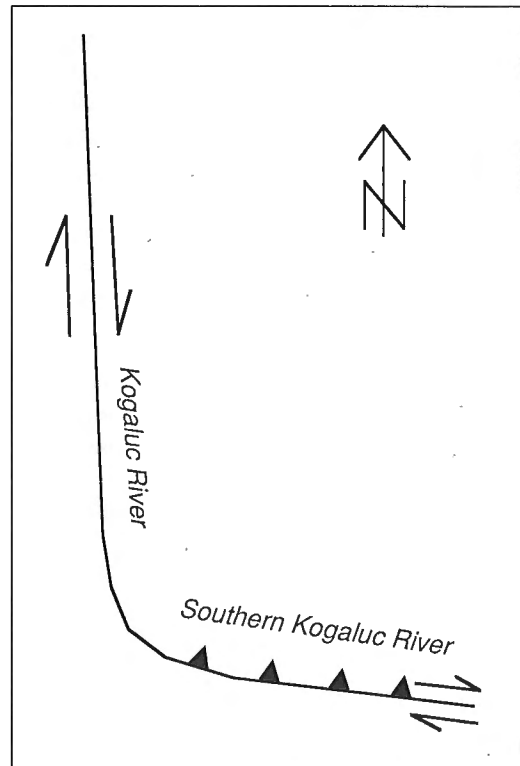


**Figure 11.** Schematic diagram showing the kinematic relationship between the D3 north-trending dextral transcurrent shear zone along the Kogaluc River and the ~east-trending north-over-south thrust along the southern Kogaluc River.

**Table 1.** Structural correlation between the Vizien belt.

Vizien belt	Kogaluc area	
	Kogaluc belt	Granulite terrane
D5 -- mesoscopic open to tight Z folds (F5) -- mylonitic foliation with subhorizontal stretching lineations -- associated with dextral transcurrent shear zone	D3 -- mesoscopic open to tight Z folds (F5) -- mylonitic foliation with subhorizontal stretching lineations -- associated with dextral transcurrent shear zone	
D4 -- mesoscopic and macroscopic open folds (F4) -- east-trending axial plane -- no associated axial planar foliation		
D3 -- macroscopic open to tight folds (F3), overprinted by F4 -- north-northwest-trending axial plane -- no associated axial planar foliation		-- macroscopic open to tight folds -- north-northwest-trending axial plane -- no associated axial planar foliation
D2 -- mesoscopic tight to isoclinal folds (F2) -- axial-planar penetrative foliation with steep lineations, folded by F3 -- associated with major shear zone, NE-over-SW(?) dip-slip	D2 -- mesoscopic and macroscopic tight to isoclinal folds (F2), doubly plunging -- axial planar penetrative foliation with steep lineations, folded by F3 -- associated with major shear zone, east-over-west dip slip	-- penetrative foliation (gneissosity), folded by macroscopic folds
D1 -- locally preserved foliation, folded by F2	D1 -- locally preserved foliation, folded by F2	-- foliation preserved in xenoliths, discordant with penetrative foliation

### *Implications for mineral exploration*

Our preliminary results indicate that the Kogaluc greenstone belt has structural features similar to the gold-mineralized breaks of the southern Superior Province, e.g., Kirkland Lake-Larder Lake-Cadillac break of the Abitibi greenstone belt (Robert, 1989, 1993; Cruden, 1990; Lin and Williams, 1992b, 1993), raising the possibility of gold mineralization in the Kogaluc belt. During our mapping, many small gossans were noted in association with iron formation (Percival et al., 1995). We suggest that the sheath-like geometry of the iron formation may be a favourable site for mineralization, possibly having trapped migrating fluid. The upward closure of the doubly plunging fold (or sheath fold) in the iron formation has the most potential for mineralization.

### **STRUCTURES IN THE HIGH-GRADE ROCKS FLANKING THE KOGALUC BELT**

The Kogaluc belt is flanked on both sides by meta-plutonic rocks and enclosed supracrustal rocks, both containing orthopyroxene beyond ~5 km to the east and west of the belt (Percival et al., 1995). Supracrustal rocks include paragneiss, mafic rocks, and iron formation of both magnetite-quartz and garnet-grunerite-quartz types. Like the Kogaluc belt, individual belts of supracrustal rocks are rarely >1 km wide. These rocks are possibly high-grade equivalents of those in the Kogaluc belt (Percival et al., 1995).

The dominant structure in the high-grade rocks is a penetrative foliation, interpreted to be correlative with S<sub>2</sub> in the Kogaluc belt. An earlier, discordant foliation is locally preserved in xenoliths. The dominant foliation is folded by map-scale upright folds without associated axial plane cleavage (Percival et al., 1995), a style similar to F<sub>3</sub> folds in the Vizien belt. These folds are probably older than the D<sub>3</sub> shear zones in the Kogaluc belt because neither the east-trending nor the north-trending shear zones are affected by the folds.

### **SUMMARY AND REGIONAL STRUCTURAL CORRELATIONS**

The structural history of the Vizien belt and the Kogaluc area is summarized in Table 1. These data show that, with the exception of crossfolding (F<sub>4</sub> in the Vizien belt), all ductile structures recognized in the Vizien belt have possible correlatives in the Kogaluc area. A tentative structural correlation between the two areas is also shown in Table 1.

Preliminary results from the Qulluivartuq-Payne Lake area indicate a similar structural history (Percival et al., 1995). This indicates that the structural sequence established in the Vizien belt has potential for serving as a structural framework for the entire Goudalie domain.

### **ACKNOWLEDGMENTS**

We thank exploration companies for information exchange, and Janet King and Cees van Staal for helpful comments on the manuscript.

### **REFERENCES**

- Cruden, A.R.**  
1990: Relative timing of pluton emplacement and fault movement in the Kirkland Lake area, S.W. Abitibi; A-G Lithoprobe Workshop Proceedings (Montreal), 1-4.
- Lin, S. and Williams, P.F.**  
1992a: The origin of ridge-in-groove slickenside striae and associated steps in an S-C mylonite; *Journal of Structural Geology*, v. 14, p. 315-321.  
1992b: The geometrical relationship between the stretching lineation and the movement direction of shear zones; *Journal of Structural Geology*, v. 14, p. 491-497.  
1993: The geometrical relationship between the stretching lineation and the movement direction of shear zones: reply; *Journal of Structural Geology*, v. 15, p. 241-242.
- Percival, J.A. and Card, K.D.**  
1992a: Vizien greenstone belt and adjacent high grade domains of the Minto block, Ungava Peninsula, Quebec; in *Current Research, Part C*; Geological Survey of Canada, Paper 92-1C, p. 69-80.  
1992b: Geology of the Vizien greenstone belt; Geological Survey of Canada, Open File 2495, scale 1:50 000.  
1994: Geology, Lac Minto-Rivière aux Feuilles, Québec; Geological Survey of Canada, Map 1854A, scale 1:500 000.
- Percival, J.A., Card, K.D., and Mortensen, J.K.**  
1993: Archean unconformity in the Vizien greenstone belt, Ungava Peninsula, Quebec; in *Current Research, Part C*; Geological Survey of Canada, Paper 93-1C, p. 319-328.
- Percival, J.A., Mortensen, J.K., Stern, R.A., and Card, K.D.**  
1992: Giant granulite terranes of northeastern Superior Province: the Ashuanipi complex and Minto block; *Canadian Journal of Earth Sciences*, v. 29, p. 2287-2308.
- Percival, J.A., Skulski, T., Lin, S., and Card, K.D.**  
1995: Granite-greenstone terrains of the northern Goudalie domain, northeastern Superior Province, Quebec; in *Current Research 1995-C*; Geological Survey of Canada, this volume.
- Percival, J.A., Stern, R.A., Skulski, T., Card, K.D., Mortensen, J.K., and Begin, N.J.**  
1994: Minto block, Superior Province: Missing link in deciphering assembly of the craton at 2.7 Ga; *Geology*, v. 22, p. 839-842.
- Robert, F.**  
1989: Internal structure of the Cadillac tectonic zone southeast of Val d'Or, Abitibi greenstone belt, Quebec; *Canadian Journal of Earth Sciences*, v. 26, p. 2661-2675.  
1993: The geometrical relationship between the stretching lineation and the movement direction of shear zones: discussion; *Journal of Structural Geology*, v. 15, p. 239-240.
- Skulski, T., Percival, J.A., and Stern, R.A.**  
1994: Oceanic allochthons in an Archean continental margin sequence, Vizien greenstone belt, northern Quebec; in *Current Research 1994-C*; Geological Survey of Canada, p. 311-320.

# Archean unconformity in the Qalluviartuuq greenstone belt, Goudalie domain, northern Quebec

P.A. Winsky<sup>1</sup>, T.M. Kusky<sup>1</sup>, J.A. Percival, and T. Skulski  
Continental Geoscience Division

*Winsky, P.A., Kusky, T.M., Percival, J.A., and Skulski, T., 1995: Archean unconformity in the Qalluviartuuq greenstone belt, Goudalie domain, northern Quebec; in Current Research 1995-C; Geological Survey of Canada, p. 131-140.*

---

**Abstract:** An unconformity in the northern Qalluviartuuq greenstone belt separates basement of metasedimentary and tonalitic rocks from conglomerate and sandstone. The basal conglomerate has tonalitic clasts, grading upward into a polymict assemblage of tonalite, basalt, andesite, granodiorite, metasedimentary and ultramafic clasts. The basalt, gabbro, and ultramafic clasts suggest that a metavolcanic terrane was being eroded in the (local) source area for the conglomerate, and yet the conglomerate passes with apparent stratigraphic continuity upwards into mafic volcanics. Either an older greenstone sequence within the basement complex contributed detritus to the conglomerate, or a tectonic break may be hidden in the complex structure of a fragmental mafic unit marking the contact between the conglomerate and metavolcanic units. In this second hypothesis, an overriding greenstone sheet would have shed clasts as it was thrust over synorogenic conglomerate deposited on basement.

**Résumé :** Une discordance dans la partie nord de la ceinture de roches vertes de Qalluviartuuq sépare le socle de roches métasédimentaires et tonalitiques du conglomérat et du grès. Le conglomérat de base contient des clastes de tonalite se transformant graduellement en un assemblage polygénique de clastes de tonalite, basalte, andésite, granodiorite, roches métasédimentaires et ultramafites. Les clastes de basalte, de gabbro et d'ultramafites font supposer que le terrane de roches vertes a subi une érosion dans la zone source (locale) du conglomérat et, pourtant, celui-ci laisse place vers le haut, avec une apparente continuité stratigraphique, à des volcanites mafiques. Ou bien une séquence plus ancienne de roches vertes au sein du complexe de socle a fourni les éléments détritiques du conglomérat, ou bien une rupture tectonique se cache peut-être dans la structure complexe d'une unité mafique clastique marquant le contact entre le conglomérat et les unités métavolcaniques. Selon cette seconde hypothèse, un feuillet de roches vertes chevauchant a déposé des clastes pendant son charriage au-dessus d'un conglomérat synorogénique déposé sur le socle.

---

<sup>1</sup> Department of Earth Sciences, Boston University, 675 Commonwealth Ave., Boston, MA 02215

## INTRODUCTION

Unconformities within Archean greenstone belts are valuable markers and provide opportunities to examine stratigraphic, structural and chronological relationships between younger and older Archean sequences. Other Archean unconformities near greenstone belts have proved significant in determining tectonic setting, including Steep Rock Lake, Ontario (Wilks and Nisbet, 1988), Belingwe, Zimbabwe (Winsky and Kusky, 1994; Kusky and Winsky, in press), Point Lake, Northwest Territories (Kusky, 1991, 1992), and the Vizien belt, Quebec (Percival et al., 1993). The Qalluviartuq greenstone belt of the Minto block (Fig. 1) was chosen to study relationships between metavolcanic rocks, basement and surrounding plutonic rocks, and to investigate the structural geometry of the branching that divides the belt into four arms (Fig. 2), similar to branching patterns within greenstone belts worldwide (Kusky and Vearncombe, in press). Possible models to account for this map-scale quadripartite division of the greenstone belt include interference folding, doming of surrounding granitoid massifs, structural juxtaposition by faulting, or inheritance and preservation of initially complex basin geometry. This year was the first year of detailed study of the Qalluviartuq greenstone belt, carried out under the auspices of a regional mapping project of the Goudalie domain (Percival et al., 1995). In this report, we summarize the geology of the northern Qalluviartuq Lake area and consider the origin and significance of the unconformity found there. Along with the structure of the belt, a detailed study of the conglomerate overlying the unconformity may help define the tectonic setting at the time of deposition.

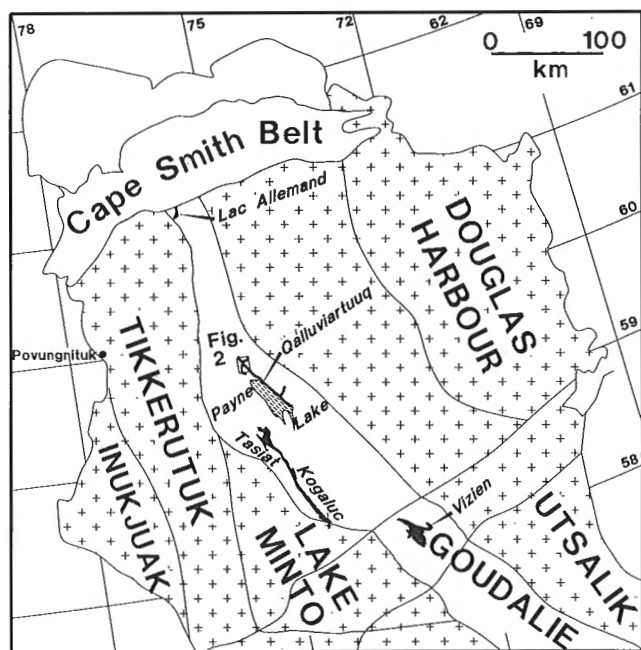


**Figure 1.** Geological domains of Ungava Peninsula, north-eastern Superior Province (modified after Percival et al., 1992), showing greenstone belts of the Goudalie domain.

## REGIONAL GEOLOGY

The Minto Block of the Superior Province is characterized by plutonic rocks and high grade gneiss with northerly trending structures and aeromagnetic anomalies (Percival et al., 1992). Recent mapping (Percival et al., 1990; 1991; 1992; Percival and Card, 1992) resulted in the division of the Minto Block into six, northwesterly trending lithotectonic domains (Fig. 1) including, from west to east, the Inukjuak, Tikkerutuk, Lake Minto, Goudalie, Utsalik, and Douglas Harbour domains. The central Goudalie domain contains abundant tonalites with supracrustal remnants, and plutons of hornblende-bearing granodiorite and granite. Greenstone belts of the Goudalie Domain include the Vizien, Kogaluc, Payne Lake, Qalluviartuq, and Lac Allemand belts (Fig. 1), each of which contains a suite of metamorphosed mafic-, intermediate- and felsic volcanic rocks, gabbro, and ultramafic rocks, as well as pelites, quartzites, and conglomerates. Granodiorite in the Kogaluc belt has been dated at  $2733 \pm 2$  Ma, and monzonite is  $2725 \pm 5$  Ma (Percival et al., 1995). Rocks of the Goudalie domain possess a strong northwest-striking foliation, with variably developed

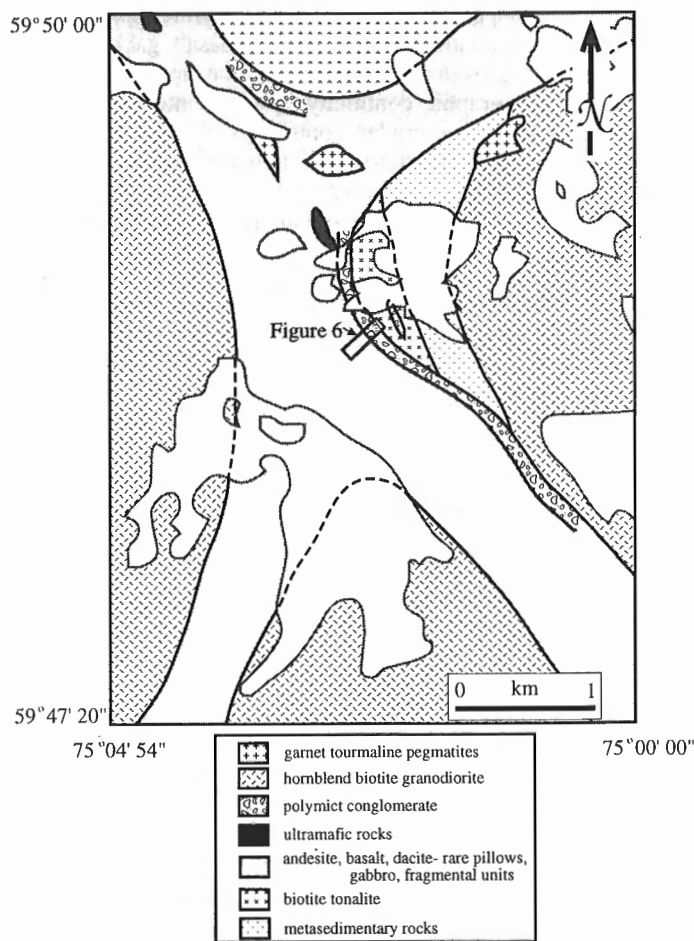


**Figure 2.** Geological map of the northern Qalluviartuq greenstone belt.

older and younger foliations (Lin et al., 1995). Rocks of the Goudalie domain have been interpreted (Percival et al., 1994; Skulski et al., 1994) as a complex assemblage of oceanic, accretionary prism, and island arc rocks caught between colliding continental arcs represented by the domains to the east and west.

In the northern Goudalie domain there are two packages of supracrustal rocks (Percival et al., 1995). The Payne Lake belt, consisting principally of migmatitic paragneiss and mafic gneiss, extends from Lac Le Breuil south to the eastern Kogaluc River. The Qalluviartuuq belt, the focus of this study, extends from north of Qalluviartuuq Lake 70 km to the south through Payne Lake.

## ROCK TYPES

### Basement units

The oldest unit in the northern Qalluviartuuq belt is a metasedimentary package interpreted to be greywacke and argillite with local, irregularly spaced, relict beds (Fig. 2). These generally schistose rocks are composed of quartz, plagioclase, and biotite with common garnet.

Intruding the metasedimentary rocks is a coarse grained, biotite-, magnetite±epidote tonalite, typically with a strong foliation (Fig. 3) and prominent mineral lineation (Fig. 4). The tonalite contains mafic enclaves (Fig. 5a) and mafic dykes with minor marginal tourmaline. A zone of tonalitic

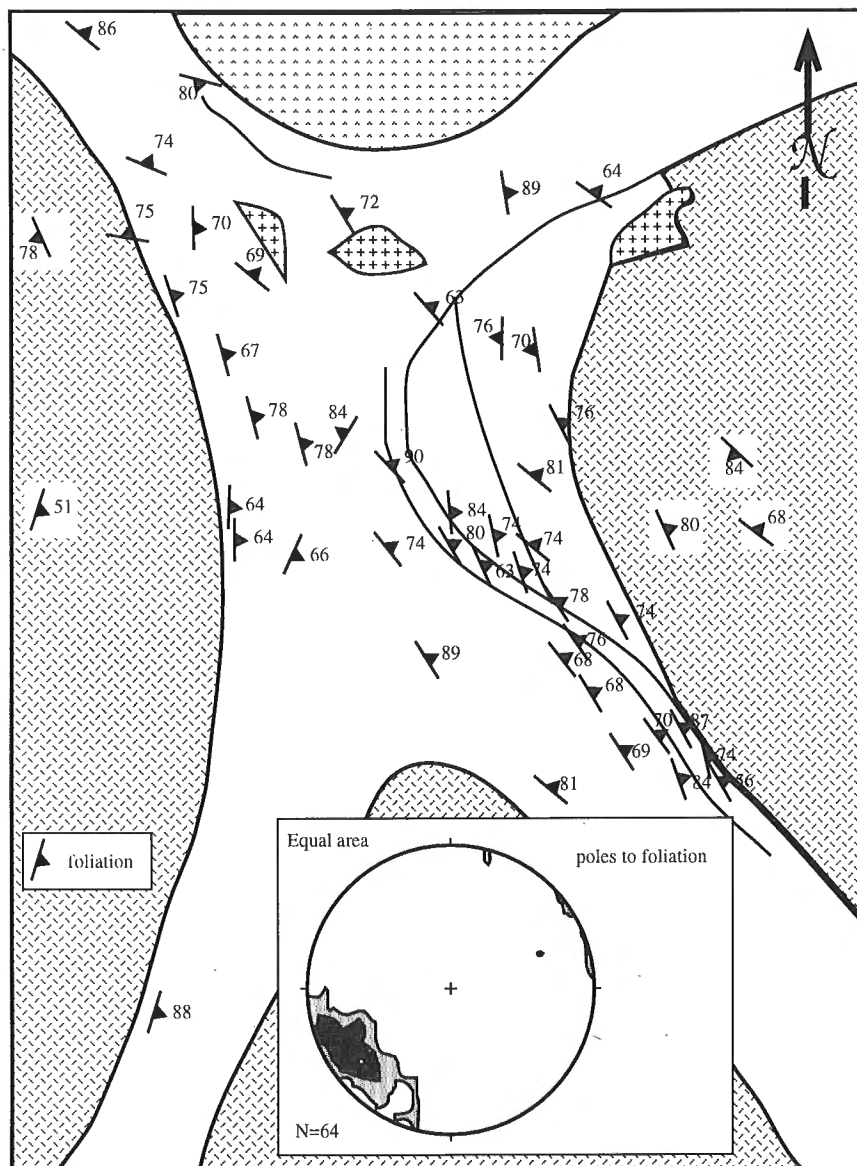


Figure 3. S<sub>2</sub> foliation of the northern Qalluviartuuq greenstone belt.

agmatitic intrusion breccia cuts tonalite/diorite in the northern part of the basement unit, suggesting a polyphase intrusion history for the magmatic rocks in the basement complex. Dykes of intermediate to mafic composition cut basement tonalite but do not appear to cross the unconformity. The basement is cut by anastomosing shear zones and by zones of epidote alteration.

**Unconformity and conglomerate**

Along the east side of the Qalluviartuuq belt near the intersection of the four arms, the older tonalite (Fig. 5a, b) is overlain unconformably by thin conglomerate (Fig. 5c, d) and sandstone units over a strike length of approximately 3 km (Fig. 2, 6). Conglomerate also occurs to the east and north

(Fig. 2), without well exposed unconformities. Beneath the exposed unconformity, the tonalite may be slightly regolithic, based on the presence of positive-weathering patches 2-4 cm in size, possibly a protoclastic texture. The discontinuous weathered zone is up to 15 cm thick. Although tectonically flattened, the unconformity appears to be relatively planar, without potholes or stream channels.

Directly overlying the unconformity is a 40 cm thick conglomerate unit containing 2-4 cm tonalite clasts. Above this, polymictic conglomerate contains clasts of dacite, andesite, metasediments and ultramafic rocks (Fig. 5c) along with clasts of tonalite up to 45 cm in diameter. The generally clast-supported conglomerate locally has a pelitic, garnet-bearing matrix. The clasts are deformed to varying degrees (e.g., Fig. 5d) with tonalite being the most resistant followed

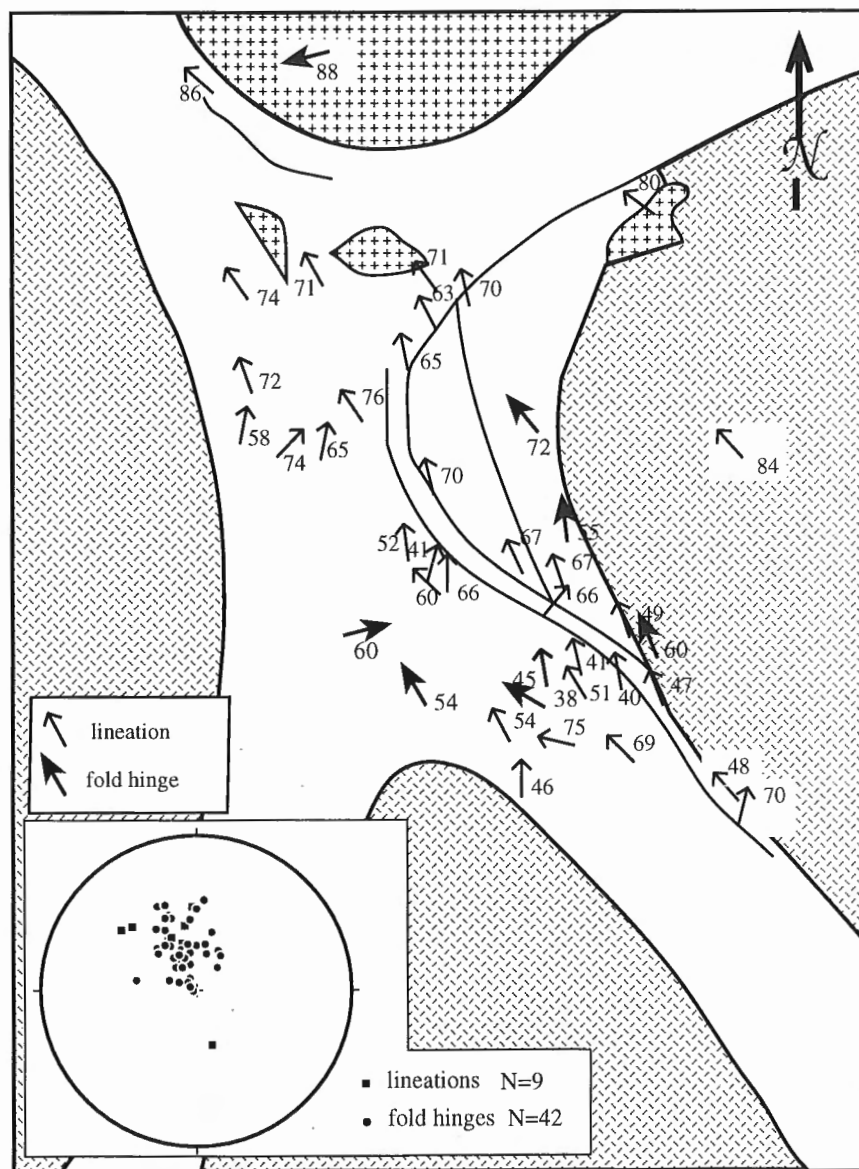
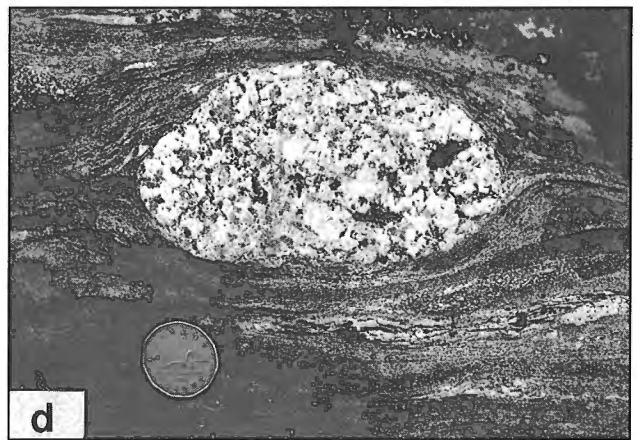
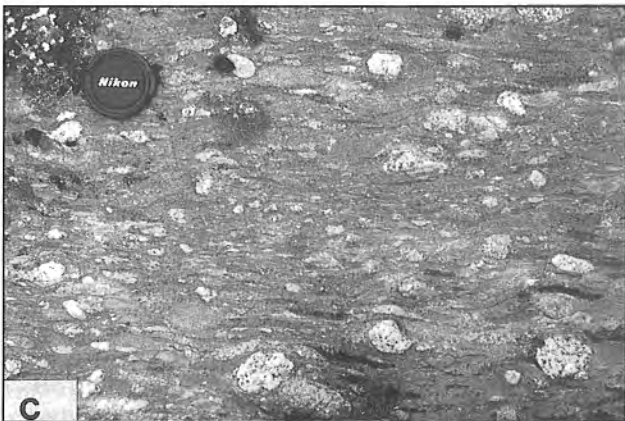
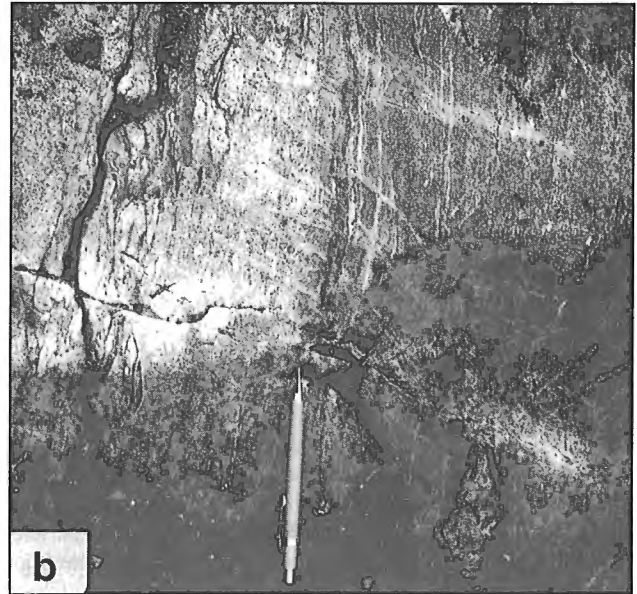
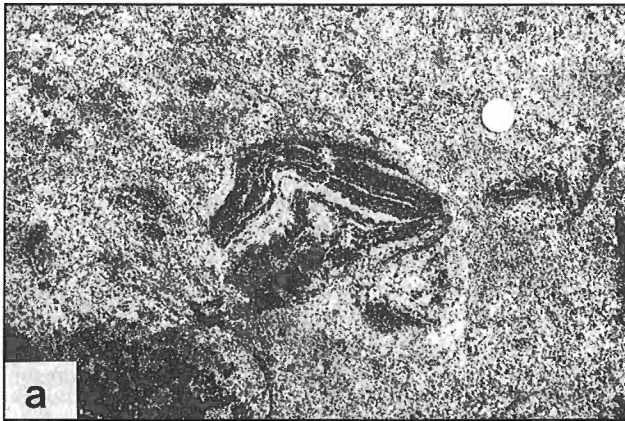


Figure 4. Lineation and fold hinges, northern Qalluviartuuq belt.



a) basement tonalite showing digested mafic enclaves; coin in this and subsequent photos is 27 mm in diameter (GSC 1994-765A);

c) conglomerate showing elliptical plutonic clasts. Material between pale-coloured clasts is matrix and deformed clasts of volcanic origin; lens cap in this and subsequent photos is 5 cm in diameter (GSC 1994-765B);

b) unconformity between tonalite (to right of pencil) and conglomerate (GSC 1994-765A);

d) conglomerate clast from Payne Lake, similar to those in the northern Qalluviartuuq belt (GSC 1994-765B).

**Figure 5.** Outcrop photographs of representative rock types.



by dacite, andesite, metasedimentary, and ultramafic clasts. Sandstone beds throughout the conglomeratic unit contain erosion-resistant quartz/sillimanite knots. Above the polymictic conglomerate lies about 6 m of quartz-rich sandstone which contains a few small clasts (Fig. 6). The sandstone is overlain by a mafic breccia unit with clasts of andesite and basalt.

**Mafic breccia**

At the base of the volcanic section and above the sandstone, a disrupted mafic unit containing structurally incoherent blocks of mafic volcanic and plutonic rocks is exposed. The breccia unit has a sharp contact with the underlying sedimentary rocks and appears conformable, although in most places the contact is intruded by a thin (5-10 cm) hornblende tonalite sill. The breccia unit contains primarily basaltic and andesitic fragments, along with subordinate gabbro, and is intruded by thin ultramafic dykes or sills. Judging by the pancake-shaped clasts, the overall state of strain is high, with zones of higher strain alternating with less-deformed, but still disrupted, areas bounded by anastomosing shear zones. A 5-10-m-thick lens of tonalite-pebble conglomerate lies above one of these high

strain zones near the unconformity location and indicates structural or stratigraphic repetition of the conglomerate/ mafic breccia contact. The upper contact of the breccia unit with the flow and pillowed units of the greenstone belt is covered by overburden. Further detailed mapping is planned along both contacts of the mafic breccia unit, as the nature of these contacts is critical for tectonic interpretations of the area.

**Greenstones**

The Qalluviartuuq greenstone belt contains units of andesite, basalt, and gabbro (Fig. 2, 7a) with lesser amounts of dacite, all metamorphosed to amphibolite facies. Small pockets of leucosome surrounded by ultramafic selvages are common, and probably represent anatectic melts generated during high-grade metamorphism (e.g., Brown, 1993). Many of the volcanic units may be fragmental (Fig. 7b), and rare pillows and pillow breccias were recognized. The stretched pillows define a lineation parallel to local mineral lineations. Minor iron-formation (Fig. 7c) occurs in association with pillow basalts. Common bodies of gabbro (Fig. 7a) probably represent deformed sills.

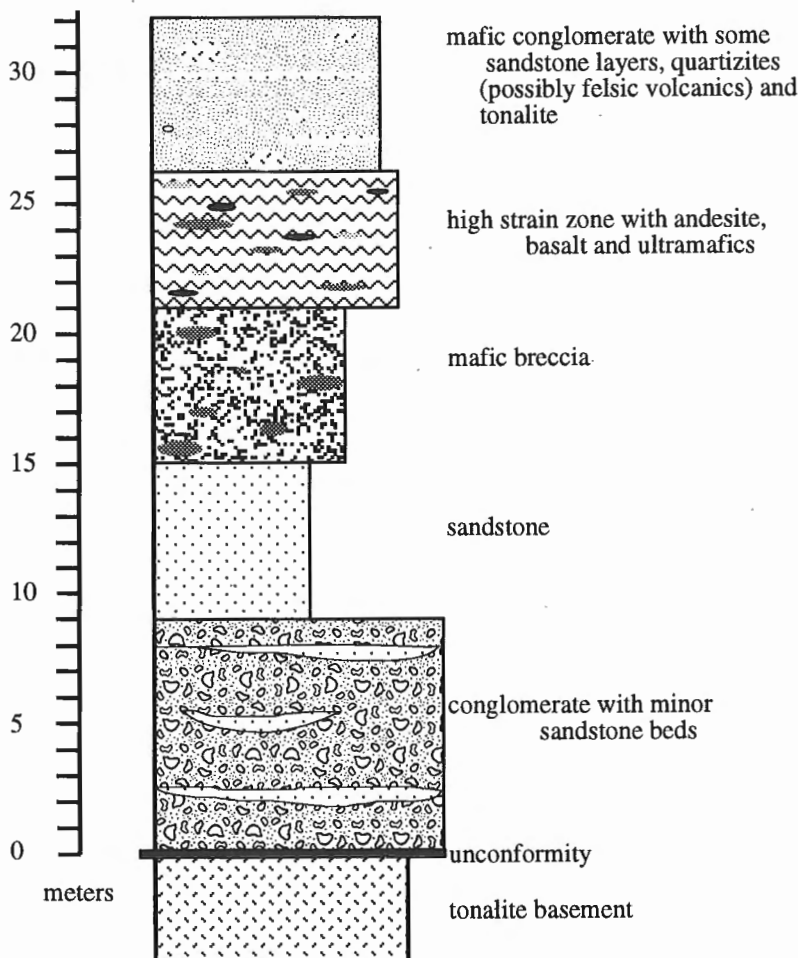


**Figure 6.**

*Schematic stratigraphic section of units above the unconformity; see Figure 2 for location of section.*

A zone containing pods and lenses of ultramafic rock occurs in the northwestern arm of the belt (Fig. 2). Two types of ultramafic rocks are recognized: large bodies with pyroxenite and dunite layers, probably layered sills; and more abundant schistose bodies containing talc, serpentine and tremolite.

### *Younger intrusions*

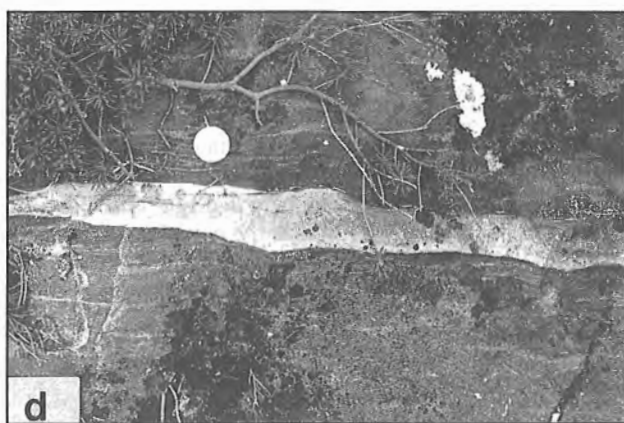
Intruding the volcanics and the disrupted unit at the base of the volcanics are rare felsic dykes (Fig. 7d) which were sampled for geochronology to provide an upper limit on the age of the greenstones. Surrounding the Qalluviartuuq belt is a variably foliated and lineated hornblende- biotite granodiorite, cutting both the greenstones and basement complex. Clasts of granodiorite in the conglomerate lithologically resemble this relatively young intrusive unit, which if supported by geochronology, would suggest that the conglomerate is one of the youngest units in the sequence.

Also cutting the belt are massive, undeformed, peraluminous pegmatites containing garnet and muscovite up to 15 cm long and tourmaline up to 10 cm across. The pegmatites appear to have intruded passively because country rock inclusions in the pegmatites have the same orientations as the host.

### STRUCTURE

The Qalluviartuuq greenstone belt has a strike length approximately 70 km (Fig. 1). Its northern termination, the subject of this study, has four arms extending to the northwest, northeast, southwest, and southeast (Fig. 2). Rocks within these arms have sustained intense deformation and amphibolite-facies metamorphism.

At the junction of the four arms (Fig. 2), the entire Qalluviartuuq belt is a zone of steeply east-dipping strong foliation (Fig. 3). The western margin of the belt is an intrusive contact with granodiorite and the northern margin is cut by



a) gabbro cutting andesite (GSC 1994-765C);

b) amphibolite, possibly of fragmental origin (GSC 1994-765C);

c) crenulated, foliated amphibolite with ankerite and iron-formation pods (GSC 1994-765D);

d) felsic dyke cutting disrupted mafic unit (GSC 1994-765D);

**Figure 7.** Outcrop photographs of representative rock types from the Qalluviartuuq greenstone belt.

pegmatites. The southern contact, in the hinge of the southern two limbs, is an intrusive contact between intermediate to mafic volcanics and coarse-grained tonalite-granodiorite.

Percival et al. (1995) described four ductile deformation events from the southern Qalluviartuuq belt. The first is expressed as a  $S_1$  foliation and migmatitic layering in the supracrustal rocks of the Payne Lake belt (Percival et al., 1995).  $S_1$  is recognized in the northern Qalluviartuuq area only as a foliation in paragneiss enclaves within the basement.

In the central section of the belt, the dominant foliation,  $S_2$  (Fig. 3), is defined by a strong lithological layering in amphibolitic mafic volcanic rocks, flattened volcanic fragments, and planar alignment of biotite (Fig. 3). The foliation strikes approximately  $330^\circ$  and dips about  $70^\circ$  to the northeast. This foliation is axial planar to the first generation of folds observed,  $F_2$  (Fig. 4), which have northwest striking, steeply east-dipping axial surfaces. To the north the  $S_2$  foliation is more variable and transected by numerous pegmatite pods (Fig. 3). Lineations defined by oriented mineral grains, stretched clast and pillow fragments are ubiquitous within the Qalluviartuuq greenstone belt, and on average plunge  $70^\circ$  toward  $340^\circ$  (Fig. 4).

The third deformation event can be seen on the outcrop scale as a local crenulation cleavage and refolding of  $S_2$ . The third generation of folds,  $F_3$ , generally has the form of south-east striking crenulation surfaces (Fig. 7c). The  $F_3$  fold hinges also plunge steeply to the north-northwest.

The fourth deformation event, defined a few kilometres to the south by a mylonite zone along the eastern edge of the belt, is not recognized in the northern Qalluviartuuq belt, where the margin is marked by an unconformity.

In areas where complex refolding causes bifurcation of lithological domains, lineation and foliation trajectories are expected to vary with position on early and late fold structures, with foliations generally following the outcrop strike, and lineations following small circle distributions or pointing inward towards structural sinks and outward from structural culminations (e.g., Veenhof and Stel, 1991). In the Qalluviartuuq greenstone belt, structural data reveal that neither the foliation nor the lineation show much variation in orientation through the quadrivial point where the four arms of the greenstone belt meet (Fig. 3, 4). This could indicate that fold interference is not the mechanism responsible for the complex map pattern, or that mesoscopic structures formed during early generations of folds ( $F_1$ ) have been obliterated or strongly transposed by younger fabrics ( $D_{2,3}$ ).

## DISCUSSION

The discovery in the 1994 field season of an unconformity between conglomerates and older basement units in the Qalluviartuuq greenstone belt has significant implications for the tectonic development of the Minto Block. There is little evidence of weathering along the unconformity surface, suggesting that the erosional surface was not exposed for a

long time prior to being buried by conglomerate. The conglomerate contains clasts of all rock types that occur in the greenstone belt and surrounding granitoid terrane, including granodiorites, suggesting that the conglomerate was deposited during a period of rapid uplift and erosion of basement and greenstone belt units, relatively late in the tectonic evolution of the Goudalie domain. In this regard the conglomerate resembles "Timiskaming-type" sequences of the southern Superior Province (e.g., Card, 1990). However, the relationship between conglomerate and the overlying volcanics requires further study. Key relationships may lie hidden within the structurally disrupted and highly strained mixed volcanic and sedimentary unit along the contact between the units. Needing explanation also is the source of metavolcanic clasts in the conglomerate unit. The most obvious source for the clasts would be the main Qalluviartuuq belt, but this sits with apparent conformity and stratigraphic continuity above the conglomerate. An alternative origin of the greenstone clasts in the conglomerate is the gneissic, potentially older Payne Lake greenstone belt (Percival et al., 1995). It is possible that this greenstone belt is exposed to the east of the northern end of the Qalluviartuuq greenstone belt, perhaps as the northeast arm. This could represent the origin of the conglomerate clasts, and explain the apparent stratigraphic continuity between the conglomerate and the mafic volcanics of the Qalluviartuuq belt. In this scenario, the mixed unit could represent an early fragmental or phreomagmatic volcanic unit deposited conformably over the conglomerates in a shallow but rapidly deepening basin.

It is alternatively possible that the overall high state of strain in the fragmental mafic unit hides a structural transition between the conglomerate and the overlying metavolcanic sequence. In this interpretation, the conglomerate may contain clasts eroded from the overlying metavolcanic units, and deposited unconformably on the older gneissic rocks, along with rocks derived from the basement complex. The ultimate interpretation will depend critically upon the age of cobbles contained within the conglomerate.

The Qalluviartuuq conglomerates can be compared on the basis of age, provenance, and structural history to other conglomerate occurrences of the Goudalie domain to determine their role in the regional tectonic evolution. Other conglomerates within greenstone belts include those of panel B in the Vizien belt to the south (Percival et al., 1993; Skulski et al., 1994; Lin et al., 1995) and Lac Allemand and Lac Inet to the north (Moorhead, 1989). Conglomerates in these belts share some similarities to those in the northern Qalluviartuuq belt: they overlie unconformities, contain granitoid clasts, and are overlain by volcanic rocks. Comparisons of the Goudalie conglomeratic units to others within the Superior craton may reveal regional patterns reflecting large-scale tectonic events.

## ACKNOWLEDGMENTS

The manuscript benefited from comments by K.D. Card, J.R. Henderson, and J.E. King.

---

**REFERENCES**


---

**Brown, M.**

1993: The generation, segregation, ascent and emplacement of granite magma: the migmatite-to-crustally-derived granite connection in thickened orogens; *Earth Science Reviews*, v. 36, p. 83-130.

**Card, K.D.**

1990: A review of the Superior Province; a product of Archean accretion; *Precambrian Research*, v. 48, p. 99-156.

**Kusky, T. M.**

1991: Structural development of an Archean orogen, western Point Lake, Northwest Territories; *Tectonics*, v. 10, p. 820-841.

1992: Relative timing of deformation and metamorphism at mid- to upper-crustal levels in the Point Lake Orogen, Slave Province, Canada; *in* *The Archean: Terranes, Processes and Metallogeny*, (ed.) J.E. Glover and S.E. Ho; Geology Department (Key Centre) and University Extension, The University of Western Australia, Publication no. 22, p. 59-71.

**Kusky, T.M. and Vearncombe, J.**

in press: Structure of Archean Greenstone Belts; *in* *Tectonic Evolution of Greenstone Belts*, (ed.) M.J. de Wit and L.D. Ashwal; Oxford Monograph on Geology and Geophysics.

**Kusky, T.M. and Winsky, P.A.**

in press: Structural relationships between a shallow water platform and an oceanic plateau, Zimbabwe; *Tectonics*.

**Lin, S., Percival, J.A., Winsky, P.A., Skulski, T., and Card, K.C.**

1995: Structural evolution of the Vizien and Kogaluc greenstone belts in Minto Block, northeastern Superior Province, northern Quebec; *in* *Current Research 1995-C*; Geological Survey of Canada, this volume.

**Moorhead, J.**

1989: Géologie de la région du Lac Chukotat, Québec (fosse de l'Ungava); Ministère de l'Énergie et des Ressources du Québec, ET87-10.

**Percival, J.A. and Card, K.D.**

1992: Vizien greenstone belt and adjacent high grade domains of the Minto block, Ungava Peninsula, Quebec; *in* *Current Research, Part C*; Geological Survey of Canada, Paper 92-1C, p. 69-80.

**Percival, J.A., Card, K.D., and Mortensen, J.K.**

1993: Archean unconformity in the Vizien greenstone belt, Ungava Peninsula, Quebec; *in* *Current Research, Part C*; Geological Survey of Canada, Paper 93-1C, p. 319-328.

**Percival, J.A., Card, K.D., Stern, R.A., and Bégin, N.J.**

1990: A geological transect of northeastern Superior Province, Ungava Peninsula, Quebec: The Lake Minto area; *in* *Current Research, Part C*; Geological Survey of Canada, Paper 90-1C, p. 133-141.

1991: A geological transect of the Leaf River area, northeastern Superior Province, Ungava Peninsula, Quebec; *in* *Current Research, Part C*; Geological Survey of Canada, Paper 91-1C, p. 55-63.

**Percival, J.A., Mortensen, J.K., Stern, R.A., and Card, K.D.**

1992: Giant granulite terranes of northeastern Superior Province: the Ashuanipi complex and Minto block, *Canadian Journal of Earth Sciences*, v. 29, p. 2287-2308.

**Percival, J.A., Skulski, T., Lin, S., and Card, K.D.**

1995: Granite-greenstone terranes of the northern Goudalie domain, northeastern Superior Province, Quebec; *in* *Current Research 1995-C*; Geological Survey of Canada, this volume.

**Percival, J.A., Stern, R.A., Skulski, T., Card, K.D., Mortensen, J.K., and Bégin, N.J.**

1994: Minto block, Superior province: missing link in deciphering assembly of the craton at 2.7 Ga; *Geology*, v. 22, p. 839-842.

**Skulski, T., Percival, J.A., and Stern, R.A.**

1994: Oceanic allochthons in an Archean continental margin sequence, northeastern Superior Province, northern Quebec; *in* *Current Research 1994-C*; Geological Survey of Canada, p. 311-320.

**Veenhof, R.P. and Stel, H.**

1991: A cleavage triple point and its mesoscopic structures: the Mustio Sink (Svecofennides of SW Finland); *Precambrian Research*, v. 50, p. 269-282.

**Wilks, M.E. and Nisbet, E.G.**

1988: Stratigraphy of the Steep Rock Group, northwest Ontario: a major Archean unconformity and Archean stromatolites; *Canadian Journal of Earth Sciences*, v. 25, p. 370-391.

**Winsky, P.A., and Kusky, T.M.**

1994: Structural relationships between a shallow water platform and an oceanic plateau, Zimbabwe; *Geological Society of America, Abstracts with Programs*, v. 26, p. A407.

---

 Geological Survey of Canada Project 890009



# Granite-greenstone terranes of the northern Goudalie domain, northeastern Superior Province, Quebec

J.A. Percival, T. Skulski, S. Lin, and K.D. Card  
Continental Geoscience Division

*Percival, J.A., Skulski, T., Lin, S., and Card, K.D., 1995: Granite-greenstone terranes of the northern Goudalie domain, northeastern Superior Province, Quebec; in Current Research 1995-C; Geological Survey of Canada, p. 141-150.*

---

**Abstract:** Reconnaissance-scale mapping of the Goudalie domain in an area up to 200 km north of the Vizien belt shows that the northwest-trending negative aeromagnetic anomaly corresponds to granite-greenstone terrane. The 110-km long, <1 km wide, Kogaluc-Tasiat belt of sheared, amphibolite-facies, mafic metavolcanic rocks, biotite schist, and iron-formation, is bordered to the east and west by 15-20 km wide zones of similar lithologies at granulite facies forming screens in pyroxene-bearing granodiorite and granite. The eastern zone of high-grade supracrustals extends north into the Payne Lake belt of paragneiss, mafic gneiss, and iron-formation, with concordant sheets of granitoid rock, cut locally by Archean dykes. To the east, the Qalluviartuuq belt of sheared, amphibolite-facies mafic metavolcanic schist, biotite schist, and conglomerate is locally unconformable on tonalitic basement. Favourable environments for VMS and shear-zone-hosted gold mineralization may be present.

**Résumé:** Une cartographie de reconnaissance du domaine de Goudalie dans une région s'étendant jusqu'à 200 km au nord de la ceinture de Vizien montre que l'anomalie aéromagnétique négative à orientation nord-ouest correspond à un terrane de granite-roches vertes. La ceinture de Kogaluc-Tasiat, qui a 110 km de longueur et <1 km de largeur, se compose de métavolcanites mafiques du faciès de amphibolites, de schiste à biotite et de formation de fer cisailés, et est limitée à l'est et à l'ouest par des zones de 15-20 km de largeur de lithologies similaires au faciès des granulites qui forment écran dans un granite et un granodiorite à pyroxène. La zone est des roches supracrustales fortement métamorphisées s'étend vers le nord jusque dans la ceinture de paragneiss, de gneiss mafique et de formation de fer de Payne Lake, avec feuillets concordants de roche granitoïde, que recourent localement des dykes archéens. À l'est, la ceinture de Qalluviartuuq, composée de schiste métavolcanique mafique du faciès des amphibolites, de schiste à biotite et de conglomérat cisailés, repose localement en discordance sur un substratum tonalitique. Des environnements favorables à la mise en place de SMV et de minéralisation aurifère dans une zone de cisaillement pourraient être présents.

## INTRODUCTION

The Goudalie granite-greenstone domain, discovered during a geological transect of the Minto block (Percival and Card, 1994), holds keys to deciphering the tectonic history of the northeastern Superior Province. Goudalie volcano-sedimentary belts preserve a more complete stratigraphic and structural record than associated granitoid domains of the Minto block. Identified on the basis of its well preserved supracrustal sequences, including the Vizien greenstone belt (Percival et al., 1992; 1993) and associated tonalitic gneisses, the domain coincides with a negative aeromagnetic anomaly that extends several hundred kilometres north and south of the transect. The Vizien belt in the central Goudalie contains ancient continental crust in the form of >2.9 Ga tonalitic gneisses (Stern et al., 1994; unless otherwise specified, cited ages are U-Pb zircon dates), overthrust by younger oceanic sequences (Skulski et al., 1994). The submarine volcanic packages have metamorphic alteration assemblages resembling modern seafloor environments (Percival and Card, 1992a) and point to significant potential for Archean greenstone-belt-hosted mineralization in the Goudalie. A multi-year project was initiated in 1994 to investigate the northern extension of the Goudalie domain, both for its economic potential, and to provide critical information on the tectonic evolution of the Minto block (e.g., Percival et al., 1994).

## REGIONAL GEOLOGY

The geology of the Minto block is known from 1:1 000 000-scale reconnaissance (Stevenson, 1968) and from the more detailed southwest-northeast transect in which several lithotectonic domains were defined. West of the Goudalie domain (Fig. 1), the Lake Minto domain consists predominantly of plutonic rocks with sparse supracrustal xenoliths, mainly paragneiss and iron formation. Major plutonic suites include pyroxene-, hornblende-bearing granodiorites ( $2725 \pm 5$  Ma; Stern et al., 1994), orthopyroxene-biotite diatexite (2712 Ma), with local enclaves of 3.1 Ga tonalitic gneiss, and granite (2690 Ma) (Percival et al., 1992). The Goudalie domain in the Leaf River area consists predominantly of tonalitic rocks, including units dated at 2.9-3.1 Ga (Percival et al., 1992; Stern et al., 1994), and variably preserved supracrustal remnants. Within the Goudalie domain, the Vizien greenstone belt (Percival and Card, 1992a; b) is a structurally complex tectonic collage of units of oceanic and continental margin affinity (Skulski et al., 1994; Lin et al., 1995). Four volcanic sequences are recognized: (1) a ~2792 Ma bimodal, continental tholeiitic, shallow marine to subaerial volcanic sequence; (2) a 2786 Ma submarine sequence of tholeiitic mafic lavas and peridotite sills; (3) a 2724 Ma calc-alkaline mafic to felsic emergent sequence; and (4) a younger (<2718 Ma) continental sequence that includes mafic and ultramafic tholeiitic volcanic rocks (Skulski et al., 1994; Percival et al., 1994). The volcanic units occur within discrete structural panels that have sustained a complex structural history (Skulski et al., 1994; Lin et al., 1995), most of which occurred between 2718 and 2693 Ma. To the east, the

Utsalik domain consists of pyroxene and hornblende-bearing granodiorite ( $2725 \pm 5$  Ma; Stern et al., 1994). Northerly structural trends are defined by kilometre-scale granite sheets.

## NORTHERN GOUDALIE DOMAIN

Using the aeromagnetic anomaly as a guide, 200 km of strike length of the Goudalie domain north of the Vizien belt was mapped at reconnaissance scale (Fig. 2). Several narrow, elongate belts of amphibolite-facies supracrustal rock occur within the region, which is otherwise dominated by pyroxene-bearing plutonic rocks containing screens of high-grade supracrustal rock.

### Supracrustal rocks of the Goudalie domain

Aside from a few scattered occurrences of gneiss of volcanic origin noted on Stevenson's (1968) map and unpublished reports of industrial reconnaissance-scale exploration, greenstone belts and their regional context have not previously been described from the northern Goudalie domain. The greenstone sequences reported here have protoliths of volcanic and sedimentary origin, including iron-formation. Pervasive shear fabrics and local mylonite zones characterize the belts over significant strike lengths.

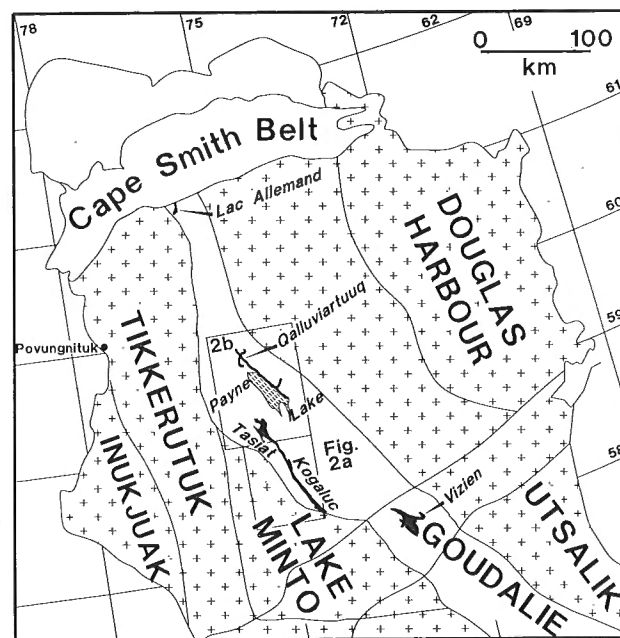
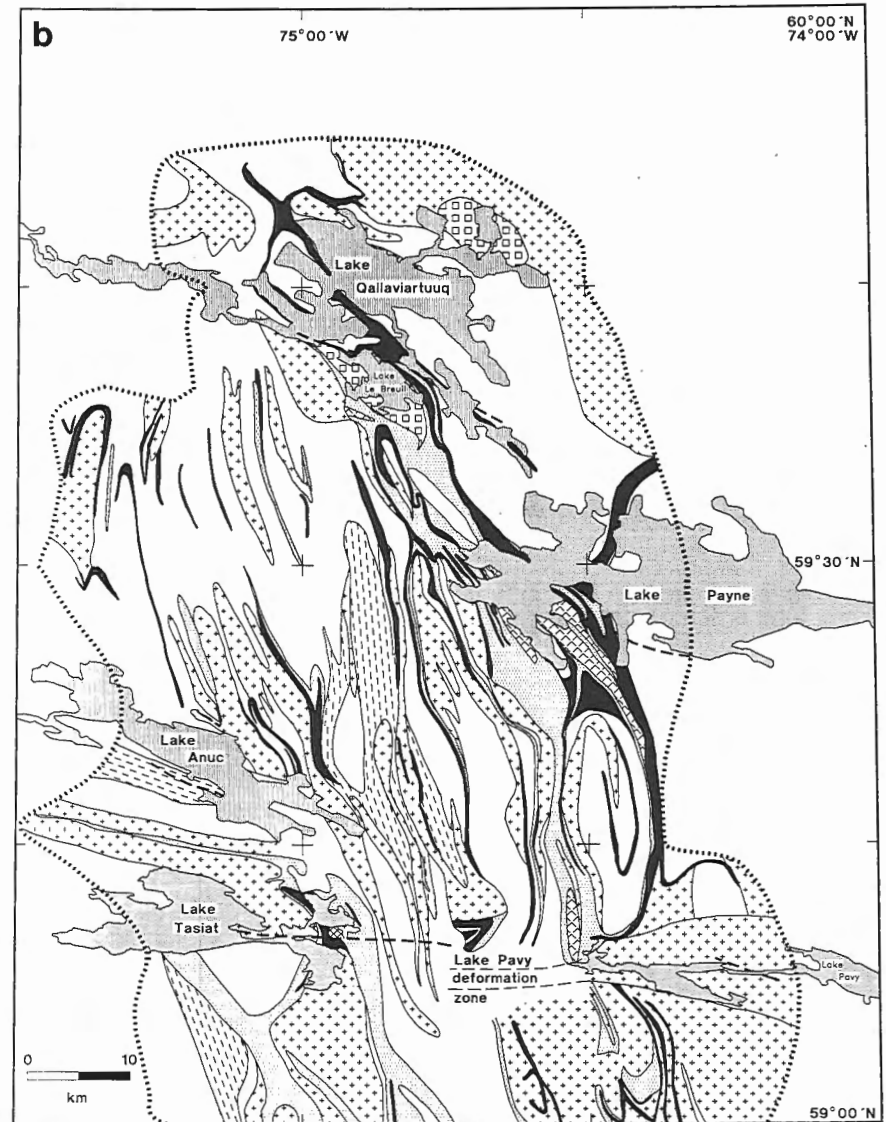
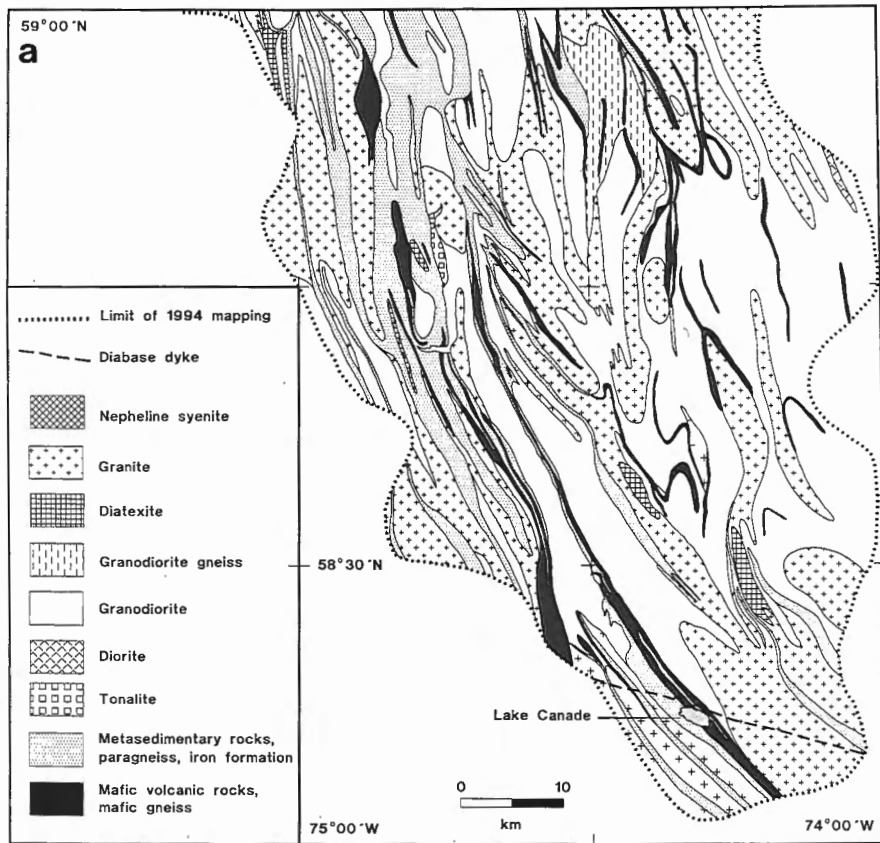


**Figure 1.** Generalized geological map of northeastern Superior Province showing domains identified in the Minto transect (Percival and Card, 1994), and negative aeromagnetic anomaly associated with Goudalie domain.

**Figure 2.** Compilation map of the Goudalie domain; **a)** southern region (NTS 34J), showing the Kogaluc – Tasiat belt; **b)** northern region (NTS 34O) showing the Payne Lake and Qalluviartuuq belts.





### ***Kogaluc – Tasiat belt***

Although metamorphic grade is lower in the <1 km wide Kogaluc – Tasiat belt (Fig. 2a) than the regional upper amphibolite to granulite facies, primary features are rarely preserved owing to the effects of at least two high-strain events. Three main units can be distinguished: rocks of volcanic origin, metasedimentary rocks, and iron-formation. Metavolcanic rocks are generally fine grained mafic schists with stretched pillows evident locally, as well as relict gabbroic textures. Primary quartz phenocrysts are locally preserved in felsic metavolcanic rocks. Metasedimentary rocks are mainly fine grained biotite and/or muscovite schist with rare quartz-rich sandstones and conglomerate. A 5-10 m thick unit of quartz-magnetite banded iron-formation (Fig. 3) with a strike length of ~15 km occurs in the northern part of the Kogaluc belt, in association with biotite schist, siliceous

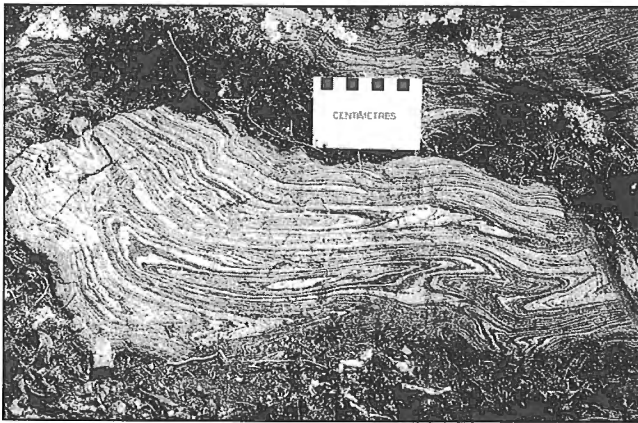


**Figure 3.** Thinly laminated magnetite-quartz iron-formation showing outcrop-scale  $D_2$  sheath folds, northern Kogaluc belt (see also Lin et al., 1995). GSC 1994-742M.



**Figure 4.** Sedimentary structures including channel scours and pebbly conglomerate, preserved in a low-strain window in the southern Kogaluc belt. Lens cap in this and subsequent photos is 5 cm in diameter. GSC 1994-759G.

metasediments and metagabbro. Discontinuous units of silicate-facies iron-formation (garnet+grunerite+quartz±magnetite rocks) occur sporadically throughout the belt.

Preserved facing directions permit local reconstruction of stratigraphic sections. In the southern Kogaluc belt, sedimentary rocks display crossbedding, channel scours and graded beds (e.g. Fig. 4), indicating that a sequence with a lower unit of plagioclase-porphyrific andesite and semi-pelite is overlain by massive and pillowed andesite with gabbro cumulate sills. These are in turn overlain by a unit of interbedded semi-pelite and mafic tuff, a sedimentary unit containing grit, semi-pelite and polymictic conglomerate, and an uppermost unit of quartz-porphyrific rhyolite tuff, with a preliminary U-Pb zircon age of  $2744 \pm 10$  Ma (T. Skulski, unpublished data). In the north-central part of the belt, basal mafic tuff and basalt is overlain by oxide-facies banded iron formation, quartz-rich siltstone, greywacke, and mafic epiclastic rocks interbedded with pelite. The well-preserved metavolcanic rocks have calc-alkaline geochemical characteristics (T. Skulski, unpublished data).

Metamorphic grade in the Kogaluc – Tasiat belt ranges from lower to middle amphibolite facies, based on the presence of local occurrences of both andalusite and sillimanite in pelitic schist and epidote-hornblende assemblages in mafic rocks. In the Lake Tasiat area regional metamorphic assemblages are overgrown by low-pressure hornfels (muscovite±andalusite±cordierite), probably related to intrusion of adjacent granodiorite. The regional assemblage garnet-plagioclase-sillimanite-quartz yields an estimate of metamorphic conditions of 0.38 GPa, 575°C using TWQ software (Berman, 1991).

High-grade supracrustal rocks occur as narrow belts of migmatitic gneiss enclosed in plutonic rocks in zones 15-20 km wide west and east of the Kogaluc – Tasiat belt. Like their lower grade neighbour, individual belts are rarely >1 km thick. The dominant rock type is paragneiss, with garnet-biotite-plagioclase-quartz±sillimanite±cordierite assemblages, and associated diatexite. Mafic rocks consist



**Figure 5.** Silicate-facies iron-formation from the southern Payne Lake belt. Modal variations of garnet-grunerite-quartz-magnetite assemblages produce the centimetre-scale layering. GSC 1994-759A.

of hornblende-plagioclase, with variable amounts of orthopyroxene, clinopyroxene and rare garnet. Primary structures are not preserved, with the possible exception of quartz-magnetite laminae in iron-formation. The mafic rocks are presumed to be of supracrustal origin based on their association with metasedimentary units. Iron-formation, both magnetite+quartz and garnet+grunerite+quartz (Fig. 5) type, occurs in lenses and layers within paragneiss and along mafic gneiss-paragneiss contacts.

Granulite-facies conditions are indicated by orthopyroxene-bearing mafic gneisses beyond 5 km east of the Kogaluc – Tasiat belt and garnet-sillimanite±cordierite assemblages occur in paragneiss. Plutonic rocks in the eastern region are dominantly foliated pyroxene-bearing granodiorite and granite. Beyond ~5 km to the west of the Kogaluc – Tasiat belt, mafic gneiss contains orthopyroxene and metasedimentary migmatites have garnet-sillimanite-cordierite assemblages. Associated granodiorite and granite contain sporadic ortho- and clinopyroxene.

### *Qalluviartuuq – Payne Lake area*

Two distinct packages of supracrustal rocks occur in the northern part of the map area (Fig. 1, 2b). The 8 km wide Payne Lake belt, dominated by migmatitic paragneiss with associated iron formation and minor mafic metavolcanic rocks, extends from western Lac Le Breuil through western Payne Lake and continues southward into the eastern Kogaluc River area as high-grade enclaves in plutonic units. The <2 km wide Qalluviartuuq belt extends from northern Qalluviartuuq Lake to central Payne Lake and consists mainly of mafic schist in the epidote amphibolite facies, with locally preserved volcanic and intrusive features.

The Payne Lake belt consists mainly of garnet-biotite±sillimanite paragneiss. Units of thinly laminated garnet-grunerite-magnetite iron-formation up to 20 m thick are locally associated with units of hornblende-plagioclase±garnet mafic gneiss up to 500 m thick. Thin discontinuous

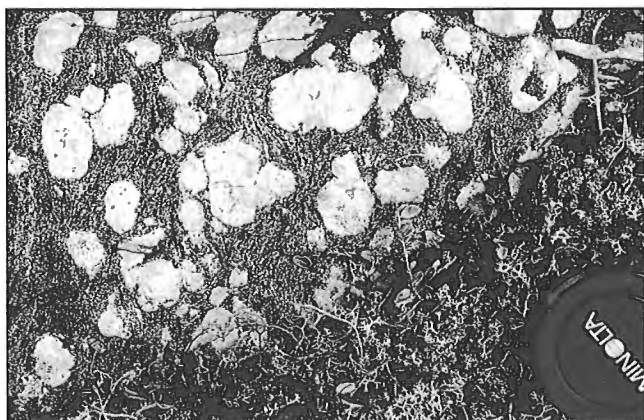


**Figure 6.** Glomeroporphyritic gabbro from the central Payne Lake belt. Variably preserved plagioclase phenocrysts constitute up to 30 per cent of the rock. GSC 1994-759H.

units of foliated oikocrystic pyroxenite are probably boudinaged sills. In an ultramafic-mafic-anorthositic gabbro intrusion and associated glomeroporphyritic gabbro, igneous layering is preserved locally (Fig. 6). Steeply dipping ferro-gabbro-magnetite peridotite underlies anorthositic gabbro, suggesting a westward-facing layered intrusion. In western Payne Lake, diorite and minor plagioclase-porphyrific andesite and dacite are the dominant rock types. Several concordant sheets of granite cut the supracrustal belt and locally form cores of tight upright antiforms. North-northwest-trending mafic dykes up to 3 m wide, with preserved chill margins, cut both supracrustal and intrusive units and are inferred to be Archean based on the presence of a penetrative foliation and sparse granitic veins. Dykes with similar trend and characteristics cut granite with pyroxenite enclaves west of Qalluviartuuq Lake. Locally plagioclase porphyritic (Fig. 7), the dykes could be high-level feeders to a younger supracrustal sequence of volcanic rocks and/or sills.

Supracrustal rocks of the Qalluviartuuq belt occur in a principal north-striking spine and several branches (Fig. 1, 2). Mafic rocks, including metavolcanic, metagabbroic and highly tectonized components, are interlayered with garnetiferous metasedimentary units. A vertically dipping unconformity north of Qalluviartuuq Lake separates a basement of medium grained biotite tonalite with paragneiss enclaves, cut by mafic dykes, from a west-facing sedimentary unit including tonalite-clast conglomerate (Fig. 8) and sandstone (Winsky et al., 1995). The sedimentary rocks are overlain by a unit of epidote-rich mafic to intermediate volcanic breccia and sill-like bodies of dacite and ultramafic schist. Coarse conglomerate occurs at several localities in western Payne Lake. At one location, granodiorite boulder conglomerate is separated by a narrow covered zone from granodiorite, presumed to be basement, and the sedimentary unit overlain by glomeroporphyritic basalt. The volcanic package includes plagioclase-glomeroporphyritic basalt, pillowed amygdaloidal basalt (Fig. 9), and fine grained mafic volcanic rocks. A lens of gabbroic anorthosite in southern Qalluviartuuq Lake is associated with alteration to cordierite-anthophyllite

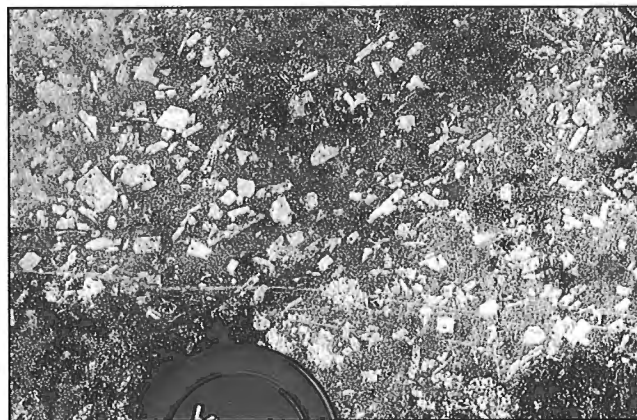


**Figure 7.** Plagioclase porphyritic mafic dyke cutting granite west of Qalluviartuuq Lake. A weak foliation and rare granitic veins suggest an Archean age for the dykes which could be high-level feeders to younger volcanic rocks. GSC 1994-759B.

assemblages. Sparse galena from a sulphide-bearing zone yielded a model lead age of 2.74 Ga (assuming a southern Superior Province two-stage lead growth model; R. Thorpe, pers. comm., 1994). Conglomerate occurs in the northern and southern extremities of the belt.

Metamorphic grade in the Payne Lake belt is generally to upper amphibolite facies, indicated by abundant migmatitic leucosome and garnet-sillimanite assemblages in paragneiss, as well as hornblende-plagioclase±garnet±clinopyroxene assemblages in mafic units. Grade is somewhat lower in the Qalluviartuuq belt, judging by the presence of widespread epidote in mafic rocks (with hornblende-plagioclase) and cordierite-anthophyllite-Mg-chlorite assemblages in alteration zones.

### ***Plutonic rocks of the Goudalie domain***

Four major and three minor plutonic suites of distinct composition, texture, and mineralogy underlie most of the region. Some are spatially restricted whereas others are widespread. The oldest plutonic suite consists of coarse grained (to 6 cm average grain size) pyroxenite and melagabbro that occur as variably net-veined enclaves (Fig. 10) within younger plutonic rocks. The podiform bodies range in size from a few to 300 m. They are generally massive clino- or orthopyroxenite with some interstitial olivine, hornblende, biotite and spinel. Although more common in granodiorite, the ultramafic pods also occur in granite. Their relationship to the sparse ultramafic sills in the Payne Lake belt is not known.

A large area east of the Kogaluc – Tasiat belt is underlain primarily by homogeneous, medium grained, variably foliated granodiorite with characteristic orthopyroxene-clinopyroxene-biotite±hornblende assemblages. Foliation is defined by mafic mineral alignment and in gneissic zones by lit-par-lit granite veins. Rare mafic phases include diorite and quartz diorite. North-striking belts of high-grade mafic gneiss and paragneiss with some iron-formation occur as screens in a 20-km-wide zone (Fig. 2a). Small enclaves of dioritic and

anorthositic rocks locally contain gneissic fabrics predating the foliation in enclosing granodiorite (Fig. 11). Pyroxene in granodiorite may be of igneous origin based on several observations: 1) dykes of pyroxene-bearing granodiorite cut amphibolite-facies rocks; 2) hornblende and biotite commonly overgrow pyroxene, suggesting a late magmatic or retrograde metamorphic origin for the hydrous minerals rather than prograde decomposition to form pyroxene; and 3) locally completely anhydrous assemblages in rocks of granodioritic and dioritic composition would require metamorphic temperatures beyond hornblende and biotite stability, for which there is no evidence in associated metabasic and metasedimentary rocks. The composition and petrographic features of the suite suggest affinity with the Leaf River plutonic suite of  $2725 \pm 5$  Ma age defined to the south (Stern et al., 1994).

A second suite of granodiorites flanks the Kogaluc – Tasiat belt. The homogeneous, medium grained, variably foliated biotite±hornblende-bearing plutons form linear



**Figure 9.** Well preserved pillows in metabasalt, southern Qalluviartuuq belt. The pillows contain plagioclase phenocrysts and quartz-filled amygdules. GSC 1994-759I.

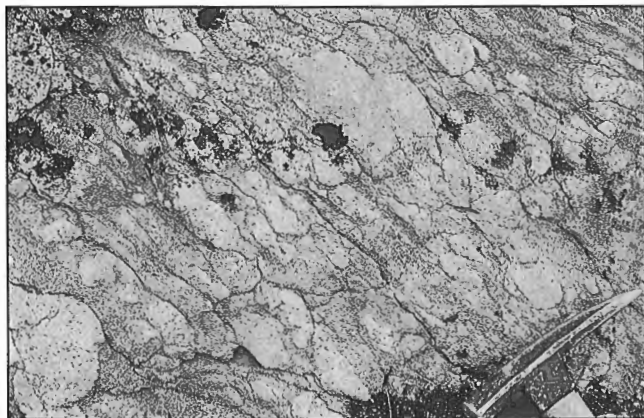


**Figure 8.** Tonalite-cobble conglomerate overlying tonalitic basement in the northern Qalluviartuuq belt. For more detail, see Winsky et al. (1995). GSC 1994-759J.

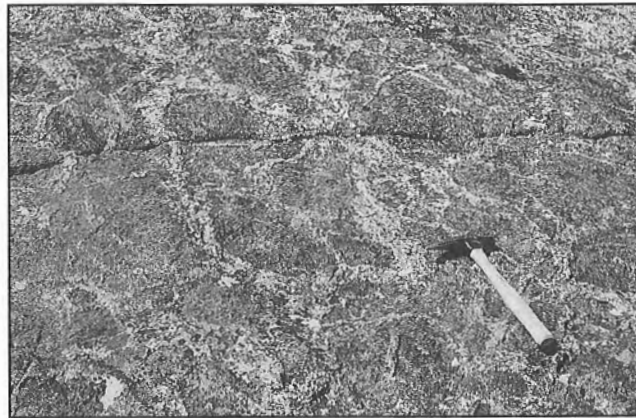


**Figure 10.** Net-veined pyroxenite enclave in granodiorite east of the Kogaluc belt. Pyroxenite pods up to a few hundred metres across are variably invaded by host granodiorite and granite. GSC 1994-759C.



**Figure 11.** Enclaves of foliated anorthosite in weakly foliated orthopyroxene-clinopyroxene granodiorite. Note variably discordant foliation in enclaves indicating a set of structures older than the granodiorite and regionally pervasive  $S_2$  foliation. GSC 1994-759D.

bodies a few kilometres wide and tens of kilometres long. One such foliated biotite granodiorite in the southern Kogaluc belt was dated at  $2733 \pm 2$  Ma, whereas a massive biotite monzonite to the north is  $2725 \pm 5$  Ma (T. Skulski, unpublished data). Lin et al. (1995) inferred a syn- $D_2$  age for foliated granodiorite in the northern Kogaluc belt. The plutons contain linear enclaves of mafic gneiss and paragneiss, locally with pyroxene-bearing assemblages, and are cut by abundant sheets of granite and pegmatite. Plutonic rocks flanking the Qalluviartuuq belt are mainly strongly foliated, mafic hornblende-biotite granodiorite, tonalite, and quartz diorite with a few mafic enclaves.

Dykes of foliated peraluminous granite occur within the Kogaluc – Tasiat and Payne Lake belts and regionally within paragneiss. The metre-scale bodies of coarse grained to pegmatitic rocks contain minor amounts of biotite, muscovite, garnet, and tourmaline. They are generally concordant and folded with layering in the host rocks. Dykes of similar composition are less abundant in the Qalluviartuuq belt. In the Vizien belt, similar peraluminous pegmatites of 2693 Ma age (U-Pb monazite age; T. Skulski, unpublished data) crosscut ductile fabrics.

A distinct suite of foliated to massive, medium- to coarse-grained granodiorite to granite occurs as plutons and dykes throughout the Kogaluc River area. It contains K-feldspar with distinctive red cores and common biotite±clinopyroxene mafic mineral assemblages. These rocks cut the previously described granitoid units and are generally less foliated.

A body of nepheline syenite approximately 2 x 3 km cuts foliated granodiorite and granite at Lake Tasiat. The medium- to coarse-grained, aegerine-augite essexite to biotite nepheline syenite has both a local igneous lamination and pervasive tectonic foliation. The pluton is cut locally by dykes of pegmatitic syenite and by east-west trending diabase dykes.

Massive, coarse grained biotite granite, leucogranite and pegmatite occur as small plutons and sheets, cutting foliated rocks. They are apparently the youngest regional unit. Local skarn replacement veins post-date granite and pegmatite. The coarse grained calcite+diopside±phlogopite veins, up to several metres thick, passively replace silicate along the layering, locally forming breccias with a carbonate matrix.

At least two sparse sets of west-northwest-trending diabase dykes of presumed Proterozoic age cut all Archean units. Green-weathering dykes of probable tholeiitic composition up to 60 m wide trend  $270-300^\circ$  and bifurcate locally. A few brown-weathering olivine diabase dykes <10 m wide trend  $\sim 290^\circ$ . A northwest-trending body of coarse grained gabbro in western Payne Lake contains granitic dykes or segregations; its age is unknown.

### Structural geology

Primary depositional structures have been recognized in a few locations. Bedding, crossbedding, graded bedding, and channel scours are preserved locally in relatively low-grade metagreywackes (e.g. Fig. 4); deformed pillows (Fig. 9), pillow breccias and amygdules represent primary volcanic structures.

In the Kogaluc – Tasiat belt (Table 1), the main fabric is a steep, synmetamorphic  $D_2$  foliation; older ( $D_1$ ) folds and cleavage are rare. The dominant, north-northwest-striking, foliation has an associated steep down-dip lineation. The kinematic sense, based on the geometry of  $D_2$  sheath folds (e.g. Fig. 3), appears to be east over west. North-northwest-trending foliation of  $D_2$  age is also evident in foliated plutonic rocks within and adjacent to the belt. Older ( $D_1$ ?) structures are only locally recognizable in enclaves as discordant foliation.

**Table 1.** Age relationships, Kogaluc River area.

$D_5$ :	E-W brittle faults; cataclasite; pseudotachylite
$D_{4b}$ :	E-W steep brittle-ductile shear zones; S over N
$D_{4a}$ :	dextral transcurrent high-strain zone- central Kogaluc belt
I:	pink pegmatite; granite
$D_3$ :	open folds in gneiss & plutonic domains
I:	red feldspar granite, granodiorite
$D_2$ :	main penetrative N-S foliation; steep lineation
I:	peraluminous pegmatite
I:	granodiorite including Leaf River suite equivalents (2725 Ma?)
$D_1$ :	early folds in Kogaluc belt; gneissosity in high-grade supracrustal rocks
P:	mafic, felsic volcanics (2744 Ma); greywacke; BIF
P=	primary depositional event
I =	intrusive event
D=	deformational event

Several sets of structures postdate the main foliation. In plutonic-dominated areas to the east and west of the Kogaluc – Tasiat belt, map-scale folds are evident from air photographs and ground observations. These open, upright,  $F_3$  folds of  $S_2$  foliation and layering are generally synforms with gently to moderately south-plunging axes and lack associated axial-planar foliation; corresponding antiforms are rare.

Within the Kogaluc – Tasiat belt, north-northwest-trending mylonite zones up to 25 m wide extend for several kilometres along strike. Developed in both mafic and felsic rock types, the steeply dipping brittle-ductile structures ( $D_{4a}$ ) include ultramylonite and cataclasite and are characterized by a sub-horizontal stretching lineation. Kinematic indicators including "z" folds (Fig. 12), C-S fabrics and shear bands indicate dextral transcurrent movement. A second set of brittle and brittle-ductile structures is evident as zones of east-west foliation and negative aeromagnetic anomalies. These deformation zones, up to 10 km wide, are developed in granite and have limited strike length in the map area; none appears to cross or offset the supracrustal belt. They include, from south to north the southern Kogaluc zone, Lac Pavy zone, and Lac Anuc – Lac Tasiat zone. The southern deformation zone extends eastward from Lac Canadé as a zone of moderately north-dipping shear fabrics including C-S mylonite indicating north-over-south dip-slip and dextral transcurrent components. The Lac Pavy zone extends east from Lac Tasiat and also indicates a north-over-south movement component in granitic C-S mylonites. These thrust-related structures are assigned a  $D_{4b}$  age on the basis that they appear kinematically related to the dextral transcurrent  $D_{4a}$  structures within the Kogaluc – Tasiat belt (Lin et al., 1995).

Evidence of brittle deformation in the Lac Anuc – Lac Tasiat zone is most pronounced near the western margin of the map area, where abundant pseudotachylite and cataclasite breccia (Fig. 13) are associated with chlorite-epidote alteration of granitoid host rocks. The brittle structures cleanly cut across the older ( $D_4$ ) east-west foliation and gneissosity, suggesting that a discrete  $D_5$  event occurred after  $D_4$  strain.

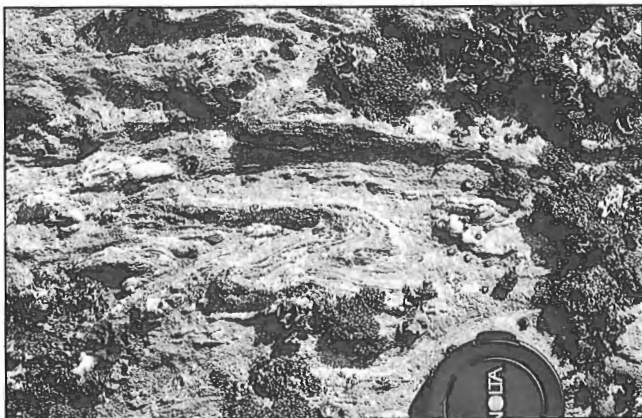


**Figure 12.** Small "z" folds in mafic schist, central Kogaluc belt. The variably plunging  $F_{4a}$  structures fold the penetrative  $S_2$  schistosity. GSC 1994-759F.

The Qalluviartuuq Lake area (Table 2) is dominated by steep, north-northwest-trending structures resulting from at least four phases of ductile deformation. The earliest ( $D_1$ ) is a foliation and migmatitic layering in supracrustal rocks of the Payne Lake belt. It may be correlative with the foliation in paragneiss enclaves in basement beneath the unconformity in the northern Qalluviartuuq belt (Winsky et al., 1995). The main penetrative foliation,  $D_2$ , defined by hornblende, plagioclase and epidote in metavolcanic rocks and by biotite in meta-sedimentary and plutonic units, dips steeply and is accompanied by a down-dip stretching lineation. The foliation trends north-northwest in the spine of the belt, and is folded by open, upright  $F_3$  folds in the arms. A strong shear fabric ( $S_4$ ) with mylonite and a gently plunging lineation defines the eastern margin of the belt over most of its length. Kinematic indicators in the fine grained mafic and granitoid mylonites, including shear bands, z folds, and C-S fabrics, indicate dextral transcurrent motion. Two sets of granitic pegmatites bracket the  $D_4$  strain: pink leucogranites are deformed whereas white peraluminous pegmatites cut the shear fabrics.

## REGIONAL CORRELATION

Broad regional correlations can be made on the basis of the similarity of lithological assemblages. In the Kogaluc River area, supracrustal rocks in the lower and high-grade zones are invariably separated by sheets of plutonic rock, but may be correlative on the basis of common lithological packages of mafic rocks, iron-formation, and clastic metasedimentary rocks although lithological proportions vary widely both across and along strike. Supracrustal belts within the eastern high-grade zone can be traced northward to the Lac Pavy deformation zone and a similar assemblage of supracrustal and plutonic rocks extends farther north to become the Payne Lake belt, although individual units are discontinuous along the 150 km of strike length represented. If these correlations are valid, the Payne Lake belt could also be ~2744 Ma, the

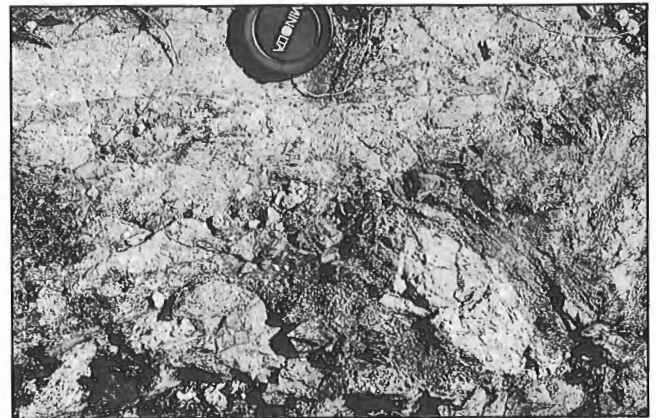


**Figure 13.** Pseudotachylite breccia in chlorite-, epidote-altered, cataclastic granite, Lac Anuc – Lac Tasiat deformation zone. These late ( $D_5$ ), brittle, east-west structures probably indicate high-level faults. GSC 1994-759E.

preliminary age available for the Kogaluc belt. Based on the presence of Archean mafic dykes in the Payne Lake belt and local unconformities in the Qalluviartuuq belt, rocks of this age could represent depositional basement to the undated Qalluviartuuq belt. Further field and geochronological work is planned to test this hypothesis.

Similarities exist among supracrustal units in the Qalluviartuuq Lake area and those in the Vizien belt, 250 km to the south (Percival et al., 1994; Skulski et al., 1994). In the Vizien belt, a relatively low-grade volcanic-sedimentary sequence, partly unconformable on dyke-riddled 2.94 Ga tonalitic basement, was complexly deformed between 2718 and 2693 Ma. Panel B of the Vizien belt, with a <2718 Ma unconformity and conglomerate overlain by tholeiitic volcanic rocks, could correspond to the unconformity-based Qalluviartuuq belt. Older (2.79, 2.78, 2.72 Ga) supracrustal rocks also occur in the Vizien belt, although in the absence of geochronology it is uncertain which, if any, of these Vizien units could correlate with the Payne Lake belt. Conglomerate, overlain by mafic volcanic rocks, occurs sporadically along the length of the Goudalie domain. In the Lac Allemand belt (Fig. 1), 150 km north of Qalluviartuuq Lake, Moorhead (1989) reported coarse tonalite-boulder conglomerate at the base of a mainly mafic volcanic succession, and a similar sequence unconformably overlying granodioritic basement to the west at Lake Inet. Detailed studies (e.g., Winsky et al., 1995) are underway to determine the age and tectonic significance of the conglomeratic units and overlying volcanic strata.

### ***Correlation of magnetic anomalies and continuity of the Goudalie domain***

A 70 km wide regional aeromagnetic negative anomaly corresponds to the Goudalie domain in the Leaf River area. It reflects the lithological contrast between weakly magnetic tonalite gneiss and supracrustal rocks and flanking magnetite-bearing plutonic rocks. The anomaly continues to the north and includes the Kogaluc – Tasiat, Payne Lake and Qalluviartuuq belts. However, tonalitic rocks are much less abundant north of the Goudalie type area. West of the Kogaluc – Tasiat belt, the western boundary of the aeromagnetic low corresponds approximately to the western limit of abundant paragneiss and to the eastern limit of orthopyroxene-bearing units. To the east are north-trending positive and negative anomalies that correspond crudely to areas underlain respectively by pyroxene-bearing plutonic units and zones containing significant amounts of supracrustal remnants. In the Qalluviartuuq – Payne Lake area, the western edge of the aeromagnetic low is locally the limit of the Payne Lake belt, however, the eastern edge occurs within granitoid rocks up to 10 km east of the belt of supracrustal rocks.

In summary, although the character of the Goudalie domain varies along strike, many lithological and structural features are common. Narrow supracrustal belts contain volcanic and sedimentary rocks, including mantle-derived units and unconformity-related conglomerates, deposited between ~2.79 and 2.72 Ga. Ancient (~3.0 Ga) tonalites are common in the Leaf River area and more potassic granitoid plutons (2.73-2.69 Ga) are widespread to the north. The

**Table 2.** Age relationships, Qalluviartuuq Lake area.

I:	pegmatite dykes
D <sub>4</sub> :	N-S dextral transcurrent high-strain zone(s); mylonite
D <sub>3</sub> :	open regional folds
I:	pegmatite pods, dykes
D <sub>2</sub> :	main penetrative N-S foliation in Qalluviartuuq belt; steep lineation; epidote-amphibolite facies metamorphism
P:	conglomerate; mafic volcanic, ultramafic, sedimentary rocks; anorthosite (Qalluviartuuq belt); associated Archean dykes in basement
P:	erosional unconformity
I:	granodiorite, pyroxenite, granite
D <sub>1</sub> :	penetrative N-S foliation in Payne Lake belt; metamorphism
P:	older supracrustals (Payne Lake belt); tonalite sheets
P= primary depositional event	
I= intrusive event	
D= deformational event	

domain is characterized by a pervasive north-south foliation and protracted deformation history, including high-strain events that are particularly well expressed in the elongate supracrustal belts. Based on evidence from the Vizien belt, Percival et al. (1994) suggested that the Goudalie domain contains a suture that separated the Lake Minto and Utsalik domains. Relationships to the north confirm a protracted deformation history including significant shear deformation. Geochronology in progress will help define the order of assembly of belts along the length of this complex margin.

### **ECONOMIC POTENTIAL**

In the Kogaluc – Tasiat belt, many small gossans were noted in association with both oxide- and silicate-facies iron-formations. These sulphide-bearing zones are rarely exposed over more than 1 m in width and a few metres in length. Similar zones occur in association with iron-formation in the higher-grade supracrustal belts to the east. Shear zones in the Kogaluc – Tasiat belt have a similar structural history to the gold-mineralized breaks of the southern Superior Province (Lin et al., 1995), raising the possibility of lode gold mineralization.

To the north, the Payne Lake belt contains numerous, mainly silicate-facies, iron-formations, some with rusty zones. Although not yet assayed, iron-formation-hosted gold mineralization is possible. Part of the Qalluviartuuq belt is characterized by coarse cordierite-anthophyllite assemblages, suggesting early magnesium alteration, subsequently metamorphosed to amphibolite facies. Similar alteration zones surround many metamorphosed massive sulphide deposits and could indicate the presence of VMS mineralization in the Qalluviartuuq belt.

## ACKNOWLEDGMENTS

We thank A. Still, L. Tulk, and P. Winsky for dedicated field assistance and some independent mapping. Efficient logistical support was provided by A. Tulugak (Povungituk), Viking Helicopters (through Polar Continental Shelf Project) and Johnny May's Air Charters. P. McKay and O. Ijewliw drafted Figure 2. Tim Kusky is thanked for stimulating discussions in the field. Access to unpublished maps, reports and data of exploration companies active in the region is gratefully acknowledged. S. Hanmer is thanked for an insightful review.

## REFERENCES

### Berman, R.G.

1991: Thermobarometry using multi-equilibrium calculations: a new technique, with petrological applications; *Canadian Mineralogist*, v. 29, p. 833-855.

### Lin, S., Percival, J.A., Winsky, P.A., Skulski, T., and Card, K.D.

1995: Structural evolution of the Vizien and Kogaluc greenstone belts in Minto block, northeastern Superior Province, northern Quebec; *in* Current Research 1995-C; Geological Survey of Canada, this volume.

### Moorhead, J.

1989: Géologie de la région du lac Chukotat (fosse de l'Ungava); Ministère de l'Énergie et des Ressources, Québec, ET87-10.

### Percival, J.A. and Card, K.D.

1992a: Vizien greenstone belt and adjacent high grade domains of the Minto block, Ungava Peninsula, Quebec; *in* Current Research, Part C; Geological Survey of Canada, Paper 92-1C, p. 69-80.

### Percival, J.A. and Card, K.D. (cont.)

1992b: Geology of the Vizien greenstone belt; Geological Survey of Canada, Open File 2495, scale 1:50 000.

1994: Geology, Lac Minto – Rivière aux Feuilles, Québec; Geological Survey of Canada, Map 1854A, scale 1:500 000.

### Percival, J.A., Mortensen, J.K., Stern, R.A., and Card, K.D.

1992: Giant granulite terranes of northeastern Superior Province: the Ashuanipi complex and Minto block; *Canadian Journal of Earth Sciences*, v. 29, p. 2287-2308.

### Percival, J.A., Card, K.D., and Mortensen, J.K.

1993: Archean unconformity in the Vizien greenstone belt, Ungava Peninsula, Quebec; *in* Current Research, Part C; Geological Survey of Canada, Paper 93-1C, p. 319-328.

### Percival, J.A., Stern, R.A., Skulski, T., Card, K.D., Mortensen, J.K., and Begin, N.J.

1994: Minto block, Superior Province: Missing link in deciphering assembly of the craton at 2.7 Ga; *Geology*, v. 22, p. 839-842.

### Skulski, T., Percival, J.A., and Stern, R.A.

1994: Oceanic allochthons in an Archean continental margin sequence, Vizien greenstone belt, northern Quebec; *in* Current Research 1994-C; Geological Survey of Canada, p. 311-320.

### Stern, R.A., Percival, J.A., and Mortensen, J.K.

1994: Geochemical evolution of the Minto block: a 2.7 Ga continental magmatic arc built on the Superior proto-craton; *Precambrian Research*, v. 65, p. 115-153.

### Stevenson, I.M.

1968: Geology of the Leaf River area; Geological Survey of Canada, Memoir 356.

### Winsky, P.A., Kusky, T.M., Percival, J.A., and Skulski, T.

1995: Archean unconformity in the Qalluivartuq greenstone belt, Goudalie domain, northern Quebec; *in* Current Research 1995-C; Geological Survey of Canada, this volume.

Geological Survey of Canada Project 89009

# Polymetallic unconformity-related uranium veins in lower Proterozoic Amer Group, Pelly Lake map area, northern Thelon Basin, Churchill Province, Northwest Territories

A.R. Miller

Mineral Resources Division

*Miller, A.R., 1995: Polymetallic unconformity-related uranium veins in lower Proterozoic Amer Group, Pelly Lake map area, northern Thelon Basin, Churchill Province, Northwest Territories; in Current Research 1995-C; Geological Survey of Canada, p. 151-161.*

---

**Abstract:** In the Garry Lake area, the northern margin of the 1.72 Ga Thelon Basin overlies the lower Proterozoic Amer Group, and Archean gneisses and plutonic rocks. Northeast- to north-northeast- and northwest-striking faults record post-Thelon Formation displacement. A uranium-bearing boulder train was located near the erosional edge of the Thelon Basin. Polymetallic calcite-bearing veins containing native silver-altaite-clausthalite-pitchblende, are hosted by lower greenschist grade arkosic wacke belonging to the upper Amer Group clastic sedimentary sequence. Based on the polymetallic elemental signature in the veins, thin argillic alteration envelopes mantling crack-and-fill veins, and calcite as the principal gangue mineral in veins, this occurrence resembles the clay-bounded subtype of unconformity-related uranium deposits. Recognition of this subdeposit type in the northern Thelon Basin extends its known areal distribution and signals this segment of the basin to be prospective for unconformity-related uranium deposits.

**Résumé :** Dans la région du lac Garry, la marge nord du bassin de Thelon (1,72 Ga) surmonte le Groupe d'Amer du Protérozoïque inférieur et des gneiss et des plutonites de l'Archéen. Des failles à direction nord-est à nord-nord-est et à direction nord-ouest témoignent d'un déplacement postérieur à l'accumulation de la Formation de Thelon. Une traînée de blocs uranifères a été localisée près de la marge d'érosion du bassin de Thelon. Des veines de calcite polymétalliques contenant argent natif-altaïte-clausthalite-pechblende sont contenues dans un grauwaacke arkosique du faciès des schistes verts inférieur appartenant à la séquence sédimentaire clastique de la partie supérieure du Groupe d'Amer. En raison de la signature polymétallique élémentaire observée dans les veines, des minces enveloppes d'altération argillique couvrant les veines de fissure et de remplissage et de la présence de calcite comme principal minéral de gangue dans les veines, cette occurrence s'apparente au sous-type, limité par de l'argile, des gisements d'uranium associés à une discordance. La découverte de ce type de sous-gisement dans la partie nord du bassin de Thelon augmente son aire de distribution connue et indique que ce segment du bassin contient peut-être des gisements d'uranium associés à une discordance.



## **INTRODUCTION**

Erosional remnants of two areally extensive, unmetamorphosed siliciclastic basins, Athabasca and Thelon basins, having similar ages circa 1.72 - 1.7 Ga (Cumming et al., 1987; Miller et al., 1989) are preserved in the southwestern and central Churchill Province respectively. Even though these basins are separated by approximately 300 km, striking similarities such as the position of each basin with respect to a Proterozoic orogen and crustal-scale mylonite zones, timing of crustal stabilization, creation and geochemical signature of pre-basin paleosols, the succession from widespread siliciclastic into carbonate sedimentation and sedimentation characterized by fining upward sequences, have led to numerous comparisons and regional correlations. (Donaldson, 1967, 1969; Curtis and Miller, 1980; Miller and LeCheminant, 1985).

These regional lithostratigraphic correlations coupled with similar uranium metallogeny suggest that both isolated basins can be viewed as a single and the youngest metallogene in the Churchill Province. In particular, the discovery of unconformity-related uranium deposits adjacent to the eastern margin of the Thelon basin – Kiggavik (Lone Gull) deposit (Fuchs et al., 1986; Miller and LeCheminant, 1985) and the Boomerang prospect beneath the southwestern portion of the basin (Davidson and Gandhi, 1989) – have analogs in the uranium-rich Athabasca Basin.

This research is part of ongoing regional uranium metallogenetic studies that focus on the three Proterozoic basins of the central Churchill Province, north of 60°. This report presents petrographic and mineralogical data with electron microprobe analyses of unconformity-related uranium mineralization from the northern margin of the Thelon Basin (Fig. 1). Host rock composition, metamorphic grade and structural style displayed in mineralized specimens are discussed in light of the regional geology of lower Proterozoic sedimentary basins, tectonics, classification of this unconformity-related occurrence and uranium metallogeny of the Thelon Basin.

## **EXPLORATION HISTORY**

Encouraged by discoveries in the early 1970s of significant unconformity-related uranium deposits in the southwestern and northeastern Thelon Basin, numerous companies focused their uranium exploration activities to the northeastern and northern Thelon basin and immediately adjacent basement during the late 1970s and early 1980s (Brophy et al., 1985). Because elements of both Thelon and basement regional geology appeared to be similar to the southeastern margin of the Athabasca Basin, the exploration model at that time was the "Key Lake" deposit type. The critical characteristics of this model were polydeformed lower Proterozoic supracrustal belts with infolded Archean basement, lower Proterozoic graphitic metasedimentary rocks and post-sandstone fault zones.

In the northern Thelon Basin, the scarcity of outcrops due to widespread Pleistocene deposits necessitated boulder train prospecting complemented with a wide array of geochemical and ground and airborne geophysical surveys. These techniques led to the discovery of several uranium-bearing boulder trains. One of those trains, termed the Garry Lake boulder train, was found by Kidd Creek Mines Ltd., later Falconbridge Ltd. The Garry Lake boulder train is narrow and associated with a soil geochemical anomaly that was traced for 3 km (Brophy et al., 1985; Jewett et al., 1983; Jewett and Duncan, 1983). This report is based on and up-dated from an unpublished research document written by the author and submitted to Kidd Creek Mines Ltd. in March 1983, at which time they held claim to the area being discussed. The claims have since lapsed.

## **REGIONAL GEOLOGY**

The basement adjacent to the northeastern and northern margin of the Thelon Basin comprises three northeast-trending synclinoria which consist of lower Proterozoic Amer Group metasedimentary rocks. These metasedimentary rocks have been infolded with and faulted against an Archean gneissic and plutonic complex (Tella, 1994). The geology in the area south of Garry Lake and the location of the Garry Lake boulder train are represented in Figure 1.

Immediately south of lower Garry Lake (NTS 66F/9), Tella et al., (1984) outlined a poorly exposed narrow northeast-trending syncline that has an exposed strike length of approximately 14 km. The syncline is bounded to the northwest by the Garry Lake complex, an Archean gneiss complex dominated by quartz-feldspar-biotite gneiss and porphyroblastic K-feldspar augen gneiss. Southeast of the syncline is Archean massive to well foliated granite.

The stratigraphic column in the Garry Lake Syncline lacks the relatively thin transitional clastic sequence that is present in the Amer Group synclinorium to the southeast (Tella et al., 1983, 1984). White orthoquartzite, base of the Amer Group, is exposed in one locality on the southwestern limb of the syncline and was intersected in drill core on the northwestern limb of the syncline (Jewett et al., 1983). The dominant lithological unit in the Garry Lake Syncline belongs to the upper Amer Group. Arkosic wacke and calcareous arkose are the most abundant rocks and are interbedded with siltstone-graphitic slate-mudstone.

An airborne VLF survey identified weak conductors within the upper Amer Group strata (Lechow, 1982). The geophysical signature of these conductors has been interpreted to be graphite in slate interbeds within the lower sections of the upper Amer Group sequence (Lechow, 1982; Jewett and Zang, 1982). The trace of these conductors shown in Figure 1 outlines the approximate margin of the Garry Lake syncline, south of Garry Lake. Closure of conductive strata towards the northeast and southwest suggests that the syncline is doubly plunging.

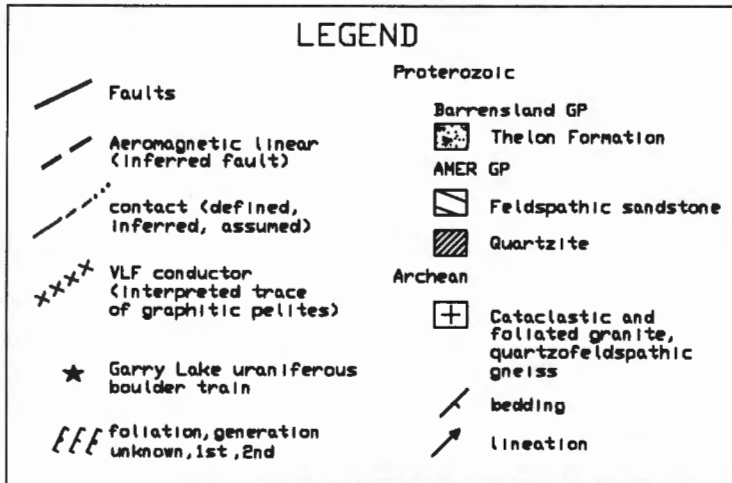
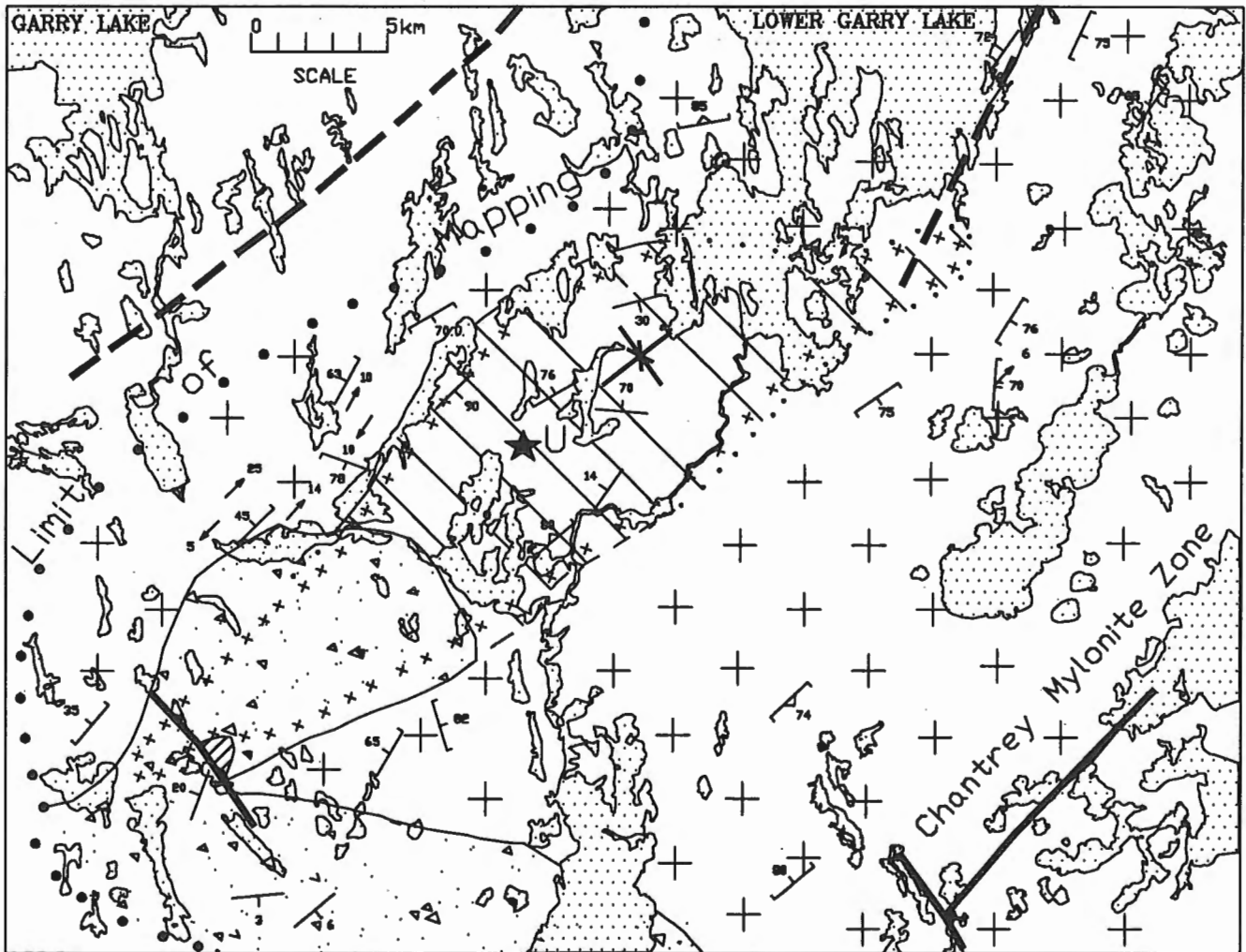


*Figure 1.*

*Geology of the northern Thelon Basin (from Tella, 1994), location of the Garry Lake uranium boulder train (from Jewett et al., 1983) and trace of geophysical conductors (from Lechow, 1982).*



Pebbly sandstone with minor interbedded conglomerate of the Thelon Formation, Barrenland Group, Dubawnt Supergroup (Gall et al., 1992), overlie Amer Group meta-sedimentary rocks in the Garry Lake Syncline. Based on the geometry of the conductive strata shown in Figure 1, approximately 40 per cent of the Garry Lake Syncline lies beneath the Thelon sandstone.

Two regional structural elements, both displaying post-Thelon Formation movement are present throughout the northern and northeastern portions of the Thelon Basin (Tella, 1994). Their presence in the Garry Lake area are important criteria in evaluating and prioritizing areas for the presence of unconformity-related uranium mineralization. Regionally, the Garry Lake area lies within a faulted domain between the uplifted high-grade gneissic terrane of the Queen Maud block to the west and a block to the southeast that has preserved in it lower and middle Proterozoic supracrustal sedimentary rocks. This tectonic zone is characterized by parallel northeast-to north-northeast-striking aeromagnetic linears which have been identified as mylonite zones (Geological Survey of Canada, 1982; Tella, 1994). The Garry Lake Syncline is located between two of these structures, the Chantrey mylonite zone to the southeast and a unnamed aeromagnetic linear to the northwest (Fig. 1). Weak northeast-trending VLF conductors within the Garry Lake syncline are interpreted as fault-fracture zones (Jewett et al., 1983; Jewett and Duncan, 1983) and probably related to this regional structural fabric. A northwest-trending brittle fault set, possibly not as well developed as the former system, displaces Thelon Formation sandstone against Archean and Proterozoic strata.

### **PETROGRAPHY OF UNMINERALIZED HOST ROCK**

Unmineralized host rocks in the vicinity of the Garry Lake boulder train are red to red-maroon calcareous lithic arkosic wacke. This sandstone is medium grained, well sorted with both framework grains and lithic clasts ranging in size from 0.3 to 0.5 mm. Feldspars constitute approximately 25-30 per cent of the framework grains with a ratio of plagioclase ( $An_{1-2}$ ) to microcline equal to 3:1. Quartz, feldspars and lithic clasts are commonly subangular to subrounded with a minor, proportion of rounded framework grains. The wacke is clast supported; interclast volumes are filled by very fine grained intergrowth of hydromuscovite and clinocllore, minor carbonate and hematite. Accessory detrital phases include muscovite, zircon, tourmaline, apatite, magnetite, and ilmenite.

Hematite, present as sparsely disseminated ultra-fine grains, <0.05 mm, is variably coalesced into aggregates as large as 0.15 mm. Hematite is distributed unevenly throughout the phyllosilicate-rich matrix. Hematite partially mantles detrital quartz and feldspar, and is disseminated through matrix phyllosilicates. These textures suggest that a portion of this iron oxide is a diagenetic cement. Aggregates of hematite locally follow the foliation; this texture is similar to phyllosilicate-hematite textures associated with 1.72 Ga paleosol formation and diagenesis (Albert, 1984; Miller et al., 1992). Consequently it is probable that some of the hematite

infiltrated into paleoweathered material and/or was remobilized by paleoweathering processes. The northeastern segment of the Garry Lake Syncline must lie at or near the exhumed sub-Thelon paleosurface considering the proximity of the Thelon Formation.

Metasedimentary rocks have a weak penetrative fabric defined by the alignment of very fine intergrowths of hydromuscovite-clinocllore and to a lesser extent the alignment of framework quartz and feldspars. Selected analyses of these host-rock phyllosilicates are represented in Table 2. The very fine grained intergrowth of these phases is represented by chlorite analyses having greater than 1 wt.%  $K_2O$ . A metamorphic grade of lower greenschist, chlorite grade, is established based on this stable assemblage and is in agreement with the regional gradient, lower to subgreenschist facies, along the southwestern margin of the exposed Amer synclinorium (Tella et al., 1983, 1984).

### **PETROGRAPHY AND MINERALOGY OF URANIUM-BEARING ARKOSIC WACKE**

Five fractured and uranium-bearing samples were examined from the Garry Lake boulder train; the results are summarized in Table 1. Fine grained pitchblende with lead selenide and trace amounts of lead telluride, native silver and a copper-arsenic-sulphur phase partially filling micro- and macrofractures, some fractures are as wide as 2-3 mm. Trace amounts of an ultra fine grained uranium-bearing phase is present in pitchblende-veined Amer sandstones. Electron microprobe energy dispersive spectra show that this phase contains the elements titanium-uranium or silicon-titanium-uranium. It is assumed to be a brannerite-like compound. Canary yellow secondary uranium phases pseudomorph pitchblende and fill microfractures.

Uranium-bearing fractures are discordant to the metamorphic fabric. Macroscopic pitchblende-bearing fractures are locally associated with a close-spaced fracture cleavage in wall-rock quartz and feldspar (Fig. 2, 3). Grain-size reduction associated with microfracturing was noted in only one sample, GL-82-11, but this texture is minor. The abundance of micro- and macroscopic open-space filling textures and fracture cleavage suggest that mineralization is coeval with brittle deformation. Bleached envelopes are present adjacent to some pitchblende-bearing veins. These envelopes are light pink, 1-2 mm wide, discontinuous and are similar to the subtle reaction envelopes adjacent to unconformity-related mineralization in the Baker Lake Basin (Miller, 1980, Plate 2).

The intensity of hydrothermal alteration in the host rock is very low to non-existent in spite of abundant pitchblende-filled fractures (Fig. 2). The lack of illite replacement of framework plagioclase grains in the host rock indicates negligible pervasive host rock alteration. However, framework feldspar in the wallrock immediately adjacent to pitchblende-bearing fractures has been completely degraded to very fine grained hydromuscovite (Table 2). The subtle colour variations recognized in hand specimens correspond to such alteration envelopes.

Table 1. Mineral assemblage summary, Garry Lake boulder train.

Sample	Host rock	Formation	Diagnostic metamorphic assemblage	Host rock alteration	Ore mineralogy	Gangue mineralogy	Control on mineralization	Type of mineralization	Secondary uranium minerals
GL-82-1	sericitic arkosic wacke	upper Amer Group	hydromuscovite, clinocllore, calcite	increased hydro-muscovite content adjacent to carbonate-bearing fractures	none in section	coarse-grained calcite filled fractures	fractures	—	uranophane $\text{Ca}(\text{UO}_2)_2[\text{SiO}_3(\text{OH})]_2 \cdot 5\text{H}_2\text{O}$
GL-82-4	sericitic arkosic wacke	upper Amer Group	hydromuscovite, clinocllore, calcite	increased hydro-muscovite content adjacent to carbonate- and pitchblende-bearing fractures	<b>Vein filling:</b> Banded pitchblende claustralite, altaite, native silver; sooty pitchblende, a Cu-As-S phase, trace coffinite, silica-bearing Ti-U phase (brannerite?)	coarse-grained calcite fills the centre of pitchblende-lined fractures; coarse-grained calcite filled fractures; uranium-bearing calcite; trace Mg-bearing calcite	fractures	unconformity-related	beta-uranophane
GL-82-7	sericitic arkosic wacke	upper Amer Group	hydromuscovite, clinocllore, calcite	increased hydro-muscovite content adjacent to carbonate- and pitchblende-bearing fractures	<b>Vein filling:</b> pitchblende, claustralite Stage 2: Ti-U phase (brannerite?)	calcite interstitial to colloform pitchblende	fractures	unconformity-related	uranophane
GL-82-11	sericitic arkosic wacke	upper Amer Group	hydromuscovite, clinocllore, calcite	hydromuscovite veinlets with claustralite grains up to 0.35mm	<b>Vein filling:</b> claustralite	coarse-grained calcite veins; well developed fracture cleavage; very minor grain size reduction in fractures	uranophane in fractures	unconformity-related	uranophane
GL-82-19	sericitic arkosic wacke	upper Amer Group	hydromuscovite, clinocllore, calcite	increased hydro-muscovite content adjacent to carbonate- and pitchblende-bearing fractures	<b>Vein filling:</b> banded pitchblende, claustralite, native silver, uranium-bearing calcite	coarse-grained calcite veins; calcite brecciates pitchblende	fractures	unconformity-related	uranophane, an amorphous uranium-bearing phase

**Table 2.** Selected electron microprobe analyses of hydromuscovite and clinocllore.

<b>CHLORITE</b>						
SAMPLE	GL-82-1	GL-82-1	GL-82-1	GL-82-11	GL-82-11	GL-82-19
SiO <sub>2</sub>	27.95	35.78	29.84	31.20	28.89	31.37
Al <sub>2</sub> O <sub>3</sub>	21.76	24.75	21.56	23.27	21.71	20.46
TiO <sub>2</sub>	0.00	0.12	0.10	0.04	0.05	0.00
Cr <sub>2</sub> O <sub>3</sub>	0.02	0.05	0.03	0.02	0.00	0.02
FeO	12.64	8.96	11.41	10.29	12.44	10.98
MNO	0.19	0.19	0.25	0.23	0.21	0.29
MGO	22.78	14.07	22.06	19.96	22.76	22.62
CAO	0.08	0.03	0.03	0.03	0.02	0.05
NA <sub>2</sub> O	0.05	0.07	0.04	0.04	0.05	0.03
K <sub>2</sub> O	0.46	4.78	1.11	2.01	0.65	0.58
TOTAL	85.93	88.80	86.43	87.09	86.78	86.40
Formula based on 28 oxygen						
Si	5.609	6.800	5.908	6.086	5.728	6.162
Al	2.391	1.200	2.092	1.914	2.272	1.838
Total	8.000	8.000	8.000	8.000	8.000	8.000
Al	2.757	4.344	2.940	3.436	2.801	2.900
Ti	0.000	0.018	0.015	0.005	0.007	0.000
Cr	0.003	0.007	0.005	0.003	0.000	0.002
Fe	2.121	1.424	1.889	1.679	2.062	1.804
Mn	0.032	0.030	0.042	0.039	0.035	0.048
Mg	6.815	3.986	6.513	5.804	6.728	6.624
Ca	0.016	0.006	0.007	0.007	0.005	0.010
Na	0.021	0.025	0.015	0.015	0.020	0.010
K	0.119	1.160	0.279	0.500	0.164	0.146
Total	11.884	11.000	11.705	11.488	11.822	11.544
<b>HYDROMUSCOVITE</b>						
SAMPLE	GL-82-1	GL-82-4	GL-82-7	GL-82-11	GL-82-19	GL-82-19
SiO <sub>2</sub>	45.71	45.61	46.50	46.83	45.42	45.61
Al <sub>2</sub> O <sub>3</sub>	31.48	27.99	29.00	29.06	28.66	29.56
TiO <sub>2</sub>	0.18	0.20	0.11	0.31	0.30	0.29
Cr <sub>2</sub> O <sub>3</sub>	0.01	0.03	0.05	0.03	0.05	0.00
FeO	2.42	4.69	3.96	3.91	4.49	4.41
MNO	0.00	0.06	0.01	0.00	0.01	0.04
MGO	1.49	2.97	2.36	2.27	2.68	1.97
CAO	0.04	0.08	0.03	0.06	0.08	0.00
BAO	0.00	0.00	0.00	0.00	0.00	0.00
NA <sub>2</sub> O	0.28	0.20	0.15	0.16	0.22	0.18
K <sub>2</sub> O	10.21	10.22	10.84	10.85	10.08	10.80
TOTAL	91.82	92.05	93.01	93.48	91.99	92.86
Formula based on 22 oxygen						
Si	6.348	6.423	6.458	6.467	6.385	6.364
Al	1.652	1.577	1.542	1.533	1.615	1.636
Ti	0.000	0.000	0.000	0.000	0.000	0.000
Total	8.000	8.000	8.000	8.000	8.000	8.000
Al	3.500	3.069	3.204	3.197	3.134	3.227
Ti	0.018	0.021	0.011	0.032	0.032	0.031
Cr	0.001	0.003	0.006	0.003	0.005	0.000
Fe	0.281	0.552	0.460	0.452	0.527	0.515
Mn	0.000	0.007	0.001	0.000	0.002	0.004
Mg	0.308	0.624	0.489	0.466	0.562	0.410
Total	4.108	4.276	4.171	4.150	4.262	4.187
Ca	0.005	0.011	0.005	0.008	0.012	0.000
Ba	0.000	0.000	0.000	0.000	0.000	0.000
Na	0.076	0.054	0.039	0.042	0.059	0.050
K	1.809	1.835	1.920	1.911	1.808	1.923
Total	1.890	1.900	1.964	1.961	1.879	1.973

### Uranium minerals and associated metallic phases

Two textural forms of pitchblende fill fractures. Colloform pitchblende, the more common, is present as crusts on fracture walls; in some fractures opposing bands are coalesced to form massive pitchblende filled fractures (Fig. 4). Calcite and minor very fine grained sooty pitchblende are present only within the central portions of pitchblende-lined veins. Both varieties exhibit polygonal and radial cracks. This texture is due to dehydration and is in agreement with low analytical totals on pitchblende that indicate variable structurally bound water (Table 3). Preservation of microbanding in pitchblende, undeformed contacts between banded pitchblende and weak hydrothermally altered wallrock, and coarse grained unstrained gangue minerals record the absence of any penetrative tectonic overprint.

The oxides of lead and calcium vary from core to rim within individual pitchblende polyhedra (Table 3). These variations are consistent with the associated gangue mineral, calcite, and the inferred paragenetic sequence. Uniform CaO abundances in pitchblende indicate calcium substitution for uranium which is consistent with calcite-pitchblende textures that indicate carbonate precipitation was pre-, syn- and post-colloform pitchblende. Paired analyses of pitchblende record a variable but generally increased PbO content toward the outer margin of a polyhedron. This cryptic variation coupled with lead selenide and telluride in late stage calcite suggests an evolution from uranium to lead-bearing phases from the hydrothermal fluid.

The distribution of rare earth elements (REEs) in particular Ce, La, Sm, Nd and Gd, is uniform across individual polyhedra. The highly variable fluorine distribution within and between grains is real but the analytical-mineralogical-chemical significance of this distribution is unresolved. Vast resources of phosphorus, primarily in fluorapatite, were captured as an early diagenetic cement in the Thelon sandstone (Miller, 1983; Miller et al., 1989). Fluorapatite textures, U-Pb geochronology and the presence of anomalous phosphorus in unconformity-related deposit attests to the mobility of phosphorus during protracted diagenesis and ore-forming events (Binns et al., 1980; Miller, unpublished report, 1981; Pagel and Ruhlmann, 1985, Tables 1 and 2; Ruhlmann, 1985, Table 4). Could fluorine have been scavenged from diagenetic cements by a basinal brine that migrated in response to post-sandstone tectonism?

The accessory and diagnostic metallic assemblage accompanying pitchblende include clausthalite, altaite and native silver. Abundant clausthalite and minor altaite, both having a grain size between 10-80  $\mu\text{m}$ , characteristically are present in calcite-filled syneresis cracks in botryoidal pitchblende and in calcite which has filled the central portions of veins lined by colloform pitchblende (Fig. 5). Minute grains, <20  $\mu\text{m}$ , of native silver are hosted in calcite and adjacent to sooty pitchblende in the central portions of calcite-filled veins (Fig. 6). In one sample, an unidentified phase having an energy dispersive spectra of Cu-As with minor S, is associated with sooty pitchblende and coffinite.

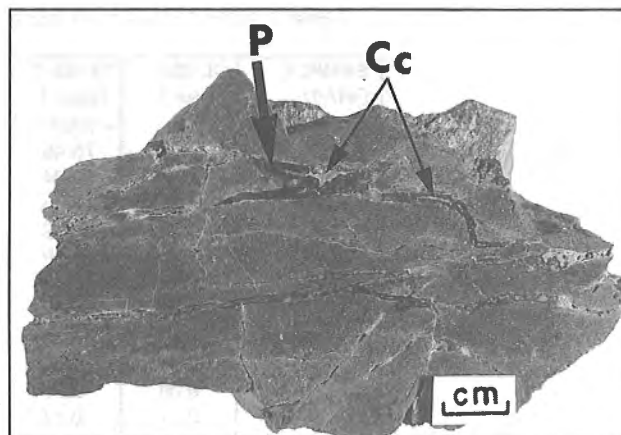


**Figure 2.** Photograph of highly fractured radioactive boulder, GL-82-7. Pitchblende (P) coats fracture walls and the centres of veins are filled with calcite (Cc).

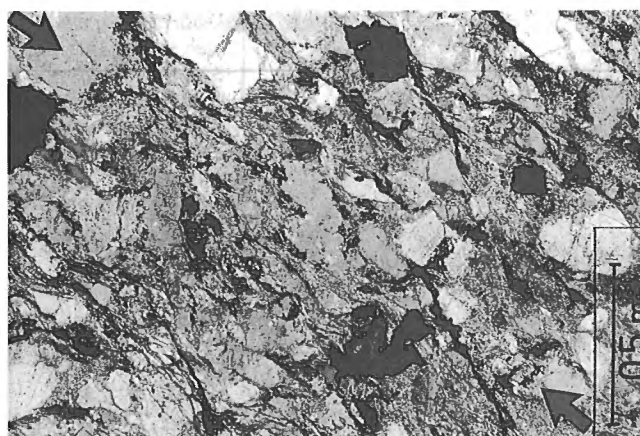


**Figure 3.** Photomicrograph of close-spaced fracture cleavage (marked by arrows) in framework quartz and feldspar, sample GL-82-19.

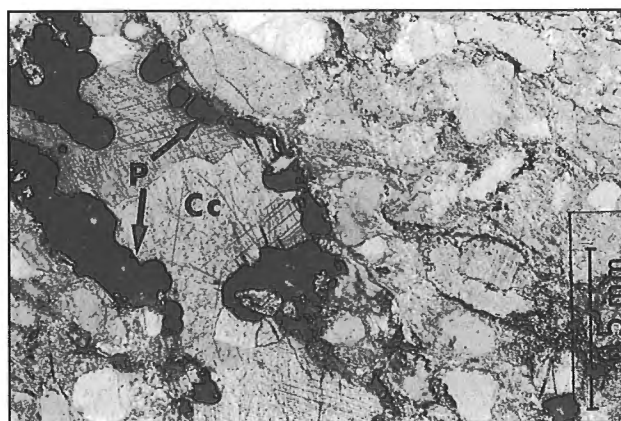


**Figure 4.** Photomicrograph, transmitted light, of mineralized vein containing undeformed colloform pitchblende (P) lining fracture walls and the centre of the vein filled by undeformed coarse grained calcite (Cc), sample GL-82-7.

**Table 3.** Selected electron microprobe analyses of pitchblende.

<b>SAMPLE</b>	<b>GL-82-7</b>	<b>GL-82-7</b>	<b>GL-82-7</b>	<b>GL-82-7</b>	<b>GL-82-19</b>	<b>GL-82-19</b>
<b>GRAIN</b>	Grain 1	Grain 1	Grain 2	Grain 2	Grain 10	Grain 10
	centre	edge	centre	edge	centre	edge
UO <sub>2</sub>	77.46	75.46	81.32	79.69	80.41	80.58
PbO	8.16	10.24	6.15	5.89	7.89	7.15
CaO	6.04	6.06	5.31	5.28	6.77	6.83
SiO <sub>2</sub>	1.04	1.08	1.50	1.39	1.10	1.15
ThO <sub>2</sub>	0.04	0.02	0.07	0.00	0.00	0.12
La <sub>2</sub> O <sub>3</sub>	0.13	0.02	0.11	0.04	0.04	0.07
Ce <sub>2</sub> O <sub>3</sub>	0.66	0.42	0.99	0.93	0.39	0.25
Nd <sub>2</sub> O <sub>3</sub>	0.40	0.30	0.43	0.39	0.20	0.25
P <sub>2</sub> O <sub>5</sub>	0.06	0.09	0.06	0.08	0.09	0.00
Sm <sub>2</sub> O <sub>3</sub>	0.06	0.07	0.13	0.13	0.00	0.06
Y <sub>2</sub> O <sub>3</sub>	0.17	0.17	0.14	0.19	0.11	0.10
Pr <sub>2</sub> O <sub>3</sub>	0.00	0.03	0.20	0.04	0.01	0.00
Eu <sub>2</sub> O <sub>3</sub>	0.08	0.22	0.10	0.02	0.00	0.12
Gd <sub>2</sub> O <sub>3</sub>	0.06	0.14	0.05	0.12	0.01	0.12
Dy <sub>2</sub> O <sub>3</sub>	0.07	0.00	0.14	0.16	0.11	0.19
F	0.35	0.39	0.18	0.20	1.25	0.51
TOTAL	94.78	97.71	96.88	94.52	98.38	97.49
<b>SAMPLE</b>	<b>GL-82-19</b>	<b>GL-82-19</b>	<b>GL-82-19</b>	<b>GL-82-19</b>	<b>GL-82-19</b>	<b>GL-82-19</b>
<b>GRAIN</b>	Grain 11	Grain 11	Grain 12	Grain 12	Grain 13	Grain 13
	centre	edge	centre	edge	centre	edge
UO <sub>2</sub>	81.20	79.96	79.05	78.93	81.23	78.32
PbO	7.51	8.97	8.23	9.34	7.90	9.99
CaO	6.74	6.42	6.49	6.55	6.61	6.12
SiO <sub>2</sub>	1.42	1.22	1.20	1.17	1.36	1.01
ThO <sub>2</sub>	0.00	0.07	0.07	0.10	0.06	0.02
La <sub>2</sub> O <sub>3</sub>	0.07	0.10	0.06	0.10	0.17	0.07
Ce <sub>2</sub> O <sub>3</sub>	0.27	0.33	0.37	0.31	0.30	0.29
Nd <sub>2</sub> O <sub>3</sub>	0.11	0.16	0.22	0.18	0.21	0.13
P <sub>2</sub> O <sub>5</sub>	0.05	0.00	0.05	0.05	0.08	0.00
Sm <sub>2</sub> O <sub>3</sub>	0.12	0.05	0.01	0.08	0.00	0.26
Y <sub>2</sub> O <sub>3</sub>	0.13	0.05	0.18	0.15	0.15	0.13
Pr <sub>2</sub> O <sub>3</sub>	0.18	0.01	0.15	0.00	0.12	0.06
Eu <sub>2</sub> O <sub>3</sub>	0.13	0.17	0.18	0.00	0.24	0.15
Gd <sub>2</sub> O <sub>3</sub>	0.03	0.12	0.16	0.08	0.10	0.10
Dy <sub>2</sub> O <sub>3</sub>	0.10	0.21	0.00	0.09	0.09	0.00
F	0.00	0.96	1.57	1.54	0.00	0.33
TOTAL	98.05	98.79	97.99	98.65	98.60	97.00

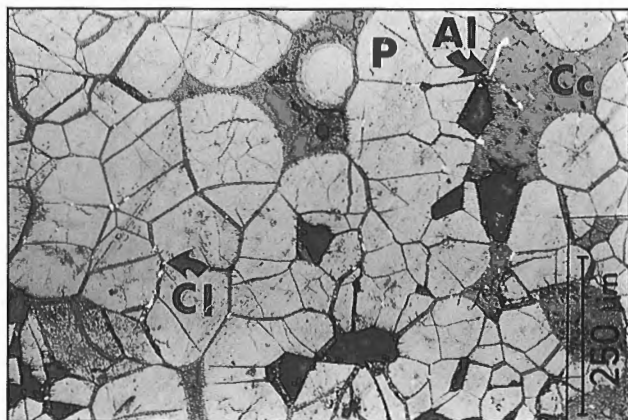


**Figure 5.** Photomicrograph, reflected light, of botryoidal pitchblende (P) with disseminated clauthalite (Cl) and altaite (Al). Selenide and telluride minerals are present in calcite-filled syneresis cracks and in matrix calcite (Cc), sample GL-82-4.

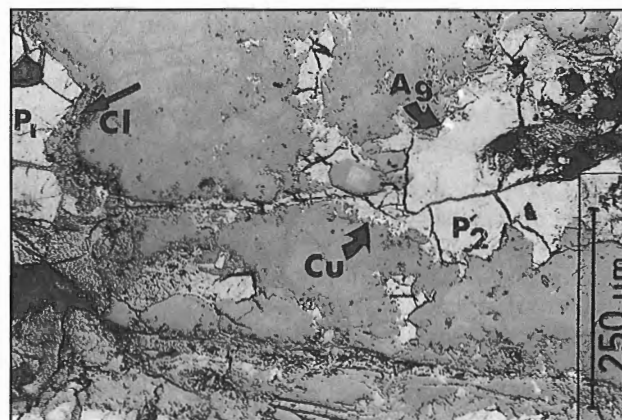


**Figure 6.** Photomicrograph, reflected light, of sooty pitchblende (P2) with accessory clauthalite (Cl), native silver (Ag) and Cu-As-S phase (Cu). Botryoidal pitchblende (P1) on left side of photograph, sample GL-84-4.

## Calcite

Excluding the thin hydromuscovite-bearing alteration envelopes adjacent to pitchblende-bearing veins, coarse grained unstrained calcite is the diagnostic and only hydrothermal non-metallic gangue mineral associated with the preceding metallic assemblages (Fig. 4). The composition of this carbonate is pure end-member calcite. Two carbonates were identified in only one specimen, GL-82-4 and that included pure end member calcite with very fine grained intergrowths of magnesium-bearing calcite.

Two generations of calcite veins were recognized based on calcite vein geometry and calcite-pitchblende textures. Calcite commonly occupies the central portions of veins which contain symmetrical crusts of colloform and botryoidal pitchblende adhering to vein walls (Fig. 4, 7). This variety of calcite is characterized by a dusty or clouded appearance in transmitted light and can brecciate colloform pitchblende (Fig. 8). The distribution of this calcite type within any vein is highly variable and controlled by vein width and thickness of colloform pitchblende bands on opposing sides of the vein. Second generation calcite is commonly clear and colourless in transmitted light, contains angular fragments of colloform pitchblende and occurs adjacent to earlier calcite-pitchblende veins (Fig. 7, 8). The above geometrical and textural descriptions suggest crack and fill type veins.

The energy dispersive spectra on calcite within the central portions of pitchblende-bearing veins indicate that uranium is present in calcite. Fine grained pitchblende was not observed in the calcite. It is possible that "invisible pitchblende", probably sooty pitchblende as in GL-82-7, may be present in calcite. Since calcium has substituted for uranium in colloform pitchblende (Table 3), the reverse substitution appears plausible considering calcite is paragenetically syn- and post-colloform pitchblende.

## METALLOGENETIC SIGNIFICANCE

One unique feature of the central portion of the Churchill Province, Northwest Territories is the preservation of three overlapping Proterozoic sediment-dominated supracrustal sequences that span the interval from approximately 2.45 to 1.7 Ga. Even though these three supracrustal sequences, represented by the Amer and Hurwitz groups, Baker Lake and Wharton groups and the Barrenland Group, record markedly different sedimentology, tectonics and magmatism, they are linked together by a common metallogenic theme - formation of the central Churchill Proterozoic uranium province. Each of these time-lithostratigraphic sequences in the central Churchill Province is host to a distinctive uranium deposit type or types (Curtis and Miller, 1980; Miller and LeCheminant, 1985).

On a regional perspective, the overlap of commonly two and rarely three of these supracrustal sequences implies that uranium deposit types should and do overlap. The following uranium deposit types are recognized in the area of the northeastern Thelon basin: stratabound and stratiform uranium in the Amer Group, Beaverlodge-type structurally

controlled uranium in ductile fault zones and unconformity-related in the Archean basement and cover sandstone. Therefore in the central Churchill uranium province, imbrication of these uranium deposit types in space and time is of considerable importance. This overlapping dictates that each occurrence be analyzed to ascertain the type and whether superposition of uranium events is present. The above mineralogical and structural features displayed by the Garry Lake samples are typical of unconformity-related mineralization (Miller, 1980; Curtis and Miller 1980).

Dahlkamp (1991) subdivided Proterozoic unconformity-related uranium deposits into two classes: fracture-bound deposits and clay-bound deposits. This classification is based on the position with respect to the unconformity, host rock, metallic signature, paragenesis and ore grade. The two

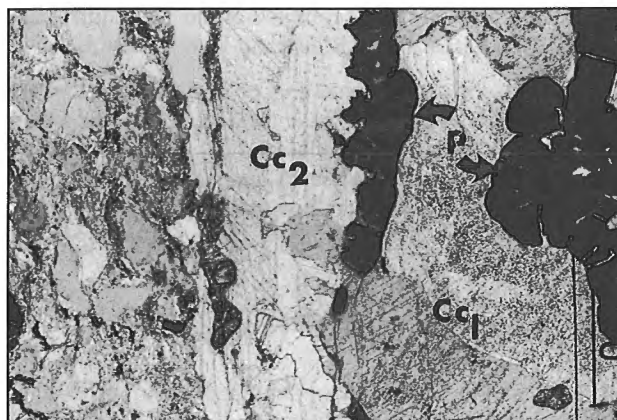


*Figure 7. Photomicrograph, transmitted light, of mineralized vein containing undeformed colloform pitchblende (P) filled with dusty calcite (Cc1). A second generation crack-and-fill vein represented by colourless calcite (Cc2) invaded along the vein/wallrock interface and brecciated colloform pitchblende, sample GL-82-7.*

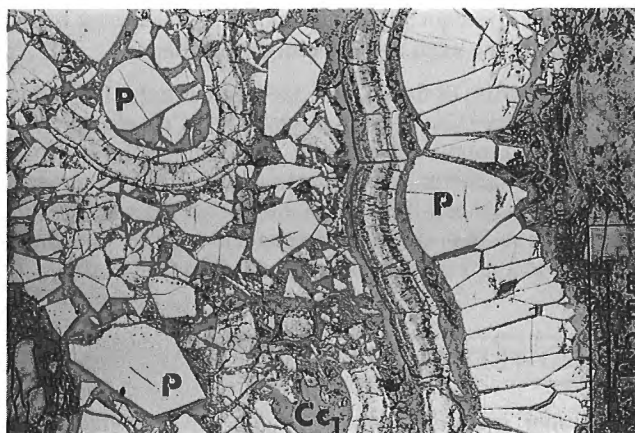


*Figure 8. Photomicrograph, reflected light, brecciated colloform pitchblende (P) in dusty calcite (Cc1), sample GL-82-19.*



unconformity-related deposits with the Thelon Basin are representative of the two categories: Kiggavik and satellite deposits are of the fracture-bound subtype and the Boomerang prospect of the clay-bound subtype.

The Kiggavik and satellite deposits are hosted entirely within the basement near the faulted margin of the north-eastern Thelon Basin and are classified as fracture-bound subtype. Basement lithologies that host uranium include ortho-quartzite-pelite-metagreywacke belonging to the 2796 to 2752 Ma Woodburn Lake Group, early Proterozoic fluorite-bearing granite complex and Archean gneisses (Roddick et al., 1992; Wollenberg, 1991). The intersection and reactivation of both Archean and Proterozoic brittle and ductile fault systems control the geometry of alteration envelopes and monomineralic ore zones (Miller, 1981, unpublished report to Urangescellschaft Canada Ltd., Lone Gill Uranium Deposit, 150 p.). Aspects of the regional and local geology of the Kiggavik deposit draw a comparison to the Cluff Lake deposits, Athabasca Basin (Blaise and Koning, 1985).

The gold-uranium Boomerang prospect belongs to the clay-bound category (Davidson and Gandhi, 1989) as are the U-Se-Cu-Ag-Au occurrences hosted in various basement units near the erosional margin of the eastern Thelon Basin (Miller, 1980; Miller and LeCheminant, 1985; Miller et al., 1986).

## SUMMARY

Attributes of the Garry Lake pitchblende-bearing boulders integrated with the regional geology indicate this mineralization is of the clay-bounded subcategory. There has not been a superposition of uranium deposit types. The potential for this subdeposit type is areally more extensive than previously known. The boulder train hosted by lower greenschist Aphebian metasedimentary rocks is located only 5 km northeast of the Thelon unconformity and must be near or within the paleoweathered zone. The presence of graphitic pelite in the Amer sequence represents a structurally incompetent unit that could accommodate strain associated with post-Barrenland faulting and consequently brittle fracturing in adjacent lithologies can be the locus for uranium deposition.

The signature of the Garry Lake boulder train, U-Pb-Se-Te-Ag with trace Cu-As-S, is polymetallic. Clay alteration is minimal and is restricted to vein walls. However the distribution of multi-generation carbonate as the principal gangue mineral in crack-and-fill veins is diagnostic and supports the interpretation that this occurrence belongs to the clay-bounded unconformity-related deposit subtype.

## ACKNOWLEDGMENTS

The author gratefully acknowledges the following GSC colleagues for their support: A.C. Roberts for X-ray identification of secondary uranium minerals, John Stirling for electron microprobe analyses of pitchblende, S. Tella for permission to reproduce a portion of the Pelly Lake map area geology,

and S. Alvarado for computer assistance. The author thanks certain individuals in the exploration community whose enthusiasm and interest in the Thelon Basin prompted the writeup of this research.

## REFERENCES

- Albert, R.**  
1984: Precambrian weathering on acid metaplutonic rocks at Rumble Lake, District of Keewatin, N.W.T.; BSc. thesis, University of Ottawa, Ottawa, Ontario, 101 p.
- Binns, R.A., Ayers, D.E., Wilmshurst, J.R. and Ramsden, A.R.**  
1980: Petrology and geochemistry of alteration associated with uranium mineralization at Jabiluka, Northern Territory, Australia; in Uranium in the Pine Creek Geosyncline, Proceedings of the International Uranium Symposium on the Pine Creek Geosyncline, (ed.) J. Ferguson and A.B. Goleby; International Atomic Energy Agency, Vienna, p. 417-438.
- Blaise, J.R. and Koning, E.**  
1985: Mineralogy and structural aspects of the Dominique-Peter uranium deposit; in The Carswell Structure Uranium Deposits, Saskatchewan; (ed.) R. Laine, D. Alonso and M. Svab; Geological Society of America, Special Paper 29, p. 139-152.
- Brophy, J.A., Crux, J.C., Gibbins, W.A., Laporte, P.J., Lord, C.C., Padgham, W.A. and Seaton, J.B.**  
1985: Chapter 5: Keewatin region by P.J. Laporte, in Mineral Industry Report 1982-83, Northwest Territories; Department of Indian and Northern Affairs, EGS-1985-4, p. 188-199.
- Cumming, G.L., Krstic, D. and Wilson, J.A.**  
1987: Age of the Athabasca Group, Northern Saskatchewan; Geological Association of Canada-Mineralogical Association of Canada, Joint Annual Meeting, Program with Abstracts, v. 12. p. 35.
- Curtis, L. and Miller, A.R.**  
1980: Uranium geology in the Amer-Dubawnt-Yathkyed-Baker Lake region, Keewatin District, N.W.T., Canada; in Uranium in the Pine Creek Geosyncline, Proceedings of the International Uranium Symposium on the Pine Creek Geosyncline, (ed.) J. Ferguson, and A.B. Goleby; International Atomic Energy Agency, Vienna, p. 595-616.
- Dahlkamp, F.J.**  
1991: Uranium Ore Deposits; Springer Verlag, 460 p.
- Davidson, G.I. and Gandhi, S.S.**  
1989: Unconformity-related U-Au mineralization in the Middle Proterozoic Thelon sandstone, Boomerang Lake prospect, Northwest Territories, Canada; Economic Geology, v. 84, p. 143-157.
- Donaldson, A.J.**  
1967: Two Proterozoic clastic sequences: a sedimentological comparison; Geological Association of Canada, Proceedings, v. 18, p. 33-54.  
1969: Descriptive notes (with particular reference to the Late Proterozoic Dubawnt Group) to accompany a geological map of central Thelon Plain, Districts of Keewatin and Mackenzie; Geological Survey of Canada, Paper 68-49, 4 p.
- Fuchs, H.D., Hilger, W., and Prosser, E.**  
1986: Geology and exploration history of the Lone Gull property; Canadian Institute of Mining and Metallurgy, Special Volume 33, p. 286-292.
- Gall, Q., Peterson, T.D., and Donaldson, J.A.**  
1992: A proposed revision of Early Proterozoic stratigraphy of the Thelon and Baker Lake basins, Northwest Territories; in Current Research, Part C; Geological Survey of Canada, Paper 92-1C, p.129-137.
- Geological Survey of Canada**  
1982: International Map of the World, Magnetic anomaly map, Thelon River, Northwest Territories; Geological Survey of Canada, NQ-12/13/14-AM, scale 1:1 000 000.
- Jewett, D.A. and Duncan, D.R.**  
1983: Kidd Creek Mines Ltd., Garry Lake area, Keewatin; Department of Indian and Northern Affairs, Yellowknife, Mining Assessment Report 081640.
- Jewett, D.A. and Zang, M.W.**  
1982: Kidd Creek Mines Ltd., Garry Lake area, Keewatin; Department of Indian and Northern Affairs, Yellowknife, Mining Assessment Report 081468.

- Jewett, D.A., Duncan, D.R., Slankis, J.A. and Zang, M.W.**  
1983: Kidd Creek Mines Ltd., Garry Lake area, Keewatin; Department of Indian and Northern Affairs, Yellowknife, Mining Assessment Report 081630.
- Lechow, W.R.**  
1982: Kidd Creek Mines Ltd., Garry Lake-Consul River area, Keewatin; Department of Indian and Northern Affairs, Yellowknife, Mining Assessment Report 081450.
- Miller, A.R.**  
1980: Uranium geology of the eastern Baker Lake Basin, District of Keewatin, Northwest Territories; Geological Survey of Canada, Bulletin 330, 63 p.  
1983: A progress report: Uranium-phosphorous association in the Helikian Thelon Formation and sub-Thelon saprolite, central District of Keewatin; *in* Current Research, Part A; Geological Survey of Canada, Paper 83-1A, p. 449-456.
- Miller, A.R. and LeCheminant, A.N.**  
1985: Geology and uranium metallogeny of Proterozoic supracrustal successions, central District of Keewatin, N.W.T. with comparisons to northern Saskatchewan; *in* Geology of Uranium Deposits, (ed.) T.I.I. Sibbald and W. Petruk; Canadian Institute of Mining and Metallurgy, Special Volume 32, p. 167-185.
- Miller, A.R., Cumming, G.L., and Krstic, D.**  
1989: U-Pb, Pb-Pb and K-Ar isotopic study and petrography of uraniferous phosphate-bearing rocks in the Thelon Formation, Dubawnt Group, Northwest Territories, Canada; Canadian Journal of Earth Sciences, v. 26, p. 867-880.
- Miller, A.R., Needham, R.S. and Stuart-Smith, P.G.**  
1992: Mineralogy and geochemistry of the pre-1.65 Ga Paleosol under Komolgie Formation sandstone of the Pine Creek Geosyncline, Northern Territory, Australia; *in* Early Organic Evolution: Implications for Mineral and Energy Resources, (ed.) M. Schidlowski, S. Golubic, M.M. Kimberley, D.M. McKirdy and P.A. Trudinger; Springer-Verlag, p. 76-106.
- Miller, A.R., Stanton, R.A., Cluff, G.R., and Male, M.J.**  
1986: Uranium deposits and prospects of the Baker Lake Basin and subbasins, central District of Keewatin, Northwest Territories; *in* Uranium Deposits of Canada, (ed.) E.L. Evans; Canadian Institute of Mining and Metallurgy, Special Volume 33, p. 263-285.
- Pagel, M. and Ruhlmann, F.**  
1985: Chemistry of uranium minerals in deposits and showings of the Carswell Structure (Saskatchewan-Canada); *in* The Carswell Structure Uranium Deposits, Saskatchewan; (ed.) R. Laine, D. Alonso and M. Svab; Geological Society of America, Special Paper 29, p. 153-164.
- Roddick, J.C., Henderson, J.R., and Chapman, H.J.**  
1992: U-Pb ages from the Archean Whitehills-Tehek lakes supracrustal belt, Churchill Province District of Keewatin, Northwest Territories; *in* Radiogenic Age and Isotopic Studies: Report 6; Geological Survey of Canada, Paper 92-2, p. 31-40.
- Ruhlmann, F.**  
1985: Mineralogy and metallogeny of uraniferous occurrences in the Carswell Structure; *in* The Carswell Structure Uranium Deposits, Saskatchewan, (ed.) R. Laine, D. Alonso and M. Svab; Geological Society of America, Special Paper 29, p. 105-120.
- Tella, S.**  
1994: Geological map of the Amer Lake (66H), Deep Rose Lake (66G), and parts of Pelly Lake (66F) Areas, District of Keewatin, Northwest Territories; Geological Survey of Canada, Open File 2969.
- Tella, S., Ashton, K.E., Thompson, D.L., and Miller, A.R.**  
1983: Geology of the Deep Rose Lake map area, District of Keewatin; *in* Current Research, Part A; Geological Survey of Canada, Paper 83-1A, p. 403-409.
- Tella, S., Thompson, D.L., and James, D.T.**  
1984: Geology of parts of the Deep Rose Lake and Pelly Lake map areas, District of Keewatin; *in* Current Research, Part A; Geological Survey of Canada, Paper 84-1A, p. 313-322.
- Wollenberg, P.**  
1991: Application and results of geophysical surveys for unconformity type uranium deposits in the Thelon Basin, District of Keewatin, N.W.T.; *in* Exploration Overview 1991 Northwest Territories, (ed.) J.A. Brophy; N.W.T. Geology Division, Department of Indian and Northern Affairs, Yellowknife, p. 40.

---

Geological Survey of Canada Project 810024



# Oxide iron-formation-hosted lode gold, Meliadine Trend, Rankin Inlet Group, Churchill Province, Northwest Territories<sup>1</sup>

A.R. Miller, M.J. Balog<sup>2</sup>, and S. Tella<sup>3</sup>

Mineral Resources Division

*Miller, A.R., Balog, M.J., and Tella, S., 1995: Oxide iron-formation-hosted lode gold, Meliadine Trend, Rankin Inlet Group, Churchill Province, Northwest Territories; in Current Research 1995-C; Geological Survey of Canada, p. 163-174.*

---

**Abstract:** Oxide iron-formation in the ca 2.66 Ga lower- to middle-greenschist facies Rankin Inlet Group defines a pronounced discontinuous 65 km long northwest-trending aeromagnetic linear, the Meliadine Trend. Quartz+carbonate veined iron-formation is host to lode gold prospects that are spatially associated with a 1-2 km wide ductile to brittle high strain zone. Two types of lode gold are recognized based on: 1) regional and local lithological variations, 2) type of oxide iron-formation, 3) deformation style, 4) differences in silicate-carbonate-sulphide assemblages, and 5) gold compositions. A Proterozoic hydrothermal event is indicated by Ar-Ar and Pb-Pb isotopic ages from silicate and sulphide alteration minerals. Widespread Proterozoic thermotectonism in the eastern Churchill Province reactivated pre-existing Archean shear zones during the early Proterozoic. Hydrothermal fluids channeled along these structures are postulated to have formed Proterozoic lode gold deposits in Archean rocks.

**Résumé :** Les formations de fer oxydées dans le Groupe de Rankin Inlet du faciès inférieur à intermédiaire des schistes verts, qui date de 2,66 Ga environ, définissent une direction linéaire aéromagnétique prononcée, à direction nord-ouest, discontinue sur 65 km, appelée direction Meliadine. Les formations de fer à veines de quartz+carbonate renferment des prospects d'or filonien qui sont spatialement associés à une vaste zone de déformation ductile à cassante de 1 à 2 km de largeur. On a établi deux types d'or filonien en se basant sur : 1) les variations régionales et locales de la lithologie, 2) le type de formation de fer oxydée, 3) le style de déformation, 4) les différences entre les assemblages de silicates-carbonates-sulfures et 5) les compositions de l'or. Un épisode hydrothermal protérozoïque est révélé par les datations par Ar-Ar et Pb-Pb de minéraux d'altération silicatés et sulfurés. Au Protérozoïque précoce, un thermotectonisme étendu dans l'est de la Province de Churchill a eu pour effet de réactiver les zones de cisaillement archéennes. Les fluides hydrothermaux canalisés le long de ces structures auraient formé des gisements d'or filonien au Protérozoïque dans des roches archéennes.

---

<sup>1</sup> Contribution to Canada-Northwest Territories Mineral Initiatives (1991-1996), an initiative under the Canada-Northwest Territories Economic Development Cooperative Agreement.

<sup>2</sup> Comaplex Minerals Corp., 901-1015 4<sup>th</sup> Street S.W., Calgary, Alberta T2R 1J4

<sup>3</sup> Continental Geoscience Division

## INTRODUCTION

The Churchill Province has many lithostructural attributes that differentiate it from adjacent structural provinces (Davidson, 1972). These identify this terrane as crucial to understanding the architecture of the Canadian Shield. Three Archean greenstone belts of contrasting ages, ca 2.8, 2.7, and 2.66 Ga, are distributed across the province. Seldom appreciated is the long and varied Proterozoic history that has affected these Archean rocks. Crustal-scale imprints from bounding Proterozoic orogens are preserved across the Archean belts, and three distinct Proterozoic lithostratigraphic sequences spanning the interval ca. 2.45 to 1.72 Ga overlie the Archean crust. A spectrum of mineral deposit types spans the interval from ca 2.7 to 1.4 Ga. Proterozoic mineral deposit types are particularly diverse because of specific combinations of magmatism, sedimentation, and/or tectonism. Because Proterozoic thermotectonism affected the Archean crust, Proterozoic metallogenic studies must evaluate both Proterozoic and Archean strata. This report discusses the geological setting, alteration mineralogy, metasomatic processes, and Proterozoic geochronology associated with two contrasting types of oxide iron-formation-hosted lode gold in the Archean Rankin Inlet Group.

## EXPLORATION HISTORY

The Meliadine Trend comprises several units of deformed auriferous oxide iron-formation that lie within and adjacent to a major structural zone, the Pyke fault zone (PFZ; Fig. 1). Despite the Trend's proximity to the hamlet of Rankin Inlet, and to a past-producing nickel mine, regional geological mapping and exploration of the Meliadine iron-formations were only undertaken in the early 1990s. Early mapping projects by Wright (1967) and Laporte (1983) either concentrated south of the Trend or were at too large a scale to identify the structural features unique to the area. Active exploration by industry for both shear zone and iron-formation-hosted gold deposits is continuing.

## REGIONAL GEOLOGY OF THE RANKIN INLET GROUP

The term Rankin Inlet Group was first used by Bannatyne (1958) to describe a sequence of intrastratified metamorphosed and polydeformed Archean felsic and mafic volcanics, related pyroclastic equivalents, oxide iron-formation, greywacke-argillite, and ultramafic intrusions exposed in the Rankin Inlet area. Subsequent regional mapping subdivided

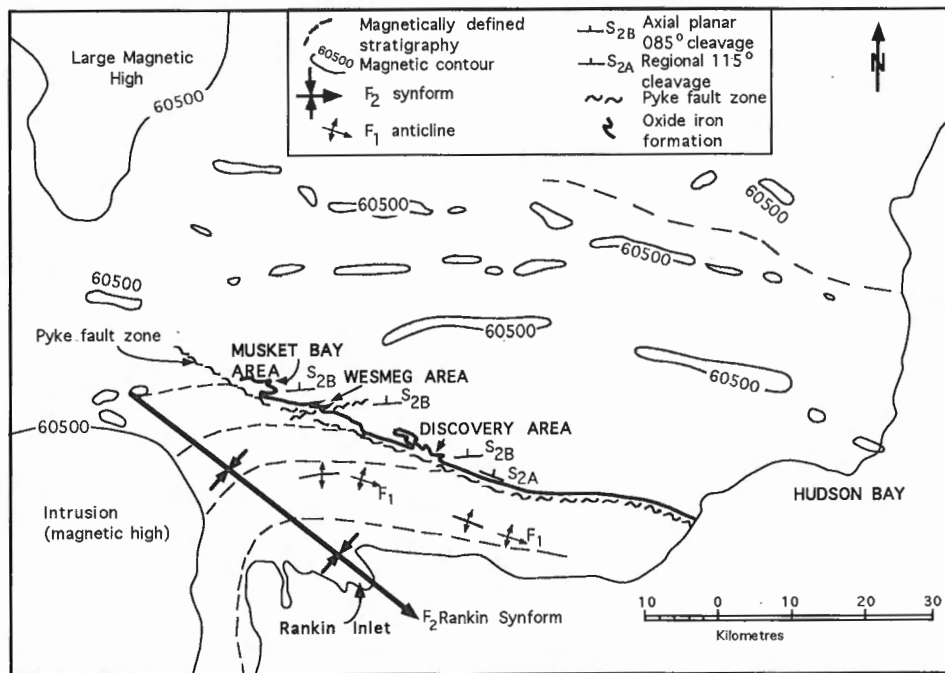


**Figure 1.** Aeromagnetic map of the Meliadine Trend showing the distribution of iron-formation, the Pyke fault zone (PFZ), and the location of significant auriferous iron-formation. Derived from Geological Survey of Canada Magnetic Anomaly Map NP 15-16-M.

the Rankin Inlet Group into two major cycles of mafic volcanic rocks separated by greywacke-turbidite containing banded oxide iron-formation (Tella et al., 1986). A U/Pb zircon age of 2665  $\pm$  3 Ma from a dacitic porphyry within the Rankin Inlet Group establishes a minimum age for volcanism (Tella, 1994).

At least two periods of Archean deformation and one Proterozoic deformational event are recognized in the Rankin Inlet Group. Archean deformation resulted in the development of an east-southeast-dipping regional  $F_1$  homocline that was refolded by a shallowly southeast-plunging  $F_2$  syncline. Proterozoic deformation involved tectonic interleaving of Archean metavolcanic rocks with Proterozoic Hurwitz orthoquartzite. Metamorphic grade is within the lower to middle greenschist facies. Gabbro and diabase intruded the Archean sequence during the late Archean to early Proterozoic and were followed by post-tectonic granitoid plutons, relatively younger phlogopite lamprophyre, and finally northwest-trending gabbro dikes (Mackenzie swarm).

## GEOLOGY OF THE MELIADINE TREND

The Meliadine Trend is characterized by a regional pervasive structural zone located at the southern edge of a pair of locally auriferous oxide iron-formations (Fig. 1). This structure, informally called the Pyke fault zone (PFZ), is interpreted to be a zone several kilometres wide of ductile to brittle strain with apparent dextral displacement. High strain is concentrated along the southern margin of the two iron-formations and decreases northward across a 1-2 km wide zone. The fault zone is considered to be an Archean thrust that underwent subsequent late Archean to Proterozoic reactivation (Balog, 1993; Tella, 1994). The PFZ itself lacks a distinct geophysical signature, but the two iron-formations display pronounced linear northwest-trending aeromagnetic anomalies along the 65 km long Meliadine exploration property. The northern iron-formation (Fig. 1) is magnetite rich, whereas the southern one is leaner and quartz rich with corresponding lower magnetic susceptibility.

### Facies variation

A regional-scale facies change is interpreted along the north side of the Meliadine Trend. Variation in the proportion of clastic sedimentary and volcanic rocks indicates a sediment-dominated domain over the central and eastern portions of the trend, from Discovery Area to the east. Volcanic rocks dominate the second domain over the western half of the trend, including the Wesmeg and Musket Bay areas. Both domains host auriferous oxide iron-formation (Fig. 1). In the Discovery area, iron-formation is interstratified with graded fine grained greywacke-pelite, subordinate mafic volcanic flows, and tuff. In the Wesmeg area, iron-formation is interstratified with sheared and carbonatized massive and pillowed metabasalt and very minor schistose magnesite-talc-chlorite rock, probably metakomatiite. Fine grained buff to black argillite-phyllite, commonly graphitic and sulphidic, is interlayered with siliceous iron-formation in the Wesmeg area.

## Metamorphism

Supracrustal rocks of the Rankin Inlet Group and equivalent strata that extend north to Chesterfield Inlet have been poly-deformed and regionally metamorphosed under greenschist to amphibolite facies conditions (Tella et al., 1986, 1992, 1993). This metamorphism is presumed to be Archean as Lower Proterozoic strata near Rankin Inlet are not metamorphosed. Mineral assemblages in volcanic and clastic sedimentary rocks within the trend indicate lower to middle greenschist metamorphic conditions. In the northwest and central parts of the trend, the mineral assemblage in sheared unaltered metabasalt is actinolite-chlorite-carbonate-albite-epidote-calcite. Pelitic rocks in metaturbidite from the central part contain muscovite-chlorite-biotite. Iron-formation, typical of the Archean Algoma type, is composed of recrystallized and transposed layers containing variable proportions of quartz, magnetite, and chlorite. Chlorite-rich layers in banded magnetite-quartz iron-formation contain the assemblage chlorite- $\pm$ -biotite, possibly stilpnomelane.

## Structural history

Detailed structural analysis of the Meliadine Trend has been hampered by the very limited outcrop. Property-scale mapping (Gochnauer and Dickson, 1991, 1992) and structural studies (Barkley, 1991, 1992) in the Discovery area, and regional mapping and structural analysis by Tella et al. (1992, 1993), Tella (1994), and Armitage et al. (1993) have indicated that several increments of deformation are recorded in the rocks. These studies form the framework for interpretation of the structure of the Trend.

Deformation of the Rankin Inlet Group originated with the development of an east-southeast-dipping  $F_1$  homocline and extensive bedding-parallel thrusts (Tella et al., 1986). Northeast-plunging mineral-stretching lineations suggest that the transport direction on interleaving tectonic sheets was either to the northeast or to the southwest, or both.

The Archean sequence was refolded into a southeast-plunging synform in early to mid- $D_2$  (Fig. 2). A regional shear fabric,  $S_{2A}$ , oriented 285/53NE, and developed on  $F_1$  folds and thrusts (Barkley, 1992). It is parallel to the regional trend of both the fault zone and iron-formation and is best expressed in metavolcanic and metasedimentary schists that envelop the iron-formation. Progressive strain may have produced apparent dextral movements on a portion of one or several pre-existing  $F_1$  thrust planes along the Meliadine Trend. Propagation of these displacements westward with time in mid- $D_2$  resulted in development of the Pyke fault zone. Primary bedding and  $F_1$  fabrics near the fault zone are generally transposed into  $S_{2A}$ .

Syn- to late- $D_2$  folding of  $S_{2A}$  foliation in response to apparent dextral shearing on the PFZ is extremely well developed over the western half of the trend. Asymmetrical Z-folds plunging 064/49NE predominate, with S-folds confined to local overturned limbs (Balog, 1993). Individual folds range from centimetre- to kilometre-scale structures and are well developed in the northern oxide iron-formation (Fig. 1, 2, 3, 4). Fold interference patterns in iron-formation reflect refolding

of early folds developed during  $F_1$  thrusting (Tella et al., 1992; Barkley, 1992; Armitage et al., 1993). Reorientation of early  $F_1$  folds about a  $270/67N$  axial plane ( $S_{2B}$ ) is also recorded in iron-formation across the entire strike length of the Trend (Barkley, 1992). The  $15^\circ$  difference between  $S_{2A}$  and  $S_{2B}$  foliations is consistent over 35 km from the Discovery to Musket Bay areas (Fig. 2). On a regional scale, as shown on Figure 1, bedding planes south of the PFZ define the large

$F_2$  syncline and are truncated by the fault north of the PFZ. Stratigraphic layering as reflected by iron-formation is parallel to the fault east of Discovery area, but is discordant and intensely folded west of it. Airborne geophysical maps indicate that the point where this folding of iron-formation increases is precisely where the fault zone exhibits discordance with strata to the south of it (Balog, 1993).

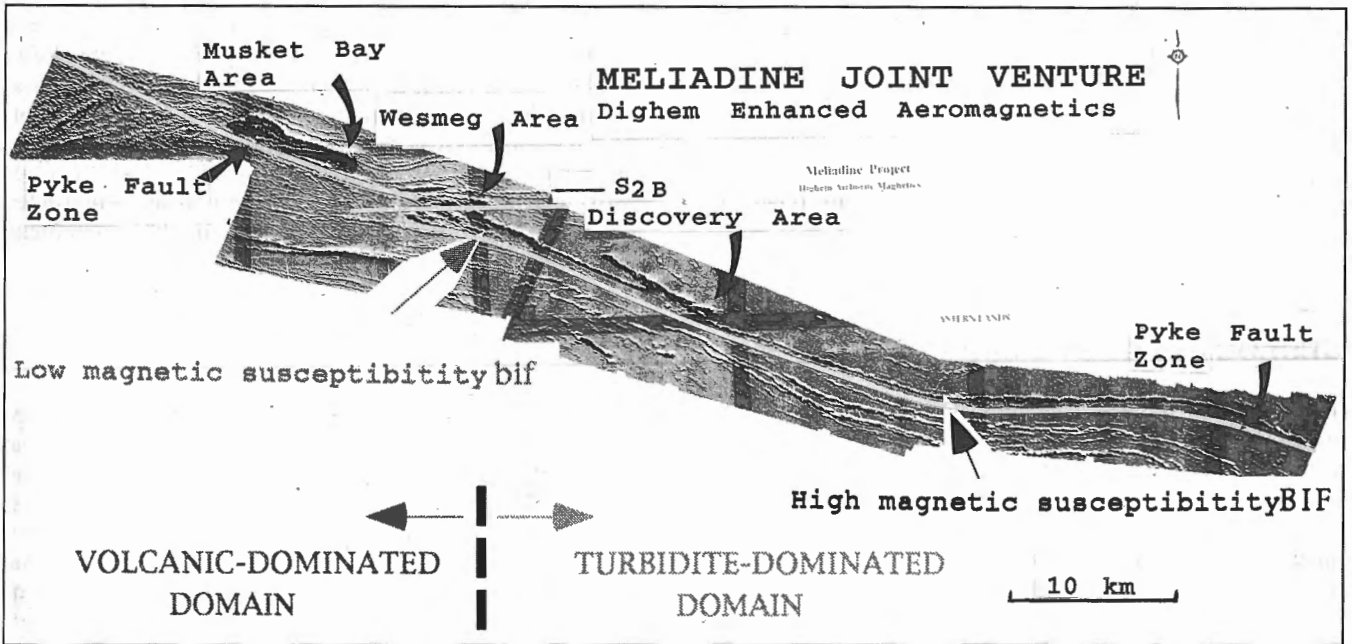


Figure 2. Schematic aeromagnetic map, Rankin-Meliadine area.

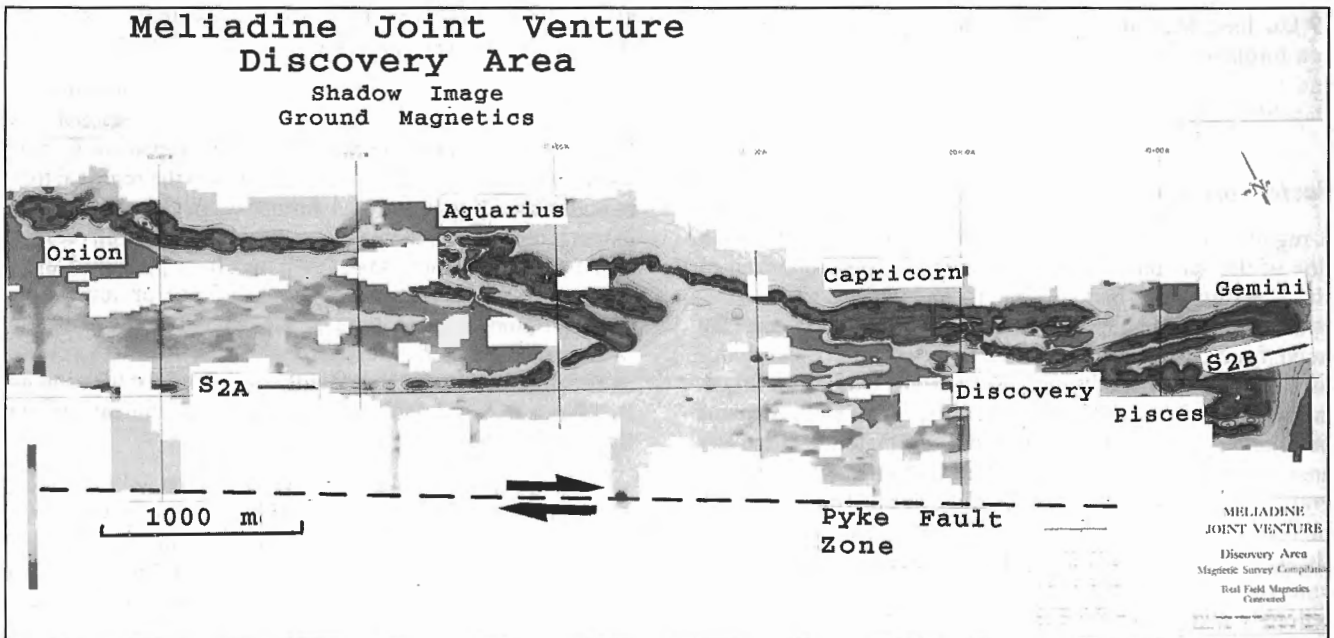


Figure 3. Ground magnetic map of the Discovery area.

The regional presence of  $S_{2B}$ , superimposed on  $S_{2A}$  foliation in iron-formation along the Trend, indicates continued shortening and eventual coaxial flattening of  $F_1$  and  $F_{2A}$  folds into the 270/67N  $S_{2B}$  direction (Barkley, 1992). Progressive strain along the fault zone in late  $D_2$  to  $D_3$  time resulted in brittle failure along a west-trending,  $S_{2B}$ -parallel cross fault that offset stratigraphy in the Wesmeg area. This offset, the Wesmeg fault, is the only recognized ductile-brittle fault that affected both iron-formation and the PFZ along the Trend (Fig. 4).

$S_3$  crenulations in the Meliadine area are locally well developed on  $S_2$  foliation planes in some metapelite and argillite adjacent to iron-formation. Orientations of the  $D_3$  crenulations are difficult to determine given the lack of outcrop along the Pyke fault zone and problems orienting the core. Both steep and shallow sets have been observed. Regional structural studies outside of the trend have shown an increase in  $S_3$  intensity adjacent to  $F_1$  thrust planes. By inference, this increase may indicate proximity to  $F_1$  structures and  $D_3$  movement on them. The presence of Archean metavolcanics thrust onto Proterozoic orthoquartzite in the eastern part of the Trend may be a reflection of this  $D_3$  movement. Timing of this Proterozoic thrusting relative to dextral movement is not yet known.

## DISCOVERY-TYPE LODE GOLD

The central Z-folded section of the Trend, referred to as the "Discovery area", is the locus for significant iron-formation-hosted lode gold mineralization and lies 0.75 km north of the fault zone (Fig. 1). This 6.5 km long section of the northern oxide iron-formation and adjacent greywacke-pelite is folded into a series of asymmetric Z-folds that step down to the southeast. Extreme shortening of the iron-formation has led to tectonic thickening in hinge zones and attenuation of limbs (Fig. 3). Numerous gold occurrences have been identified in individual hinge and limb segments of the folded iron-formation (Capricorn, Orion, Gemini, Pisces, as well as Discovery and Snowgoose zones).

Polydeformed banded magnetite+quartz iron-formation is host to 'Discovery-type' lode gold mineralization (Tella et al., 1992; Armitage et al., 1993). This iron-formation consists of 85 per cent banded quartz+magnetite oxide iron-formation, and 15 per cent foliated chlorite schist, silicate iron-formation. Silicate iron-formation bands consist of Fe-chlorite, variety ripidolite, +/- magnetite with accessory quartz, apatite, and rare biotite. Due to ductility contrasts during polyphase folding, the thicknesses of individual layers of the two subunits are highly variable with hinge zones being the loci of significant thickening (Tella et al., 1992, Fig. 6). Discontinuous turbidite beds identical to the enclosing greywacke-pelite are present within the Discovery area iron-formation.

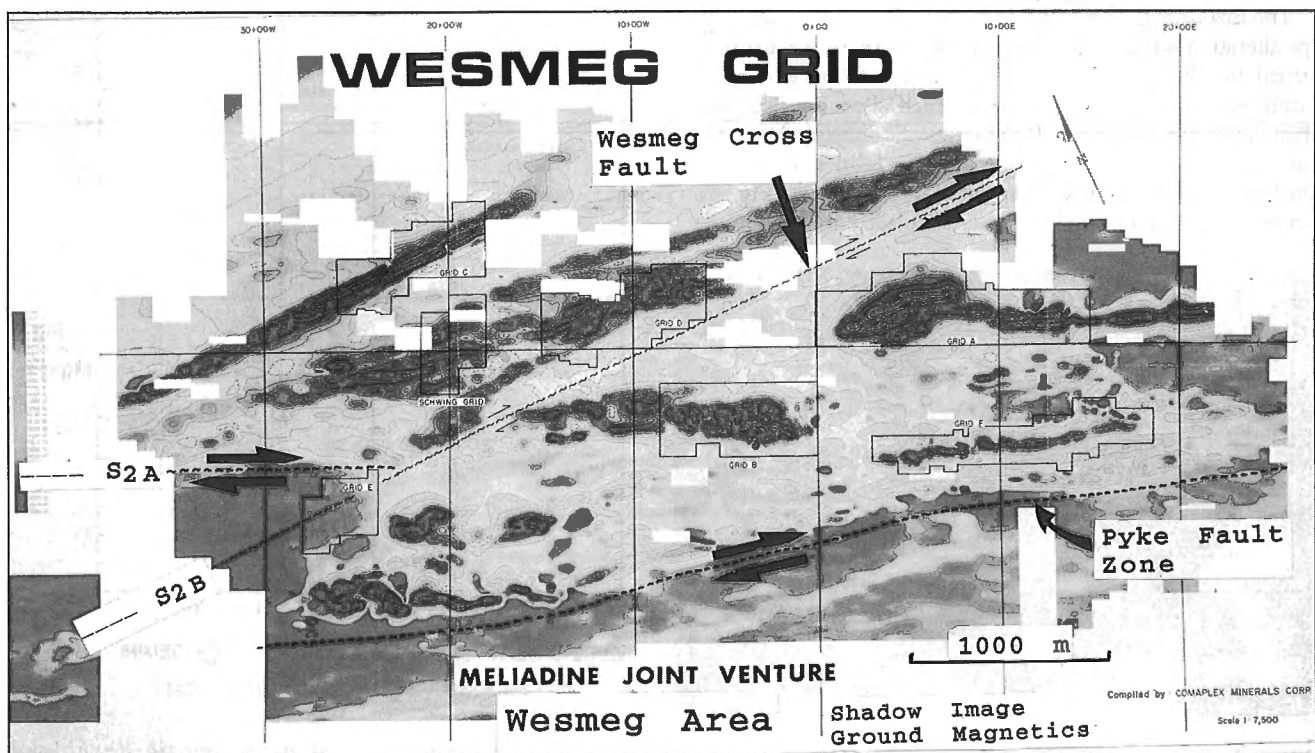


Figure 4. Ground magnetic map of the Wesmeg area.



Quartz+carbonate veins are associated with each phase of folding in the iron-formation-turbidite sequence but vein formation associated with Z-folds is proportionally the most abundant. Variable recrystallization of vein quartz records ongoing vein development during polyphase folding. Veins formed during the latest phase of folding are sulphide bearing and auriferous. In long limbs of folds, quartz+carbonate veins up to 10 cm in width are commonly parallel and at low angles to compositional layering. Irregular-shaped quartz+carbonate flood zones, 1 to 3 m in width, preferentially occupy F<sub>2</sub> fold hinges, brecciate the iron-formation, and are responsible for intense hydrothermal replacement of silicate and oxide iron-formation.

**Alteration**

Discovery-type hydrothermal alteration has been examined from Orion, the most westerly prospect, through the Discovery Zone to Snowgoose in the east, a 13 km strike distance along the Trend. Alteration envelopes adjacent to gold-calcite-sulphide-bearing quartz vein networks are in the order of 5-6 m. Quartz flood zones up to 3 m are found in the iron-formation and to a lesser degree in the greywacke-pelite structurally below the iron-formation. Vein systems constitute up to 25 per cent of auriferous iron-formation compared to 5-10 per cent in the unmineralized equivalent. Alteration assemblages overprint pre-existing fabrics and replace greenschist facies assemblages in iron-formation and turbiditic sedimentary rocks (Fig. 5). The discordant relationship of alteration minerals to older fabrics (S<sub>2B</sub>) indicates that metasomatism and gold are late- to post-Z-fold formation.

The metasomatic assemblage that characterizes Discovery-type alteration is fine- to medium-grained, very weakly to undeformed hornblende+biotite+grunerite+calcite+/-trace allanite. Hornblende is diagnostic of hydrothermal alteration in greenschist facies iron-formation. Porphyroblastic subhedral to euhedral hornblende prisms overgrow older fabrics in silicate iron-formation and banded magnetite-quartz layers (Fig. 5). Banded quartz+magnetite layers are replaced by circular to

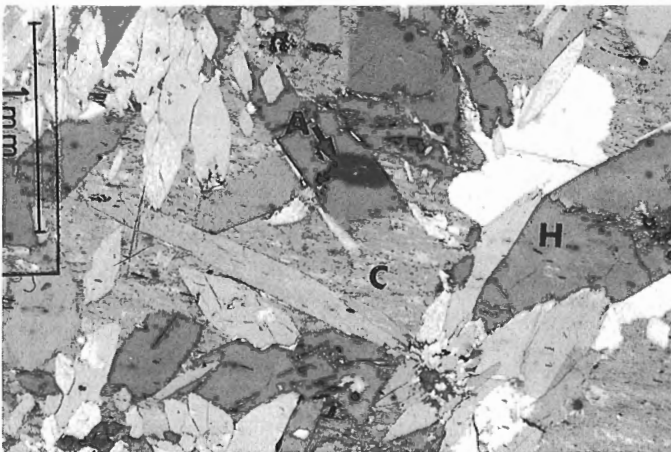


**Figure 5.** Photomicrograph of hornblende (H) with allanite (A inside pleochroic halo) overgrowing fabric (S<sub>2A</sub>) and replacing foliated metamorphic chlorite (C) schist, Discovery Zone.

slightly oblong fine grained radiating aggregates of hornblende+grunerite+calcite. Poikiloblastic hornblende occurs in and adjacent to quartz+carbonate veins in footwall metaturbidite. Fine grained allanite is present only in altered iron-formation and as inclusions in porphyroblastic hornblende and biotite. The rare assemblage garnet+biotite+hornblende is present adjacent to quartz+carbonate veins. The absence of retrogression of, and strain within, any hydrothermal minerals indicates that alteration was late peak metamorphism and deformation.

**Geochemistry of alteration minerals**

**Hornblende**

Representative electron microprobe analyses of metasomatic hornblende from altered iron-formation and underlying turbidite are plotted in Figure 6. Aluminum-rich hornblende, averaging 15.3 wt% Al<sub>2</sub>O<sub>3</sub>, displays a limited compositional range that clusters within the ferro-tschermakite field and extends into the ferro-tschermakitic hornblende field. Metasomatic hornblende of similar composition, yet from widely spaced prospects, indicates that large volumes of iron-formation interacted with hydrothermal fluid in the Discovery area.

Metasomatic hornblende coexisting with albite (An<sub>0</sub>) is present in and adjacent to sulphide-bearing quartz-carbonate veins in footwall metaturbidite. This hornblende is compositionally distinct from iron-formation hornblende (Fig. 6). Reaction between markedly different rock

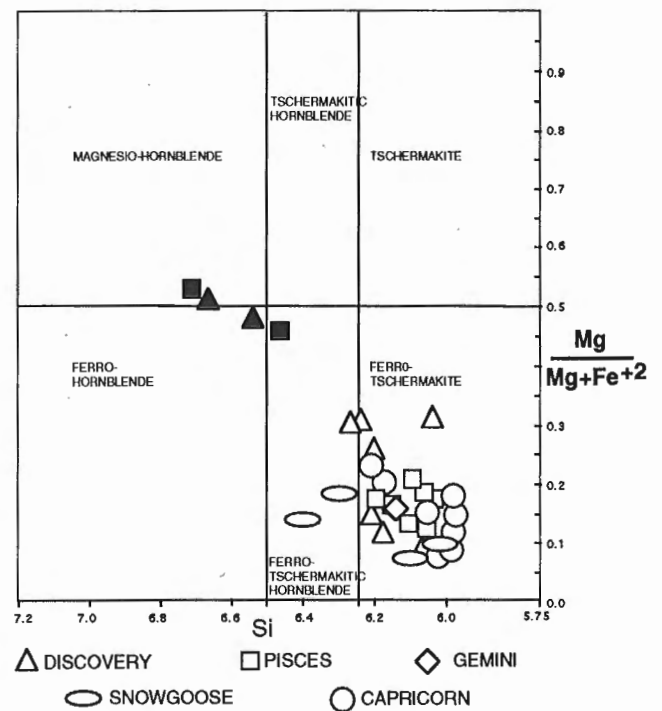


**Figure 6.** Composition of metasomatic hornblende, Discovery area. (open symbol: iron formation; filled symbol: greywacke-pelite)

types and hydrothermal fluid accounts for this variation. Widespread hydrothermal hornblende indicates calcium, sodium, and potassium metasomatism of the oxide iron-formation.

### Grunerite

Grunerite is ubiquitous in altered hornblende+/-biotite+sulphide+gold-bearing iron-formation but is not present in recrystallized unaltered iron-formation. It has replaced chlorite in chlorite schist and magnetite in banded oxide iron-formation. The Mg/Fe ratio in grunerite varies from 0.74 to 0.86 with lower values in magnetite-quartz layers. Development of grunerite records a critical oxidizing hydrothermal reaction represented by equation 1 (Table 1).

### Carbonate

Calcite is the only carbonate mineral in altered iron-formation. It occurs in sulphide-bearing quartz+carbonate veins in altered iron-formation and in footwall greywacke-pelite, and is disseminated amongst metasomatic amphiboles in altered iron-formation. Calcite composition range in veins and altered iron-formation is restricted and calcite contains up to 5.5 wt% FeO (Fig. 7). Calcite coexisting with hornblende+/-grunerite implies low  $X_{CO_2}$  in the hydrothermal fluid.

### Chlorite

Foliated, fine grained metamorphic chlorite in chlorite schist is the variety ripidolite (Fig. 5, 8). Chlorite acted as a reactant with hydrothermal fluid to form amphiboles, as represented by equation 2 (Table 1), and underwent minor recrystallization during hydrothermal alteration.

### Sulphides and gold

Sulphides in metasomatized auriferous iron-formation are the same as those contained in quartz+carbonate veins in altered iron-formation and footwall rocks. The diagnostic 'Discovery-type' sulphide assemblage, pyrrhotite with minor chalcopyrite, is directly associated with amphibole-bearing iron-formation. Sulphidization of magnetite is suggested by embayed magnetite-pyrrhotite contacts, islands of pyrrhotite in magnetite, and replacement of magnetite bands by pyrrhotite.

Accessory pyrite, a critical phase in some gold zones, replaces pyrrhotite. Pyrite indicates increased  $F_{S_2}$  in altered iron-formation. The import of pyrite and the oxidizing amphibole-forming reaction would lower gold solubility in the hydrothermal fluid.

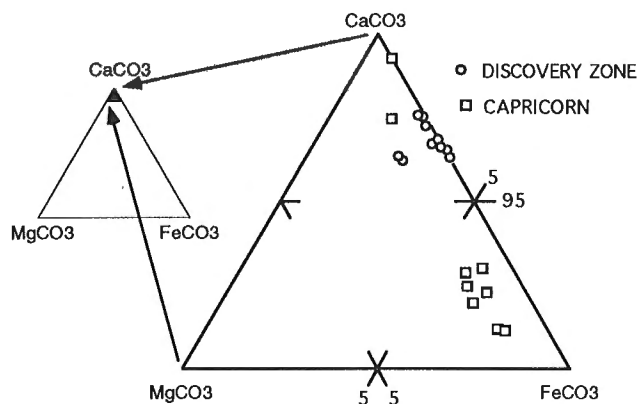


Figure 7. Composition of hydrothermal calcite, Discovery area.

Table 1. Proposed hydrothermal reactions for Discovery- and Wesmeg-type lode gold.

<b>Discovery-type lode gold</b>	
$7Fe_3O_4 + 24SiO_2 + 3H_2O = 3Fe_7Si_8O_{22}(OH)_2 + 3.5O_2$	(1)
$(Fe_{4.5}, Mg_{4.5}, Al_{2.6}) (Si_{5.4}, Al_{2.6}) O_{20}(OH)_{16} + Ca + K + Na =$ chlorite + fluid	
$(Na, K)_{29} Ca_{2.0} (Mg_{6.6}, Fe_{2.63}, Fe_{.95}, Al_{.81}) (Si_{6.1}, Al_{1.8}) O_{22}(OH)_2 + 8H_2O + 2O_2 + 3.84Mg + 0.92Fe$	(2)
<b>Wesmeg-type lode gold</b>	
actinolite + epidote + $CO_2 + H_2O =$ chlorite + calcite + quartz	(3)
albite + chlorite + calcite + $K^+ + CO_2 =$ muscovite + ankerite + quartz + fluid + $Na^+$	(4)
chlorite + $H_2S + H_2O =$ muscovite + pyrite + quartz + $Mg^{++}$	(5)
$7Fe_3O_4 + 24SiO_2 + 3H_2O = 3Fe_7Si_8O_{22}(OH)_2 + 3.5O_2$	(6)

Coarse grained porphyroblastic arsenopyrite, accompanied by trace amounts of sphalerite, is texturally late and overgrew pyrrhotite-magnetite and amphiboles. Porphyroblastic textures in arsenopyrite represent a late or possibly separate hydrothermal event. Arsenopyrite and amphibole indicate altered iron-formation, but gold does not directly correlate with arsenic.

Free gold occurs intergranular to pyrrhotite and metamorphic amphibole and as fracture fillings, inclusions in and coatings on porphyroblastic arsenopyrite, disseminated in altered chlorite layers and in sulphide-bearing

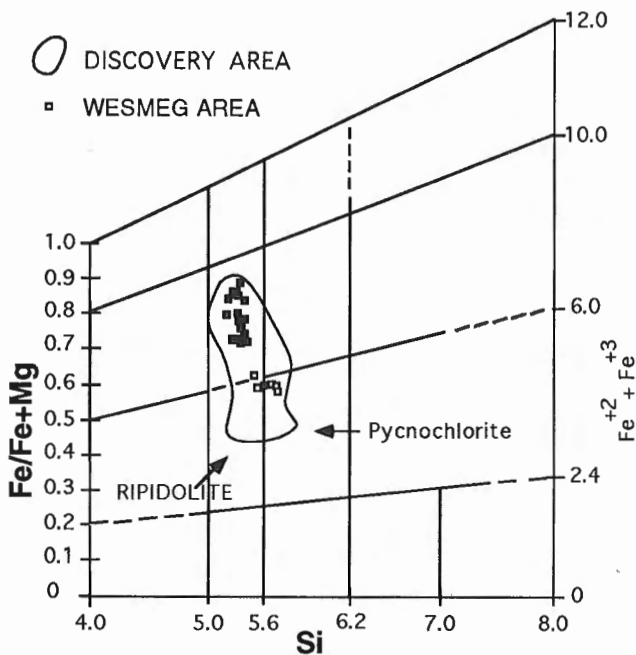


Figure 8. Chlorite compositions, Discovery and Wesmeg areas. (open square: metamorphic; filled square: hydrothermal).



Figure 9. Transposed, quartz-veined (Q), and sulphidized (S) siliceous iron-formation, Wesmeg area.

carbonate+quartz veins. The average gold grain composition Au/Ag ratio in Discovery-type prospects is 85/15, irrespective of the textural form of the gold.

### WESMEG-TYPE LODE GOLD

The Wesmeg area, 8 km west of the Discovery area and adjacent to the PFZ, is defined as the central of three areas of structural deformation on the west end of the Trend (Fig. 1). To date, exploration and study over the 7 km long auriferous region has concentrated on the lower siliceous iron-formation and not the northern iron-formation explored in the Discovery area, although both iron-formations are present in the Wesmeg area. 'Wesmeg-type' gold mineralization has been documented from drill core examination of eight drill-tested anomalies. Alteration envelopes in wallrock, up to 20 m wide, are invariably associated with zones of strong penetrative fabrics related to transposition of contacts between volcanic rocks and iron-formation, and to ductile-brittle movement along the Wesmeg fault and PFZ.

Like the Discovery-type, 'Wesmeg-type' lode gold is hosted in veined, complexly folded and transposed sulphidized siliceous iron-formation (Fig. 9). However Wesmeg-type lode gold is distinguished from Discovery-type lode gold by deformational style and silicate, carbonate, sulphide, and gold compositions. Hydrothermal alteration products consist of carbonate, chlorite, sericite, and quartz in auriferous iron-formation and metavolcanic wallrocks in the Wesmeg area. Quartz+carbonate vein systems are preferentially developed in or near iron-formation contacts and to a much lesser degree in adjacent metabasalt.

### Alteration

Carbonatization, chloritization, sericitization, and silicification of wallrock metabasalt are typical of shear-zone-related lode gold deposits (Clark et al., 1986). Destruction of fine grained metamorphic actinolitic hornblende, epidote, albite, and porphyroblastic magnetite is a cryptic indicator of the outer parts of the altered envelope. Carbonatization together with sericitization and silicification account for colour variations from green to dark green unaltered to grey altered metabasalt. Auriferous iron-formation is marked by hydrothermal grunerite with carbonates, chlorite sericite, and quartz.

### Geochemistry of alteration minerals

#### Carbonate

Carbonatization of metabasalt is recorded by 8 to 13 wt% CO<sub>2</sub> compared to background values of 0.5 to 1.0 wt%. Unaltered metabasalt contains veinlets and disseminated fine grained calcite (Fig. 10). With increasing strain and CO<sub>2</sub> introduction, metamorphic calcite is replaced by Fe-dolomite-ankerite, as 1-2 mm porphyroblasts in grey-green altered metabasalt.

### Muscovite and biotite

The alignment of these phyllosilicates and hydrothermal carbonates and chlorite in the foliation plane indicates alteration was synchronous with deformation. The presence of fine grained muscovite and red-brown biotite records moderate to intense wallrock alteration. Increased modal abundances of muscovite correlates with the destruction of albite, especially in intensely carbonatized metabasalt.  $\text{Na}_2\text{O}$  contents in muscovite ranging from 0.28 to 1.02 wt% indicate paragonitic compositions. Phyllosilicate replacement of carbonatized metabasalt and iron-formation and mica-bearing quartz+carbonate veins in these lithologies indicates that potassium metasomatism accompanied  $\text{CO}_2$ .

### Chlorite

Two generations of ripidolitic chlorite are present, based on textural variations and optical characteristics. With increasing alteration and strain towards the iron-formation contact, metamorphic chlorite with a  $\text{Fe}/\text{Fe}+\text{Mg} = \sim 0.5$  is replaced by hydrothermal chlorite having a ratio of 0.7-0.8 (Fig. 9).

### Sulphides and gold

Two generations of sulphides are recognized in auriferous siliceous iron-formation. Discontinuous streaky laminations of fine grained pyrrhotite+pyrite+/-chalcopyrite are present with disseminated fine grained magnetite. This assemblage, similar to sulphides in adjacent argillite-graphitic phyllite, could be in part syngenic.

Hydrothermal sulphides mantle quartz+carbonate veins and consist of medium- to coarse-grained arsenopyrite with pyrrhotite+/-chalcopyrite+/-pyrite+/-sphalerite+/-galena. A rare assemblage of arsenopyrite+gersdorffite+pyrrhotite with magnesite+siderite (Fig. 10) is associated with quartz+carbonate veins in metakomatiite.

Free gold in iron-formation has the same textural associations as in Discovery-type lode gold. However, Wesmeg gold is consistently finer,  $\text{Au}/\text{Ag} = 90/10$  to  $95/5$ . Silicate-carbonate and sulphide assemblages indicate that the Wesmeg hydrothermal system is clearly different from the Discovery system and was  $\text{CO}_2$ -dominated.

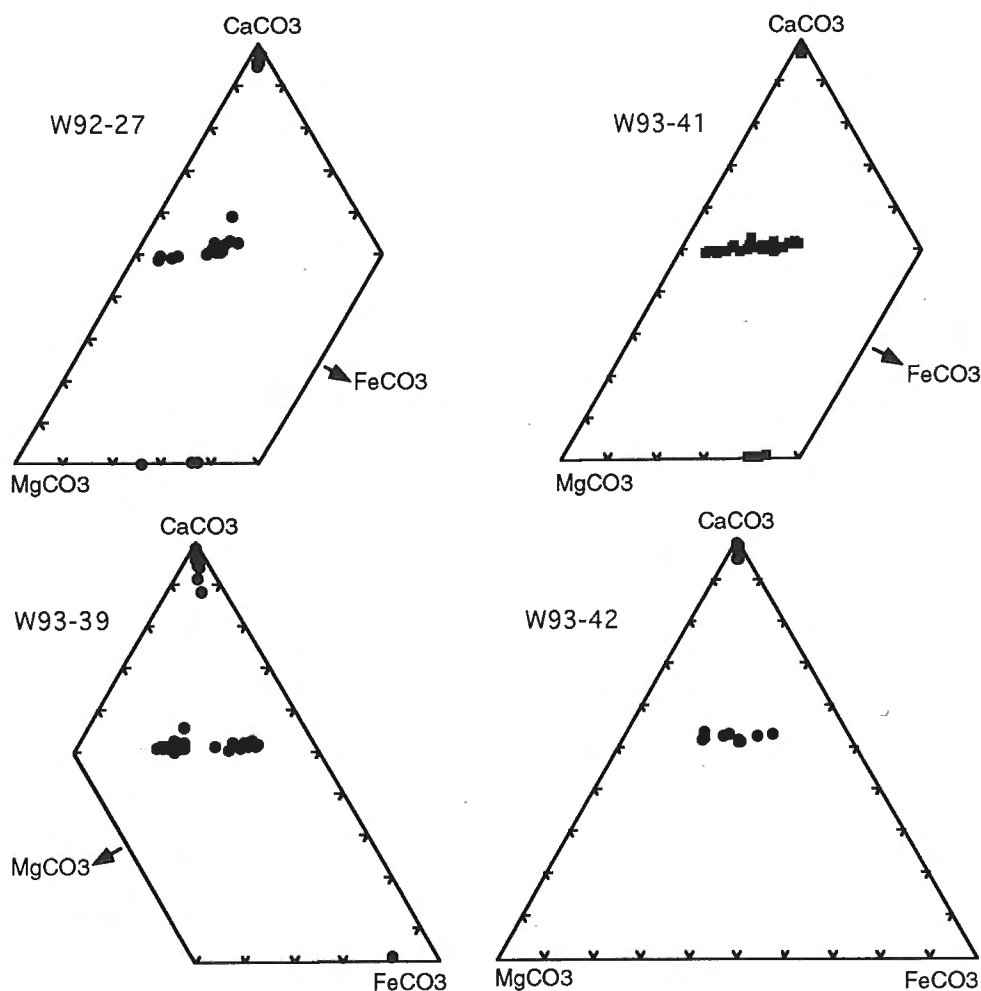


**Figure 10.** Compositional variation of carbonates from hydrothermally altered metabasalt, Wesmeg area.

## RELATIONSHIP BETWEEN MINERALIZATION AND DEFORMATION

It is apparent that mineralizing processes occurred as continuations of similar events rather than as series of unrelated episodes. Multiple injections of gold, sulphur, arsenic, and silica into these systems appear to be due to overlapping deformational and hydrothermal events. Textural relationships suggest that the quartz+carbonate+pyrrhotite+pyrite+gold phase of mineralization associated with sulphidization of magnetite occurred prior to introduction of gold-bearing porphyroblastic arsenopyrite. Folding of the pyrrhotite-dominated mineralization suggests a mid- to late-D<sub>2</sub> event, coincident with or postdating Z-fold development.

The arsenopyrite-gold-quartz-iron carbonate-bearing phase of mineralization displays little evidence of postdepositional strain. The S<sub>2A</sub> (285°) alignment of rounded quartz+carbonate vein fragments hosting undeformed arsenopyrite in a healed siliceous matrix indicates that the gold-arsenopyrite phase of mineralization was associated with events that culminated in late, post-F<sub>2</sub> apparent dextral movement along the PFZ. It is postulated that gold-arsenic-silica-rich fluids were introduced into a predominantly ductile deformational regime in the Discovery area and into a brittle deformational regime in the Wesmeg area during displacements along the fault zone.

## GEOCHRONOLOGY

<sup>40</sup>Ar-<sup>39</sup>Ar isotopic analyses of metasomatic hornblende from the Discovery Zone, and Pb-Pb analyses of galena from the Wesmeg area, were initiated in order to constrain the timing of hydrothermal alteration and gold mineralization. The <sup>40</sup>Ar-<sup>39</sup>Ar incremental-release spectrum for Discovery Zone hornblende provides a plateau age of 1780 ± 20 Ma. This age represents cooling through about 500°C, the Ar closure temperature for hornblende. The <sup>40</sup>Ar-<sup>39</sup>Ar spectrum has no Archean signature. Garnet-biotite geothermometry on this Discovery area alteration assemblage yielded a temperature estimate of 520 ± 30°C at 3 kbars, which suggests that the above cooling age is close to the crystallization age.

Pb-Pb galena model ages using Stacey-Kramer method on galena intergrown with pyrrhotite+porphyroblastic arsenopyrite from the Wesmeg area have yielded ages between 2140-2055 Ma. These first age determinations from silicate and opaque alteration minerals indicate Proterozoic mineralization in the ca 2.665 Ga Rankin Inlet Group.

## METALLOGENIC SIGNIFICANCE

Regional-scale brittle to ductile greenschist-grade fault zones, characterized by the Amer, Wager, Snowbird, and Great Slave shear zones, record early Proterozoic movement histories throughout the Churchill Province. In the eastern Churchill Province north of the Meliadine region, two juxtaposed granulite-grade mylonitic events have been recognized - an Archean (ca. 2.59 Ga) event overprinted by an Early Proterozoic

(ca 1.94 Ga) event (Tella et al., 1992, 1993). Tella et al. (1994) suggested that greenschist grade fault zones at relatively higher crustal levels may be temporarily linked to deep-crustal ductile fault zones reactivated during the Early Proterozoic. Metamorphic fluids formed during Proterozoic thermotectonism may be focused along these reactivated fault zones.

Approximately 360 km southwest of the Rankin Inlet Group, Proterozoic thrusts and related faults are the critical elements that provided conduits for Proterozoic auriferous hydrothermal fluids (Miller et al., 1994). Overlapping Archean-Proterozoic gold metalotects in the Churchill Province are comparable to overlapping Archean-Proterozoic gold districts in the Quadrilatero Ferrifero, Brazilian Shield (Scarpelli, 1991; Ladeira, 1991). Reactivated faults or newly formed Proterozoic shear zones such as the Pyke fault zone may focus hydrothermal fluids and form Proterozoic lode gold deposits in Archean rocks. In the Meliadine area, Proterozoic imbricate thrust stacking of Archean and Proterozoic strata (Tella, 1994) and Proterozoic ages from gold-related hydrothermal minerals suggest that the Meliadine Trend is part of the Proterozoic gold metalotect in the eastern Churchill Province.

## ACKNOWLEDGMENTS

A.R. Miller and S. Tella thank Comaplex Minerals Corp. and Cumberland Resources Ltd. for giving access to the property, logistical support, and permission to publish. ARM thanks John Stirling for electron microprobe support and C. Roddick, Geochronology and Paleomagnetism Section, for <sup>40</sup>Ar-<sup>39</sup>Ar analyses. This research is part of the project "Metallogeny of the Churchill Province" and has been funded under this and the 1987-1991 MDA agreements. ARM gratefully acknowledges the careful and constructive review by F. Robert.

## REFERENCES

- Armitage, A.E., Tella, S., and Miller, A.R.**  
1993: Iron-formation-hosted gold mineralization and its geological setting, Meliadine Lake area, District of Keewatin, Northwest Territories; in *Current Research, Part C*; Geological Survey of Canada, Paper 93-1C, p. 187-195.
- Balog, M.J.**  
1993: Studies, compilations, and reinterpretation of the geology of the Meliadine Project; Internal report for Comaplex Minerals Corporation.
- Bannatyne, B.B.**  
1958: The geology of the Rankin Inlet area and North Rankin Nickel Mines Limited, Northwest Territories; MSc. Thesis, University of Manitoba, Winnipeg.
- Barkley, W.A.**  
1991: Structural mapping and analysis, Meliadine River Project; Internal report for Asamera Minerals Inc.  
1992: Report on inspection of selected drill core and reconnaissance regional mapping for the Meliadine Project; Internal report for Asamera Minerals Inc.
- Clark, M.E., Archibald, N.J., and Hodgson, C.J.**  
1986: The structural and metamorphic setting of the Victory gold mine, Kambalda, Western Australia; in *Proceedings of Gold '86*, an International Symposium on the Geology of Gold, (ed.) A.J. Macdonald; Toronto, 1986, p. 243-254.

**Davidson, A.**

1972: The Churchill Province; in *Variations in Tectonic Styles in Canada*, (ed.) R.A. Price and R.J.W. Douglas; Geological Association of Canada, Special Paper 11, p. 381-434.

**Gochnauer, K.M. and Dickson, G.D.**

1991: Report on the 1991 Exploration Results, Meliadine Project, Discovery Area and Eastern Lands, District of Keewatin, Rankin Inlet, N.W.T.; Internal report for Asamera Minerals Inc.

1992: Report on geological mapping; geophysical surveys, litho-geochemistry and diamond drilling results; Internal report submitted for assessment purposes to Indian and Northern Affairs Canada.

**Ladeira, E.A.**

1991: Genesis of gold in Quadrilatero Ferrifero: A remarkable case of permanency, recycling and inheritance - A tribute to Djalma Guimaraes, Pierre Routhier and Hans Ramberg; in *Brazil Gold '91: The economics, geology, geochemistry and genesis of gold deposits*, (ed.) E.A. Ladeira; A.A. Balkema, Rotterdam, p. 11-30.

**Laporte, P.J.**

1983: Geology of the Rankin Inlet area, District of Keewatin, Northwest Territories, NTS 55K/16, parts of 55J/13. K/9; Open File Report 1983-4, Department of Indian Affairs and Northern Development, Canada.

**Miller, A.R., Balog, M.J., Barham, S.A., and Reading, K.L.**

1994: Geology of the Early Proterozoic Gold Metallotect, Central Churchill Structural Province: Hurwitz Group in the Cullaton-Griffin lakes area, Northwest Territories, Canada; in *Current Research 1994-C*; Geological Survey of Canada, p. 135-146.

**Scarpelli, W.**

1991: Aspects of gold mineralization in the Iron Quadrangle, Brazil; in *Brazil Gold '91: The economics, geology, geochemistry and genesis of gold deposits*, (ed.) E.A. Ladeira; A.A. Balkema, Rotterdam, p. 151-159.

**Tella, S.**

1994: Geology, Rankin Inlet (55K/16), Falstaff Island (55J/13), and Marble Island (55J/11); Geological Survey of Canada, Open File 2968, scale 1:250 000.

**Tella, S., Annesley, I.R., Borradaile, G.J., and Henderson, J.R.**

1986: Precambrian geology of parts of Tavani, Marble Island, and Chesterfield Inlet map areas, District of Keewatin: a progress report; Geological Survey of Canada, Paper 86-13, 20 p.

**Tella, S., Schau, M., Armitage, A.E., and Loney, B.C.**

1993: Precambrian geology and economic potential of the northeastern parts of Gibson Lake map area, District of Keewatin, Northwest Territories; in *Current Research, Part C*; Geological Survey of Canada, Paper 93-1C, p. 197-208.

**Tella, S., Schau, M., Armitage, A.E., Seemayer, B.E., and Lemkow, D.**

1992: Precambrian geology and economic potential of the Meliadine Lake-Barbour Bay region, District of Keewatin, Northwest Territories; in *Current Research, Part C*; Geological Survey of Canada, Paper 92-1C, p. 1-11.

**Tella, S., Schau, M., Roddick, J.C., and Mader, U.**

1994: Significance of juxtaposed mid-crustal mylonite zones of contrasting ages, Uvauk Complex, Churchill Structural Province, District of Keewatin, N.W.T., Canada; *Abstracts Geological Society of America, Abstracts with Programs*, v. 26, 7, p. A135.

**Wright, G.M.**

1967: Geology of the southeastern barren grounds, parts of the Districts of Mackenzie and Keewatin; Geological Survey of Canada, Memoir 350, 91 p.

---

Geological Survey of Canada Project 810024



# Stratigraphic setting of semiconformable alteration in the Spi Lake area, Kaminak greenstone belt, Churchill Province, Northwest Territories

A.R. Miller and S. Tella<sup>1</sup>

Mineral Resources Division

*Miller, A.R. and Tella, S., 1995: Stratigraphic setting of semiconformable alteration in the Spi Lake area, Kaminak greenstone belt, Churchill Province, Northwest Territories; in Current Research 1995-C; Geological Survey of Canada, p. 175-186.*

---

**Abstract:** The Spi Lake Zn-Cu-Pb-Ag prospect is a proximal volcanic-hosted volcanogenic massive sulphide within ca 2.69 Ga tholeiitic-calc-alkaline volcanic rocks of the Kaminak greenstone belt. The volcanic rocks were deformed and metamorphosed under lower greenschist facies conditions. The prospect consists of irregular pods of massive and disseminated galena-chalcopyrite-sphalerite in rhyolite breccia and tuff. Two alteration zones are recognized at different stratigraphic levels in the Spi Lake area. A discordant sericite-chlorite alteration transects host rock rhyolite and tuff, underlying porphyritic rhyolite flows, and nearby tonalite. Semiconformable quartz-chlorite-epidote-albite alteration overprints stratigraphically higher basaltic pillow lava, interflow sediments and andesitic breccia. The semiconformable alteration zones stratigraphically above the Spi Lake base metal prospect suggests that stacked alteration zones are present and massive sulphide exploration might be focused upsection, to the west and southwest.

**Résumé :** Le prospect de Zn-Cu-Pb-Ag de Spi Lake est un massif sulfuré volcanogène proximal logé dans des volcanites calco-alkalines et tholéiitiques d'environ 2,69 Ga qui faisaient partie de la ceinture de roches vertes de Kaminak. Les volcanites ont été déformées et métamorphosées dans des conditions caractéristiques du faciès des schistes verts inférieur. Le prospect est composé d'amas irréguliers de galène-chalcopyrite-sphalérite sous forme massive et disséminée dans de la brèche rhyolitique et du tuf. Deux zones d'altération s'observent à différents niveaux stratigraphiques dans la région du lac Spi. Une zone d'altération discordante à séricite-chlorite recoupe la rhyolite et le tuf hôtes, des coulées sous-jacentes de rhyolite porphyrique et une tonalite adjacente. Une altération semi-concordante de quartz-chlorite-épidote-albite se surimprime stratigraphiquement à des laves de basalte en coussins plus élevées, à des sédiments intercalés à des coulées et à une brèche andésitique. Des zone d'altération semi-concordantes qui se trouvent stratigraphiquement au-dessus du prospect de métaux communs de Spi Lake laissent supposer que des zones d'altération superposées sont présentes et que la prospection des sulfures massifs pourrait être dirigée vers le haut du profil, vers l'ouest et le sud-ouest.

---

<sup>1</sup> Continental Geoscience Division



**INTRODUCTION**

Understanding the geometry of alteration zones associated with volcanogenic massive sulphide deposits will result in better models for their formation and provide a more comprehensive framework with which to explore for this ore deposit type. It has long been recognized that proximal volcanogenic massive sulphide deposits are commonly underlain by a discordant footwall alteration pipe (Franklin et al., 1981). In the late 1970s to early 1980s, the identification of semiconformable alteration zones at variable depths below massive sulphide deposits provided new insights into the source of metals and sulphur for these deposits generated from hydrothermal convection systems, and most importantly into the type of reactions and physiochemical conditions for these reservoir rocks (Hodgson and Lydon, 1977; Franklin et al., 1981; Gibson et al., 1983; Galley, 1993). Semiconformable alteration beneath, and associated with, massive sulphide deposits characterized by silicification, epidotization, carbonatization, and albitization have been identified within Archean massive sulphide districts such as the Matagami and Noranda regions (MacGeehan, 1978; Gibson et al., 1983) and the Proterozoic Snow Lake districts (Galley et al., 1993; Skirrow and Franklin, 1994).

**OBJECTIVE AND SCOPE OF THE PROJECT**

This project was initiated following a reinterpretation of lithological and mineralogical descriptions presented in Barrett (1981). In the Spi Lake area pillowed felsic flows were described near the Spi Lake Zn-Cu-Pb-Ag prospect in the Archean Kaminak greenstone belt (Fig. 1). The reinterpretation of Barrett's data suggest pervasive alteration of mafic volcanic rocks and the presence of a semiconformable alteration zone in the area of the Spi Lake prospect.

The area around the Spi Lake prospect was remapped in order to address the following questions: 1) are these rocks altered? 2) what are the alteration assemblages? 3) if altered, what was the protolith? and 4) what is the geometric and stratigraphic relationship of this alteration to the Spi Lake massive sulphide prospect?

**ARCHEAN GREENSTONE BELTS, CHURCHILL PROVINCE**

Archean granite-greenstone belts in the central and north-eastern segments of the Churchill Province are subdivided into three time-lithostratigraphic sequences, on the basis of rock association and/or age of volcanism (Fig. 1). Greenstone belt nomenclature north of the Snowbird Tectonic Zone follows that of Frisch (1982), Schau (1982), and

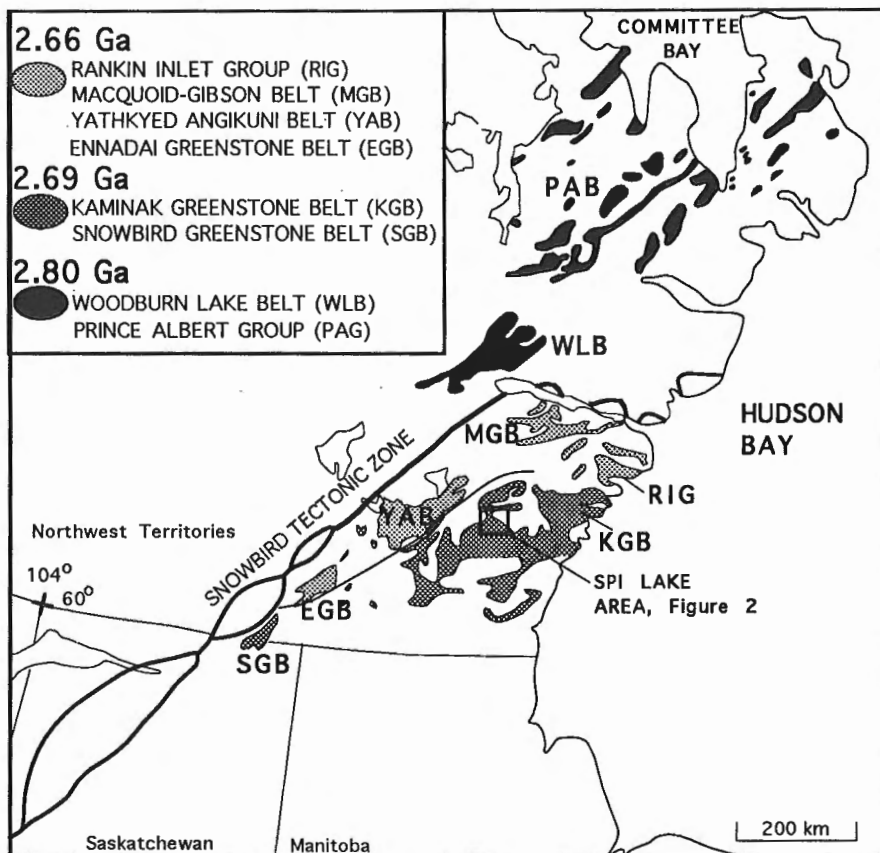


*Figure 1.*  
Distribution of Archean greenstone belts in the Churchill Province.

Henderson et al. (1991). East of the Snowbird Tectonic Zone, a subdivision is proposed for the two northeast-trending Archean supracrustal belts.

The southern belt, termed the Rankin-Ennadai greenstone belt (Ridler, 1973, 1974), is the best understood and, as a consequence, other greenstone belts have been correlated with the Kaminak Group or Rankin-Ennadai greenstone belt. The term Rankin-Ennadai greenstone belt refers to three unconnected Archean greenstone belts in the Rankin Inlet, Kaminak Lake, and Ennadai Lake areas. Because of the lack of continuity between these segments and the recent recognition of two ages of volcanism, the term Rankin-Ennadai greenstone belt should be discontinued. Each individual granite-greenstone entity should be referred to by a prominent geographic name (i.e. Kaminak greenstone belt; Fig. 1).

North of the Snowbird Tectonic Zone, the ca 2.79 Ga Woodburn Lake and Prince Albert groups are characterized by mafic-ultramafic volcanic rocks, shallow water quartzose arenite, and minor felsic volcanic rocks (Frisch 1982; Schau 1982; Henderson et al., 1991; Roddick et al., 1992). East of the Snowbird Tectonic Zone, two multicyclic greenstone belts are recognized: the ca 2.69 Ga Rankin-Ennadai greenstone belt (Mortensen and Thorpe, 1987; Park and Ralser, 1992) and the ca 2.665 Ga Rankin Inlet Group (Tella, 1994; Fig. 1).

The Kaminak greenstone belt, the largest and most continuous of the ca 2.69 Ga supracrustal sequences, extends from Pistol Bay on the Hudson Bay coast southwestward for approximately 480 km. The Snowbird greenstone belt is an equivalent Archean supracrustal sequence to the southwest (Fig. 1; Taylor, 1963; Chiarenzelli and Macdonald, 1986).

The youngest greenstone terrane lies north and northwest of the Kaminak and Ennadai belts. These belts define a broad arc that extends from Ennadai Lake to Chesterfield Inlet. The best understood of the three is the ca 2.665 Ga Rankin Inlet Group northeast of the Kaminak belt (Tella et al., 1986; Tella, 1994). The east- to southeast-trending MacQuoid-Gibson belt, north of the Rankin Inlet Group, is interpreted to be a higher grade equivalent of the Rankin Inlet Group (Tella et al., 1992, 1993). The Yathkyed-Angikuni (Eade, 1986) and Ennadai Lake (Eade, 1971) belts are the southwestward extension of the ca 2.66 Ga greenstone terrane.

Both the ca 2.69 and ca 2.66 Ga belts display characteristics common to mid-Archean granite-greenstone terranes: multicyclic mafic to felsic volcanic piles, intercalated clastic and chemical sedimentary rocks, and composite tonalitic to granitic plutons. These features and the presence of Archean volcanogenic massive sulphide occurrences and structurally-controlled lode gold deposit types in the Kaminak greenstone belt have drawn comparisons to the metal-rich Abitibi belt, Superior Province (Ridler, 1973, 1974; Franklin and Thorpe, 1982).

Based on these plutonic and lithostratigraphic similarities, the ca 2.69 and ca 2.66 Ga greenstone belts of the central Churchill Province are regarded as favourable environments for volcanic massive sulphide deposits. Prospects and deposits are present in greenstone belts of both

ages and are associated with felsic volcanic centres. Examples include prospects near Heninga and Spi lakes in the ca. 2.69 Ga Kaminak belt (Ridler, 1974; Franklin and Thorpe, 1982) and the ca 2.66 Ga belts, Rochon Lake prospect in the Ennadai Lake belt (Franklin and Thorpe, 1982), and Sandhill prospect in the MacQuoid-Gibson belt (Armitage et al., 1995).

## REGIONAL GEOLOGICAL SETTING

This overview highlights aspects of the geology of the Spi Lake area. The reader is referred to the following references for additional details (Davidson, 1970; Ridler, 1973, 1974; Ridler and Shilts, 1974; Laporte et al., 1981; Irwin, 1993). Felsic volcanic rocks in the Spi Lake area are part of a more extensive felsic volcanic accumulation that extends up to 35 km southwestward into the Heninga Lake area (Davidson, 1970; Bell, 1971). The present study area (Fig. 2) is located near the southwestern contact of the composite northeast-trending Kaminak batholith. This batholith, approximately 60 km long and 15 km wide, parallels the trend of the Kaminak greenstone belt.

Davidson (1970) identified two unconformable sedimentary sequences north and north-northeast of Spi Lake, both of which rest unconformably on volcanic rocks. The belt of north-trending metasedimentary rocks has been previously assigned to different ages - Archean (Davidson, 1970) and Aphebian (Laporte et al., 1981; Irwin, 1993). These sedimentary rocks are better correlated with widely distributed and fault-bounded remnants of late Archean arenaceous and conglomeratic strata referred to as the Mackenzie Lake metasediments (Davidson, 1970), Montgomery Lake Group (Eade, 1974), and as arenaceous sediments exposed north of Heninga Lake (Miller and Cavell, 1993). They overlie Archean meta-volcanic and volcanoclastic rocks and were intruded by late Archean plutons (P.A. Cavell, pers. comm., 1994).

Proterozoic tectono-thermal events are best recorded by the pre-Hurwitz Group Kaminak diabase dyke swarm (Davidson, 1970). Volcanic and plutonic rocks in the Spi Lake area were metamorphosed to greenschist grade during the Archean and subsequently overprinted by Proterozoic greenschist grade, metamorphism.

## GEOCHRONOLOGY OF THE KAMINAK GREENSTONE BELT

Several felsic volcanic centres have been identified within the Kaminak belt, most notably thick accumulations at Quartzite and Spi lakes (Davidson, 1970; Ridler, 1973). Zircon geochronology on rhyolitic rocks hosting the Spi Lake massive sulphide prospect have yielded an age of  $2697 \pm 1.4$  Ma (Mortensen and Thorpe, 1987).

The deformed volcano-sedimentary sequence in the Spi Lake area is part of a widespread felsic volcanic sequence that was intruded by three composite circular to lobate intrusions, informally termed the Kaminak, Turquetil and Heninga batholiths (Ridler, 1973). Emplacement ages range from

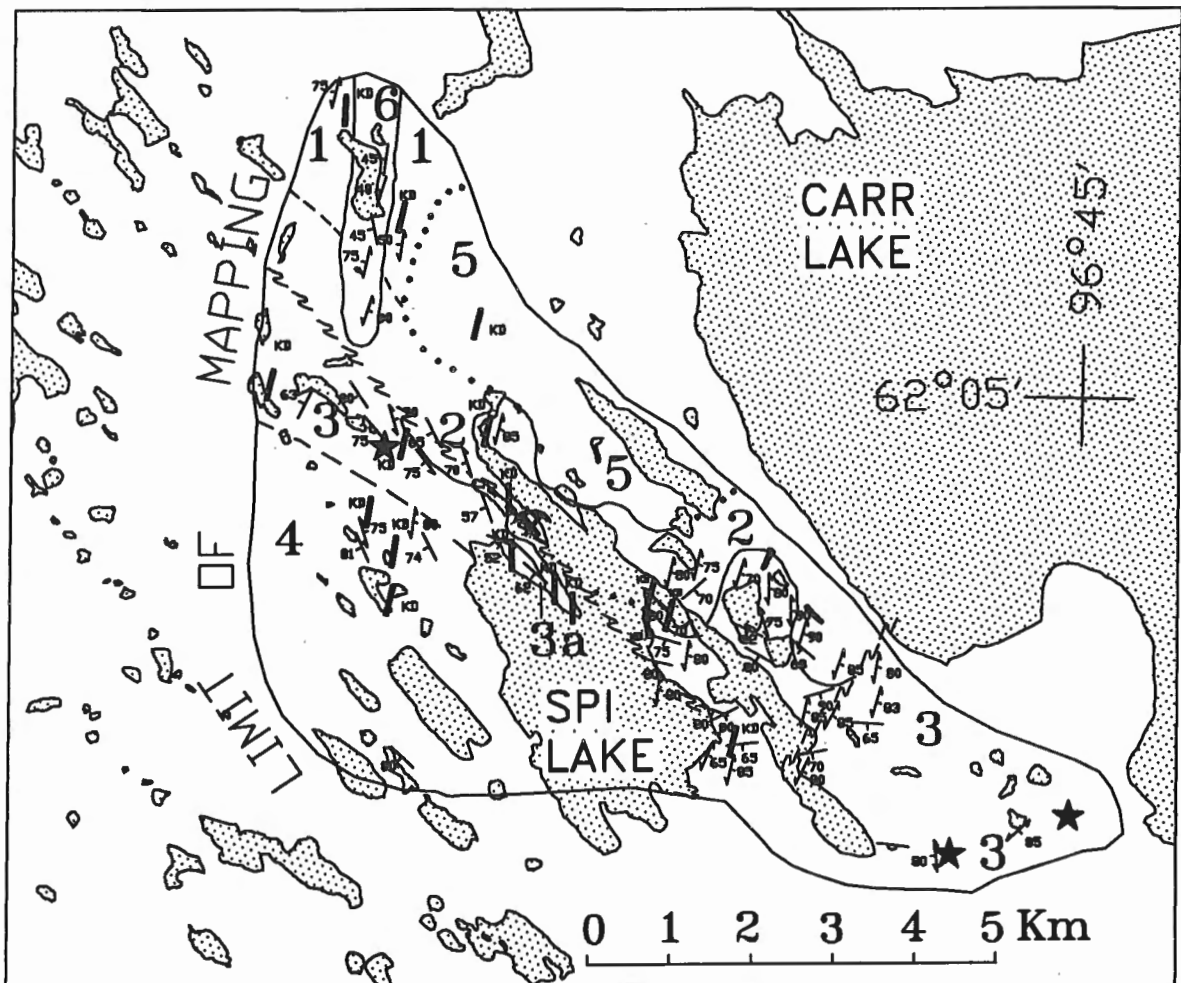
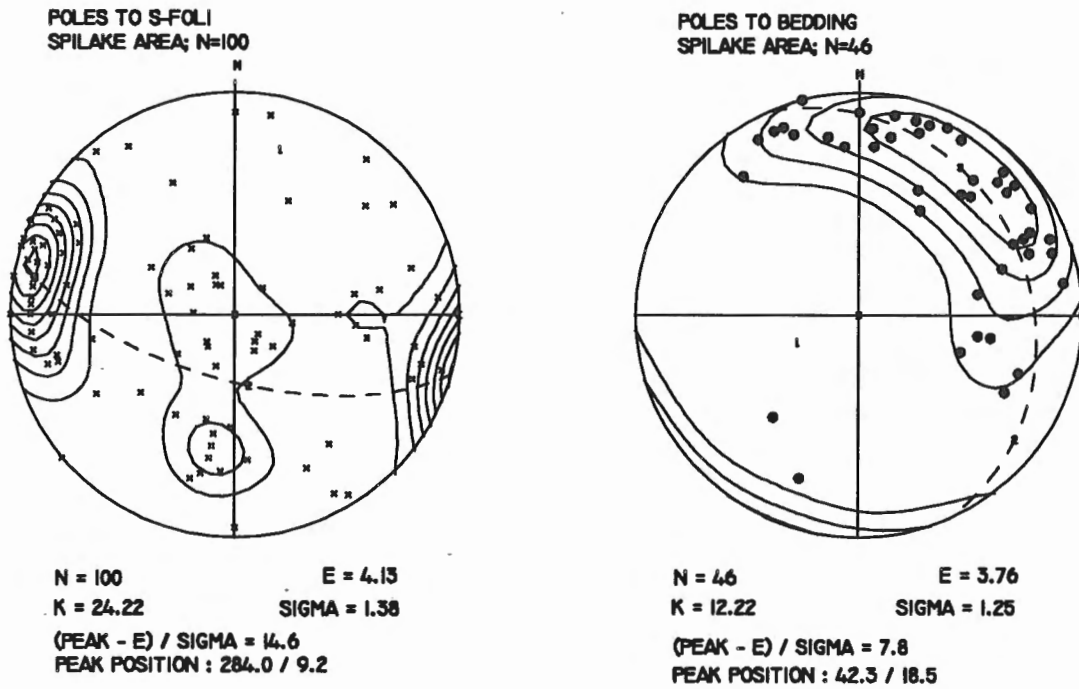


Figure 2. Geology of the Spi Lake area, Kaminak greenstone belt.

2680 to 2700 ± 11 Ma, In particular an age of ca 2700 Ma for the Kaminak batholith (Cavell et al., 1992; Cavell, pers. comm., 1994) overlaps ages from felsic volcanic rocks at Spi Lake. This implies some plutons in the Kaminak belt are synvolcanic. This temporal relationship between volcanism and plutonism appears to be a critical element in the identification and evaluation of a granite-greenstone terrane as a potential host for volcanogenic massive sulphide deposits.

## GEOLOGY OF THE SPI LAKE AREA

### Archean

#### Volcanic and volcanoclastic rocks (units 1 to 4)

The volcanic stratigraphy in the study area has been subdivided into four lithological units that are upright and dip steeply to the southwest (Fig. 2). The lowest stratigraphic unit, unit 1, is poorly exposed in the northern part of the area. It comprises sheared mafic volcanic flows and was intruded by tonalite, unit 5, and overlain by conglomerate, unit 6.

Unit 2 is a heterolithic felsic volcanic unit that hosts the Spi Lake Ag-Pb-Cu-Zn massive sulphide prospect. It comprises massive quartz- and feldspar-phyric rhyolite flows, well bedded rhyolitic to dacitic agglomerate, lapilli and crystal tuff, and minor basalt flows.

A felsic breccia hosts the Spi Lake base-metal-rich prospect. The diversity in texture and morphology of monolithic breccia clasts, bedding attitudes, and megascopic geometry of felsic blocks suggests a felsic dome. The gossan lies at or

near the stratigraphic top of unit 2. The sulphide-bearing outcrop is composed of angular blocks, up to 5-8 m, of massive dacite to rhyolite, well bedded tuff, and pyritic siliceous exhalite. Bedding strike and dip are variable over the outcrop. This contrasts with attitudes in the laterally equivalent overlying stratigraphic units. Semimassive to massive galena-chalcopyrite-sphalerite-pyrite-pyrrhotite, locally banded, occurs as pods and disseminations along the north-east side of the outcrop. On fresh surface, all rocks are green due to moderate chlorite alteration.

Megascopic and macroscopic textures are well preserved throughout except in local areas where well developed D<sub>1</sub> axial planar schistosity and shearing in fault zones has destroyed primary features. In addition, hydrothermal alteration interpreted as synvolcanic overprints specific portions of the lower volcanic stratigraphy (see "Hydrothermal alteration").


The Spi Lake rhyolite (unit 2) is overlain by a mafic volcanic sequence, unit 3. Based on well constrained facing directions, a generalized stratigraphic column through unit 3 consists of massive flows with interflow mafic tuff at the base, which grade upward into polyolithic mafic breccia, pillow basalt, andesitic pillow breccia, and minor mafic tuff and laminated chert. Minor rhyolite tuff and fine laminated chert, unit 3a, are intercalated with massive mafic flows immediately west and stratigraphically above the Spi Lake prospect. Polyolithic mafic breccia, interpreted as a debris flow deposit, overlies sulphide-bearing tuff and massive quartz-phyric rhyolite just southeast of the Spi Lake gossan. This breccia extends southeastward onto a small island in Spi Lake (designated island 'A' in Ridler, 1974). Here it contains small

massive sulphide clasts, presumably derived from the Spi Lake massive sulphide. The assumed lateral equivalents to the southeast and northwest are basaltic flows, pillow lava, and pillow breccias. Barrett (1981) described two localities of pillowed rhyolite within these laterally equivalent rocks types. Our observations at these two localities indicate that these felsite rocks are pervasively altered basaltic pillow lavas, breccia, and interflow sediments.

Approximately 2 km northwest of the Spi Lake prospect, extensive silicification is superimposed on perfectly preserved, unstrained pillow and massive basalt, interflow mafic tuff, and chert. Alteration is confined to pillowed basalt flows and interflow sediments on the western side of this outcrop area whereas massive flows on the eastern, stratigraphically lower, portion of the same outcrop are unaltered. Alteration is indicated by a distinctive white- to grey-weathering hue in amygdaloidal pillow basalt (Fig. 3) and pink to greenish-pink hue and conchoidal fracture habit in laminated interflow sediments. The freshly broken surface of altered basalt has a mottled texture formed by irregular shaped, dark to light green and creamy white blotches.

#### Legend for Figure 2.

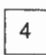
##### PROTEROZOIC

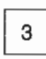
 Kaminak diabase/gabbro (K<sub>D</sub>)

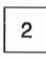
##### ARCHEAN

 Tonalite cobble conglomerate, minor feldspathic quartzite

 Tonalite

 Pillowed and massive basalt, polyolithic volcanoclastic debris flows.

 Pillow basalt and breccia, massive basalt flows, mafic tuff and laminated mafic tuff-ash; 3a laminated rhyolite tuff, chert.

 Quartz and quartz-feldspar phyric rhyolite, rhyodacitic agglomerate, lapilli and crystal tuff, chert, minor basalt.

 Massive basalt flows

 Semiconformable alteration zone  foliation, bedding, pillows

--- ····· Contacts; inferred, assumed  Fault Zone

 Spi Lake Massive Sulphide

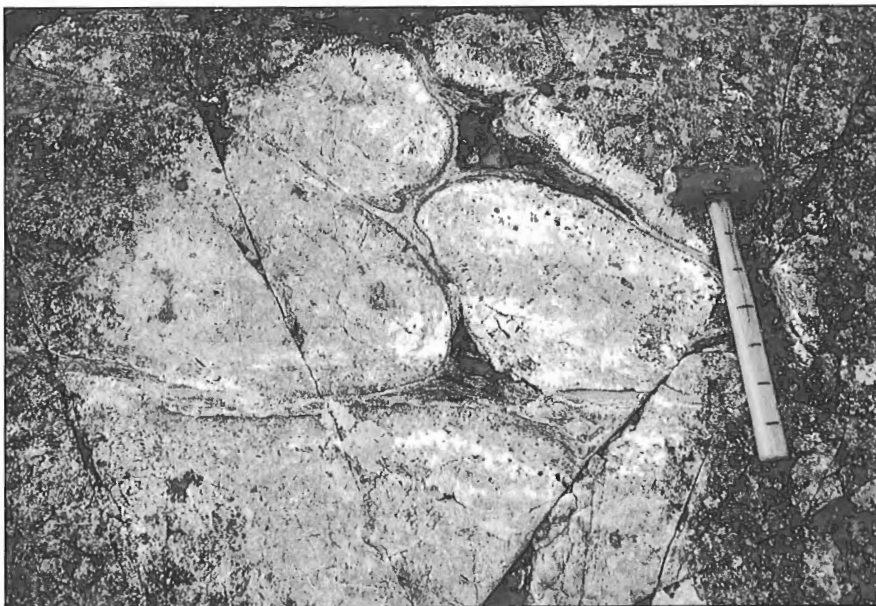


**Figure 3.**  
*Altered amygdaloidal pillow lava (unit 3), northwest of Spi Lake.*

The second locality is approximately 7 km to the southeast along strike of the Spi Lake prospect, and is approximately 1 km above the contact with felsic volcanic rocks of unit 2. This well developed alteration zone is at least 1.5 km long and 0.75 km wide and overprints a monolithic fragmental pillow breccia that weathers ash white. In the eastern part of this zone, fragments are on average 10-15 cm and display equant rounded to blocky rounded form (Fig. 4). The western part of this outcrop area contains oblong fragments up to 40 cm long amongst smaller breccia fragments. Pillow forms with selvages are recognizable, and southwest-facing directions are consistent with directions elsewhere in the study area. This unit resembles a felsic breccia, however the presence of pillow fragments suggests that this thick breccia unit is the lateral equivalent of andesitic flows along strike. A variation in fragment colour occurs from south to north across this breccia deposit, with ash white in the south changing to grey green in the north. This breccia pile overlies unaltered green to dark green massive basalt and pillow breccia.

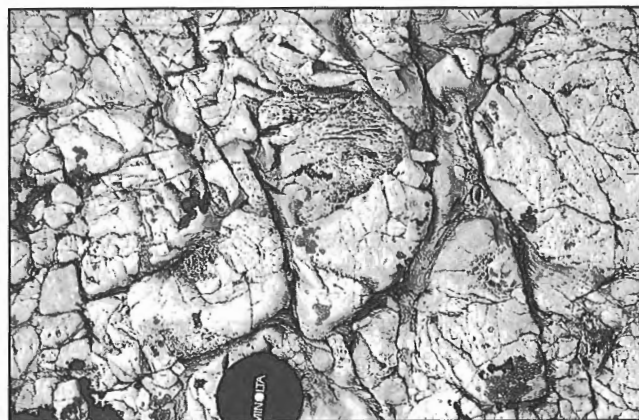


**Figure 4** *Altered pillow breccia (unit 3), southeast of Spi Lake.*

Rocks in the uppermost lithostratigraphic sequence (unit 4) consist of polyolithic breccias, with minor basaltic flows. These breccias are interpreted as debris flows based on the presence of basalt, rhyolite-dacite and chert clasts with angular irregular to rounded elongate shapes, and massive to graded bedforms (Fig. 5). The mineral assemblage, carbonate-sericite-actinolite-chlorite, from flows within this unit is consistent with regional metamorphic patterns (Davidson, 1970; Eade, 1980).

#### **Tonalite - Kaminak batholith (unit 5)**

The northeastern portion of the area is underlain by medium grained grey to very pale green-grey leucocratic, equigranular tonalite (unit 5), which is intrusive into unit 2 porphyritic felsic volcanic rocks. A well developed intrusive contact zone, up to tens of metres wide, is composed of an intersecting network of fine- to coarse-grained tonalite veins and dykes.



**Figure 5.** *Graded debris flow (unit 4).*

The tonalite is composed of equigranular quartz and plagioclase with minor intergranular chloritized biotite. Numerous alteration textures such as replacement of plagioclase by sericite-epidote-carbonate and of chlorite by epidote-carbonate, and the presence of disseminated pyrite, chalcopyrite, and trace sphalerite, titanite and tourmaline, suggest that the intrusion has undergone hydrothermal alteration, possibly coeval with hydrothermal alteration of the overlying volcanic pile.

### Conglomerate (unit 6)

The youngest lithological unit (unit 6) is a clast-supported cobble- to pebble-conglomerate that unconformably overlies units 1 and 2. Fine grained arenaceous sediments at the base of the conglomerate are in contact with sheared mafic volcanic rocks. Tonalite clasts, compositionally and texturally identical to the Kaminak batholith (unit 5) constitute 90 per cent of this conglomerate. The rest includes amygdaloidal and massive mafic volcanic clasts similar to underlying mafic volcanics and tuffs (Fig. 6). The conglomerate matrix is composed of finer grained lithic clasts of tonalite and coarse- to fine-grained quartz, feldspar, and sericite.

The absence of Proterozoic Kaminak dyke clasts, the presence of north-trending penetrative planar fabric similar to that noted in the underlying volcanic sequence, and similarities to other conglomerate-arenite sequences in the Kaminak greenstone belt suggest a late Archean age for this unit rather than a previously assigned early Proterozoic age (Laporte et al., 1981; Irwin, 1993).

## Proterozoic

### Kaminak dykes

The Spi Lake area lies within a broad 20 km wide northeast-trending, biotite-grade greenschist facies Proterozoic metamorphic zone. This belt overlaps folded Hurwitz Group strata in the Kaminak Lake map area. Davidson (1970) noted that the north- to north-northeast-trending, regionally pervasive Kaminak diabase dyke swarm was deflected to the northeast in areas affected by higher Proterozoic strain and metamorphism. In the Spi Lake area Kaminak dykes trend 000-020° and were not affected by significant Proterozoic tectonism. Locally sheared dyke margins and adjacent mafic metavolcanic rocks are commonly the loci for discontinuous pyrite- and chalcopyrite-bearing quartz veins. Dykes, up to 20-30 m in width, anastomose and incorporate rafts of country rock. They cut all Archean rock units and contain xenoliths of granite, granodiorite, and tonalite, phases assumed to be part of the Kaminak batholith.

## STRUCTURE

Preservation of graded bedding, scour channels, amygdaloidal flow tops, and pillow structures in each stratigraphic unit indicates that volcanic stratigraphy in the Spi Lake area is upright and faces southwest with moderate to steep dips (Fig. 2). Bedding ( $S_0$ )-cleavage ( $S_1$ ) relationships (Fig. 7) indicate the stratigraphic sequence in the Spi Lake area forms part of the western limb of a 70° southwest-plunging anticline (Fig. 2). The axial trace of this fold lies east of Spi Lake.

Two directions of late subvertical faults were recognized, northwest and east-northeast. The east-northeast fault is characterized by a wide zone of chlorite and quartz-sericite schists

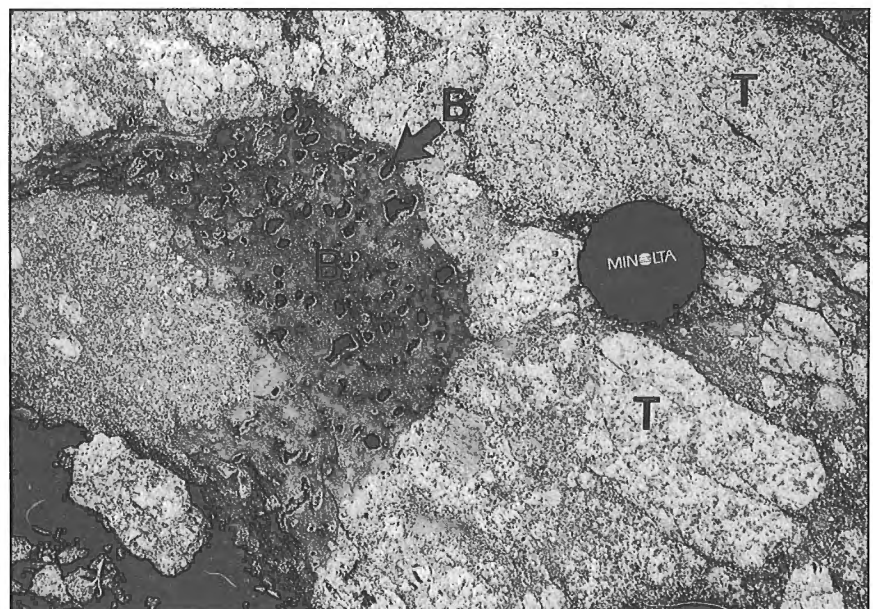


**Figure 6.**

Tonalite (T) and amygdaloidal basalt (B) clasts in conglomerate (unit 6).

and locally contains fine grained disseminated pyrite. The northwest-trending fault at the contact of units 2 and 3 is defined by a narrow zone of pyrite-pyrrhotite-bearing sericitic schist (Fig. 2).

## HYDROTHERMAL ALTERATION

Two types of alteration zones were recognized in the Spi Lake area, discordant and semiconformable. This subdivision is based on geometry and stratigraphic position relative to the Spi Lake massive sulphide prospect. Discordant footwall alteration is present in felsic flows and tuffs that contain the prospect, and in underlying porphyritic rhyolite flows and tonalite northeast of the prospect. Semiconformable alteration, not directly related to the Spi Lake prospect, is present in unit 3 basaltic pillow lava, mafic tuff, and andesitic pillow breccia that lie stratigraphically above and laterally to the prospect.

### Discordant alteration

Sulphide-bearing hydrothermally altered rocks that host the Spi Lake prospect consist of sericite+epidote+chlorite±carbonate. This assemblage is typical of metamorphosed hydrothermally altered rocks at greenschist grade and is consistent with greenschist facies assemblages elsewhere in the study area. Northeast of the prospect, rhyolite and tonalite are replaced by anomalously high modal abundances of fine- to medium grained epidote+sericite+chlorite±carbonate. Altered tonalite also contains titanite intergrown with medium grained epidote+chlorite, mantling rutile/anatase and disseminated base metal sulphides. Both mineralogy and stratigraphic position suggest that the area northeast of the prospect is part of the discordant alteration zone.

### Semiconformable alteration

Mottled textures observed in hand specimens from the alteration zone in pillow basalt northwest of Spi Lake result from the uneven distribution of ultrafine grained, <0.1 mm, sericite+chlorite+epidote+quartz+albite+ rutile/anatase and disseminated chalcopyrite and pyrrhotite. In places, this assemblage totally replaces primary textures; however plagioclase crystallites are preserved in areas of weaker alteration. Interflow-laminated sediments, resembling chert, consist of epidote+chlorite+actinolite+albite with subordinate quartz+sericite.

Southwest of Spi Lake, the metamorphosed alteration assemblage in white silicified pillow breccia is quartz-albite+epidote+carbonate+chlorite+rutile/anatase. Altered rock consists of albite phenocrysts in a fine grained groundmass of quartz and albite. Sericite+carbonate+epidote replace the groundmass and phenocrysts. This texture is similar to altered silicified andesite of the upper Amulet formation, Noranda (Gibson et al., 1983, Fig. 16).

## GEOCHEMISTRY

A cation plot of whole rock data from Ridler (1974) shows a trend line extending from the komatiite field along a line that straddles the tholeiitic-calc-alkalic intersection (Fig. 8). The same general trend is shown by analyses from this study; however, this trend lies within the calc-alkalic field (Fig. 9). The Zr/Y range of 6.48 to 13.5 for the latter sample set is consistent with a calc-alkaline differentiation trend (Barrett and Maclean, 1994). Higher than normal Zr abundances in least altered basalt, units 3 and 4, may be due to the calc-alkalic differentiation trend (Table 1).

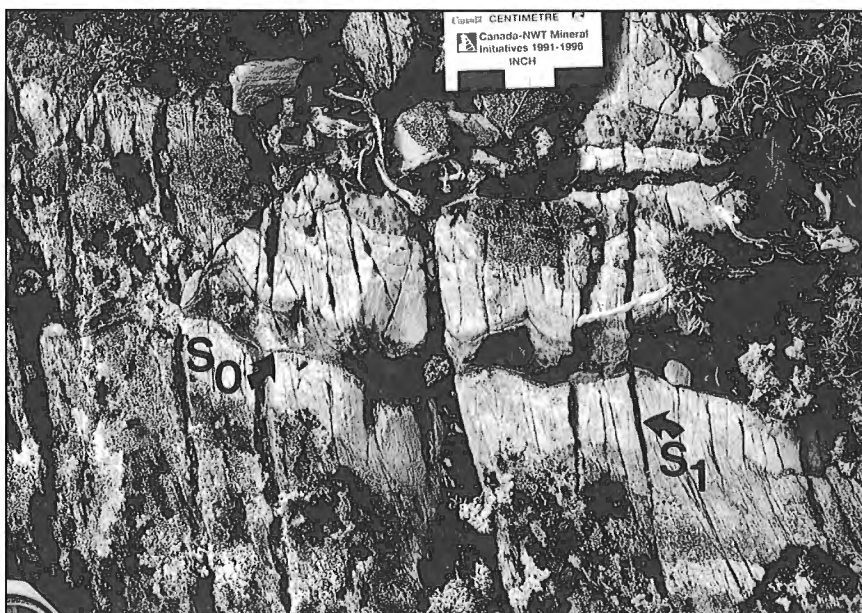


Figure 7.  
*S<sub>0</sub>-S<sub>1</sub> relationship in rhyolitic tuff (unit 2).*

Table 1. Major and trace element abundances for rocks, Spi Lake area.

SAMPLES	Northwest Alteration Zone, Unit 3			Southeast Alteration Zone, Unit 3				Unaltered Unit 2		Unaltered Unit 3
	94MYAA22-3	94MYAA23-1	94MYAA57-6	94MYAA49-1	94MYAA49-3	94MYAA50-1	94MYAA51-1	94MYAA64-2	94MYAA55-1	
SiO2	62.70	55.80	59.30	73.70	68.70	74.50	73.90	74.40	66.90	
Al2O3	17.40	22.10	19.40	13.60	15.60	12.60	13.30	13.00	12.50	
Fe2O3	5.36	4.76	5.88	2.53	1.44	1.09	0.94	2.29	4.61	
CaO	3.44	4.70	3.80	1.10	2.81	2.21	2.78	1.91	4.13	
MgO	1.80	1.57	1.68	1.15	0.36	0.29	0.22	0.57	2.53	
Na2O	5.52	4.90	5.24	4.56	4.65	5.14	4.97	2.07	3.51	
K2O	1.10	2.60	1.81	0.58	1.20	0.58	0.84	3.08	0.85	
TiO2	0.96	1.17	1.10	0.42	0.45	0.35	0.35	0.28	0.40	
P2O5	0.11	0.17	0.13	0.15	0.09	0.09	0.09	0.03	0.09	
MnO	0.10	0.14	0.12	0.01	0.01	0.04	0.05	0.04	0.08	
Cr2O3	0.02	0.07	0.02	<0.01	<0.01	<0.01	<0.01	<0.01	<0.01	
LOI	1.85	2.25	1.95	2.10	3.15	2.35	2.90	2.35	4.75	
SUM	100.36	100.23	100.43	99.9	98.46	99.24	100.34	100.02	100.35	
V	213.00	339.00	223.00	60.00	63.00	22.00	31.00	8.00	68.00	
Cu	32.00	18.20	48.00	20.60	28.40	12.60	16.60	12.10	29.00	
Zn	74.40	120.00	64.50	46.10	28.40	34.20	26.00	26.20	91.90	
Pb	<2	21.00	<2	<2	<2	<2	<2	<2	<2	
Ag	0.30	0.10	0.40	<0.1	0.20	0.50	0.30	<0.1	<0.1	
Ni	112.00	134.00	101.00	26.00	9.00	<1	6.00	<1	62.00	
Co	33.00	27.00	27.00	13.00	8.00	3.00	2.00	3.00	15.00	
Sr	137.00	195.00	162.00	103.00	180.00	119.00	149.00	57.90	104.00	
Ba	24.00	71.00	45.00	14.00	33.00	3.00	20.00	47.00	13.00	
Th	260.00	400.00	359.00	140.00	252.00	165.00	213.00	1540.00	128.00	
U	1.00	NA	NA	NA	NA	1.70	NA	NA	NA	
Nb	0.40	NA	NA	NA	NA	0.50	NA	NA	NA	
Zr	4.00	7.00	5.00	5.00	7.00	3.00	3.00	16.00	3.00	
Y	50.50	89.70	51.70	131.00	151.00	105.00	114.00	301.00	111.00	
La	11.60	16.90	14.10	8.80	8.50	5.20	5.20	37.50	8.20	
Ce	14.70	15.30	9.80	17.90	16.30	7.80	12.40	39.10	12.40	
Nd	16.70	NA	NA	NA	NA	19.70	NA	NA	NA	
Sm	11.00	NA	NA	NA	NA	8.90	NA	NA	NA	
Eu	3.00	NA	NA	NA	NA	2.00	NA	NA	NA	
Gd	0.88	NA	NA	NA	NA	0.56	NA	NA	NA	
Tb	2.80	NA	NA	NA	NA	1.60	NA	NA	NA	
Dy	0.50	NA	NA	NA	NA	0.20	NA	NA	NA	
Ho	2.80	NA	NA	NA	NA	1.10	NA	NA	NA	
Er	0.53	NA	NA	NA	NA	0.20	NA	NA	NA	
Tm	1.50	NA	NA	NA	NA	0.50	NA	NA	NA	
Yb	0.20	NA	NA	NA	NA	-0.10	NA	NA	NA	
Lu	1.50	NA	NA	NA	NA	0.40	NA	NA	NA	
Fr	0.21	NA	NA	NA	NA	0.06	NA	NA	NA	
	2.30	NA	NA	NA	NA	2.20	NA	NA	NA	

NA = not analyzed



High Na<sub>2</sub>O contents (4.9 to 5.2 wt %) and low MgO contents (1.5 to 1.8 wt %) suggest spilitization of altered pillow basalt northwest of Spi Lake (Table 1). In Figure 9, these analyses are shifted toward more felsic rock types when compared to least altered protolith. Southeast of Spi Lake, altered breccia exhibits high SiO<sub>2</sub> and Na<sub>2</sub>O, low K<sub>2</sub>O, and higher TiO<sub>2</sub>, compared to unaltered unit 2 rhyolite (Table 1). In Figure 9, these analyses plot within rhyolite and dacite fields. This pseudo calc-alkaline trend as defined by the shift between unaltered and altered rocks is common in volcanogenic massive sulphide camps (MacGeehan and MacLean, 1980) and is evidence for broad-scale hydrothermal alteration resulting from regional seawater convection systems (Gibson, 1989). An incompatible element plot of a representative analysis from each alteration zone shows 20-30x chondrite values, shallow negative slopes and minor heavy rare-earth element depletion (Fig. 10). The protolith for each alteration zone is interpreted to have been a mafic rock: basalt in the northwest zone and possibly andesite in the southeast zone.

**CONCLUSIONS**

Based on widespread sulphide-bearing exhalites associated with felsic volcanic centres, Ridler (1974) stated that the Kaminak greenstone belt should possess a high potential for volcanogenic massive sulphide deposits, similar to the Abitibi belt. This study has recognized several new aspects of magmatic-hydrothermal evolution in the Spi Lake area that are critical in assessing this belt for volcanogenic massive sulphide deposits. Rocks with komatiitic affinities are present and their distribution may be more widespread in thick mafic volcanic sequences than the few known occurrences (Eade, 1974). The overlap in isotopic dates between the Kaminak batholith and felsic volcanic rocks suggests that the former is a synvolcanic pluton. Base metal occurrences in marginal phases of the batholith and adjacent volcanic rocks (Davidson, 1970; Miller, unpub.

data) are characteristic of synvolcanic plutons. Furthermore the calc-alkaline trend in the volcanic sequence suggests a high potential to host base metal deposits (Campbell et al., 1981; MacGeehan and MacLean., 1980).

The Spi Lake prospect, hosted in massive dacitic to rhyolitic flows and tuff, and underlying volcanic rocks to the northeast are overprinted by a discordant alteration zone. Semiconformable alteration zones developed on basaltic to andesitic volcanic rocks and interflow sediments are stratigraphically above and laterally distant from the prospect. The presence of semiconformable alteration suggests that hydrothermal alteration systems may be stacked in the Spi Lake area, and that massive sulphide exploration might be focused upsection, to the west and southwest.

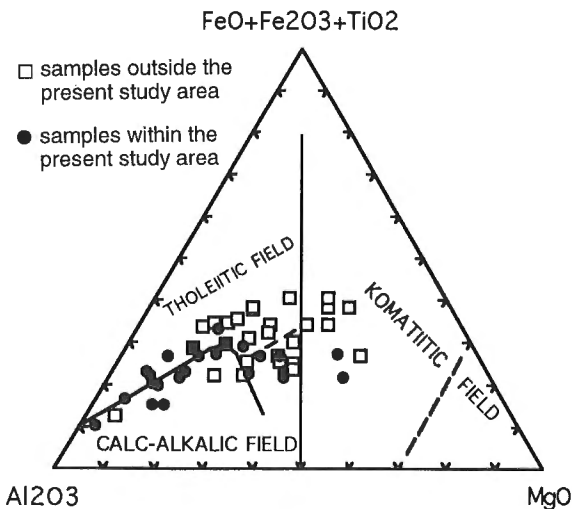


Figure 8. Jensen cation plot of volcanic and intrusive rocks (from Ridler, 1974).

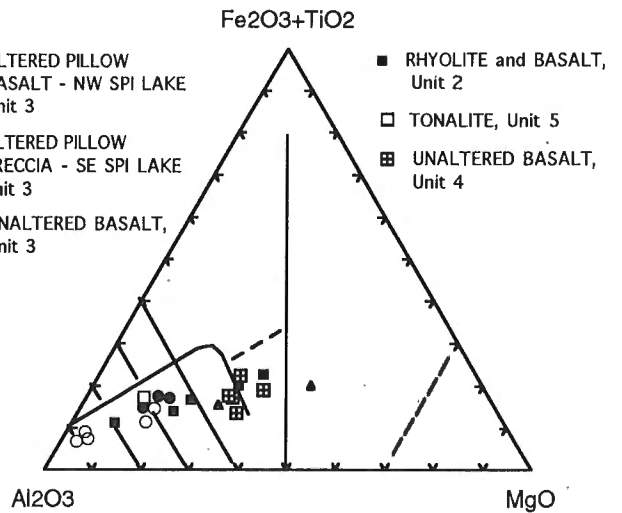


Figure 9. Jensen cation plot of volcanic and intrusive rocks from this study.

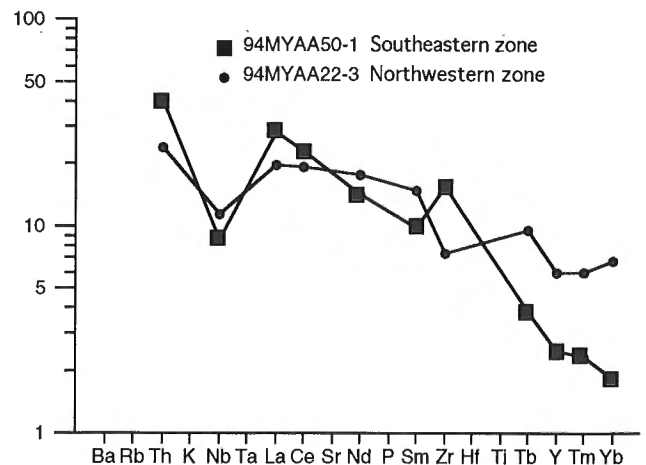


Figure 10. Incompatible element plot of rocks from semiconformable alteration zones.

## ACKNOWLEDGMENTS

The authors thank BHP Minerals Canada Ltd. and Royal Oak Mines Inc. for permission to publish data. John Lindel of Eskimo Point Lumber, Arviat, Northwest Territories, provided excellent logistical support. This research benefited from a critical review by A. Galley. S. Alvarado is thanked for computer assistance.

## REFERENCES

- Armitage, A.E., Miller, A.R., and MacRae, N.D.**  
1995: Geological setting of the Sandhill Zn-Cu-Pb-Ag prospect in the Gibson-MacQuoid lakes area, District of Keewatin, Northwest Territories; in *Current Research 1995-C*; Geological Survey of Canada, this volume.
- Barrett, K.R.**  
1981: The volcanology and sedimentology of the Kaminak Group, Carr Lake. District of Keewatin, Northwest Territories, MSc. thesis, University of Manitoba, 63 p.
- Barrett, T.J. and Maclean, W.H.**  
1994: Chemostratigraphy and hydrothermal alteration in exploration for VHMS deposits in greenstones and younger volcanic rocks; in *Alteration and alteration Processes associated with ore-forming systems*, (ed.) D.R. Lentz; Geological Association of Canada, Short Course Notes, v. 11, p. 433-467.
- Bell, R.T.**  
1971: Geology of Henik Lakes (east half) and Ferguson Lake (east half) map-areas, District of Keewatin; Geological Survey of Canada, Paper 70-61, 31 p.
- Campbell, I.H., Franklin, J.M., Gorton, M.P., Hart, T.R., and Scott, S.D.**  
1981: The role of subvolcanic sills in the generation of massive sulfide deposits; *Economic Geology*, v. 76, p. 2248-2252.
- Cavell, P.A., Wijbrans, J.R., and Baadsgaard, H.**  
1992: Archean magmatism in the Kaminak Lake area, District of Keewatin, Northwest Territories: ages of the carbonatite-bearing alkaline complex and some host granitoid rocks; *Canadian Journal Earth Sciences* v. 29, p. 896-908.
- Chiarenzelli, J.R. and Macdonald, R.**  
1986: A U-Pb zircon age for the Ennadai Group; in *Summary of Investigations 1986*, Saskatchewan Geological Survey; Saskatchewan Energy and Mines, Miscellaneous Report 86-4, p. 112-113.
- Davidson, A.**  
1970: Precambrian geology, Kaminak Lake map-area, District of Keewatin; Geological Survey of Canada, Paper 69-51, 27 p.
- Eade, K.E.**  
1971: Geology of Ennadai Lake map-area, District of Keewatin; Geological Survey of Canada, Paper 70-45.  
1974: Geology of Kognak River area, District of Keewatin, Northwest Territories; Geological Survey of Canada, Memoir 377, 66 p.  
1980: Notes on metamorphism in southern District of Keewatin; in *Metamorphism in the Canadian Shield*, (ed.) J.A. Fraser and W.W. Heywood; Geological Survey of Canada, Paper 78-10, p. 191-194.  
1986: Precambrian Geology of the Tulemalu Lake-Yathkyed Lake Area, District of Keewatin; Geological Survey of Canada, Paper 84-11, 31 p.
- Franklin, J.M. and Thorpe, R.I.**  
1982: Comparative metallogeny of the Superior, Slave, and Churchill Provinces; in *Precambrian Sulphide Deposits*, (ed.) R.W. Hutchison, C.D. Spence, and J.M. Franklin; H.S. Robinson Memorial Volume, Geological Association of Canada, Special Paper 25, p. 3-90.
- Franklin, J.M., Sangster, D.F., and Lydon, J.W.**  
1981: Volcanic-associated massive sulfide deposits; *Economic Geology* 75th Anniversary Volume, p. 485-627.
- Frisch, T.**  
1982: Precambrian geology of the Prince Albert Hills, western Melville Peninsula, Northwest Territories; Geological Survey of Canada, Bulletin 346, 70 p.
- Gibson, H.L.**  
1989: The mine sequence of the central Noranda volcanic complex: geology, alteration, massive sulphide deposits and volcanological reconstruction; Ph.D. thesis, Carleton University, Ottawa, Ontario, 715 p.
- Gibson, H.L., Watkinson, D.H., and Comba, C.D.A.**  
1983: Silicification: Hydrothermal alteration in an Archean geothermal system within the Amulet Rhyolite Formation, Noranda, Quebec. *Economic Geology*, v.78, p. 954-971.
- Hodgson, C.J. and Lydon, J.W.**  
1977: The geologic setting of volcanogenic massive sulphide deposits and active hydrothermal systems: some implications for exploration; *Canadian Mining and Metallurgy Bulletin*, v. 70, p. 95-106.
- Galley, A.G.**  
1993: Characteristics of semi-conformable alteration zones associated with volcanogenic massive sulphide districts; *Journal of Geochemical Exploration*, v. 48, p. 175-200.
- Galley, A.G., Bales, A.H., and Kitzler, G.**  
1993: Geological setting and hydrothermal evolution of the Chisel Lake and North Chisel Zn-Pb-Cu-Ag-Au massive sulfide deposits, Snow Lake, Manitoba; *Exploration Mining Geology*, v. 2, no. 4, p. 271-295.
- Henderson, J.R., Henderson, M.N., Pryer, L.L., and Cresswell, R.G.**  
1991: Geology of the Whitehills-Tehek area, District of Keewatin: an Archean supracrustal belt with iron-formation hosted gold mineralization in central Churchill Province; in *Current Research, Part C*; Geological Survey of Canada, Paper 91-1C, p. 149-156.
- Irwin, D.A.**  
1993: Mineral occurrences and preliminary geology of the Kaminak-Carr lakes area, District of Keewatin; in *Exploration Overview: Northwest Territories*, (ed.) S.P. Goff; Canadian Department of Indian Affairs and Northern Development, Northern Affairs Program (Canada).
- Laporte, P.J., Barrett, K.R., and Leggett, S.R.**  
1981: Geology of the Heninga-Turquetil-Carr Lakes area, N.W.T.; Department of Indian Affairs and Northern Development, EGS 1981-4.
- MacGeehan, P.J.**  
1978: The geochemistry of altered volcanic rocks at Matagami, Quebec: A geothermal model for massive sulphide genesis; *Canadian Journal of Earth Sciences*, v. 15, p. 551-570.
- MacGeehan, P.J. and MacLean, W.H.**  
1980: An Archean sub-seafloor geothermal system, 'calc-alkali' trends, and massive sulphide genesis; *Nature*, v. 286, p. 767-771.
- Miller, A.R. and Cavell, P.A.**  
1993: Geology of the Proterozoic Heninga Lake syenite complex and surrounding Proterozoic and Archean supracrustal rocks: Implication for a lower limit to early Proterozoic sedimentation in the southern Churchill Structural Province, north of 60°, District of Keewatin, Northwest Territories; in *Current Research, Part C*; Geological Survey of Canada, Paper 93-1C, p. 171-178.
- Mortensen, J.K. and Thorpe, R.I.**  
1987: U-Pb zircon ages of felsic volcanic rocks in the Kaminak Lake area, District of Keewatin; in *Radiogenic Age and Isotopic Studies: Report 1*; Geological Survey of Canada, Paper 87-2, p. 123-128.
- Park, A.F. and Ralsler, S.**  
1992: Precambrian geology of the southwestern part of the Tavani map area, District of Keewatin, Northwest Territories; Geological Survey of Canada, Bulletin 416, 81 p.
- Ridler, R.H.**  
1973: Volcanic stratigraphy and metallogeny: Rankin Inlet - Ennadai belt, District of Keewatin; in *Report of Activities, Part A*; Geological Survey of Canada, Paper 73-1A, p. 165-174.  
1974: Volcanic stratigraphy and metallogeny of the Kaminak Group, Spi Lake area, District of Keewatin; in *Report of Activities, Part A*; Geological Survey of Canada, Paper 74-1A, p. 181-185.
- Ridler, R.H. and Shilts, W.W.**  
1974: Exploration for Archean polymetallic sulphide deposits in permafrost terranes: an integrated geological/geochemical technique; Geological Survey of Canada, Paper 73-34, 33p.
- Roddick, J.C., Henderson, J.R., and Chapman, H.J.**  
1992: U-Pb ages from the Archean Whitehills-Tehek lakes supracrustal belt, Churchill Province, District of Keewatin, Northwest Territories; in *Radiogenic Age and Isotopic Studies: Report 6*; Geological Survey of Canada, Paper 92-2, p. 31-40.

**Schau, M.**

1982: Geology of the Prince Albert Group in parts of Walker Lake and Laughlin Lake map area, District of Keewatin; Geological Survey of Canada, Bulletin 337, 62 p.

**Skirrow, R.G. and Franklin, J.M.**

1994: Silicification and metal leaching in semi-conformable alteration beneath the Chisel Lake massive sulfide deposit, Snow Lake, Manitoba; *Economic Geology*, v. 89, p. 31-50.

**Taylor, F.C.**

1963: Snowbird Lake Map-Area, District of Mackenzie; Geological Survey of Canada, Memoir 333, 23p.

**Tella, S.**

1994: Geology, Rankin Inlet (55K/16), Falstaff Island (55J/13), and Quartzite Island (55J/11), District of Keewatin, Northwest Territories; Geological Survey of Canada, Open File 2968, scale 1:50 000.

**Tella, S., Annesley, I.R., Borradié, G.J., and Henderson, J.R.**

1986: Precambrian geology of parts of Tavani, Marble Island and Chesterfield Inlet map areas, District of Keewatin, N.W.T.; Geological Survey of Canada, Paper 86-13, 20 p.

**Tella, S., Schau, M., Armitage, A.E., and Loney, B.C.**

1993: Precambrian geology and economic potential of the northeastern parts of Gibson Lake map area, District of Keewatin, Northwest Territories; in *Current Research, Part C*; Geological Survey of Canada, Paper 93-1C, p. 197-208.

**Tella, S., Schau, M., Armitage, A.E., Seemayer, B.E., and Lemkow, D.**

1992: Precambrian geology and economic potential of the Meliadine Lake-Barbour Bay region, District of Keewatin, Northwest Territories; in *Current Research, Part C*; Geological Survey of Canada, Paper 92-1C, p. 1-11.

---

Geological Survey of Canada Project 810024

# Lamprophyre dykes of the Christopher Island Formation, Thirty Mile Lake, District of Keewatin, Northwest Territories

A.L. Jones<sup>1</sup>, A.R. Miller, A.E. Armitage<sup>1</sup>, and N.D. MacRae<sup>1</sup>

Mineral Resources Division

*Jones, A.L., Miller, A.R., Armitage, A.E., and MacRae, N.D., 1995: Lamprophyre dykes of the Christopher Island Formation, Thirty Mile Lake, District of Keewatin, Northwest Territories; in Current Research 1995-C; Geological Survey of Canada, p. 187-194.*

---

**Abstract:** The Thirty Mile Lake area is underlain by upper amphibolite to granulite grade para- and orthogneiss and by Archean megacrystic alkali feldspar megacrystic granite. Paleoproterozoic gabbro, lamprophyre, and feldspar porphyry dykes intrude basement rocks. A thick hematitic saprolite was developed in the gneiss prior to deposition of South Channel Formation sharpstone conglomerate. The lamprophyre dykes, equated to the Christopher Island Formation of the Baker Lake Group, are of two types. The first contains phlogopite phenocrysts in a groundmass consisting of phlogopite, alkali feldspar, and apatite; the second contains phlogopite±amphibole in a groundmass consisting of amphibole, alkali feldspar, and apatite. The lamprophyre dykes intrude along a northwest-trending joint set and east-trending mylonite zones. Oblate xenoliths of granitoid and less abundant mafic-ultramafic compositions occur in the dykes; some xenoliths display recessive rims indicating reactions with the host rock. The lamprophyres are being thoroughly studied in order to evaluate their diamond potential.

**Résumé :** La région du lac Thirty Mile repose sur des paragneiss et orthogneiss allant du faciès des amphibolites supérieur à celui des granulites et sur un granite mégacristallin à feldspath alcalin de l'Archéen. Des dykes de gabbro, de lamprophyre et de porphyre feldspathique du Paléoprotérozoïque recoupent les roches du socle. Une saprolite hématitique épaisse s'est formée dans le gneiss avant le dépôt du conglomérat à fragments anguleux de la Formation de South Channel. Les dykes de lamprophyre, assimilés à la Formation de Christopher Island du Groupe de Baker Lake, sont de deux types. Le premier type contient des phénocristaux de phlogopite dans une matrice de phlogopite, de feldspath alcalin et d'apatite; le second contient phlogopite±amphibole dans une matrice d'amphibole, de feldspath alcalin et d'apatite. Les dykes de lamprophyre longent une série de joints à direction nord-ouest et des zones de mylonite à direction est. Ils renferment des xénolites de granitoïde aplatis aux pôles et, en moindre abondance, de roches mafiques-ultramafiques; certains xénolites présentent une bordure récessive indiquant des réactions avec la roche hôte. Les lamprophyres font actuellement l'objet d'études approfondies afin d'évaluer leur potentiel diamantifère.

---

<sup>1</sup> Department of Earth Sciences, University of Western Ontario, London, Ontario N6A 5B7

## INTRODUCTION AND REGIONAL GEOLOGY

The study area is located approximately 90 km southwest of Baker Lake in the central Churchill Structural Province (Fig. 1). Field mapping in 1994 focused on a 100 km<sup>2</sup> area near the western end of Thirty Mile Lake (Fig. 2) in which lamprophyre dykes of the Christopher Island Formation (Baker Lake Group) are abundant. This preliminary report describes lithological units underlying the area, with emphasis on dykes in order to document their distribution and structural controls.

It has been proposed that minette and lamproitic lavas and dykes of the Christopher Island Formation were intruded following subduction of oceanic crust beneath the Churchill protocontinent at ca. 2.0-1.9 Ga (Peterson and Rainbird, 1990; Peterson, 1994). Crustal thickening and mantle metasomatism resulting from contemporaneous collisions of the Superior and Slave cratons at ca. 1.9-1.85 Ga produced ultrapotassic magmas beneath the Churchill Province (Peterson and Rainbird, 1990). The ascent of these magmas along brittle fractures led to widespread subaerial volcanism at ca. 1.84 Ga (Peterson and Rainbird, 1990; Roddick and Miller, in press). Lamprophyre dykes in the Thirty Mile area are similar in composition to Christopher Island Formation flows and have been interpreted as feeder dykes for the lavas (Blake, 1980; LeCheminant et al., 1987). Both the flows and dykes have previously been described in the Angikuni Lake area by Blake (1980), in the Dubawnt Lake area by Peterson

et al. (1989) and Peterson and Rainbird (1990), and in the Thirty Mile Lake area by LeCheminant et al. (1976, 1977, 1979) and Blake (1980).

Helmstaedt and Gurney (1994) note that, assuming mantle roots defined by tomography (Anderson et al., 1992) beneath both the Slave and Churchill provinces are Archean, post-Archean kimberlites (and lamproites) in these areas should have a reasonable diamond potential. In 1992 one microdiamond was recovered from a small diatreme 225 km southwest of Baker Lake (Davis, 1993) and in 1993 a 270 μ diamond was found in a lamprophyre dyke in the Gibson Lake area 100 km southeast of Baker Lake (Armitage et al., 1994a). A primary aim of this study is to examine, through detailed petrology and mineralogy, the diamond potential of Christopher Island Formation lamprophyres.

## BASEMENT ROCKS

The Thirty Mile Lake area is underlain by Archean upper amphibolite to granulite facies migmatized metasedimentary and metavolcanic rocks. These rocks were intruded by megacrystic alkali feldspar granite ca. 2.6 Ga (LeCheminant and Roddick, 1991) and by Paleoproterozoic gabbro dykes. Albite+epidote+carbonate metamorphic assemblages in the gabbro dykes and similar retrograde assemblages in the Archean gneisses are associated with regional Proterozoic deformation.

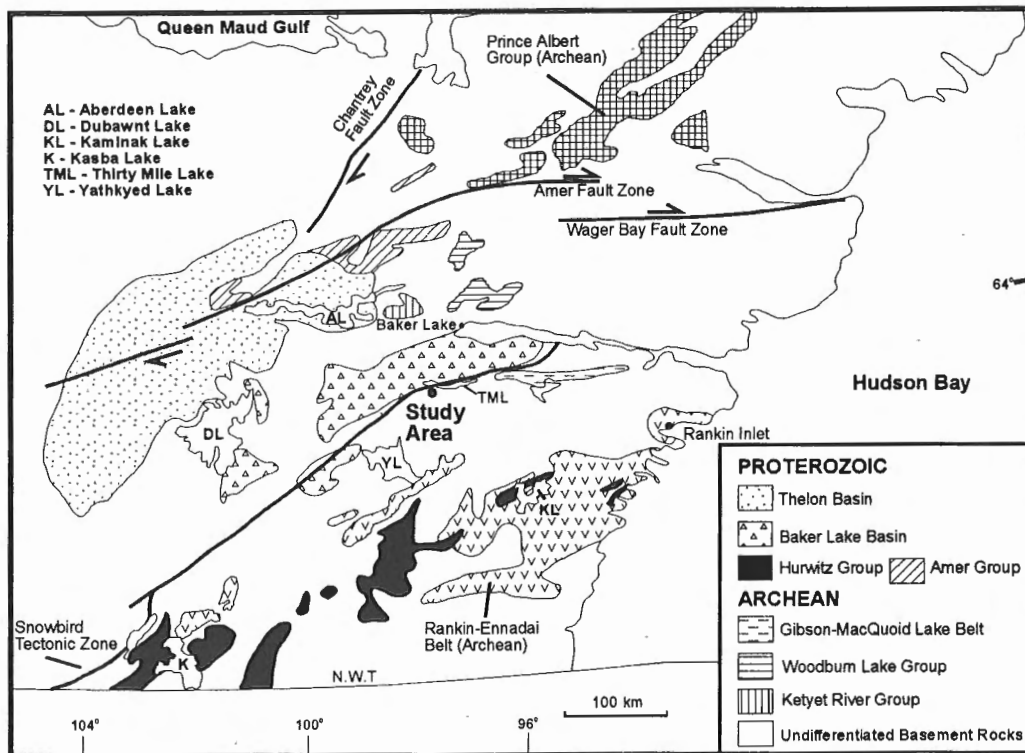


Figure 1. Regional setting of Thirty Mile Lake (TML), central Churchill Province (modified from Gebert and Irving, 1993).

### Archean gneisses

Whereas gneisses are diverse in character, a number of predominant rock types were distinguished. Most dominant are the 'black and white' gneisses previously described by LeCheminant et al. (1979). They are thinly and irregularly banded, well exposed, and locally strongly mylonitized. The leucocratic portion (approximately 60 per cent by volume) is granitic to granodioritic, medium- to coarse-grained, weathers white to pink, and exhibits multiple generations of crosscutting granitic leucosomes. The melanocratic portion is highly variable in both mineralogy and form, ranging from rusty-weathering garnet-rich pods to contorted layers of medium- to coarse-grained garnet-hornblende-rich gneiss and amphibolite. The rocks are interpreted as mafic volcanic

or volcanogenic sedimentary rocks (LeCheminant et al., 1977, 1979). These volcanic rocks may be part of a more continuous greenstone belt in the Gibson-MacQuoid Lake area (Miller and Tella, 1995; Armitage et al., 1994b). Rare metamorphosed iron-formation, consisting of garnet+quartz+magnetite, is interlayered with biotite+muscovite+garnet-bearing quartzofeldspathic gneiss interpreted here to have been turbiditic sedimentary rocks.

Regional gneissosity trends east to southeast with flat to moderate dips to the north. Two generations of folding are observed:  $F_1$  are centimetre-scale isoclinal folds in the gneissic layering (Fig. 3) and  $F_2$  are metre-scale, east-verging, open folds. East- and northeast-striking subvertical mylonites with dextral or sinistral sense of movement, recognized

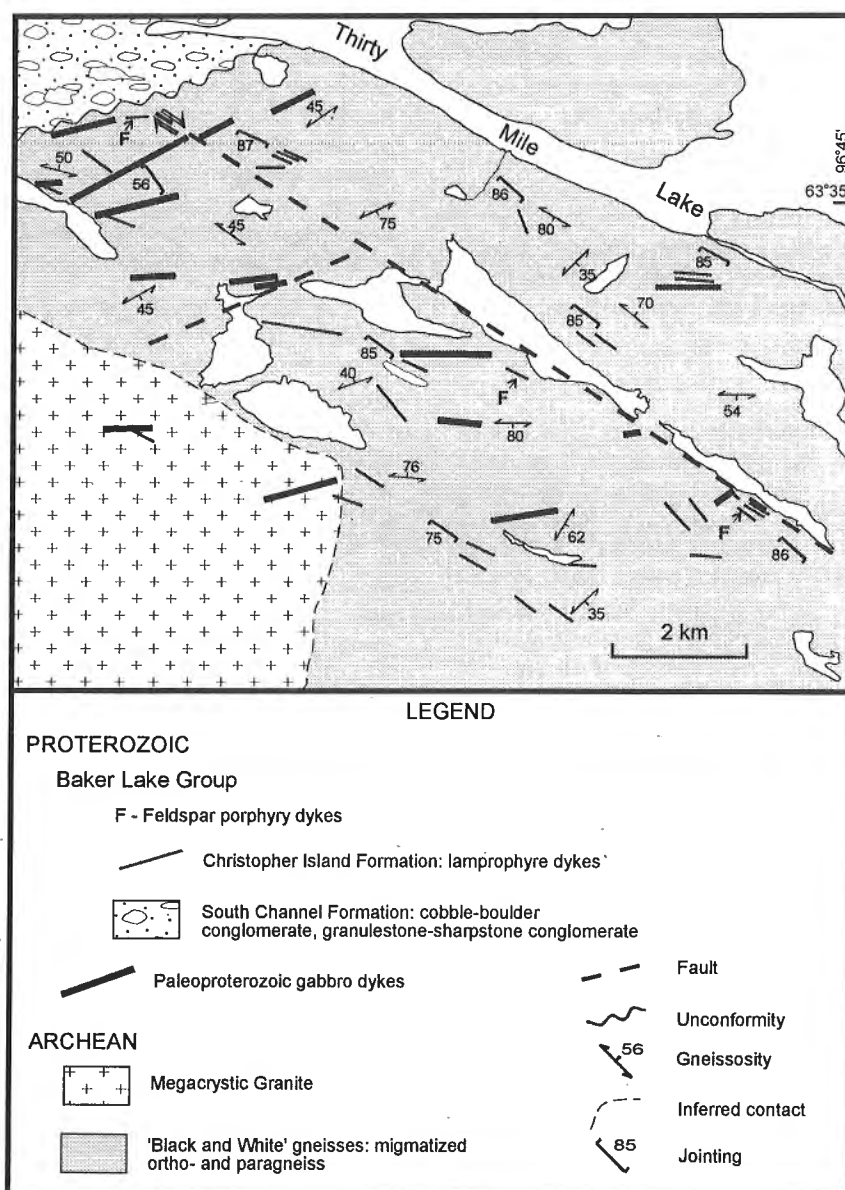
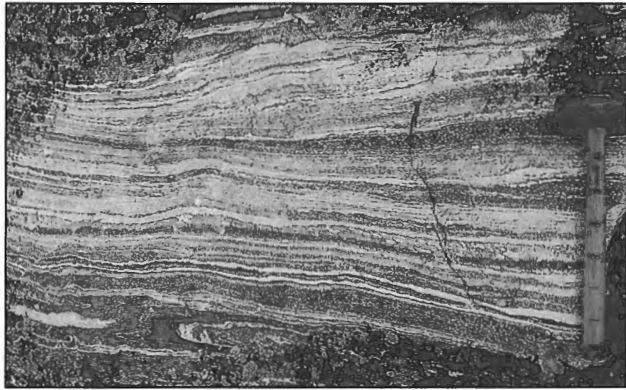


Figure 2. Geological map of the Thirty Mile Lake study area.



**Figure 3.** Centimetre-scale layering and isoclinal folding ( $F_1$ ) in paragneiss. Hammer is 40 cm long.

throughout the study area, cause variations in regional gneissosity. These mylonite zones are part of a regional ductile deformation zone recognized by LeCheminant et al. (1977) in the basement south of the Baker Lake Group.

Metamorphism in the study area is upper amphibolite to granulite facies, with widespread but incomplete lower greenschist facies retrogression. Partial to complete replacement of garnet by feldspar and epidote+chlorite+carbonate assemblages adjacent to mylonite zones and brittle fractures are the most obvious evidence of retrograde metamorphism.

### **Megacrystic granite**

In the southwest corner of the study area (Fig. 2), a unit of foliated pink- to white-weathering alkali feldspar megacrystic granite intrudes the 'black and white' gneisses. This pluton may be related to the 2.6 Ga megacrystic granites that are widespread across the central Churchill Province (LeCheminant and Roddick, 1991). Contact relations with supracrustal rocks are undetermined due to limited exposure. However, an increase in the abundance of granitic pegmatites in the immediate area of the contact suggests an intrusive relationship.

### **Paleoproterozoic gabbro/diabase dykes**

Both the 'black and white' gneisses and megacrystic granite are crosscut by prominent ridge-forming gabbroic dykes. The dykes are northeast- to east-trending, medium- to coarse-grained, variably deformed and range from 5 to 40 m in width. Fine grained margins are common and the centres of the largest dykes locally retain primary textures. Associated with deformation is extensive alteration to epidote+chlorite+carbonate±hematite along sheared and schistose contacts, with extensive development of secondary amphibole and biotite in the central portion of dykes. Eade (1986) describes a similar regional dyke swarm in the Tulemalu Lake-Yathkyed Lake area and refers to this swarm as the "Tulemalu dykes". The age of the Tulemalu dykes is not constrained. However, gabbroic dykes in the Thirty Mile Lake area may be related to gabbro intrusions dated at

2111 ± 0.6 Ma (Heaman and LeCheminant, 1993) and 2094 +26/-17 Ma (Patterson and Heaman, 1991) that intruded the Hurwitz Group.

## **BAKER LAKE GROUP: PALEOSOL AND THE SOUTH CHANNEL FORMATION**

In the northwest corner of the study area (Fig. 2), Archean gneisses are overlain by the South Channel Formation (Baker Lake Group). Both the lower sharpstone conglomerate unit and the upper pebble/cobble conglomerate unit of the South Channel Formation type section (Donaldson, 1965; Miller and LeCheminant, 1985) are represented. However, in contrast to an extremely thin or nonexistent paleosol marking the unconformity with underlying Archean gneisses in most locations, the paleosol in the study area is well exposed in a continuous section.

Thickness of up to 2 m of weakly hematitized gneisses below the South Channel conglomerates were previously interpreted as truncated paleosols (Miller, 1980). The thin paleoweathered zones were attributed to high-energy fluvial systems apparent in the eastern segment of the Baker Lake Group; thick paleosol sections were preserved only where low-energy sedimentation conditions preceded development of South Channel conglomerates (Miller, 1993).

The Thirty Mile Lake paleosol is exposed over an outcrop width of 10-12 m measured south from the east-striking unconformity. Bedding dips of 50-60° to the north, in coarse grained granulestone overlying the paleosol, indicate significant post-South Channel block rotation. This dip indicates a true exposed width of 8-10 m through the paleosol, making it undoubtedly the best paleosol exposure in the eastern Baker Lake Basin.

The protolith is a biotite leucogranitic gneiss with locally abundant granitic pegmatites. The first imprints of paleoweathering in the lowest portion of unaltered gneiss are thin hematite haloes along some fractures and joints (Fig. 4). Higher in the paleosol, the haloes become wider and more

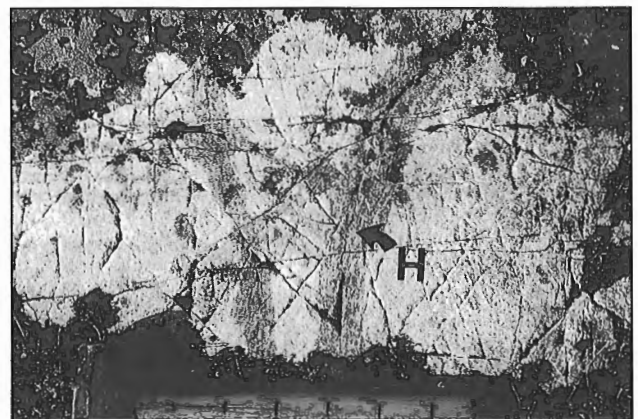


**Figure 4.** Weak hematitization(H) along fractures at the base of the paleosol.

abundant. Also, discolouration intensifies from light pink to red pink due to hematite impregnation. At one locality, several different directions of hematitized joints form a pink-red polygonal shape about an unhematitized white central core. This geometric form is reminiscent of the corestone textures or onion-skin weathering features of modern weathering profiles. Strongly hematitized gneiss (Fig. 5) is a deep red maroon due to pervasive disseminated hematite interstitial to quartz and feldspar as well as 'clotted' hematite resulting from coalesced aggregates of iron oxide along foliation planes.

The basal unit of the South Channel Formation, directly overlying the paleosol, is a hematitic, nonbedded, clast-supported sharpstone conglomerate (Fig. 6) interstratified with pebbly arkose to even-bedded granulestone (Fig. 7). The upper unit of the South Channel Formation is a rounded pebble to cobble conglomerate, and is interstratified with the basal unit about 5 to 8 m above the unconformity. Clast

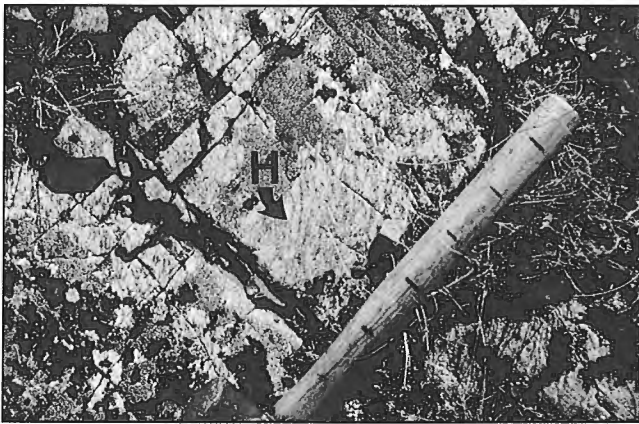


**Figure 5.** Intensely hematitized leucocratic biotite granitic gneiss about 1 m from the unconformity. Note the clotted texture of hematite (H) in foliation planes.



**Figure 6.** Sharpstone conglomerate at the base of the South Channel Formation contains clasts of hematitic gneiss (G) and hematitic metagabbro (Mg). Clotted hematite texture (H) in angular clasts is similar to hematite in the paleosol (see Fig. 5).

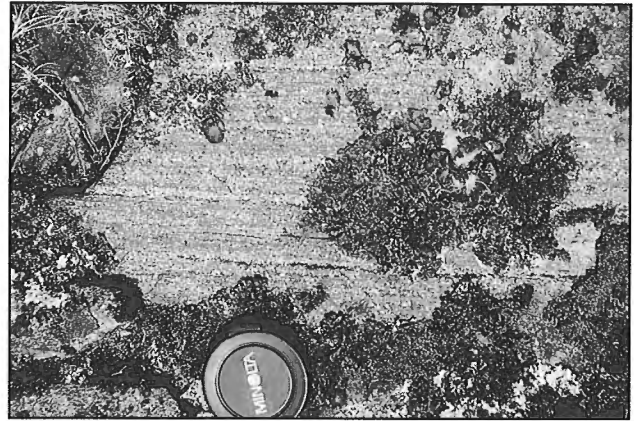


**Figure 7.** Parallel-bedded granulestone at the base of the South Channel Formation.

lithology in the lower sections is dominated by intensely weathered leucocratic gneiss with subordinate weakly foliated hematitized diabase and vein quartz. Based on angularity, type of clast, and hematite textures in the clasts (the latter are identical to those of the underlying paleosol), these clasts were locally derived. The granulestone is cemented by carbonate, quartz, and white mica and the fine grained white mica may, in part, be derived from saprolitic basement. With increasing stratigraphic height above the unconformity, gneiss clasts in conglomerate exhibit a greater degree of rounding and a decrease in or lack of intense hematitization.

The immaturity, roundness, restricted clast compositions, and bed forms in these sedimentary rocks suggest that these deposits are debris flows that reworked a regolith developed from the immediately underlying hematitic saprolitic gneiss. These highly immature sedimentary rocks record the earliest phase of tectonism related to the formation of fault-bounded basins into which the Baker Lake Group was deposited.

Several narrow phlogopite- and phlogopite+pyroxenophytic dykes, identical to the dykes in the basement, intrude the South Channel Formation and are interpreted, because of their composition and mineral content, to correlate with lamprophyre dykes of the Christopher Island Formation.

### **CHRISTOPHER ISLAND FORMATION: LAMPROPHYRE DYKES**

Lamprophyre dykes are abundant and widespread in the study area and are interpreted to be feeder dykes to the overlying lavas of the Christopher Island Formation because of their similar composition (Blake, 1980). These dykes have been termed "minettes" by LeCheminant et al. (1987) and "lamproite-minette" by Peterson and Rainbird (1990), on the basis of their ultrapotassic, calc-alkaline composition and mineralogy of phlogopite+clinopyroxene+sanidine. A minimum age of 1753  $\pm$  3/2 Ma has been established for the Christopher Island Formation by U-Pb dating of zircon from a granitic pluton intruding Christopher Island Formation lavas in the Carruthers Lake-Kamilukuak Lake area



(Loveridge et al., 1987). Roddick and Miller (in press) dated hornblende ( $^{40}\text{Ar}$ - $^{39}\text{Ar}$ ) from the ultrapotassic Enekatcha plutonic suite (located approximately 100 km south of Dubawnt Lake) at  $1825 \pm 12$  Ma; this suite, linked geochemically to the Christopher Island Formation, establishes the age of ultrapotassic magmas in the western portions of the Baker Lake Group.

Christopher Island Formation dykes are undeformed. They truncate albite-epidote alteration of Archean gneisses and deformed northeast-striking gabbroic dykes. They were intruded along pre-existing structures, particularly northwest joint sets (Fig. 2) and subordinate east-west mylonites, and typically bifurcate to enclose 'rafts' of gneissic wall rock. Dykes range from 10 cm to approximately 10 m in width, are subvertical, chill against basement wall rock, and occur as recessive trenches which crosscut the more resistant gneisses. They are almost always xenolithic (inclusions ranging from 1-2 mm to 80 cm; Fig. 8) and contain abundant phlogopite, pyroxene, and amphibole xenocrysts.

Field observations and mapping identified two major types of lamprophyre dykes in the study area. The first is a buff- to dark brown-weathering rock, steel grey on fresh surface, consisting of 0.1 to 0.75 cm phlogopite crystals (approximately 25 per cent by volume) in a fine grained to aphanitic groundmass of alkali feldspar, phlogopite, apatite, and carbonate. Phlogopite phenocrysts are invariably kinked and are considered to be xenocrysts (see below); their tendency to be aligned parallel to dyke margins results in a 'ribbed' texture on weathered surface (Fig. 9). The second type is medium- to coarse-grained, weathers pink to orange and is extremely rich in alkali feldspar. It consists of approximately 40 per cent by volume of phlogopite and amphibole phenocrysts, in approximately equal proportions, in a fine grained matrix of chlorite, potassic feldspar, mica, carbonate, and apatite. Chlorite and other fine grained secondary minerals replace all but about 20-40 per cent of the clinopyroxene phenocrysts. Locally, aggregates of phlogopite phenocrysts weather out to produce a pitted, 'leopard skin' appearance in outcrop (Fig. 10).



**Figure 8.** Large rounded xenoliths within a recessive lamprophyre dyke.

### *Xenoliths-xenocrysts*

Macroxenoliths are dominated by rounded to oblate spheroids of crustal felsic gneisses and mylonites. These crustal xenoliths lack albite-epidote-carbonate assemblages typical of gneissic host rocks in the study area. It is suggested that they were entrained from a somewhat deeper crustal level. Xenoliths in most of the dykes have their long axes aligned subparallel to parallel with the dyke margins, consistent with alignment of phlogopite phenocrysts. They are commonly concentrated in the central portions of dykes and in places are aligned to form a 'train' parallel with the dyke walls. These features suggest flow concentration.

The characteristic equant to oblong rounded form of the xenoliths suggests sufficient residency time in the magma to produce extensive alteration and ablation; pink alteration envelopes on the margins of some felsic xenoliths clearly indicate reaction with the host magma (Fig. 11). In addition, vermiform intergrowths of alkali feldspar and quartz suggest that the xenoliths approached conditions of anatexis. Ultramafic rocks, now largely serpentine, gabbro, amphibolite, and chloritized hornblende, form a minor proportion of



**Figure 9.** 'Ribbed' texture in a K-feldspar-rich lamprophyre dyke produced by weathering of aligned phlogopite xenocrysts. Hammer is parallel to the alignment.



**Figure 10.** 'Leopard skin' weathering texture in lamprophyre dyke. Scale bar is in 1 cm increments.



**Figure 11.** Reaction envelope on a 6 cm granitoid xenolith within a lamprophyre dyke.

the xenoliths. Mafic inclusions are rounded to angular with thick recessively weathered reaction rims against the ultrapotassic host rock.

Xenocrysts are predominantly phlogopite with lesser amphibole and quartz. Curved and kinked phlogopite, with some grains as large as 1 cm, are very diagnostic and noteworthy, considering that the groundmass to these phenocrysts is undeformed. Phlogopite can occur as clots suggestive of incipient 'superegg' or 'glimmerite' formation (Peterson and LeCheminant, 1993). Spherical quartz xenocrysts up to 0.5 cm in diameter commonly contain inclusions of calcite.

### **Feldspar porphyry dykes**

Three porphyritic dykes were identified in the study area (Fig. 2). They vary from 2 to 12 m in width. The widest dyke is symmetrically zoned with chill margins of approximately 1 m in width. Their characteristic and diagnostic feature is a phenocryst population which includes 0.25 to 2.0 cm alkali feldspar phenocrysts along with subordinate 1.0 to 4.0 mm pale green, saussuritized plagioclase laths, and biotite weakly aligned within a reddish-orange aphanitic matrix. The edges of the feldspar phenocrysts are rounded and partially replaced by calcite. Prismatic aggregates from 1 to 3 mm in length consisting of chlorite, phlogopite, muscovite, and carbonate are thought to have been primary clinopyroxene. Similar dykes occur near Parker Lake to the southeast and are probably related to the Martell syenite intrusive suite (LeCheminant et al., 1976). All of the dykes are undeformed and appear to be emplaced along fault zones within extremely sheared and fractured gneissic basement rocks.

### **SUMMARY**

The Christopher Island Formation of the Baker Lake Group is represented in the study area by undeformed, xenolith-rich, northwest- to east-west-trending lamprophyre dykes. Both the phlogopite-rich and alkali feldspar-rich types intruded along joint sets and mylonite zones within basement gneisses. Phlogopite xenocrysts locally display aggregate textures and

preferred alignment, indicating flow. Feldspar porphyry dykes are thought to represent more evolved members of the Christopher Island Formation. An extremely well exposed paleoweathering horizon, separating basement Archean gneisses and the South Channel Formation, is the best preserved paleosol in the eastern Baker Lake Basin.

Future work will focus on petrological and geochemical classification of Christopher Island Formation lamprophyre dykes in the Thirty Mile Lake area, to better understand the upper mantle-lower crust processes that formed the Christopher Island Formation's rocks and to address their diamond-bearing potential.

### **ACKNOWLEDGMENTS**

The following agencies are thanked for providing additional financial assistance for this project: Indian and Northern Affairs Canada (Contract No. YK 94-95-029) and Natural Sciences and Engineering Research Council of Canada (Grant No. OGP0005539). Cogema Resources Inc. and PNC Exploration (Canada) Co. Ltd. are thanked for their logistical support in the field. We thank Liz and Boris Kotelewetz of the Baker Lake Lodge for excellent expediting services, S. Alvarado for computer assistance, and A.N. LeCheminant for constructive suggestions for manuscript improvement.

### **REFERENCES**

- Anderson, D.L., Tanimoto, T., and Zhang, Y-S.**  
1992: Plate tectonics and hotspots: The third dimension; *Science*, v. 256, p. 1645-1651.
- Armitage, A.E., MacRae, N.D., and Miller, A.R.**  
1994a: Diamond-bearing potential of alkaline dykes in the Gibson Lake area, District of Keewatin, Northwest Territories; *Geological Survey of Canada, Minerals Colloquium, Program with Abstracts*; Appendix.
- Armitage, A.E., Miller, A.R., and MacRae, N.D.**  
1994b: Geology of the Sandhill Zn-Cu showing in the Gibson Lake area, District of Keewatin, Northwest Territories; in *Current Research 1994-C*; Geological Survey of Canada, p. 147-155.
- Blake, D.H.**  
1980: Volcanic rocks of the Paleohelikian Dubawnt Group in the Baker Lake-Angikuni Lake area, District of Keewatin, N.W.T.; *Geological Survey of Canada, Bulletin 309*, 39 p.
- Davis, J. W.**  
1993: Diamond exploration in the Dubawnt region, District of Keewatin, Northwest Territories; in *Exploration Overview 1993 Northwest Territories, Mining, Exploration and Geological Investigation*, (ed.) S.P. Goff; Northwest Territories Geology Division, p. 27.
- Donaldson, J.A.**  
1965: The Dubawnt Group, Districts of Keewatin and Mackenzie; *Geological Survey of Canada, Paper 64-20*, 11 p.
- Eade, K.E.**  
1986: Precambrian Geology of the Tulemalu Lake-Yathkyed Lake area, District of Keewatin; *Geological Survey of Canada, Paper 84-11*, 31 p.
- Gebert, J.S. and Irving, M.**  
1993: Principal mineral deposits and active prospects of the NWT; Department of Energy, Mines, and Petroleum Resources, Government of the Northwest Territories.
- Heaman, L.M. and LeCheminant, A.N.**  
1993: Paragenesis and U-Pb systematics of baddeleyite (ZrO<sub>2</sub>); *Chemical Geology*, v. 110, p. 95-126.

**Helmstaedt, H.H. and Gurney, J.J.**

1994: Geotectonic controls on the formation of diamonds and their kimberlitic and lamproitic host rocks: Applications to diamond exploration; in *Kimberlites, Related Rocks and Mantle Xenoliths*, Volume 2, (ed.) H.O.A. Meyer and O.H. Leonardos; Fifth International Kimberlite Conference, Companhia de Pesquisa de Recursos Minerais Special Publication 1/A, p. 236-250.

**LeCheminant, A.N. and Roddick, J.C.**

1991: U-Pb zircon evidence for widespread 2.6 Ga felsic magmatism in the central District of Keewatin, N.W.T.; in *Radiogenic Age and Isotopic Studies: Report 4*; Geological Survey of Canada, Paper 90-2, p. 91-99.

**LeCheminant, A.N., Blake, D.H., Leatherbarrow, R.W., and deBie, L.**

1977: Geological studies: Thirty Mile Lake and MacQuoid Lake map-areas, District of Keewatin; in *Report of Activities, Part A*; Geological Survey of Canada, Paper 77-1A, p. 205-208.

**LeCheminant, A.N., Hews, P.C., Lane, L.S., and Wolff, J.M.**

1976: MacQuoid Lake (55 M west half) and Thirty Mile Lake (65 P east half) map areas, District of Keewatin; in *Report of Activities, Part A*; Geological Survey of Canada, Paper 76-1A, p. 383-386.

**LeCheminant, A.N., Leatherbarrow, R.W., and Miller, A.R.**

1979: Thirty Mile Lake map area, District of Keewatin; in *Current Research, Part B*; Geological Survey of Canada, Paper 79-1B, p. 319-327.

**LeCheminant, A.N., Miller, A.R., and LeCheminant, G.M.**

1987: Early Proterozoic alkaline igneous rocks, District of Keewatin, Canada: petrogenesis and mineralization; in *Geochemistry and Mineralization of Proterozoic Volcanic Suites*, (ed.) T.C. Pharoah, R.D. Beckinsale, and D. Rickard; Geological Society Special Publication No. 33, p. 219-240.

**Loveridge, W.D., Eade, K.E., and Roddick, J.C.**

1987: A U-Pb age on zircon from a granite pluton, Kamilukuak Lake area, District of Keewatin, establishes a lower limit for the age of the Christopher Island Formation, Dubawnt Group; in *Radiogenic Age and Isotopic Studies: Report 1*; Geological Survey of Canada, Paper 87-2, p. 67-71.

**Miller, A.R.**

1980: Uranium geology of the eastern Baker Lake Basin, District of Keewatin, Northwest Territories; Geological Survey of Canada, Bulletin 330, 63 p.

1993: Redbed copper occurrences in the Lower Proterozoic Baker Lake Group, Dubawnt Supergroup, District of Keewatin, Northwest Territories; in *Current Research, Part C*; Geological Survey of Canada, Paper 93-1C, p. 159-170.

**Miller, A.R. and LeCheminant, A.N.**

1985: Geology and uranium metallogeny of Proterozoic supracrustal successions, central District of Keewatin, N.W.T., with comparisons to northern Saskatchewan; in *Geology of Uranium Deposits*, (ed.) T.I.I. Sibbald and W. Petruk; Canadian Institute of Mining and Metallurgy, Special Volume 32, p. 167-185.

**Miller, A.R. and Tella, S.**

1995: Semiconformable alteration of basaltic pillow lavas and sediments, Spi Lake area, Kaminak greenstone belt, Churchill Province, Northwest Territories; in *Current Research 1995-C*; Geological Survey of Canada, this volume.

**Patterson, J.G. and Heaman, L.M.**

1991: New geochronological limits on the depositional age of the Hurwitz Group, Trans-Hudson hinterland, Canada; *Geology*, v. 19, p. 1137-1140.

**Peterson, T.D.**

1994: Early Proterozoic ultrapotassic volcanism of the Keewatin Hinterland, Canada; in *Kimberlites, related rocks and mantle xenoliths*, Volume 1; (ed.) H.O.A. Meyer and O.H. Leonardos; Fifth International Kimberlite Conference, Companhia de Pesquisa de Recursos Minerais, Special Publication 1/A, p.221-235.

**Peterson, T.D. and LeCheminant, A.N.**

1993: Glimmerite xenoliths in early Proterozoic ultrapotassic rocks from the Churchill Province; *The Canadian Mineralogist*, v. 31, p. 801-819.

**Peterson, T.D. and Rainbird, R.H.**

1990: Tectonic and petrological significance of regional lamproite-minette volcanism in the Thelon and Trans-Hudson hinterlands, Northwest Territories; in *Current Research, Part C*; Geological Survey of Canada, Paper 90-1C, p.69-79.

**Peterson, T.D., LeCheminant, A.N., and Rainbird, R.H.**

1989: Preliminary report on the geology of northwestern Dubawnt Lake area, District of Keewatin, N.W.T.; in *Current Research, Part C*; Geological Survey of Canada, Paper 89-1C, p. 173-183.

**Roddick, J.C. and Miller, A.R.**

1994: An  $^{40}\text{Ar}$ - $^{39}\text{Ar}$  age from the REE-enriched Enekatcha ultrapotassic intrusive suite and implications for timing of ultrapotassic magmatism in the central Churchill Structural Province, N.W.T.; in *Radiogenic Age and Isotopic Studies: Report 8*; Geological Survey of Canada, *Current Research 1994-F*, p. 69-74.

# Paleomagnetism of 779 Ma Hottah gabbro sheets of the Wopmay Orogen, Northwest Territories

John K. Park, Kenneth L. Buchan, and Sunil S. Gandhi<sup>1</sup>

Continental Geoscience Division

*Park, J.K., Buchan, K.L., and Gandhi, S.S., 1995: Paleomagnetism of 779 Ma Hottah gabbro sheets of the Wopmay Orogen, Northwest Territories; in Current Research 1995-C; Geological Survey of Canada, p. 195-200.*

---

**Abstract:** A preliminary paleomagnetic study of the 779 Ma Hottah gabbro sheets of the western part of the Wopmay Orogen in the northwestern Canadian Shield yields a primary direction of magnetization at  $D, I = 286^\circ, +16$  ( $N = 3$  sheets (6 sites),  $k = 34$ ,  $\alpha_{95} = 21^\circ$ ) with corresponding paleomagnetic pole at  $141^\circ E, 13^\circ N$  ( $\delta p, \delta m = 11^\circ, 22^\circ$ ). This paleopole is close to another of the same age from diabase intrusions of the Outer Fold Belt of the Mackenzie Mountains in the northern Cordillera, suggesting that there has been no appreciable relative rotation between the Wopmay Orogen of the Canadian Shield and the Outer Fold Belt of the Mackenzie Mountains since 779 Ma.

**Résumé :** Une étude paléomagnétique préliminaire des feuillets de gabbro de Hottah datés à 779 Ma dans la partie ouest de l'orogène de Wopmay, dans le nord-ouest du Bouclier canadien, indique une direction primaire d'aimantation à  $D, I = 286^\circ, +16$  ( $N = 3$  feuillets (6 sites),  $k = 34$ ,  $\alpha_{95} = 21^\circ$ ) avec un pôle paléomagnétique correspondant à  $141^\circ E, 13^\circ N$  ( $\delta p, \delta m = 11^\circ, 22^\circ$ ). Ce paléopôle se trouve proche d'un autre du même âge dans des intrusions de diabase de la zone de plissement d'Outer dans les monts Mackenzie (Cordillère septentrionale), indiquant qu'il n'y a pas eu, depuis 779 Ma, de rotation relative appréciable entre l'orogène de Wopmay du Bouclier canadien et la zone de plissement d'Outer dans les monts Mackenzie.

---

<sup>1</sup> Mineral Resources Division

## INTRODUCTION

Few paleomagnetic poles of Neoproterozoic age have been obtained from the Canadian Shield for the interval 850 to 600 Ma. A notable exception is the paleopole (e.g., Fahrig et al., 1971) from the 723  $\pm$  4/-2 Ma (Heaman et al., 1992) Franklin mafic magmatism of northern Canada.

In this paper we describe preliminary paleomagnetic results from gabbro sheets of the Wopmay Orogen of the northwestern Canadian Shield, which are about 60 Ma older than the Franklin igneous events, according to recent high-precision U-Pb geochronology (Rainbird et al., 1992; LeCheminant and Heaman, 1994). This study establishes a well-dated paleopole for the Canadian Shield in the Neoproterozoic, based on a combination of new paleomagnetic data and previously published results (Park, 1974; Fahrig et al., 1971), whose significance was previously unrecognized. This paleopole can be directly compared with a paleopole of precisely the same age from a gabbro sill that intrudes the Mackenzie Mountains Supergroup in the Outer Fold Belt of the Mackenzie Mountains, thus allowing for the test of relative rotation between the Outer Fold Belt of the Mackenzie Mountains and the Canadian Shield.

## GEOLOGY

In the area between Great Bear and Great Slave lakes, a set of gently dipping northeast-trending gabbro sheets (Fahrig and West, 1986; Fahrig, 1987; Hoffman and Hall, 1993) intrude Paleoproterozoic rocks of the western part of the Wopmay Orogen (Fraser et al., 1972) (Fig. 1). These sheets, labelled from north to south the Gunbarrel, Calder, Margaret, and Faber sheets, together with vertical northeast-trending diabase dykes in the same region, are termed the Hottah intrusions (Fahrig and West, 1986; Fahrig, 1987). A U-Pb baddeleyite date of 779  $\pm$  2 Ma is available from two Hottah sheets and from two other gabbro intrusions in the northern Cordillera, a sill in the Outer Fold Belt of the Mackenzie Mountains and a dyke in the Muskwa Ranges (Rainbird et al., 1992; LeCheminant and Heaman, 1994). One of the dated Hottah samples is from paleomagnetic sampling site 2 (Fig. 1), which was collected in 1962 by W.F. Fahrig and which forms part of the paleomagnetic collection maintained at the Geological Survey of Canada. No reliable isotopic age is available for the northeast-trending diabase dykes of the study area. They have been tentatively correlated with north-trending dykes (Fahrig and West 1986; Fahrig 1987), that transect rocks of the Mesoproterozoic Hornby Bay and Dismal Lakes groups northeast of Great Bear Lake.

Hottah sheets generally are composed of coarse gabbro, but more mafic and felsic zones occur in some places. The two sheets, Gunbarrel and Calder, which have been studied in detail, have a tholeiitic subalkaline basaltic composition, consisting of 40-50 per cent labradorite to andesine phenocrysts, 30-35 per cent subhedral to anhedral augite, and 5-10 per cent anhedral grains of iron-titanium oxides (Perrier, 1988). Sheets have chilled margins that are typically a few tens of centimetres thick. They are gently inclined, with the

two northern sheets dipping no more than about 15° to the northwest (R.S. Hildebrand, pers. comm.), and southern sheets dipping to the southeast (site 7 has a dip of about 5°). The four major sheets range in thickness from a few tens of metres up to 100 m and in width of exposure from a few hundred metres to 1 km. More irregular surface exposures characterize the Margaret sheet near Rebesca and Ingray lakes (Fig. 1). Subsidiary thin sheets and dykes occur in the vicinity of the major sheets.

The northeasterly trend of Hottah sheets is subparallel to Paleoproterozoic right-lateral transcurrent faults. The sheets cut the faults as well as the major north-trending medial zone (Hildebrand et al., 1990). Although some later minor movements on pre-existing faults may have affected the sheets, they are nondeformed and the following geological evidence suggests that they have not been subjected to appreciable tilting since intrusion. First, Hottah dykes, which together with the sheets postdate all other consolidated rocks in the region, are described as nearly vertical (Lord and Parsons, 1952) and as vertical or nearly so (Wilson and Lord, 1942). Second, strata of the Mesoproterozoic Hornby Bay Group, which abut the Gunbarrel sheet to the northwest (Fig. 1), have dips of less than 10° to the northwest (Hildebrand et al., 1983). Third, the younger Cambrian and overlying strata immediately to the west have dips of less than 5° (Douglas et al., 1974). Assuming that these arguments restrict possible tilting of the Hottah sheets to 10° or less, we have not applied a tilt correction to the magnetic directions and their associated paleopoles.

## SAMPLING AND LABORATORY METHODS

In this study, paleomagnetic results are derived from three gabbro sheets (Fig. 1; Table 1). Sites 4 and 5 from the Calder sheet were reported previously by Park (1974), and site 7 from the Margaret sheet by Fahrig et al. (1971) in paleomagnetic studies that focused on the 723 Ma Franklin magmatic episode. Data from site 1 in the Gunbarrel sheet were provided by P.J. Wynne. In addition, the samples measured in this study from sites 2 and 3 of the Calder sheet were obtained from the 1962 collection of W.F. Fahrig.

In the present study, block samples or drilled cores were oriented in the field by sun and magnetic compasses, and prepared for analysis in the laboratory by cutting cylindrical specimens (2.2 cm in length, 2.5 cm in diameter). Natural remanent magnetizations (NRMs) of samples were measured with Schonstedt DSM-1 or Geofyzika JR-4 spinner magnetometers. The NRMs were analyzed with alternating field (AF) or thermal (TH) demagnetization techniques. Several samples, collected by W.F. Fahrig in 1962 and previously subjected to AF treatment at 10 mT, were thermally demagnetized in the present study.

AF studies were carried out with a Schonstedt GSD-1 demagnetizer using a procedure whereby specimens were treated at peak fields along each of the three orthogonal axes of the specimen in succession. After each single-axis demagnetization, specimens were measured along that axis. Axes were reversed on alternate treatment steps. TH studies were

conducted using Schonstedt TSD-1 ovens that had been modified to provide temperature control of  $\pm 2^\circ\text{C}$ . Both AF and TH treatments were carried out in incremental steps until remanent magnetizations became too weak to measure or exhibited unstable behaviour. Present measurements and demagnetizations were carried out in a shielded room with ambient fields of less than 3000 gammas. Magnetic components were analyzed by means of vector diagrams and the LINEFIND program of Kent et al. (1983).

## RESULTS

TH or AF demagnetization of the NRM yielded either one or two magnetic components. A steeply dipping downward component, with a direction near the present Earth's field in the region, was removed below about  $500^\circ\text{C}$ . It is assumed to be a viscous remanent magnetization and therefore is not discussed further. At temperatures up to  $560^\circ\text{C}$  a shallowly

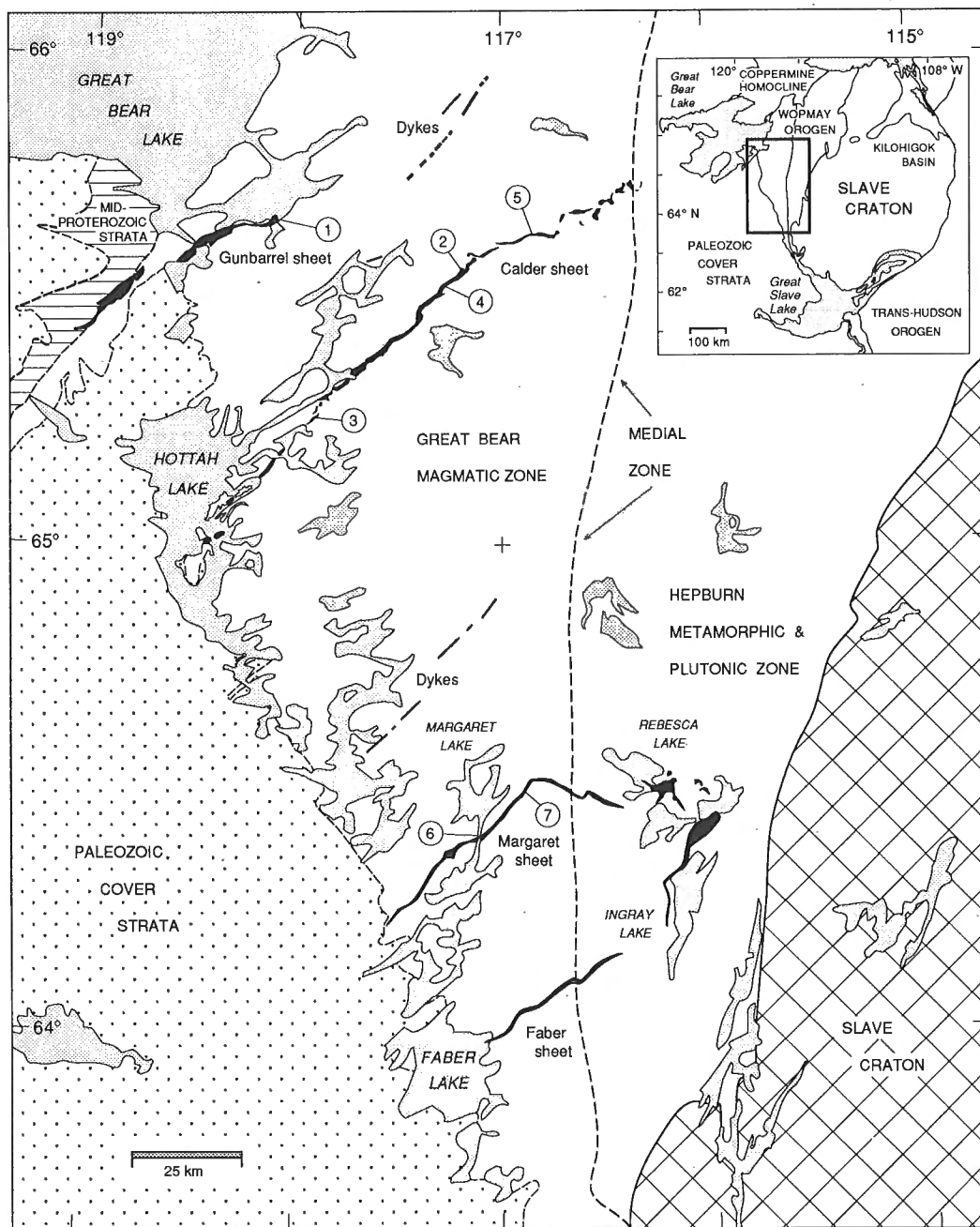


**Figure 1.** Paleomagnetic sampling sites in the Hottah gabbro sheets. Site coordinates are given in Table 1. Hottah sheets and selected northeast trending dykes compiled from Kidd (1936), Lord (1942), Lord and Parsons (1952), Fraser (1967), Hildebrand (1984), Hildebrand et al. (1984), Hildebrand et al. (1987), Hildebrand and Bowring (1988), and Reichenbach (1991).

**Table 1.** Magnetization directions.

Si	Treatment		N	D°, I°	R	k	$\alpha_{95}^\circ$	Ref
	AF (mT)	TH (°C)						
<i>Gunbarrel sheet</i>								
1	20-70	300-550	7	281, +03	6.94	95	6	-1
<i>Calder sheet</i>								
2/3	13-45	450-560	2 <sup>1</sup>	288, +21	2	-	-	-2
4	20 <sup>2</sup>	-	6	292, +27	5.86	36	10	-3
5	20 <sup>2</sup>	-	4	307, +24	3.54	7	26	-4
<i>Margaret sheet</i>								
6	5-50	400-560	4 <sup>3</sup>	283, +12	3.97	101	9	-5
6C	AF	100-520	2 <sup>4</sup>	285, +20	-	-	-	-6
		350-565						
7	25 <sup>2</sup>	-	4	278, +20	3.96	80	8	-7
<i>Mean of sheets</i>			3	286, +15		34	21	
<i>Mean of sites</i>			6	288, +18		38	11	

Notes: Si, site; N, samples; AF, alternating field; TH, thermal; D°, I°, declination and inclination of direction with respect to the present horizontal; R, vector resultant;  $\alpha_{95}^\circ$ , half-angle of the circle of 95% confidence about the direction; Ref, references: (1) this study, unpublished data of P.J. Wynne; (2) this study, samples collected by W.F. Fahrig in 1962; (3), (4) Park (1974); (5), (6) this study, samples collected by SSG; (7) Fahrig et al. (1971), site 29 (incorrect site locality listed in original study is shown correctly in Park (1974)). Site coordinates: 1 - 118° 08' 34" W, 65° 40' 00" N; 2 - 117° 10' 29" W, 65° 34' 37" N; 3 - 117° 56' 07" W, 65° 15' 25" N; 4 - 117° 18' 17" W, 65° 31' 37" N; 5 - 116° 51' 53" W, 65° 38' 23" N; 6 - 117° 07' 54" W, 64° 24' 04" N; 7 - 116° 54' 15" W, 64° 30' 00" N. <sup>1</sup>Two sites, each with one sample, combined. <sup>2</sup>Magnetic cleaning field. <sup>3</sup>Results from 3 samples not used. Extremely high magnetic intensities and scattered directions indicated a probable lightning strike. <sup>4</sup>From quartz monzonite host rocks, 4 and 8 m from diabase.

dipping downward component, directed to the west, was removed (Fig. 2). This hard component also was removed in AF's of 70 mT or by TH treatment between 450 and 560°C in samples that had been previously AF demagnetized to 10 mT. Both the resistive coercive forces and unblocking temperatures (T<sub>UBS</sub>) of the hard component are characteristic of a magnetite or low-titanium titanomagnetite host. Results are listed in Table 1 and plotted in Figure 3.

Samples of the host rock at site 6C, within 8 m of the Margaret sheet (site 6), yield a component on thermal demagnetization that is within 10° of the hard component from the gabbro (Table 1, Fig. 3). The host rock component has T<sub>UBS</sub> from 350-565°C suggestive of a low-titanium titanomagnetite host. We interpret this component to have been acquired as an overprint at the time of gabbro intrusion.

**ANALYSIS AND DISCUSSION**

The Hottah gabbro sheets carry a stable characteristic magnetic remanence, likely residing in magnetite or low-titanium titanomagnetite. Magnetic directions determined from the three Hottah sheets form groupings that are distinct (Fig. 3). Although the data are insufficient for a truly definitive secular variation test to establish if the remanence is primary (see description of the test in Buchan and Halls, 1990), this pattern likely represents secular variation during the period over which the sheets were intruded. Additional evidence for the primary nature of the Hottah remanence direction and other

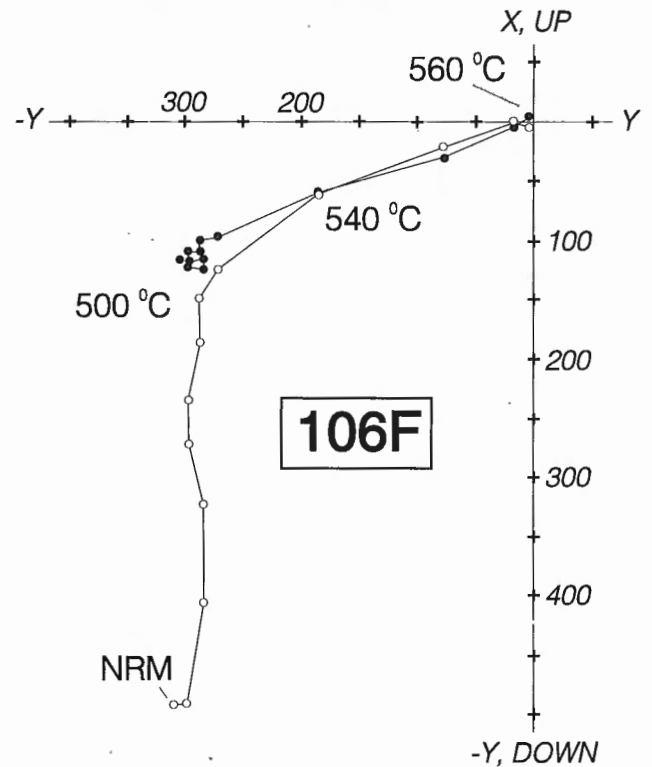


**Figure 2.** Vector diagram of the thermal demagnetization of a typical specimen from site 6 of the Margaret sheet showing viscous and hard magnetization components. Closed (open) symbols represent directions plotted in the X-Y (UP-Y) horizontal (vertical) plane. Magnetic intensity is in mA/m.

directions from mafic intrusions of the same age elsewhere in western North America was summarized by Park et al. (in prep.).

Of particular importance in the interpretation of the Hottah paleopole is the fact that one of the U-Pb baddeleyite ages reported for the sheets was obtained from material collected at a paleomagnetic sampling site. Direct correlation of the paleomagnetic and dating localities ensures that the primary paleopole determined for the Hottah sheets can be directly dated by the 779 Ma isotopic age.

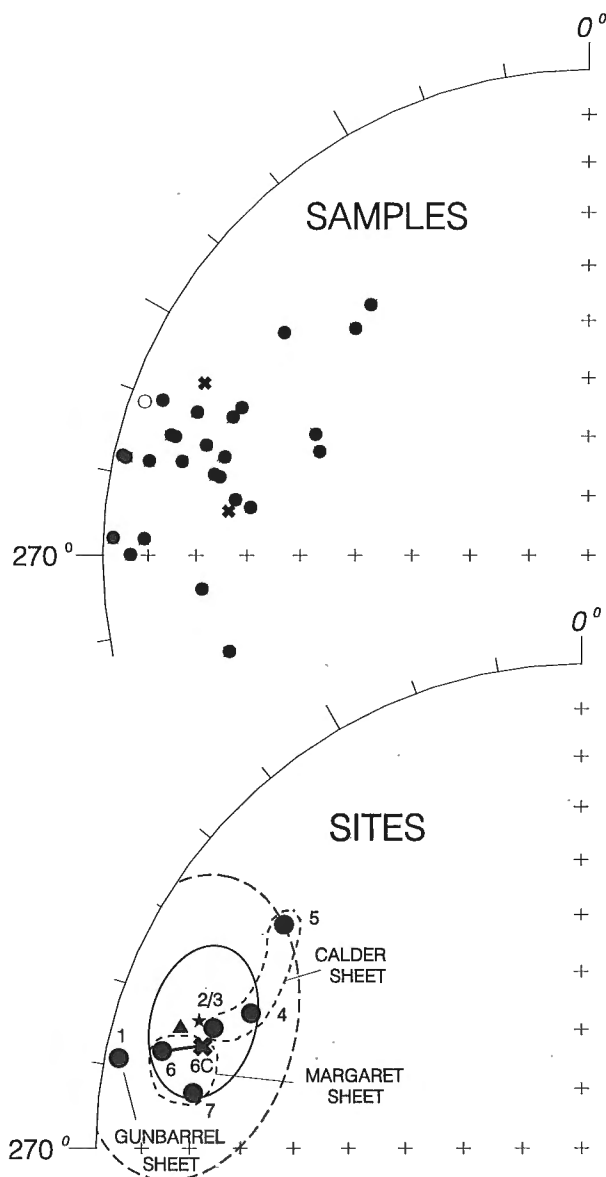


**Figure 3.** In situ sample and site directions from the Hottah sheets plotted on an equal area stereographic projection. Closed (open) symbols represent downward (upward) directions. Crosses represent the contact rocks of site 6C. Site (sheet) mean is represented by star (triangle) with  $\alpha_{95}$  error by solid (dashed) ellipse. Small, dashed lines enclose sites within each sheet.

Mean directions and corresponding ovals of confidence based on six Hottah sites or three sheets are shown in Figure 3 and Table 1. A paleopole at  $141^\circ\text{E}$ ,  $13^\circ\text{N}$  ( $\delta p$ ,  $\delta m = 11^\circ$ ,  $22^\circ$ ) corresponding to the mean direction from three sheets is plotted in Figure 4. The paleopole based on sheet rather than site data yields a more conservative estimate of the uncertainty involved. This is considered important since there are an insufficient number of individual intrusions studied to fully average out secular variation. For example, Buchan and Halls (1990) noted that secular variation is unlikely to be averaged out with less than four dykes. A better defined paleopole for the Hottah sheets must await the opportunity for further sampling in this remote area.

The 779 Ma Hottah paleomagnetic pole is similar to paleopoles reported from mafic intrusions of about 780 Ma in two other widely separated areas of western North America (Fig. 4): the Outer Fold Belt of the Mackenzie Mountains of the northern Cordillera (Park, 1981; Park et al., 1989) and the Wyoming Province of Montana (Harlan, 1993; Harlan et al., in prep.). Notwithstanding the larger error on the Hottah pole, the 780 Ma paleopoles form a grouping that falls west of the well-defined 723 Ma paleopoles for the Franklin magmatic episode, suggesting movement of the Canadian Shield in the 60 Ma interval between emplacement of Hottah and Franklin intrusions.

The coincidence of 780 Ma paleopoles from western North America led Park et al. (in prep.) to suggest that little or no significant relative rotation or translation of these areas has taken place since that time.

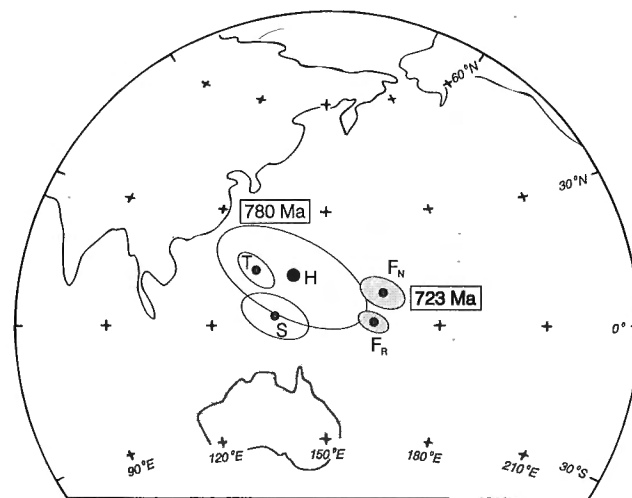


**Figure 4.** Paleopole plot for 780 and 723 Ma intrusions: FN, Franklin intrusions normal (grand mean calculated in Park and Rainbird, in prep.); FR, Franklin intrusions reverse (Park and Rainbird, in prep.); H, Hottah sheets (this study); S, diabbases of the northern Cordillera (Park, 1981; Park et al., 1989); T, dykes of Tobacco Root Mountains, Montana (Harland 1993; Harland et al., in prep.). Paleopoles are based on unit weight to intrusion. Error ellipses are defined by the semi-axes ( $\delta m$ ,  $\delta p$ ) of 95% confidence about the poles.



## ACKNOWLEDGMENTS

We would like to thank P.J. Wynne for contributing the data from site 1, which she collected in a collaborative study (project 860094) with E. Irving and R.S. Hildebrand. W.F. Fahrig kindly provided individual sample directions from site 7 for use in Fig. 3. R.H. Rainbird, A.N. LeCheminant, R.S. Hildebrand, S.S. Harlan, and R.R. Parrish provided helpful discussions, and R.H. Rainbird and L. Tanczyk reviewed the manuscript.

## REFERENCES

- Buchan, K.L. and Halls, H.C.**  
1990: Paleomagnetism of Proterozoic mafic dyke swarms of the Canadian Shield; in *Mafic Dykes and Emplacement Mechanisms*, (ed.) A.J. Parker, P.C. Rickwood, and D.H. Tucker; Balkema, Rotterdam, p. 209-230.
- Douglas, R.J.W., Norris, A.W., and Norris, D.K.**  
1974: Geology of Horn River, District of Mackenzie; Geological Survey of Canada, Map 1372A, scale: 1 to 500,000.
- Fahrig, W.F.**  
1987: The tectonic settings of continental mafic dyke swarms: failed arm and early passive margin; in *Mafic Dyke Swarms*, (ed.) H.C. Halls and W.F. Fahrig; Geological Association of Canada, Special Paper 34, p. 331-348.
- Fahrig, W.F. and West, T.D.**  
1986: Diabase dyke swarms of the Canadian Shield; Geological Survey of Canada, Map 1627A.
- Fahrig, W.F., Irving, E., and Jackson, G.D.**  
1971: Paleomagnetism of the Franklin diabases; *Canadian Journal of Earth Sciences*, v. 8, p. 455-467.
- Fraser, J.A.**  
1967: Geological map, Hardisty Lake (West Half); District of Mackenzie, Northwest Territories; Geological Survey of Canada, Map 224A, scale 1 inch to 4 miles.
- Fraser, J.A., Hoffman, P.F., Irvine, T.N., and Mursky, G.**  
1972: The Bear Province; in *Variations and Tectonic Styles in Canada*, (ed.) R.A. Price and R.J.W. Douglas; Geological Association of Canada, Special Paper 11, p. 454-503.
- Harlan, S.S.**  
1993: Paleomagnetic results from Middle and Late Proterozoic intrusive rocks of the central and southern Rocky Mountains; Geological Society of America, Abstracts with Programs, v. 25, 48p.
- Heaman, L.M., LeCheminant, A.N., and Rainbird, R.H.**  
1992: Nature and timing of Franklin igneous events, Canada: Implications for a late Proterozoic mantle plume and the breakup of Laurentia; *Earth and Planetary Science Letters*, v. 109, p. 117-131.
- Hildebrand, R.S.**  
1984: Geology of the Rainy Lake-White Eagle Falls area, District of Mackenzie: Early Proterozoic cauldrons, stratovolcanoes and subvolcanic plutons; Geological Survey of Canada, Paper 83-20, p. 1-41.
- Hildebrand, R.S., and Bowring, S.A.**  
1988: Geology of parts of the Calder River map area, central Wopmay Orogen, District of Mackenzie; in *Current Research, Part C*; Geological Survey of Canada, Paper 88-1C, p. 199-205.
- Hildebrand, R.S., Annesley, I.R., Bardoux, M.V., Davis, W.J., Heon, D., Reichenbach, I.G., and Van Nostrand, T.**  
1984: Geology of the Early Proterozoic rocks in parts of the Leith Peninsula map area, District of Mackenzie; in *Current Research, Part A*; Geological Survey of Canada, Paper 84-1A, p. 217-221.
- Hildebrand, R.S., Bowring, S.A., Andrew, K.P.E., Gibbins, S.F., and Squires, G.C.**  
1987: Geological investigations in Calder River map area, central Wopmay Orogen, District of Mackenzie; in *Current Research, Part A*; Geological Survey of Canada, Paper 87-1A, p. 699-711.
- Hildebrand, R.S., Bowring, S.A., and Housh, T.**  
1990: The medial zone of Wopmay Orogen, District of Mackenzie; in *Current Research, Part C*, Geological Survey of Canada, Paper 90-1C, p. 167-176.
- Hildebrand, R.S., Bowring, S.A., Steer, M.E., and Van Schmus, W.R.**  
1983: Geology and U-Pb geochronology of parts of the Leith Peninsula and Riviere Grandin map areas, District of Mackenzie; in *Current Research, Part A*; Geological Survey of Canada, Paper 83-1A, p. 329-342.
- Hoffman, P.F.**  
1989: Precambrian geology and tectonic history of North America; in *The Geology of North America: An Overview*, (ed.) A.W. Bally and A.R. Palmer; Geological Society of America, *Geology of North America*, v.A, Boulder, Colorado, p. 447-512.
- Hoffman, P. and Hall, L.**  
1993: Geology, Slave craton and environs, District of Mackenzie, Northwest Territories; Geological Survey of Canada, Open File 2559, scale 1:1 000 000.
- Kent, J.T., Briden, J.C., and Mardia, K.V.**  
1983: Linear and planar structure in ordered multivariate data as applied to progressive demagnetization of paleomagnetic remanence; *Geophysical Journal of the Royal Astronomical Society*, v. 75, p. 593-621.
- Kidd, D.F.**  
1936: Rae to Great Bear Lake, Mackenzie District, N.W.T.; Geological Survey of Canada, Memoir 187, 44 p.
- LeCheminant, A.N. and Heaman, L.M.**  
1994: 779 Ma mafic magmatism in the northwestern Canadian Shield and northern Cordillera: a new regional time-marker; Eighth International Conference on Geochronology, Cosmochronology and Isotope Geology, Berkeley, California, in *United States Geological Survey Circular 1107, Program with Abstracts*, 187 p.
- Lord, C.S.**  
1942: Snare River and Ingray Lake map-areas, Northwest Territories; Geological Survey of Canada, Memoir 235, 35 p.
- Lord, C.S. and Parsons, W.H.**  
1952: Camsell River map area, District of Mackenzie, Northwest Territories; Geological Survey of Canada, Map 1014A, scale: 1 inch to 4 miles.
- Park, J.K.**  
1974: Paleomagnetism of miscellaneous Franklin and Mackenzie diabases of the Canadian Shield and their adjacent country rocks; *Canadian Journal of Earth Sciences*, v. 11, p. 1012-1017.
- 1981: Paleomagnetism of the Late Proterozoic sills in the Tsezotene Formation, Mackenzie Mountains, Northwest Territories, Canada; *Canadian Journal of Earth Sciences*, v. 18, p. 1572-1580.
- Park, J.K., Norris, D.K., and Laroche, A.**  
1989: Paleomagnetism and the origin of the Mackenzie Arc of northwestern Canada; *Canadian Journal of Earth Sciences*, v. 26, p. 2194-2203.
- Perrier, C.**  
1988: Etude comparative de deux intrusions gabbroïques dans la zone magmatique du Grande Lac de l'Ours, Province de l'Ours, Territoires du Nord-Ouest; B.Sc. Thesis, Université de Montréal, p. 1-46.
- Rainbird, R.H., Heaman, L.M., Jefferson, C.W., and LeCheminant, A.N.**  
1992: Refined correlation of Neoproterozoic stratigraphy in northwestern Canada; in *Exploration Overview*, Yellowknife Geoscience Forum, Yellowknife, N.W.T., 39 p.
- Reichenbach, I.G.**  
1991: The Bell Island Bay Group, remnant of an early Proterozoic ensialic marginal basin in Wopmay Orogen, District of Mackenzie; Geological Survey of Canada, Paper 88-28, 43 p.
- Wilson, J.T. and Lord, C.S.**  
1942: Ingray Lake map area, District of Mackenzie, Northwest Territories; Geological Survey of Canada, Map 697A, scale: 1 inch to 4 miles.

# Geological setting of Bode copper and Damp polymetallic prospects, central Great Bear magmatic zone, Northwest Territories<sup>1</sup>

Sunil S. Gandhi and Nirankar Prasad  
Mineral Resources Division

*Gandhi, S.S. and Prasad, N., 1995: Geological setting of Bode copper and Damp polymetallic prospects, central Great Bear magmatic zone, Northwest Territories; in Current Research 1995-C; Geological Survey of Canada, p. 201-212.*

---

**Abstract:** A dacite-rhyodacite assemblage containing some basalt, andesite, rhyolite and sedimentary rocks, underlies a 30 x 15 km area between Isabella and Longtom lakes. It is intruded by related porphyries and younger granitic plutons. The volcanic assemblage is lithologically comparable with, and lies on the regional trend of, the LaBine Group 50 km to the north-northwest at Great Bear Lake, and belongs to the 1.87-1.84 Ga old Great Bear magmatic zone.

The Bode copper prospect near Isabella Lake to the south is in an east-trending shear zone in dacite, and contains pyrite-chalcopyrite aggregates and disseminations, with minor quartz and bornite. The Damp prospect at the northern tip of the assemblage is hosted by a breccia zone in rhyodacite, containing magnetite-hematite as matrix, and pyrite, chalcopyrite, cobalt-nickel sulphides and uraninite. It is regarded as an example of an Olympic Dam-type deposit.

**Résumé :** Un assemblage de dacite-rhyodacite contenant un peu de basalte, d'andésite, de rhyolite et de roches sédimentaires repose sous une zone de 30 km sur 15 km entre les lacs Isabella et Longtom. Il est recoupé par des intrusions de porphyres associés et des plutons granitiques plus récents. L'assemblage volcanique est lithologiquement comparable au Groupe de LaBine, situé à 50 km au nord-nord-ouest du Grand lac de l'Ours, groupe sur la direction duquel il s'étend, et il fait partie de la zone magmatique du Grand lac de l'Ours de 1,87-1,84 Ga.

Le prospect de cuivre de Bode, près du lac Isabella au sud, se situe dans une zone de cisaillement à direction est dans des dacites, et contient des agrégats et des disséminations de pyrite-chalcopyrite et un peu de quartz et de bornite. Le prospect de Damp, à l'extrémité nord de l'assemblage, est encaissé dans une zone bréchique dans une rhyodacite, contenant de la magnétite-hématite comme matrice, et de la pyrite, de la chalcopyrite, des sulfures de cobalt-nickel et de l'uraninite. C'est un exemple de gisement de type Olympic Dam.

---

<sup>1</sup> Contribution to Canada-Northwest Territories Mineral Initiatives (1991-1996), an initiative under the Canada-Northwest Territories Economic Development Cooperation Agreement.

## INTRODUCTION

The Isabella-Longtom lakes area is of interest with regard to the regional metallogeny of the whole Great Bear magmatic zone because of the Damp prospect, which is one of the few examples of breccia-hosted Olympic Dam-type polymetallic (Fe-Cu-U-Au-Ag) occurrences in a volcanic assemblage (Cannuli et al., 1989). Others are the Sue- Dianne, Mar and Fab prospects in the Faber Lake area more than 150 km to the south, and like the Damp prospect they are hosted by volcanic rocks (Gandhi, 1994). The Bode copper prospect near Isabella Lake, on the other hand, is of vein and disseminated-type in a shear zone in the volcanic assemblage. The present study was undertaken to better define the volcanic setting and mineralization of the Bode and Damp prospects. This paper summarizes the results of mapping in 1994 around Bode Lake, and of an examination of the two prospects. It

incorporates earlier observations on the Damp prospect and in its vicinity by the first author, made in the late 1980s in the company of the exploration crews of the Central Electricity Generating Board Exploration (Canada) Limited (CEGBE (Canada) Ltd.). The recent work was carried out as part of a project on the metallogeny of the southern Great Bear magmatic zone (viz. south of latitude 65°), under the Canada-Northwest Territories Minerals Initiative Program 1991-1996.

## PREVIOUS WORK

During early reconnaissance geological mapping of the area Kidd (1936), Fraser (1967), and Lord and Parsons (1947) recognized the presence of a volcanic assemblage in the Isabella-Longtom lakes area (Fig. 1). More recent mapping

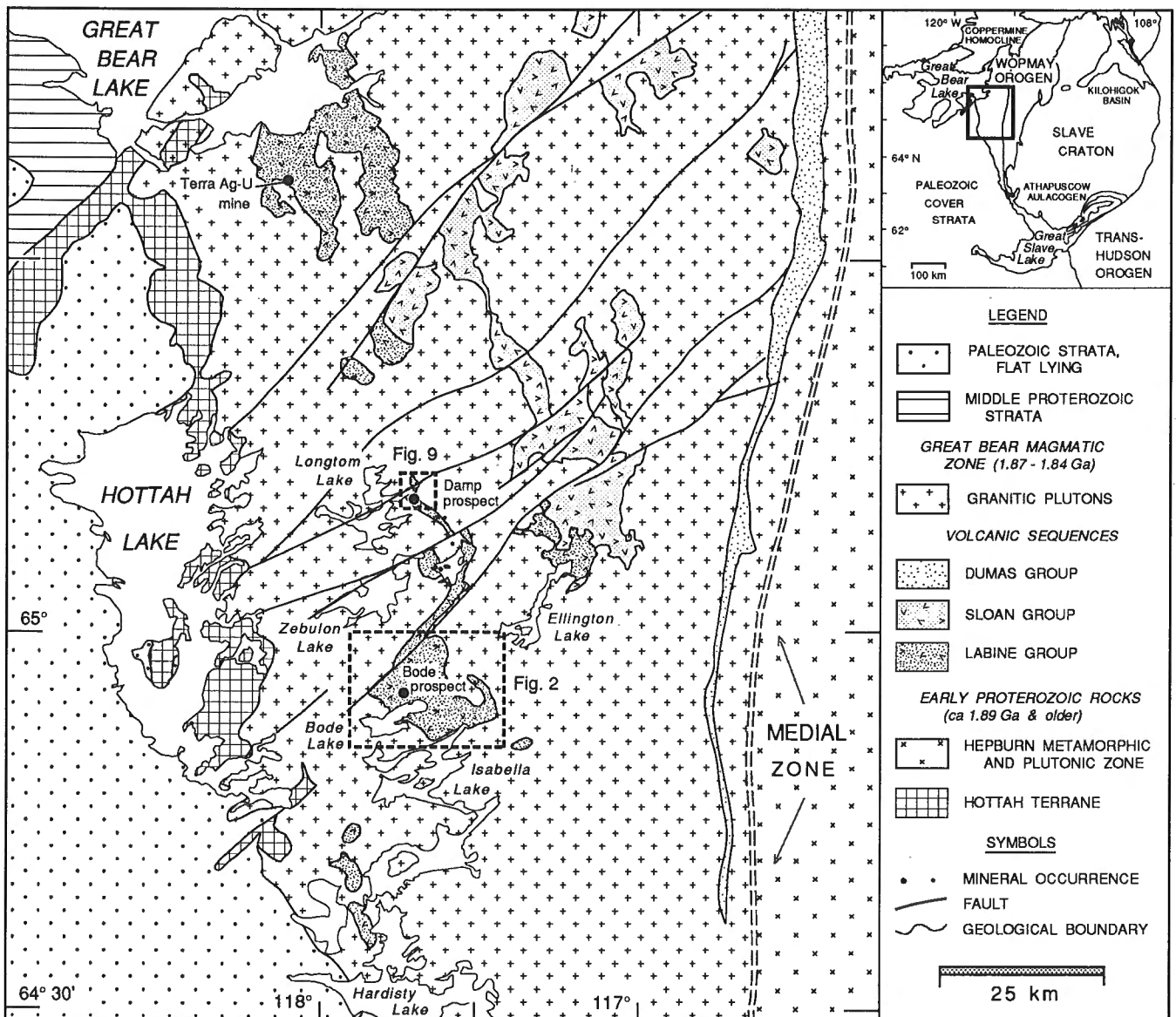


**Figure 1.** Volcanic assemblages of the central Great Bear magmatic zone, and location of the Bode and Damp prospects.

to the north has led to the interpretation of the volcanic and related plutonic rocks as part of a continental magmatic arc formed 1870-1840 Ma ago, during the late stages of Wopmay orogeny (Hoffman, 1980, 1984; Hildebrand et al., 1987). Detailed mapping of the volcanic assemblages in the region has been carried out by Hildebrand (1981, 1984) near Great Bear Lake, Pelletier (1985) in the Ellington Lake area east of Longtom Lake, and Reichenbach (1991) in the Hottah Lake area to the west.

The Cent claims were the first ones staked in the area (Baykal, 1968), and on these very weak radioactivity and galena were reportedly found in a quartzite-argillite zone. This zone, however, turns out to be, as learned from the present work, a giant quartz vein with chloritic alteration that contains abundant specular hematite and spotty weak radioactivity. An airborne scintillometer survey in 1968 by Shield Resources Limited did not detect any radioactivity, but located the gossan zone of the Bode copper prospect, which was trenched and drilled in the following year (Curry, 1969). The Geological Survey of Canada conducted a regional geochemical survey in 1973 (Allan and Cameron, 1973), and an airborne spectrometric survey on 25 km line spacing in 1974 (GSC Open Files 140 and 188). During the mid-1980s, CEGBE (Canada) Limited extended their exploration from Great Bear Lake to the Longtom Lake area, and discovered the Damp prospect in 1985, and several other occurrences in the area within 15 km to the south (Cannuli et al., 1989; Cannuli, 1989; Sawiuk et al., 1989).

## GENERAL GEOLOGY

The Great Bear magmatic zone is a continental volcano-plutonic zone more than 800 km long and 100 km wide (Hoffman, 1980, 1984; Hildebrand et al., 1987). Aggregate thickness of the volcanic assemblage in the northern and central parts of the magmatic zone is in the order of 10 km. It is divided into the LaBine Group in the west, overlying Sloan Group in the middle, and the Dumas Group along the eastern boundary (Fig. 1). Large granitic plutons mark the late stages of the magmatic activity. These were followed by brittle faulting, along northeast-trending right lateral faults that affected the whole magmatic zone.

The volcanic assemblage of the Isabella-Longtom lakes area is isolated from the larger volcanic area to the north by younger granitic plutons, which are even more extensive in the south (Fig. 1). Geographically closest are the rocks of the LaBine Group in the Camsell River area to the north and the Ellington Lake area to the east (Hildebrand, 1981, 1984; Pelletier, 1985). Extrusive rocks that range from basalt to rhyolite in composition, and associated sediments, occur in both areas, and are intruded by quartz monzonite-monzodiorite. The overlying Sloan Group, dominated by dacite-rhyodacite-rhyolite, postdates these intrusions (Hildebrand et al., 1987). The lower assemblage at Ellington Lake has been regarded as equivalent to the LaBine Group and the upper assemblage to the northeast as part of the Sloan Group by Hildebrand and Bowring (1988). The assemblage

of the Isabella-Longtom lakes area is also lithologically comparable with the LaBine Group, and is intruded by quartz monzonite-monzodiorite.

The basement on which the Isabella-Longtom lakes assemblage was deposited is not exposed. In the north, the LaBine Group rests unconformably on the Hottah terrane, which is an early Proterozoic terrane of granitic rocks with metasedimentary remnants, and a 1.9 Ga volcanic assemblage of the Bell Island Bay Group exposed along Hottah Lake (Hildebrand et al., 1987; Reichenbach, 1991).

The volcanic assemblage of the Isabella-Longtom lakes area is discussed here in two parts. The southern part near Isabella Lake (Fig. 2) is described first, based mainly on the fieldwork done by the writers in 1994. The northern part near Longtom Lake is reviewed briefly to provide the geological setting for the Damp prospect.

## GEOLOGY OF THE ISABELLA LAKE AREA

Following the regional mapping by Fraser (1967) that outlined an area of 'porphyries', a more detailed stratigraphic and structural study was done near Bode Lake, on a scale of 1 inch to 1/2 mile by Curry (1969). He recognized two subunits to the assemblage, one rhyolitic and the other dacitic. This was confirmed by the present work, which in addition identified the Bode Lake dacite porphyry as a subvolcanic intrusive phase rather than as part of the dacitic volcanic subunit. Curry (1969) interpreted moderately tight folds about east trending axes in the western part of the area, which has been substantiated by the present study, but the structure is complex and needs further study. The two volcanic subunits are referred to here as the Swan Lake and Isabella Lake sequences (Fig. 2).

### *Swan Lake rhyolitic sequence*

This sequence is well exposed on the eastern large peninsula of Swan Lake and forms northeast-trending ridges that extend for more than 5 km. The sequence has variable dips because of minor folds, but commonly has gentle dips to the east and southeast. The lowermost unit on the tip of the peninsula is an aphanitic rhyolite with a few small quartz eyes less than 1 mm in diameter. It is overlain by a siltstone 7 m thick that dips 35° to the north. The siltstone is followed farther to the northeast by several ignimbrite units that are tens of metres thick. They display variations in texture from well foliated due to compaction/flowage (Fig. 3 and sample 401, Table 1), to relatively massive and lithic fragmental. These are overlain by a banded to massive rhyolite that forms the top of a ridge few hundred metres northeast of sample 401 (Fig. 2). The rhyolite is distinctive because of its aphanitic texture, the presence of a few small quartz eyes (< 1 mm diameter) and white weathering surface (sample 626, Table 1). It is in turn overlain by a thinly bedded siltstone 60 m thick (Fig. 4). They have been folded into a syncline which is well exposed on the top of the ridge.

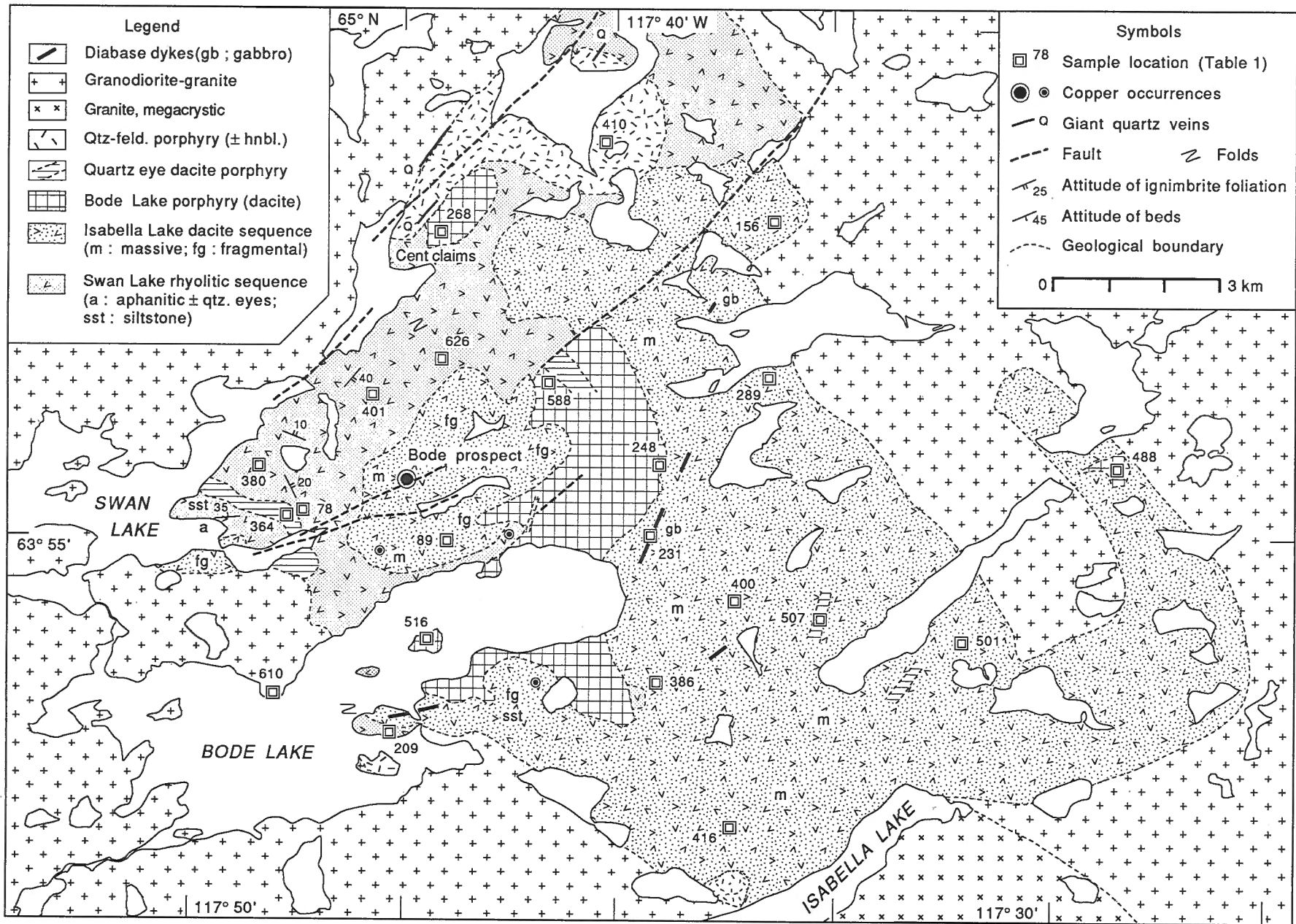


**Figure 2.** Geology and mineral occurrences of the Bode Lake-Isabella Lake area. Analyses of the samples given in Table 1. Abbreviations: qtz. - quartz; hnb. - hornblende; feld. - feldspar.

The rhyolite sequence outcrops discontinuously on the north and south sides of Bode Lake. A few exposures contain dark grey vitreous rhyolite. Rhyodacites with well developed ignimbritic foliation (sample 209, Table 1), and banded rhyolite are also encountered in some places. Thin siltstone beds occur locally.

The overall distribution and attitude of the rocks of the Swan Lake sequence suggest a broad syncline plunging gently to the east. Subsidiary folds and minor folds at a scale of a metre to tens of metres are recognizable in several places. The aggregate thickness of the sequence is estimated to be in the order of 500 m.

### *Isabella Lake dacitic sequence*

Grey massive and fragmental dacitic rocks of this sequence are areally extensive, and form most of the ridges in the area north of Isabella Lake (Fig. 2). They are porphyritic, with 25-30 per cent plagioclase as euhedral to subhedral laths 2 to 4 mm long, set in a dark to medium grey matrix. Thin sections reveal that mafic silicates, mainly hornblende, are highly altered to chlorite. Some of them contain highly altered



**Figure 3.** Rhyolitic ignimbrite, showing moderate dip of flowage/compaction foliation. Near sample 401 (Fig. 2). Looking southwest. (GSC 1994-750Y)



**Figure 4.** Current bedding in siltstone, 400 m northeast of sample 401 (Fig. 2). Looking southwest. (GSC 1994-750L)

octagonal sections of pyroxene. Somewhat more felsic rocks contain sparsely distributed quartz grains. This is reflected in their chemical compositions which show a range of 62 to 69 per cent silica (analyses 7 to 13, Table 1).

The stratigraphic succession in these rocks is difficult to determine because of the lack of marker units, and obscure unit boundaries. Fragmental rocks are widely distributed and are thick in some places, but their boundaries with massive rocks are commonly gradational. The fragmental rocks contain subangular to rounded fragments of rocks close in composition to the host rock. The fragments commonly have coarser but fewer feldspar phenocrysts and a finer and darker grey matrix. They range in size from a few millimetres to a few tens of centimetres (Fig. 5). In some places they are elongate lensoid, as much as a metre long. In a few places a concentration of such stretched lenses give a flow banded appearance (Fig. 6). Faintly developed layering has been observed at many localities in commonly massive looking rocks. In many cases this layering dips gently to the northeast. The massive rocks also have sparsely distributed fragments similar in composition to those in the fragmental rocks (Fig. 7).

Dacitic rocks of this type were also observed southwest of Isabella Lake during the present study, in the northernmost of the three isolated volcanic areas west of Hardisty Lake (Fig. 1). In the northeastern corner of this area, a siltstone unit is overlain by polymictic conglomerate containing some magnetite-rich quartzite boulders. This in turn is overlain by rhyodacite ignimbrite (analysis 14, Table 1). Bedding in siltstone and flowage/compaction foliation in ignimbrite dip 25 to 40° to the north. These rocks have been intruded by a large body of Bode Lake porphyry (analyse 20, Table 1).

### *Bode Lake porphyry*

A massive feldspar porphyritic dacite forms a large intrusive body exposed on the north and south sides of Bode Lake, and smaller bodies are found elsewhere (Fig. 2). It is characterized by well formed feldspar phenocrysts 8 to 10 mm long, set in a dark grey fine- to medium-grained matrix comprising pyroxene, hornblende, quartz, feldspar, and iron oxides



**Figure 5.** Coarse fragmental dacite, near sample location 89 (Fig. 2). (GSC 1994-750N)

Table 1. Chemical analyses of selected rocks from the Bode Lake-Isabella Lake area, Northwest Territories.

Analysis	1	2	3	4	5	6	7	8	9	10	11	12	13	14	15	16	17	18	19	20	21	22	23	24	25	26
Sample #	401	78	209	380	626	D8:13	400	386	89	416	289	501	156	333'	248	268	588	488	516	338'	364	507	410	325'	610	231
Rock unit	Swan Lake rhyolites					Rhyd*	Isabella Lake dacites							Dacite	Bode Lake porphyry					BL por.	Qz-eye porph.	QF por.	Qz-mo.	Grd.	Gabbro	
SiO <sub>2</sub> %	70.90	71.00	71.50	71.70	72.70	61.90	62.80	63.80	64.10	64.20	64.50	64.50	65.70	66.10	61.90	63.00	62.00	63.30	61.60	61.80	68.30	69.10	70.40	73.10	69.40	53.80
TiO <sub>2</sub>	0.25	0.27	0.41	0.26	0.24	0.39	0.62	0.62	0.63	0.58	0.60	0.55	0.57	0.53	0.67	0.65	0.66	0.58	0.65	0.76	0.39	0.37	0.32	0.23	0.42	0.61
Al <sub>2</sub> O <sub>3</sub>	14.70	14.90	16.50	14.40	14.60	18.30	15.60	15.50	15.20	15.10	15.40	15.70	15.50	15.20	17.00	15.40	15.50	15.30	16.70	15.60	16.10	15.20	15.20	14.30	14.50	11.10
Fe <sub>2</sub> O <sub>3</sub>	1.10	2.10	2.00	1.60	0.90	5.60	2.50	2.10	4.20	2.10	2.30	3.20	2.50	2.10	4.30	4.70	3.90	2.70	2.10	4.70	2.30	1.90	1.30	0.70	1.60	2.40
FeO	1.20	0.50	0.70	1.00	1.10	1.10	2.70	3.00	1.20	3.00	2.50	1.70	1.90	2.30	2.00	0.90	2.40	2.70	3.10	1.90	0.90	1.30	1.10	1.20	1.80	5.80
MnO	0.08	0.05	0.03	0.06	0.04	0.04	0.09	0.10	0.07	0.07	0.09	0.09	0.06	0.06	0.06	0.11	0.06	0.12	0.05	0.10	0.06	0.05	0.04	0.05	0.07	0.15
MgO	0.53	0.32	0.69	0.51	0.36	0.84	2.95	2.97	2.39	3.02	2.61	1.88	1.45	2.18	2.75	3.11	2.51	2.63	2.99	2.92	0.99	1.24	0.91	0.47	1.73	12.63
CaO	1.89	1.26	0.17	1.56	1.24	1.08	4.62	4.56	4.03	4.40	3.86	4.48	3.69	4.21	5.43	4.62	4.27	4.80	3.55	4.80	2.89	2.52	1.97	1.80	1.88	6.28
Na <sub>2</sub> O	2.00	3.70	0.40	1.50	1.90	9.40	2.60	3.00	2.80	3.30	2.60	2.90	3.10	2.70	2.60	2.30	2.80	2.40	2.80	2.90	2.40	2.70	3.30	2.90	3.00	1.20
K <sub>2</sub> O	5.76	4.71	5.23	5.20	5.75	0.07	3.61	3.56	3.66	2.74	4.09	3.61	3.72	2.82	2.01	3.37	3.56	3.76	4.66	3.56	4.00	5.00	4.77	4.94	4.70	3.34
P <sub>2</sub> O <sub>5</sub>	0.06	0.07	0.10	0.06	0.05	0.15	0.16	0.15	0.15	0.15	0.15	0.14	0.15	0.13	0.16	0.15	0.16	0.13	0.17	0.19	0.09	0.09	0.08	0.06	0.12	0.20
LOI	1.00	0.70	2.40	1.30	1.20	0.90	1.30	0.60	1.40	0.80	1.40	1.20	1.10	1.00	0.90	2.20	1.80	1.20	1.20	0.70	1.30	0.60	1.00	0.80	1.40	1.60
Total	98.60	99.10	97.80	98.10	99.00	99.00	98.40	99.60	98.50	98.80	98.80	98.90	98.50	98.70	99.10	98.50	98.00	98.60	98.50	99.40	98.50	99.70	99.60	99.90	99.40	97.70
Ba ppm	939	1006	401	1008	983	61	774	725	704	443	889	773	806	1811	410	748	757	630	726	712	790	790	746	772	827	687
Be	22	22	22	21	22	23	16	20	16	16	19	18	15	14	15	17	16	19	19	15	17	19	18	19	17	18
Co	254	213	338	267	237	21	183	185	176	136	157	180	137	157	157	119	142	186	202	174	195	220	193	222	197	175
Cr	214	217	28	202	152	45	364	332	294	339	311	306	320	397	430	386	287	196	317	310	271	255	237	186	278	266
Cu	272	344	258	326	268	148	219	211	204	215	218	237	211	198	195	197	182	194	231	220	238	201	193	198	208	137

Notes :

- Analyses by the Analytical Chemistry Section, Mineral Resources Division, Geological Survey of Canada, Ottawa; All analyses by x-ray fluorescence method except FeO and LOI (Loss on ignition) by rapid chemical methods; Fe<sub>2</sub>O<sub>3</sub> is calculated using formula :  $Fe_2O_3 + Fe_2O_3(xrf) - 1.11134 X FeO$  (volumetric).
- Location of samples in Figure 2, except for # 325', 333' and 338' (analyses 8,14 and 20) from the north end of the volcanic area southwest of Isabella Lake (Fig. 1), and for the # D8:13 (Rhyd\* : analysis 6) which is from the Damp prospect drill hole Zeb-88-8 at approximately 13.0 m; all sample numbers except the drill core sample, are of GFA-94 series collected in 1994.
- Abbreviations : Rhyd\* - Rhyodacite, altered, from the Damp prospect; BL por. - Bode Lake porphyry; Qz-eye porph. - Quartz eye porphyry; QF por. - Quartz-feldspar porphyry; Qz-mo. - quartz monzonite, marginal phase; Grd. - Granodiorite.

(Fig. 8). Feldspar phenocrysts make up approximately 20 per cent of the rock, and are randomly oriented. Quartz phenocrysts occur in most of the rocks but they are few, and make up less than 5 per cent of the rock. Because they are sparsely distributed in the rock and are greyish in colour, they are not readily apparent in the field. The chemical data show a small range in composition for the Bode Lake porphyry (analyses 15 to 19, Table 1).

### ***Quartz-eye dacite porphyry***

Large dyke-like bodies of grey, quartz-eye dacite porphyry are found at a few localities in the area (Fig. 2). These are difficult to distinguish from the Bode Lake porphyry in the field, but an abundance of quartz phenocrysts, which make up 15 to 20 per cent of the rock, is their distinguishing feature. Sharp chilled margins of the dykes are observed against the dacites and the Bode Lake porphyry. A sheet of this type of porphyry occurs on the peninsula of Swan Lake, and is subparallel to the gently dipping siltstone and ignimbrites (analysis 21, Table 1).



**Figure 6.** Dacite with stretched lenticular pyroclasts, 1 km northeast of Bode prospect. Looking north. Note glacial strike dipping gently to the east. (GSC 1994-7500)



**Figure 7.** Massive dacite with sparsely distributed dacite fragments. At sample site 386 (Fig. 2). (GSC 1994-750Q)

### ***Quartz-feldspar porphyry***

A large body of porphyry containing well formed phenocrysts of quartz and feldspar in a pale cream coloured aphanitic matrix, occurs northeast of Swan Lake (Fig. 2; analysis 23, Table 1). Numerous dykes and irregular bodies of similar porphyries occur near Swan and Bode lakes, but are too small to show on the map (Fig. 2). Some of them are quartz poor and contain phenocrystic hornblende, and a few others appear to be transitional to quartz monzonite.

### ***Quartz monzonite-monzodiorite***

Several dykes of quartz monzonite, monzonite and monzodiorite cut the volcanic rocks of the area, but no large intrusions of these types have been found. They are characterized by well formed coarse feldspar crystals and contain medium to coarse interstitial hornblende, feldspars, quartz and accessory minerals. Southwest of Isabella Lake, an intrusion of this type in the sedimentary-volcanic sequence has a siliceous marginal phase (analysis 24, Table 1).

### ***Granodiorite-granite***

Medium- to coarse-grained hornblende-biotite granodioritic rocks surround the volcanic assemblage. Sharp intrusive contacts of the plutons with the volcanic rocks are observed on the south side of Bode Lake. Irregular dyke-like patches of finer grained granitic rock occur in the volcanic rocks near the contact. Locally aggregates of pyrite, as much as 25 cm long, occur in granite at the contact, as seen east of sample site 209 (Fig. 2). Fine grained granite and aplitic dykes occur in the plutons. The western body is hornblende- and biotite-bearing granodiorite (analysis 25, Table 1). It is apparently an extension of the large Yen pluton east of Hottah Lake (Fig. 1) mapped by Reichenbach (1991).

### ***Megacrystic granite***

A large pluton of coarse feldspar porphyritic granite occurs in the Isabella-Hardisty Lake area (Fraser, 1967). Curry (1969) projected its contact along the north shore of the lake



**Figure 8.** Bode Lake porphyry. East end of island, sample 516 (Fig. 2). (GSC 1994-750K)



through an overburden covered area on the south side of a high ridge of dacite (Fig. 2). At the southwest end of this ridge, near sample site 416, a 50 m dyke of coarse porphyritic monzonite was observed during the present work. It may have been regarded by him as megacrystic granite.

**Diabase dykes**

A number of diabase dykes occur in the area, but only a few are shown on the map (Fig. 2). Most of the dykes trend in directions between north and east-northeast. They range to as much as 10 m in width. They are fresh, diabase to diorite in composition, but a noteworthy exception is a coarse grained magnesium-rich gabbroic dyke, approximately 10 m wide, located on a ridge northeast of Bode Lake (analysis 26, Table 1). Smaller porphyritic dykes related to it occur along the east side of the northeast-trending ridge.

**GEOLOGY OF THE LONGTOM LAKE AREA**

The Longtom Lake area north of 65° N (Fig. 1) was mapped on a regional scale by Lord and Parsons (1947), and geologists of CEGBE (Canada) Limited carried out more detailed mapping (at a scale of 1 : 12 500) of most of this area in the 1980s (Cannuli, 1989). This work showed a northeast-trending zone of dacitic and rhyodacite ignimbrites in the south which forms a continuation of the Swan Lake rhyolitic sequence. There is a small gap in detailed mapping between the two map areas, and further fieldwork is needed to determine a stratigraphic sequence common to both. Basaltic and andesitic flows occur near the Damp prospect (Fig. 9) and to the southwest of it.



Figure 9. General geology of the Damp prospect area. After Cannuli (1989).

Sedimentary rocks are extensive southwest of the Damp prospect (Cannuli, 1989). They include sandstones which contain variable amounts of feldspar and mafic minerals, siltstones and argillaceous beds. They are regarded as fluvial, and largely volcanoclastic. They trend commonly to the southeast and dip to the southwest. Folding and shearing are noted in the sedimentary and volcanic rocks at several places.

Large bodies of quartz monzonite-monzodiorite-monzonite intrusions occur near the Damp prospect (Fig. 12) and to the southwest of it. Their contacts, where determinable, appear to be concordant with the volcano-sedimentary assemblage, and are commonly marked by intense albitization (Cannuli, 1989).

**MINERAL OCCURRENCES**

**Bode copper prospect**

During a helicopter-borne scintillometer survey carried out in 1968 by Shield Resources Limited, a conspicuous gossan zone was found at the site of the Bode copper prospect. It contained aggregates and disseminations of pyrite with some chalcopyrite, and some quartz stringers that contain local concentrations of the two minerals (Curry, 1969). It was staked as the BL claim group, and in the following year it was mapped in detail, and explored further by 3 trenches and 5 drillholes totalling 533 m (Fig. 10). Assay results of trench and drill core samples are summarized in Table 2.

The sulphides are hosted by a shear zone in massive dacite. The sulphide zone is best exposed in Trench 1 (Fig. 11). The shear zone trends approximately east-northeast and is nearly vertical. It contains disseminated pyrite that forms as much as 10 per cent of the rock. Stringers and veins of coarse pyrite, quartz and chalcopyrite occur mainly in the zone of pyrite dissemination, but a few extend beyond it. Chalcopyrite is paragenetically later than pyrite, and in part

Table 2. Assays of selected drill core sections from the Bode prospect, Isabella Lake area, Northwest Territories.

Hole No.	From	To	Length	Cu %	Bi %
BL-69-1	37.95 m	58.06 m	20.11 m	0.66	0.029
BL-69-1	36.42 m	66.60 m	30.18 m	0.52	0.019
BL-69-2	15.55 m	21.64 m	6.09 m	0.18	
	33.22 m	38.10 m	4.88 m	0.36	
	44.44 m	114.30 m	69.86 m	0.28	0.018
BL-69-3	79.40 m	86.87 m	7.47 m	0.09	
BL-69-4	51.76 m	60.97 m	9.20 m	0.10	tr
BL-69-4	87.02 m	93.27 m	6.25 m	0.09	tr
BL-69-5	31.55 m	36.62 m	8.07 m	0.16	0.006

Notes: i) Drill holes shown in Figure 9; ii) tr = traces; iii) Ag assays ranged from traces to 10 ppm (0.3 oz/l) and Au contents in traces only; iv) Source: Curry (1969).

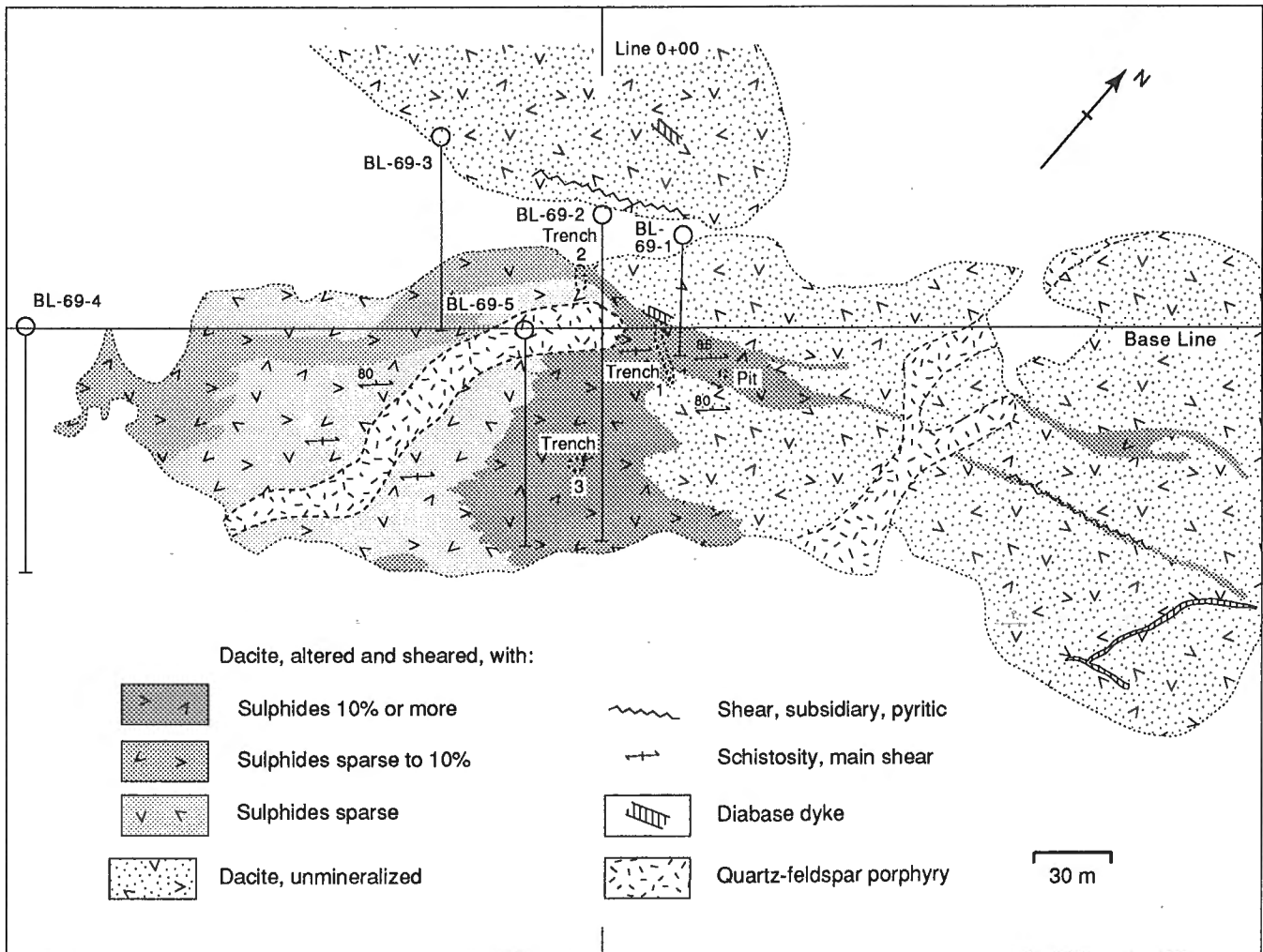


**Figure 10.** Geology, trenches and diamond drillhole locations of the Bode Lake copper prospect. After Curry (1969).

replaces it. Other minerals present in varying amounts are hematite, specularite, calcite, and locally bornite in sulphide aggregates. The host rock is intensely altered to chlorite, and in places it is highly silicified and contains abundant sericite.

**Damp polymetallic prospect**

The Damp prospect was discovered in 1985 by CEGBE (Canada) Limited during exploration for Port Radium-type U-Ag veins through application of a model based on mapping by the Geological Survey of Canada (Sawiuk et al., 1989). The model emphasizes the zone of intense albitization at the boundary of high level quartz monzonitic intrusions in the LaBine Group, and this is flanked by a zone of magnetite-apatite-actinolite veins and pods and an outer sulphide halo (Hildebrand, 1984). U-Ag occurrences of the Port Radium-Camsell River mining camp are spatially associated with this alteration zoning. The magnetite concentration provided an



**Figure 11.** Trench 1 of the Bode prospect (Fig. 9). Looking southeast. Note quartz-sulphide veins in schistose sulphide-rich zone. (GSC 1994-750 C)

exploration guide. The aeromagnetic data published by the Geological Survey of Canada were digitized and colour plotted by consultants Peterson, Grant and Watson Limited, and the magnetic anomalies were selected for ground follow-up (Sawiuk et al., 1989).

The polymetallic (Cu-U-Co-V ± Zn-Pb) mineralization occurs in a breccia zone within a rhyodacite ignimbrite (Fig. 12, 13). The dips of the primary foliation in the host unit and the distribution pattern of the associated volcanic units show a moderately tight synform about a southeast-trending axis (Fig. 9). The breccia zone also strikes in the same direction, dips steeply to the southwest, and is broadly concordant with the host unit. Strongly albitized rhyodacite occurs as fragments in a hematite-specularite-magnetite matrix (Fig. 13). Strong albitization is reflected in a drill core sample in the vicinity of the breccia zone that contains 9.4 per cent soda and 0.07 per cent potash, accompanied by some iron enrichment (analysis 6, Table 1). Veins of iron oxides occur

in the host rock in and adjacent to the breccia zone, and commonly form a network or framework breccia. Surface exposures show brick red hematite, green malachite stains, and yellow uranium secondary minerals.

Samples of outcrops and trenches, and drill core from 8 holes totalling 660 m, done during 1986-1988 show significant contents of Cu, U, Co, V, and locally Zn and Pb (Table 3). Au and Ag are present in many of the samples; the best value encountered was 6 g/t over 0.75 m in the upper part of the mineralized section in drillhole Z-88-14 (Cannuli, 1989). Mineral phases identified to date are chalcopyrite, pitchblende, pyrite, covellite, bornite, siegenite (NiCo<sub>2</sub>S<sub>4</sub>), violarite ((Ni,Fe)<sub>3</sub>S<sub>4</sub>), hematite, specularite, magnetite, albite, chlorite, epidote, garnet, and an unidentified vanadium mineral (Cannuli, 1989; Sawiuk et al., 1989). Hematite and specularite predominate over magnetite. Calcite occurs in some veins, and molybdenite is reported by Cannuli in what appear to be younger veins near the breccia zone. Galena and

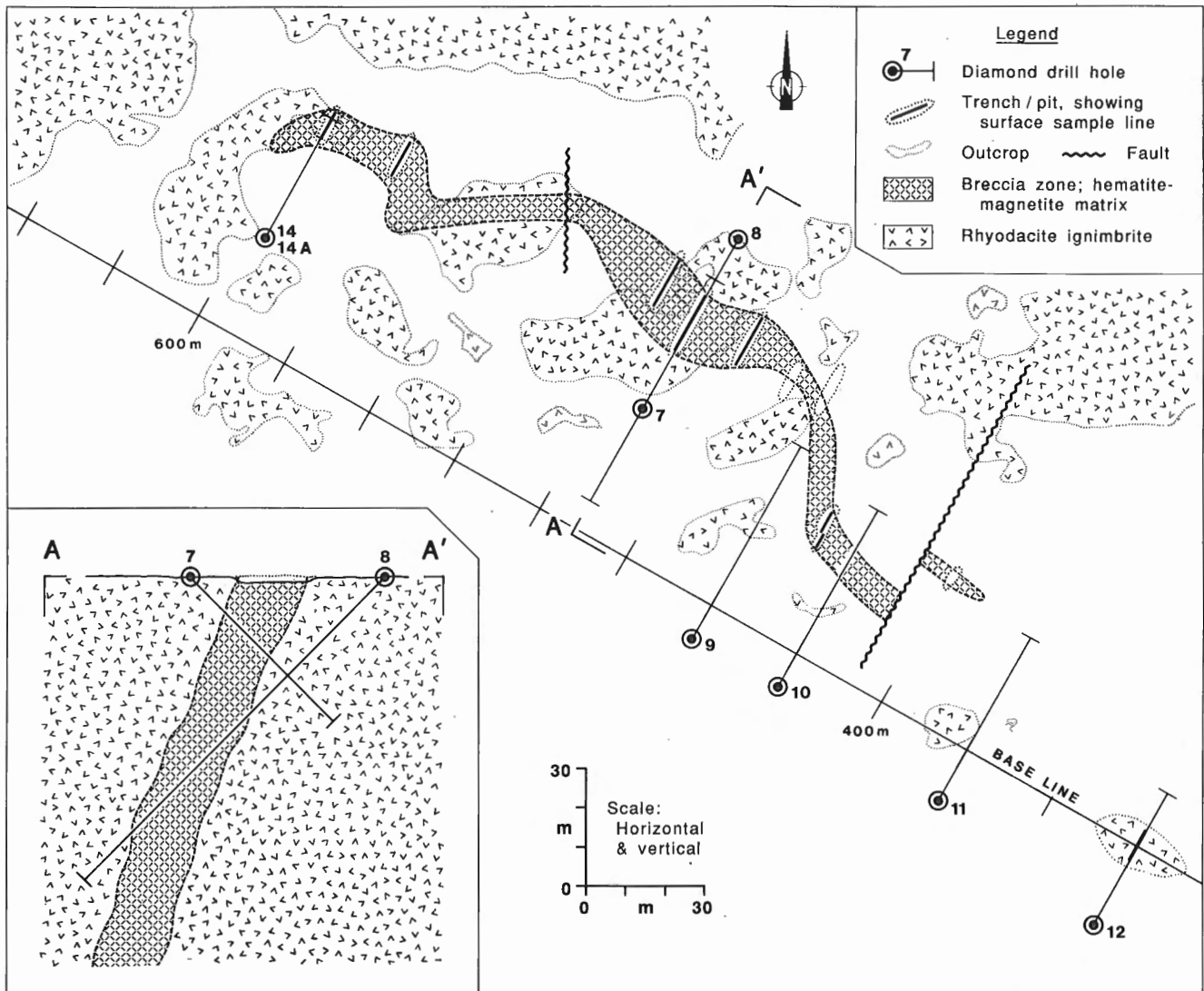


Figure 12. Geology, trenches and diamond drillhole locations of the Damp prospect. After Cannuli (1989).

spalerite occur to the southeast along the trend of the breccia zone (Fig. 12; Table 3), which has abundant pyrite but little or no iron oxide and uranium. The southeast extension thus represents a different style of mineralization from the main breccia zone. Uranium is concentrated in veins and fractures near surface in the breccia zone, and its contents decline to low values at depth as revealed by drilling (Cannuli, 1989).

**Table 3.** Selected assay results for the surface and drill core samples from the Damp prospect, Longtom Lake, Northwest Territories.

Sample Location	Width	Cu %	U %	Co %	V %	Pb %	Zn %
<b>Surface :</b>							
595 W : 55-62 m N	7.00 m	0.13	0.220	0.190	0.120		
575 W : 55-57 m N	2.00 m	0.10	0.021	0.150	0.130		
575 W : 62-65 m N	3.00 m	0.27	0.011	0.057	0.021		
500 W : 59-68 m N	9.00 m	0.25	0.246	0.059	0.033		
500 W : 78-75 m N	7.00 m	0.20	0.280	0.040	0.021		
490 W : 52-68 m N	16.00 m	0.32	0.161	0.058	0.037		
475 W : 56-70 m N	14.00 m	0.75	0.012	0.071	0.084		
434 W : 26-30 m N	4.00 m	0.48	1.187	0.052	0.077	0.29	0.08
435 W : 30-36 m N	6.00 m	0.39	0.806	0.065	0.110	0.21	0.06
325 W : 0-5 m N	5.00 m	0.79		0.051			1.98
325 W : 0-4 m S	4.00 m	0.97		0.052			1.82
<b>Diamond Drill Core :</b>							
88- 7 : 13.3-28.6 m	9.00 m*	0.45	0.019	0.071	0.023		
88- 8 : 48.5-92.4 m	12.00 m*	0.20	0.016	0.055	0.025		
88- 9 : 40.5-72.2 m	28.00 m*	0.17	0.006	0.072	0.017		
88-10 : 37.5-61.2 m	23.50 m*	0.29	0.008	0.061	0.028		
88-14 : 21.0-28.0 m	6.75 m*	0.22	0.040	0.180	0.048		
88-14A: 29.4-48.4 m	13.00 m*	0.01	0.002	0.013	0.012		
Notes: i) Surface samples from outcrops and trenches, and core samples from holes drilled at -45° during 1988 (Fig. 12); ii) * denotes true width of the mineralized zone; iii) Source : Cannuli (1989).							



**Figure 13.** Breccia in the central part of the Damp prospect near section A-A' (Fig. 12). Note grey colour of hematite-rich matrix and light coloured rhyodacitic fragments; darker area to the right has yellow uranium and green malachite stains. (GSC 1994 -750J)

### Other mineral occurrences

Several small uranium occurrences have been discovered by CEGBE (Canada) Limited near the Damp prospect (Fig. 9). Two of these, the Fog and DW, were each tested by a 52 m long drillhole. Two additional holes totalling 104 m tested a conductor zone at the northwest corner of Seahorse Lake, but did not reveal any significant mineralization. Surface exploration by the company during 1988 in the area to the south led to the discovery of several occurrences (Fig. 1), including one of polymetallic and one of Cu-Mo type, on an island and on the west shore of Devil's Lake, 9 km south-southeast of the Damp prospect. In the Bode Lake area, the present study revealed several small occurrences of chalcopyrite in quartz and quartz-hematite veins and along fractures, with or without pyrite (Fig. 2). Disseminated pyrite is common along and in the vicinity of the shear zone that hosts the Bode copper prospect, and forms gossans at several localities.

### DISCUSSION

This study reveals a preponderance of dacite-rhyodacite-rhyolite in the Isabella-Longtom lakes area (Table 1). More mafic rocks are restricted to the north near Longtom Lake (Fig. 9). The latter have been regarded as andesites and basalts mainly from the field observations, but it is possible that some of them are dark grey dacites like those found to the south. In any case, the true andesites and basalts are not known in the south at Isabella and Hardisty lakes, nor in the area farther to the south in the Faber Lake volcanic belt (Gandhi, 1994). If these southern volcanic rocks are coeval with those of the LaBine Group near Great Bear Lake, as appears to be the case from the geochronological data and field observations (Gandhi, 1994), then it is apparent that progressively more siliceous volcanism occurred in the Great Bear magmatic zone from north to south. This implies the differences in the involvement of the sialic crust during subduction, and in the compressional and extensional regimes during the magmatic activity.

A metallogenically significant aspect is the proximity of the quartz monzonitic plutons to the Olympic Dam-type polymetallic deposits exemplified by the Damp prospect and the Kiruna-type magnetite-apatite-actinolite veins and irregular bodies near Great Bear Lake (Hildebrand, 1984, 1986; Reardon, 1993; Gandhi, 1994). This implies a direct or indirect genetic link between the plutons and these magmatogenic mineral occurrences. The intense albitization associated with these occurrences, however, is not seen in occurrences farther to the south, although some alkali exchange is observed (Gandhi, 1994). The breccia zone of the Damp prospect has been regarded by Sawiuk et al. (1989) as crudely analogous to hydrothermal breccia associated with porphyry copper style mineralization in continental arc settings of Phanerozoic age. In the writers' opinion, however, the differences outweigh the similarities in terms of the metal contents and alteration. The Bode copper prospect displays greater similarities with porphyry copper-type deposits, as pointed out by Curry (1969), than with the Damp prospect. But it is one of

the few small occurrences of its kind in the whole of the Great Bear magmatic zone. Some other Cu-Mo occurrences noted in this zone are small granite-related veins (Gandhi, 1994).

## ACKNOWLEDGMENTS

Able assistance provided by Edward Williah, a native of Rae-Edzo, is greatly appreciated by the authors. The first author received excellent guidance and co-operation from exploration crews of the CEGBE (Canada) Limited during his visits to the Damp prospect during 1986-1989, in particular A. Climie, M. Cannuli, and M. Sawiuk. This paper benefited from the critical review by R.I. Thorpe of the Geological Survey of Canada.

## REFERENCES

- Allan, R.J. and Cameron, E.M.**  
1973: Lake sediment geochemical survey, Bear-Slave operation, District of Mackenzie; Geological Survey of Canada, Maps 1-1972 to 9-1972.
- Baykal, O.**  
1968: Preliminary geological report on Cent #1 to #12 mineral claims, Bode Lake, N.W.T.; Report prepared for M and M Silver Syndicate; Department of Indian and Northern Affairs, Document 018851; 15 p.
- Cannuli, M.**  
1989: CEGB Exploration (Canada) Ltd., Zebulon Project, Geological, geochemical and diamond drilling report, Permits 1098 and 1099 N.T.S. 86 F/04; Department of Indian and Northern Affairs, Document 082733.
- Cannuli, M., Climie, J.A., Sawiuk, M., and Gandhi, S.S.**  
1989: Cu-Co-Au-U mineralization in magnetite-specularite matrix of rhyodacite breccia at Damp prospect and its metallogenic significance to the Great Bear magmatic zone; in Exploration Overview 1989, Northwest Territories; Department of Indian and Northern Affairs, Abstracts of talks and posters, p. 30.
- Curry, J.D.**  
1969: BL Group Exploration Program - 1969; Report to Shield Resources Limited; Department of Indian and Northern Affairs, Document 080799, p. 11.
- Fraser, J.A.**  
1967: Geological map, Hardisty Lake (West Half); District of Mackenzie, Northwest Territories; Geological Survey of Canada, Map 224A, scale 1 inch to 4 miles.
- Gandhi, S.S.**  
1994: Geological setting and genetic aspects of mineral occurrences in the southern Great Bear magmatic zone, Northwest Territories; in Studies of Rare-Metal Deposits in the Northwest Territories, (ed.) W.D. Sinclair and D.G. Richardson; Geological Survey of Canada, Bulletin 475, p. 63-96.
- Hildebrand, R.S.**  
1981: Early Proterozoic LaBine Group of Wopmay orogen: remnant of a continental volcanic arc developed during oblique convergence; in Proterozoic Basins of Canada, (ed.) F.H.A. Campbell; Geological Survey of Canada, Paper 81-10, p. 133-156.  
1984: Geology of the Rainy Lake-White Eagle Falls area, District of Mackenzie: Early Proterozoic cauldrons, stratovolcanoes and subvolcanic plutons; Geological Survey of Canada, Paper 83-20, 42 p.  
1986: Kiruna-type deposits: their origin and relationship to intermediate subvolcanic plutons in the Great Bear magmatic zone, northwest Canada; Economic Geology, v. 81, no. 3, p. 640-659.
- Hildebrand, R.S. and Bowring, S.A.**  
1988: Geology of parts of the Calder River map area, District of Mackenzie; in Current Research, Part C; Geological Survey of Canada, Paper 88-1C, p. 199-205.
- Hildebrand, R.S., Hoffman, P.F., and Bowring, S.A.**  
1987: Tectono-magmatic evolution of the 1.9-Ga Great Bear magmatic zone, Wopmay orogen, northwestern Canada; Journal of Volcanology and Geothermal Research, v. 32, p. 99-118.
- Hoffman, P.F.**  
1980: Wopmay Orogen: a Wilson cycle of Early Proterozoic age in the northwest of the Canadian Shield; in Continental Crust and its Mineral Deposits; (ed.) D.W. Strangway; Geological Association of Canada, Special Paper 20, p. 523-549.  
1984: Geology, Northern Internides of Wopmay Orogen, District of Mackenzie, Northwest Territories; Geological Survey of Canada, Map 1576A, scale 1:250 000.
- Kidd, D.F.**  
1936: Rae to Great Bear Lake, Mackenzie District, N.W.T.; Geological Survey of Canada, Memoir 187, 44 p.
- Lord, C.S. and Parsons, W.H.**  
1947: Camsell River, District of Mackenzie, N.W.T.; Geological Survey of Canada, Map 1014A, scale 1 inch to 4 miles.
- Pelletier, K.S.**  
1985: Preliminary geology of Ellington Lake area, N.W.T. (86 F/3); Northwest Territories Geology Division, Department of Indian and Northern Affairs, Yellowknife; Map EGS 1985-9, with marginal notes, scale 1:50 000.
- Reardon, N.C.**  
1993: Magmatic-hydrothermal systems and associated magnetite-apatite-actinolite deposits, Echo Bay, Northwest Territories; MSc. thesis, University of Ottawa, Ottawa, Ontario, 154 p.
- Reichenbach, I.G.**  
1991: The Bell Island Bay Group, remnant of an early Proterozoic ensialic marginal basin in Wopmay orogen, District of Mackenzie; Geological Survey of Canada, Paper 88-28, 43 p.
- Sawiuk, M., Cannuli, M. and Climie, J.A.**  
1989: The Damp prospect: volcanic-hosted polymetallic (Cu-Fe-Co-U) breccia mineralization; in Exploration Overview 1989, Northwest Territories; Department of Indian and Northern Affairs, Abstracts of talks and posters, p. 51.

---

Geological Survey of Canada Project 750010

# Geological setting of the Sandhill Zn-Cu-Pb-Ag prospect in the Gibson-MacQuoid Lake area, District of Keewatin, Northwest Territories<sup>1</sup>

A.E. Armitage<sup>2</sup>, A.R. Miller, and N.D. MacRae<sup>2</sup>

Mineral Resources Division

*Armitage, A.E., Miller, A.R., and MacRae, N.D., 1995: Geological setting of the Sandhill Zn-Cu-Pb-Ag prospect in the Gibson-MacQuoid Lake area, District of Keewatin, Northwest Territories; in Current Research 1995-C; Geological Survey of Canada, p. 213-224.*

---

**Abstract:** The Gibson-MacQuoid Lake area is underlain by a polydeformed amphibolite grade Archean sequence of mafic to felsic volcanic rocks, sedimentary rocks, and orthogneiss; Proterozoic pyroxenite, gabbro, lamprophyre, and diabase intrusions are common. Geochemistry of the mafic volcanic rocks indicates a back-arc rift depositional environment. Stratabound Zn-Cu-Pb-Ag mineralization of the Sandhill prospect occurs within an envelope of hydrothermally altered rhyodacitic tuff; altered by the loss of Na and Ca and by the addition of Mn and Fe. Fine- to medium-grained sphalerite occurs as multiple bands (4 mm to 8 cm wide) associated with a highly aluminous assemblage of muscovite+quartz+garnet+staurolite+gahnite+biotite; coarse grained, sphalerite+galena associated with fine grained, disseminated, chalcopyrite occurs in discontinuous, concordant chert horizons. These features identify the Sandhill prospect as a metamorphosed volcanogenic massive sulphide deposit type.

**Résumé :** La région des lacs Gibson et MacQuoid repose sur une séquence archéenne polydéformée du faciès des amphibolites composée de volcanites mafiques à felsiques, de roches sédimentaires et d'orthogneiss; les intrusions de pyroxénite, de gabbro, de lamprophyre et de diabase du Protérozoïque sont nombreuses. La géochimie des volcanites mafiques indique un milieu de dépôt dans un rift d'arrière-arc. La minéralisation stratoïde de Zn-Cu-Pb-Ag du prospect de Sandhill loge dans une enveloppe de tuf rhyodacitique altérée par des fluides hydrothermaux (altérée par la perte de Na et de Ca et par l'ajout de Mn et de Fe). De la sphalérite à grain fin à moyen forme des bandes multiples (de 4 mm à 8 cm de largeur) associées à un assemblage très alumineux de muscovite+quartz+grenat+staurolite+gahnite+biotite; de la sphalérite+galène à grain grossier associée à une chalcopyrite disséminée à grain fin se rencontre dans des horizons de chert concordants discontinus. Ces caractéristiques concourent à qualifier le prospect de Sandhill de gisement de sulfures massifs volcanogènes métamorphisés.

---

<sup>1</sup> Contribution to Canada-Northwest Territories Mineral Initiatives (1991-1996), an initiative under the Canada-Northwest Territories Economic Development Cooperation Agreement.

<sup>2</sup> Department of Earth Sciences, University of Western Ontario, London, Ontario N6A 5B7

## INTRODUCTION

The Sandhill base metal prospect in the Gibson-MacQuoid Lake area occurs within the Gibson-MacQuoid Lake belt (GMLB), a predominantly west-trending Archean/ Proterozoic granite-greenstone-gneiss belt in the northern Churchill Structural Province of the Canadian Shield (Fig. 1). The Sandhill prospect, located approximately 120 km northwest of Rankin Inlet, is the focus of a four year program (1992-1996) to study its geological, mineralogical, geochemical and structural features. This study will provide useful guidelines for further exploration for base metal deposits in this belt.

This report summarizes the initial results of two years of bedrock mapping (1:30 000 scale) of parts of the Gibson Lake (55N/12) and MacQuoid Lake (55M/9) map sheets; mapping began during the 1993 field season (Armitage et al., 1994) and was completed during the 1994 field season. Field data were processed using field-based portable PC and pocket computers and the FIELDLOG (Brodaric and Fyon, 1989) v2.83 software application.

## REGIONAL GEOLOGY

The geology of the Gibson-MacQuoid Lake belt was initially outlined during a regional mapping program (Operation Baker) by the Geological Survey of Canada in 1954 (Wright, 1967). Subsequent mapping programs by Reinhardt et al. (1980), LeCheminant et al. (1976, 1977), Tella et al. (1993) and Tella and Schau (1994) further defined the Gibson-MacQuoid Lake belt. The belt is approximately 150 km long and reaches a maximum width of approximately 25 km in the MacQuoid Lake area (Reinhardt and Chandler, 1973; Fig. 1). It comprises a polydeformed sequence of interbedded mafic to felsic volcanic and volcanoclastic rocks and clastic and chemical sediments, all metamorphosed to the amphibolite facies. Smaller gabbro and syenite bodies of uncertain age intrude the volcanic and sedimentary rocks. The supracrustal sequence is bounded to the north and south by granite gneiss, migmatite and younger granitoids. The lithological and structural pattern of the Gibson-MacQuoid Lake belt is similar to the better understood Archean Rankin- Ennadai Greenstone Belt, south of the study area (Tella and Annesley, 1987; Tella et al. 1986, 1989, 1990, 1992).

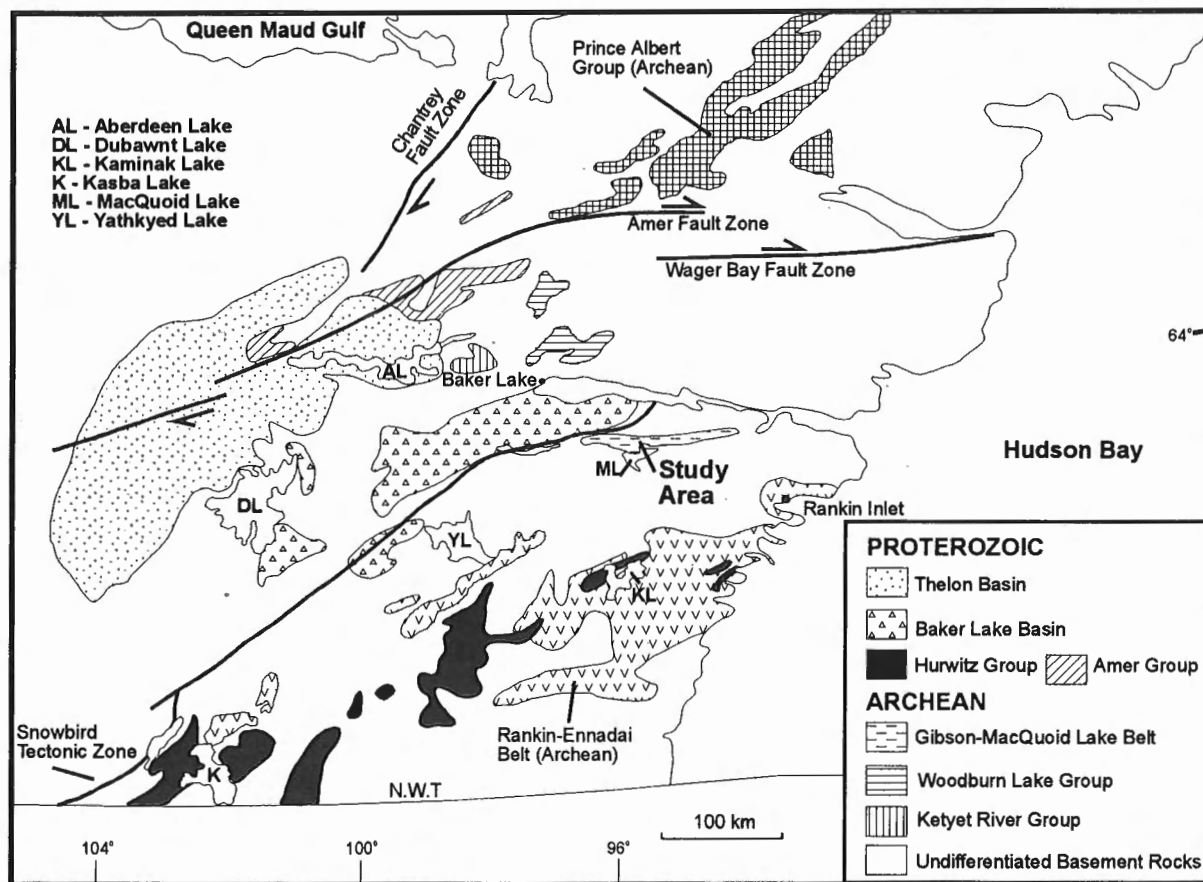


Figure 1. Map showing the location of the major supracrustal belts in the central part of the Churchill Structural Province and the study area.

## **GEOLOGY OF THE GIBSON-MACQUOID LAKE AREA**

The study area is underlain by a polydeformed sequence of mafic to intermediate massive to pillowed flows, volcanic breccias and interflow agglomerates and tuffs, felsic volcanic tuffs, and sedimentary rocks, all of the Gibson-MacQuoid Lake belt; tuff refers to a grain size of what are interpreted to be volcanoclastic rocks. Pyroxenite and gabbro intrusions and lamprophyre and diabase dykes are common throughout the map area. Outcrop is good with 50-70 per cent exposure in most areas.

### **VOLCANIC ROCKS**

#### ***Mafic volcanic rocks (unit 1)***

In the eastern part of the map area (Fig. 2), mafic volcanic rocks (unit 1) form linear continuous to discontinuous bands up to 500 m wide in plan view. These rocks are massive to banded, strongly foliated to sheared and consist of fine- to medium-grained hornblende+plagioclase+garnet; banding in the rocks is defined by variable hornblende and plagioclase content. Garnet occurs as crystals 0.1-8 mm in diameter, partially replaced by plagioclase, and forms up to 30 per cent by volume of the rock. The same mafic unit is thicker in map view, and displays primary volcanic features in an area near Grizzly Lake (Fig. 2). These rocks consist of interlayered massive to pillowed flows, tuffs and agglomerates. Massive layers of fine- to medium-grained hornblende+plagioclase+garnet schist, 2-4 m wide, are bounded by mafic volcanic breccias; mildly deformed pillows up to 1 m in diameter are well developed north and east of Grizzly Lake. Volcanic breccias are typically several metres thick and consist of angular hornblende+plagioclase-rich fragments set in a carbonate-rich matrix. Mafic tuffs form 1-2 m thick bands and consist of 0.4-1 cm plagioclase clasts, partially flattened parallel to the foliation, in a fine grained matrix of hornblende and plagioclase. Mafic agglomerates are common in the western part of the map area. They form 1-2 m wide layers with rounded to subrounded clasts, 5-20 cm in diameter, consisting of plagioclase+hornblende+garnet in a hornblende+garnet-rich matrix. Massive, weakly to strongly foliated gabbro sills are common in the mafic volcanic unit, especially in the western part of the map area. The gabbro is dark green, and contains medium- to coarse-grained hornblende and plagioclase; in the western part of the map area, plagioclase may form 0.5-2 cm phenocrysts.

The mafic volcanic rocks are basaltic to andesitic in composition (Fig. 3a) and show a tholeiitic chemical affinity (Fig. 3b). These rocks show flat (7-20x chondrite) to slightly light rare earth element (LREE)-enriched profiles (Fig. 3c)  $(Ce/Yb=1.45)_N$  with no discernible Eu anomaly. The mafic rocks also show a LIL element enrichment when normalized to N-type Mid-Ocean Ridge Basalt (MORB) (Fig. 4). The pattern defined by the Gibson-MacQuoid Lake mafic rocks is consistent with a back-arc basin depositional environment.

#### ***Intermediate volcanic rocks (unit 2)***

In the central and western parts of the map area, the mafic volcanic rocks grade northwards into a predominantly intermediate volcanic unit consisting of interlayered agglomerates and crystal tuffs. Agglomerates contain 5-50 cm long plagioclase-rich clasts, aligned parallel to foliation, which occur in a fine- to medium-grained matrix of hornblende+plagioclase+garnet. Crystal tuffs are characterized by 2-10 per cent subhedral plagioclase and minor quartz crystals in a plagioclase+quartz+biotite+garnet matrix. Several metre scale layers in a 50-100 m wide transition zone between the mafic and intermediate rocks consist of 20-40 per cent medium- to coarse-grained, randomly oriented, acicular needles of hornblende in a predominantly white plagioclase-rich matrix.

#### ***Felsic volcanic rocks (unit 3)***

A linear belt of felsic volcanic rocks dominated by crystal tuffs extends from the east to the central part of the map area (Fig. 2); this unit terminates at a major northwest-trending fault. The rocks are light grey to pink, well laminated to layered on a millimetre to centimetre scale and consist of quartz, feldspar, biotite and chlorite with minor 1-2 cm thick hornblende-rich bands. Discontinuous lenses, 5-10 cm thick, in the tuff contain angular 2-5 mm plagioclase clasts. Garnet, 1-5 mm in diameter, may form as much as 5 per cent in some layers. In an outcrop at the western end of the belt, a 0.5 m wide felsic agglomerate consists of 6-30 cm long felsic clasts, parallel to foliation, set in a fine grained plagioclase+quartz+biotite matrix.

The felsic volcanic rocks are dacitic to rhyolitic in composition (Fig. 3a) and show a calc-alkaline chemical affinity (Fig. 3b). The rocks show LREE-enriched profiles (Fig. 3d)  $(Ce/Yb=5.85)_N$ , and, like the mafic volcanic rocks, show no significant Eu anomaly.

A second less extensive belt of felsic volcanic rocks occurs adjacent to a granodiorite intrusion west of Grizzly Lake (Fig. 2). These rocks are light-grey to white-weathering, well layered, crystal tuffs and consist predominantly of plagioclase and quartz with lesser biotite, white-mica and garnet; quartz and/ or plagioclase may form 2-8 mm clasts. Several 1-2 m wide layers contain 5-10 per cent medium grained hornblende.

#### ***Sedimentary rocks (unit 4)***

Sedimentary rocks in the map area (Fig. 2) are dominated by wacke, psammitic to semi-pelitic in composition. In the eastern and central parts of the map area, these rocks are grey to red-brown, gritty, fine- to medium-grained and consist of quartz+biotite+plagioclase+white-mica+garnet. Several horizons of semi-pelitic to pelitic rocks, in the central to western parts of the map area, are characterized by staurolite and andalusite-bearing assemblages (Fig. 2). Staurolite and andalusite occur as 0.4-5 cm long porphyroblasts (Fig. 5) in a fine- to medium-grained quartz+plagioclase+biotite+garnet



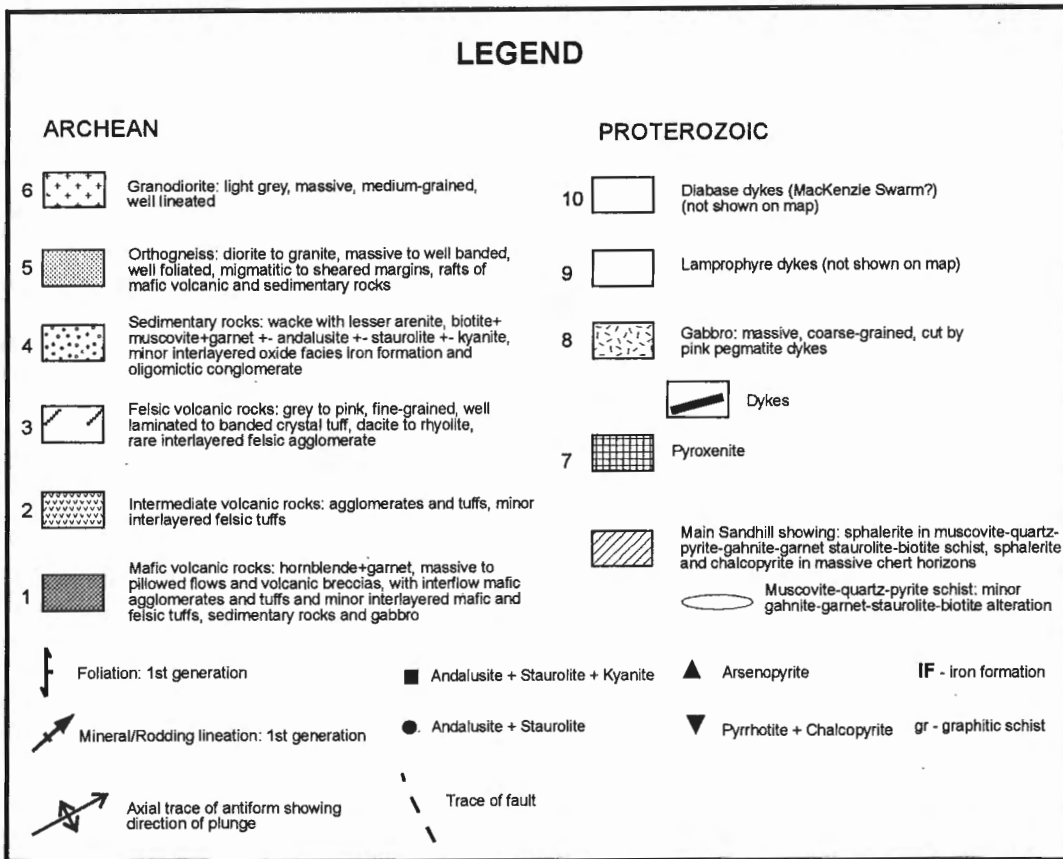
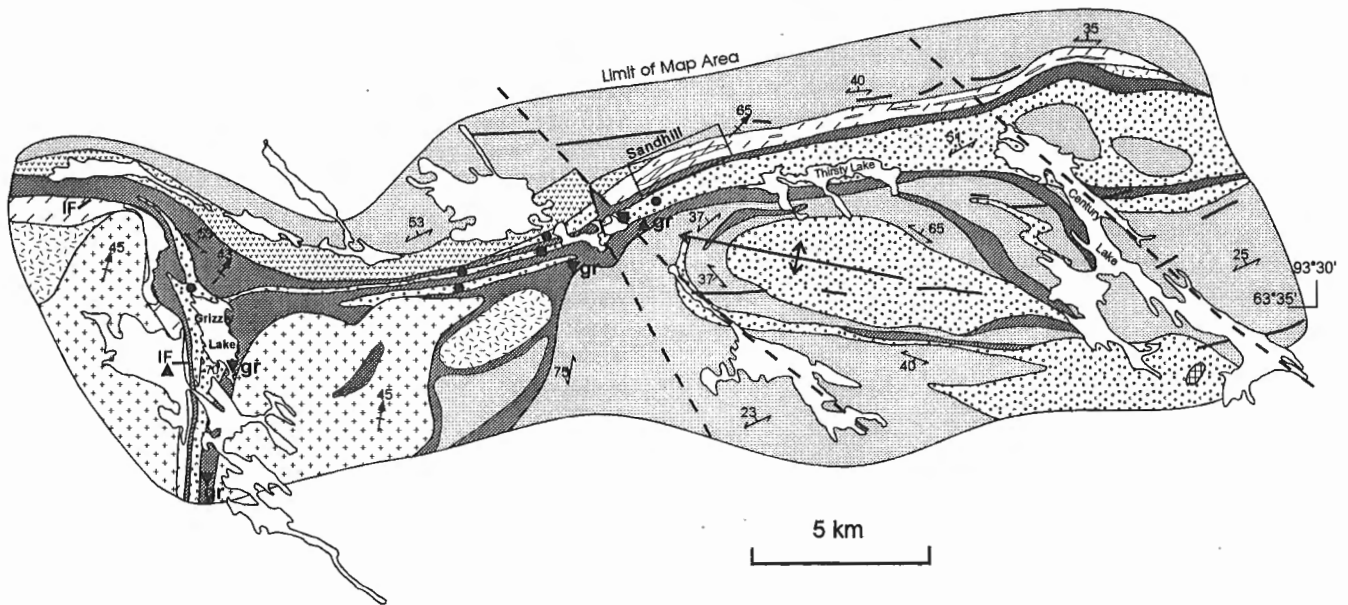


Figure 2. Geological map of the Gibson-MacQuoid Lake area.

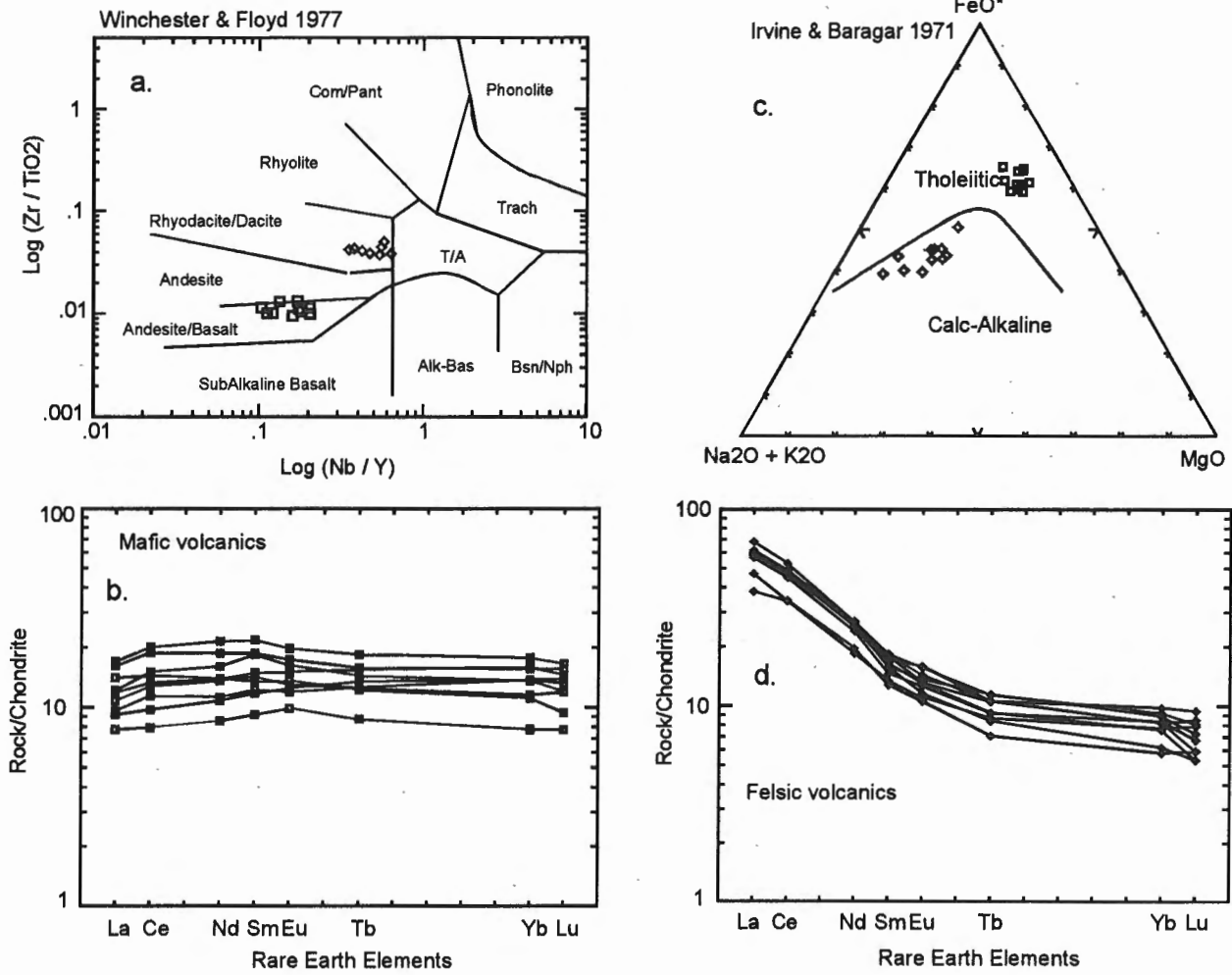


Figure 3. a) Trace element and b) major element (AFM) discrimination plots, and c) and d) Chondrite-normalized REE plots for the relatively unaltered mafic and felsic volcanic rocks respectively. REE normalization values after Taylor and McLennan (1985).

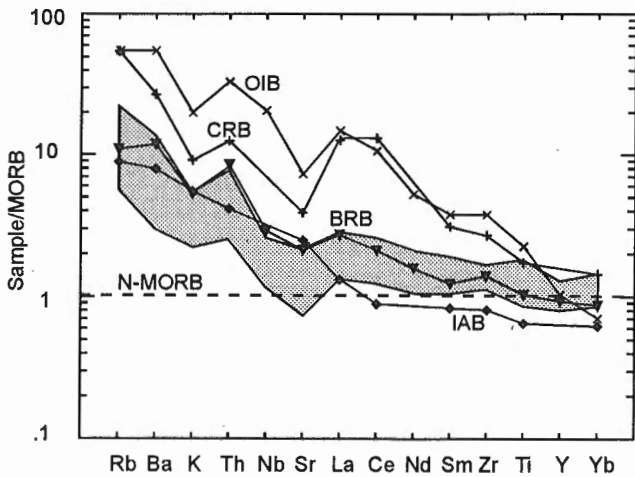


Figure 4.

Multi-element diagram for the relatively unaltered mafic volcanic rocks (shaded area) normalized against N-type MORB. Normalizing values from Sun and McDonough (1989). The mafic volcanic rocks are compared with an average composition for Continental Rift Basalt (CRB) and Island Arc Basalt (IAB) (Condie, 1982), Ocean Island Basalt (OIB) (Sun and McDonough, 1989), and Back-arc Basin Basalt (BRB) (Saunders and Tarney, 1991).

matrix. Porphyroblasts form in 5-10 cm wide foliation-parallel layers which alternate with relatively aluminosilicate-poor layers. This layering may represent primary compositional banding.

In the eastern and central parts of the map area, pelitic to semi-pelitic rocks typically grade northward into light-grey weathering, fine- to medium-grained psammite to quartzite.



**Figure 5.** Porphyroblasts of andalusite and staurolite in the pelitic rocks (unit 4). The porphyroblasts have been reoriented during the development of a northerly-plunging crenulation.

Psammitic rocks consist of quartz+plagioclase+muscovite with minor (< 5%) biotite and garnet; white-weathering quartzite forms discontinuous 3-8 m wide bands structurally below and in sheared contact with mafic volcanic rocks (unit 1). Minor discontinuous layers of oligomictic conglomerate occur in the psammitic layers, are 0.5-1 m wide, and contain pebbles and cobbles of granite and quartzite. Framework clasts show variable degrees of flattening.

Iron-formation (IF) is typically hosted by semi-pelitic rocks (unit 4) in the southern and central parts of the map area. Iron-formation forms 1-8 m wide bands consisting of 25-40 per cent garnet, 0.2-3.0 cm in diameter, in a quartz+magnetite+amphibole+biotite matrix. The iron-formation has a pronounced aeromagnetic signature (Geological Survey of Canada, 1971a). The most extensive band of iron-formation occurs at the contact between mafic (unit 1) and felsic (unit 3) volcanic rocks in the western part of the map area (Fig. 2). It strikes discontinuously for more than 10 km, ranges from 2-8 m wide, and is siliceous with only minor (10-15%) magnetite+pyrrhotite±grunerite laminae.

**Orthogneiss (unit 5)**

Orthogneiss comprises several ages of variably deformed and metamorphosed intrusive rocks that range in composition from diorite through granodiorite to granite; contacts of orthogneiss and supracrustal rocks are typically migmatitic

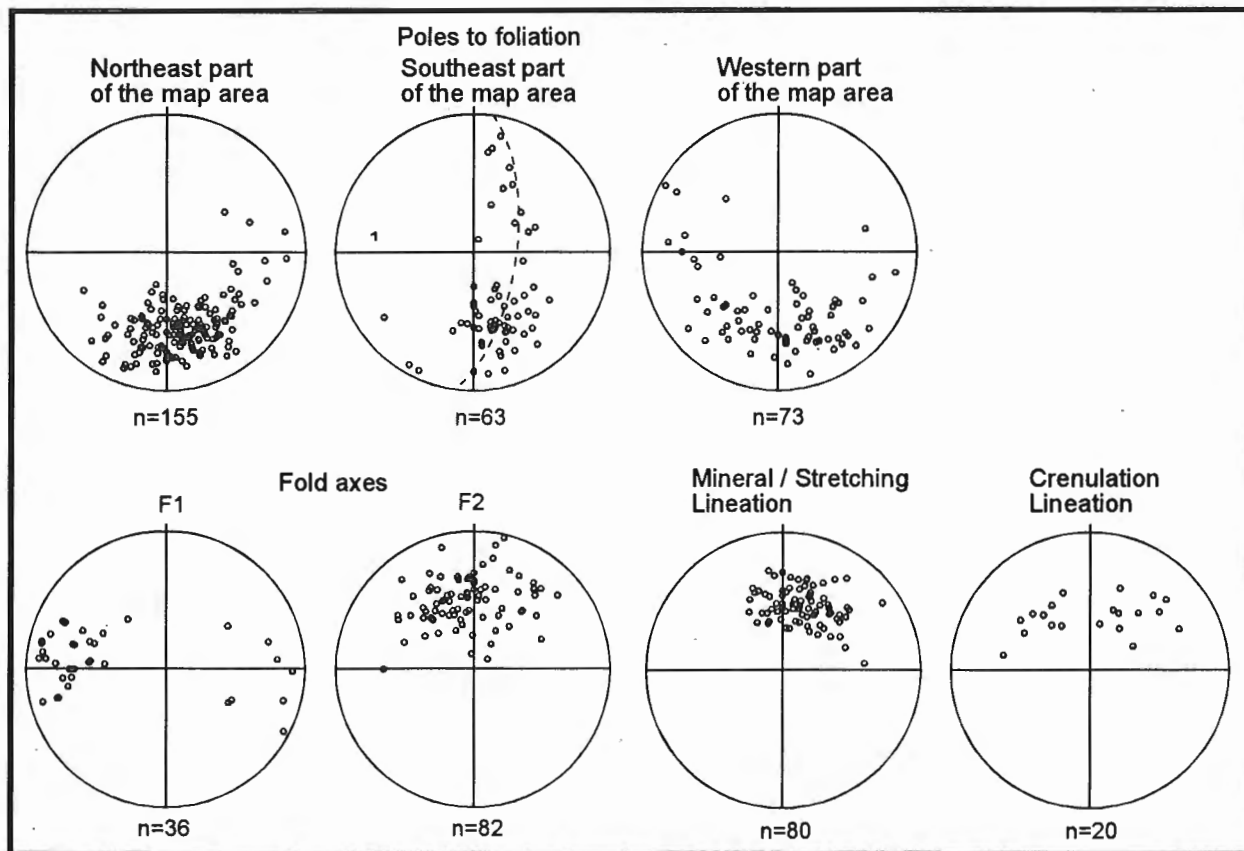


**Figure 6.** Orientation of planar and linear fabrics from the Gibson-MacQuoid Lake area.

and/or highly strained. Ages of the intrusions, which make up the orthogneiss unit, are uncertain and some may be older than the supracrustal rocks.

### **Granodiorite (unit 6)**

Two large white to grey-weathering granodiorite intrusions occur in the western part of the map area (Fig. 2). Contacts with the supracrustal rocks are sharp, well foliated to sheared and contain rafts of the supracrustal rocks. Typically, the granodiorite is massive and unfoliated, but contains a well developed lineation defined by elongated biotite aggregates. The granodiorite consists of medium grained quartz+feldspar+biotite±hornblende and minor fine grained, euhedral 1-2 per cent magnetite.

### **Mafic and felsic intrusions (units 7-10)**

Relatively undeformed mafic and felsic intrusions of probable Proterozoic age are common throughout the map area. In the southeast part of the map area (Fig. 2), a 750 m long elliptical plug of pyroxenite (unit 7) intrudes the sedimentary rocks (unit 4). Gabbro (unit 8) occurs as numerous east-trending dykes which form prominent topographic ridges up to 300 m wide throughout the map area, and as two large masses in the western part of the map area. These rocks are dark green, massive, and contain medium- to coarse-grained pyroxene/amphibole+plagioclase-bearing assemblages. Several of the gabbro intrusions contain 1-2 per cent disseminated, fine grained pyrrhotite.

Light to dark brown-weathering, northwest-trending (340°-350°) lamprophyre dykes (unit 9), up to 2 m wide, are common throughout the map area. These dykes are typically porphyritic with phlogopite±pyroxene phenocrysts set in a fine grained amphibole+K-feldspar+apatite-bearing matrix. Several dykes contain inclusions of country rock which include granite, orthogneiss, and metasediments. Lamprophyres are correlated with the 1.84 Ga alkaline igneous province defined by the distribution of the Christopher Island Formation (CIF) of the Baker Lake Group (LeCheminant et al., 1987; Peterson and Rainbird, 1990; Gall et al., 1992).

In the eastern part of the map area, three northwest-trending diabase dykes (unit 10), up to 1 m wide, cut the volcanic and sedimentary rocks and are probably related to the 1267 ± 2 Ma Mackenzie dyke swarm (LeCheminant and Heaman, 1989).

Foliated and boudinaged white tourmaline-bearing pegmatite dykes are common in the orthogneiss (unit 5), sedimentary rocks (unit 4), and mafic volcanic rocks (unit 1). Relatively undeformed white to pink tourmaline±beryl pegmatite dykes are common in the central to western parts of the map area; they cut all units previously described. White tourmaline pegmatite dykes are assigned to the Archean and the pink tourmaline dykes to the Proterozoic based on style and intensity of deformation.

## **STRUCTURE AND REGIONAL METAMORPHISM**

Bedding ( $S_0$ ) in the study area is indicated by compositional layering in the sedimentary and felsic volcanic rocks, and by the interlayering of flows, breccias, tuffs and agglomerates in the mafic and intermediate volcanic rocks. Facing directions are poorly preserved; however, in the western part of the map area, weakly deformed pillows indicate a younging to the north; crossbedding in a quartz arenite directly below the Sandhill prospect (Fig. 2) also indicates younging to the north. Regional foliation ( $S_1$ ) is parallel to bedding/layering ( $S_0=S_1$ ) and is defined by micas in the sedimentary and felsic volcanic rocks and orthogneiss, and by amphibole in the mafic volcanic unit. In the northeastern part of the map area (Fig. 2),  $S_1$  foliation strikes consistently west and dips moderately to the north (Fig. 6).  $S_1$  foliations define shallow to moderate east- and west-plunging isoclinal folds ( $F_1$ ) (Fig. 6, 7) in the mafic and felsic volcanic rocks and sedimentary rocks.

In the southeastern part of the map area,  $S_1$  foliations (Fig. 6) define a regional shallow northwest-plunging anti-form (Fig. 2); the generation of this fold is unknown, however, the fold axis is parallel to the  $F_1$  isoclinal folds (Fig. 6). In the western part of the map area (Fig. 2),  $F_1$  foliations in the supracrustal rocks wrap around and dip away from two large granodiorite intrusions (Fig. 6).

Moderate northwest- to northeast-plunging  $F_2$  folds (Fig. 6) show S- and Z- asymmetry. Moderate northwest- to northeast-plunging crenulations (Fig. 6), locally well developed, define a second cleavage ( $S_2$ ) which is axial planar to the  $F_2$  folds (Fig. 8). Locally, aluminosilicate porphyroblasts in the sedimentary rocks, have been rotated into the plane of the  $S_2$  foliation (Fig. 5).

Moderate north- to northeast-plunging mineral and rod-ding lineations (Fig. 6) are weakly developed along the mafic volcanic-sedimentary contact and the felsic volcanic-orthogneiss contact in the eastern and central parts of the map



**Figure 7.** Moderate west-plunging isoclinal fold in the sedimentary rocks in the central part of the map area.

area (Fig. 2). This lineation is well developed in the supra-crustal rocks (Fig. 9) and the two large unfoliated granodiorite intrusions (unit 6) in the western part of the map area. Late north- to northwest-trending brittle faults crosscut the map area. A major fault, part of the Baker Lake Cataclastic Zone, in the central part of the map area shows variable dextral offset (Fig. 2); the felsic volcanic rocks terminate on the east side of the fault and a sedimentary rock sequence is terminated on the west side of the fault. A second major fault in the eastern part of the map area is identified by extensive block faulting. Numerous smaller scale faults not shown on the map (Fig. 2) display limited offset of both sinistral and dextral movement. Deformation associated with these faults affected all rock units, including the gabbro dykes and lamprophyre dykes; epidote and K-feldspar retrogression is commonly associated with late brittle faults.

Lower amphibolite facies metamorphism is indicated by biotite+garnet±andalusite±staurolite in sedimentary rocks and hornblende+garnet in the mafic volcanic rocks. An estimate of the P-T conditions for regional metamorphism is in the order of 2-3 kbars and 520-580°C based on the stability

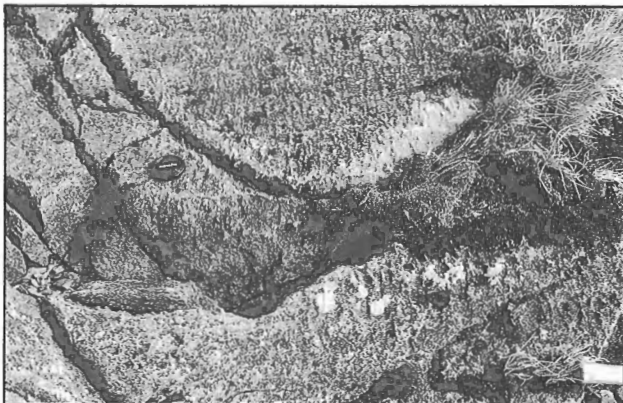


Figure 8. The hinge zone of a northeast-plunging F2 fold in the sedimentary rocks and well developed axial plane cleavage.



Figure 9. Well developed rodding in a felsic volcanic tuff from the western part of the map area.

of Fe-staurolite and the aluminosilicate triple point (Yardley, 1989). Kyanite in the sedimentary rocks in the central part of the map area adjacent to the northwest-trending fault (Fig. 2) indicates different conditions of metamorphism in this area. However, the relationship between kyanite, andalusite and staurolite has not been determined.

## MINERALIZATION AND ALTERATION

The Sandhill mineralization is hosted by coarse grained, white-weathering pyritic quartz+paragonitic muscovite schist (Fig. 2, 10; Table 1). The strike length of the concordant mineralized zone and enclosing alteration envelope in the Sandhill is approximately 2000 m and it has a maximum width of 200 m zone (Fig. 10). This schist contains medium- to coarse-grained sphalerite as discontinuous 2-8 cm wide bands and fine grained disseminated sphalerite. Zinc values range from 0.02-9.3 wt % (average of 1.6 wt %) in 28 selected samples; 15 of these samples ran > 0.5 g/tonne silver and averaged 10 g/tonne. This mineralization is associated with the highly aluminous assemblage manganiferous garnet+ zirconian staurolite+biotite+gahnite (Table 1). Several discontinuous concordant chert horizons, 0.5-1.5 m thick, contain discontinuous 1-4 cm wide bands of coarse grained sphalerite±galena with associated 2-10 per cent disseminated

Table 1. Average compositions of alteration minerals, Sandhill prospect.

	Muscovite		Garnet			Staurolite	Gahnite	Biotite
	Core	Mantle	Rim					
SiO <sub>2</sub>	45.58	37.17	37.46	37.30	27.30	0.09	37.01	
TiO <sub>2</sub>	0.67	0.03	0.04	0.03	0.51	0.00	1.26	
Al <sub>2</sub> O <sub>3</sub>	34.07	21.21	21.28	21.25	53.55	56.77	18.32	
Cr <sub>2</sub> O <sub>3</sub>	0.01	0.00	0.02	0.02	0.03	0.06	0.02	
MnO	0.56	19.47	18.80	19.81	0.58	0.18	0.30	
FeO	2.06	12.00	13.29	9.65	9.18	6.89	16.41	
MgO	0.51	8.69	8.04	9.87	1.61	1.86	13.13	
ZnO	----	----	----	----	4.86	34.37	----	
CaO	0.01	1.61	1.54	2.56	0.00	----	0.01	
BaO	0.25	----	----	----	----	----	0.17	
K <sub>2</sub> O	9.41	----	----	----	0.00	----	8.90	
Na <sub>2</sub> O	1.08	----	----	----	0.00	----	0.24	
F	0.02	----	----	----	----	----	0.97	
Cl	0.01	----	----	----	----	----	0.05	
Total	94.24	100.18	100.47	100.49	97.62	100.22	96.79	
Si	6.16	5.97	5.99	5.98	7.98	0.02	5.45	
Al <sub>IV</sub>	1.84	0.04	0.02	0.03	0.03	11.92	2.55	
Al <sub>VI</sub>	3.59	3.98	3.99	3.98	18.41	----	0.63	
Ti	0.07	0.01	0.01	0.01	0.11	0.01	0.14	
Cr	0.00	0.00	0.01	0.01	0.01	0.00	0.00	
Fe	0.25	3.00	2.92	3.15	2.25	1.03	2.02	
Mg	0.11	0.75	0.76	0.65	0.70	0.03	2.88	
Mn	0.07	1.99	2.04	1.79	0.14	0.49	0.04	
Zn	----	----	----	----	1.05	4.52	----	
Ca	0.00	0.28	0.27	0.04	0.00	----	0.00	
Ba	0.01	----	----	----	----	----	0.01	
K	1.62	----	----	----	0.00	----	1.67	
Na	0.29	----	----	----	0.00	----	0.07	
F	0.01	----	----	----	----	----	0.45	
Cl	0.01	----	----	----	----	----	0.01	
O	22.00	24.00	24.00	24.00	48.00	24.00	22.00	
Fe	----	49.90	48.79	52.23	54.28	16.95	41.24	
Mg	----	12.46	12.74	10.80	16.90	0.46	58.76	
Ca	----	4.61	4.42	7.34	----	----	----	
Mn	----	33.03	34.05	29.63	----	8.14	----	
Zn	----	----	----	----	25.36	74.45	----	
K	0.85	----	----	----	----	----	----	
Na	0.15	----	----	----	----	----	----	

fine grained chalcopyrite. Two selected samples from a chert horizon averaged 3.9 wt % Zn, 0.9 wt % Cu, 0.2 wt % Pb, 185 g/tonne Ag, and 0.2 g/tonne Au.

Hydrothermally altered rhyodacitic tuffs enclosing the Sandhill mineralization (Fig. 10) are grey to red-brown weathering and characterized by an increase in the abundance of garnet from 2-5 per cent in relatively unaltered felsic tuffs to 15-25 per cent in altered equivalents. Garnet is associated with plagioclase+biotite+muscovite+staurolite+gahnite. A comparison of the geochemistry of the altered and relatively unaltered felsic volcanic rocks (Fig. 11) indicates hydrothermal alteration resulted in a loss in Na and Ca, a gain in Mn and Fe<sub>T</sub>, and no variation in Mg, Si, and K. These elements were ratioed against Al and Ti because Al and Ti are typically immobile during VHMS alteration (Barrett and MacLean, 1994).

Alteration assemblages, similar to those that host the Sandhill mineralization, persist for up to 12 km eastward along strike (Fig. 2). Discontinuous pyritic quartz+muscovite schist contains intermittent, fine- to medium-grained manganese garnet+zincian staurolite+gahnite+biotite±kyanite.

Although sphalerite and/or chalcopyrite were rarely observed, the presence of gahnite as well as zincian staurolite are good indicators of massive sulphide mineralization (Spry, 1986; Spry and Scott, 1986). Thirteen samples from the eastern horizons averaged 0.1 wt % Zn and negligible Cu and Pb. Despite the low base metal values in these zones thirteen samples averaged 8.2 g/tonne Ag.

Numerous other gossans are sporadically distributed throughout the map area (Fig. 2). A 0.5-1.0 m wide band of massive pyrrhotite with 10-15 per cent chalcopyrite (Fig. 2) extends discontinuously for up to 1 km in the central part of the map area. Coarse grained arsenopyrite (Fig. 2) with pyrite, and minor chalcopyrite and galena in quartz veins occur in the central to west parts of the map area. One sample from a quartz vein, south of Sandhill analyzed 8.4 wt % As, 0.14 wt % Zn, 223 ppm Cu, 682 ppm Pb, and 12.7 g/tonne Ag. Several of these gossans define a discontinuous graphitic schist in the mafic volcanic rocks (Fig. 2). The graphitic schist is interpreted to be a primary, sulphidic, carbonaceous shale which has been modified during regional metamorphism. The southern showing in the western iron-formation (Fig. 2) is cut by numerous arsenopyrite-bearing quartz veins.

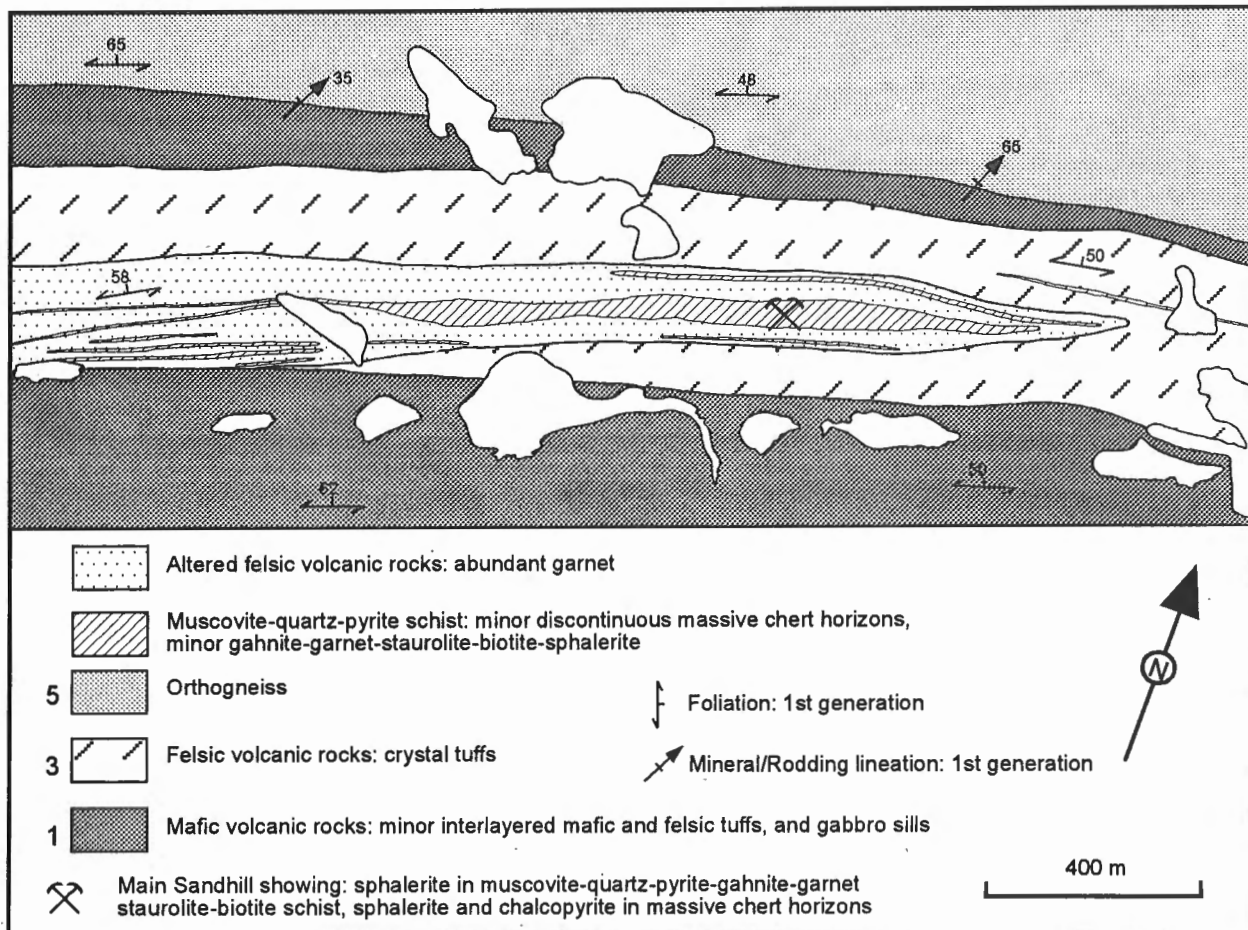


Figure 10. Geology of the Sandhill Zn-Cu-Pb-Ag prospect.

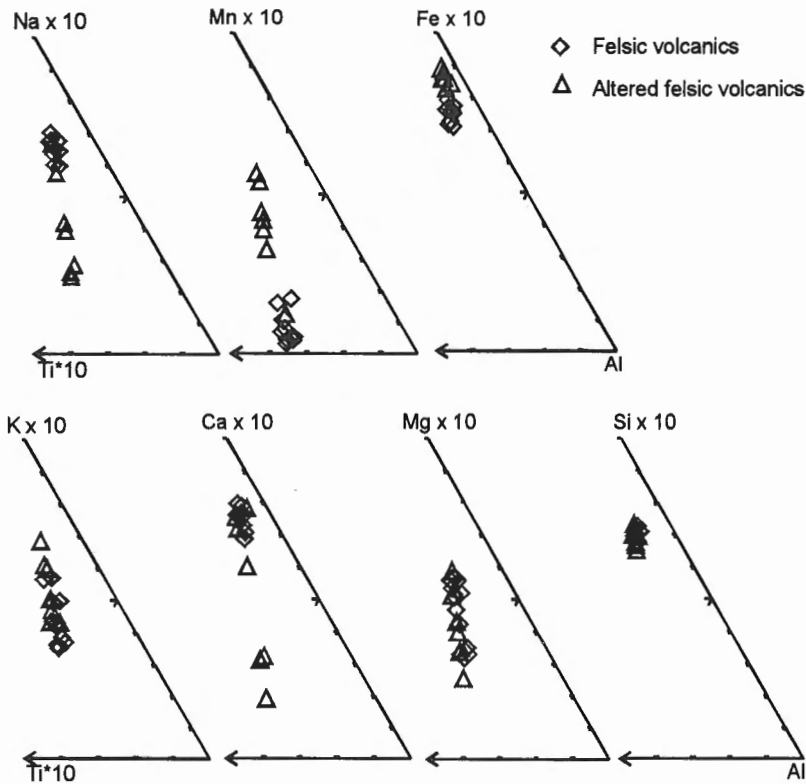


Figure 11.

Ternary diagrams displaying the chemical changes between altered and unaltered felsic volcanic rocks (unit 4), Sandhill project.

## SUMMARY

Felsic volcanic host rocks and aluminous alteration assemblages with disseminated and massive base metal sulphides are common features in well studied metamorphosed volcanogenic massive sulphide districts (Walford and Franklin, 1982; Bailes, 1987; Zaleski, 1989, 1991; Morton et al., 1991; Barrett and MacLean, 1994). The formation of these deposits is attributed to submarine seafloor alteration related to syn-volcanic hydrothermal systems.

The Sandhill Zn-Cu-Pb-Ag prospect is hosted within a polydeformed amphibolite grade Archean greenstone belt. The belt comprises north facing and dipping, interlayered semi-pelitic to arenaceous sedimentary rocks and tholeiitic basalt and calc-alkaline rhyodacitic tuff. The association of fine grained well laminated tuffs, arenaceous sediments with rare crossbeds, and interlayered mafic pillowed volcanic rocks and agglomerates indicates a shallow subaqueous to subaerial depositional environment. The geochemistry of the mafic volcanic rocks suggests a back-arc rift tectonic setting.

The Sandhill mineralization and associated alteration envelope are stratabound in rhyodacitic tuff. Sphalerite occurs within a quartz+muscovite schist and are associated with a highly aluminous assemblage. The aluminous schist is interpreted as the metamorphosed equivalent of a quartz-sericite hydrothermally altered felsic tuff. Base metal-bearing quartz-rich layers within the schist are interpreted as recrystallized siliceous exhalite. The quartz+muscovite schist is enveloped by weakly altered felsic tuffs characterized by plagioclase+biotite+garnet+muscovite± staurolite±gahnite. Geochemistry of the altered felsic volcanic rocks indicates

losses in Na and Ca and gains in Mn and Fe<sub>T</sub> during alteration. These characteristics identify the Sandhill prospect as a metamorphosed volcanogenic massive sulphide deposit-type.

The sulphidic, graphitic schist and the highly aluminous nature of the metasediments in the western part of the map area define a western extension of the Sandhill lithostratigraphic sequence. The bimodal volcanism in the Sandhill area, intense hydrothermal alteration with base and precious metals, and a wide expression of base and precious metal occurrences in stratigraphically equivalent rocks indicates that the Gibson-MacQuoid greenstone belt has a high metal potential.

Whole rock and mineral chemistry studies will continue in order to further evaluate the hydrothermal alteration, importance of concordant and discordant alteration zones, and the role of exhalative versus replacement processes in the Sandhill prospect.

## ACKNOWLEDGMENTS

We thank the following agencies for additional financial support for this project: Indian and Northern Affairs Canada (Contract No. YK-94-95-029) and Natural Sciences and Engineering Research Council of Canada (Grant No. OGP 0005539). We thank Adrienne Jones and Sergio Alvarado for field assistance; Subhas Tella, Continental Geoscience Division, for his advice and support in the field, specifically on the structural aspects of this study; P. Mudry and M. Pyke of Comaplex Minerals Corp. for making available

unpublished data from the Sandhill area and logistical support; Melinda Tatty of M&T Enterprises Ltd., Rankin Inlet for excellent expediting services.

Whole rock chemistry was partially determined at the University of Western Ontario analytical chemistry laboratory; major and trace elements by XRF on fused and powdered disks respectively, and REE data by INAA. The remainder of the data were determined by X-RAY Assay Laboratories, Don Mills Ontario; major elements by XRF, trace elements by ICP-ES, and REE by ICP-MS. Mineral chemical compositions were determined using a JEOL JXA-8600 Superprobe fitted with four automated wavelength dispersion spectrometers at the University of Western Ontario. The thorough review by Doreen Ames improved the manuscript

## REFERENCES

- Armitage, A.E., Miller, A.R. and MacRae, N.D.**  
1994: Geology of the "Sandhill" Zn-Cu showing in the Gibson Lake Area, District of Keewatin, Canada; in *Current Research 1994-C*; Geological Survey of Canada, p. 147-155.
- Bailes, A.H.**  
1987: Chisel-Morgan Lake project; in *Report of Field Activities*, Manitoba Energy and Mines, p. 70-80.
- Barrett, T.J. and MacLean, W.H.**  
1994: Chemostratigraphy and hydrothermal alteration in exploration for VHMS deposits in greenstones and younger volcanic rocks; in *Alteration and Alteration Processes Associated with Ore-forming Systems*, (ed.) D.R. Lentz; Geological Association of Canada-Mineralogical Association of Canada, Short Course notes, v. 11, p. 433-465.
- Brodaric, B. and Fyon, J.A.**  
1989: OGS FIELDLOG: A Microcomputer-based Methodology to Store, Process and Display Map-related data; Ontario Geological Survey, Open File Report 5709, 73 p. and 1 diskette.
- Condie, K.C.**  
1982: *Plate Tectonics and Crustal Evolution*; Pergamon, Great Britain, 476 p.
- Gall, Q., Peterson, T.D., and Donaldson, J.A.**  
1992: A proposed subdivision of Early Proterozoic stratigraphy of the Thelon and Baker Lake basins, Northwest Territories; in *Current Research, Part C*; Geological Survey of Canada, Paper 92-1C, p. 129-137.
- Geological Survey of Canada**  
1971a: Sheet 55N/12; Geophysical Series (Aeromagnetic) Map 6800G.  
1971b: Sheet 55M/9; Geophysical Series (Aeromagnetic) Map 6801G.
- Irvine, T.N. and Barager, W.R.A.**  
1971: A guide to the chemical classification of the common volcanic rocks; *Canadian Journal of Earth Sciences*, v. 8, p. 523-548.
- LeCheminant, A.N., Hews, P.C., Lane, L.S., and Wolff, J.M.**  
1976: MacQuoid Lake (55M west half) and Thirty Mile Lake (65P east half) map areas, District of Keewatin; in *Report of Activities, Part A*; Geological Survey of Canada, Paper 76-1A, p. 383-386.
- LeCheminant, A.N., Blake, D.H., Leatherbarrow, R.W., and deBie, L.**  
1977: Geological studies: Thirty Mile Lake and MacQuoid Lake map areas; in *Report of Activities, Part A*; Geological Survey of Canada, Paper 77-1A, p. 205-208.
- LeCheminant, A.N., Roddick, J.C., and Henderson, J.R.**  
1987: Geochronology of Archean and Early Proterozoic magmatism in the Baker Lake-Wager Bay region, N.W.T.; in *Geological Association of Canada/Mineralogical Association of Canada, Program with Abstracts*, v. 12, p. 66.
- LeCheminant, A.N. and Heaman, L.M.**  
1989: Mackenzie igneous events, Canada: Middle Proterozoic hotspot magmatism associated with ocean opening; *Earth and Planetary Science Letters*, v. 96, p. 38-48.
- Morton, M.L., Hudak, G.C., Walker, J.S., and Franklin, J.M.**  
1991: Physical volcanology and hydrothermal alteration of the Sturgeon Lake caldera complex; in *Mineral Deposits in the Western Superior Province, Ontario*, (ed.) J.M. Franklin, B.R. Schneiders, and E.R. Koopman; 9th IAGOD Field Trip Guidebook, Geological Survey of Canada, Open File 2164, p. 74-94.
- Peterson, T.D. and Rainbird, R.H.**  
1990: Tectonic and petrological significance of regional lamproite-minette volcanism in the Thelon and Trans-Hudson hinterlands, Northwest Territories; in *Current Research, Part C*; Geological Survey of Canada, Paper 90-1C, p. 69-79.
- Reinhardt, E.W. and Chandler, F.W.**  
1973: Gibson-MacQuoid Lake map area, District of Keewatin; in *Report of Activities, Part A*; Geological Survey of Canada, Paper 73-1A, p. 162-165.
- Reinhardt, E.W., Chandler, F.W., and Skippen, G.B.**  
1980: Geological map of the MacQuoid Lake (NTS 55M, E1/2) and Gibson Lake (NTS 55N, W1/2) map area, District of Keewatin; Geological Survey of Canada, Open File 703; compiled by G.B. Skippen.
- Saunders, A. and Tarney, J.**  
1991: Back-arc basins; in *Oceanic Basalts*, (ed.) P.A. Floyd; Blackie, New York, p. 219-263.
- Spry, P.G.**  
1986: The stability of zincian spinels in sulphides systems and their potential as exploration guides for metamorphosed massive sulphide deposits; *Economic Geology*, v. 81, p. 1446-1463.
- Spry, P.G. and Scott, S.D.**  
1986: Zincian spinel and staurolite as guides to ore in the Appalachians and Scandinavian Caledonides; *Canadian Mineralogist*, v. 24, p. 124-163.
- Sun, S.S. and McDonough, W.F.**  
1989: Chemical and isotopic systematics of ocean basalts: implications for mantle composition and processes; in *Magmatism in the Ocean Basins*, (ed.) A.D. Saunders and M.J. Norry; Geological Society of London Special Publication 42, p. 313-345.
- Taylor, S.R. and McLennan, S.M.**  
1985: *The Continental Crust: Its Composition and Evolution*; Blackwell, Oxford, 312 p.
- Tella, S. and Annesley, I.R.**  
1987: Precambrian Geology of parts of the Chesterfield Inlet map area, District of Keewatin; in *Current Research, Part A*; Geological Survey of Canada, Paper 86-13, 20 p.
- Tella, S., and Schau, M.**  
1994: Geology, Gibson Lake east-half, District of Keewatin, Northwest Territories, Geological Survey of Canada, Open File 2737, Scale 1:250 000.
- Tella, S., Annesley, I.R., Borradaile, G.J., and Henderson, J.R.**  
1986: Precambrian geology of parts of Tavani, Marble Island and Chesterfield Inlet map areas, District of Keewatin, N.W.T.; Geological Survey of Canada, Paper 86-13, 20 p.
- Tella, S., Roddick, J.C., Bonardi, M., and Berman, R.G.**  
1989: Archean and proterozoic tectonic history of the Rankin Inlet-Chesterfield Inlet region, District of Keewatin, N.W.T.; *Geological Society of America, Abstracts with Programs*, v. 21, no. 6, p. 22.
- Tella, S., Roddick, J.C., Park, A.F., and Ralsler, S.**  
1990: Geochronological constraints on the evolution of the Archean and Early Proterozoic terrane in the Tavani-Rankin Inlet region, Churchill Structural Province, N.W.T.; *Geological Society of America, Abstracts with Programs*, v. 22, no. 7 p. A174.
- Tella, S., Schau, M., Armitage, A.E., and Loney, B.C.**  
1993: Precambrian geology and economic potential of the northeastern parts of the Gibson Lake (55N) map area, District of Keewatin, Northwest Territories; in *Current Research, Part C*; Geological Survey of Canada, Paper 93-1C, p. 197-208.
- Tella, S., Schau, M., Armitage, A.E., Seemayer, B.E., and Lemkow, D.**  
1992: Precambrian geology and economic potential of the Meliadine Lake-Barbour Bay region, District of Keewatin, Northwest Territories; in *Current Research, Part C*; Geological Survey of Canada, Paper 92-1C, p. 1-11.
- Walford, P.C. and Franklin, J.M.**  
1982: The Anderson Lake Mine, Snow Lake, Manitoba; in *Robinson Symposium Volume*, (ed.) R.W. Hutchinson, C.D. Spence, and J.M. Franklin; Geological Association of Canada, Special Paper 25, p. 481-524.



**Winchester, J.A. and Floyd, P.A.**

1977: Geochemical discrimination of different magma series and their differentiation products using immobile elements; *Chemical Geology*, v. 20, p. 325-343.

**Wright, G.M.**

1967: Geology of the southeastern barren grounds, Parts of the Districts of Mackenzie and Keewatin; Geological Survey of Canada, Memoir 350.

**Yardley, B.W.D**

1989: *An Introduction to Metamorphic Petrology*; Longman, England, 248 p.

**Zaleski, E.**

1989: Metamorphism, structure and petrogenesis of the Linda Petrology of the Linda volcanogenic massive sulphide deposit, Snow Lake, Manitoba; PhD. thesis, University of Manitoba, Winnipeg, Manitoba, 344 p.

1991: Metamorphic Petrology of Fe-Zn-Mg-Al alteration at the Linda volcanogenic massive sulphide deposit, Snow Lake, Manitoba; *Canadian Mineralogist*, v. 29, p. 995-1017.

---

Geological Survey of Canada Project 810024

# Granitoid plutons and major structures in the Iskwasum Lake sheet, Manitoba: a portion of the Flin Flon Domain of the Trans-Hudson Orogen<sup>1</sup>

D.W. Morrison<sup>2</sup> and J.B. Whalen  
Continental Geoscience Division

*Morrison, D.W. and Whalen, J.B., 1995: Granitoid plutons and major structures in the Iskwasum Lake sheet, Manitoba: a portion of the Flin Flon Domain of the Trans-Hudson Orogen; in Current Research 1995-C; Geological Survey of Canada, p. 225-234.*

---

**Abstract:** Six major granitoid plutons intrude mafic volcanic rocks, mafic tectonites and older plutonic rocks within the Iskwasum Lake sheet of Manitoba (NTS 63K/10). Three of these plutons are contiguous with plutons of the adjoining Elbow Lake sheet, which range in age from 1.876 Ga to 1.826 Ga, and in composition from granodiorite to quartz diorite. The Iskwasum Lake sheet is structurally complex, containing four major shear zones and many minor faults. Except for the late east-west-trending Berry Creek fault in the south, most of these structures are apparently early and long-lived, north-northeast-trending structures. Based on geochemical studies of correlative volcanic assemblages bounding these structures to the north, some probably represent important internal boundaries or sutures within the Flin Flon Domain of the Paleoproterozoic Trans-Hudson Orogen.

**Résumé :** Six plutons granitoïdes importants recoupent des volcanites mafiques, des tectonites mafiques et des plutonites plus anciennes dans la région cartographique du lac Iskwasum, au Manitoba (SNRC 63K/10). Trois de ces plutons sont contigus aux plutons de la région cartographique adjacente du lac Elbow, dont l'âge varie entre 1,876 Ga et 1,826 Ga, et dont la composition va de granodiorite à diorite quartzique. La région cartographique du lac Iskwasum est structuralement complexe et contient quatre zones de cisaillement majeures et de nombreuses failles mineures. À l'exception de la faille tardive de Berry Creek à orientation est-ouest dans le sud, la plupart de ces structures semblent être des structures précoces de longue durée, à orientation nord-nord-est. Selon des études géochimiques des assemblages volcaniques corrélatifs limitant ces structures au nord, certaines représentent probablement d'importantes frontières ou sutures internes au sein du Domaine de Flin Flon de l'orogène trans-hudsonien paléoprotérozoïque.

---

<sup>1</sup> Contribution to the Shield Margin NATMAP Project and Canada-Manitoba Partnership Agreement on Mineral Development (1990-1995), a subsidiary agreement under the Canada-Manitoba Economic and Regional Development Agreement.

<sup>2</sup> Ottawa-Carleton Geoscience Centre, University of Ottawa, Ontario K1N 6N5

## INTRODUCTION

The central part of the Flin Flon Domain of the Paleoproterozoic Trans Hudson Orogen, interpreted as an amalgamation of 1.91-1.88 Ga oceanic and arc tectonostratigraphic assemblages, termed the Flin Flon tectonic collage, is stitched together by 1.87-1.84 Ga granitoid plutons, and overlain by 1.85-1.84 Ga sedimentary rocks (Lucas and Stern, 1994; Lucas et al., in prep.) (Fig. 1). Critical evaluation of this model requires a better understanding of key elements, such as the volumetrically significant (>60%) granitoid plutons and major structures separating portions of the collage. Recent studies in the Elbow Lake sheet (63K/15) (e.g., Syme and Whalen, 1992; Syme, 1992; Whalen, 1993a,b; Ryan and Williams, 1993; Whalen and Hunt, 1994) have provided a better understanding of some of these elements. Geochemical and structural studies of volcanic and plutonic rocks, within and adjacent to the Elbow Lake shear zone (Fig. 1), show that it represents a long-lived deformation zone, separating ca. 1.9 Ga tectonostratigraphic assemblages (Syme, 1992; Stern et al., 1994; Ryan and Williams, 1993; Stern et al., in prep.).

This study in the Iskwasum Lake map sheet (NTS 63K/10), which forms part of a M.Sc. thesis at the University of Ottawa, was initiated in 1994 with the objective of

extending geological mapping and the study of granitoid plutons southward from the Elbow Lake sheet to the Shield Margin. Mapping was undertaken jointly with E.C. Syme (Manitoba Geological Services Branch), who was responsible for reconnaissance mapping of the supracrustal rocks in the Iskwasum Lake sheet (Syme, 1994). Geochronology of the granitoid plutons is part of a collaborative project with N. Machado (GÉOTOP, Université du Québec à Montréal).

The study area is located 50 km east-southeast of Flin Flon and 45 km west-southwest of Snow Lake, lying entirely within the Grass River Provincial Park. Geological mapping during the summer of 1994, at a scale of 1:50 000, outlined six major granitoid bodies (Fig. 2), three of which are correlative with plutons in the Elbow Lake sheet. These plutons together comprise approximately 60 per cent of the Precambrian bedrock in the map area. The southern portion of the area is underlain by Paleozoic cover rocks. Some of the major shear zones and faults from the Elbow Lake sheet were mapped through the study area (cf. Syme, 1994), and a previously unrecognized major shear zone was identified. Future field and laboratory studies will better constrain age relationships between important structural/tectonic events and pluton emplacement mechanisms and their tectonic setting.

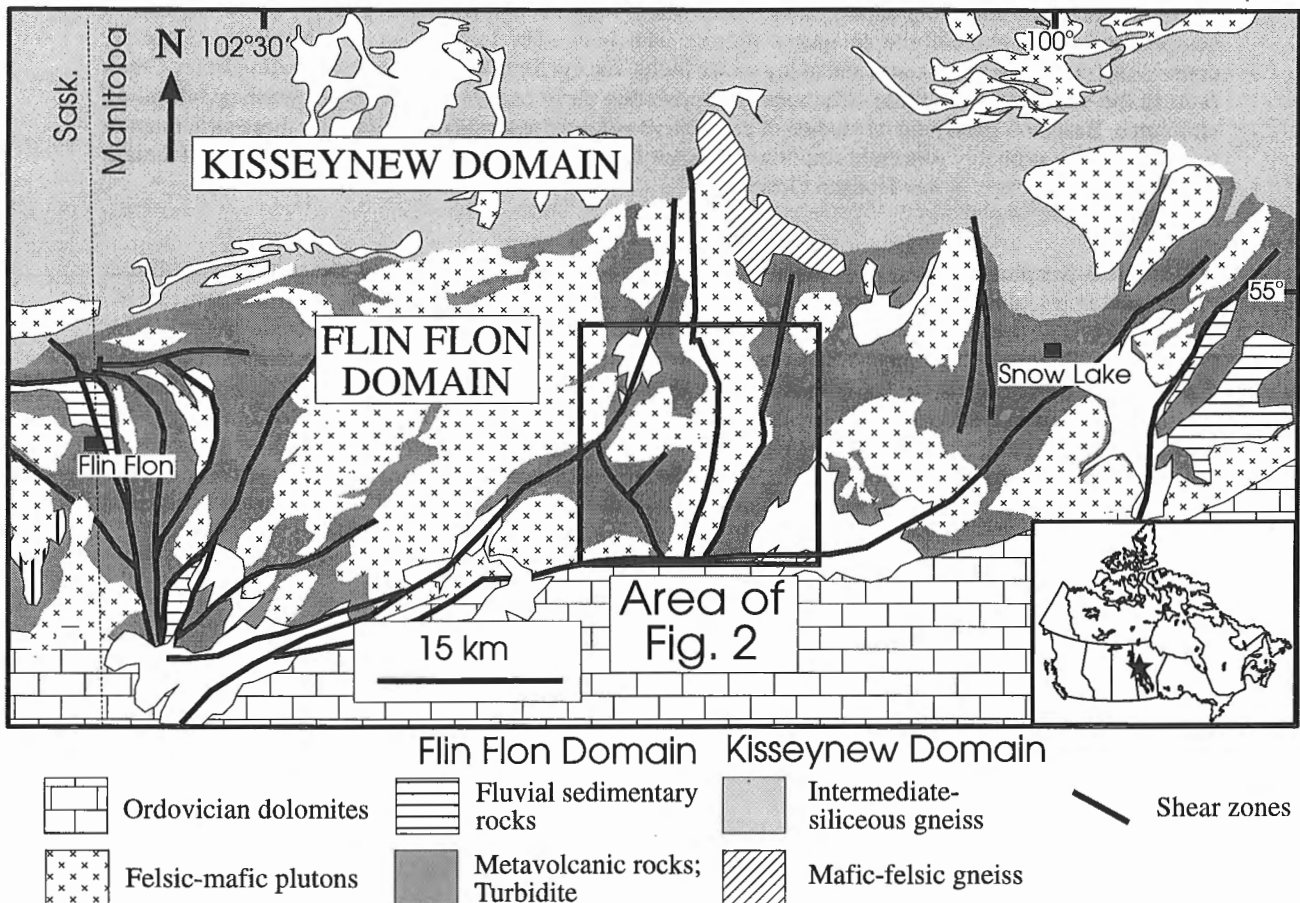


**Figure 1.** Location of the Iskwasum Lake sheet (NTS 63K/10), Manitoba, in the Flin Flon Domain of the Paleoproterozoic Trans-Hudson Orogen.

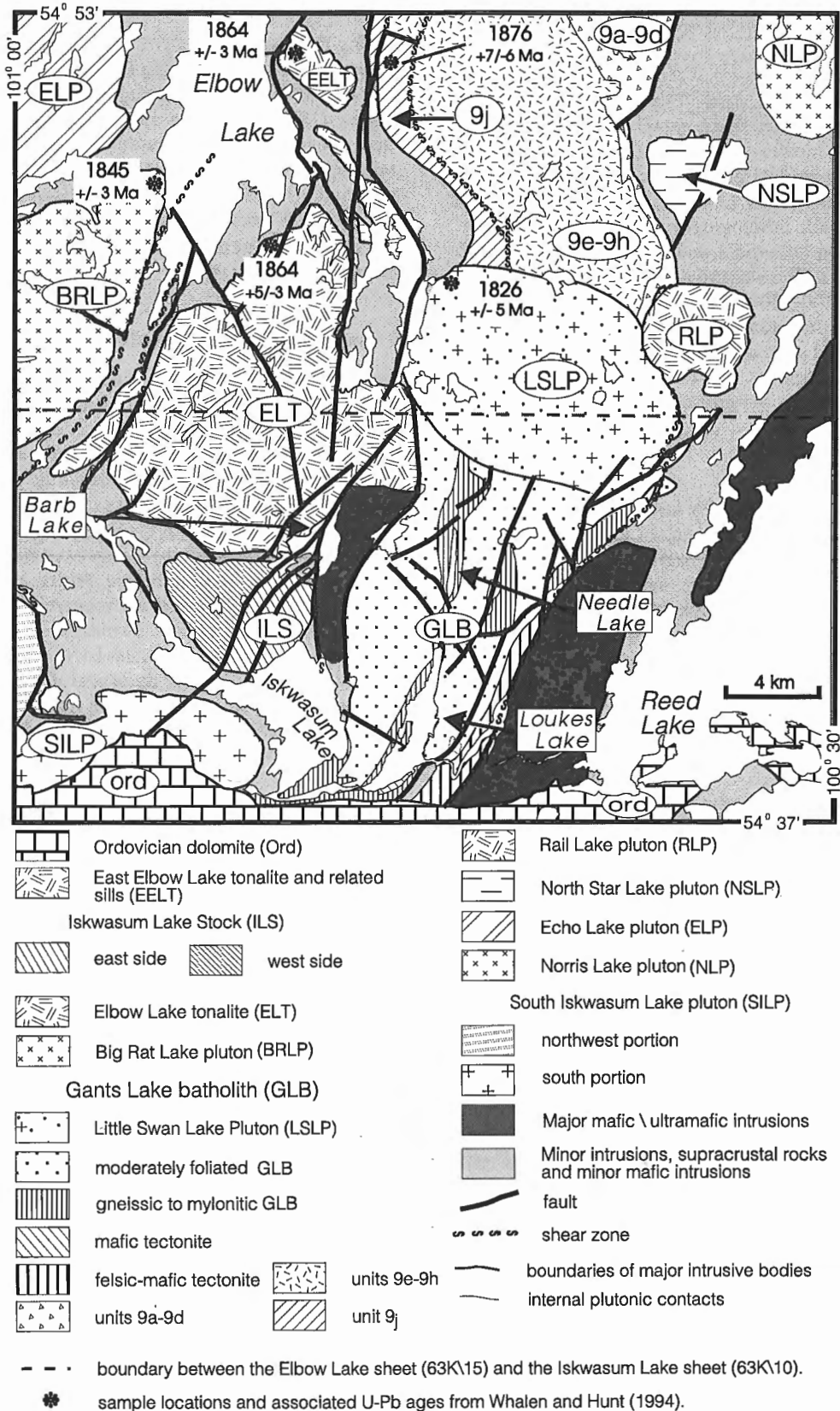


**Figure 2.** Simplified geological map of the Iskwassum Lake (NTS 63K/10) and the adjoining Elbow Lake (NTS 63K/15) sheets showing major granitoid intrusions. Abbreviations for plutons used in figure and text are given in legend. Elbow Lake sheet portion modified after Whalen (1993b) and Whalen and Hunt (1994); unit numbers within the Gants Lake batholith refer are map units of Whalen (1993a).

## PETROGRAPHY OF GRANITOID PLUTONS

### 1. *Iskwasum Lake stock*

The ovoid Iskwasum Lake stock (ILS) consists mainly of leucocratic, biotite tonalite. Mafic minerals generally make up <10 per cent, and locally <5 per cent of the rock. Pervasive and fracture-related epidote alteration of plagioclase occur east and west of the Barb Lake fault, respectively. The Iskwasum Lake stock lithologically resembles the Elbow Lake tonalite. Pluton host rocks include mafic tectonite and mafic volcanic rocks. The western and northern edges of the pluton consist of a 100-200-m-wide zone of tonalite rich (up to 75%) in wallrock inclusions. The fabric in mafic tectonite inclusions was folded prior to incorporation in the tonalite. A later moderate foliation in the Iskwasum Lake stock is oriented concentric to the margins of the pluton.

### 2. *Elbow Lake tonalite*

The Elbow Lake tonalite (ELT) straddles the boundary between the Elbow Lake and Iskwasum Lake sheets (Fig. 2). The northern portion, which was described by Whalen (1992, 1993a,b), yielded the U-Pb zircon age of 1864±5/-4 Ma (Whalen and Hunt, 1994). Although this pluton can be compositionally, texturally, and structurally variable at the outcrop scale, at the map scale it is predominantly a quartz-biotite porphyritic, biotite±hornblende tonalite. Locally, the pluton varies from quartz diorite to granodiorite, and from porphyritic to equigranular. Quartz and biotite phenocrysts range from 2-20 mm.

The Elbow Lake tonalite is cut by mafic dykes and quartz stockworks which cannot be traced from one outcrop to the next, suggesting discontinuous preservation of primary features within the pluton. Brittle north-northeast-trending faults which crosscut the Elbow Lake tonalite are the dominant structural features within the pluton. These faults, typically recognizable as topographic lineaments and as areas with distinct fracture patterns, are associated with a relative decrease in grain size.

In portions of the Elbow Lake tonalite, compositional zoning appears to have escaped disruption by the prevalent, north-northeast-trending brittle faults. At the pluton's western margin, an ovoid granodiorite unit grades outwards to equigranular tonalite, and finally to quartz-biotite porphyritic tonalite. At the pluton's centre, a hornblende-rich tonalite unit has been outlined.

In general, the margins of the Elbow Lake tonalite appear to be intrusive rather than structural. The best evidence in support of this is the presence of abundant wall rock xenoliths. Two distinct xenolith-rich zones contain large, angular fragments of proximal wall-rock lithologies. However, the contact between the Elbow Lake tonalite and Gants Lake batholith (Fig. 2, 3) is interpreted as a sheared contact. It is marked by a thin (<50 m) zone of banded gneisses and mylonites probably derived from felsic intrusive and mafic supracrustal rocks.

### 3. *Big Rat Lake pluton*

The Big Rat Lake pluton (BRLP) occupies only about 10 km<sup>2</sup> in the northwest corner of the Iskwasum Lake sheet (Fig. 2). Only two of the phases mapped in the Elbow Lake sheet by Whalen (1993a) continue into the Iskwasum Lake sheet. These consist of a fine- to medium-grained biotite granite to granodiorite, and a medium- to coarse-grained, biotite granite to granodiorite. Based on field relationships in the Elbow Lake sheet (Whalen, 1993a,b) these units intrude into a Big Rat Lake pluton unit that has an U-Pb zircon age of 1845 ± 3 Ma (Whalen and Hunt, 1994).

### 4. *South Iskwasum Lake pluton*

The exposed South Iskwasum Lake pluton (SILP) is separated into lithologically distinct southern and northwestern portions (Fig. 2). Its southern end is overlain by Paleozoic rocks. Its southern portion, located south of Iskwasum Lake, consists of homogeneous, moderately foliated, biotite-hornblende granodiorite. South of Iskwasum Lake, relatively undeformed granodiorite of the South Iskwasum Lake pluton and mafic tectonite occur in close proximity. It is notable that north-northeast-trending brittle faults and shear zones, ubiquitous in other plutons, are relatively rare in this body. However, the Barb Lake fault is a notable exception (Figs. 2, 3). This suggests that either the South Iskwasum Lake pluton was emplaced after much of the deformation, or that deformation was concentrated in less competent mafic host rocks. Given the low state of deformation in other plutons in the area adjacent to deformed supracrustal rocks, we favour the latter suggestion.

The northwestern portion of the South Iskwasum Lake pluton is lithologically more complex than the southern portion (Fig. 2). At its southern end, it contains a small zone of K-feldspar-porphyritic granodiorite. K-feldspar is poikilitic with quartz and mafic mineral inclusions. This unit, which is volumetrically more significant in the adjoining Cranberry Portage sheet, grades towards the north into equigranular biotite-hornblende granodiorite. Farther north, this unit grades into hornblende quartz-monzonite and, finally, near its northernmost wall-rock contact, into hornblende-biotite granodiorite. The northern contact with mafic tectonite is characterized by a thin (<150 m wide) zone of intrusive breccia which contains at least seven different xenolith lithologies. Xenoliths include mafic tectonite, moderately deformed to massive mafic volcanic rock, various intrusive rocks, and cognate xenoliths. The southern margin of the northwestern portion of the pluton is overlain by an outlier of Ordovician dolomite. The eastern margin is in intrusive contact with moderately deformed pillow basalt.

The northwestern portion of the South Iskwasum Lake pluton also differs from its southern counterpart in its structural complexity. A shear zone, which forms its northeastern contact with mafic volcanic rocks, crosscuts the pluton to the south (Fig. 3). This ductile shear zone is 150-200 m wide within the pluton, and appears to truncate the zone of intrusive breccia in the north. Rocks at the margins of the shear zone

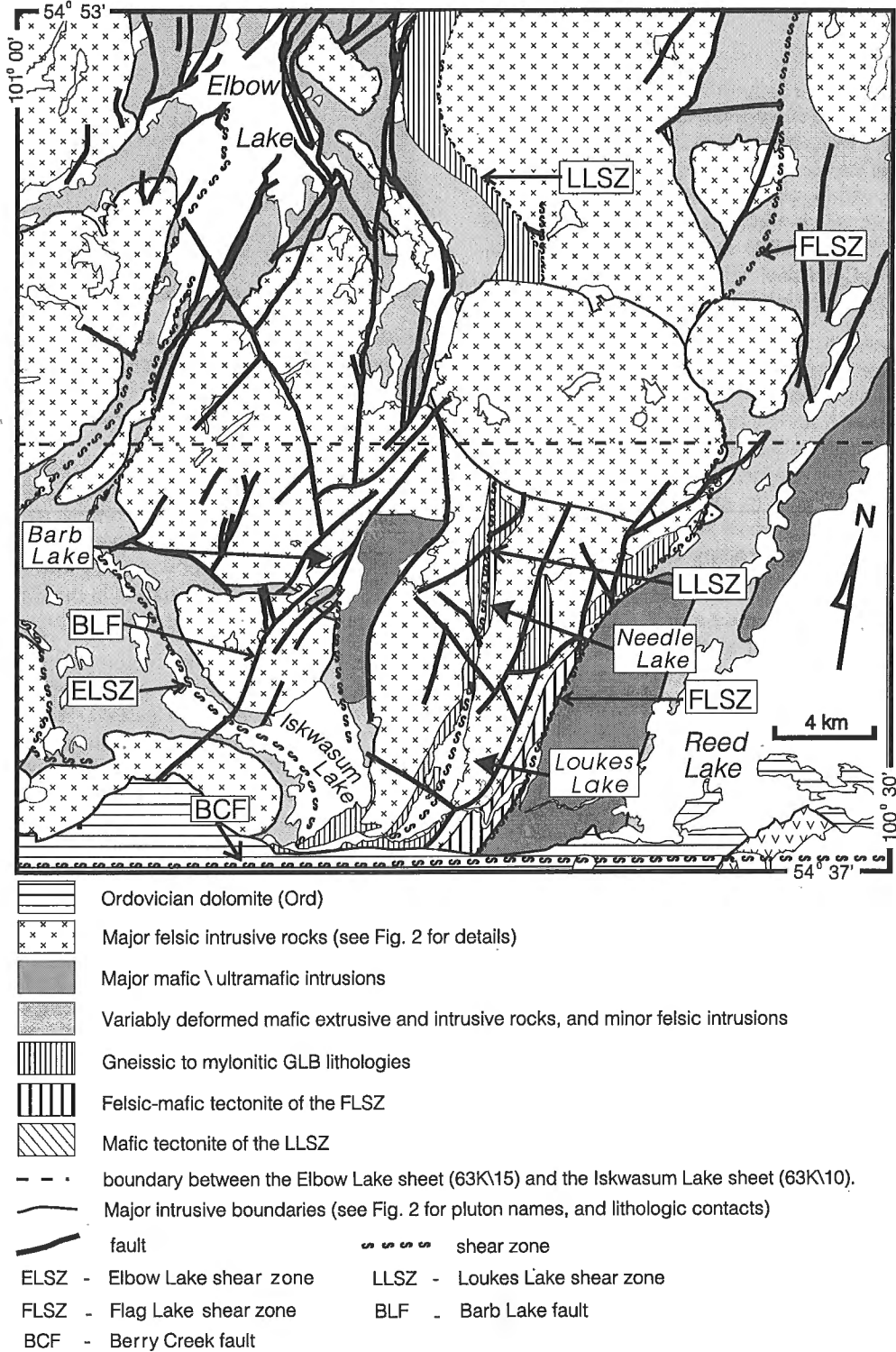


**Figure 3.** Simplified structural map of the Iskwasum Lake (NTS 63K/10) and the adjoining Elbow Lake (NTS 63K/15) sheets. Abbreviations of faults and shear zones used in figure and text are given in the legend.

are recognizable as sheared equivalents of South Iskwasum Lake pluton units, but there is some evidence that mafic sheets have also been deformed within the shear zone.

### 5. Gants Lake batholith

The bulk of the Gants Lake batholith (GLB) crops out in the Elbow Lake sheet, where it was mapped and subdivided by Whalen (1993a,b). Two or three main intrusive units appear to continue into the Iskwasum Lake sheet. Significant structural complexities, within and at the margins of the GLB, are mainly related to the north-northeast-trending Loukes Lake (LLSZ) and Flag Lake (FLSZ) shear zones and the east-west-trending Berry Creek fault (BCF) (Fig. 3). These structural features are described below.

The southern portion of the Gants Lake batholith is dominated by plagioclase porphyritic, hornblende-biotite granodiorite. A similar plagioclase- porphyritic granodiorite phase mapped in the Elbow Lake sheet (map unit 9j of Whalen, 1993a,b) (Fig. 2), yielded an U-Pb zircon age of  $1876 \pm 7/-6$  Ma (Whalen and Hunt, 1994). The deformation state of this phase varies from slightly foliated to gneissic, and may reflect proximity to the Loukes Lake shear zone (Fig. 3). At present, however, the age of phases bounding the shear zone is not known.

In a well-exposed area northwest of Loukes Lake, and away from deformation related to the Loukes Lake shear zone, five texturally different intrusive lithologies were recognized in the Gants Lake batholith. Crosscutting relationships, where all five phases coexist, suggest that all phases were approximately comagmatic. Where these lithologies are present on the west shore of Needle Lake, the Loukes Lake shear zone has obliterated all crosscutting relationships. East of the Loukes Lake shear zone, the Flag Lake shear zone separates the Gants Lake batholith from the Reed Lake mafic/ultramafic complex and mafic intrusive and extrusive rocks to the south and north, respectively. Two large xenolith-rich zones suggest that the Gants Lake batholith intruded both mafic volcanic rocks and gabbros. These zones, one of which is fault-bounded, consist of large (up to 10 m wide) angular fragments of both mafic intrusive and extrusive lithologies within quartz-porphyritic granodiorite. Fragments in both areas occupy 50-80 per cent of the outcrop area. The Gants Lake batholith granodiorite east of the Loukes Lake shear zone includes one ~150-200m wide block of mylonitic felsic intrusive rock within relatively undeformed granodiorite. Two of the three sides of this block are faulted bounded (see Fig. 2).

At the northern margin of the map sheet, the ovoid Little Swan Lake pluton (LSLP) intrudes the Gants Lake batholith. The northern half of this pluton, located in the Elbow Lake sheet (map units 9n to 9s of Whalen (1993a), yielded a U-Pb titanite age of  $1826 \pm 5$  Ma (Whalen and Hunt, 1994), significantly younger than the  $1876 \pm 7/-6$  Ma U-Pb zircon age obtained for its plagioclase porphyritic granodiorite wall rock. Consistent with this apparent age gap, north-trending structures within the elongate Gants Lake batholith terminate at the Little Swan Lake pluton contact (Fig. 3). The Little

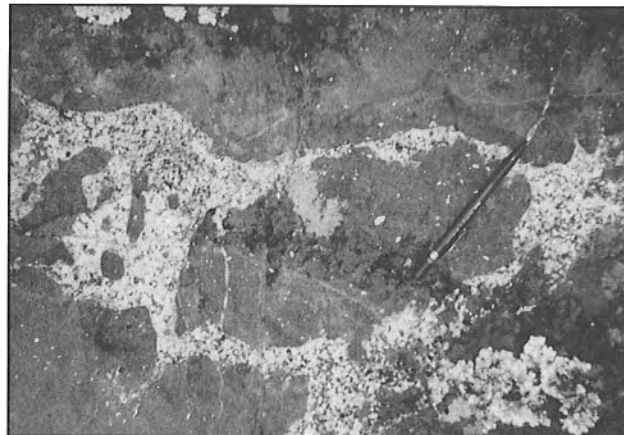


**Figure 4.** Lobate, comagmatic inclusions of quartz diorite in porphyritic granodiorite of the Little Swan Lake pluton; note the incorporation into the quartz diorite of plagioclase phenocrysts from the granodiorite. (GSC 1994-743E)

Swan Lake pluton typically exhibits a moderate foliation, parallel to the margin of the pluton. A second, similarly oriented, foliation is developed within the Gants Lake batholith parallel to its contact with the Little Swan Lake pluton. Intensity of this second foliation in the Gants Lake batholith increases toward its contact with the Little Swan Lake pluton.

The Little Swan Lake pluton is dominated by coarse grained, hornblende-biotite granodiorite, but also includes quartz diorite, diorite, and gabbro. Field relations, such as small (<10 cm) lobate mafic inclusions (Fig. 4) as well as much larger (1500 m wide) mafic zones within granodiorite, indicate coexisting mafic and felsic magmas (see also Whalen, 1993a,b).

## STRUCTURAL GEOLOGY

The Iskwasum Lake sheet is dominated by three northerly trending shear zones (the Loukes Lake shear zone (LLSZ) (Syme, 1994), Flag Lake shear zone (FLSZ), and the Elbow Lake shear zone (ELSZ) (Syme, 1994)), and a late east-west-trending shear zone (the Berry Creek fault (BCF); Syme, 1993, 1994)) (Fig. 3). In addition, smaller faults, with a dominant north-northeast-trending orientation, are common throughout the area. These north-northeast-trending structures typically truncate earlier NW trending faults, but this is not always the case. Of these brittle features, the Barb Lake fault (BLF) is an important feature and will be discussed further.

### 1. Elbow Lake shear zone

The Elbow Lake shear zone (ELSZ) is a prominent structure in the Elbow Lake sheet (Syme, 1991, 1992). Ryan and Williams (1993) interpreted it as a complex and long-lived structure, which began to form prior to the 1864 Ma emplacement of the Elbow Lake tonalite and which outlasted peak metamorphic conditions at 1820 to 1805 Ma (David et. al.,

1993; Ansdell and Norman, in press). Mapping by Syme (1991,1992) and Syme and Whalen (1992) and geochemical investigations by Stern et al. (in press, in prep.) have shown that the Elbow Lake shear zone juxtaposes various ocean floor and arc tectonostratigraphic assemblages.

In the Elbow Lake sheet, the Elbow Lake shear zone narrows to both the north and south, from its maximum width of about 2.2 km in the middle of Elbow Lake, to approximately 50 m at the Grass River outlet at the lake's southwest end (Syme, 1991). Reconnaissance geology by Syme (1994) suggests that the Elbow Lake shear zone continues southward from Elbow Lake to Iskwasum Lake and is eventually dragged into, and terminated against the Berry Creek fault. On Iskwasum Lake, the Elbow Lake shear zone is localized primarily within various mafic extrusive and intrusive units. Although often strongly foliated/gneissic, granitoid rocks exposed on the northeast shore of Iskwasum Lake (the only granitoid rocks to outcrop on Iskwasum Lake) are not as deformed as the mafic rocks within the Elbow Lake shear zone. Deformation on the margin of the Gants Lake batholith can be attributed to the shear zone, as the intensity of deformation rapidly decreases away from the shore of the lake (Fig. 3). The Elbow Lake shear zone does not appear to affect other large granitoid plutons (i.e., Elbow Lake tonalite, Iskwasum Lake stock, South Iskwasum Lake pluton) in the area to the same degree as the Gants Lake batholith.

## 2. Loukes Lake shear zone

Previously unrecognized, the Loukes Lake shear zone is a  $\leq 1500$  m wide zone of variably mylonitic granitoid rocks. Only one thin ( $< 200$  m wide) sliver of mafic tectonite was recognized within the shear zone on the southeast shore of Loukes Lake. The Loukes Lake shear zone, which separates eastern and western portions of the Gants Lake batholith, is an anastomosing shear zone. To the north it first pinches out, then reappears on Needle Lake, and to the south it is dragged into the Berry Creek fault (Fig. 3). Intensity of deformation generally decreases away from the centre of Loukes Lake. An abrupt westward change from mylonitic to strongly foliated granitoid rocks is attributed to late north-northeast brittle structures along the edge of the Loukes Lake shear zone. These brittle structures, as well as primary strain deviations, may account for the anastomosing nature of the shear zone. Granitoid rocks east of the Loukes Lake shear zone are mylonitic only at the extreme northern end of Loukes Lake, and other exposures of the Gants Lake batholith on the east shore are less deformed (see Fig. 3).

As the Loukes Lake shear zone thins to the north, it becomes gneissic rather than mylonitic. Farther north on Needle Lake, the mylonite reappears, and continues north until it is cut by the Little Swan Lake pluton at the northern margin of the map sheet. Deformation intensity gradually decreases laterally, from gneissic to strongly foliated 500 m east and west of Needle Lake. To the north in the Elbow Lake sheet, the Loukes Lake shear zone is correlated with a mylonite zone within the Gants Lake batholith outlined by Whalen (1993a,b). Except for a few minor east-west offsets, the Loukes Lake shear zone appears to continue in a

north-south-direction, from the north side of the Little Swan Lake pluton to the northern edge of the Elbow Lake sheet (see Fig. 3), where it was mapped as a mylonite belt by Whalen and Syme (1992).

The Loukes Lake shear zone appears to postdate Gants Lake batholith emplacement, as the shear zone cuts across lithological boundaries, including quartz diorite, quartz diorite to tonalite and granodiorite from south to north. The porphyritic granodiorite, which occurs on the western side of the Loukes Lake shear zone near Loukes Lake, resembles a major plutonic unit on the northwest side of the Gants Lake batholith in the Elbow Lake sheet (unit 9j) (Fig. 2). In the Elbow Lake sheet, this unit is bounded on its eastern side by the proposed continuation of the Loukes Lake shear zone. The granodiorite unit with a dominant north-northeast-trending orientation yielded an U-Pb zircon age of  $1876 \pm 7$ -6 Ma (Whalen and Hunt, 1994), which puts a maximum age constraint on the Loukes Lake shear zone. A  $1826 \pm 5$  Ma U-Pb titanite age was obtained on the crosscutting Little Swan Lake pluton (Whalen and Hunt, 1994), which cuts off the Loukes Lake shear zone. This places a minimum age constraint on the Loukes Lake shear zone, for the Little Swan Lake pluton is only moderately foliated and truncates all major structures in the Gants Lake batholith.

Pegmatite dykes and veins intrude the Loukes Lake shear zone and are variably deformed, suggesting that they have been syntectonically emplaced. Narrow pegmatite veins (1-3 cm wide) have been deformed in the shear zone to the point where they consist of K-feldspar porphyroclasts strung out 1-10 cm apart (Fig. 5). Although unambiguous shear sense indicators are relatively rare, locally present winged porphyroclasts generally indicate dextral shear, although some are sinistral. Thin section study of the Loukes Lake shear zone mylonite will attempt to validate such field observations and further identify shear sense indicators.

## 3. Flag Lake shear zone

The Flag Lake shear zone, a north-northeast-trending zone of banded mafic-felsic mylonite on the Grass River east of Loukes Lake, separates the Gants Lake batholith to the west from the Reed Lake layered mafic-ultramafic complex to the east (Fig. 2, 3). Although interpretation of protoliths is equivocal, this 500-750 m wide belt of tectonite probably contains sheared equivalents of both intrusive bodies. The Flag Lake shear zone is unconformably overlain to the south by Paleozoic cover, and passes along strike into a felsic mylonite to the north, where it is eventually truncated by a north-northwest-trending fault. Tectonites along the Flag Lake shear zone are typically fine grained with a dominant banded appearance. No shear sense indicators were identified in the field. The Flag Lake shear zone is predominately concentrated in supracrustal rocks, but immediately north of the northwest-trending fault, which truncates the tectonite belt, is an area of mylonitic felsic intrusive rock. Although this unit is along strike with the tectonite, it is not certain whether deformation in this unit was due to the Flag Lake shear zone, or whether it is an unrelated fault-bounded block.



The eastern portion of the Gants Lake batholith contains two fault-bounded blocks of felsic mylonite, juxtaposed against relatively undeformed granodiorite (Fig. 2). The mylonitic blocks (~0.15-0.9 km) have no context with respect to large-scale structures in the area and do not continue along strike. However, the mylonitic fabric generally has a similar orientation to the north-northeast-trending structures in the area. The blocks may represent fragmented parts of the Flag Lake shear zone or an earlier, similarly orientated structure. The Flag Lake shear zone may continue north-northwest into

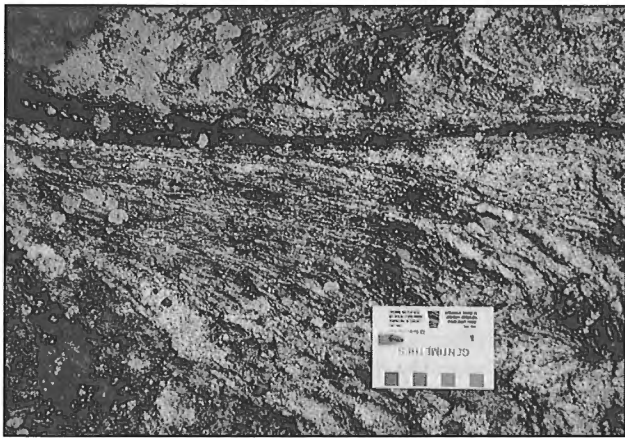


**Figure 5.** *Folded and strung out pegmatite veins near the margin of the Loukes Lake shear zone; note the extremely attenuated nature of the veins, some are folded, others form strung out lines of K-feldspar porphyroclasts. (GSC 1994-743C)*

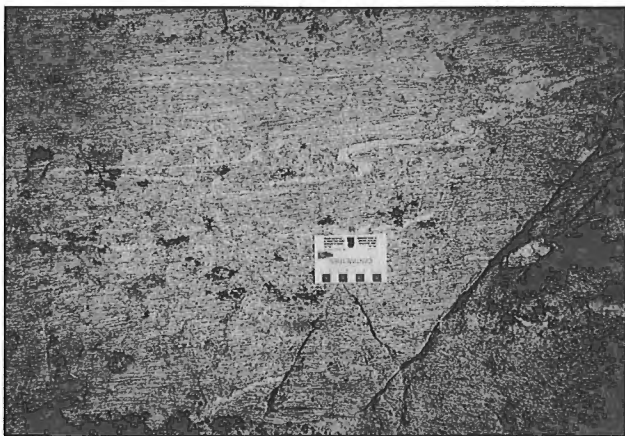


**Figure 6.** *Complex folds of a thin pegmatite vein in the Loukes Lake shear zone. Folds are tight to isoclinal, and appear to show some signs of polyphase folding. Shear zone fabric trends approximately north, while Berry Creek fault fabric can be seen as late brittle fractures. (GSC 1994-743G)*

the Elbow Lake sheet, linking with a shear zone which crosses North Star Lake and continues northward west of the Norris Lake pluton (see Fig. 3).

#### 4. Berry Creek fault

The Berry Creek fault is a major west-east trending structure which extends from Athapapuskow Lake to the west shore of Wekusko Lake. Although it is entirely covered by Palaeozoic rocks in the Iskwasum Lake sheet, associated deformation has been recognized up to 5 km to the north of it. The Berry Creek fault has a north-side-down or normal dip slip component south of Athapapuskow Lake (Syme, 1992) and, in the Cranberry Lake area, an apparent sinistral sense of displacement associated with brittle deformation (Syme, 1993). However, in the map area, ductile deformation has transposed north-northeast-trending structures and lithologies into a westerly orientation, suggesting a dextral sense of horizontal shear. The Berry Creek fault is, therefore, a complex structure with an apparently long-lived deformational history, and further work is required to integrate observations along strike length.

On a hand-specimen scale, fabrics of the Berry Creek fault overprint earlier fabrics within the Gants Lake batholith, and its shear zones (Elbow Lake shear zone, Loukes Lake shear zone, Flag Lake shear zone). This overprinting is so intense that, adjacent to the fault, earlier fabrics are completely transposed into the Berry Creek fault fabric (Fig. 6). Farther away, for up to 5 km north, the Berry Creek fault foliation can be recognized as an axial planar foliation to minor open to isoclinal folds of earlier foliations and compositional layering. Late brittle faults also appear to be axial planar to the Berry Creek fault-related folds (see Fig. 7). Isoclinal folds are commonly located nearer to the Berry

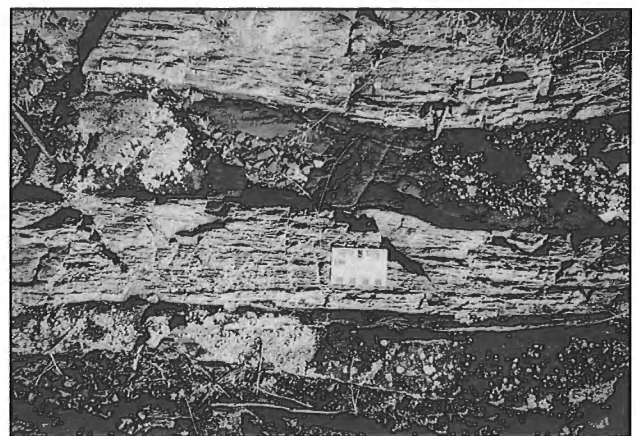


**Figure 7.** *Sheet of ultramafic rock within the Loukes Lake shear zone, near the Berry Creek fault; note that the felsic host rock is so extremely attenuated that few kinematic indicators are preserved. Although the Loukes Lake shear zone is a north-northwest-trending structure, the fabric at this location is east-west-trending due to the later east-west Berry Creek fault. (GSC 1994-743H)*

Creek fault and typically have an east-northeast orientation with Z-fold asymmetry (Fig 7), consistent with the map-scale relations.

### 5. Barb Lake fault

The Barb Lake fault, one of the most significant north-northeast-trending brittle faults, is a large structure with associated distinct fracture sets. These structures are best recognized on aerial photographs and can be recognized by mapping of lithological offsets. The Barb Lake fault cuts the Iskwasum Lake stock (ILS), extends north through Barb Lake, and south through Iskwasum Lake, where it cuts the Elbow Lake shear zone (Syme, 1994) and the South Iskwasum Lake pluton (Fig. 2, 3). The Barb Lake fault is best seen within the Iskwasum Lake stock, where it separates highly altered rocks from less altered equivalents. Large cliff faces are found on either side of the fault, and associated fracture patterns are recognizable up to 1 km away. These fractures trend parallel to the fault (010-020°) and dip east at about 80°. Such brittle deformation is common throughout the Iskwasum Lake sheet but is rarely as pronounced. The eastern portion of the Iskwasum Lake stock has fracture-related alteration of plagioclase to epidote while alteration on the west side is much more pervasive. This is thought to reflect shallow- (east-side) and deeper- (west-side) level exposures of the Iskwasum Lake stock, assuming that late-stage hydrothermal alteration is due to fluids which have had a greater effect on the upper portions of the pluton. Because the juxtaposition of these two different alteration patterns requires that the east side be moved up with respect to the west, this fault is interpreted as having a predominantly dip-slip component. Lateral offset on the Barb Lake fault appears minimal, given the minor displacement of the steeply dipping contact between the Iskwasum Lake stock and host rocks.

## DISCUSSION

Correlatives of both main plutonic rock units and major structures, which are well defined in the Elbow Lake sheet to the north (e.g., Syme and Whalen, 1992; Syme, 1992; Whalen, 1993a,b), have been mapped in the Iskwasum Lake sheet. The Iskwasum Lake sheet probably represents a similar complex and tectonically important portion of the Flin Flon Domain.

The Elbow Lake shear zone, which juxtaposes diverse volcanic assemblages, is interpreted as an early structure (pre-1864 Ma) with a protracted movement history (Syme, 1992; Ryan and Williams, 1993). The Loukes Lake shear zone is localized almost entirely within plutonic rocks of the Gants Lake batholith in both the Iskwasum and Elbow Lake sheets. Geochemical characterization of volcanic rocks (E.C. Syme, 1994, pers. comm.) indicates that the Gants Lake batholith is bounded by ocean-floor assemblages to the west and arc-type assemblages to the east. Based on this evidence, Whalen and Hunt (1994) suggested that the Gants Lake batholith may be localized along a significant tectonic boundary. The Loukes Lake shear zone, like the Elbow Lake shear zone, may represent the reworked trace of such a boundary. More

detailed investigation is required to determine the age, tectonic significance, and relationship of shear zones in the Iskwasum-Elbow Lake area to other map scale structures in the Flin Flon Domain.

## ACKNOWLEDGMENTS

The senior author would like to acknowledge the able field assistance of Trevor Bohay. Field work was facilitated by the hospitality and helpful advice of Eric Syme and other staff of Manitoba Energy and Mines. The authors benefited from discussions with Eric Syme and Andre Lalonde. A number of careful and thorough critical editings of the manuscript by Steve Lucas greatly improved its quality. Critical reviews by John Percival and Edgar Froese were greatly appreciated.

## REFERENCES

- Ansdell, K.M. and Norman, A.R.,**  
in press: The timing of magmatism, deformation and metamorphism along the southern flank of the Kiseynew Domain; Precambrian Research (in press).
- David, J., Machado, N., Bailes, A., and Syme, E.**  
1993: U-Pb geochronology of the Proterozoic Flin Flon Belt-Snow Lake Belt: New results.
- Lucas, S.B. and Stern, R.A.**  
1994: Significance of accretion and melting processes for the development of Paleoproterozoic continental lithosphere; Geological Association of Canada, Program with Abstracts, v. 19, p. A67.
- Ryan, J.J. and Williams, P.F.**  
1993: Structural mapping in the Elbow Lake area, Flin Flon-Snow Lake Belt, central Manitoba; in Manitoba Energy and Mines, Minerals Division, Report of Activities, 1993, p. 84-85.
- Stern, R.A., Syme, E.C., Bailes, A.H., and Lucas, S.B.**  
in press: Paleoproterozoic (1.90-1.86 Ga) arc volcanism in the Flin Flon Belt, Trans-Hudson Orogen, Canada; Contributions to Mineralogy and Petrology.
- Syme, E.C.**  
1991: Elbow Lake project - Part A: supracrustal rocks and structural setting; in Manitoba Energy and Mines, Minerals Division, Report of Activities, 1991, p. 14-27.  
1992: Elbow Lake project - Part A: Supracrustal rocks; in Manitoba Energy and Mines, Minerals Division, Report of Activities, 1992, p. 32-46.  
1993: Cranberry-Simonhouse reconnaissance; in Manitoba Energy and Mines, Minerals Division, Report of Activities, 1993, p. 61-66.  
1994: Supracrustal rocks of the Iskwasum Lake area (63K/10W); in Manitoba Energy and Mines, Minerals Division, Report of Activities, 1994, p.xx-xx.
- Syme, E.C. and Whalen, J.B.**  
1992: Elbow Lake (part 63K/15): Manitoba Energy and Mines, Preliminary Map 1992F-1; 1:20 000.
- Whalen, J.B.**  
1992: Elbow Lake project - Part B: Granitoid rocks; in Manitoba Energy and Mines, Minerals division, Report of Activities, 1992, p. 47-51.  
1993a: Geology, Elbow lake (NTS 63K/15), Manitoba; Geological Survey of Canada, Open File 2709, scale 1:50 000.  
1993b: Granitoid rocks of the Elbow Lake Sheet (NTS 63K/15); in Manitoba Energy and Mines, Minerals Division, Report of Activities, 1993, p. 86-89.
- Whalen, J.B. and Hunt, P.A.**  
1994: Geochronological study of granitoid rocks in the Elbow Lake Sheet (NTS 63K/15), Manitoba: a portion of the Flin Flon Domain of the Paleoproterozoic Trans Hudson Orogen; in Radiogenic Age and Isotopic Studies: Report 8; Geological Survey Canada, Current Research 1994-F, p. 1-10.



# Preliminary diatom analysis of selected samples from Lake Abitibi and Glacial Lake Ojibway, Ontario and Quebec

Clément L. Prévost, Jean J. Veillette, and Paul B. Hamilton<sup>1</sup>

Terrain Sciences Division

*Prévost, C.L., Veillette, J.J., and Hamilton, P.B., 1995: Preliminary diatom analysis of selected samples from Lake Abitibi and Glacial Lake Ojibway, Ontario and Quebec; in Current Research 1995-C; Geological Survey of Canada, p. 235-242.*

---

**Abstract:** In August 1993, fourteen long cores were collected from various parts of Lake Abitibi in order to identify and date the transition periods between Glacial Lake Ojibway, ancestral Lake Abitibi, and modern Lake Abitibi. Ongoing geochemical, pedological, and paleoecological studies are conducted to find traces of extreme lake-level fluctuations and dry lake bed conditions in postglacial time. Diatom (algae) analysis is one paleoecological method used. Preliminary results from 8 samples of Lake Ojibway varved clay and Cochrane till reveal that the diatom flora of Glacial Lake Ojibway was poor, since only 15 diatom species from 8 genera were identified. This low number is likely the result of several factors (turbidity, high rates of sedimentation, lack of nutrients, icebergs) that created poor growing conditions in the cold paleowaters and hampered the successful development of diatom communities. The diatom flora of Lake Abitibi is much more developed: 149 species from 39 genera were identified in modern surficial material from the top of 14 cores. This preliminary study indicates that diatom analyses can successfully be used to help characterize the sedimentary transition from Glacial Lake Ojibway to Lake Abitibi.

**Résumé :** En août 1993, 14 carottes ont été prélevées à divers endroits dans le lac Abitibi, afin d'identifier et de dater les périodes de transition entre le Lac glaciaire Ojibway, le protolac Abitibi et le lac Abitibi actuel. Des études géochimiques, pédologiques et paléoécologiques sont en cours afin de trouver des indices postglaciaires pouvant témoigner de variations extrêmes du niveau du lac, voire de son assèchement complet. Parmi les différentes méthodes paléoécologiques, on a inclus l'analyse de diatomées (algues). Les résultats préliminaires obtenus suite à l'analyse de huit échantillons d'argile du Lac glaciaire Ojibway et de till de Cochrane révèlent que la flore de diatomées du lac glaciaire était pauvre, puisque seulement 15 espèces réparties dans 8 genres ont été identifiées. Ce petit nombre d'espèces résulte vraisemblablement d'une combinaison de facteurs (turbidité, taux de sédimentation élevés, pénurie d'éléments nutritifs, icebergs) qui ont créé un milieu défavorable au développement des communautés de diatomées dans les eaux froides du lac glaciaire. La flore moderne du lac Abitibi est beaucoup plus riche : au total, 149 espèces réparties dans 39 genres ont été identifiées lors de l'analyse des échantillons de surface prélevés au sommet des 14 carottes. Cette étude préliminaire montre que l'analyse des diatomées peut servir à la caractérisation des unités sédimentaires du Lac glaciaire Ojibway et du lac Abitibi.

---

<sup>1</sup> Canadian Museum of Nature, Research Division, P.O. Box 3443, Station D, Ottawa, Ontario, K1P 6P4

## INTRODUCTION

Lake Abitibi is a large shallow lake (average depth 3 m) straddling the Quebec-Ontario border in the southern Hudson Bay watershed (Fig. 1). Like many lakes below 300 m elevation in the northwestern Quebec and northeastern Ontario Clay Belt, it occupies a basin consisting entirely of varved clay deposited in Glacial Lake Ojibway. This huge glacial lake emptied into Hudson Bay approximately 8000 years BP when ice retreat reached the James Bay area (Hardy, 1976). Well defined wave-cut benches on the eastern and northern sides of Lake Abitibi indicate that in early postglacial time, the lake was at least 15 m higher and occupied a much larger basin (ancestral Lake Abitibi) than now. Several small rivers drain the surrounding flat clay plain, and the main outlet to James Bay, the Abitibi River, is located at the western end of the lake. The shallow depth of Lake Abitibi makes it especially sensitive to regional fluctuations in groundwater level. In warmer and drier periods throughout the Holocene, it may have experienced severe drops in level and even have dried up completely. A dam, built at the turn of the century on the Abitibi River to facilitate the floating of timber, raised its level by about 1.5 m, thus the pre-anthropogenic average depth of the lake is less than its present average depth of 3 m.

In August 1993, a two-week coring program was carried out in various parts of the lake basin with the following objectives: (1) identify and date transition periods between Glacial Lake Ojibway, ancestral Lake Abitibi, and modern Lake Abitibi before and after artificial damming of the lake, using geochemical and paleoecological methods, and (2) examine fossil lake bottom sediments for traces of

extreme lake-level fluctuations, namely for physical, geochemical, pedological, or paleoecological indications of dry lake bed conditions in postglacial time. One interesting physical characteristic of Lake Abitibi is that it drains northward through the Abitibi River, and isobases are oriented northwest-southeast so that uplift is greatest along the north shore of the lake. With the outlet rising at about the same rate as the north shore, the lake should be transgressing its southern shore. The possibility of finding physical evidence for this process should therefore be greatest in cores obtained in the southern part of the lake.

Diatom analysis is one paleoecological method used in the project. Because of their specific habitat requirements and life strategies (Patrick, 1977; Smol, 1990), diatoms are successfully used in a variety of sedimentary studies. For example, in southeastern Minnesota, stratigraphic analyses of diatom assemblages have shown the persistence of glacial ice (Florin and Wright, 1969), as well as the development of a small lake above a forest soil (Florin, 1970). The recession of Glacial Lake Agassiz was successfully reconstructed through the use of diatom stratigraphy (Ritchie and Koivo, 1975). The transgression of that same glacial lake (Emerson Phase) was later identified by Björck and Keister (1983) on the basis of diatom and pollen data.

The diatom component in this study is twofold. In order to correctly interpret changes in sedimentary diatom assemblages in Lake Abitibi cores, we have to (1) document the fossil diatom flora of Glacial Lake Ojibway, and (2) examine the modern diatom flora of Lake Abitibi. In this paper, we present some interesting results from preliminary investigations of selected samples.

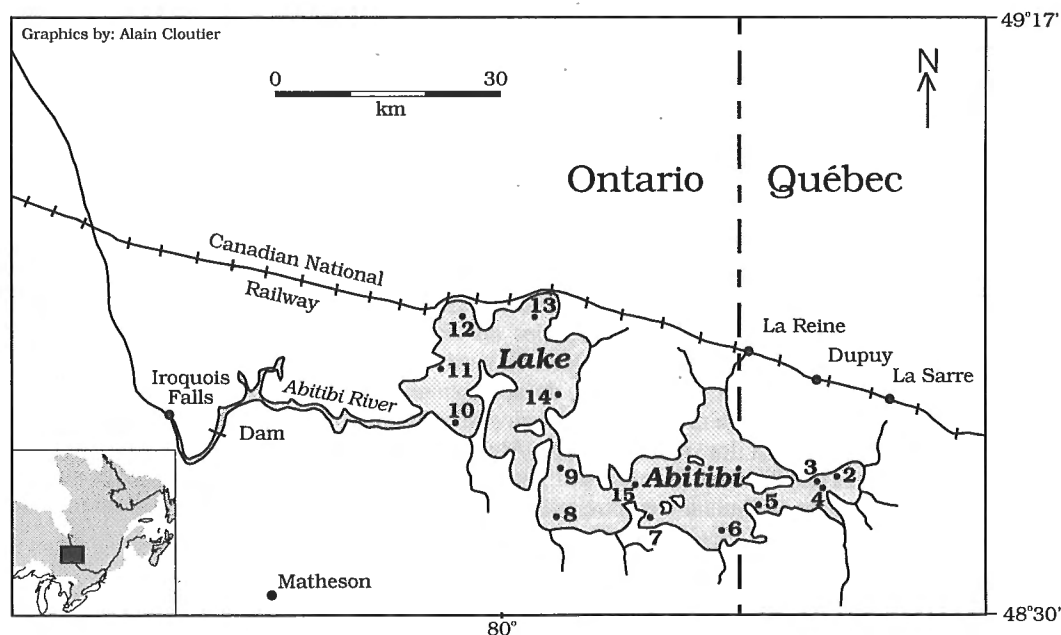


Figure 1. Location map of the study area, with ABI coring sites.

## MATERIAL AND METHODS

### Sampling procedures

Modern material analysed for diatoms was taken from the top of 14 cores collected in Lake Abitibi (Fig. 1). The cores ranged in length from 2.21 to 9.47 m, for a total of 71 m. Coring was conducted from a 30-foot houseboat anchored with wooden poles. Standard piston-type Livingstone aluminum coring tubes 5.0 cm in diameter and 1.5 and 2.0 m in length were pushed through the clay by hand using Mg-Zr, E-size drilling rods in a 10 cm plastic casing pushed 30 cm or more into lake bottom sediments. In all cases core recovery was 100 per cent. The cores were sealed with ethafoam plugs and brought to the laboratory where they were later split in half using a cutting tool. Split cores were described and sampled for moisture content, grain-size analysis, carbonate content (using Chittick and Leco methods), and geochemical analysis of 32 elements. Wood fragments were set aside for dating and selected sections of core were chosen for pollen and diatom analysis. Most results are not in yet.

Surficial geology mapping programs carried out in the general area of Lake Abitibi (Veillette, 1989; Veillette et al., 1991, 1992a, 1992b) have supplied abundant data on physical and geochemical characteristics of Glacial Lake Ojibway sediments. Eight subsamples of this fossil material were selected for diatom analysis, including both Ojibway varved clay and Cochrane till.

### Diatom analysis

Modern and fossil samples were processed according to standard procedures. Approximately 1 g of material was treated with 10% HCl to remove carbonates. Because of carbonate input by late southeast-flowing ice from the James Bay and Hudson Bay lowlands (Fig. 2; Veillette et al., 1992b), Lake Abitibi lies within the zone of carbonate-rich clays of western Abitibi. Organic matter was eliminated by boiling the samples in a 1:1 mixture of nitric and sulfuric acids. Samples were washed 5 to 7 times with distilled water to remove all traces of acid, with settling periods of 24 hours between washes. Slides for random scanning were prepared by pipetting approximately 0.3 ml of a homogeneous diatom suspension onto a 18 x 18 mm cover glass. The cover glasses were subsequently dried on a slide warmer at 75°C, and mounted on permanent slides using Hyrax<sup>R</sup>. Diatom identification was performed on a Leitz DM-RB microscope, using a PL-Fluotar 100 X oil-immersion objective with Leica L-Plan 10 X oculars.

Identifications were based on the studies of Patrick and Reimer (1966, 1975), Foged (1981), Germain (1981), and Kramer and Lange-Bertalot (1986, 1988, 1991a, 1991b). We also followed the generic revision of Round et al. (1990). For synonymy and authorship, we consulted the catalogue of Van Landingham (1967-1979), along with the checklist of Hartley (1986) and the compilation of Hamilton et al. (1994a). To facilitate reading, the authorities are not attached to the species names in the text, but appear in a compiled list of diatom species available upon request from the senior author.

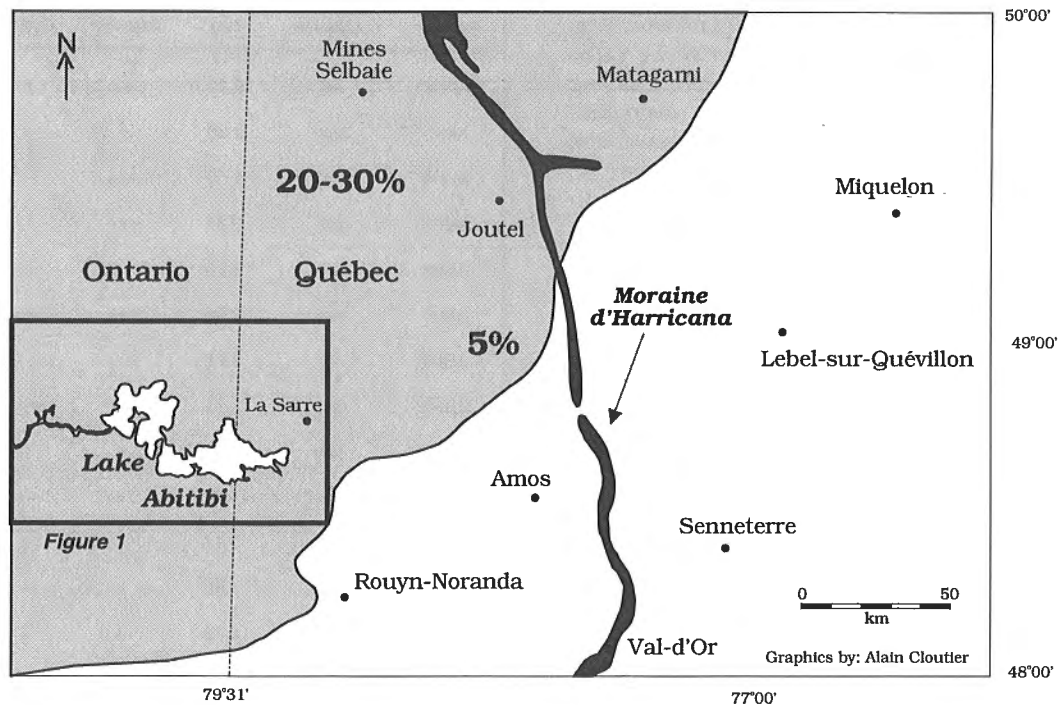


Figure 2. Approximate dispersal limit of Paleozoic carbonates, and carbonate content of Ojibway varved clays (%); modified from Veillette et al., 1992b.

## RESULTS

### Glacial Lake Ojibway sediments

Five samples of Cochrane till and three of Ojibway clay were analyzed a few years ago to compare the diatom flora of both types of sediments, and to verify the presence of a potential marine flora in Cochrane till (Prévost, 1992). The samples are from a wide area in Abitibi and are representative of Glacial Lake Ojibway fine-grained sediments. The same samples have been re-examined here (using new mounted slides and with a different purpose in mind), and the results match the 1992 findings. Diatom diversity and relative abundance were low in every sample (Table 1). In a standard diatom enumeration, a minimum of between 500 and 600 diatom valves are counted in order to provide adequate interpretation (Battarbee, 1986). Diatoms were not abundant in the Ojibway samples: counts were done using microslides with a dense layer of material, and the highest count obtained was 106 diatom valves. Four of the eight samples analyzed showed a freshwater diatom assemblage consisting predominantly of periphytic/benthic (associated with shallow water) species. Only two planktonic (deep water) taxa were found. Three other samples contained a few intact frustules along with isolated freshwater diatom fragments. One sample lacked the presence of diatom valves and fragments. Chrysophycean cysts were found in low abundance in three of the eight samples. No sponge spicules were found in any of the samples examined in this preliminary study (Table 1).

Only 15 diatom species from 8 genera were identified in Glacial Lake Ojibway material. The samples were dominated by *Achnanthes minutissima* (sensu lato) and *Achnanthes petersenii*, cosmopolitan diatoms widespread in all fresh waters. Subdominant in the samples were two planktonic taxa, identified as *Synedra delicatissima* and *Synedra radians*. Other periphytic diatoms found in lower numbers were *Diatoma tenuis*, *Nitzschia* cf. *perminuta*, *Nitzschia amphibia*, *Nitzschia* cf. *flexoides*, *Eunotia praerupta*, *Navicula vulpina*, *Navicula radiosa*, *Cymbella* cf. *arctica*, *Cymbella descripta*, *Cymbella microcephala*, and *Cymbella cistula*. Undifferentiated species of *Achnanthes*, *Gomphonema*, *Navicula*, and *Nitzschia* were also encountered.

### Lake Abitibi sediments

The 14 surface samples collected from the top of the core sections were randomly scanned. Diatom diversity and relative abundance differ from site to site and are related to sediment type (Table 2). Only two clay samples showed a significant diatom component (ABI-4 and ABI-7). The five remaining clay samples comprised a scarce diatom flora. Diatoms were particularly abundant in all sand and silt samples. Samples ABI-11 and ABI-15 had the most abundant and diverse diatom floras. Chrysophycean cysts were particularly abundant in samples ABI-7 and ABI-15, and moderately abundant in four other samples. Sponge spicules were abundant in samples ABI-2 and ABI-5, and moderately abundant in seven other samples (Table 2).

**Table 1.** Relative abundance of diatoms and other siliceous microfossils from Glacial Lake Ojibway sediments.

Sample	Type of sediment	Diatoms	Cysts	Sponge spicules
OJIB-1	till	++	+	-
OJIB-2	till	++	+	-
OJIB-3	clay	++	-	-
OJIB-4	clay	++	-	-
OJIB-5	clay	+	-	-
OJIB-6	till	+	+	-
OJIB-7	till	-	-	-
OJIB-8	till	+	-	-

Key to codes: - absent  
+ present, poor, scarce  
++ moderately abundant

**Table 2.** Relative abundance of diatoms and other siliceous microfossils from Lake Abitibi surface samples.

Sample	Type of sediment	Water depth (m)	Diatoms	Cysts	Sponge spicules
ABI-2	silt	2.29	++	+	+++
ABI-3	clay	2.80	+	+	+
ABI-4	clay	2.55	+++	++	++
ABI-5	silt	2.84	+++	+	+++
ABI-6	silt	3.23	++	+	+
ABI-7	clay	3.00	+++	+++	++
ABI-8	silt	3.71	+++	++	++
ABI-9	silt	3.21	++	++	++
ABI-10	clay	3.39	+	+	+
ABI-11	sand	1.80	+++	++	++
ABI-12	clay	3.47	+	+	+
ABI-13	clay	3.68	+	+	+
ABI-14	clay	3.48	+	+	++
ABI-15	sand	2.90	+++	+++	++

Key to codes: + present, poor, scarce  
++ moderately abundant  
+++ abundant

A total of 149 diatom species from 39 genera were identified in present-day Lake Abitibi. These numbers will obviously change as future systematic counts are completed. The diatom flora is represented by numerous periphytic/benthic and planktonic taxa. *Aulacoseira* spp. were amongst the most common planktonic diatoms, being present in essentially every sample. Other frequent planktonic species included *Asterionella formosa* and *Fragilaria crotonensis* and occurred mainly in sample ABI-4. Species of *Cyclotella* and *Stephanodiscus* (mostly *S. niagarae*) were also common. The periphyton was well represented, with the genus *Navicula* (sensu lato) abundant, especially in samples ABI-11 and ABI-15. Species of *Amphora*, *Cymbella* (sensu lato), *Neidium*, *Nitzschia*, and *Pinnularia* were also common in most samples. A more detailed outline of the diatom flora of present-day Lake Abitibi, as a complete alphabetical species list, may be requested from the senior author.

## DISCUSSION

Preliminary results reveal that Glacial Lake Ojibway sediments are relatively poor in diatoms. The flora consists of a limited number of periphytic/benthic taxa, *Achnanthes minutissima* and *Achnanthes petersenii* being the dominant diatoms. These two species are found in abundance in modern alkaline lakes and ponds on Ellesmere Island (Hamilton et al., 1994b). *Achnanthes minutissima* is a widespread taxon and is tolerant of a wide range of pH levels, as it thrives in waters of pH 6.5 to 9.0 (Patrick and Reimer, 1966). It also has a preference for well aerated waters and epiphytic habitats, and is considered an aerophilic/bryophytic species (Björck et al., 1993). Thus it is regarded as one of the best indicators of oxygen-rich conditions (Florin, 1970; Gasse, 1986). The autecology of *A. petersenii* is not as well known. Krammer and Lange-Bertalot (1991b) report it as being most abundant in oligotrophic, circumneutral waters. *Synedra delicatissima* and *Synedra radians* were the only two planktonic diatoms found in the Ojibway samples. These two species are a common component of the plankton of many fresh waters (Patrick and Reimer, 1966; Gasse, 1986). *Synedra radians* is often found in slightly alkaline waters with relatively high conductance (Patrick and Reimer, 1966). Both taxa have an optimum pH preference that falls between 7.4 and 7.8 (Gasse, 1986).

It is not surprising that relatively few diatom taxa, cysts, and spicules were found in the Ojibway sediments. The low number may result from several factors, which create the poor growing conditions that likely existed in the cold paleowaters of Glacial Lake Ojibway. The first factor, turbidity, was likely the most important limiting, since the amount of light is restricted in turbid waters (Patrick, 1977; Vannote et al., 1980), resulting in limited algal growth and subsistence. The meltwaters of the Laurentide Ice Sheet provided large amounts of suspended clay to this immense glacial lake, as shown by the thick deposits of Ojibway clay. A clay thickness of 20 m or more is common in Lake Abitibi area, as determined from boreholes drilled for mineral exploration purposes by the Ontario Geological Survey (1989). Light penetration must have been considerably attenuated in

Glacial Lake Ojibway, resulting in poor diatom growth. Björck and Keister (1983) have advanced this factor to explain the low diatom concentration in varved clays of Glacial Lake Agassiz. Rawlence (1988) also suggested a similar reason for the lack of diatom valves in a basal clay layer of Splan Lake, New Brunswick. A second factor, high rates of sedimentation, associated with profuse suspended clay would certainly have hampered diatom productivity in Glacial Lake Ojibway. High sedimentation rates produce an adverse biotic environment, with sediments characterized by scarcity of diatoms (Björck and Keister, 1983). Another factor is the lack of essential nutrients, especially nitrogen and phosphorus. Low nutrient levels dramatically reduce the growth rate of diatoms and lower species diversity (Reynolds, 1984). Alpine streams and glacier lakes typically have oligotrophic, nutrient-depleted waters (Patrick and Reimer, 1966). In Glacial Lake Ojibway, relatively poor nutrient conditions during and after glacial retreat would have hampered algal productivity, a scenario currently observed in ice-covered Lake Hazen, Ellesmere Island. Icebergs and ice rafts should also be taken into consideration. They were abundant on Glacial Lake Ojibway: over 8300 scars were mapped in the northern part of the Abitibi region (Veillette et al., 1992a). Ice scars, gauges, and furrows of up to 4 m deep, 100 m large, and 10 km long have been measured. The numerous icebergs and ice rafts more than likely inhibited growth of planktonic diatoms by restricting light penetration. Smol (1990) states that on present-day arctic lakes, the proportion of ice cover determines the area of a lake that can be colonized by photosynthetic organisms, thus when the deep parts of lakes are ice covered, only shallow water, littoral diatoms are able to flourish. He mentions that when the ice cover recedes, most of the lake becomes colonized by diatoms, allowing deeper water floras to develop. As Smol (1990) points out, this could explain the abundance of shallow water taxa in late-glacial and early postglacial sediments of many lakes. Numerous studies of lakes have revealed such a diatom flora in basal core sediments, characterized by a lack of planktonic and an abundance of littoral taxa (Brugam, 1980; Smol, 1983; Wolfe and Butler, 1994). The planktonic diatom communities could not develop appropriately because of a reduced growing season, and they became competitive only when the lake ice cover was less extensive (Smol, 1990). By introducing icebergs as elements limiting light penetration, the same argument may be used to explain in part the poor plankton component of Glacial Lake Ojibway. Also, intense ice rafting and scouring are a good indication of strong winds. Statistical analyses performed on iceberg scars of the Abitibi area indicate that paleowinds with a strong southeast gradient (110°) prevailed on Glacial Lake Ojibway (Veillette et al., 1992a). Such winds would certainly have provoked high turbidities, clay resuspension, and disruption of benthic microhabitats.

Although Glacial Lake Ojibway was undoubtedly deep enough to have supported planktonic diatom communities, all the limiting factors mentioned are sufficient to have inhibited diatom growth. The result is a glaciolacustrine sediment with a poor planktonic component compared to littoral/benthic diatoms (these latter taxa also being relatively poor). Amongst benthic diatoms, we expected to find small species of the *Fragilaria* cluster (sensu Hustedt, 1930), such as



**Table 3.** Comparative summary of information from fossil (Glacial Lake Ojibway) and modern (Lake Abitibi) samples.

Environment	Cysts	Sponge spicules	Diatom abundance	Diatom diversity	Planktonic species
Glacial Lake Ojibway	scarce	absent	low	low	<i>Synedra delicatissima</i> <i>Synedra radians</i>
Lake Abitibi	abundant	abundant	high	high	<i>Asterionella formosa</i> <i>Fragilaria crotonensis</i> <i>Aulacoseira</i> spp. <i>Cyclotella</i> spp. <i>Stephanodiscus</i> spp.

*Staurosirella pinnata* and *Staurosira construens*, but the Ojibway clay samples lacked these taxa (although few samples have been analyzed). These are pioneering diatoms usually found in late-glacial and early postglacial material (Smol, 1983) and they frequently dominate floristic assemblages of early Holocene core sediments (e.g. Florin, 1970; Brugam, 1980; Rawlence, 1992; Wolfe and Butler, 1994). They are also a major component of modern-day diatom communities in high-latitude Arctic lakes (Koivo and Ritchie, 1978; Smol, 1983; Hamilton et al., 1994b), and even in moraine lakes of the Yukon (Bradbury and Whiteside, 1980). Foged (1981) and Rawlence (1988) suggest that *Fragilaria* communities require alkaliphilous conditions. They often colonize newly deglaciated lakes, since their sediments release significant amounts of base cations (Smol, 1983). Since alkaline sediments seem to trigger the development of these pioneering diatoms, they should be found in Glacial Lake Ojibway clays (moderate carbonate content; Fig. 2). However, cold paleowaters may have provided conditions unsuitable for growth of such communities (deep water, reduced light penetration, turbidity, high rate of sedimentation, and lack of nutrients). Further investigations may reveal the presence of these diatoms higher in the Lake Abitibi cores, perhaps within the sedimentary sequence of ancestral Lake Abitibi. These small *Fragilaria* are found in surface samples of present-day Lake Abitibi, but they are not numerous.

It is interesting to note that Björck and Keister (1983) have recorded a subaerial diatom component from sediments of Glacial Lake Agassiz. In one stratigraphic unit, they found a significant number of *Hantzschia amphioxys*, a well accepted terrestrial/subaerial taxon universally present on soils (Round et al., 1990). Its presence combined with that of planktonic species lead Björck and Keister (1983) to interpret the glacial lake environment as typified by deep waters surrounded by unstable soils easily eroded by wave action. No typical terrestrial diatoms have yet been found in Glacial Lake Ojibway sediments, although only a limited number of samples have been analyzed. However, some taxa encountered are regarded as ecologically tolerant to subaerial conditions (e.g. *Nitzschia amphibia*, *Achnanthes minutissima*, and *Eunotia praerupta*). *Nitzschia amphibia* was reported to be very common on damp soil habitats from Caylor Prairie, Iowa (Reimer, 1970). Even if its preferred growth area is the littoral zones of lakes, *N. amphibia* can occur in great numbers on slightly moist walls, in stagnant waters, and on mosses and other plants

(Florin, 1970). Other species found in the Ojibway sediments, such as *Achnanthes minutissima* and *Eunotia praerupta*, are also known as atmophytic diatoms and are frequently observed on wet rocks and mosses, as well as in mud from small moist depressions (Bock, 1970; Florin, 1970; Gasse, 1986; Björck et al., 1993). The ecological tolerance of *E. praerupta* makes it a typical nordic-alpine taxon (Patrick and Reimer, 1966).

Contrary to Glacial Lake Ojibway samples, Lake Abitibi surface sediments show an abundant and diverse diatom flora. The planktonic population is well represented, comprising *Asterionella formosa*, *Fragilaria crotonensis*, and species of *Aulacoseira*, *Cyclotella*, and *Stephanodiscus*. Periphytic communities are also well developed. Of note is the presence of *Melosira undulata* and its variety *normannii*. This taxon is restricted to surface sample ABI-15, in which it is common. It is worth noting that *M. undulata* has not often been recorded in the literature. Germain (1981) found it in France from lake samples collected in 1931, but noted its absence from the same lake's modern flora (i.e. 1981), making it a recently extinct diatom. McLaughlin and Stone (1986) analyzed two Late Pleistocene lake deposits along the shores of Cook Inlet (Alaska) and noted that *M. undulata* was occasional to common at one site. Other rare diatoms are found in sample ABI-15, namely *Gomphonema grovei*, *Cymbella hilliardii*, *Encyonema triangulum*, and *Pinnularia rostellata*. Amongst these taxa, *P. rostellata* and *G. grovei* are considered fossil diatoms (Krammer and Lange-Bertalot, 1986; Kociolek et al., 1988). Surface sample ABI-15 consists of a sand layer directly overlying Glacial Lake Ojibway varved clay. This sand layer might be a key sample for the interpretation of future stratigraphic diatom analyses. It appears to represent an in situ sedimentary unit of fossil diatoms, rather than a reworked deposit. Further investigations will address this issue.

## CONCLUSIONS

From the analysis of sedimentary diatoms and other siliceous microfossils, it appears that it is possible to distinguish Glacial Lake Ojibway sediments from those of ancestral and modern Lake Abitibi. In light of the results and discussion, diatom populations of fossil and modern sediments are obviously

quite different (Table 3). In Glacial Lake Ojibway sediments, sponge spicules are virtually absent, cysts are rather rare, and diatom abundance and diversity are low. In Lake Abitibi surface samples, sponge spicules and cysts are prominent features, and diatom communities (periphytic and planktonic) are well developed. Planktonic species may be a key component in the interpretation of past diatom assemblages. Planktonic diatoms found in Glacial Lake Ojibway sediments seem to be limited to only two species, *Synedra radians* and *Synedra delicatissima*. The plankton of Lake Abitibi is much more developed, being abundant and diverse (*Asterionella formosa*, *Fragilaria crotonensis*, and species of *Aulacoseira*, *Cyclotella*, and *Stephanodiscus*).

Additional modern samples will be collected and analyzed to better understand Lake Abitibi's diatom flora (surficial sediments, aquatic macrophytes, scrapings from submerged rocks and wood detrital material, plankton tows). Also, subsequent Ojibway sediments will be analyzed for diatoms. During the Abitibi-Témiscamingue surficial geology mapping programs, more than 600 Ojibway clay samples were collected, primarily for carbonate content and grain-size analysis (Veillette et al., 1992b). More of these samples must be examined to enhance our knowledge of the diatom flora once supported by Glacial Lake Ojibway. Although the study is still at its investigative stage, preliminary results are promising and indicate that diatom analyses can successfully be applied to characterize the sedimentary transition from Glacial Lake Ojibway to Lake Abitibi.

## ACKNOWLEDGMENTS

The thoughtful comments and suggestions of Sheridan Hipwell and Roger McNeely greatly improved earlier drafts of this manuscript. Jean-Marc Moisan and Alexandre French provided invaluable assistance in the field (lake bottom sampling). Roger Paulen's contribution to the description of cores in the laboratory is greatly appreciated. The personnel of the Ontario Ministry of Natural Resources, Cochrane Division, is acknowledged for providing us with a bathymetry map of Lake Abitibi. Alain Cloutier prepared the two figures. Part of this manuscript was written under the funding of GSC Project 920049-HJ.

## REFERENCES

- Battarbee, R.W.**  
1986: Diatom analysis; in *Handbook of Holocene Palaeoecology and Palaeohydrology*, (ed.) B.E. Berglund; John Wiley & Sons, Toronto, p. 527-570.
- Björck, S. and Keister, C.M.**  
1983: The Emerson Phase of Lake Agassiz, independently registered in northwestern Minnesota and northwestern Ontario; *Canadian Journal of Earth Sciences*, v. 20, p. 1536-1542.
- Björck, S., Håkansson, H., Olsson, S., Barnekow, L., and Janssens, J.**  
1993: Palaeoclimatic studies in South Shetland Islands, Antarctica, based on numerous stratigraphic variables in lake sediments; *Journal of Paleolimnology*, v. 8, p. 233-272.
- Bock, W.**  
1970: Felsen und Mauern als Diatomeenstandorte; *Nova Hedwigia*, v. 31, p. 395-441.
- Bradbury, J.P. and Whiteside, M.C.**  
1980: Paleolimnology of two lakes in the Kutlan Glacier region, Yukon Territory, Canada; *Quaternary Research*, v. 14, p. 149-168.
- Brugam, R.B.**  
1980: Postglacial diatom stratigraphy of Kirchner Marsh, Minnesota; *Quaternary Research*, v. 13, p. 133-146.
- Florin, M.-B.**  
1970: Late-glacial diatoms of Kirchner Marsh, S.E. Minnesota; *Nova Hedwigia*, v. 31, p. 667-756.
- Florin, M.-B. and Wright, H.E.**  
1969: Diatom evidence for the persistence of stagnant glacial ice in Minnesota; *Geological Society of America Bulletin*, v. 80, p. 695-704.
- Foged, N.**  
1981: Diatoms in Alaska; *Bibliotheca Phycologica*, v. 53, 317 p.
- Gasse, F.**  
1986: East African diatoms. Taxonomy, ecological distribution; *Bibliotheca Diatomologica*, v. 11, 292 p.
- Germain, H.**  
1981: Flore des diatomées, eaux douces et saumâtres du Massif Armoricaïn et des contrées voisines d'Europe occidentale; *Société des Nouvelles Éditions Boubée*, Paris, 444 p.
- Hamilton, P.B., Douglas, M.S.V., Fritz, S.C., Pienitz, R., Smol, J.P., and Wolfe, A.P.**  
1994a: A compiled freshwater diatom taxa list for the Arctic and Subarctic regions of North America; in *Proceedings of the Fourth Arctic-Antarctic Diatom Symposium*, Canadian Museum of Nature, Ottawa, (ed.) P.B. Hamilton; *Canadian Technical Report of Fisheries and Aquatic Sciences*, v. 1957, p. 85-102.
- Hamilton, P.B., Poulin, M., Prévost, C., Angell, M., and Edlund, S.A.**  
1994b: *Americanarum Diatomarum Exsiccata*: fascicle II (CAN), voucher slides representing 34 lakes, ponds and streams from Ellesmere Island, Canadian High Arctic, North America; *Diatom Research*, v. 9, in press.
- Hardy, L.**  
1976: Contribution à l'étude géomorphologique de la portion québécoise des basses terres de la Baie de James; PhD. thesis, McGill University, Montreal, 264 p.
- Hartley, B.**  
1986: A check-list of the freshwater, brackish and marine diatoms of the British Isles and adjoining coastal waters; *Journal of the Marine Biology Association of United Kingdom*, v. 66, p. 531-610.
- Hustedt, F.**  
1930: Bacillariophyta (Diatomeae); in *Die Süsswasser-Flora Mitteleuropas*, (ed.) A. Pascher; v. 10, p. 1-466.
- Kociolek, J.P., Jing-Rong, Y. [sic], and Stoermer, E.F.**  
1988: Taxonomy, ultrastructure and systematic position of the *Gomphonema grovei* M. Schm. - species complex (Bacillariophyceae); *Nova Hedwigia*, v. 47, p. 145-158.
- Koivo, L.K. and Ritchie, J.C.**  
1978: Modern diatom assemblages from lake sediments in the boreal-arctic transition region near the Mackenzie Delta, N.W.T., Canada; *Canadian Journal of Botany*, v. 56, p. 1010-1020.
- Krammer, K. and Lange-Bertalot, H.**  
1986: Bacillariophyceae. 1. Teil: Naviculaceae; in *Süsswasserflora von Mitteleuropa*, (ed.) H. Ettl, J. Gerloff, H. Heynig, and D. Mollenhauer; Gustav Fischer Verlag, Stuttgart, Band 2/1, 876 p.
- 1988: Bacillariophyceae. 2. Teil: Bacillariaceae, Epithemiaceae, Surirellaceae; in *Süsswasserflora von Mitteleuropa*, (ed.) H. Ettl, J. Gerloff, H. Heynig, and D. Mollenhauer; Gustav Fischer Verlag, Stuttgart, Band 2/2, 596 p.
- 1991a: Bacillariophyceae. 3. Teil: Centrales, Fragilariaceae, Eunotiaceae; in *Süsswasserflora von Mitteleuropa*, (ed.) H. Ettl, J. Gerloff, H. Heynig, and D. Mollenhauer; Gustav Fischer Verlag, Stuttgart, Band 2/3, 576 p.
- 1991b: Bacillariophyceae. 4. Teil: Achnantheaceae; in *Süsswasserflora von Mitteleuropa*, (ed.) H. Ettl, J. Gerloff, H. Heynig, and D. Mollenhauer; Gustav Fischer Verlag, Stuttgart, Band 2/4, 576 p.
- McLaughlin, R.B. and Stone, J.L.**  
1986: Some Late Pleistocene diatoms of the Kenai Peninsula, Alaska; *Nova Hedwigia*, v. 82, 149 p.
- Ontario Geological Survey**  
1989: Sonic drillholes 88-17, 88-18, and 88-19, Abitibi 1 and Abitibi 2 Townships, District of Cochrane; OGS Map 81-152.

- Patrick, R.**  
1977: Ecology of freshwater diatoms and diatom communities; *in* The biology of diatoms, (ed.) D. Werner; University of California Press, Los Angeles, p. 284-332.
- Patrick, R. and Reimer, C.W.**  
1966: The diatoms of the United States, exclusive of Alaska and Hawaii. Volume I: Fragilariaceae, Eunotiaceae, Achnantheaceae, Naviculaceae; Academy of Natural Sciences of Philadelphia Monographs, No. 13, 688 p.  
1975: The diatoms of the United States, exclusive of Alaska and Hawaii. Volume II, Part 1: Entomoneidaceae, Cymbellaceae, Gomphonemaceae, Epithemiaceae; Academy of Natural Sciences of Philadelphia Monographs, No. 13, 213 p.
- Prévost, C.L.**  
1992: Identification of diatoms in eight samples of Ojibway clay and Cochrane till from Abitibi, Québec; Diatom report, Geological Survey of Canada, Ottawa, 5 p.
- Rawlence, D.J.**  
1988: The post-glacial diatom history of Splan Lake, New Brunswick; *Journal of Paleolimnology*, v. 1, p. 51-60.  
1992: Paleophycology of Long Lake, Saint-John County, New Brunswick, Canada, based on diatom distribution in sediments; *Canadian Journal of Botany*, v. 70, p. 229-239.
- Reimer, C.**  
1970: Some diatoms (Bacillariophyceae) from Cayler Prairie; *Nova Hedwigia*, v. 31, p. 235-249.
- Reynolds, C.S.**  
1984: The ecology of the freshwater phytoplankton; Cambridge University Press, Cambridge, 384 p.
- Ritchie, J.C. and Koivo, L.K.**  
1975: Postglacial diatom stratigraphy in relation to the recession of Glacial Lake Agassiz; *Quaternary Research*, v. 5, p. 529-540.
- Round, F.E., Crawford, R.M., and Mann, D.G.**  
1990: The diatoms. Biology and morphology of the genera; Cambridge University Press, New York, 747 p.
- Smol, J.P.**  
1983: Paleophycology of a high arctic lake near Cape Herschel, Ellesmere Island; *Canadian Journal of Botany*, v. 61, p. 2195-2204.
- Smol, J.P. (cont.)**  
1990: Freshwater algae; *in* *Methods in Quaternary Ecology*, (ed.) B.G. Warner; Geoscience Canada Reprint Series, No. 5, p. 3-14.
- Van Landingham, S.L.**  
1967- Catalogue of the fossil and recent genera and species of diatoms and their synonyms, Parts 1 to 8; J. Cramer, Vaduz.  
1979: **Vannote, R.L., Minshall, G.W., Cummins, K.W., Sedell, J.R., and Cushing, C.E.**  
1980: The river continuum concept; *Canadian Journal of Fisheries and Aquatic Sciences*, v. 37, p. 130-137.
- Veillette, J.J.**  
1989: Ice movements, till sheets and glacial transport in Abitibi-Témiscamingue, Québec and Ontario; *in* *Drift Prospecting*, (ed.) R.N.W. Dilabio and W.B. Coker; Geological Survey of Canada, Paper 89-20, p. 139-154.
- Veillette, J.J., Paradis, S.J., Thibaudeau, P., and Pomarès, J.-S.**  
1991: Distribution of distinctive Hudson Bay erratics and the problem of the Cochrane limit in Abitibi, Québec; *in* *Current Research, Part C*; Geological Survey of Canada, Paper 91-1C, p. 135-142.
- Veillette, J.J., Paradis, S.J., Thibaudeau, P., Pilon, J.A., and de Bellefeuille, C.**  
1992a: Les sillons d'icebergs du nord de l'Abitibi; Association québécoise pour l'étude du Quaternaire (AQQUA), VIIe Congrès quadriennal, 1992; Recueil des résumés de communications, *Bulletin de l'Association québécoise pour l'étude du Quaternaire*, vol. 18, p. 77.  
1992b: La géomorphologie et la géologie du Quaternaire de l'Abitibi-Témiscamingue; Association québécoise pour l'étude du Quaternaire (AQQUA), VIIe Congrès quadriennal, Rouyn-Noranda, Québec, livret-guide des excursions, 252 p.
- Wolfe, A.P. and Butler, D.L.**  
1994: Late-glacial and early Holocene environments at Pine Hill Pond, Newfoundland, Canada: evidence from pollen and diatoms; *Boreas*, v. 23, p. 53-65.

---

Geological Survey of Canada Project 860020

# The spectacular cross-striated outcrops of James Bay, Quebec

J.J. Veillette and M. Roy  
Terrain Sciences Division

*Veillette, J.J. and Roy, M., 1995: The spectacular cross-striated outcrops of James Bay, Quebec; in Current Research 1995-C; Geological Survey of Canada, p. 243-248.*

---

**Abstract:** Bedrock on the east coast and on some James Bay islands shows spectacular examples of cross-striations that reveal a shift from initial northwestward ice flow, followed by westward, southwestward, and local southeastward and southwestward flows related to the opening of James Bay during deglaciation of the region. The high quality of striated outcrops is attributed to their freshness, which results from a combination of postglacial uplift, the protective effect of glacial deposits, and recent erosion of these deposits by wave action. Photographs and schematic illustrations are used to explain the processes at work in this particular marine environment.

**Résumé :** Le substratum de la côte est et de certaines îles de la baie James montre des exemples spectaculaires de stries transversales révélant un changement de direction dans l'écoulement glaciaire initial vers le nord-ouest, suivi d'écoulements vers l'ouest et le sud-ouest, puis d'écoulements locaux vers le sud-est et le sud-ouest reliés à l'ouverture de la baie James au cours de la déglaciation de la région. La grande qualité des affleurements striés est attribué au fait qu'ils ne sont pas altérés et ce, en raison d'une combinaison de facteurs comme le soulèvement postglaciaire, l'effet protecteur des dépôts glaciaires et la récente érosion de ces dépôts par l'action des vagues. Des photographies et des illustrations schématiques sont utilisées pour expliquer les processus en action dans cet environnement marin particulier.

## INTRODUCTION

The James Bay coast and islands were visited during summer 1994 to look for bedrock-inscribed ice flow evidence related to the presence of an old northwestward ice flow associated with the expansion of the Laurentide Ice Sheet (see Veillette, 1995). Spectacular, multifaceted, cross-striated outcrops were found to be widespread along the east coast of James Bay and in the rocky islands in the northern part of the bay. This report describes particular site-specific conditions which, through a combination of bedrock lithology, isostatic uplift, and wave erosion, have produced unique conditions for the study of palimpsest features formed by ice flows of different ages and directions.

The bedrock of James Bay occupies parts of three geological provinces, and lithology largely controls the quality of striated outcrops (Fig. 1). A narrow band along the east coast, extending 25 to 100 km offshore, consists predominantly of Archean gneiss and migmatites, massive and foliated granitoids and gneisses of the Superior Province with rare basalt occurrences (Avramtchev, 1983). It contains most of the cross-striated sites examined. The west coast and central part of the bay are underlain by Hudson Bay Platform carbonates, and outcrops are rare and of poor quality for striations. Most large islands in James Bay are underlain by carbonates and are composed predominantly of unconsolidated deposits. A narrow, pie-shaped, southern extension of Proterozoic sedimentary rocks of the Churchill Province from southeastern Hudson Bay penetrates into the eastern half of James Bay and includes most of the remote islands where striations were measured.

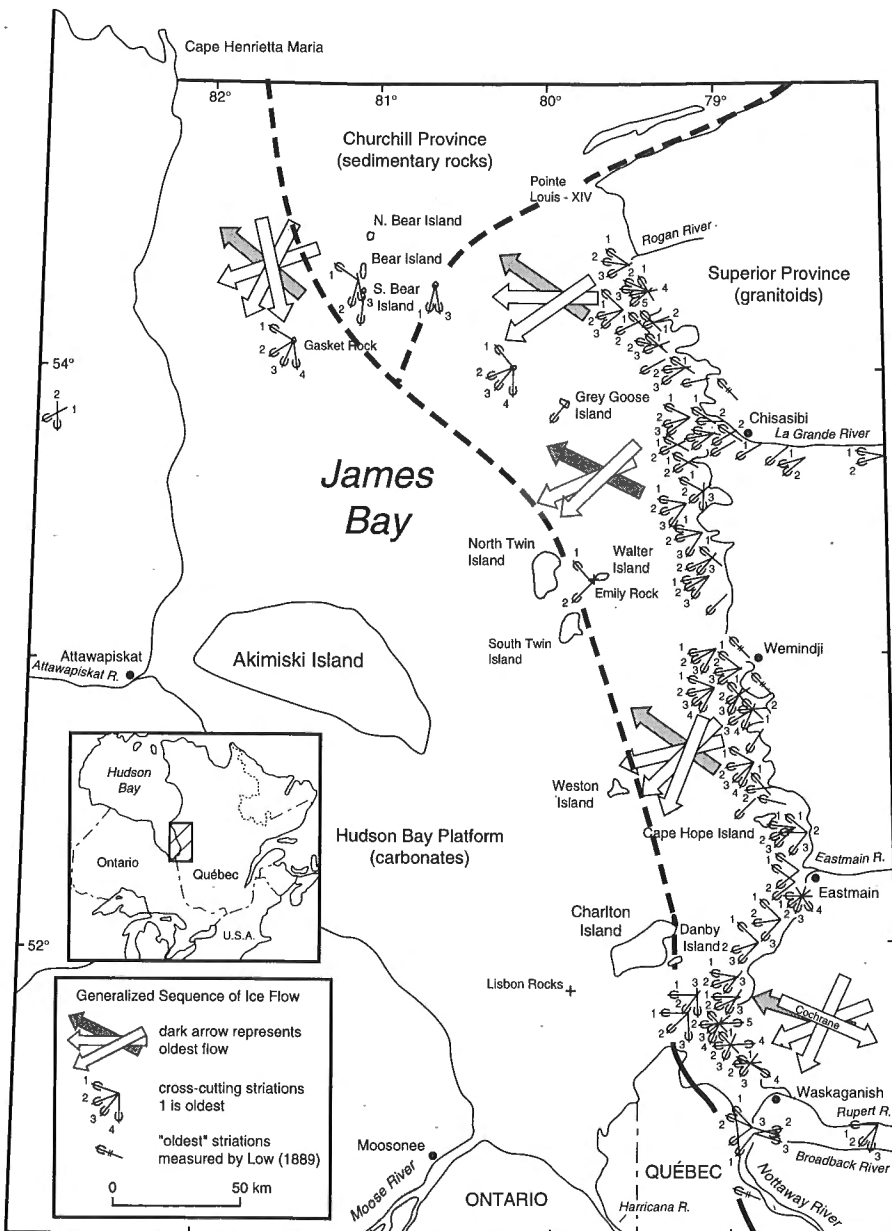


**Figure 1.**  
Location of study area, geological provinces, and map of striations in James Bay (adapted from Veillette, 1995). Geology from Avramtchev (1983) and Energy Mines, and Resources Canada (1987).

## ISLANDS ARE BEST

The eastern coast is dotted with numerous rock islands with little or no vegetation, especially between Pointe Louis-XIV and Eastmain (Fig 1). Small (a few hundred square metres to a few hectares) islands less than 10 m above sea level were found to be the most favourable areas to study bedrock-inscribed features left by the passage of multiple ice flows (Fig. 2A). Their small size allows for rapid and detailed inspection on foot of their periphery, near the waterline. This is of particular importance since many old northwestward striations found in this survey are located in the intertidal zone or slightly above the high water mark. In an area of multiple ice flows of different ages and directions, such as here, all facets of these islands, which in themselves constitute large isolated outcrops, can be fully and rapidly examined and described. Because of their low elevation above sea level, they show large expanses of bare unweathered bedrock (Fig. 2B). From the distribution of floated debris (mostly driftwood) and the maximum level of the wave-washed zone

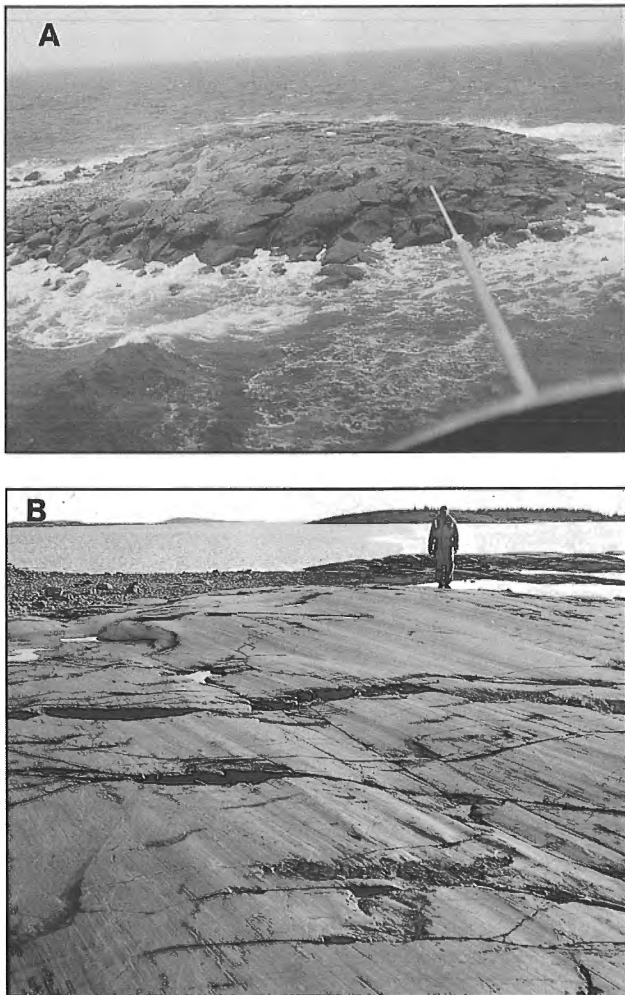


**Figure 2.** A) Small bare wave-washed bedrock (gneiss) island (GSC 1994-752A); and B) large unweathered striated surfaces, typical of many islands visited on the east coast of James Bay. (GSC 1994-752G)

that in places is exposed to vast expanses of water, the storm beach level was found to reach up to 7-10 m above the high water mark. A broad wave-washed zone, coupled with a rapidly emerging coastline (about 1 m/100 yr, Hillaire-Marcel, 1976) that continuously brings "fresh" rock to the surface of the sea, creates an environment highly favourable for the preservation of striated surfaces. Large concentrations of locally derived boulders visible at low tide (tidal range 1.5-2.0 m) and aligned on the down-ice (last ice flow) side of many bedrock islands, testify to the erosive action of waves on what used to be crag and tail and drumlinoid landforms composed of boulders and sandy till.

## SELECTED EXAMPLES

Figures 3A and B show examples of old northwestward striations commonly encountered during the survey. Sketches are used because of the difficulty of adequately photographing such features. Foliated granitoids and gneisses of the eastern James Bay coast are conducive to the development of extensive quarrying faces on the lee sides of outcrops associated

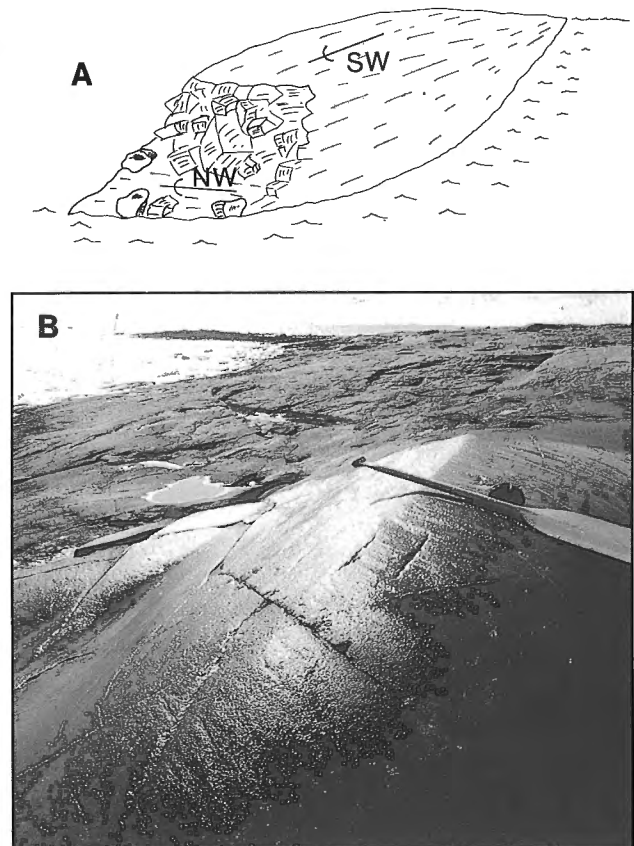


**Figure 3.** A) Sketch of a common type of sheltered site on islands where old northwestward striations were preserved below the plucked face, near the water line, and down ice from westward and southwestward flows; B) Photograph of sheltered striated surfaces indicating northwestward ( $305^\circ$ ) flow, found on the lee side of a striated surface oriented  $250^\circ$  (paddle). (GSC 1994-752B)

with the last dominant ice movement. The upper walls of sheltered striated faces have often been destroyed by the plucking action of the last flow (or flows). Because of this, but also because of the greater freshness of old striations exposed near sealevel, the base of the lee side of ice-moulded outcrops was found to be the most favourable place to search for old striated surfaces.

The most striking type of bedrock-inscribed ice-flow indicators found down ice from bedrock hills are whole patches of striated roches moutonnées indicating northwestward movement whose upper surfaces are devoid of erosive marks from subsequent ice flows to the west and southwest (Fig. 4). This excellent preservation implies that the roches moutonnées were covered by unconsolidated deposits laid down by the ice flow that shaped them. The deposits were then eroded by wave action in the last few hundred years as they emerged through isostatic uplift.

Striations on glacially polished, light coloured, and dry granitoids can be extremely difficult to see without proper light and moisture conditions. A low sun angle that enhances shadows of small linear depressions brings out fine striations, grooves, and truncations on a slightly wet surface (excessive water causes a bright glare) that would not be visible otherwise (Fig. 5A). Striations on mafic intrusives, such as those in the Wemindji area, are easy to see on wet surfaces (Fig. 5B).

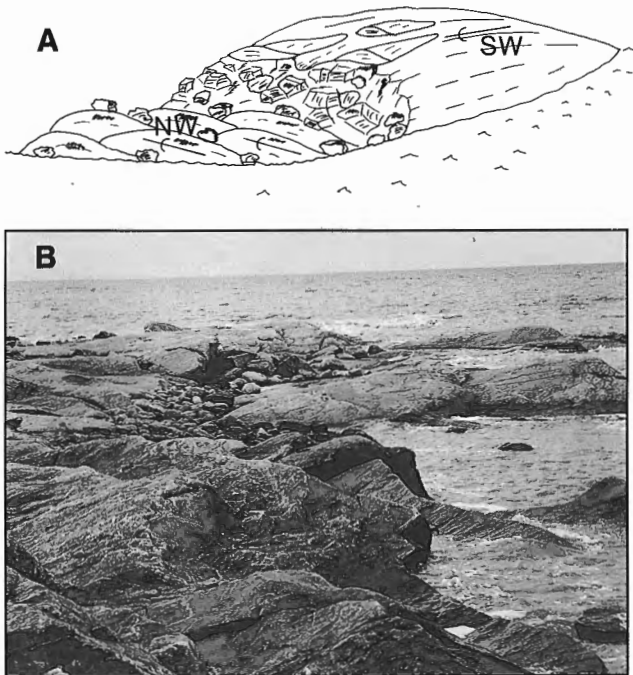


**Figure 4.** A) Sketch of a bedrock island illustrating the exceptional preservation of large surfaces of roches moutonnées that indicate northwestward ice flow, preserved below the plucked face, near the water line, and down ice from bedrock shaped by southwestward flows; B) Photograph of roches moutonnées indicating movement toward 300°(left to right) preserved on lee side of island moulded and striated toward 250°. (GSC 1994-752R)

## THE VANISHED PROTECTOR

Site-specific conditions favourable to the preservation of striations largely compensate for the widespread presence of granitoids along the east coast of James Bay. The term "vanished protector" is used here to refer to a protective deposit (such as till) or a bedrock knob that has prevented the destruction of a striated surface by subsequent ice flow or flows, and that has been later removed by natural or artificial means. Outcrops on James Bay islands show excellent examples of vanished protectors. The protector was usually till that was removed by wave action. Figure 6 (A-F) illustrates the

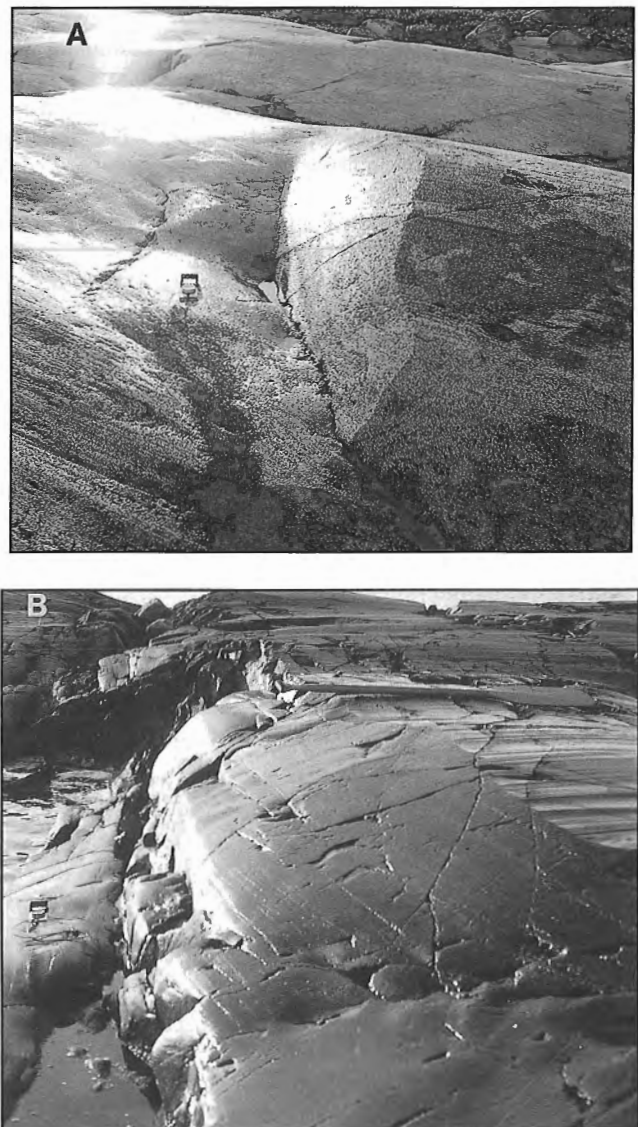
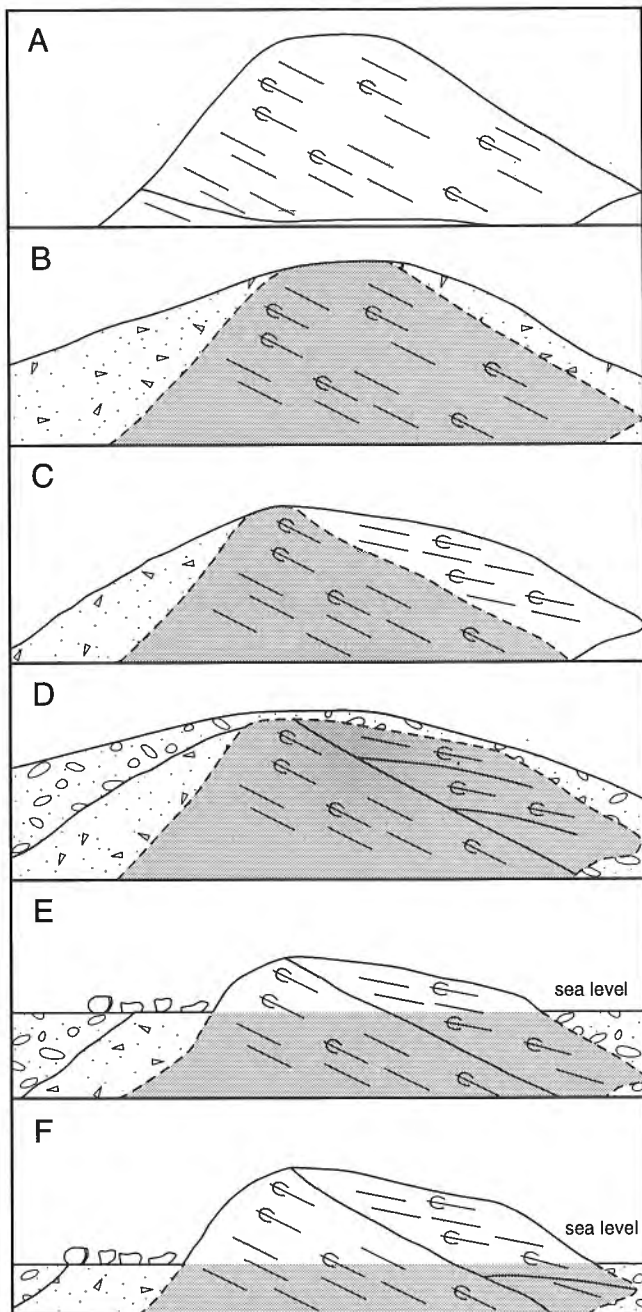


**Figure 5.** Striated surfaces showing the effect of lithology, light, and moisture conditions: A) granitoids, striations toward 310° (compass) crosscut by striations toward 240° (right to left) (GSC 1994-752J); B) mafic intrusives of Wemindji area, northwestward striations (compass) preserved on lee side of outcrop shaped by southwestward flow (right to left). (GSC 1994-752S)

process taking place in this particular marine environment where postglacial uplift, the masking effect of till, and the erosive action of waves combine to produce an uninterrupted source of fresh striated surfaces at the surface of the sea.

This explains why at several locations, the low islands of James Bay show fresh, striated surfaces, some associated with growth of the last ice sheet and others with late deglaciation of the area. Where the elevation exceeds about 10 m, the youngest striations on higher parts of islands are usually more weathered and less distinct than older striations found near sea level. Several sites visited during the course of this survey illustrate the preservation potential of large patches of till



located on the down-ice side (last ice flow) of bedrock knobs; the best examples include large areas of roches moutonnées (see Fig. 4).

## DISCUSSION

The numerous examples seen in recent years in James Bay and northwestern Quebec and involving different aspects of the vanished protector suggest answers to questions often raised about the sharp contacts between striated surfaces of various ages and directions observed on many outcrops (G. Boulton, pers. comm., 1987; T. Brennand, pers. comm., 1993; D. R. Grant, pers. comm., 1994). Why do many outcrops show sharp contacts between striated surfaces when a gradual, continuous shift in a given direction is involved? In fact, this is not always the case and, as seen on the James Bay outcrops (Fig. 1), several sets of striations are present on outcrops at some locations, indicating a gradual shift from an initial northwestward flow to a last south-southwestward flow. Often, however, striations indicating a gradual shift are lacking. The most likely causes are (1) prolonged ice flow capable of eroding a new surface and erasing previous ones, or (2) the presence of the vanished protector. In the general area southeast of James Bay, several large crag and tail in till have been excavated for logging road material and the bedrock exposed at the base of the excavation (for general location see Veillette, 1995, Fig. 2). In places, exposed bedrock only shows striations associated with an earlier northwestward flow and none associated with the last southwestward flow that formed the crag and tail. In other places, striated surfaces from both flows are present on the same outcrop while elsewhere, only the last movement is represented. This indicates that till associated with the early northwestward flow was not always entirely removed by the last southwestward flow and protected the old striated surfaces from this last flow. This hiatus in the erosional record produces sharp contacts between striated surfaces, in spite of a gradual change in the direction of ice flow. These anomalies can usually be explained by differences in bedrock topography on the pit floor.

**Figure 6.** Schematic reconstruction illustrating the evolution of a hypothetical roche moutonnée on a bedrock island in James Bay; the roche moutonnée was first moulded and striated by a northwestward flow (A) and left covered with till (B). It was then eroded, mainly in its upper part, and remoulded by a second, southwestward flow (C). In the process, till associated with the early northwestward flow was eroded and the old northwestward striations were erased from the new up-ice face, but not from the sheltered side of the outcrop (C). A second till sheet associated with southwestward flow was deposited on the outcrop (D). During deglaciation, the site was flooded first by Lake Ojibway, then by the Tyrrell Sea and present-day James Bay (Hardy, 1976). Isostatic uplift brought the outcrop and its till protector to the surface of the sea in the last few hundred years (E). Wave erosion removed the till and exposed both older and younger striated surfaces at the same time (F).



## **ACKNOWLEDGMENTS**

Staff from Hydro-Québec at LG-1 assisted with radio communication and provided accomodation during preparation for the boat traverse. Several individuals from LG-1, and from the Chisasibi, Wemindji, and Waskaganish Band councils assisted with logistics and navigation along the east coast of James Bay. A.S. Dyke suggested the term vanished protector. J. Aylsworth read the paper and T. Barry drew Figures 1 and 6. Sincere thanks to all.

## **REFERENCES**

### **Avramtchev, L.**

1983: Carte des gîtes minéraux du Québec; Série des cartes minérales, région de la baie James, ministère de l'Énergie et des Ressources, cartes 32 M, 33D, 33E, DPV 940, échelle de 1/250 000.

### **Energy, Mines, and Resources Canada**

1987: Principal mineral areas of Canada; Canadian Department of Energy, Mines, and Resources, Mineral Policy Sector and Geological Survey of Canada, Map 900A, scale 1: 7 603 200.

### **Hardy, L.**

1976: Contribution à l'étude géomorphologique de la portion québécoise des basses terres de la baie de James; Thèse de doctorat, Université McGill, Montréal, 264 p.

### **Hillaire-Marcel, C.**

1976: La déglaciation et le relèvement isostatique sur la côte est de la baie d'Hudson; Cahiers de géographie du Québec, vol. 20, p. 185-200.

### **Low, A.P.**

1889: Report on exploration in James Bay, and country east of Hudson Bay, drained by the Big, Great Whale and Clearwater Rivers. 1887-1888; Geological and Natural History Survey of Canada, Annual Report, v. 3, Part II, Report J, 62 p.

### **Veillette, J.J.**

1995: New evidence for northwestward glacial ice flow, James Bay region, Quebec; in Current Research 1995-C; Geological Survey of Canada, this volume.

---

Geological Survey of Canada Project 860020

# New evidence for northwestward glacial ice flow, James Bay region, Quebec

Jean J. Veillette

Terrain Sciences Division

*Veillette, J.J., 1995: New evidence for northwestward glacial ice flow, James Bay region, Quebec; in Current Research 1995-C; Geological Survey of Canada, p. 249-258.*

---

**Abstract:** At several hundred sites in the James Bay region of west-central Quebec and northeastern Ontario, bedrock-inscribed indicators of generally northwestward ice flow were measured on lee sides of outcrops heavily striated by younger westward and southwestward flows. The consistent position and orientation of old northwestward striations at the base of the ice-flow sequence suggests an association with the inception and expansion of the Laurentide Ice Sheet from an initial growth zone extending northwestward from an area southeast of James Bay. This new model is in agreement with glacial transport data east and west of James Bay and has direct implications for the application of drift sampling to mineral exploration. Stratigraphic evidence and a similar former direction of ice movement in the Severn River area of northern Ontario support an Early Wisconsinan age for this event.

**Résumé :** À plusieurs centaines d'emplacements situés dans la région de la baie James, dans le centre ouest du Québec et le nord-est de l'Ontario, des indicateurs gravés dans le substratum d'un écoulement glaciaire dans une direction générale nord-ouest ont été mesurés sur les faces aval d'affleurements fortement striés par des écoulements plus récents vers l'ouest et le sud-ouest. La position et l'orientation constantes de ces anciennes stries orientées au nord-ouest à la base de la séquence d'écoulement glaciaire suggèrent une association avec la création et l'expansion de l'Inlandsis laurentidien à partir d'une zone de croissance initiale allant d'une région au sud-est de la baie James. Ce nouveau modèle est compatible avec les données de transport glaciaire recueillies tant à l'est qu'à l'ouest de la baie James et il a des répercussions directes sur l'échantillonnage des débris glaciaires aux fins de l'exploration minérale. Des indices stratigraphiques et une direction antérieure similaire de mouvement glaciaire dans la région de la rivière Severn, dans le nord de l'Ontario, concourent à dater cet événement au Wisconsinien inférieur.

**INTRODUCTION**

A systematic investigation of bedrock-inscribed ice-flow features and lithological indicators of long-distance glacial transport in west-central Quebec and northern Ontario has been conducted in recent years. The area (Fig. 1) is at the geographic centre of the area once covered by the Labrador sector of the Laurentide Ice Sheet (Prest, 1984). An early ice-flow pattern was determined from striations preserved on lee sides of outcrops shaped and striated toward the west and the southwest. New data demonstrate the existence of a major early northwestward ice flow extending from the Lake Mistassini area in central Quebec and the Kuujuarapik area in southeast Hudson Bay, and correlate with evidence from

the Big Trout Lake, Winisk, and Nelson River areas of northern Ontario and northern Manitoba (Fig. 1). There, it was first attributed to the Patrician Ice Sheet by Tyrrell (1913, 1914, 1935) and later assigned to an older Wisconsinan flow of the Laurentide Ice Sheet by Prest (1963) and Thorleifson et al. (1992, 1993). This flow is here attributed to northwestward expansion of the Laurentide Ice Sheet across the James Bay basin from an initial growth zone south and southeast of James Bay. This body of information constitutes the first coherent evidence that allows mapping of expansion of the Labrador Sector of the Laurentide Ice Sheet from a 1500 km axis in Quebec. This new information has important implications for ice-sheet modeling and for drift sampling for mineral exploration purposes.

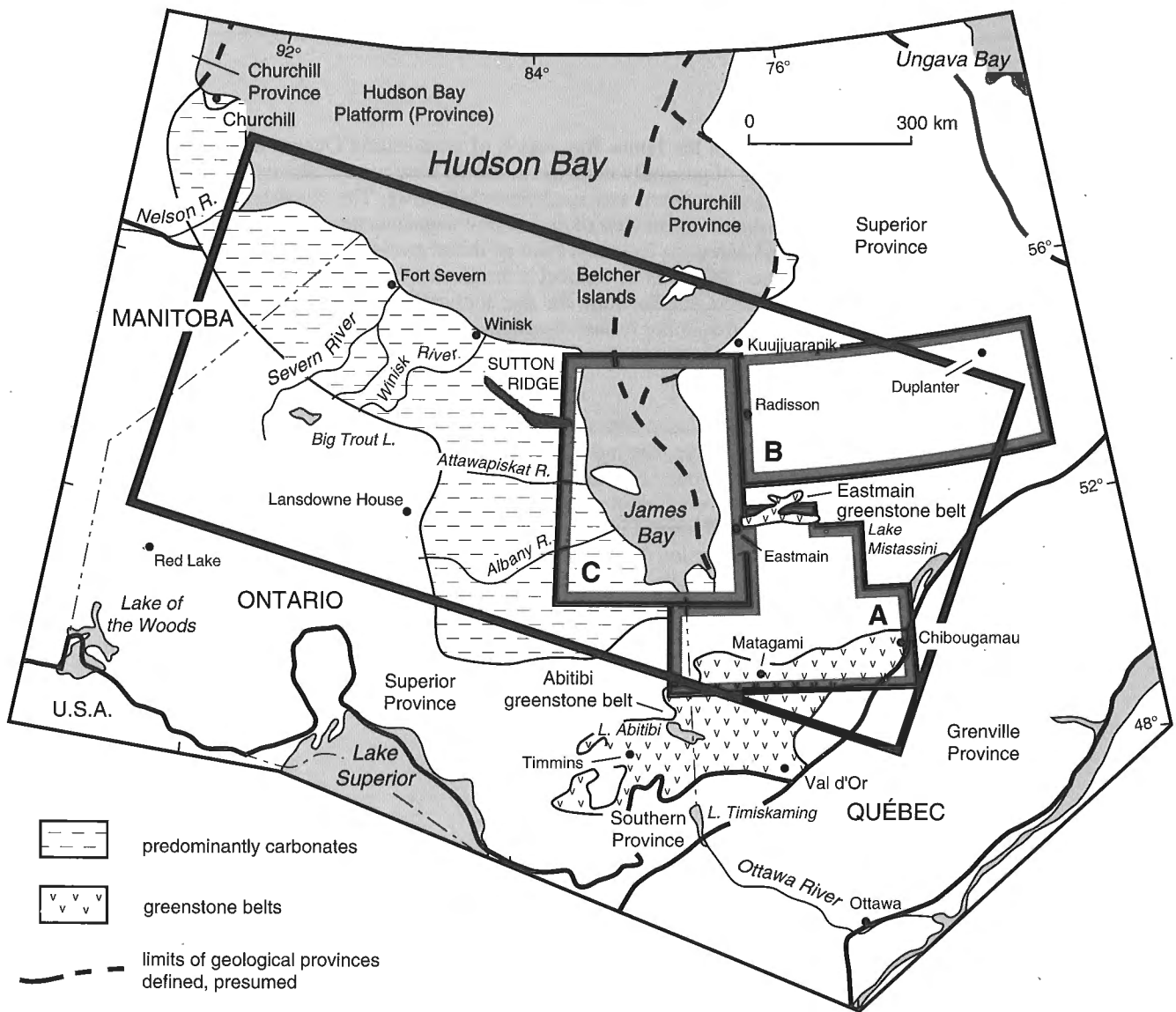


**Figure 1.** Location of study area showing bedrock geology and the location of detailed study areas. Geology adapted from Energy, Mines, and Resources (1987) and ministère de l'Énergie et des Ressources du Québec/Ontario Geological Survey (1983).

## PREVIOUS WORK

Low (1889, 1903) was the first to propose that an "old" ice movement had flowed northwestward across the east coast of James Bay and southern Hudson Bay. He assigned the oldest rank of ice-flow chronology to a few striated surfaces indicating northwestward ice flow ( $300^\circ$ ) crossed by striations assigned to the older rank and indicating west-southwest flow ( $250^\circ$ - $270^\circ$ ). Striations indicating south-southwestward ( $200^\circ$ - $230^\circ$ ) flow were considered to be the third and youngest flow. Low (1903, p. 81) associated northwestward flow with growth of the ice sheet:

"Along the east coast of Hudson Bay, three marked sets of striae are found, and from these it is seen that the earliest ice flow started from a central gathering ground between the 50th and 51st parallels of N. latitude, near the centre of the peninsula. The second set of striae shows that the centre of glaciation had moved in a north-west direction to beyond the 54th parallel, while the latest set shows a continuation of the north-west movement leaving the centre of dispersion between the 55th and 56th parallels..."

Tyrrell (1913, 1914, 1935) did not attempt to correlate Low's old northwestward striations in James Bay to those of the Big Trout Lake area. Only one site showing northwestward striations on the east coast of James Bay is shown on the 1958 glacial map of Canada (Wilson et al., 1958) and none is shown on the last version of the map (Prest et al., 1968). Recently however, Thorleifson et al. (1992, 1993) suggested a possible link with old northwestward striations reported by Veillette and Pomares (1991) in the Matagami area of northwestern Quebec (Area A, Fig. 1) to those of the Big Trout Lake area and to those reported by Prest (1963) for the Lansdowne House region. Thorleifson et al. (1992, 1993) also reported northwest fabrics in older tills on the Nelson and Severn Rivers. Composition of these tills indicates generally westward and not eastward transport.

In the James Bay basin, Low's early observations were until recently the only report ever made of an old northwestward flow. Sites showing northwestward striations ( $300^\circ$ ) crossed by striations to the southwest were first observed by the author in 1986 near Matagami, and in 1987 on an island in the estuary of the Eastmain River near Eastmain (Fig. 1). Numerous crossstriated sites, showing roughly the same sequence and sense of ice-flow as these two sites, were measured in the Matagami area during the summer of 1990 (Veillette and Pomares, 1991). In 1992 outcrops along the main James Bay road, the Némaska road joining the James Bay road to Hydro-Québec Albanel relay station, logging roads, borrow pits, and the shores of the large lakes of the area (Area A, Fig. 1 and 2) revealed the same sequence of ice flow. In 1993, outcrops along the James Bay road in the Eastmain River area and along the new road joining the Chibougamau area to the Albanel post (Area A, Fig. 1 and 2) were also examined to determine the southern extent of the northwestward ice flow. Recent work by Paradis and Boisvert (1995) has added new measurements north of Chibougamau related

to a pre-Late Wisconsinan flow to the southeast. These findings led to a closer scrutiny of Low's observations on ice-flow sequence in James Bay.

## THE MATAGAMI-CHIBOUGAMAU-NÉMISKA AND EASTMAIN AREA

In the region southeast of James Bay (Fig. 2), the area south of  $50^\circ\text{N}$  and west of Desmaraisville was examined in greatest detail as part of a surficial geology mapping program (Veillette, 1989; Veillette et al., 1992). North of  $50^\circ\text{N}$  access is limited to main roads and shorelines of large lakes and rivers. In the Chibougamau-Chapais area, representative sites were chosen from those reported by Prichonnet and Beaudry (1990).

A distinct northwestward oldest flow is present northwest of a broad axis extending northeast of Desmaraisville. Southeast of this axis, all "old" striated surfaces show southeastward movement (Bouchard and Martineau, 1985; De Corta, 1988; Prichonnet and Beaudry, 1990; S.J. Paradis, pers. comm., 1994) and proposed ice divide positions were generally east of James Bay or further north (Bouchard and Martineau, 1985; Prichonnet and Beaudry, 1990). Southeast striations are crossed by flows to the southwest that correspond to orientation of deglaciation landforms.

In the western part of the area, west of the Cochrane limit, striations formed by the old northwestward flow presumably were destroyed or obscured by competing flows of the Cochrane and Rupert east-southeastward surges that occurred toward the end of the deglaciation of the area (Hardy, 1976). This may explain why traces of the old northwestward flow had escaped the attention of earlier investigators along the main James Bay road. Evidence for northwestward ice movement can still be found at favourable outcrops within the Cochrane limit.

West of the Harricana Moraine (Fig. 2), evidence for northwest-flowing ice is thin and west-southwestward ( $240^\circ$ - $260^\circ$ ) striations form the base of the ice-flow sequence (Veillette, 1989; Veillette et al., 1989). This is due either to a real shift in ice-flow direction from  $300^\circ$  to a more westerly direction, or traces of the northwestward flow have been destroyed by subsequent flows. However, at two locations northeast of Lake Abitibi ( $49^\circ 15'\text{N}$  and  $78^\circ 15'\text{W}$ , see Fig. 5), outcrops showing good stoss and lee relationships toward  $295^\circ$ - $315^\circ$  have been preserved in sheltered positions from later southwestward and southeastward flows. These sites are the southernmost occurrences of the old northwestward flow.

## THE RADISSON-DUPLANTER ROAD

Figure 3 (Area B, Fig. 1) shows the location of representative striation measurements obtained along the road linking Hydro-Québec dam sites between Radisson (LG-2) and Duplantière and on service roads around the reservoirs. Road side outcrops, floors of abandoned borrow pits, and the area

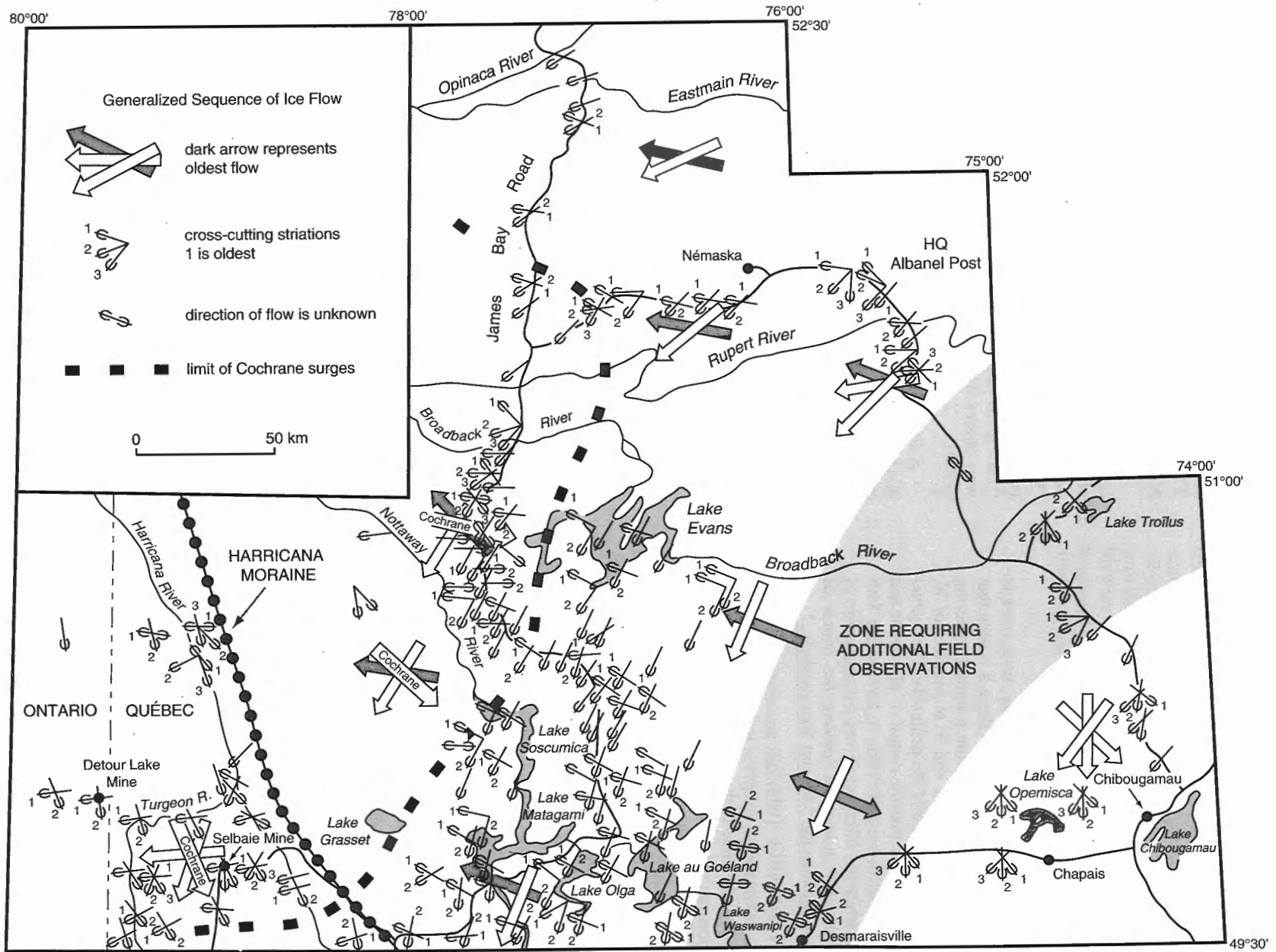


Figure 2. Ice flow sequence in the Matagami-Eastmain-Némiska and Chibougamau area (Area A of Figure 1).

around quarries where glacial deposits had been stripped away were examined for cross-striations, and till sections were checked for the presence of indicator erratics, Lake Mistassini Proterozoic clasts in particular. Areas in the immediate vicinity of main dam sites proved to be the most informative because unweathered bedrock was exposed during construction. On the other hand, floors of large borrow pits in till excavated for roads and earth dams proved the least informative due to site rehabilitation.

The traverse covered about 1000 km of road and revealed crosscutting relationships that, in the area west of Brisay, are basically the same as those of area A to the south and as those along the James Bay coast. An old northeastward flow, unique to this area, predates all west-southwestward striations and, in the Brisay area, is crossed by a last flow to the northeast associated with final deglaciation of the area south of Ungava Bay (see Fig. 1). These old northeastward striations are present at Radisson, La Grande 3 (LA-3), and Laforge 2 (LA-2).

## JAMES BAY

Striations were measured along the east coast of James Bay during a two-week Zodiac boat traverse in July and August 1994. Outcrops along a 700-km stretch of coastline, mostly on islands, were examined between the Rogan River area in the north and the village of Waskaganish in the south (Fig. 4). Several spectacular sites showing unequivocal evidence of old northwestward flow ( $290^{\circ}$ - $320^{\circ}$ ) were observed. These striations are crossed by those of later flows fanning out counterclockwise to a final south-southwest direction in southeastern James Bay (Fig. 4). Some outcrops in southeastern James Bay also show striations from the last Cochrane flows to the east-southeast, superimposed on older striations. These crosscutting relationships are similar to those previously described within the Cochrane limit along the James Bay road

(Fig. 2). Islands in the northern part of the bay, including the Bear islands, present impressive examples of outcrops shaped by the same succession of ice flows as that observed along the east coast (Fig. 4); however striations record a distinct shift from an initial northwestward flow to a final south-southeastward flow. This shift, ending to the south-southeast, differs from that observed along the east coast at comparable latitudes, which ends to the southwest. These late convergent ice flows confirm the presence of a zipper-like opening in the ice sheet proposed for the final deglaciation of the area (Hardy, 1976; Vincent and Hardy, 1979). This deglaciation model calls for the northward progression of a reentrant in the ice sheet a few kilometres offshore along the east coast of James Bay, with slower ice retreat east and west of this position. Until now, evidence for southeast flow associated with retreat of the west flank of the reentrant was lacking. The large islands in the east-central part of the bay are composed primarily of drift (Fig. 4) and may relate to the northward extension of the Harricana Moraine, along the central axis of the reentrant.

The east coast of James Bay is an exceptional environment for studying bedrock-inscribed indicators of ice flow because of its bedrock morphology, rapid emergence, and intensive erosion by wave action. Examples of processes and features in this environment are discussed by Veillette and Roy (1995). The south and west coasts of James Bay were examined by helicopter, but outcrops of soft carbonates of the Hudson Bay Platform are absent in the south, rare along the west coast, and where present, are weathered. Traverses were conducted along the Attawapiskat River to an exploration camp about 180 km inland from the James Bay coast. Striations indicating westward- and northwestward-flowing ice crossed by younger striations toward the southwest were observed at only two locations west of James Bay, both on hard Precambrian lithologies protruding above flat-lying carbonates: one on the eastern extension of the Sutton ridge and the other on volcanics in the upper Attawapiskat River area (Fig. 5).

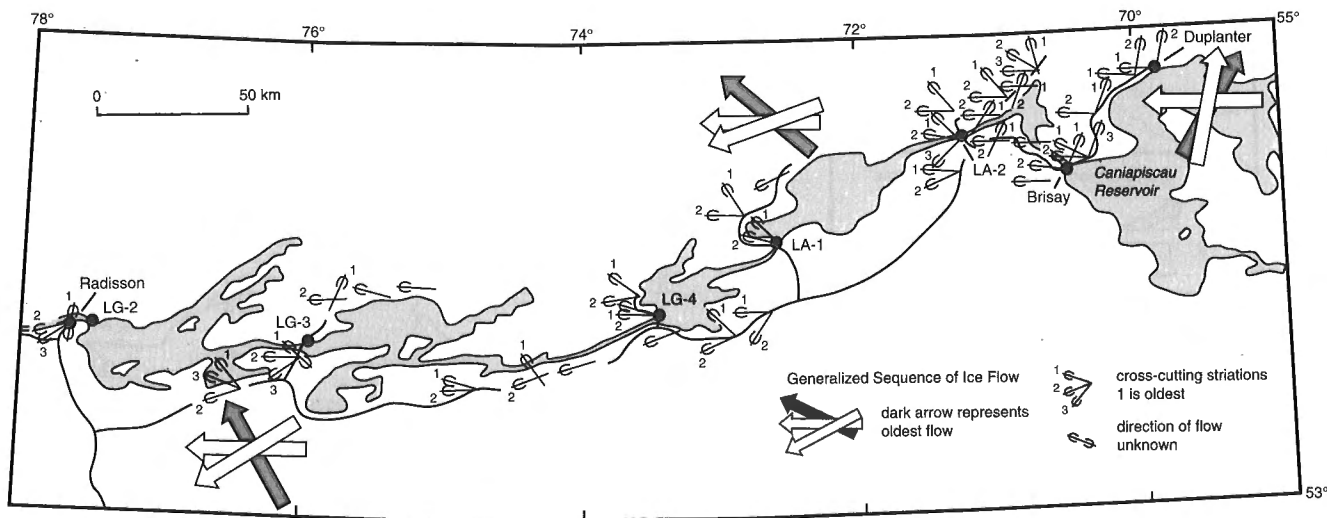


Figure 3. Ice flow sequence along the Radisson-Duplanter road (Area B of Figure 1).

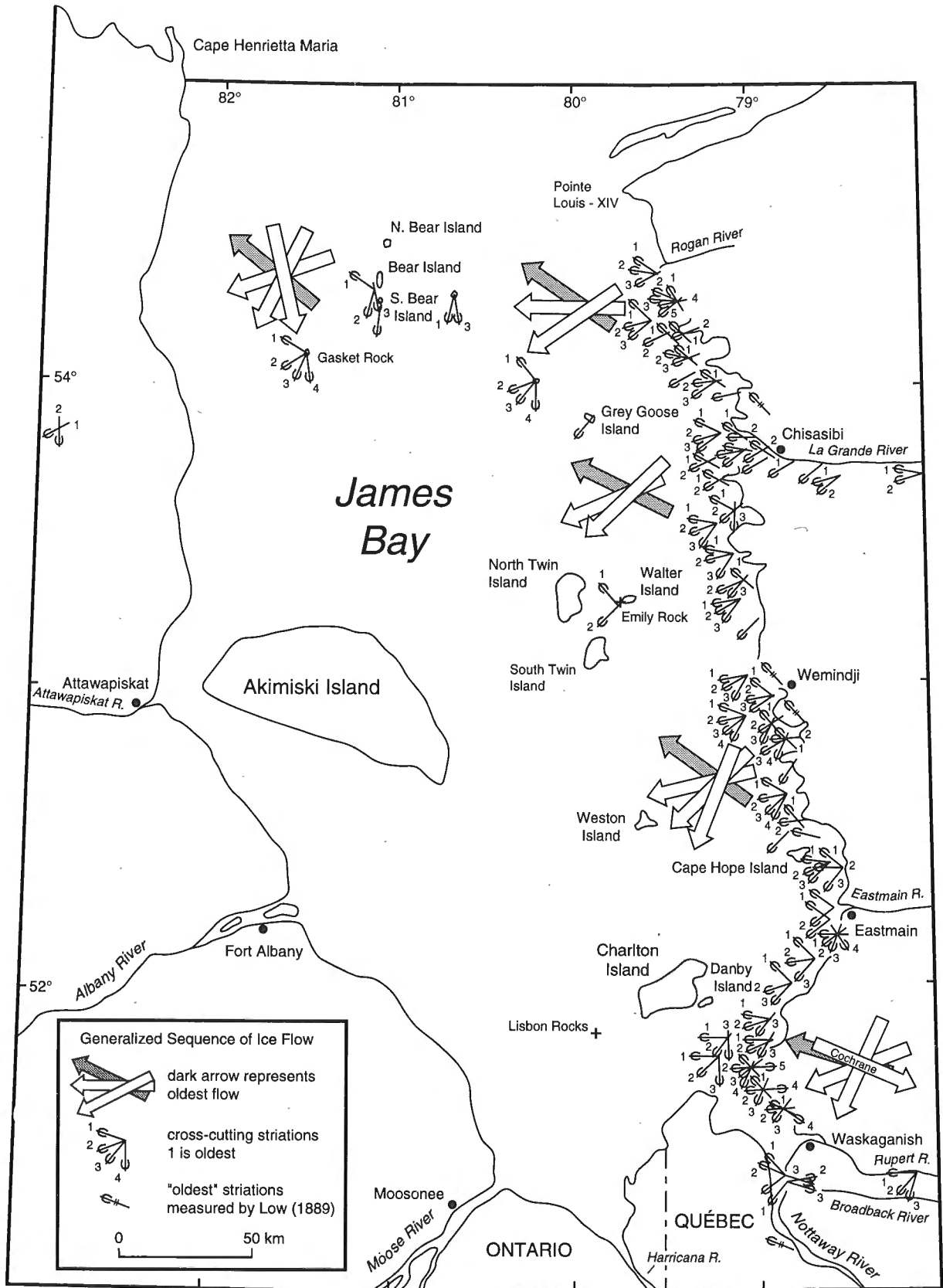
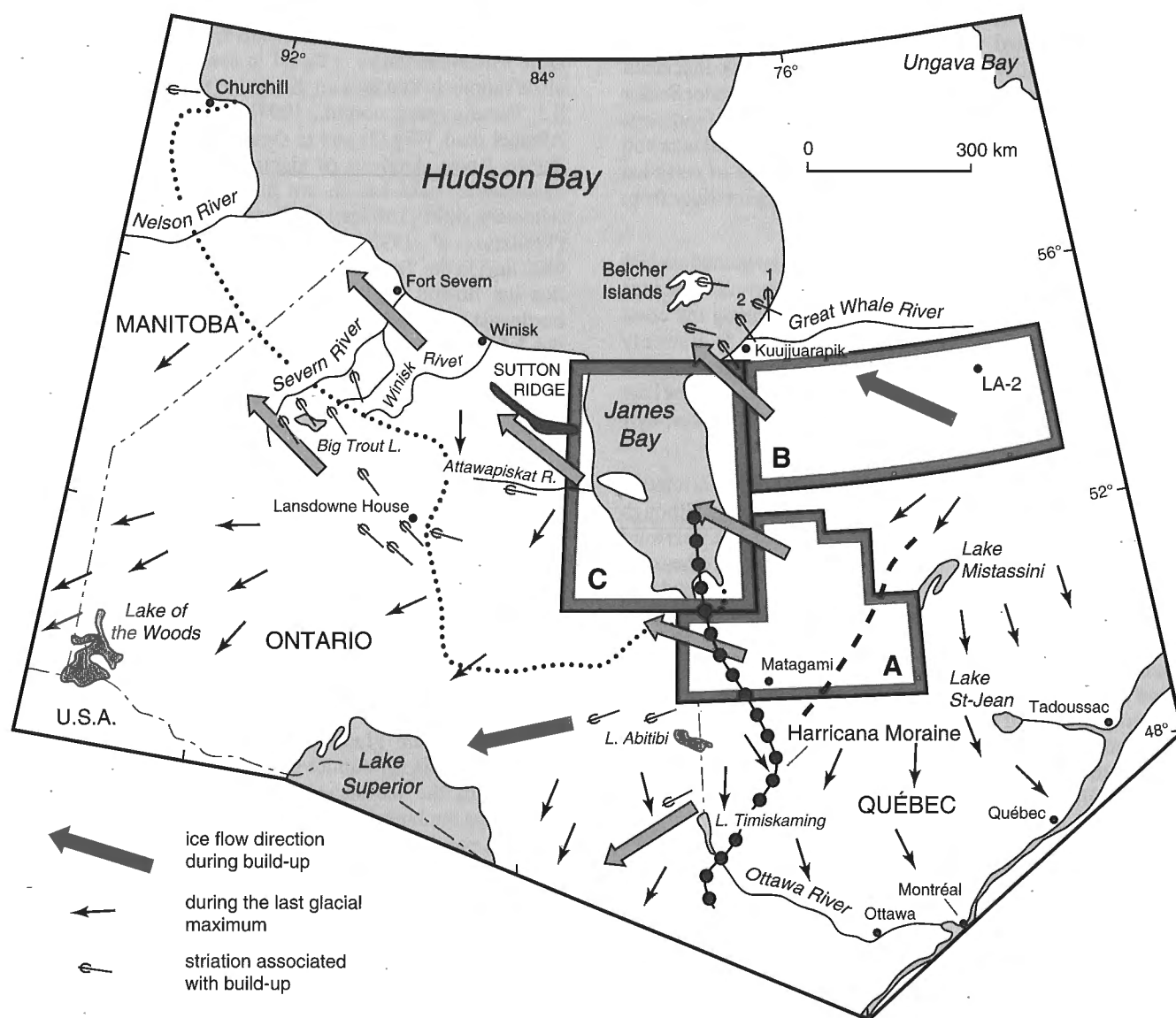


Figure 4. Ice flow sequence along the coast and within James Bay (Area C of Figure 1).

## NORTHWESTWARD EXTENT OF THE FLOW

Figure 5 shows new data presented in this paper combined with relevant ice-flow data from surrounding areas. Information from Prest (1963) and Thorleifson et al. (1993) is of particular significance because it indicates extension of the old northwestward flow across Ontario. According to Thorleifson et al. (1993), the Rocksand Till, which is present at four sites along the Severn River, contains abundant Proterozoic fragments derived from the east and a very low red carbonate content derived from Hudson Bay, and shows northwest-oriented till fabrics, is correlative with the northwestward striations at Big Trout Lake first measured by Tyrrell (1913), which Prest (1963) assigned to an Early Wisconsin ice flow

from the east. Amino acid analysis of shell fragments contained in Rocksand Till yielded ratios similar to those of Bell Sea (Skinner, 1973) sediments of the Hudson Bay Lowland. Rocksand Till was therefore attributed to mid-stage 5 glaciation. Rocksand Till lies at the base of the depositional stratigraphic sequence, in agreement with the lower position in the erosional sequence of bedrock-inscribed indicators of northwestward flow in a large area east of the Rocksand Till occurrence. Thorleifson et al. (1993) correlated Rocksand Till with Amery Till on the Nelson River (Nielsen et al., 1986), on the basis of stratigraphic position and west-northwest till fabrics (Fig. 5), although Nielsen et al. (1986) had suggested southwestward flow for this unit. The presence of Early Wisconsin or Late Sangamonian ice flowing from Quebec that



**Figure 5.** Extent of northwestward ice flow mapped from cross-striated surfaces. Later ice flow are shown separately. Heavy broken line marks the southeast limit of old northwestward striations. Dotted line shows contact between Precambrian and younger bedrock.



far to the northwest (Nelson River) prompts a re-examination of Tyrrell's unexplained old striations in the Churchill area of Manitoba, due north of the Nelson River:

"The only observation which is at a variance with this general rule is the existence of an early set of striae, pointing westward, on the rocks at Churchill. Whether these striae were made by a glacier flowing from a centre near at hand, or at a distance, was not determined. They do not accord with the striae attributed to the Labradorian glacier along Nelson River and further south, for which the west-pointing striae at Churchill were earlier than those of the Keewatin glacier, those of the Nelson River and further south are clearly later." (Tyrrell, 1898, p. 178).

The general rule Tyrrell was referring to at Churchill was the direction of flow toward Hudson Bay indicated by striations associated with Keewatin ice. The old westward striations at Churchill may represent bedrock-inscribed evidence for maximum early extension of the Labrador Sector of the Laurentide Ice Sheet. A close examination of outcrops along the west coast of Hudson Bay in the Churchill area and to the north is required to ascertain the presence of early ice flow from central Quebec, possibly predating ice flow from a Keewatin centre.

The northeast flank of this flow appears to be in southeastern Hudson Bay where Low (1889) reported several outcrops with striations to the northwest ( $280^{\circ}$ - $325^{\circ}$ ) along the coast and along rapids of the Great Whale River (Fig. 5). Recently Parent and Paradis (1993) measured striations at several sites along the coast in the Kuujjuarapik area, which record the later westward and southwestward sequence. At isolated sites, they reported traces of an older flow to the north-northwest.

In the area between  $50^{\circ}$ N and Lake Abitibi, correlative flow may have been to the west and to the southwest, although the presence of a northwestward flow preceding a westward flow remains a real possibility at two locations northeast of Lake Abitibi (Fig. 5). At Selbaie Mine (Fig. 2), fresh bedrock exposed at the base of a large open pit provided solid evidence for an early, widespread west-southwest flow ( $260^{\circ}$ ). Bedrock-inscribed features associated with that early flow were preserved under a thick till sheet of low carbonate content, the base of which is undisturbed by younger flows to the southwest and finally to the southeast, the last one having shaped the glacial landscape of the region (Veillette, 1986, 1989; Veillette et al., 1992).

The extension of west-southwestward flow across northeastern and northwestern Ontario has been verified by mapping of striations and by glacial transport studies (Skinner, 1973; Veillette, 1986; Thorleifson and Kristjansson, 1990; C.A. Kaszycki, pers. comm., 1993; B. McClenaghan, pers. comm., 1994). Thorleifson and Garrett (1993) have mapped the westward dispersal of carbonates across the Prairie region.

## GLACIAL TRANSPORT EVIDENCE

A strong and sustained initial northwestward ice flow across James Bay and southeast Hudson Bay best explains the dispersal pattern of Belcher Islands erratics (Prest, 1990, p.130, Fig. 27). Omarolluk Formation greywacke and oolitic jasper were probably first transported from the east coast of Hudson Bay to the Churchill area during expansion of the ice sheet, and redistributed to the west and southwest during the Late Glacial maximum and decay of the Laurentide Ice Sheet. The widespread occurrence of these lithological indicators across the Prairie Provinces supports this multidirectional dispersal pattern. The same applies to dispersal patterns of carbonate erratics from the Hudson Bay Lowland (Shilts, 1980), which as pointed out by Thorleifson et al. (1993) are the result of several directions of flow.

No evidence of northwestward transport of Proterozoic Lake Mistassini rocks is found in central Quebec, although observations in that area are limited to those of the author and S.J. Paradis (pers. comm., 1994) along the Chibougamau-Albanel road, (Fig. 2) and to those of Low (1885) along the Rupert River. Analysis of glacial transport using the same Proterozoic rocks has shown that transport distances were relatively short (150 km) to the southwest in Abitibi region (Veillette et al., 1992), compared with those to the southeast (400 km) in the Tadoussac area (Dionne, 1994). This implies that ice flowed for a longer period from a source north-northwest of Lake Mistassini than from a source northeast of the lake (deglaciation). No evidence has been found for eastward glacial transport on the east coast of James Bay except for ice-rafted material in Lake Ojibway and Tyrrell Sea (Veillette et al., 1991).

## CONCLUSION

A northwestward ice flow present at the base of the recognized ice-flow sequence and extending about 1500 km from central Quebec across northwestern Ontario and northern Manitoba has been mapped using cross-striated surfaces supported by stratigraphic and glacial transport evidence. This flow is attributed to early expansion of the Wisconsin Laurentide Ice Sheet. Well known major glacial events such as Cochrane late glacial surges documented from stratigraphic analysis, photointerpretation, and glacial transport, or opening of the ice sheet along the Harricana interlobate moraine in the James Bay Lowland are also represented in the striation record. It therefore seems improbable that glacial events of even greater magnitude, such as multiple deglaciations of the Hudson Bay Lowlands during the Wisconsin, proposed by Andrews et al. (1983), occurred without leaving any traces in the striation record. In fact bedrock-inscribed ice-flow data imply continuous ice cover throughout the period covering deposition of Rocksand Till and the last deglaciation. The opening of Hudson Bay during that period would have most likely induced northward and northeastward ice flows, which would have left striations that should be found crossing those of the northwestward flow.

The data presented here clearly demonstrate the importance of a detailed cross-striation record for reconstructing past glacial events and evaluating data supplied by glacial transport and more local stratigraphic studies. Such work is possible on the vast peneplains of the Precambrian Shield where ice movements appear to have been as consistent over large areas during the early life of the ice sheet as they were during deglaciation. Because of the lack of stratigraphic control in most Shield areas, it is necessary to focus on the erosional record. If enough time and effort are spent on regional mapping of cross-striated surfaces, a greatly enhanced ice-flow history would be obtained for areas underlain by crystalline bedrock.

It is apparent that the last ice sheet began in a more southerly position than is generally thought (Fig. 5). Ice flowed northwestward from an area along a line extending roughly from Lake Mistassini to Lake Abitibi. The hypothetical growth model presented by Vincent and Prest (1987, Fig. 4) for the Laurentide Ice Sheet following the last interglaciation represents a reasonably good approximation of ice-flow conditions for the intermediate and distal parts of the flow lines, precisely because the authors assigned the old northwestward striations of northern Ontario to the expansion phase of the ice sheet; however, locations of growth centres as indicated by the present data remain problematic.

These new findings have important implications for mineral exploration based on drift sampling. Northwestward-flowing ice advancing across a land surface that had been subjected to the prolonged ice-free period of the last interglacial would have been effective in eroding and transporting weathered material produced during this period. Several companies are involved in tracing indicator minerals for kimberlite sources in the James Bay basin. The entire Eastmain greenstone belt and a good part of the Abitibi greenstone belt come under the ice-flow system described here (Fig. 1).

Much more field work on ice-flow chronology could be done in central and southeastern Quebec and in Labrador to determine locations of growth centres and migration of ice divides during the Wisconsin. This knowledge is essential for a satisfactory understanding of the inception phase of the last ice sheet.

## ACKNOWLEDGMENTS

The field assistance of P. Thibaudeau, J.-S. Pomares, C. Prévost, M. Roy, and H. Karam is appreciated. Discussion with GSC colleagues H. Thorleifson, V.K. Prest, M. Parent, and A.S. Dyke, who also participated in the Radisson-Duplanter road traverse, were most helpful. S.J. Paradis supplied new measurements from the Chibougamau area. R. Martineau from La Société d'Énergie de la baie James (SEBJ) was most cooperative in lending equipment to sample some outcrops near Brisay, and SEBJ supplied free room and board at their facilities at Laforge-2 and Brisay. Several individuals from LG-1, Chisasibi, Wemindji, and Waskaganish assisted with logistics and navigation along the east coast of James Bay. N. Novak from KWG Resources provided camp facilities in the Attawapiskat area and showed the location of

striated outcrops. A. Bertrand, pilot with Abitibi Helicopters, made the difficult flight across James Bay a pleasant experience. H. Thorleifson critically read the manuscript. Sincere thanks to all.

## REFERENCES

- Andrews, J.T., Shilts, W.W., and Miller, G.H.**  
1983: Multiple deglaciations of the Hudson Bay Lowlands, Canada, since deposition of the Missinaibi (last interglacial?) Formation; *Quaternary Research*, v. 19, p. 18-37.
- Bouchard, M.A. and Martineau, G.**  
1985: Southeastward ice flow in central Quebec and its paleogeographic significance; *Canadian Journal of Earth Science*, v. 22, p. 1536-1541.
- De Corta, H.**  
1988: Les dépôts quaternaires de la région du lac Rohault - Lac Boisvert (sud de Chibougamau): aspect de la dispersion glaciaire clastique; *Mémoire de maîtrise, Université de Québec à Montréal*, 112 p.
- Dionne, J.-C.**  
1994: Les erratiques lointains de l'embouchure du Saguenay, Québec. *Géographie physique et Quaternaire*, vol. 48, p. 179-194.
- Energy, Mines, and Resources Canada**  
1987: Principal mineral areas of Canada; Canadian Department of Energy, Mines and Resources, Mineral Policy Sector and Geological Survey of Canada, Map 900 A, scale 1:7 603 200.
- Hardy, L.**  
1976: Contribution à l'étude géomorphologique de la portion québécoise des basses terres de la baie de James; Thèse de doctorat, Université McGill, Montréal, 264 p.
- Low, A.P.**  
1889: Report on exploration in James Bay, and country east of Hudson Bay, drained by the Big, Great Whale and Clearwater Rivers. 1887-1888; *Geological and Natural History Survey of Canada, Annual Report*, v. 3, Part II, Report J, 62 p.  
1903: On an exploration of the east coast of Hudson Bay from Cape Wolstenholme to the south end of James Bay; *Geological Survey of Canada, Annual Report, Report D*, v. 13, p. 5-82.
- Ministère de l'Énergie et des Ressources du Québec/ Ontario Geological Survey**  
1983: Carte lithostratigraphique de la sous-province de l'Abitibi; ministère de l'Énergie et des Ressources du Québec/Ontario Geological Survey, carte cataloguée "DV 83-16" à Québec et "Map 2484" en Ontario, échelle de 1/500 000.
- Nielsen, E., Morgan, A.V., Morgan, A., Mott, R.J., Rutter, N.W., and Causse, C.**  
1986: Stratigraphy, paleoecology, and glacial history of the Gillam area, Manitoba; *Canadian Journal of Earth Science*, v. 23, p. 1641-1661
- Paradis, S.J. et Boisvert, E.**  
1995: Séquence des écoulements glaciaires dans le secteur de Chibougamau-Némiscau, Québec; dans *Recherches en cours 1995-C*; Commission géologique du Canada, ce volume.
- Parent, M. et Paradis, S.J.**  
1993: Interprétation préliminaire des écoulements glaciaires dans la région de la Petite Rivière de la Baleine, région subarctique du Québec; dans *Recherches en cours, Partie C*; Commission géologique du Canada, Étude 93-1C, p. 359-365.
- Prest, V.K.**  
1963: Red Lake-Lansdowne House area, northwestern Ontario - surficial geology; *Geological Survey of Canada, Paper 63-6*, 23 p.  
1984: The late Wisconsinan glacier complex; in *Quaternary stratigraphy of Canada - a Canadian contribution to IGCP Project 24*, (ed.) R.J. Fulton; *Geological Survey of Canada, Paper 84-10*, p. 21-36, Map 1584A, scale 1:7 500 000.  
1990: Laurentide ice-flow patterns: a historical review, and implications of the dispersal of Belcher Islands erratics; *Géographie physique et Quaternaire*, v. 44, p. 113-136.
- Prest, V.K., Grant, R.R., and Rampton, V.N.**  
1968: Glacial map of Canada; *Geological Survey of Canada, Map 1253A*, scale 1:5 000 000.

**Prichonnet, G. et Beaudry, L.M.**

1990: Évidences d'un écoulement glaciaire sud, antérieur à l'écoulement sud-ouest du Wisconsinien supérieur, région de Chapais, Québec; dans *Recherches en cours, Partie C*; Commission géologique du Canada, Étude 90-1C, p. 331-338.

**Shilts, W.W.**

1980: Flow patterns in the central North American ice sheet; *Nature (London)*, v. 286, p. 213-218.

**Skinner, R.C.**

1973: Quaternary stratigraphy of the Moose River Basin, Ontario; *Geological Survey of Canada, Bulletin 225*, 77 p.

**Thorleifson, L.H. and Garrett, R.J.**

1993: Prairie kimberlite study-till matrix geochemistry and preliminary indicator mineral data; *Geological Survey of Canada, Open File 2745*.

**Thorleifson, L.H. and Kristjansson, F.J.**

1990: Geochemical, mineralogical and lithological analyses of glacial sediments for gold, base metal, and kimberlite exploration, Beardmore-Geraldton area, District of Thunder Bay, northern Ontario; *Geological Survey of Canada Open File 2266, Contribution to Canada-Ontario Mineral Development Subsidiary Agreement under the Economic and Regional Development Agreement, 1985-1990*.

**Thorleifson, L.H., Wyatt, P.H., and Warman, T.A.**

1993: Quaternary stratigraphy of the Severn and Winisk drainage basins, northern Ontario; *Geological Survey of Canada, Bulletin 442*, 59 p.

**Thorleifson, L.H., Wyatt, P.H., Shilts, W.W., and Neilsen, E.**

1992: Hudson Bay Lowland stratigraphy: Evidence for early Wisconsinan glaciation centered in Québec; in *The Last Interglacial-Glacial Transition in North America: Boulder, Colorado*, (ed.) P.U. Clark and P.D. Lea; *Geological Society of America, Special Paper 270*.

**Tyrrell, J.B.**

1898: Report of the Doobaunt, Kazan and Ferguson Rivers and the northwest coast of Hudson Bay; *Geological Survey of Canada, Annual Report*, v. IX, Report F, p.51-193.

1913: Hudson Bay exploration expedition 1912; *Ontario Bureau of Mines, 22nd Annual Report*, v. 22, Part 1, p.161-209.

1914: The Patrician glacier south of Hudson Bay, *Congrès géologique international, Compte rendu de la XII<sup>e</sup> session, Canada*, p. 523-534.

1935: Patrician centre of glaciation; *Pan-American Geologist*, v. 63, p. 1-5.

**Veillette, J.J.**

1986: Former southwesterly ice-flows in Abitibi-Témiscamingue: implications for the configuration of the Late Wisconsinan ice sheet; *Canadian Journal of Earth Science*, v. 23, p. 1724-1741.

1989: Ice movements, till sheets and glacial transport in Abitibi-Timiskaming, Québec and Ontario; in *Drift Prospecting*, (ed.) R.N.W. Dilabio and W.B. Coker; *Geological Survey of Canada, Paper 89-20*, p. 139-154.

**Veillette, J.J. and Pomares, J.-S.**

1991: Older ice flows in the Matagami-Chapais area, Québec; in *Current Research, Part C*; *Geological Survey of Canada, Paper 91-1C*, p. 143-148.

**Veillette, J.J. and Roy, M.**

1995: The spectacular cross-striated outcrops of James Bay, Québec; in *Current Research 1995-C*; *Geological Survey of Canada*, this volume.

**Veillette, J.J., Averill, S.A., LaSalle, P., and Vincent, J.-S.**

1989: Quaternary geology of Abitibi-Témiscamingue and mineral exploration; *Geological Association of Canada, Field Trip Guidebook B1*, 112 p.

**Veillette, J.J., Paradis, S.J., Thibaudeau, P., and Pomares, J.-S.**

1991: Distribution of distinctive Hudson Bay erratics and the problem of the Cochrane limit in Abitibi, Québec; in *Current Research, Part C*; *Geological Survey of Canada, Paper 91-1C*, p. 135-142.

**Veillette, J.J., Paradis, S.J., Thibaudeau, P., Daigneault, R.A. et Richard, P.J.H.**

1992: La géomorphologie et la géologie du Quaternaire de l'Abitibi-Témiscamingue; *Association québécoise pour l'étude du Quaternaire (AQQUA), VII<sup>e</sup> Congrès quadriennal, Rouyn-Noranda, Québec, livret-guide des excursions*, 252 p.

**Vincent, J.-S. and Hardy, L.**

1979: The evolution of Glacial Lakes Barlow and Ojibway, Québec and Ontario; *Geological Survey of Canada, Bulletin 316*, 18 p.

**Vincent, J.-S. and Prest, V.K.**

1987: The Early Wisconsinan history of the Laurentide Ice Sheet; *Géographie physique et Quaternaire*, v. 41, p. 199-213.

**Wilson, J.T., Falconer, G., Mathews, W.H., and Prest, V.K.**

1958: Glacial map of Canada; *Geological Association of Canada*, scale 1:3 801 600.

---

Geological Survey of Canada Project 860020

# Séquence des écoulements glaciaires dans le secteur de Chibougamau-Némiscau, Québec<sup>1</sup>

Serge J. Paradis et Eric Boisvert

Centre géoscientifique de Québec, Sainte-Foy

*Paradis, S.J. et Boisvert, E., 1995 : Séquence des écoulements glaciaires dans le secteur de Chibougamau-Némiscau, Québec; dans Recherches en cours 1995-C; Commission géologique du Canada, p. 259-264.*

---

**Résumé:** Un levé des marques d'érosion glaciaire dans la région comprise entre Chibougamau et Némiscau a permis de reconnaître la présence de vieilles marques d'écoulement glaciaire vers l'ouest-nord-ouest jusque dans le secteur des lacs Dompierre et Villebois, à 50 km au nord de Chibougamau. Ces nouvelles observations portent les auteurs à s'interroger sur l'existence et la localisation d'une ligne de partage des glaces dans la région de Matagami-Chibougamau-Némiscau. Ce vieux mouvement vers l'ouest-nord-ouest les mène à formuler une nouvelle interprétation des séquences d'écoulement glaciaire pour le secteur à l'étude: un premier mouvement glaciaire dirigé vers l'ouest-nord-ouest, a été suivi, dans la région au sud de la rivière Broadback, par un mouvement glaciaire vers le sud-est, lequel pourrait être relié à la formation d'une ligne de partage glaciaire située quelque part au nord de Némiscau. Cette phase a été suivie par un dernier mouvement régional dirigé vers le sud-ouest et présent dans l'ensemble du secteur à l'étude.

**Abstract:** A survey of glacial erosion indicators in the area between Chibougamau and Nemiscau has revealed the presence of ancient ice-flow indicators in a west-northwesterly direction as far as the Dompierre and Villebois lakes sector, 50 km north of Chibougamau. These new observations indicate a possible ice divide in the Matagami-Chibougamau-Nemiscau region. This ancient movement to the west-northwest suggests a new interpretation of the ice-flow sequences: an initial glacial movement to the west-northwest, followed, in the area south of Broadback River, by a glacial movement toward the southeast, which could be linked to the formation of an ice divide located somewhere north of Nemiscau. This phase was followed by a final regional movement in a southwesterly direction which is present in the entire study area.

---

<sup>1</sup> Contribution au Programme de soutien du secteur minier de la région de Chapais-Chibougamau (1992-1995), entente négociée en vertu de l'Entente auxiliaire Canada-Québec sur le développement économique des régions du Québec.

## INTRODUCTION

La route du Nord, dont la construction du tronçon reliant le poste Albabel et Chibougamau a été complétée à l'automne 1993, s'étend sur environ 260 km à partir de Chibougamau jusqu'à l'intersection de la route de la baie James (fig. 1).

Au mois de juin 1994, un levé systématique des marques d'érosion glaciaire a été entrepris le long de la route du Nord afin d'établir la séquence des écoulements glaciaires. Les données recueillies lors de cette étude seront comparées aux interprétations antérieures de Bouchard et Martineau, 1985; Prichonnet et Beaudry, 1990; Veillette et Pomares, 1991 pour le secteur de Mistassini-Chapais-Matagami. En se basant sur des marques d'écoulement glaciaire, principalement des recoupements de stries, ces différents auteurs suggèrent qu'une ligne de partage des glaces existait avant la dernière phase régionale d'écoulement glaciaire dans le secteur Matagami-Chibougamau. Les données préliminaires de la présente étude laissent supposer que cette ligne de partage glaciaire orientée plus ou moins nord-est-sud-ouest se serait formée au nord de ce secteur, probablement au nord de Némiscau.

Le substrat rocheux pour l'ensemble du secteur à l'étude (fig. 1) est constitué de roches granitiques et gneissiques archéennes, recoupé par la ceinture volcanosédimentaire archéenne de Protet-Evans, laquelle est constituée de basaltes massifs ou coussinés et de volcanoclastites. Cette bande de roches, dites vertes, est localisée à 120 km au nord de Chibougamau.

## MÉTHODOLOGIE

Le levé est constitué de 134 affleurements rocheux striés dont 60 montrent des recoupements (fig. 1, rosette). Pour faciliter la présentation cartographique à grande échelle et en raison de la proximité de plusieurs des sites, seuls 58 de ces sites de mesures d'orientation sont présentés sur la figure 1. De ce nombre, 29 comportaient des stries glaciaires orientées dans plusieurs directions.

La polarité des stries glaciaires a été définie en se basant sur deux types de critères: 1) la présence de micro-formes telles les queues-de-rat et les broutures; 2) la présence de roches moutonnées.

La chronologie relative des écoulements glaciaires a été établie à partir des recoupements et surimpositions observés sur les surfaces striées. Dans le cas d'un recoupement, une surface striée antérieure est préservée, en position relativement abritée, de l'érosion causée par un mouvement glaciaire subséquent. Typiquement, le recoupement est marqué par une troncature séparant deux surfaces striées selon des directions distinctes (Veillette, 1983), la plus ancienne étant celle qui est située en contrebas de la troncature. Dans le cas d'une surimposition, les stries les plus récentes sont formées à même une surface striée antérieure, mais sans qu'il y ait oblitération complète de cette dernière (Parent et Paradis, 1993).

## RÉSULTATS

L'inventaire des mesures de stries glaciaires le long de la route du Nord, de Chibougamau au km 274 de la route de la baie James, permet de diviser le secteur en trois zones représentées par des séquences distinctes d'écoulement glaciaire (fig. 1). La zone la plus au nord s'étend du km 274 à l'ouest jusqu'aux environs du poste Albabel en passant par Némiscau. Ce secteur est caractérisé par un vieux mouvement vers le nord-ouest ( $290^\circ$  à  $310^\circ$ ). Le mouvement nord-ouest a été suivi par le mouvement régional récent vers le sud-ouest ( $190^\circ$  à  $240^\circ$ ), avec forte concentration des mesures aux environs de  $220^\circ$  à  $230^\circ$ . Du km 274 au lac Jolliet, le socle rocheux est essentiellement constitué de gneiss et de migmatite moyennement à très altérés où il a été difficile de retrouver des indicateurs fiables de direction d'écoulement glaciaire.

Entre le poste Albabel et le lac Villon au sud, s'étend la deuxième zone. Elle se caractérise par une diminution marquée du nombre de bons affleurements rocheux et par le fait que seul le mouvement régional récent vers le sud-ouest ( $200^\circ$  à  $240^\circ$ ) ait été détecté, avec une concentration des mesures aux environs de  $220^\circ$  à  $230^\circ$ .

La troisième zone s'étend du lac Villon au nord jusqu'à Chibougamau au sud. Ce secteur est marqué par la présence d'un vieux mouvement vers le sud-est ( $120^\circ$  à  $130^\circ$ ), suivi par un mouvement intermédiaire sud ( $160^\circ$ ) qui est lui-même suivi par le mouvement régional récent vers le sud-ouest ( $200^\circ$  à  $240^\circ$ ), avec concentration des mesures aux environs de  $210^\circ$  à  $220^\circ$ . Un vieux mouvement ouest-nord-ouest ( $260^\circ$  à  $290^\circ$ ) a aussi été noté à quelques sites au sud et au nord du lac Villon ainsi que dans le secteur des lacs Dompierre et Villebois, au sud de la rivière Broadback.

## INTERPRÉTATION DES RÉSULTATS

Les différentes marques d'écoulement glaciaire permettent l'identification de trois phases d'écoulement glaciaire distinctes. Une première phase démontrant un écoulement vers l'ouest-nord-ouest, visible sur tout le territoire, est présente du km 274 jusqu'au nord du lac Chinsuu, à 50 km au nord de Chibougamau (fig. 2: écoulement ancien vers l'ouest-nord-ouest). Ce mouvement marquerait la phase de croissance de l'Inlandsis laurentidien et serait antérieur aux autres mouvements. Ce mouvement aurait été suivi, au pléniglaciaire, par un écoulement glaciaire vers le sud-est retrouvé seulement dans le secteur au sud de la rivière Broadback, suivant la formation d'une ligne de partage glaciaire quelque part dans le secteur au nord de Némiscau (fig. 2: écoulement intermédiaire vers le sud-est). Des travaux récents effectués l'été dernier au nord de Némiscau (Jean Veillette, communication personnelle, 1994) dans les secteurs de la baie James et du chemin de Brisay, pourraient permettre de retracer la contrepartie nord-ouest de cette phase d'écoulement qui n'a pas été retrouvée dans le secteur d'étude du présent rapport. Par contre, l'inventaire des mesures de marques d'érosion

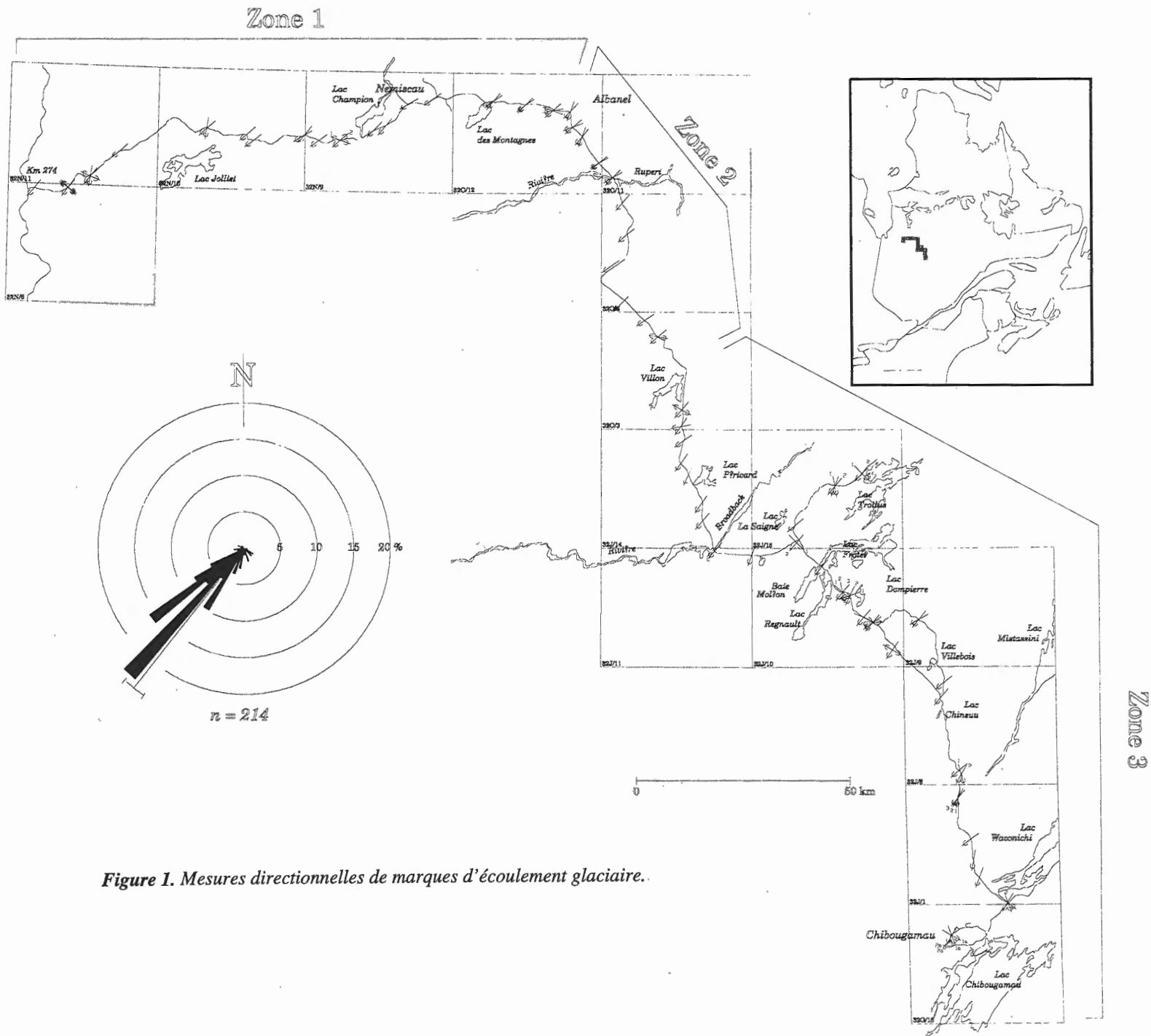


Figure 1. Mesures directionnelles de marques d'écoulement glaciaire.

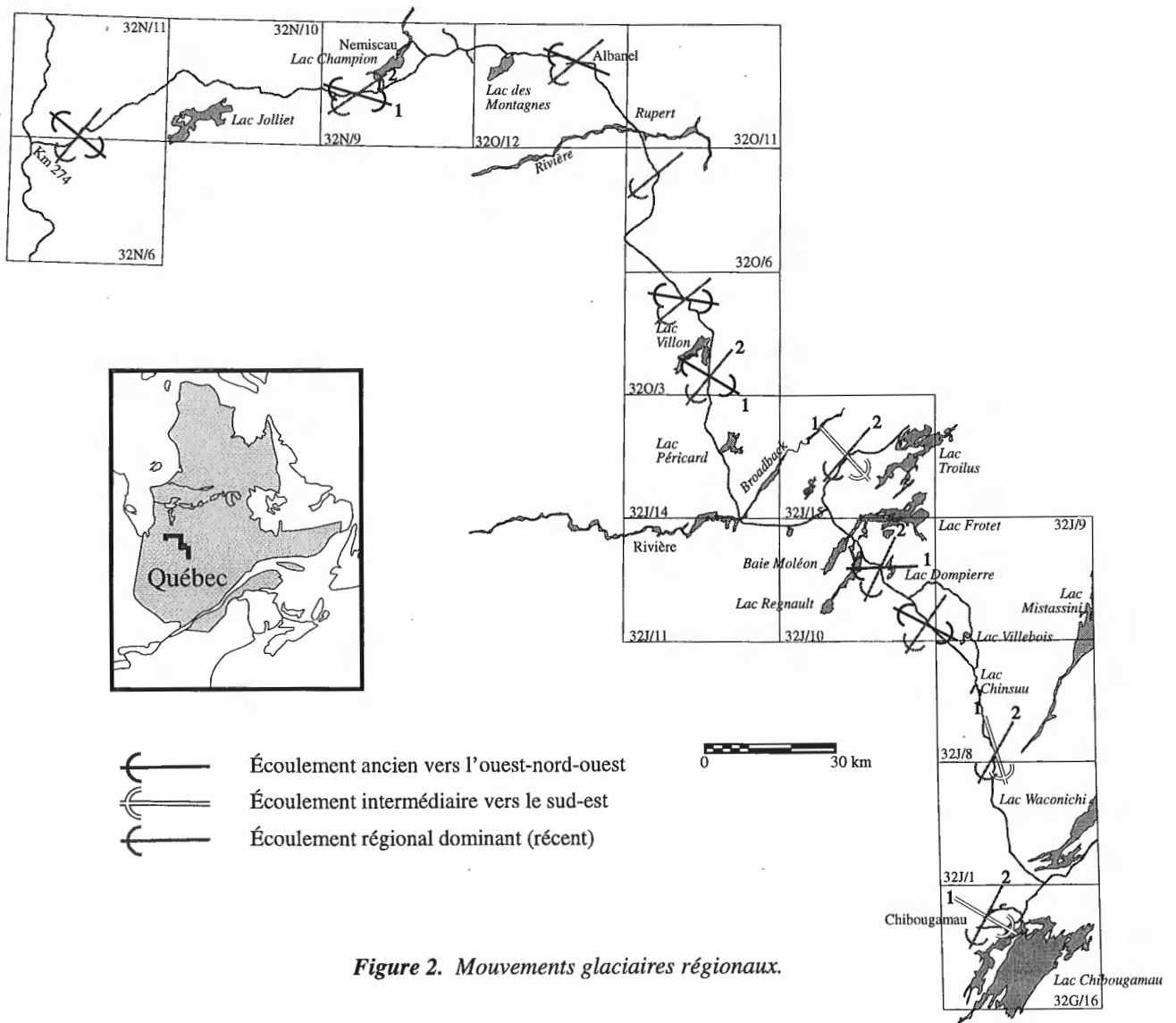
glaciaire dans le secteur de la Petite rivière de la Baleine, effectué par Parent et Paradis (1993), démontre la présence d'un vieux mouvement glaciaire vers le nord qui pourrait être la contrepartie distale de ce mouvement sud-est retrouvé dans le secteur de Chapais-Chibougamau. D'autres mesures de stries effectuées en 1993-1994 (Parent et Paradis, 1994) au nord et au sud de la Petite rivière de la Baleine, c'est-à-dire dans les secteurs de Inukjuak, Kuujuarapik-Whapmagoostui et Long Island corroborent aussi la présence de ce vieux mouvement vers le nord-ouest. L'écoulement vers le sud-est a été suivi par une troisième phase, celle du mouvement régional vers le sud-ouest. Ce dernier mouvement, très dominant sur l'ensemble du territoire, s'est poursuivi jusque lors du retrait de l'Inlandsis laurentidien.

**DISCUSSION**

Les données préliminaires de cette étude ont été comparées aux travaux effectués par différents auteurs dans les secteurs de Chapais-Chibougamau.

Bouchard et Martineau (1985) ont été les premiers à repérer des empreintes directionnelles d'érosion glaciaire de direction sud-est sur des affeurements rocheux dans les régions de Chibougamau et du lac Mistassini. La position de ces marques d'écoulements ainsi que leur bon état de conservation leur permettent de croire qu'elles sont d'âge wisconsinien. Ils proposent que ce vieil écoulement glaciaire vers le sud-est aurait été alimenté par un centre de dispersion localisé du côté est de la baie James, s'étendant possiblement comme une crête à l'est de la baie d'Hudson. La reconnaissance de blocs de tillite et de dolomie à stromatolites par Dionne (1986, 1994) sur les rivages du Saint-Laurent appuie l'hypothèse selon laquelle un écoulement glaciaire se serait produit du nord-ouest vers le sud-est dans l'axe des lacs Mistassini, Albanel, Québec et Tadoussac au cours du Wisconsinien.

Dans le secteur de Chapais, Prichonnet et Beaudry (1990) déduisent que les centres de dispersion ou les lignes de partage des glaces se sont déplacés, dans le sens horaire, depuis un secteur situé au sud de la baie James vers le centre du Nouveau-Québec.



En se basant sur des données préliminaires, Veillette et Pomares (1991) suggèrent l'existence, à une époque antérieure à la dernière déglaciation, d'une ligne de partage des glaces dans le secteur de Matagami-Chapais.

Dans la présente étude, la reconnaissance d'un vieux mouvement vers l'ouest-nord-ouest jusque dans les secteurs des lacs Dompierre et Villebois (fig. 2) fait que l'on est porté à s'interroger sur l'existence et sur la localisation de la ligne de partage des glaces, telle que décrite par les différents auteurs.

Une hypothèse est inhérente à l'interprétation des écoulements glaciaires de Veillette et Pomares (1991). Ce modèle, basé sur l'existence d'une ligne de partage des glaces située entre Matagami et Chapais, présuppose que le vieux mouvement vers le nord-ouest, retrouvé dans le secteur de Matagami, est plus ou moins synchrone avec le vieux mouvement vers le sud-est reconnu dans le secteur de Chapais et du lac Mistassini. En acceptant cette hypothèse dans le contexte de la présente étude, on pourrait présumer que l'ensemble des stries glaciaires, possiblement de direction nord-ouest, retrouvées dans la zone 1 entre le km 274 et le poste Albanel, est contemporain des stries glaciaires de direction sud-est cartographiées dans la zone 3, entre le lac Villon et Chibougamau

(fig. 1); à partir de quoi on peut ensuite supposer l'existence d'une ligne de partage des glaces qui aurait possiblement occupé la zone 2, localisée entre le poste Albanel et le lac Villon. Cette dernière serait l'extension vers le nord-est de la ligne de partage des glaces présentée par Veillette et Pomares (1991, fig. 2).

En se basant sur la distribution schématisée des séquences de marques d'écoulement glaciaire pour le secteur à l'étude, on ne peut valider l'hypothèse du synchronisme des marques d'écoulement glaciaire représentant le vieux mouvement vers le nord-ouest du secteur de Némiscau avec celles représentant le vieux mouvement vers le sud-est de la région de Chibougamau. La présence de marques d'écoulement glaciaire vers l'ouest-nord-ouest sur l'ensemble du territoire, entre le lac Chinsuu et le km 274, permet donc d'avancer l'interprétation suivante du modèle d'écoulement glaciaire pour le secteur à l'étude (fig. 3):

1. Sur l'ensemble du territoire situé entre le lac Chinsuu au sud et le km 274 (fig. 2), le long de la route de la baie James au nord de Matagami, on retrouve des marques d'écoulement glaciaire qui représentent un vieux mouvement glaciaire qui s'est effectué vers l'ouest-nord-ouest. Ce

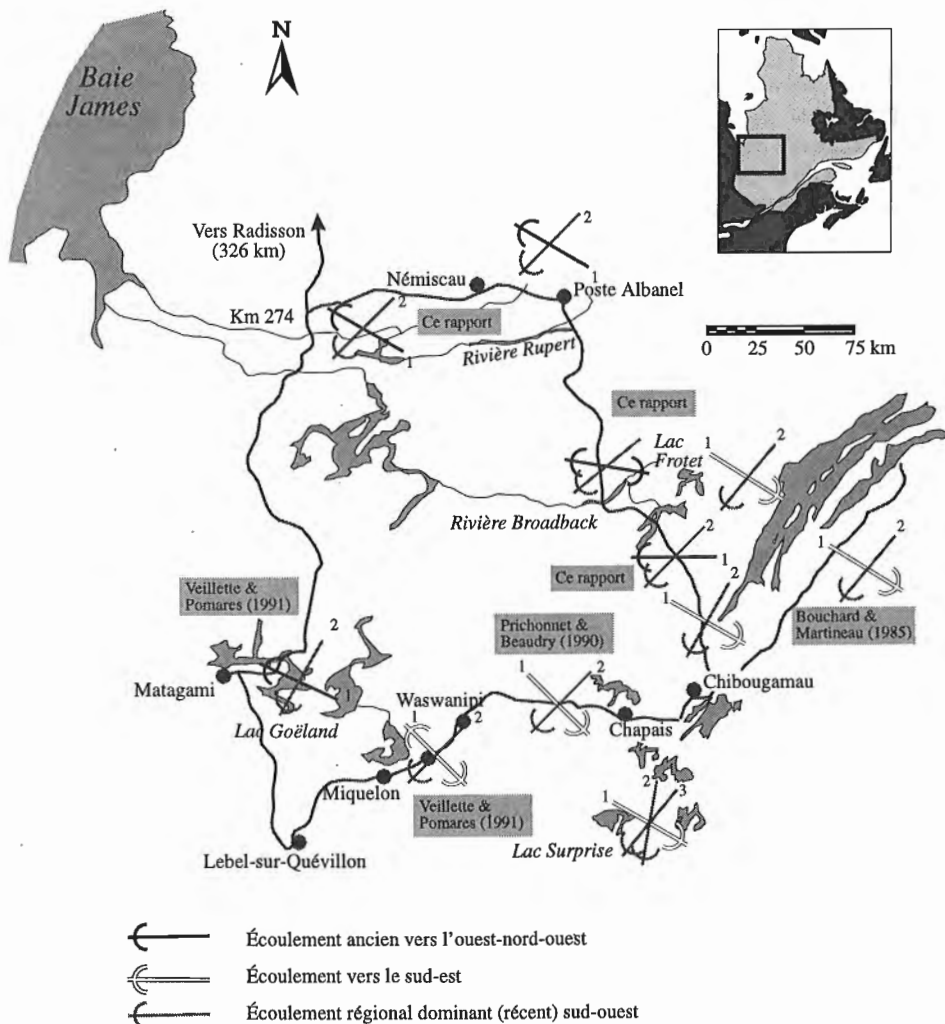


**Figure 3.**

*Comparaison des données du présent rapport et de travaux antérieurs.*



vieux mouvement a pu être de longue durée et pourrait être associé à la phase de croissance de l'Inlandsis laurentidien.

2. Par la suite, il y aurait eu formation d'une ligne de partage glaciaire, orientée plus ou moins nord-est-sud-ouest, dans une région située au nord de Némiscau. Les marques d'écoulement glaciaire vers le sud-est, dans le secteur au sud de la rivière Broadback, se seraient formées alors que cette ligne de partage des glaces était active. Le vieux mouvement vers le nord-ouest, identifié dans la région de la Petite rivière de la Baleine (Parent et Paradis, 1993) et dans les secteurs de Inukjuak au nord et de Kuujjuarapik-Whapmagoostoi et Long Island au sud (Parent et Paradis, 1994) pourrait être l'équivalent distal du vieux mouvement sud-est retrouvé dans le secteur de Chapais-Chibougamau.
3. Les marques d'écoulement glaciaire, présentes sur l'ensemble du secteur, et la morphologie dominante du paysage actuel vers le sud-ouest marqueraient le retrait de l'Inlandsis laurentidien et le début de la déglaciation.

## IMPLICATIONS POUR LA PROSPECTION

En se basant sur les données préliminaires recueillies en juin 1994 et en comparant ces résultats avec l'interprétation du contexte régional développé depuis quelques années par différents auteurs, il est nécessaire d'envisager la possibilité d'un transport glaciaire effectué par le mouvement ouest-nord-ouest. Ce nouveau modèle d'écoulement glaciaire pourrait servir de trame de base pour de futures études de traçage de blocs et de dispersion glaciaire dans le secteur de Chibougamau-Némiscau.

D'autre part, il faut se rappeler que l'ensemble du territoire entre le km 274 et Chibougamau se trouvait sous la limite maximum (450 m) du niveau d'eau atteint par le lac Ojibway lors de la phase tardive Kinocévis (Vincent et Hardy, 1979; Veillette, en préparation) juste avant la déglaciation finale. Ceci pourrait impliquer que certains blocs retrouvés en surface soient en fait des blocs de délestage glacial. Ces blocs glaciels pourraient avoir été transportés par les glaces et se trouver ainsi très loin de leur lieu d'origine.

D'autres travaux seront nécessaires pour encore mieux définir et comprendre la dynamique de l'Inlandsis laurentidien au Wisconsinien dans le secteur de la présente étude.

## REMERCIEMENTS

Les auteurs remercient le Programme du secteur minier de la région Chapais-Chibougamau (1992-1995), dans le cadre de l'Entente auxiliaire Canada-Québec sur le développement économique des régions du Québec, pour leur contribution financière et le ministère des Ressources naturelles du Québec pour le support logistique au Camp du lac Caché. Un sincère remerciement est aussi adressé à M. Charles Gosselin, géologue régional, pour le prêt de photos aériennes d'une partie du secteur à l'étude. Merci également à Michel Parent et Jean Veillette pour leurs commentaires comme lecteurs critiques.

## RÉFÉRENCES

- Bouchard, M.A. and Martineau, G.**  
1985: Southeastward ice flow in central Québec and its paleogeographic significance; *Canadian Journal of Earth Sciences*, v. 22, p. 1436-1541.
- Dionne, J.-C.**  
1986: Blocs de dolomie à stromatolites sur les rives de l'estuaire du Saint-Laurent, Québec; *Géographie physique et Quaternaire*, vol. 40, p. 93-98.  
1994: Les erratiques lointains de l'embouchure du Saguenay, Québec; *Géographie physique et Quaternaire*, vol. 48, p. 179-194.
- Parent, M. et Paradis, S.J.**  
1993: Interprétation préliminaire des écoulements glaciaires dans la région de la Petite rivière de la Baleine, région subarctique du Québec; dans *Recherche en cours, Partie C; Commission géologique du Canada, Étude 93-1C*, p. 359-365.  
1994: Géologie du Quaternaire et dynamique tardiglaciaire dans le sud-est de l'Hudsonie; ACFAS, 62<sup>e</sup> congrès, *Recueil des résumés de communications, Annales de l'ACFAS*, volume 62, p. 562.
- Prichonnet, G. et Beaudry, L.M.**  
1990: Évidences d'un écoulement glaciaire sud, antérieur à l'écoulement sud-ouest du Wisconsinien supérieur, région de Chapais, Québec; dans *Recherche en cours, Partie C; Commission géologique du Canada, Étude 90-1C*, p. 331-338.
- Veillette, J.J.**  
1983: Déglaciation de la vallée supérieure de l'Outaouais, le lac Barlow et le sud du lac Ojibway, Québec; *Géographie physique et Quaternaire*, v. 37, p. 67-84.
- Veillette, J.J. and Pomares, J.-S.**  
1991: Older ice-flows in the Matagami-Chapais area, Québec; in *Current Research, Part C; Geological Survey of Canada, Paper 91-1C*, p. 135-142.
- Vincent, J.-S. and Hardy, L.**  
1979: The evolution of glacial Lakes Barlow and Ojibway, Quebec and Ontario; *Geological Survey of Canada, Bulletin 316*, 18 pages.

# Accuracy of low porosity measurements in granite

T.J. Katsube and N. Scromeda  
Mineral Resources Division

*Katsube, T.J. and Scromeda, N., 1995: Accuracy of low porosity measurements in granite; in Current Research 1995-C; Geological Survey of Canada, p. 265-270.*

---

**Abstract:** Effective porosity ( $\phi_E$ ) of 32 granite samples from the Canadian Shield has been measured and compared with similar measurements previously made on the same samples, using slightly different measurement procedures. The purpose was to investigate measurement accuracy of previous low porosity measurements. Effective porosity is determined by taking the difference between a water-saturated and oven-dried sample.

Results show that  $\phi_E$  values (0.27-0.64%) obtained in this study are similar to those (0.16-0.60%) obtained in the past. A comparison of individual values show that previous values are lower by 10-40%. Results also indicate that reduced water saturation time and drying temperatures, used previously, account for up to about 12% of that 40% and that other explanations must be found for the remaining 28%. The currently used saturation time and drying temperature are 300 minutes and 116°C, respectively, in compared to 40 minutes and 100-105°C used in the past.

**Résumé :** Les mesures de la porosité effective ( $\phi_E$ ) de 32 échantillons de granite prélevés dans le Bouclier canadien ont été comparées à des mesures semblables antérieures des mêmes échantillons, en utilisant des méthodes de mesure légèrement différentes. L'objectif visé était d'analyser l'exactitude des mesures antérieures de porosité faible. La porosité effective est déterminée en prenant la différence de cette valeur entre un échantillon saturé en eau et un échantillon séché au four.

Les résultats indiquent que les valeurs de  $\phi_E$  (0,27-0,64 %) obtenues dans cette étude sont semblables à celles (0,16-0,60 %) obtenues dans le passé. Une comparaison des valeurs individuelles révèle que les valeurs antérieures sont de 10 à 40 % plus faibles. Les résultats indiquent en outre qu'une réduction de la période de saturation en eau et des températures de séchage, utilisées antérieurement, représente 12 % environ de ce 40 % et qu'il faut trouver d'autres explications pour le 28 % restant. La période de saturation et la température de séchage actuellement utilisées sont respectivement de 300 minutes et de 116 °C comparativement à 40 minutes et à 100-105 °C dans le passé.

## INTRODUCTION

Effective porosity ( $\phi_E$ ) of 32 granite samples from Lac du Bonnet (Manitoba) have been measured and compared with similar measurements made on the same samples in the past (Katsube et al., 1985; Katsube and Walsh, 1987). Granites are one of the rock types being considered for hosting repositories for permanent storage of high-level radioactive waste in Canada and in many other countries. Therefore, their petro-physical characteristics (e.g., porosity, permeability, and pore structure) are of importance for assessing their barrier quality for retarding radionuclide migration. Effective porosity represents the pore space of all interconnected pores. Slightly different measurement procedures were used for these samples in the past, mainly water saturation and drying methods. The method used today by us is described in recent publications (e.g., Scromeda and Katsube, 1993, 1994). The purpose of this study was to investigate the effect that longer saturation and drying time had on results, and to re-examine the measurement accuracy of earlier low-porosity measurements. This paper reports the results of recent effective porosity ( $\phi_E$ ) measurements and their comparison with previous measurements.

## MEASUREMENT METHOD

### *Samples and previous studies*

The 32 granite samples (numbers: W-1 to W-32) are half-disks with a diameter of 4.10-4.56 cm and a thickness of 0.91-1.05 cm, from depths ranging from 24 to 928 m in three drillholes. Previous effective porosity ( $\phi_E$ ) measurements were made in 1978 (including 1979) on all 32 identical samples, and the results reported in Katsube and Walsh (1987). Subsequently, five (W-4, W-5, W-21, W-24 and W-31) of the 32 samples were remeasured and part of the results reported by Katsube and Scromeda (1991). Recently, W-24 and W-31 were measured again and the results reported in Scromeda and Katsube (1993). These results are compiled in Table 1. Geochemical, petrographic, sampling location, and other information on these 32 samples can be found in Katsube and Hume (1987a). Bulk density ( $\delta$ ) data required for these porosity measurements were previously determined by Katsube and Hume (1987b) using the calliper method (American Petroleum Institute, 1960), i.e., by measuring dimensions and weight of the samples (Table 1).

### *Effective porosity measurement procedure*

In these studies, effective porosity ( $\phi_E$ ) is determined by taking the difference in weight between a water-saturated and oven-dried rock specimen. Experimental procedures used in these studies are similar to those used in Scromeda and Katsube (1993). The American Petroleum Institute (1960) recommended practice for core-analysis procedures has generally been followed, with details of the procedures as follows:

### 1. Vacuum saturation

The rock specimen is placed in a dry beaker using tweezers, and the beaker is then placed in a vacuum chamber. Vacuum is then applied at a pressure of 760 mm Hg for 15 minutes, to degas the specimen before it is saturated by introducing purified, deionized water into the chamber. After saturation, vacuum is applied for another 15 minutes for additional degassing, and the immersed specimen is left under atmospheric pressure for up to 4300 minutes (approximately 24 hours), or until a constant weight is reached. A constant weight is attained when specimen weight variation is less than 0.1 mg per hour. Before determining wet weight ( $W_W$ ), the sample is removed from the beaker using tweezers and surface moisture films are removed using a kimwipe. This procedure is repeated until constant weight is obtained. Considerable care is taken to maintain a consistent surface-drying process. The specimen is then placed in a dry beaker for vacuum drying.

**Table 1.** Effective porosity ( $\phi_E$ ) and bulk density ( $\delta$ ) data for 32 granite samples, including a comparison with previous effective porosity ( $\phi_E$ ) measurements.

Sample	h (m)	$\delta$ (g/mL)	1978	$\phi_E$ (%)		1994	Mean*
				1991	1993		
W-1	24	2.61	0.26			0.40	
W-2	55	2.70	0.16			0.27	
W-3	85	2.73	0.18			0.28	
W-4	124	2.62	0.28	0.41	0.46	0.37	0.41±0.05(±12%)
W-5	138	2.63	0.35	0.39		0.35	0.37±0.03 (±8%)
W-6	145	2.63	0.28			0.34	
W-7	160	2.63	0.29			0.32	
W-8	223	2.63	0.43			0.44	
W-9	245	2.63	0.36			0.44	
W-10	294	2.64	0.40			0.46	
W-11	303	2.63	0.33			0.51	
W-12	345	2.62	0.35			0.43	
W-13	384	2.63	0.31			0.43	
W-14	410	2.62	0.34			0.46	
W-15	460	2.63	0.37			0.48	
W-16	408	2.65	0.33			0.45	
W-17	468	2.65	0.27			0.49	
W-18	482	2.65	0.36			0.47	
W-19	505	2.64	0.39			0.48	
W-20	551	2.65	0.36			0.51	
W-21	603	2.65	0.33	0.50		0.45	0.47±0.03 (±6%)
W-22	631	2.64	0.38			0.51	
W-23	659	2.65	0.46			0.57	
W-24	692	2.64	0.40	0.55		0.59	0.57±0.03 (±5%)
W-25	719	2.64	0.45			0.52	
W-26	746	2.66	0.46			0.56	
W-27	789	2.65	0.54			0.64	
W-28	809	2.66	0.56			0.63	
W-29	840	2.65	0.53			0.62	
W-30	863	2.62	0.60			0.63	
W-31	906	2.65	0.49	0.67	0.62	0.60	0.64±0.04 (±6%)
W-32	928	2.65	0.50			0.58	

h = depth  
 $\phi_E$  = effective porosity  
 $\delta$  = bulk density  
 1978 = Katsube and Walsh (1987)  
 1991 = Katsube and Scromeda (1991)  
 1993 = Scromeda and Katsube (1993)  
 1994 = this study  
 \* = mean value of the 1991 to 1994 studies

## 2. Vacuum drying

The saturated specimen is now in a dry beaker and is placed in the vacuum chamber to evacuate the moisture. It is left under vacuum for periods from 195 to about 720 minutes. After each specified period, the sample is weighed. This procedure is repeated until a constant weight is obtained. This weight is represented by  $W_{rD}$ .

## 3. Vacuum-oven drying

Once the sample has been removed from the vacuum chamber at room temperature, it is placed in the vacuum oven under a vacuum of 760 mm of Hg. Vacuum-oven drying is carried out at 116°C for up to 2160 minutes, or until a constant weight (<0.1 mg/hour) is obtained. The sample is then removed from the oven and cooled in a desiccator for approximately 10 minutes at room temperature, before the dry weight ( $W_D$ ) is measured.

Katsube et al. (1992) provide a relatively comprehensive overview of this method, including the advantages and limitations of the various procedures applied.

### Effective porosity determination

The duration times for drying and degassing under vacuum, for saturating under atmospheric pressure, and for oven drying under vacuum are represented by  $t_f$ ,  $t_s$ , and  $t_D$ , respectively, and are expressed in minutes. Duration of saturation,  $t_s$ , is measured once 15 minutes of vacuum drying and 15 minutes of vacuum degassing of the immersed sample are completed. The weight of a specimen at any given time is represented by  $W_r$ , in grams. After  $W_r$  reaches a constant value during the saturation process, the specimen is considered to be fully saturated and its weight is represented by  $W_W$ . When  $W_r$  reaches a constant value during oven drying at 116°C, the specimen is considered to be completely dried and its weight is represented by  $W_D$ . The weight difference between  $W_r$  and  $W_D$  is  $\Delta W_r$ :

$$\Delta W_r = W_r - W_D \quad (1)$$

The effective porosity ( $\phi_E$ ) is determined using the following equation:

$$\phi_E = (W_W - W_D)\delta / (W_D\delta_W) \quad (2)$$

where  $\delta_W$  is the bulk density of the pore water (usually considered to be unity) saturating the sample. Degree of saturation,  $S_r$ , is a parameter used in this study to monitor water content in the specimen. It is defined as follows:

$$S_r = \Delta W_r / (W_W - W_D) \quad (3)$$

where  $\Delta W_r$  (equation 1) is the weight of free and bound (or adsorbed) water at any given time during the test. The  $W_r$  will reach a constant value after prolonged drying times ( $t_D$ ) at room temperature (23°C). This value is represented by  $W_{rD}$ . Similarly, the degree of saturation ( $S_r$ ) will eventually also reach a constant value, represented by constant saturation,  $S_{rD}$ , and derived by the following equation:

$$S_{rD} = (W_{rD} - W_D) / (W_W - W_D) \quad (4)$$

It represents the pore space occupied by bound or adsorbed water on pore surfaces, at room temperature (23°C) and atmospheric pressure.

### Previous measurement procedures

Shorter vacuum-drying ( $t_f$ ), saturating ( $t_s$ ), and oven-drying ( $t_D$ ) times were applied in previous measurements (Katsube and Walsh, 1987). They were set at 15, 40, and 240 minutes, respectively. Katsube et al. (1992) provide a relatively comprehensive review of these measurements. Drying temperatures were 100-105°C for all measurements carried out in the 1991 study (Katsube and Scromeda, 1991) and prior to that (e.g., Katsube and Walsh, 1987).

## EXPERIMENTAL RESULTS

Results of the effective porosity ( $\phi_E$ ) and constant degree of saturation ( $S_{rD}$ ) determinations, using equations (1) to (4), are listed in Table 2. Effective porosity ( $\phi_E$ ) values are also listed in Table 1, to enable comparison with previous data. Results

Table 2. Results of effective porosity ( $\phi_E$ ) measurements.

Sample	$\delta$ (g/mL)	$W_W$ (g)	$W_D$ (g)	$S_{rD}$ (%)	$\phi_E$ (%)
W-1	2.61	17.5225	17.4956	18.	0.40
W-2	2.70	19.4288	19.4095	29.	0.27
W-3	2.73	20.6481	20.6267	24.	0.28
W-4	2.62	18.7833	18.7570	13.	0.37
W-5	2.63	18.8848	18.8595	17.	0.35
W-6	2.63	18.3582	18.3342	15.	0.34
W-7	2.63	17.9177	17.8957	13.	0.32
W-8	2.63	18.8907	18.8595	13.	0.44
W-9	2.63	18.6943	18.6632	17.	0.44
W-10	2.64	19.6632	19.6291	11.	0.46
W-11	2.63	18.9661	18.9294	14.	0.51
W-12	2.62	17.9846	17.9553	8.2	0.43
W-13	2.63	19.0186	18.9873	13.	0.43
W-14	2.62	17.1992	17.1691	11.	0.46
W-15	2.63	17.9718	17.9389	13.	0.48
W-16	2.65	19.5010	19.4678	9.0	0.45
W-17	2.65	21.6965	21.6566	13.	0.49
W-18	2.65	22.1246	22.0852	8.4	0.47
W-19	2.64	21.1690	21.1305	9.9	0.48
W-20	2.65	19.3618	19.3247	17.	0.51
W-21	2.65	19.0541	19.0216	6.8	0.45
W-22	2.64	21.1854	21.1442	7.5	0.51
W-23	2.65	23.6459	23.5949	13.	0.57
W-24	2.64	22.6043	22.5543	7.4	0.59
W-25	2.64	22.7312	22.6869	9.0	0.52
W-26	2.66	21.5034	21.4579	7.9	0.56
W-27	2.65	19.1730	19.1270	8.5	0.64
W-28	2.66	19.4635	19.4179	12.	0.63
W-29	2.65	19.9777	19.9311	6.2	0.62
W-30	2.62	21.6817	21.6294	5.4	0.63
W-31	2.65	19.0778	19.0347	9.3	0.60
W-32	2.65	21.5061	21.4589	9.5	0.58

$\delta$  = bulk density (Equation 2)  
 $W_w$  = wet weight  
 $W_D$  = dry weight  
 $S_{rD}$  = constant degree of saturation  
 $\phi_E$  = effective porosity

**Table 3a.** Results of vacuum drying granite samples at 23°C.

Sample	$t_v$ (min)	$W_t$ (g)	$\Delta W_t$ (mg)	$S_t$ (%)
W-5	0	18.8714	4.7	17.1
	45	18.8714	4.7	17.1
	120	18.8712	4.5	16.4
	240	18.8709	4.2	15.3
	300	18.8708	4.1	14.9
	390	18.8708	4.1	14.9
	4270	18.8708	4.1	14.9
W-21	0	19.0330	7.6	21.2
	45	19.0326	7.2	20.1
	120	19.0300	4.6	12.9
	240	19.0295	4.1	11.5
	300	19.0293	3.9	10.9
	390	19.0292	3.8	10.6
	4270	19.0292	3.8	10.6
W-24	0	22.5660	4.4	9.3
	60	22.5657	4.1	8.7
	120	22.5656	4.0	8.5
	240	22.5654	3.8	8.1
	300	22.5653	3.7	7.9
	360	22.5653	3.7	7.9
	1396	22.5653	3.7	7.9

$t_v$  = vacuum drying time  
 $W_t$  = weight of specimen at time t  
 $\Delta W_t$  = weight difference between  $W_t$  and  $W_0$  of the oven-dried specimen  
 $S_t$  = degree of saturation

**Table 3c.** Results of oven-drying saturated granite samples at 116°C.

Sample	$t_o$ (min)	$W_t$ (g)	$\Delta W_t$ (mg)	$S_t$ (%)
W-5	0	18.8906	23.9	86.9
	30	18.8689	2.2	8.0
	60	18.8679	1.2	4.4
	105	18.8673	0.6	2.2
	180	18.8667	0.0	0.0
	240	18.8667	0.0	0.0
	300	18.8667	0.0	0.0
W-21	0	19.0564	31.0	86.6
	30	19.0266	1.2	3.4
	60	19.0262	0.8	2.2
	105	19.0260	0.6	1.7
	180	19.0256	0.2	0.6
	240	19.0254	0.0	0.0
	300	19.0254	0.0	0.0
W-24	0	22.6064	44.8	95.1
	30	22.5628	1.2	2.6
	60	22.5620	0.4	0.9
	105	22.5620	0.4	0.9
	180	22.5616	0.0	0.0
	240	22.5616	0.0	0.0
	300	22.5616	0.0	0.0

$t_o$  = oven-drying time  
 $W_t$  = weight of specimen at time t  
 $\Delta W_t$  = weight difference between  $W_t$  and  $W_0$   
 $S_t$  = degree of saturation

**Table 3b.** Results of saturating granite samples under atmospheric pressure 23°C.

Sample	$t_s$ (min)	$W_t$ (g)	$\Delta W_t$ (mg)	$S_t$ (%)
W-5	0	18.8649	2.7	9.8
	1	18.8928	26.1	94.9
	10	18.8928	26.1	94.9
	25	18.8931	26.4	96.0
	40	18.8931	26.4	96.0
	55	18.8931	26.4	96.0
	70	18.8934	26.7	97.1
	140	18.8938	27.1	98.6
	180	18.8942	27.5	100
	240	18.8942	27.5	100
	300	18.8942	27.5	100
W-21	0	19.0277	2.3	6.4
	1	19.0579	32.5	90.8
	10	19.0581	32.7	91.3
	25	19.0581	32.7	91.3
	40	19.0588	33.4	93.3
	55	19.0590	33.6	93.9
	70	19.0592	33.8	94.4
	140	19.0612	35.8	100
	180	19.0612	35.8	100
	240	19.0612	35.8	100
	300	19.0612	35.8	100
W-24	0	22.5659	4.3	9.1
	1	22.6054	43.8	93.0
	10	22.6061	44.5	94.5
	25	22.6069	45.3	96.2
	40	22.6069	45.3	96.2
	70	22.6074	45.8	97.2
	100	22.6087	47.1	100
	160	22.6087	47.1	100
	190	22.6087	47.1	100
	220	22.6087	47.1	100
	250	22.6087	47.1	100

$t_s$  = saturation time  
 $W_t$  = weight of specimen at time t  
 $\Delta W_t$  = weight difference between  $W_t$  and  $W_0$   
 $S_t$  = degree of saturation

of vacuum-drying samples W-5, W-21 and W-24 at room temperature (23°C) are listed in Table 3a. Results for saturating the same three samples are listed in Table 3b. Finally, results for vacuum-oven drying at 116°C are listed in Table 3c. The measurements for these three samples were performed in 1991 but are reported here for the first time.

## DISCUSSION AND CONCLUSIONS

Effective porosity ( $\phi_E$ ) values of 0.27-0.64% obtained in this study (Table 1) are of a range similar to those of 0.16-0.60% obtained in 1978 (Katsube and Walsh, 1987). However, values below 0.2%, such as those for W-2 and W-3 (0.16% and 0.18%) in the 1978 measurements, were not obtained this time. A comparison of effective porosity ( $\phi_E$ ) values obtained during this study and in 1978 is given in Figure 1. The 1978 values are smaller than those of this study by 0-50%, with 80% of the samples displaying values smaller by 10-40%. This raises the question of why the existence of this systematic difference?.

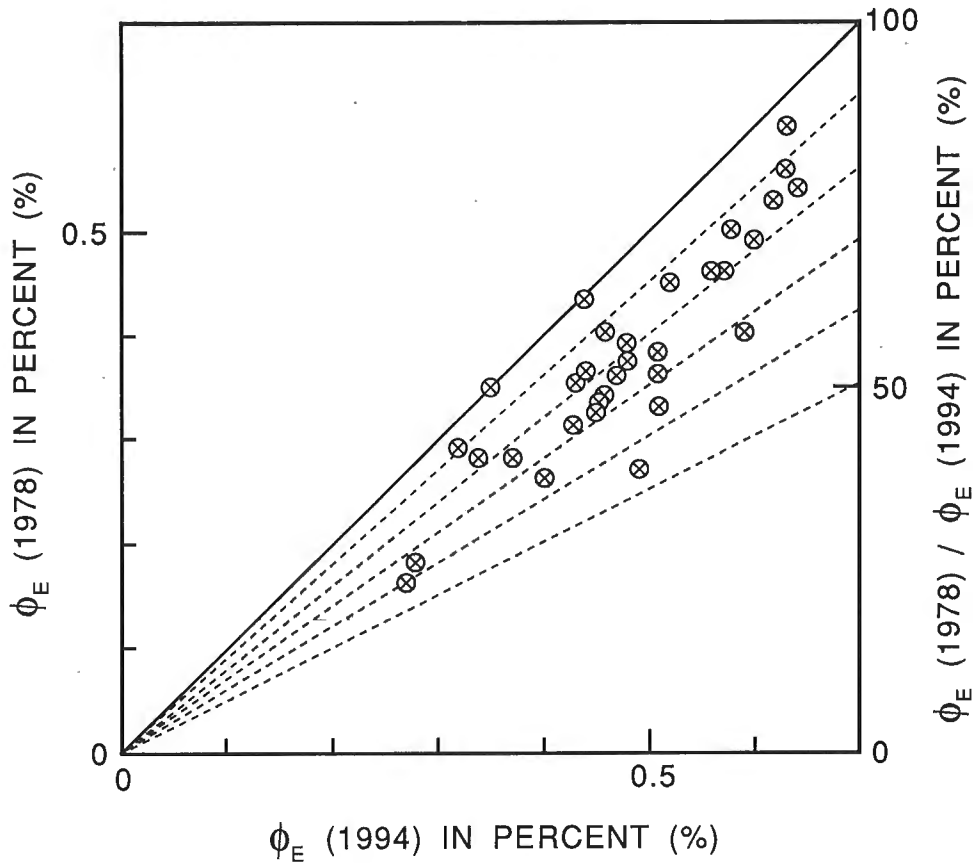


**Figure 1.** A comparison of effective porosity ( $\phi_E$ ) values obtained in this study (1994) and in 1978 (Katsube and Walsh, 1987). Results are also expressed in terms of the ratio ( $\phi_E(1978)/\phi_E(1994)$ ) of the two sets of values.

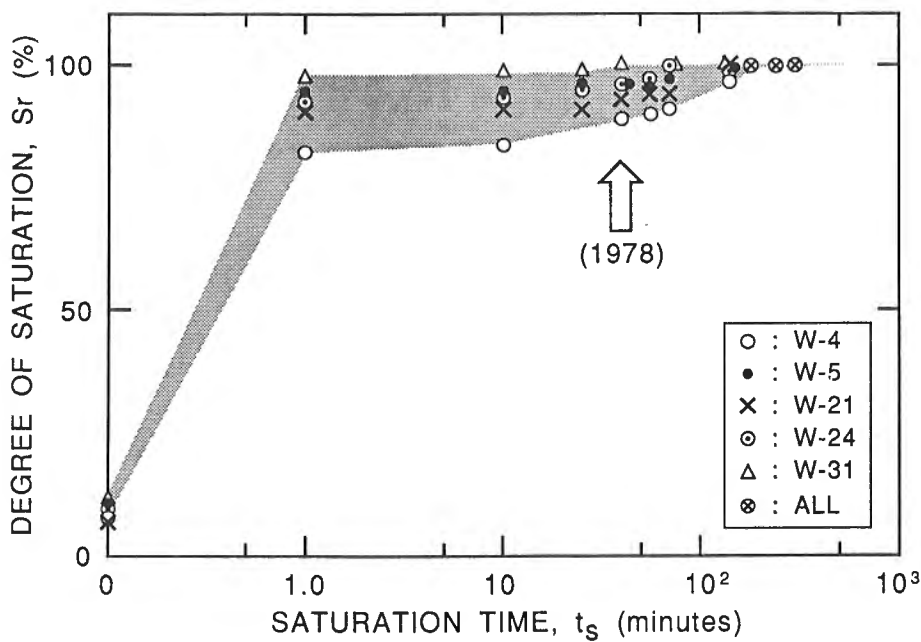


**Figure 2a.**

Degree of saturation ( $S_r$ ) as a function of saturation time ( $t_s$ ) for 5 of the 32 granite samples. Data for samples W-4 and W-31 were obtained from Katsube and Scromeda (1991).

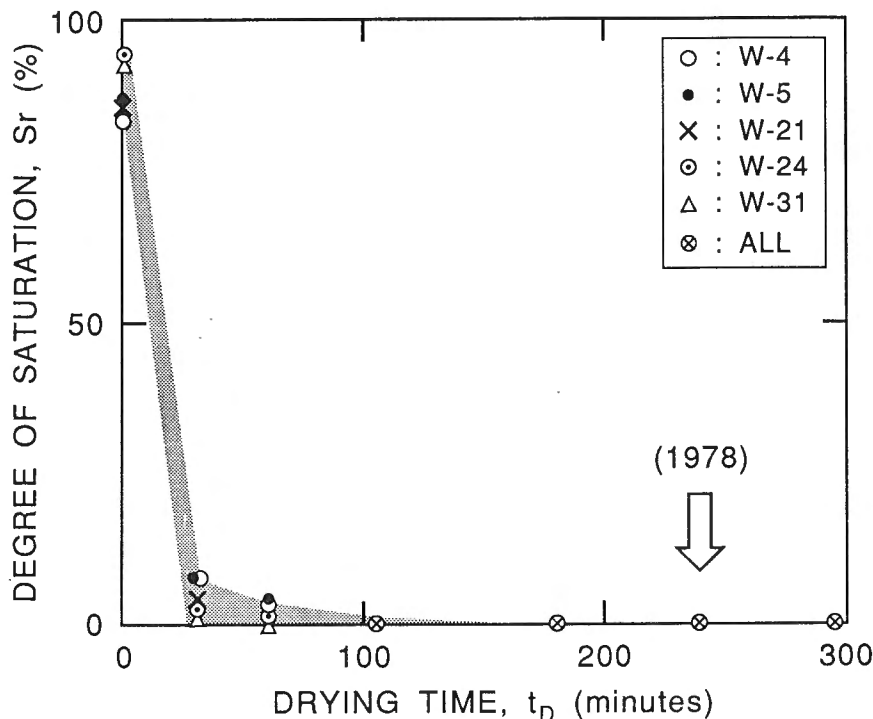


**Figure 2b.**

*Degree of saturation ( $S_r$ ) as a function of drying times ( $t_D$ ) for 5 of the 32 granite samples. Data for samples W-4 and W-31 were obtained from Katsube and Scromeda (1991).*

The degree of saturation ( $S_r$ ) as a function of saturation ( $t_s$ ) and drying times ( $t_D$ ) for five of these granite samples (Table 3b, 3c, and data in Katsube and Scromeda, 1991) is given in Figures 2a and 2b, respectively, along with the reduced saturation times (40 and 240 minutes) that were used in the 1978 study (Katsube and Walsh, 1987). These figures show that the maximum error due to reduced saturation time ( $t_s$ ) is approximately 12%, and that due to reduced drying time ( $t_D$ ) is nil.

Although lower drying temperatures (100-105°C) were used for all measurements carried out in the 1991 study (Katsube and Scromeda, 1991) and prior to that (e.g., Katsube and Walsh, 1987), the effective porosity ( $\phi_E$ ) values for the five samples used in the 1991 study (Table 1) are very similar to those of the same samples included in this study. The 1993 study (Scromeda and Katsube, 1993, Fig. 4) includes an example of a granite sample that shows a reduction in effective porosity ( $\phi_E$ ) of 4-5% with a decrease in drying temperature from 116 to 100°C.

Consequently, the reduced saturation time ( $t_s$ ) used in studies prior to 1991 could account for about 12% of the reduced effective porosity ( $\phi_E$ ) values (<40%) of the 1978 study (Katsube and Walsh, 1987). The reduced drying temperatures used in the 1991 study and prior to that might account for another 4-5%. However, other reasons should be found for the remaining 23-28% of the 40% reduced value.

## ACKNOWLEDGMENTS

The authors express their sincere thanks to Dr. S.W. Adcock (Geological Survey of Canada, Ottawa) for his constructive comments and for critically reviewing this paper.

## REFERENCES

- American Petroleum Institute**  
1960: Recommended practices for core-analysis procedure: API Recommended Practice 40 (RP 40) First Edition; American Petroleum Institute, Washington, D.C., p. 55.
- Katsube, T.J. and Hume, J.P. (editors)**  
1987a: Geotechnical studies at Whiteshell Research Area (RA-3). Canada Centre for Mineral and Energy Technology, Report MRL 87-52, 232 p.
- Katsube, T.J. and Hume, J.P.**  
1987b: Pore structure characteristics of granitic rock samples from Whiteshell Research Area; in Geotechnical Studies at Whiteshell Research Area (RA-3). Canada Centre for Mineral and Energy Technology, Report MRL 87-52, p. 111-158.
- Katsube, T.J. and Scromeda, N.**  
1991: Effective porosity measuring procedure for low porosity rocks; in Current Research, Part E; Geological Survey of Canada, Paper 91-1E, p. 291-297.
- Katsube, T.J. and Walsh, J.B.**  
1987: Effective aperture for fluid flow in microcracks; International Journal of Rock Mechanics and Mining Sciences and Geomechanics Abstracts, v. 24, p. 175-183.
- Katsube, T.J., Percival, J.B., and Hume, J.P.**  
1985: Characterization of the rock mass by pore structure parameters: Atomic Energy of Canada Limited Technical Record, TP-299, p. 375-413.
- Katsube, T.J., Scromeda, N., and Williamson, M.**  
1992: Effective porosity of tight shales from the Venture Gas Field, offshore Nova Scotia; in Current Research, Part D; Geological Survey of Canada, Paper 92-1D, p. 111-119.
- Scromeda, N. and Katsube, T.J.**  
1993: Effect of vacuum-drying and temperature on effective porosity determination for tight rocks; in Current Research, Part E; Geological Survey of Canada, Paper 93-1E, p. 313-319.
- 1994: Effect of temperature on drying procedures used in porosity measurements of tight rocks; in Current Research 1994-E; Geological Survey of Canada, p. 283-289.

## AUTHOR INDEX

Armitage, A.E. . . . .	187, 213	Morrison, D.W. . . . .	225
Balog, M.J. . . . .	163	O'Keefe, M.D. . . . .	97
Beaumont-Smith, C. . . . .	87	Paradis, S.J. . . . .	259
Bethune, K.M. . . . .	53	Park, J.K. . . . .	195
Bleeker, W. . . . .	87	Paul, D. . . . .	107
Boisvert, E. . . . .	259	Percival, J.A. . . . .	121, 131, 141
Buchan, K.L. . . . .	195	Petch, C.A. . . . .	97
Card, K.D. . . . .	121, 141	Peterson, T.D. . . . .	11, 19
Chacko, T. . . . .	77	Peterson, V.L. . . . .	35
Dehls, J.F. . . . .	97	Prasad, N. . . . .	201
Ermanovics, I. . . . .	45	Prévost, C.L. . . . .	235
Froese, E. . . . .	107	Roy, M. . . . .	243
Gandhi, S.S. . . . .	195, 201	Russell, I. . . . .	107
Godin, L. . . . .	67	Schau, M. . . . .	27
Hamilton, P.B. . . . .	235	Scammell, R.J. . . . .	53
Heather, K.B. . . . .	1	Scott, D.J. . . . .	67
Henderson, J.B. . . . .	77	Shore, G.T. . . . .	1
Henderson, J.R. . . . .	97	Skulski, T. . . . .	121, 131, 141
Henderson, M.N. . . . .	97	Tella, S. . . . .	27, 163, 175
Jones, A.L. . . . .	187	Thompson, P.H. . . . .	107
Kerswill, J.A. . . . .	97, 107	van Breemen, O. . . . .	1, 35
Kusky, T.M. . . . .	131	Veillette, J.J. . . . .	235, 243, 249
Lee, C. . . . .	11	Villeneuve, M. . . . .	97
Lin, S. . . . .	121, 141	Whalen, J.B. . . . .	225
MacRae, N.D. . . . .	187, 213	Winsky, P.A. . . . .	121, 131
Mader, U. . . . .	27	Zaleski, E. . . . .	35
Miller, A.R. . . . .	151, 163, 175, 187, 213		



## **NOTE TO CONTRIBUTORS**

Submissions to the Discussion section of Current Research are welcome from both the staff of the Geological Survey of Canada and from the public. Discussions are limited to 6 double-spaced typewritten pages (about 1500 words) and are subject to review by the Chief Scientific Editor. Discussions are restricted to the scientific content of Geological Survey reports. General discussions concerning sector or government policy will not be accepted. All manuscripts must be computer word-processed on an IBM compatible system and must be submitted with a diskette using WordPerfect. Illustrations will be accepted only if, in the opinion of the editor, they are considered essential. In any case no redrafting will be undertaken and reproducible copy must accompany the original submissions. Discussion is limited to recent reports (not more than 2 years old) and may be in either English or French. Every effort is made to include both Discussion and Reply in the same issue. Current Research is published in January and July. Submissions should be sent to the Chief Scientific Editor, Geological Survey of Canada, 601 Booth Street, Ottawa, Canada, K1A 0E8.

## **AVIS AUX AUTEURS D'ARTICLES**

Nous encourageons tant le personnel de la Commission géologique que le grand public à nous faire parvenir des articles destinés à la section discussion de la publication Recherches en cours. Le texte doit comprendre au plus six pages dactylographiées à double interligne (environ 1500 mots), texte qui peut faire l'objet d'un réexamen par le rédacteur scientifique en chef. Les discussions doivent se limiter au contenu scientifique des rapports de la Commission géologique. Les discussions générales sur le Secteur ou les politiques gouvernementales ne seront pas acceptées. Le texte doit être soumis à un traitement de texte informatisé par un système IBM compatible et enregistré sur disquette WordPerfect. Les illustrations ne seront acceptées que dans la mesure où, selon l'opinion du rédacteur, elles seront considérées comme essentielles. Aucune retouche ne sera faite au texte et dans tous les cas, une copie qui puisse être reproduite doit accompagner le texte original. Les discussions en français ou en anglais doivent se limiter aux rapports récents (au plus de 2 ans). On s'efforcera de faire coïncider les articles destinés aux rubriques discussions et réponses dans le même numéro. La publication Recherches en cours paraît en janvier et en juillet. Les articles doivent être envoyés au rédacteur en chef scientifique, Commission géologique du Canada, 601, rue Booth, Ottawa, Canada, K1A 0E8.

Geological Survey of Canada Current Research, is released twice a year, in January and July. The four parts published in January 1995 (Current Research 1995- A to D) are listed below and can be purchased separately.

Recherches en cours, une publication de la Commission géologique du Canada, est publiée deux fois par année, en janvier et en juillet. Les quatre parties publiées en janvier 1995 (Recherches en cours 1995-A à D) sont énumérées ci-dessous et sont vendues séparément.

Part A: Cordillera and Pacific Margin  
Partie A : Cordillère et marge du Pacifique

Part B: Interior Plains and Arctic Canada  
Partie B : Plaines intérieures et région arctique du Canada

Part C: Canadian Shield  
Partie C : Bouclier canadien

Part D: Eastern Canada and national and general programs  
Partie D : Est du Canada et programmes nationaux et généraux